

DISS. ETH No. 27536

**Dynamic Chemistry with
Potassium Acyltrifluoroborates (KATs)**

A thesis submitted to attain the degree of
DOCTOR OF SCIENCES of ETH ZURICH

(Dr. sc. ETH Zurich)

presented by

Yi-Chung Dzeng

Master of Science in Chemistry,
National Taiwan University

Born on 10.01.1990
Citizen of Taiwan

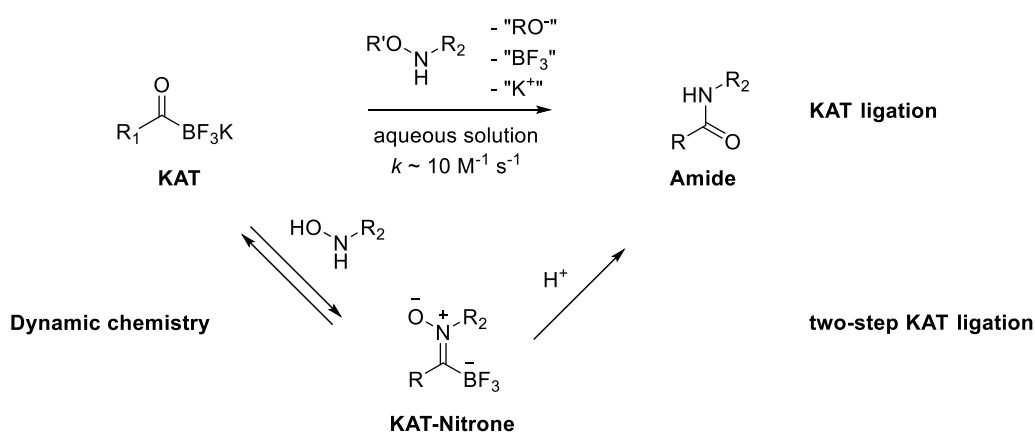
Accepted on the recommendation of

Prof. Dr. Jeffrey W. Bode and Prof. Dr. Peter Chen

2021

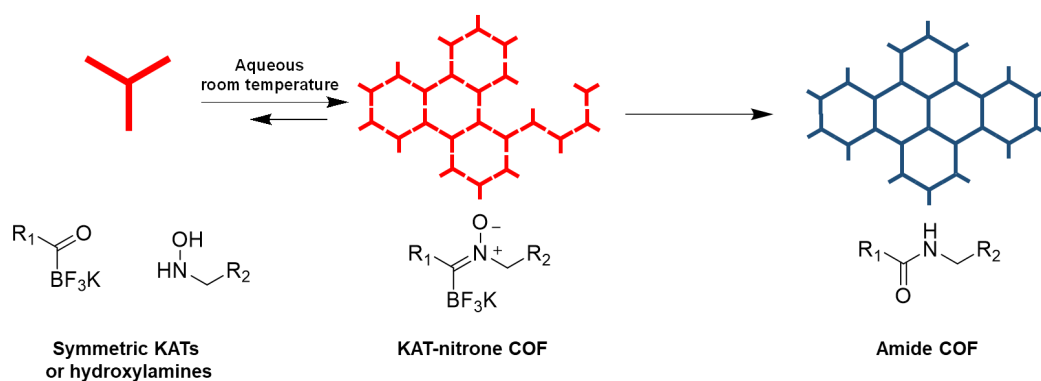
Abstract

The KAT ligation proceeds when potassium acyl trifluoroborates (KATs) couple with hydroxylamines, forming an amide bond in aqueous environment with remarkable chemoselectivity, robustness, and reaction rates. The reactivity of KAT ligation depends on both the structure of the KAT and of the hydroxylamine. Under certain circumstances, when the hydroxylamine oxygen is unsubstituted, a KAT nitron intermediate is formed reversibly between the KAT and the hydroxylamine. From this dynamic KAT nitron, a static amide bond can be formed upon acidification. This “two-step” KAT ligation via KAT-nitron formation could be a candidate for building a dynamic chemical system which can be fixed by acidification.

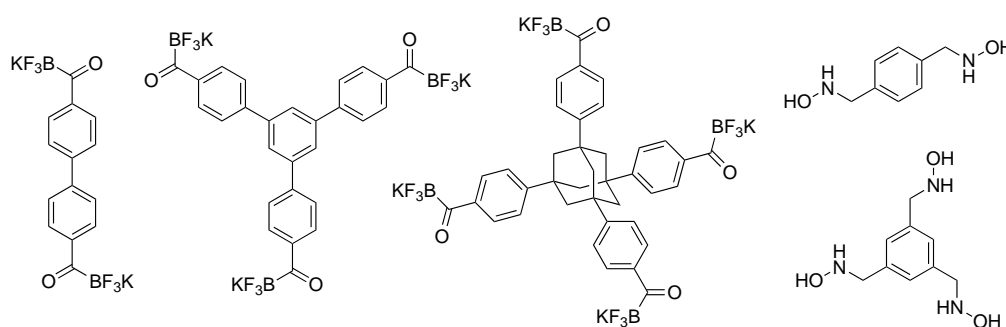


Chapter 2 of this thesis sets out to explore the properties of KAT nitrones, including their formation, spectroscopic properties, and reactivity. Mild and aqueous conditions for KAT nitron formation were identified, which enabled the investigation of the dynamic exchange of KAT-hydroxylamine pairs, as well as conditions for converting the KAT nitron into an amide. These findings supported our earlier hypothesis that KAT nitron formation was dynamic, and laid the foundation for KAT-nitrones to power dynamic chemistries.

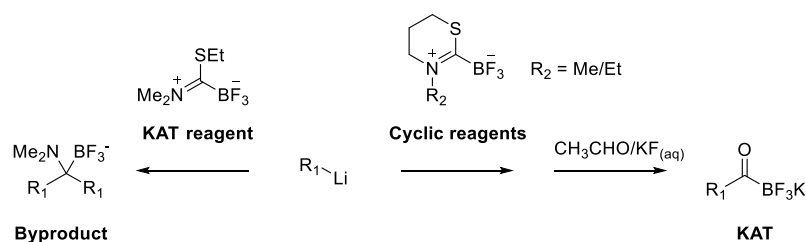
Covalent Organic Frameworks (COFs) are structure-rigid, pore-persistent, highly crystalline materials with high surface areas that have found widespread applications. The formation of COFs relies on conditions for the dynamic formation of their constituent bonds, as crystallinity arises from reversible assembly. Chemical bonds with higher dynamicity form COFs with higher crystallinity, but are also more prone to hydrolysis, setting up a trade-off between COF stability and crystallinity. We hypothesized that by building COFs with KAT-nitron bonds, the COF assembly could be performed with high dynamicity under aqueous, ambient conditions to achieve crystallinity. The resulting KAT-nitron COF could be fixed into a permanent, chemically more resistant amide COF by its acidification.



A collection of highly symmetric di-, tri-, and tetra KATs were designed and synthesized, along with the complementary bis- and tris hydroxylamines, as potential KAT-nitrone building blocks. The KAT-nitrone formation among these building blocks was facile in aqueous conditions, yet no crystalline COF products were formed in our hands. Findings related to these multivalent building block KATs and hydroxylamines were nonetheless interesting and were summarized in Chapter 3.



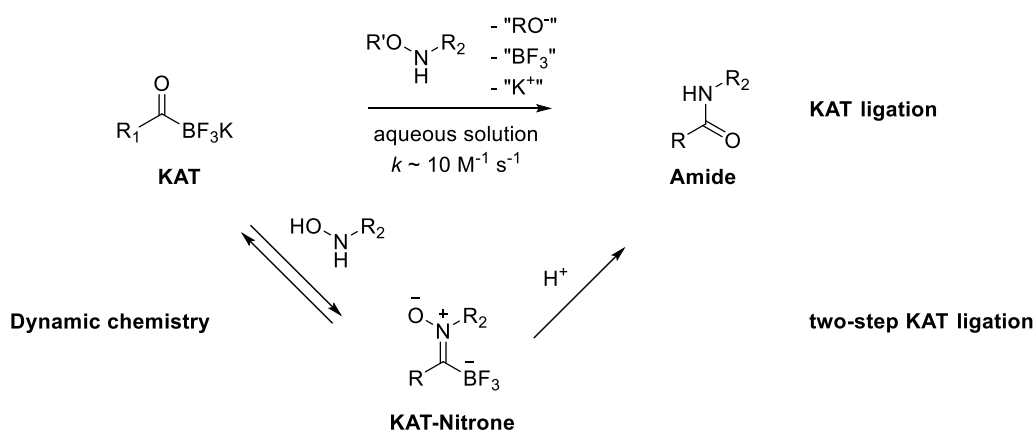
In Chapter 4 we explored the possibility of using KAT-nitrone for creating a Dynamic Covalent Library for the search of suitable PROteolysis TArgeting Chimera (PROTAC) linkers. During the preparation of the required library building blocks, we encountered the need of a new class of alkyl KATs, α -alkoxy KATs, which could not be easily synthesized with existing methods. To overcome this, new cyclic KAT reagents that expedite the synthesis of alkyl KATs from alkyllithiums were designed, evaluated, and reported in Chapter 5.



Chapter 6 collects some KAT related findings that couldn't fit in the other chapters.

Zusammenfassung

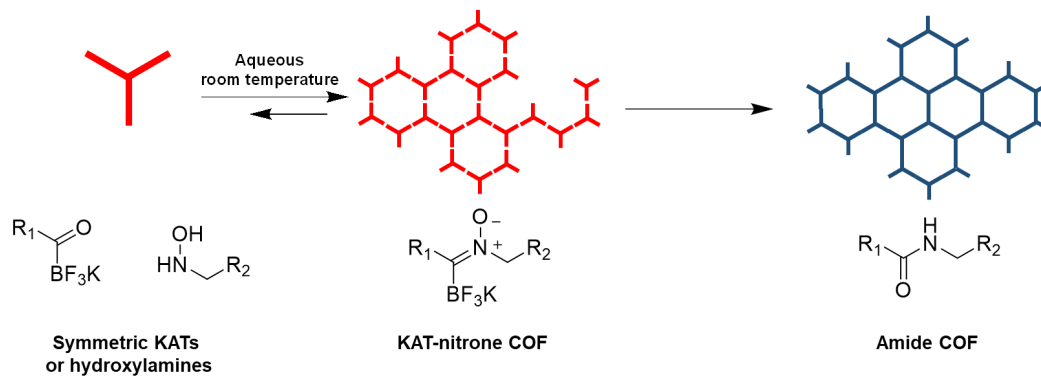
Die KAT Ligation tritt ein, wenn Kalium Acyltrifluoroborate (KATs) auf Hydroxylamine treffen und eine Amidbindung in wässrigem Medium mit einer beachtlichen Geschwindigkeit, Chemoselektivität und Robustheit formen. Die Reaktivität der KAT Ligation hängt beträchtlich von der Struktur ihrer Reaktionspartner, den KATs und den Hydroxylaminen, ab. Verwendet man N-monoalkylierte Hydroxylamine, kann ein KAT-Nitron-Intermediat reversibel mit einem KAT geformt werden. Vom KAT Nitron-Intermediat aus, kann unter Zugabe von Säure das entsprechende Amid gebildet werden. Diese "two-step" KAT Ligation, die über ein Nitron-Intermediat verläuft, könnte zum Aufbau eines Dynamic Chemical Systems verwendet werden, das unter Protonierung fixiert werden kann.



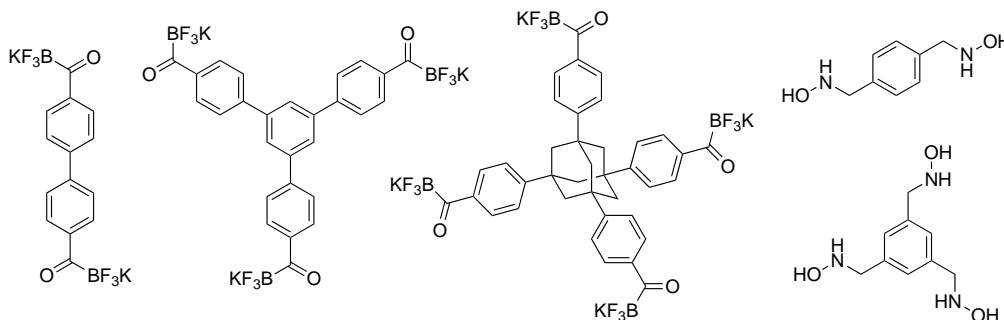
Das zweite Kapitel dieser Thesis befasst sich mit der Erkundung der Eigenschaften von KAT-Nitronen, einschliesslich ihrer Reaktivitäten und spektroskopischen Eigenschaften. Milde und wässrige Bedingungen für die Herstellung von KAT-Nitronen konnten identifiziert werden, die eine Untersuchung des dynamischen Austausch von KAT-Hydroxylamin-Paaren ermöglichten, wie auch die Umsetzung dieser Nitronen in ihre entsprechenden Amide. Diese Resultate unterstützen die Hypothese, dass die KAT-Nitron-Bildung dynamisch abläuft und gestatten ihre Nutzung für Dynamic Chemistry.

Covalent Organic Frameworks (COFs) sind strukturell harte, poröse und hochkristalline Materialien mit grossen Gesamtoberflächen und besitzen infolgedessen eine Reihe von Anwendungen. Die Bildung von COFs beruht auf der dynamischen Herstellung ihrer einzelnen Bindungen, aus der ihre Kristallinität hervorgeht. Chemische Bindungen, die sich mit hoher Dynamik formen lassen, bilden COFs mit hoher Kristallinität, sind jedoch auch anfälliger für Hydrolysen, wodurch ein Trade-off Szenario zwischen Stabilität und Kristallinität entsteht. Diese Betrachtungen führten zur Annahme kristalliner COFs mit hoher Dynamik und unter milden und wässrigen Bedingungen über eine KAT-Nitron-Bindung herstellen zu können. Das

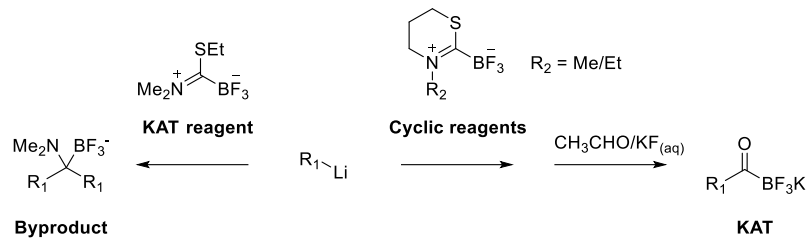
daraus resultierende KAT-Nitron-COF könnte über eine Ansäuerung in ein permanentes und chemisch resistenteres Amid-COF umgewandelt werden.



Eine Reihe von hochsymmetrischen bi-, tri-, und tetra-funktionalen KATs wurden designt und synthetisiert, wie auch ihre komplementären Hydroxylamine, die als potentielle KAT-Nitron Bausteine fungieren können. Die KAT-Nitron Bildung war einfach unter wässrigen Bedingungen herzustellen, jedoch konnten keine kristallinen COFs daraus geformt werden. Interessante Erkenntnisse konnten aus den Experimenten mit multivalenten KAT- und Hydroxylamin-Bausteinen gewonnen werden und wurden in Kapitel 3 zusammengefasst.



In Kapitel 4 wurde die Möglichkeit untersucht eine Dynamic Covalent Library mit KAT-Nitronen aufzubauen, um geeignete PROteolysis TARgeting Chimera (PROTAC) Linker zu finden. Während der Synthese der benötigten Bausteine für die Zusammenstellung einer Library, wurde eine neue Klasse vom aliphatischen KATs benötigt, den α -alkoxy KATs, die mit den zur Verfügung stehenden Methoden nicht einfach hergestellt werden konnten. Daraufhin wurde ein neues zyklisches KAT-Reagenz designt, das die Herstellung von Alkyl-KATs aus einem Alkylithium in einem Schritt ermöglicht (Kapitel 5).



Kapitel 6 beinhaltet Resultate, die mit KATs zusammenhängen und inhaltlich nicht zu den oben genannten Kapiteln passen.

Acknowledgements

And at last, here we are, at the final moment to conclude this thesis and my study at ETH. I have too many things to be thankful for and I should try my best to categorize them. The sequence of mentioning them is purely arbitrary. So let me start.

For the completion of this thesis and my doctoral exam, I need to thank Prof. Jeffrey W. Bode for everything, and Prof. Peter Chen for agreeing to be my Koreferent. Both my examiners have spent a great deal of their valuable time and effort on my thesis, and taught me a great number of things during its revision. In fact, both my dear examiners have already taught me a great deal way before participating in my exam committee. The great course of physical organic chemistry and vibrant Kolloquium discussions from Prof. Chen were among the most precious experiences I had during my stay at the Laboratorium für Organische Chemie.

I also need to express my thanks to Jeff for my entire ETH journey. From the moment Jeff accepted me into the group, his continuous support and trust has been the most empowering. These six years in his group have shaped me into a chemist I will not have imagined myself to be, before joining at October 2015. As invaluable as his mentorship is, the material support I have received under his shield is just as valuable. I still did not know which grants have supported my work even until this day, as I always had the luxury to purchase and consume materials in ways I see fit. Along with Jeff's invisible effort in raising this family, I also appreciate the generous Swiss tax-payers, and the structure of ETH and LOC as they were.

Administrative assistance from Mario Kessinger have made things running smoothly and avoided loads of trouble ahead of me. The DCHAB infrastructure has also made lab research inside the HCI building a happy lifestyle for me. I thank the HCI shop staff for keeping supplies running smoothly. The analytic departments have been wonderful and helped greatly during research. I thank Dr. Michael Wörle, Mr. Michael Solar and Dr. Nils Trapp from our Small Molecule Crystallography Center (SMoCC) for their timely, tireless, passionate, and professional support. I need to thank Dr. Wörle especially for introducing the PXRD facilities to me, and for his crystallography lecture. The NMR service is just as heartwarming and competent in maintaining our arsenal of open-access spectrometers, as well as in helping us on challenging samples while wading through waves of power, gas, and network interruptions, catching the ghost that haunts the autosamplers and maximizing the service uptime. For these I must thank Dr. Marc-Olivier Ebert, Mr. René Arnold, Rainer Frankenstein, and Stephan Burkhardt. The MoBiAS platform was indispensable for reviving our LCMS and timely HRMS

measurements. I thank Mr. Daniel Wirz, Louis Bertschi, Michael Meier and Perter Kälin for their hard work. I wish the HCI complex to stand firm and keep serving as a fortress it is now, sheltering chemists of coming generations against storms of doubt and uncertainty, during their more vulnerable stages in life.

I am also grateful to the Bode group members, past and present, for their influence on my research path in the group, including those I have met in person and those I have not. The early contributors to KAT research in Bode include Dr. Aaron Dumas, Dr. *Gábor Erős*, and Dr. Hidetoshi Noda whom I did not have the luck to meet face-to-face yet enjoyed the monologue I had with the reports they wrote and records they left behind. The later KAT subgroup members I have met have made my research days fun and resourceful. I thank Matthias Tanriver for translating the abstract of this thesis into German, as well as allowing me and my opinions into the study of KAT ligation kinetics, which to me is a long missing cornerstone of all KAT researches. Anne Schuhmacher is thanked for bring law, order, and decency to the lab, regarding research and other aspects. Philipp Schilling for great discussions stemmed from his fearlessness in stepping into the wild unknown. I also thank my ex-KAT associates: Dino Wu for witty comments on the bright sides, Alberto Osuna Gálvez for those on the dark yet not less constructive sides. Dominik Schauenburg for his wildest, constant pursuit in interesting ideas, Dmitry Mazunin for orienting me into F302 as my first Laborchef.

Yes, I thought I would have stayed at the same lab F302 throughout my stay up at Höngg. The F302 atmosphere constitutes the texture of the most part of my life in the last six years. I will remember the moments watching out the window below the G-floor bridge, overlooking the entrance hall to finger 3, during days and evenings, through snow, rain, fog or crystal sunlight, with you people being there, or possibly there. Names can then come with no explanation: Raphael Hofmann, Gaku Akimoto, Yayi Wang, Kateryna Tolmachova.

I thank Fumito Saito and Simon Baldauf, whose silent amicability and overflowing aura of chemistry penetrate the floors and walls, drawing me to pester them when I am bored. I know that I will be forgetting to mention some names of my lovely colleagues, both from the Bode group and our neighbor Yamakoshi group. I thank you all here with this single sentence, using the constraint of writing space as my alibi.

I thank the mountainous Schweiz for hosting and shaping me over the years. A large part of this thesis is completed in the alps, or on the train there. However a large part of me is already cast and set before I arrive in Zürich. The more scholarly part of me is formed first during gymnasium at Chien Kuo, and later at National Taiwan University. I have received

uncountable kindness when I messed around in both institutions. To mention two names from the NTU era: my Mastervater Prof. Tien-Yau Luh, and Prof. Murahashi with whom we worked together teaching a semester course. The six year stay with Prof. Luh is a time of absolutely no regrets as it sets me on the path to the chemist I am today. Prof. Murahashi's great hopes and care to the younger generation is a fire that I would strive to pass on. Having him joining my remote defense talk has certainly lit a corner of my heart through the day.

Further back...further...I think my blind passion for chemistry has been lit earlier than that. It is Primo Levi with his mysterious tiny book *il sistema periodico* that enchanted me to the sweet world of chemistry, even before I can write properly as a child. I thank my parents for making this encounter possible at home, and to not let me need a thing or worry a bit on life while growing up. You built a safe family for me. To talk about safe haven, family and growing up, this list must also include my wife Yuchin Sun, and some other people that widened my world at important moments: KCR, RZ, YCC, PCL, and PHH.

Finally I thank the world, including Chemistry, for being the way you are.

Table of Contents

Abstract	iii
Zusammenfassung.....	v
Acknowledgements.....	viii
Table of Contents.....	xi
List of Abbreviations.....	xv
1 Introduction.....	2
1.1. Acyl borons, acyltrifluoroborates (KATs) and KAT ligation	3
1.1.1. KAT as a keystone acylboron	3
1.1.2. KAT Ligation	5
1.1.3. Reactions at the KAT carbonyl group.....	9
1.2. KAT nitrones	10
1.3. Dynamic Chemistry	13
1.3.1. Systems chemistry and dynamic chemistry.....	13
1.3.2. Dynamic chemical bonds used in dynamic chemistry.....	15
1.3.3. Bond dynamicity enables chemical system to adapt to stimuli	18
1.4. Nitrene Chemistry.....	22
1.4.1. Nitrenes and their formation.....	22
1.4.2. Reactivity of nitrenes.....	23
1.4.3. Dynamic behavior of nitrenes.....	26
2 Properties and dynamics of KAT nitrones	29
2.1. Reactivity comparison with normal nitrenes	30
2.1.1. KAT nitrene forms easier than aldehyde nitrenes.....	30
2.1.2. Cycloaddition	32
2.1.3. Slow light promoted rearrangement	33
2.2. Spectroscopic properties of KAT nitrene	34
2.2.1. Infrared spectroscopy	34
2.2.2. Nuclear Magnetic spectroscopy	35

2.2.3.	UV-Vis spectroscopy.....	37
2.3.	Conditions for KAT-nitrone formation.....	40
2.3.1.	Solvents.....	40
2.3.2.	Effect of water.....	41
2.3.3.	Acid catalysis.....	45
2.3.4.	Acetonitrile is not always an innocent solvent.....	47
2.4.	Nitrone partner exchange.....	48
2.5.	Nitrone to amide conversion.....	49
2.5.1.	Identifying a flash acidification condition.....	49
2.5.2.	“Snapshot” experiment.....	52
2.6.	Summary.....	54
3	KAT-nitrones for covalent organic frameworks (COFs).....	55
3.1.	Covalent organic frameworks (COFs).....	56
3.2.	Synthesis of multivalent KATs.....	58
3.3.	Strong intermolecular association of multivalent KATs.....	61
3.4.	Synthesis of multivalent hydroxylamines.....	64
3.5.	Attempts on COF formation from KATs and hydroxylamines.....	67
3.5.1.	Fast formation of the nitrone.....	67
3.5.2.	Seeking crystallinity with powder XRD.....	69
3.6.	Summary and Outlook.....	78
4	Design and building block synthesis of a KAT-nitrone dynamically linked PROTAC.....	79
4.1.	PROTACs.....	80
4.1.1.	Adapter of an adapter.....	80
4.1.2.	KAT-nitrone split MZ-1 design.....	81
4.2.	Synthesis of the VHL hydroxylamine.....	83
4.3.	Synthesis of the JQ1-KAT.....	85
4.3.1.	Via a final amide coupling with amine-linker KAT.....	85

4.3.2.	Via alkylative KATylation.....	88
4.3.3.	Via photocatalytic hydroamidation with a JQ1 redox-active hydroxamic acid	90
4.3.4.	Brute-force JQ1-linker lithiation via stannane chemistry.....	94
4.4.	Summary and Outlook.....	95
5	Cyclic thiotrifluoroborate iminium reagents for alkyl KAT synthesis	97
5.1.	A need for α-alkoxy KATs, and synthetic routes of alkyl KATs.....	98
5.2.	Pyrrolidine iminiums didn't stabilize the tetrahedral intermediate enough	101
5.3.	A cyclic, N-S tethered reagent that stabilizes the intermediate.....	103
5.3.1.	Synthesis, properties and clean single addition.....	103
5.3.2.	Extraordinary stability of the KAT thioaminal after single addition	106
5.3.3.	Reactivity towards other organometallics or radical sources	109
5.3.4.	Alkyl di-KATs, potential α -leaving group KATs, and JQ1-TEG-KAT	111
5.4.	Alternative synthesis of 179 and its more soluble N-ethyl variant.....	111
5.5.	Summary	112
6	Brief journey with other KATs.....	114
6.1.	The role of a proton donor neighbor on KAT ligation rates.....	115
6.1.1.	Basicity of pyridine and quinoline KATs	115
6.1.2.	Synthesis of KATs bearing proton donors	116
6.2.	Synthesis of KATs and hydroxylamines for incorporation in polymers	118
6.2.1.	Bromomethylphenyl KATs	118
6.2.2.	KATs with polymerizable groups.....	119
7	Experimental section.....	122
7.1.	Synthetic procedures and characterization of compounds.....	123
7.1.1.	General Procedural information	123
7.1.2.	Synthesis of nitrones and amidoxime in Chapter 2	123
7.1.3.	Synthesis of multivalent KATs in Chapter 3	130

7.1.4.	Synthesis of hydroxylamines with 132	133
7.1.5.	Synthesis of MZ-1 PROTAC fragments used in Chapter 4.....	140
7.1.6.	Synthesis of KAT reagents in Chapter 5	143
7.1.7.	Synthesis of KATs with reagent (179)	149
7.1.8.	Synthesis of Compounds in Chapter 6.....	154
7.2.	Nitrone exchange experiments	156
7.2.1.	Nitrone partner exchange In Section 2.4	156
7.3.	Kinetic measurement results of KAT nitrone formation	156
7.3.1.	Butyl, p-F-phenyl and p-OMe-phenyl KAT in 1:1 DMSO-H ₂ O.....	156
7.3.2.	Nitrone 100 formation from p-Br-phenyl KAT and hydroxylamine 97 at various water concentration	158
7.3.3.	UV-Vis data of KAT nitrone 100 formation from p-bromophenyl KAT	158
7.4.	Acid-Base titration of pyridine and quinoline KATs	160
7.5.	LC-MS and IR raw data processing scripts.....	161
8	References	162
9	NMR Spectra	174

List of Abbreviations

Abbreviation	Name
KAT	potassium acyltrifluoroborate
KAHA	ketoacid-hydroxylamine (ligation)
TIM	trifluoroborate iminium
equiv	equivalances
NMR	nuclear magnetic resonance
IR	Infrared spectroscopy
quant.	quantitative
J	Coupling constant
p-	para-
Me	methyl
Et	ethyl
nBuLi	n-butyllithium
PEG	polyethylene glycol
PROTAC	proteolysis targeting chimera
COF	covalent organic framework
rt	room temperature
Cy	Cyclohexane
EtOAc	ethyl acetate
MIDA	methyliminodiacetic acid
DIPEA	N,N-diisopropylethylamine
TLC	thin-layer chromatography
LC-MS	liquid chromatography tandem mass spectroscopy
V_{int}	internal volume of silica flash chromatography columns
LDA	lithium diisopropyl amide
LN₂	liquid nitrogen
ESI	electrospray ionization
XIC	extracted ion chromatogram

DCL	dynamic combinatorial library
BET	bromo and extraterminal (domain proteins)
VHL	van Hippel-Lindau (E3 ligase)
HA	hydroxylamine(s)
calcd	calculated
POI	protein of interest
N.R.	no reaction
satd.	saturated
HFIP	hexafluoroisopropanol

1

Introduction

觸撫角獸的頭骨
閱讀殘損的詩行
可以窺見當時的
原野與年輕的
夢境嗎

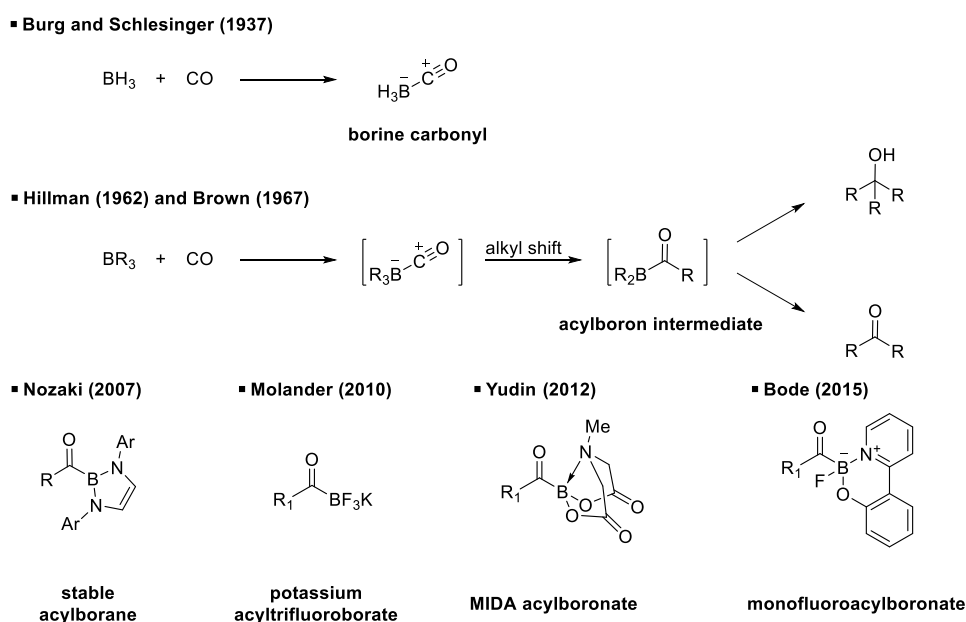
Touching the skull of a unicorn
Reading verses from a tattered page
Can this give a glimpse of the past
wilderness and of the youthful
Dreams?

羅智成一藍色時期 VI / Chih-Cheng Lo – Blue era VI

1.1. Acyl borons, acyltrifluoroborates (KATs) and KAT ligation

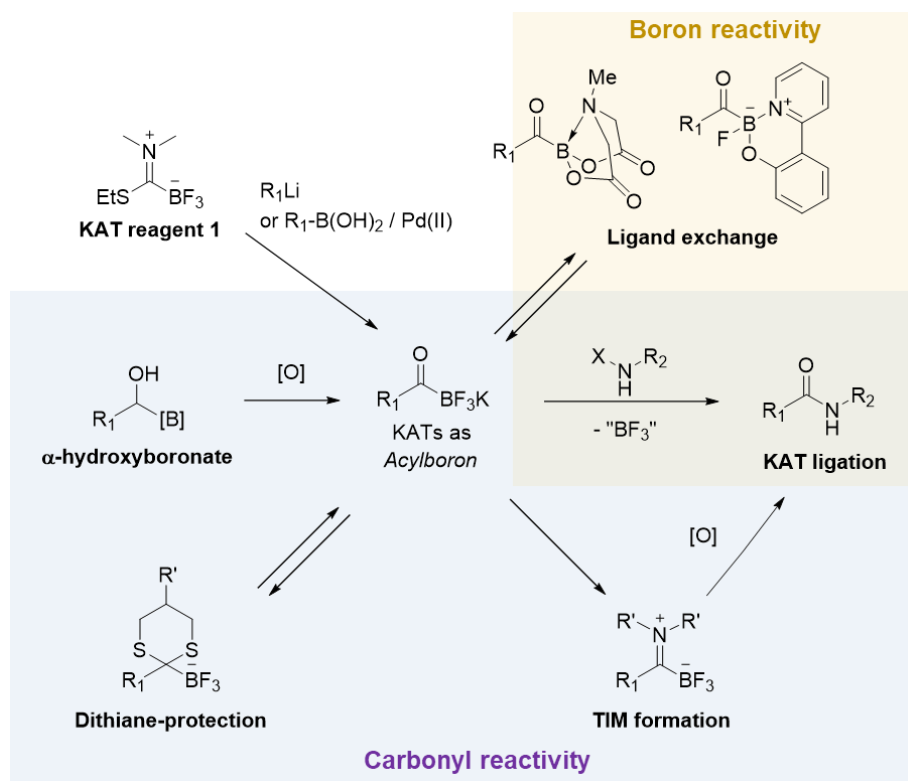
1.1.1. KAT as a keystone acylboron

The bonding between a carbonyl group and a boron atom has never been boring since their discovery in 1937, when Burg and Schlesinger prepared borine carbonyl from borane and carbon monoxide.^{1,2} The structure elucidation of borine carbonyl by vibrational spectroscopy came a decade later in the 1950s.^{3,4} In the 60s, Hillman and Brown reported that treating trialkylboranes with carbon monoxide initiated a series of boron to carbon alkyl shifts, giving trialkylcarbinol or dialkyl ketones depending on the reaction conditions,⁵⁻⁸ through a proposed acylboron intermediate. Such structures were not isolated until the first stable acylborane was reported by Nozaki et al. in 2007, where the substituent on boron was a rigid diamine that stabilized the tricoordinate borone.⁹ Shortly thereafter, tetra-coordinated acylboronates were synthesized and found to be stable. Acylboron compounds have since recently enjoyed a rapid expansion of their synthetic accessibility¹⁰⁻¹³ and gained numerous applications. **Scheme 1** summarizes these milestone structures in the development of acylboron chemistry.



Scheme 1. Milestones in the development of carbonyl-boron compounds.

The Bode group has been exploring the synthesis and applications of potassium acyl trifluoroborates (KATs) since 2012.^{14,15} KATs are usually bench-stable crystalline solids, which benefits their synthesis, purification, and handling. As of today 25 KATs are commercially available from Sigma-Aldrich, along with reagent **1**, allowing one-step synthesis of KATs from aryl halides or boronic acids.^{16,17} Its constituent parts, namely the acyl group and the trifluoroborate moiety, both have their own rich repertoire of reactivity as shown in **Scheme 2**.

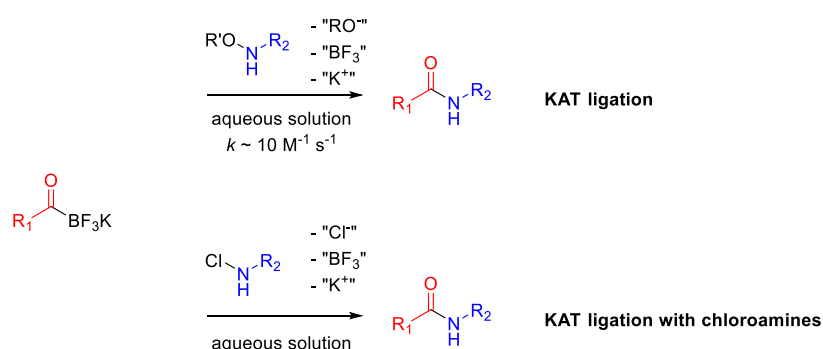


Scheme 2. KAT exhibits both reactivity at the carbonyl and the trifluoroboryl group as an acylboron.

The reactivities of KATs can also be vaguely categorized into those derived from the trifluoroborate group, and reaction of the carbonyl group. The following two sections describe briefly the current developments in both categories.

1.1.2. KAT Ligation

The KAT ligation is an amide bond forming reaction of KATs and hydroxylamines^{14,15} or chloroamines,¹⁸ during which the C–B bond and the N–O or N–Cl bond cleaves (**Scheme 3**). The chemical energy stored in KATs and hydroxylamines, both chemically stable, allows KAT ligation to operate rapidly yet selectively in the presence of unprotected nucleophilic functional groups under aqueous conditions without the need for a catalyst. This grants KAT ligations the ability to form native amide bonds quickly in complex, biological relevant environments, which is not enjoyed by most bioconjugation reactions with some exceptions such as native chemical ligation (NCL).^{19,20}



Scheme 3. KATs and acylboronates react with hydroxylamine or chloramines to form amides in aqueous environments.

Since the departure of the boron group is a pivotal event during KAT ligation, exchanging ligands on the boron provided an opportunity to alter KAT ligation reactivities. Some examples are shown in **Table 1**.^{21–24} Substituting three fluorides on the boron with a tridentate N-methyliminodiacetic acid (MIDA) ligand forming a MIDA boronate (**5**), or substituting two fluorides with a N-O bidentate forming monofluoro acylboronates (**3** and **4**) resulted in stable acylboronates with KAT ligation reactivity. Some of these acylboronates exhibited faster KAT ligation rates compared with KATs, but most of them decompose in aqueous solutions with a half-life shorter than one day. In contrast, KATs are usually stable in aqueous solutions. Both the stability and reactivity of the acyl monofluoroboronates were sensitive to the ligand structure, and ground state destabilization has been proposed to the reason of increased ligation rate.²³

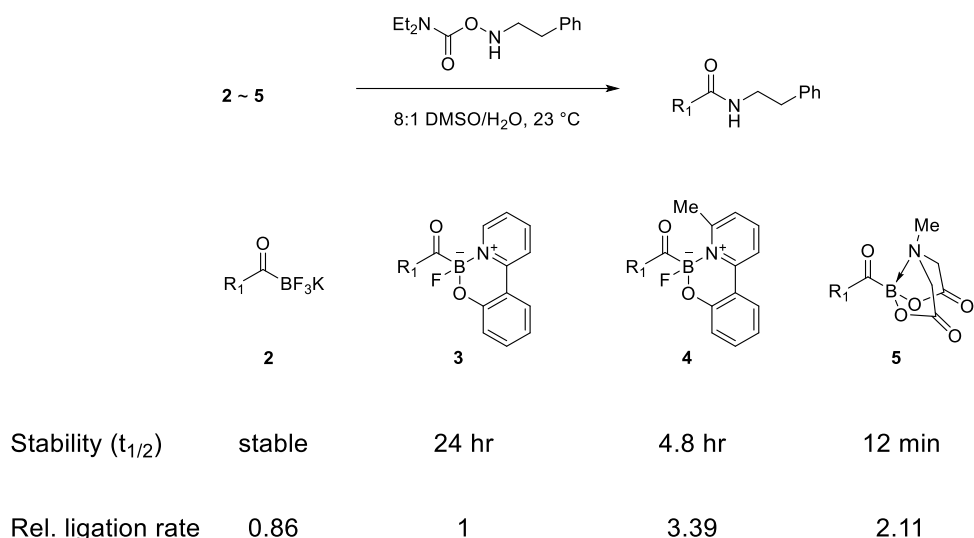
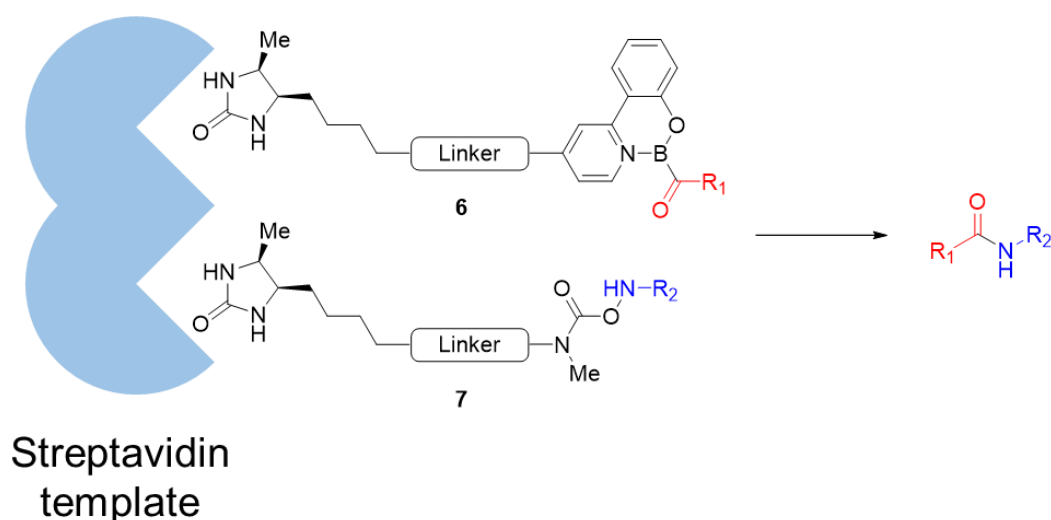


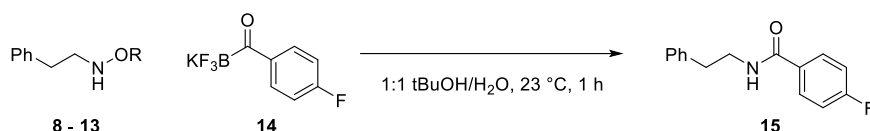
Table 1. Stability of acylboronates in aqueous solution and their relative ligation rate of acylboronates with hydroxylamine. R_1 = p-methylphenyl. KAT **2** was only slightly less reactive than the acylboronates but was significantly more stable.

Being able to substitute the ligand on boron also provided an entry point to install molecular recognition sites for template-enhanced ligations, which was demonstrated earlier in our group.²⁵ As shown in **Scheme 4**, a desthiobiotin was introduced on both the boronate ligand of a KAT-derived monofluoroacylboronate **6** and the hydroxylamine **7** O-substituent. Desthiobiotin was recognized by streptavidin, which acts as a template to bring the two reactants together and increase their mutual effective molarity. After the ligation, both desthiobiotin templates were cleaved from the ligation product, rendering this a traceless template ligation.



Scheme 4. Traceless templated KAT ligation. The streptavidin template brings the acylboronate and the hydroxylamine into proximity. The desthiobiotin and linker do not remain on the product after ligation.

A suitable O-substituent on the hydroxylamine is also crucial to its KAT ligation reactivity. It was found that hydroxylamines like **13** with N,N-diethylcarbamoyl group as the O-substituent gave the best balance between reactivity and stability,¹⁵ not unlike the situation where BF₃ substitution on the boron was the optimal balance among other substituents such as MIDA or monofluoro-pyridyl-phenol boronates mentioned above.²³



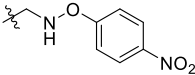
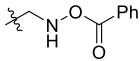
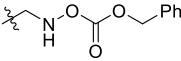
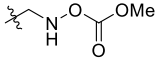
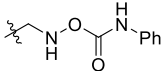
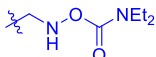
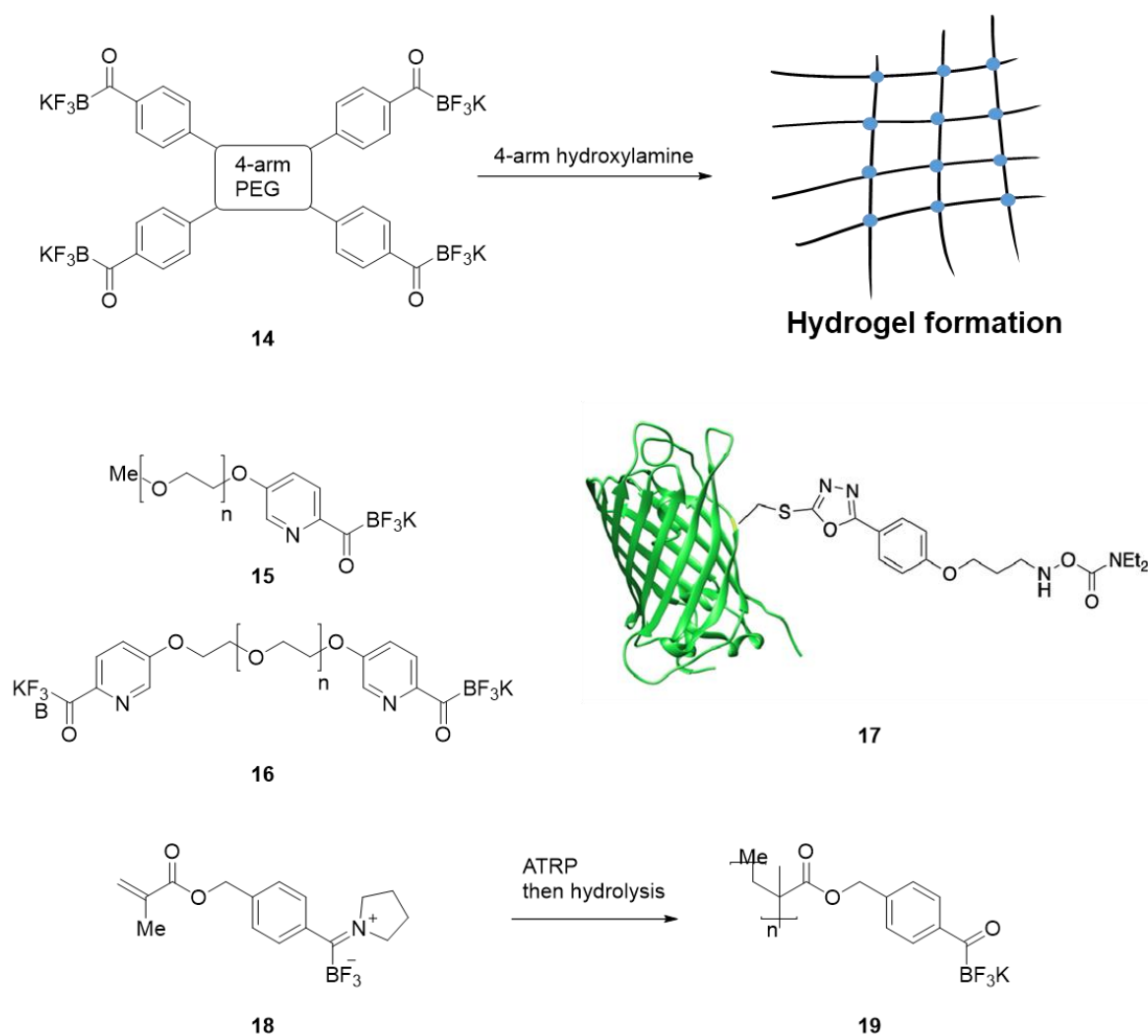
R =	relative reactivity	amine stability	acid stability
8 	14	-	-
9 	100	N	Y
10 	117	N	N
11 	124	N	N
12 	78	N	N
13 	87	Y	Y

Table 2. Relative reactivities of **8 - 13** with various R group substituent on the hydroxylamine oxygen. The amine conditions for stability test were either piperidine 20% in DMF or 10 equiv phenylethylamine in DMF. Acid condition was 50% TFA/CH₂Cl₂.

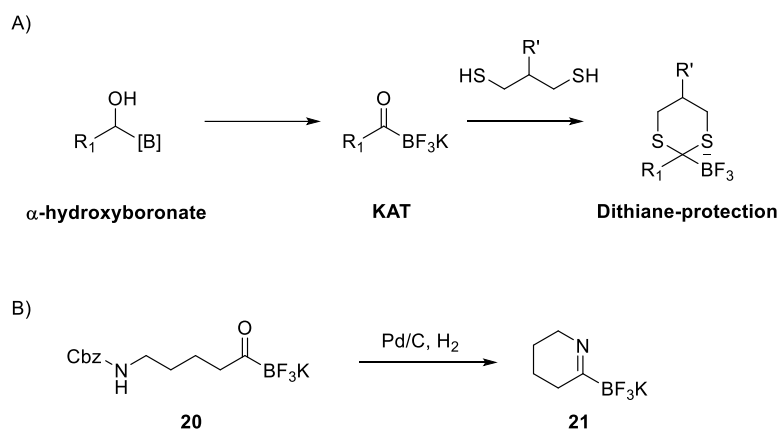
The combination of bifunctional KATs²⁶ and O-carbamoyl hydroxylamine has made KAT ligation applicable in various applications. Hydrogels can be formed and chemically decorated with KAT ligation^{27–31}. Proteins with a hydroxylamine handle such as **17** can be PEGylated by PEG-KAT **15**, dimerized with PEG-di-KAT **16** or immobilized on support via KAT ligation.^{28,32,33} Post-polymerization modification of a polymethacrylate with KAT pendant groups **19** can be achieved under dilute aqueous conditions³⁴. All of these applications were enabled by the stability of both KATs and O-carbamoyl hydroxylamines in aqueous reaction media, and the fast kinetics of KAT ligation, which have a second order rate constants as high as $10 \text{ M}^{-1} \text{ s}^{-1}$.³⁵



Scheme 5. Application of KAT ligation for hydrogel formation, protein conjugation and polymer modification.

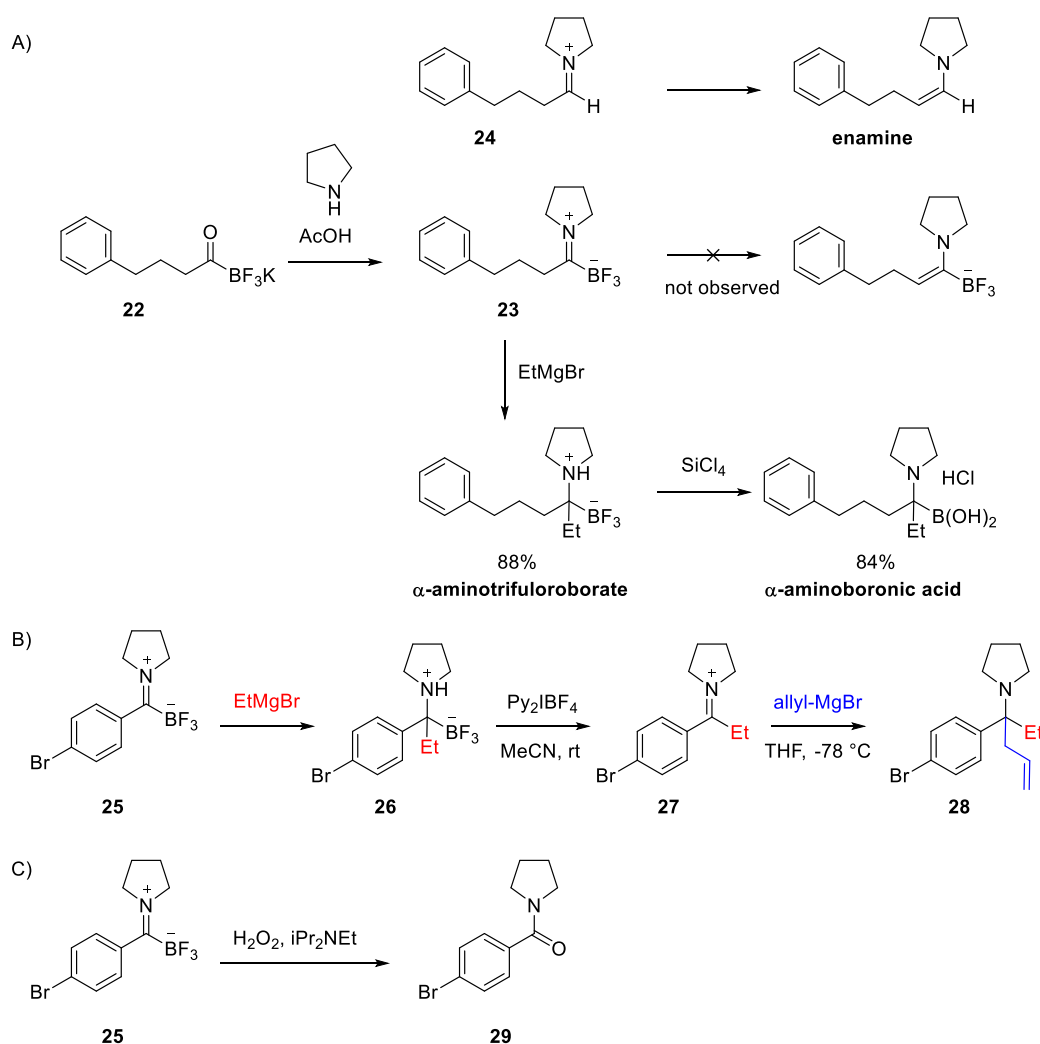
1.1.3. Reactions at the KAT carbonyl group

The carbonyl part of the KAT group can exhibit reactivities similar to ordinary carbonyl groups. For instance, they form thioacetals³¹ which was used as a protection group for KATs against ligation. They can also be formed from the oxidation of α -hydroxyboronates just like a ketone or an aldehyde can be formed from the corresponding alcohol. An example is seen in a novel KAT synthesis reported by Ito et al.^{36,37}



Scheme 6. Examples of KAT carbonyl group reactivity **A**: The KAT carbonyl can be formed by the oxidation of an α -boryl alcohol. KAT can also undergo condensation with a 1,3-dithiol to form a trifluoroboryl dithiane. **B**: KAT **20** was found to cyclize upon deprotection of its amino group, forming a trifluoroboryl imine **21**.¹²

Just as carbonyl compounds form imines and iminiums, KATs also condense with amines to form trifluoroborate iminiums (TIMs).^{12,38,39} Their formation transforms KATs, an ionic salt, into charge neutral zwitterionic compounds that are soluble in a wider range of organic solvents. TIMs are also less polar and therefore more amenable to chromatography than the corresponding KATs. The formation of TIMs occur under mild conditions when KATs were mixed with an amine and acid, and their hydrolysis require one equivalent of base be added to the reaction mixture. Unlike ordinary iminiums, iminium-enamine tautomerizations was not observed in TIMs, which makes them a suitable electrophilic synthetic intermediate to react with organometallic nucleophiles, granting synthetic access to highly substituted amine structures including α -aminoboronic acids³⁹ and N,N-alkylated α -tertiary amines³⁸. TIMs can also be oxidized swiftly into amides, affording tertiary amides that are otherwise harder to obtain.⁴⁰

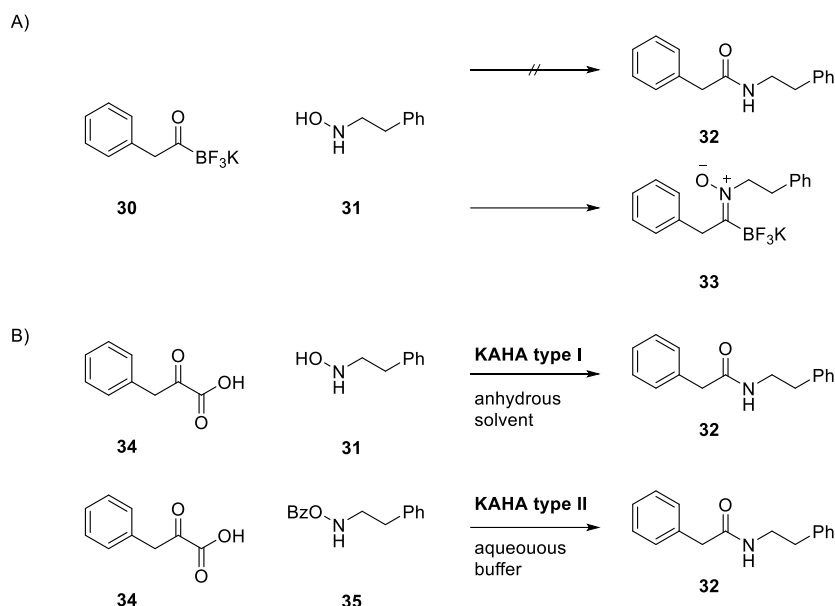


Scheme 7. Trifluoroborate iminiums (TIMs) were formed by condensing a KAT with a secondary amine. **A:** TIMs were not observed to isomerize into enamines and allowed the nucleophilic attack from Grignard reagents to occur smoothly, forming α -aminotrifluoroborates, which can be hydrolyzed with fluorophilic reagent to form α -aminoboronic acids. **B:** α -aminotrifluoroborates formed this way can also be oxidized with Barluenga's reagent to eliminate the trifluoroborate forming an iminium, which can then be treated with a second Grignard reagent to form α -tertiary amines in a three-component fashion. **C:** Oxidation of TIMs with hydrogen peroxide gives the corresponding amide.

1.2. KAT nitrones

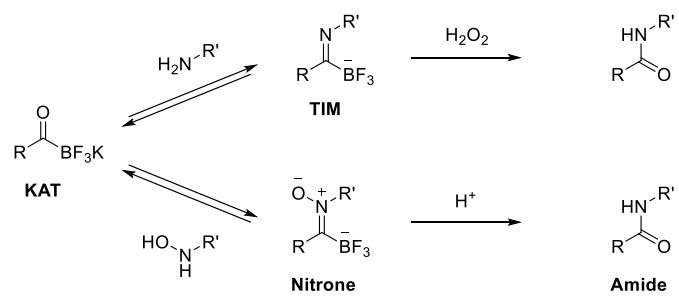
Just like TIMs, KAT nitrones also belong to the category of KAT carbonyl condensation products. Their discovery was also deeply linked with the early investigations on KAT ligation reactivity. When the first general KAT synthetic route was established,¹² it was already known that KATs can form imine like condensations such as trifluoroborate imine **21** (Scheme 21) and nitrone **33**. The original expectation was that KATs may have an amide forming reactivity towards hydroxylamines, similar to α -ketoacids in KAHA ligations.^{41–45} It turns out that under KAHA ligation type I conditions KAT **30** reacts with O-H hydroxylamine **31** only to form nitrone **33** and not amide product **32**, unlike the corresponding α -ketoacid **34** which exhibit

KAHA type I reactivity. The need to transform the hydroxylamine oxygen into a better leaving group to enable KAT ligation reactivity was only discovered shortly after. Had we realized that O-substituted hydroxylamines ligate better with KATs at before that point, O–H hydroxylamines might have not been tried, and KAT nitrones may have been overlooked for longer.



Scheme 8. Early investigation in the reactivity of KAT towards hydroxylamine and its comparison with an α -ketoacid. **A:** Benzyl KAT **30** did not form amides with O–H hydroxylamine **31** directly, unlike α -ketoacids, **B:** Phenylpyruvic acid **34** can be regarded as the carboxylate equivalent of **30** and reacts with N-phenethyl hydroxylamine **31** to form an amide. This was termed KAHA type I ligation, in contrary to KAHA type II ligation where the hydroxylamine has an O-substituent like in **35**. KAHA type I prefers the reaction media to be anhydrous.⁴⁶

While KAT nitrones are stable, isolable compounds, early studies suggested that their formation was reversible, and further acidification could convert them into the corresponding amides.⁴⁷ Similar to the amide formation from oxidation of TIMs, where a nitrogen bearing reactant condenses with KAT to form an intermediate in a reversible manner, this can be regarded as a “two-step KAT ligation.” The slow kinetics or requirement of additional reagents to initiate the subsequent second step allows the first step to reach equilibrium. We believe this feature would make KAT nitrones useful towards dynamic chemistry, which is the main theme of this thesis.

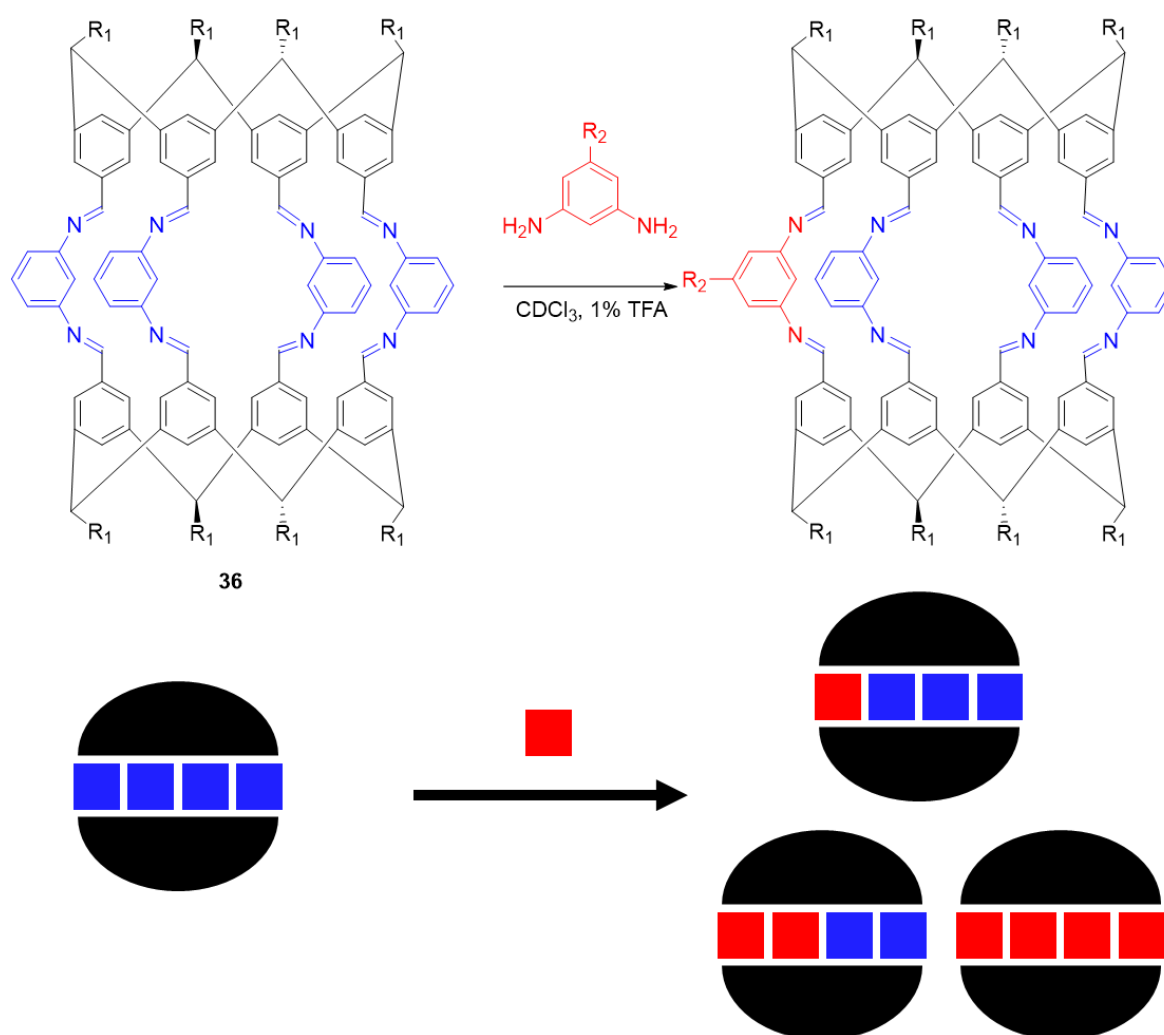


Scheme 9. Two-step amide formation reactions through an imine-like condensation products with KATs.

1.3. Dynamic Chemistry

1.3.1. Systems chemistry and dynamic chemistry

A dynamic system of chemical reactions, constantly breaking and forming chemical bonds, is what keeps us alive. Earlier this century, the term systems chemistry was proposed to describe an emerging chemical approach to analyze or create dynamic systems pertaining to the chemical origin of life, which exhibit self-organizing, self-amplifying, or energy-dissipative behaviors.⁴⁸ The scope of systems chemistry soon expanded as it grew, to cover studies towards any dynamic chemical system, as advocated by Otto.⁴⁹ These include concurrently expanding fields including dynamic combinatorial chemistry,^{50–56} dynamic combinatorial libraries (DCLs),^{57–59} and dynamic covalent chemistry.^{54,60–64}



Scheme 10. In 2000 Stoddart et al. reported⁶¹ the reversible imine bond formation allowed the components in cage compound **36** to be exchanged. They also observed that acid catalysis facilitated the imine exchange, as well as the release of the cage content. The term “dynamic covalent bond” was used to describe this kind of behavior.

Synthetic chemists spend most of their effort in the careful combination of reagents, starting materials, and operations to direct the reaction outcome to a kinetically controlled state, in a way encoding the reaction conditions into the reaction outcome⁶³. Dynamic chemistry on the other hand emphasizes another dimension of information input, relying on a common reaction condition experienced by a system of multiple possible reactants. It probes the energy landscape of all possible combinations, and finally records the result in form of chemical bonds.

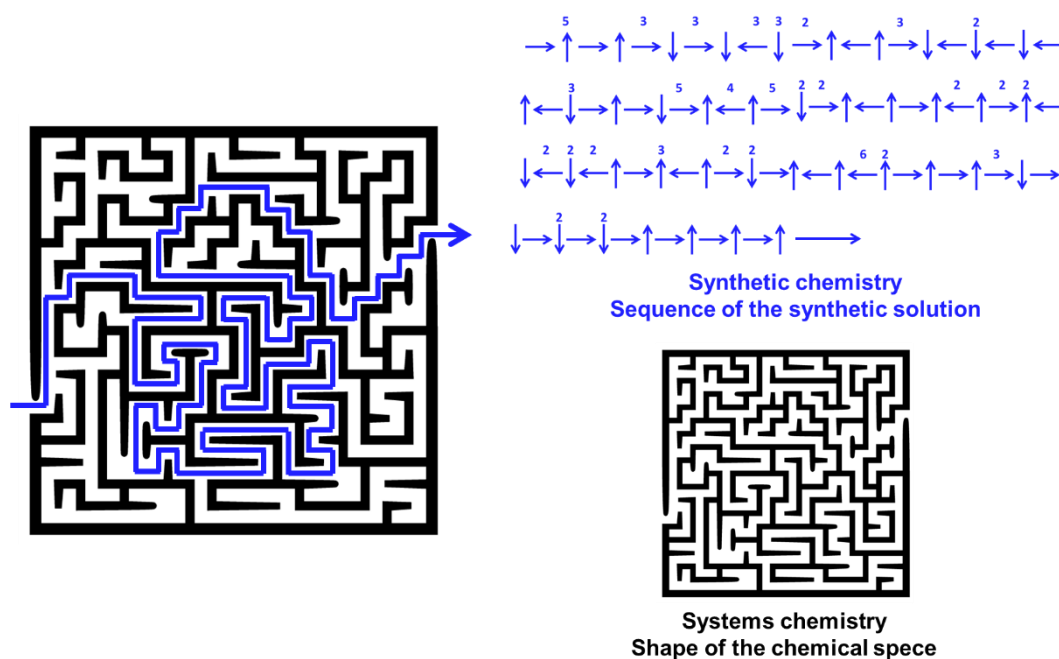
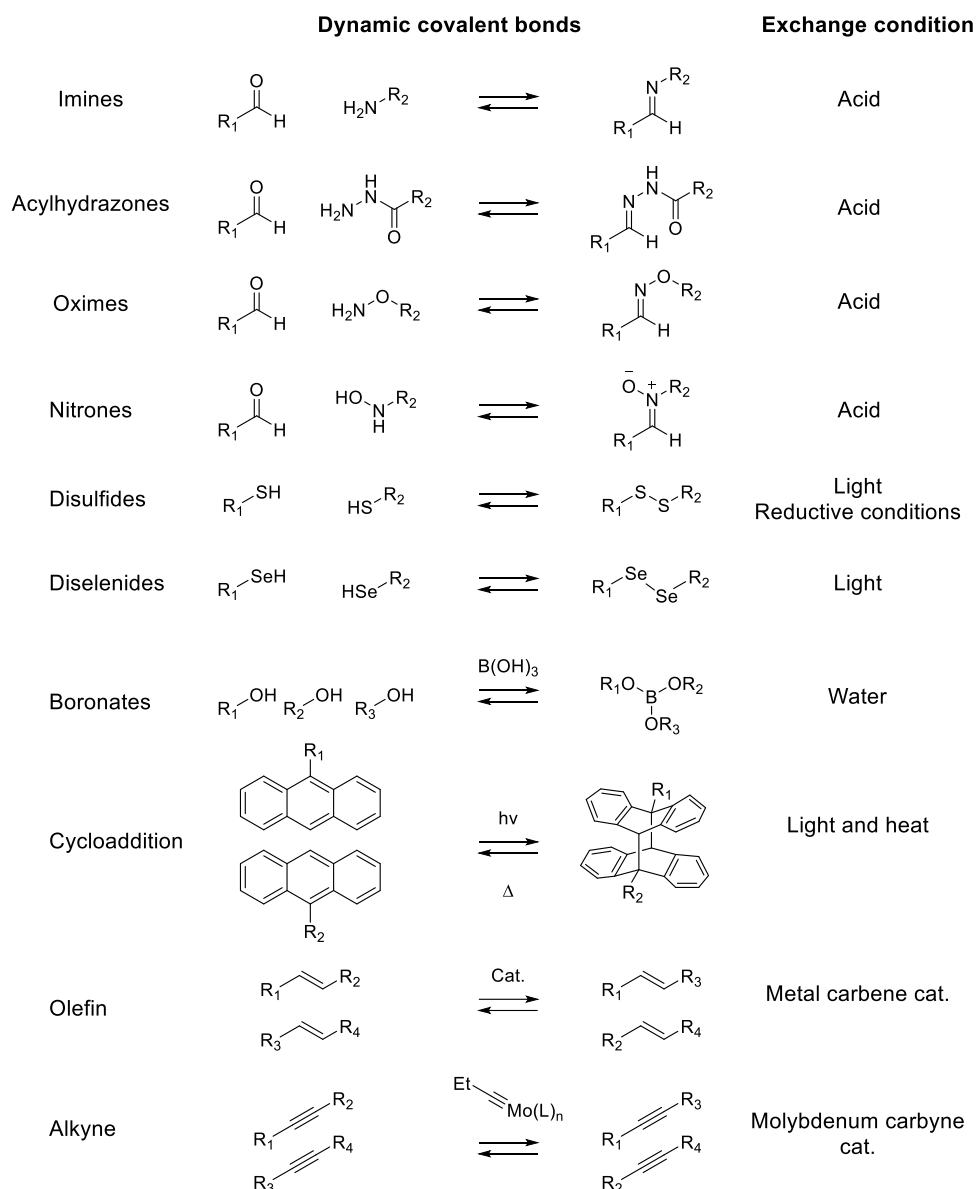


Figure 1. An analogy of chemical space as a puzzle maze. Synthetic chemists have specialized in finding the solution out to the desired target by navigating the possible paths on the potential energy surface. Where as in systems chemistry, the emphasis was turned to the attempt to sample, measure, and perhaps understand the whole maze.

The progress of dynamic chemistry was fueled by chemists' improving capability in analyzing complex mixtures in real-time, for instance as analytic techniques like ESI mass spectrometry⁶⁵ became widely accessible, or as liquid chromatography tandem mass spectrometry (LCMS) became common.⁶⁶ Methods like scanning tunneling microscopy that can reveal the collective behavior like the geometry of molecular assembly have also found application in analyzing dynamic chemical systems.⁶⁷ The development of supramolecular chemistry and molecular recognition also offered more non-covalent interactions to be studied by dynamic covalent chemistry.^{59,62,68–72} Efforts aiming at controlling supramolecular interactions eventually enabled the construction of dynamic molecular systems such as molecular machines, which was awarded the 2016 Nobel Prize in Chemistry.

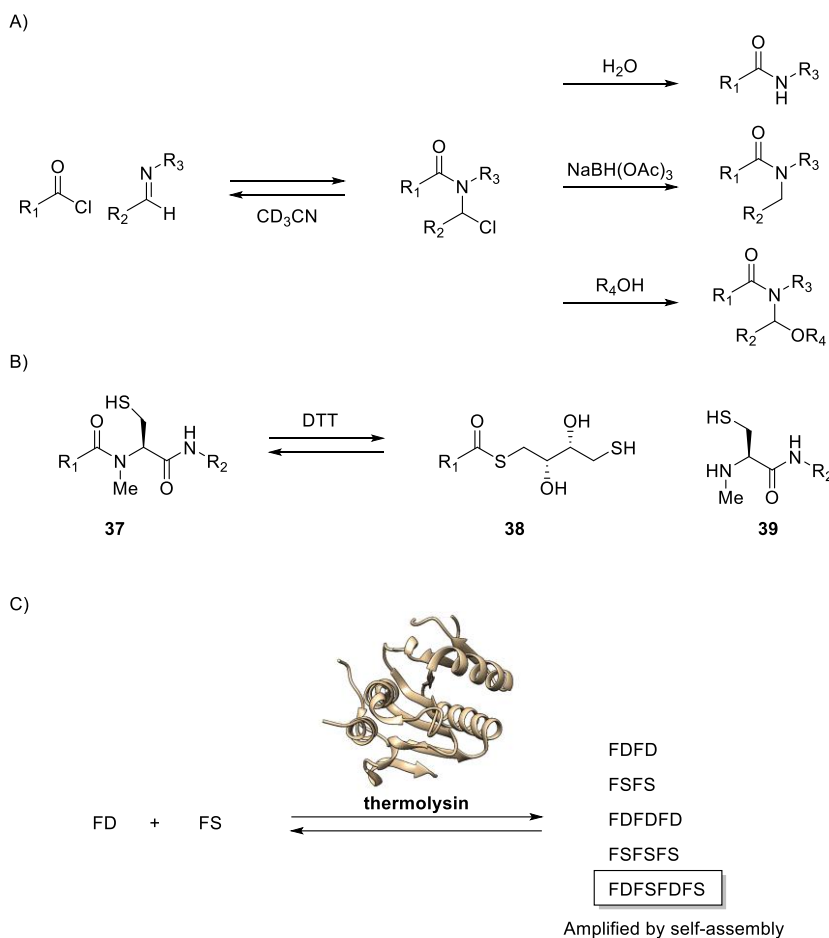
1.3.2. Dynamic chemical bonds used in dynamic chemistry

The foremost requirement of a dynamic chemical system is to have a dynamic chemical bond that can form and break reversibly. Ideally, there should also be a trigger to switch on or off the dynamicity of the chemical bonds, if one wishes to store information in the bond configurations for readout later. Imines,^{58,69,73,74} acyl hydrazones,^{75,76} oximes,⁷⁷ and nitrones⁷⁸ have been utilized for dynamic covalent chemistry. These carbonyl condensation linkages are generally dynamic at an acidic pH, and fixed when acid is removed. Disulfides^{66,79,80} have also been used in dynamic combinatorial libraries and can be fixed oxidatively, and promoted to exchange by light irradiation.⁸¹ Diselenides⁸² has been incorporated into DCC system in a similar manner. Boronate linkages also exchange readily in the presence of water by reversible hydrolysis.⁸³ The dynamic forming and breaking of C–C bonds can be seen in systems based on reversible cycloaddition, olefin and alkyne metathesis.^{84–86}



Scheme 11. Dynamic covalent bonds and the conditions to promote their exchange.

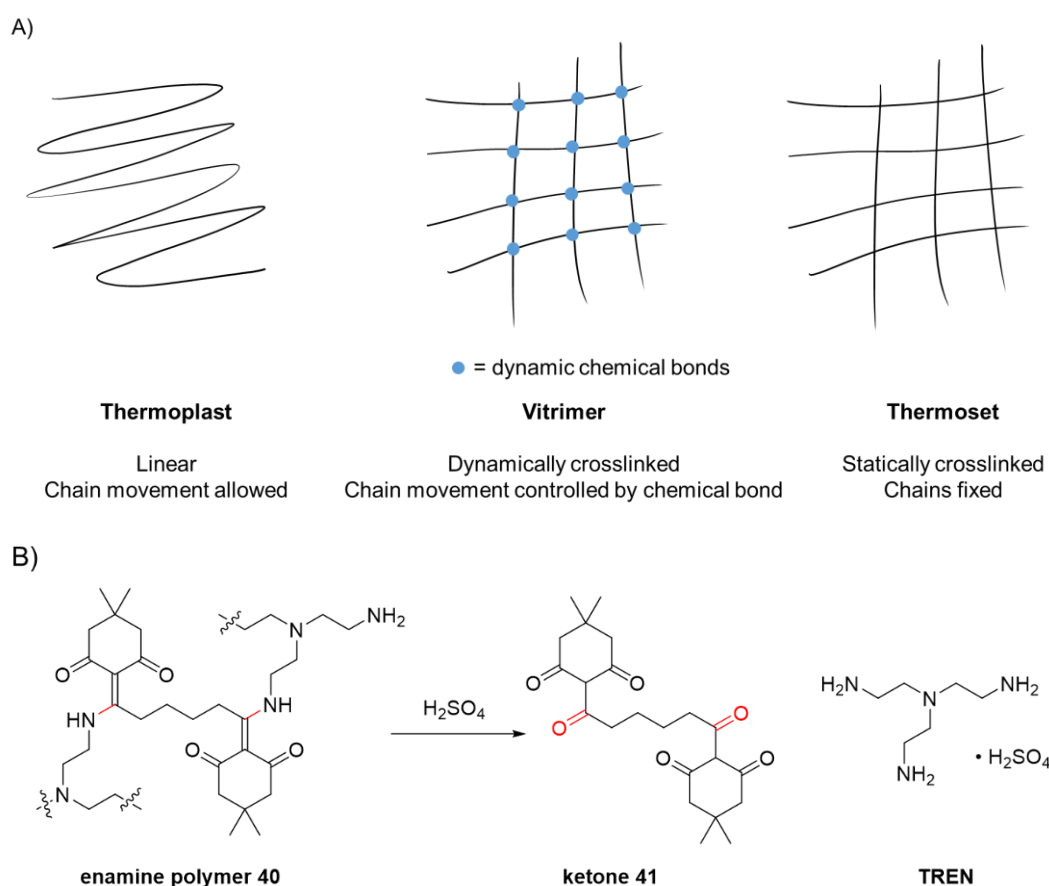
A few dynamic covalent systems can be used to form amide bonds. Dynamic imine bonds in covalent organic frameworks can be converted to a static bond by oxidation.⁸⁷ Recently Arndtsen et al. reported a dynamic N- α -chloroalkyl amide formed between imines and acylchlorides (**Scheme 12A**), which can be fixed into a static amide by either reduction, hydrolysis or alcoholysis of the α -chloride.⁸⁸ Reversible amide bond formation was also observed at specific peptidic sites in reversible native chemical ligation conditions⁸⁹ and in sortase catalyzed peptide N-terminus acylations.⁸⁹ When catalysts such as $Zr(NMe_2)_4$ or thermolysin were used, the formation and breakdown of peptide bonds could also be dynamic, with no sequence selectivity on the peptide cleavage/formation site.^{90,91}



Scheme 12. Examples of reversible amide formation. **A:** N- α -chloroalkyl tertiary amide forms reversibly when acyl chlorides were mixed with imines in CD_3CN , and can be transformed irreversibly into secondary amides by hydrolysis, tertiary amides by reductive dehalogenation or alcoholysis of the chloride.⁸⁸ **B:** When N-methyl cysteine was used at a NCL site, the NCL can be pushed in the reverse direction by addition of another thiol, in this case DTT, and give rise to dynamically formed amide bonds.⁸⁹ **C:** When dipeptide mixture FD and FS were treated with thermolysin, an endoprotease, a dynamic mixture of peptide tetramer, hexamer and octamers were formed. The octamer FDFSFD was selectively amplified due to hydrogen bond directed self-assembly.⁹¹

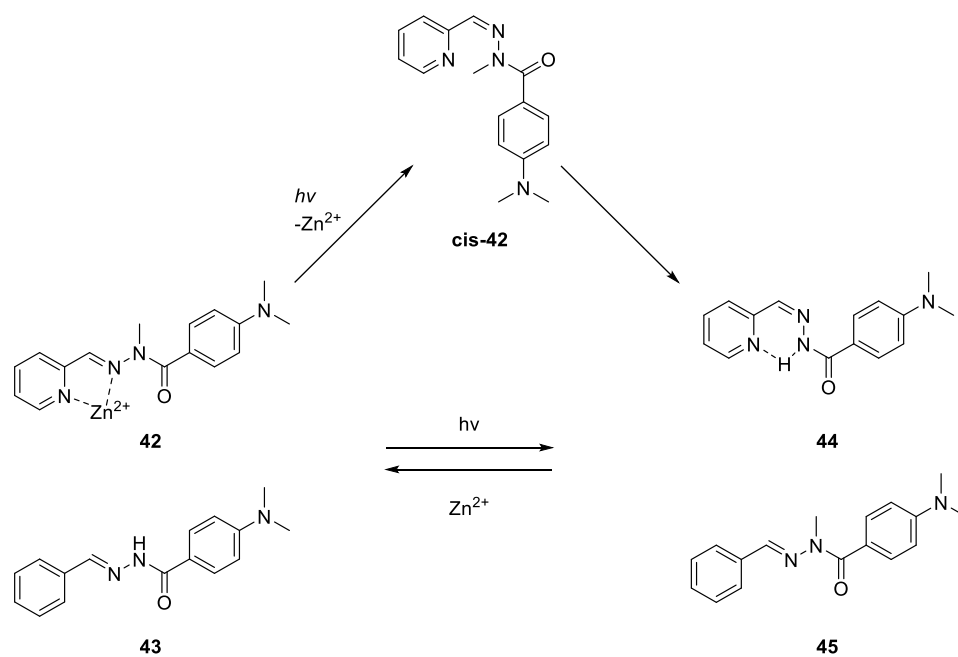
1.3.3. Bond dynamicity enables chemical system to adapt to stimuli

Dynamic chemical systems react and adapt to environmental perturbation and have enabled several applications.^{92–95} Polymer cross-links reacting to mechanical stress give rise to a class of materials termed “vitrimers” that exhibits a desirable mix of properties between a thermoplast and a thermoset.⁹⁶ Dynamic polymers connected with dynamic bonds can be degraded back to monomeric units and recycled.⁹⁷ The crystallinity of Covalent Organic frameworks (COFs) also benefits from the dynamic, reversible bond formation during its synthesis, which allows self-correction of structural defects and relaxation of stress.^{98,99}



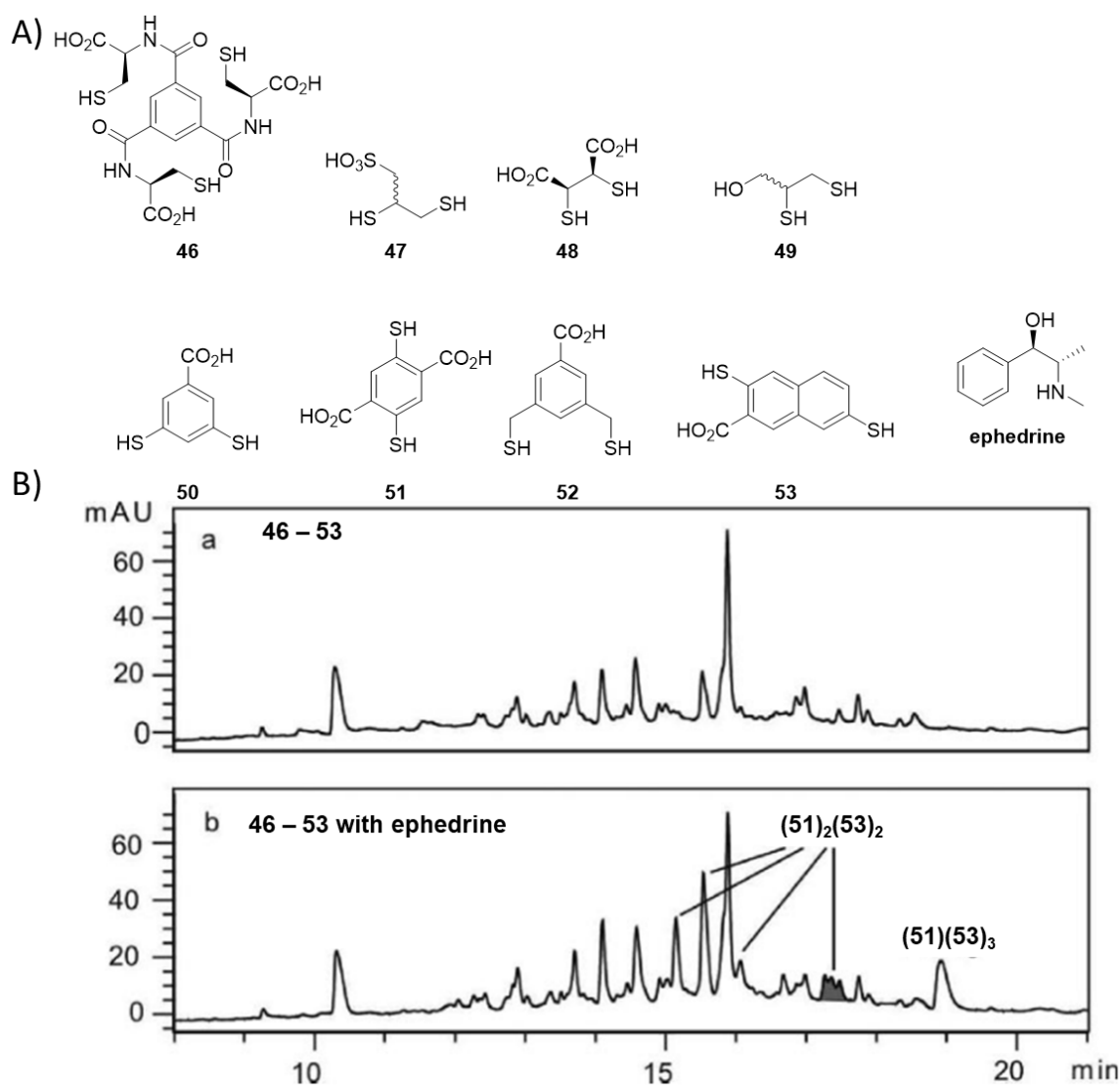
Scheme 13. Dynamic chemical linkages in polymers can be used to generate **A**: Dynamically crosslinked-polymer termed vitrimers or **B**: polymers constructed through dynamic such as enamine polymer **40**, which can be depolymerized back to separable building blocks ketone **41** and triethylene tetramine (TREN).

Lehn et al. demonstrated a dynamic library that adapts to both physical and chemical stimuli as shown in **Scheme 14**. Acylhydrazone **42** isomerizes to **cis-42** upon irradiation and loses its binding affinity to zinc ion. Hydrazone **44** in the cis form benefits from an intramolecular hydrogen bond and is stabilized. The system is shifted towards **44 + 45** under irradiation, and favors the combination **42 + 43** when Zn(II) is present.⁷⁵



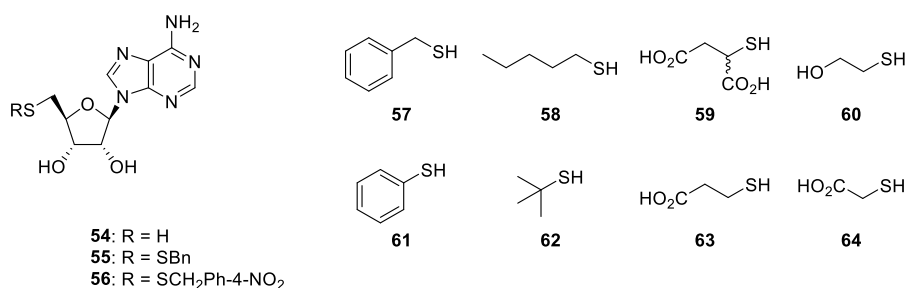
Scheme 14. A dynamic covalent chemical system that responds to light and the presence of zinc ion. **42** formed from 2-pyridinecarboxaldehyde, was stabilized in trans form when Zn(II) can be chelated, and **44** was a favored configuration when pyridine-2-yl hydrazones were driven into the cis-configuration photochemically.

Two examples of dynamic combinatorial libraries for host-guest interaction are shown below. A Dynamic Combinatorial Library from eight di-thiols has been shown by Otto et al. to contain roughly 9000 unique compounds was shown in **Scheme 15**. With the combination of HPLC and mass spectrometry two hits containing just four dithiol units were found to have micromolar affinity towards a small molecule, ephedrine, although the isomeric forms of the hits were not identified.⁶⁶



Scheme 15. A: A dynamic combinatorial library by Otto et al. contained eight dithiols **46** – **53** was added the recognition target molecule ephedrine. This library was estimated to contain 9000 unique compound. **B:** the library mixture was analyzed by HPLC, where the upper chromatogram was the blank control without no ephedrine added. Certain peaks were formed or enriched in the lower chromatogram due to template effect between the library and the target molecule. Subsequent mass spectrometry analysis disclosed the enriched peaks to have the composition $(51)_2(53)_2$ and $(51)(53)_3$, which were subjected to isothermal titration calorimetry as a mixture of isomers, and found to have binding constants of 77 μM and 67 μM respectively. The chromatogram was adapted from "Two-Vial, LC-MS Identification of Ephedrine Receptors a Solution-Phase Dynamic Combinatorial Library of over 9000 Components"⁶⁶ with permission. Copyright (2008) American Chemical Society.

Ciulli et al. used a smaller library,⁷⁹ which consisted of the components shown in **Scheme 16**, to answer a more specific question. The R group on compound **54–56** was shuffled dynamically to achieve optimal binding towards *M. tuberculosis* pantothenate synthetase. Thiols **54** and **57 – 64** were mixed in a glutathione redox buffer to form the library mixture. After adding the target protein, the intensity of the HPLC peak corresponding to disulfide **55**, which was the combination of **54** and **57** increased. The synthesized hit **55** had a binding affinity of 210 μM . Further derivatization from **55** reached their strongest protein binder **56** with 70 μM affinity.



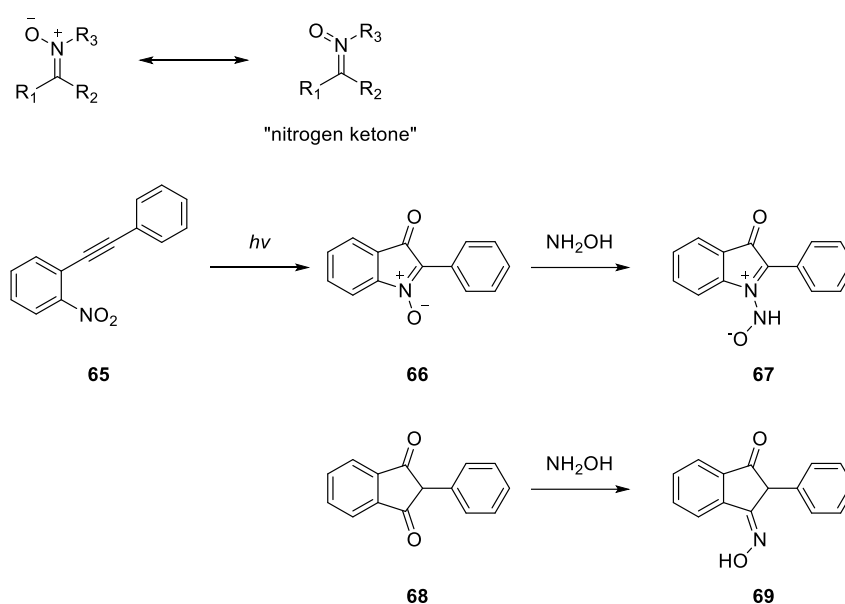
Scheme 16. A dynamic library used by Ciulli et al. to identify a binder for *M. tuberculosis* pantothenate synthetase.

Both examples shown above were based on disulfide linkages. Detection of the shift of equilibrium in the dynamic library can quickly identify tight binding hits to the target molecule. These dynamic bonds in the hits identified from a dynamic library, complicates their analysis due to their dynamic nature. Also the exchange condition for disulfide linkages may interfere with cysteine containing proteins, especially ones with important, labile disulfide bridges. We expect that KAT nitrones to be a good candidate in creating a dynamic library without these two drawbacks, since KAT nitrones form and exchange under physiological conditions, and can be converted into the amide by acidification.

1.4. Nitro Chemistry

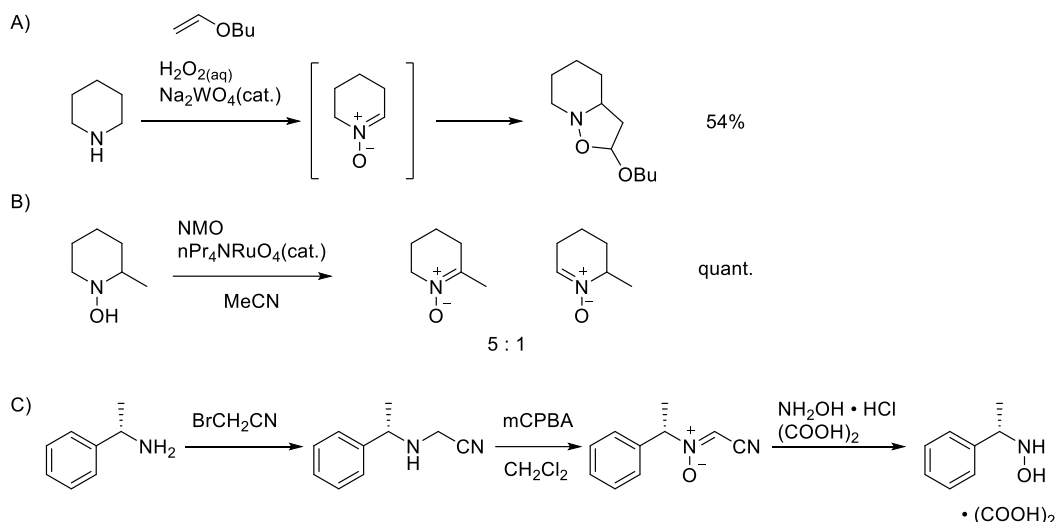
1.4.1. Nitrones and their formation

The name nitro was first used by Pfeiffer in 1916 when he was carrying out the synthesis of an indole derivative **66** from the photochemical ring closure of **65**. He identified that compound **66** has a functional group that contains a nitrogen and has similar properties to a ketone to form a condensation product **67** with hydroxylamine, just as ketone **68** forms oxime **69** when treated with hydroxylamine.¹⁰⁰



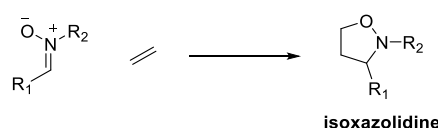
Scheme 17. Pfeiffer's nitro: nitrogen-ketone

Nitro chemistry, especially their synthesis and cycloaddition reactivity were already well studied and reviewed in the early 20th century.^{101–106} The impact of nitro chemistry continued its presence in synthetic organic chemistry till today.^{107–116} The rich redox chemistry of nitro, along with its controlled oxidation outcome compared to other nitrogen containing compounds such as hydroxylamine or nitroso compounds, also enabled a variety of nitro synthesis methods via oxidation as new oxidants and catalysts emerge.^{117–120} A few of these oxidative nitro formation methods were highlighted below in **Scheme 18**.



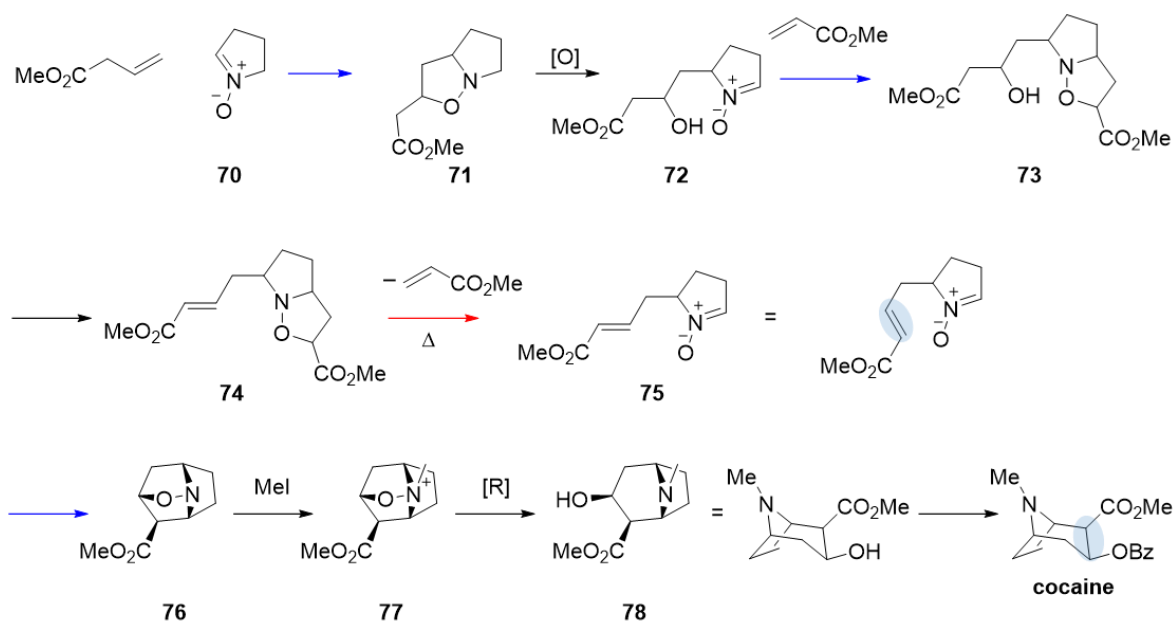
Scheme 18. Nitronium synthesis from the oxidation of nitrogen containing compounds. **A:** The catalytic oxidation of piperidine occurs in the presence of butyl vinyl ether, which traps the nitronium formed in situ. **B:** Perruthenate catalyzed hydroxylamine oxidation is sensitive to steric bulk and gave the less substituted nitronium. **C:** The Fukuyama synthesis of N-monoalkyl hydroxylamine relies on the controlled oxidation of cyanomethyl amine to the nitronium, followed by its hydroxylaminolysis.

1.4.2. Reactivity of nitroniums



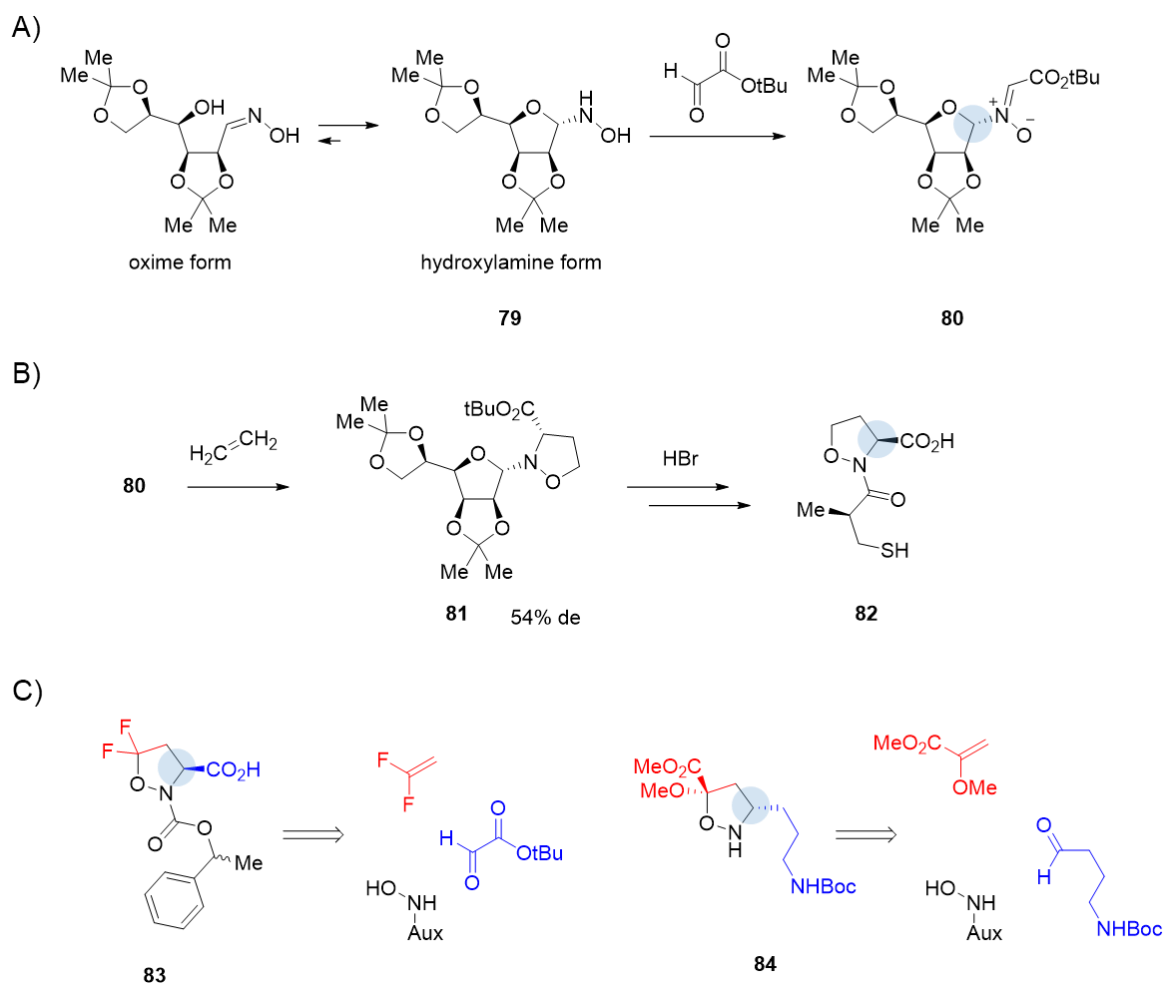
Scheme 19. Nitronium undergoes 1,3-dipolar cycloaddition to form isoxazolidines

Nitroniums are powerful synthetic intermediates, especially as 1,3-dipoles that undergo cycloaddition to form isoxazolidines.¹⁰⁸ Isoxazolidines are valuable synthetic intermediates with various downstream transformations.¹²¹ For example, a hidden 1,3-aminoalcohol can be released reductively. The stereochemical control of such cycloadditions were also well established, both in the cases of intermolecular and intramolecular reactions.¹²² The following synthesis of dl-cocaine reported by Turfariello utilized three intramolecular dipolar cycloaddition steps, in which the last one constructed the bicyclic tropane skeleton at the same time fixing the stereochemistry at position 2 and 3.



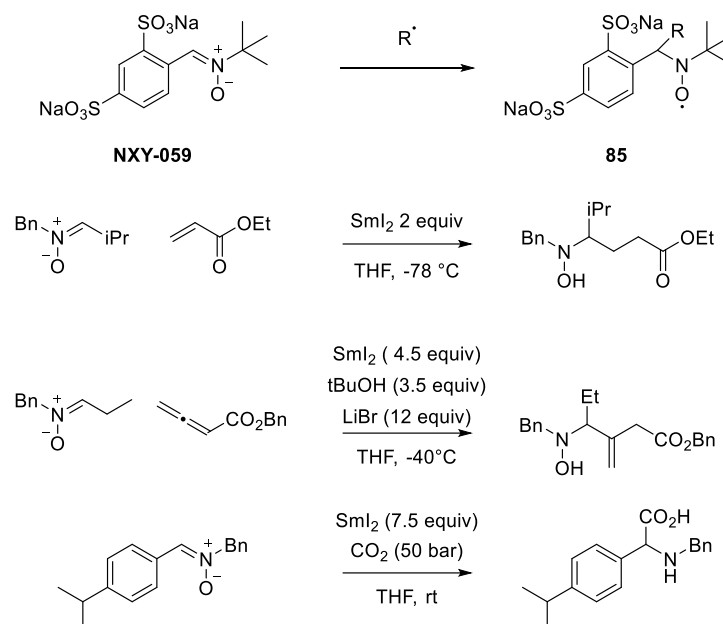
Scheme 20. The dl-cocaine total synthesis by Tufariello. In the overall sequence contained three nitronium dipolar cycloadditions steps marked in blue arrows, with one of them serving to protection nitronium **72** before the dehydration step to form **74**. The stereochemistry at position 2 and 3 (shaded in blue) was defined during the last cycloaddition (**75** – **76**).

The diastereoselectivity of intermolecular nitronium dipolar cycloadditions can be controlled by chiral auxiliary groups. Vasella has shown that a sugar derived oxime-hydroxylamine **79** condenses with aldehydes to form a nitronium, which undergoes cycloaddition with an olefin with facial selectivity, leading to the enantioselective synthesis of 5-oxaproline **82** as an analog of a proline derivative angiotensin-converting-enzyme (ACE) inhibitor. This strategy was employed by our group in the enantioselective synthesis of various oxaxoline derivatives used for KAHA ligation.



Scheme 21. Asymmetric intermolecular nitronium 1,3-dipolar cycloaddition. **A:** Treating D-mannose with hydroxylamine gives oxime **79**, which has a hydroxylamine tautomeric form that undergoes nitronium forming condensation with aldehydes to form nitronium **80**. **B:** Cycloaddition of nitronium **80** with ethylene gave isoxazolidine **81** with 54% diastereomeric excess. The stereochemical purity of **81** can be improved by repetitive crystallization before cleaving off the chiral auxiliary. **C:** Aspartic acid forming KAHA ligation monomer **83** was synthesized following a similar strategy. The cycloaddition of difluoroethylene did not have observable diastereoselectivity, but the two diastereomers are well resolved by recrystallization. α -ketoacid forming KAHA ligation monomer **84** was also prepared following the same strategy.

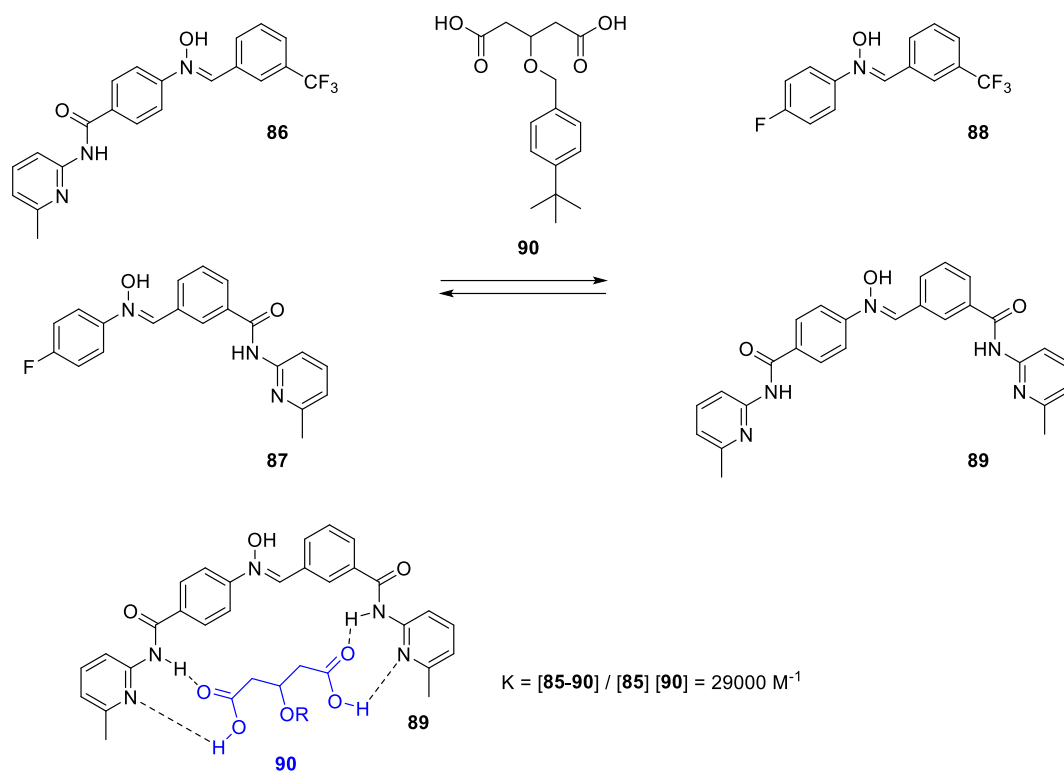
Another important aspect of nitronium reactivity is their radical trapping capability.¹²³ They readily take up a radical at the carbon to form a N-oxide, for instance nitronium **NXY-059** forms **85**. **NXY-059** was once found to have neuroprotective efficacy in preventing oxidative damage during ischemic stroke, but later found to have significance in clinical studies.^{124,125} The radical accepting reactivity, however, can be used to alkylate nitrones. Reductive coupling between nitrones and a α,β -unsaturated olefin or allenolates was reported.^{126,127} Nitrones also undergo carboxylation with CO_2 when reduced by SmI_2 .¹²⁸



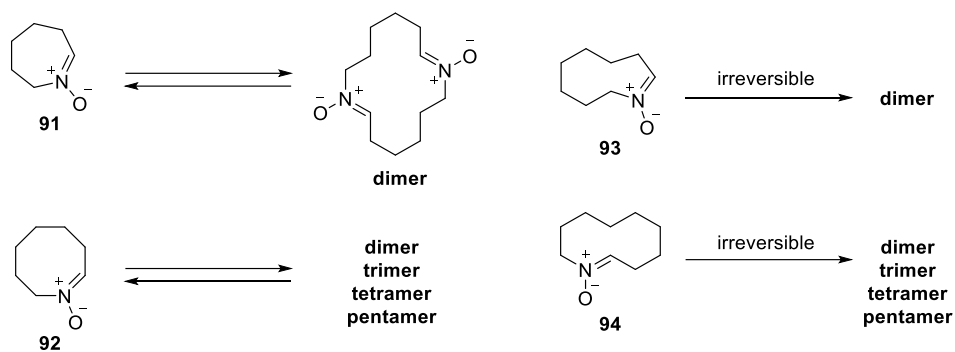
Scheme 22. Radical reactivity of nitrones

1.4.3. Dynamic behavior of nitrones

Nitrones are also known to hydrolyze back to the corresponding carbonyl compound and hydroxylamine, resulting in the exchange of aldehyde-hydroxylamine pairs. In 2008 Philp et al. prepared a dynamic nitronium system **86** and **87** in CDCl_3 in equilibrium with **88** and **89**. This system is responsive towards addition of a di-acid guest molecule that interacts strongly with nitronium **89**. Naota et al. studied the ring opening metathesis of cyclic nitrones in CHCl_3 catalyzed by tosylic acid. It is interesting to see that the ring opening of cyclic nitronium was reversible for **91** and **92**, but irreversible for 9- and 10- membered ring cyclic nitrones **93** and **94**.¹²⁹



Scheme 23. The equilibrium of a nitron dynamic chemical system was shifted by the addition of diacid **90**, which was recognized by nitron **89** with high affinity.



Scheme 24. Ring opening metathesis of cyclic nitrones.

2

Properties and dynamics of KAT nitrones

什麼是不變的呢?

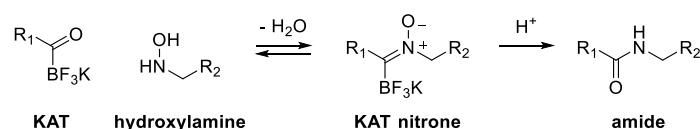
*一切記憶與書寫
不過是刻舟求劍:
我們把事件的記憶
深鏤船舷
流動的河水卻在原處
改變了事件*

What doesn't change?

All memories and writings
Are but cutting a mark for a sword overboard
Memories from an event
We carve into the hull
Yet the flowing stream where it happened
Has already altered it all
羅智成一藍色時期 XIV / Chih-Cheng Lo– Blue era XIV

Early observations have indicated that KAT nitrones could be a dynamic chemical bond, suitable for dynamic chemistry as described in 1.2. This expectation motivated us to

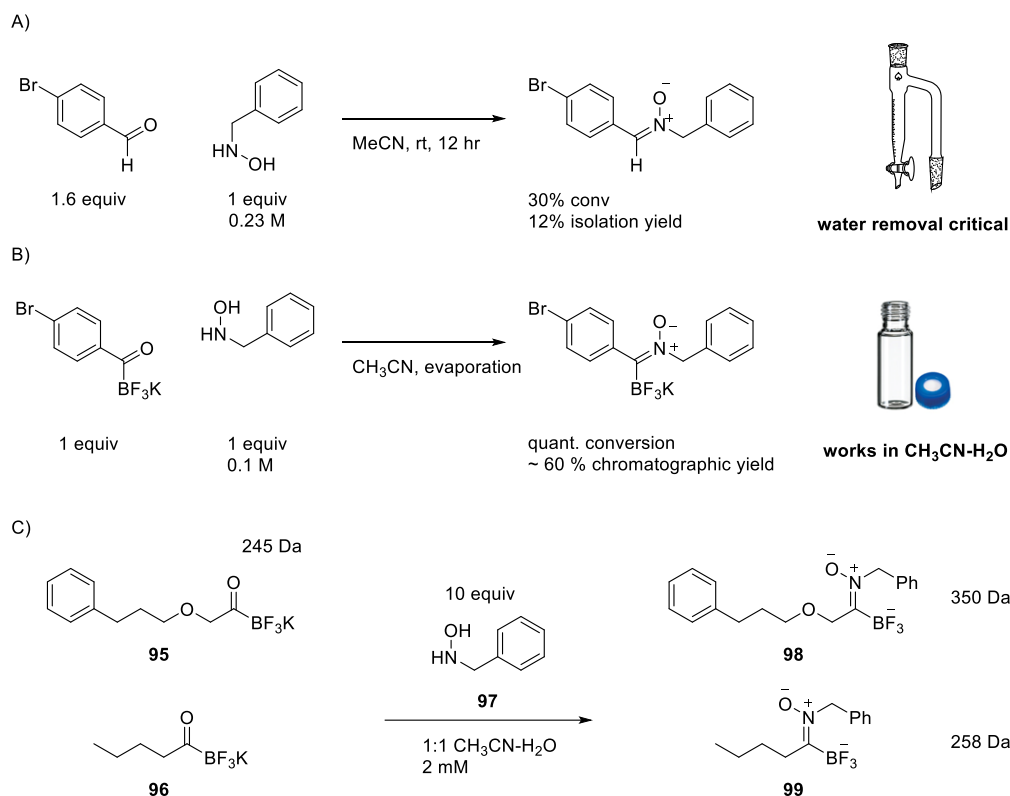
characterize the dynamic formation of KAT nitrones and their subsequent conversion to a static amide linkage, which will be described in sections **2.3** – **2.5**. Before that, a comparative account of the spectroscopic properties and reactivities of KAT nitrones, versus that of normal nitrones, will be given in sections **2.1** – **2.2**.



2.1. Reactivity comparison with normal nitrones

2.1.1. KAT nitrone forms easier than aldehyde nitrones

The most direct way to synthesize a nitrone is to mix an aldehyde or a ketone with a hydroxylamine, while using drying agents or Dean-Stark trap to remove the water formed.^{104,105,109,115} Microwave-assisted conditions¹³⁰ and ball-mill solvent-less setups¹³¹ have been developed to improve nitrone synthesis yields through this condensation route. Some nitrones hydrolyze readily in the presence of water, or even undergo solvolysis with ethanol.¹⁰⁴ On the contrary, KAT nitrones form quantitatively even when KATs and hydroxylamines were mixed in aqueous solutions without the need of desiccants or drying procedures. Adding hydroxylamine to KATs in low mM or μM concentration range in 1:1 CH_3CN -water always gives a detectable nitrone peak in the LCMS chromatogram of the mixture, and was routinely used as a rapid test to check if a hydroxylamine or a KAT was formed under a given condition. As an example, the LCMS from reaction depicted in **Scheme 25C** was shown in **Figure 2**.



Scheme 25. A: Aldonitron synthesis requires water removal. **B:** KAT nitron synthesis is less sensitive towards water in the reaction media. **C:** During the condition screening for the synthesis of **95**, which gave a mixture of KATs **95** and **96**, hydroxylamine **97** was used as a probe for KAT formation.

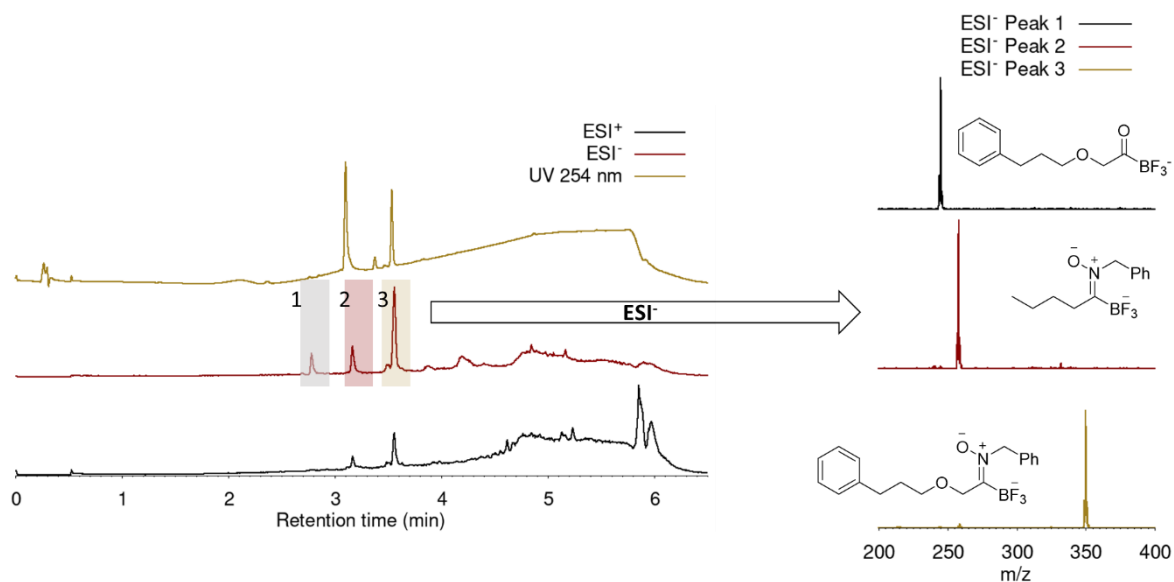


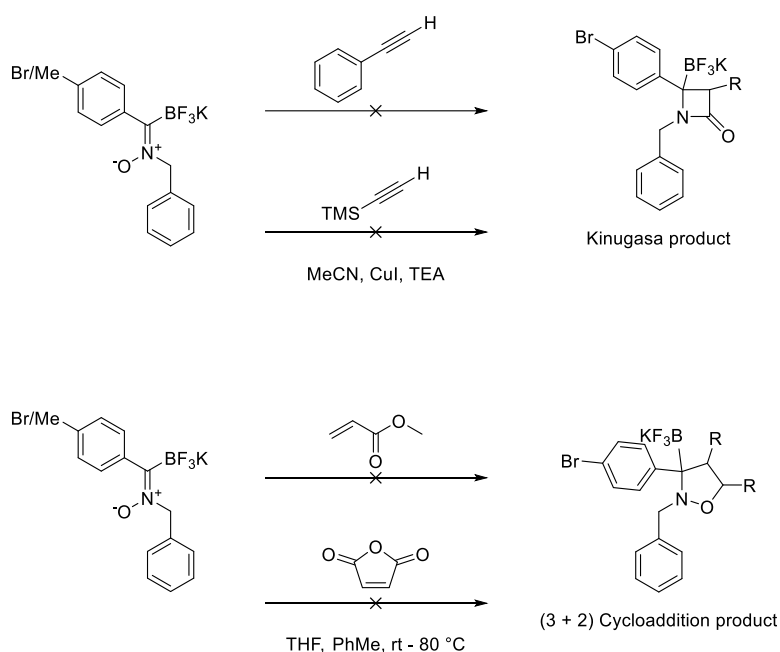
Figure 2. LCMS analysis of a mixture of KAT **95** (2 mM), **96** (trace) with hydroxylamine **97** (5 mM) in 1:1 CH₃CN showed formation of nitron **98** (Peak 3) and **99** (Peak 2) with a little remaining **95** (Peak 1)

The synthesis of KAT nitrones faces other unique challenges. The reaction solvent should dissolve the KAT, but must not react with hydroxylamines. KAT typically dissolves well in polar aprotic solvents such as DMF or DMSO, which is hard to remove after the reaction. Chromatography is often required to purify a KAT nitrone, and most of the yield loss occurred during the chromatography step.

The solvent of choice for KAT nitrone formation will be discussed further in Section 2.3.1.

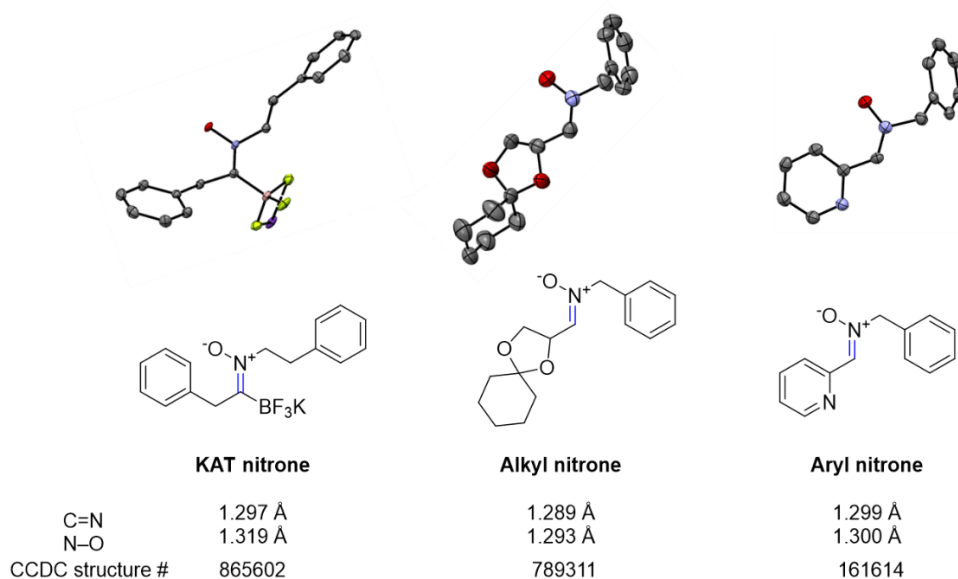
2.1.2. Cycloaddition

When KAT-nitrones were first synthesized¹² we were immediately interested in their possible cycloaddition products. The 1,3-dipolar reactivity of KAT nitrones still has not been realized today, eight years later. Simple KAT nitrones were subjected to common conditions^{108,132,133} for the addition between normal nitrones and unsaturated compounds, such as alkynes or olefins, but so far signs of the desired reactivity were not observed.



Scheme 26. KAT nitrones did not undergo cycloaddition reactions with alkyne and olefin dipolarphiles

Difference in steric bulk as well as electronic structure of KAT nitrones from typical nitrones could be responsible in the modulation of the cycloaddition reactivity. The steric size of the BF_3 group was larger than a hydride or primary alkyl group. The negative charge of the BF_3^- group as well as the difference between a C-B bond and a C-H bond could have both perturbed the frontier orbital of the $\text{C}=\text{N}^+(\text{R})\text{O}^-$ system. Some insights might be obtained from the crystal structures of nitrones and KAT nitrones.^{134,135}



Scheme 27. C=N and C–O bond lengths from crystal structures of nitrones. The C=N bond and N–O bond length in alkyl and aryl aldonitrones are more similar to each other ($\Delta < 0.005$ Å), whereas the KAT nitrone C=N / N–O length difference is 0.22 Å, suggesting that the conjugation between the C=N and N–O bonds is less prominent in a KAT nitrone.

2.1.3. Slow light promoted rearrangement

Normal nitrones are known to undergo light-triggered rearrangements to form oxaziridines, which further rearranges to amides.^{115,136} An aromatic KAT nitrone **100** was subjected to various photochemical conditions, but only 254 nm UV irradiation of a solution in quartz tube gave detectable amount of amide product **101**. The conversion was too low for light irradiation to be a practical way to fix a nitron into an amide.

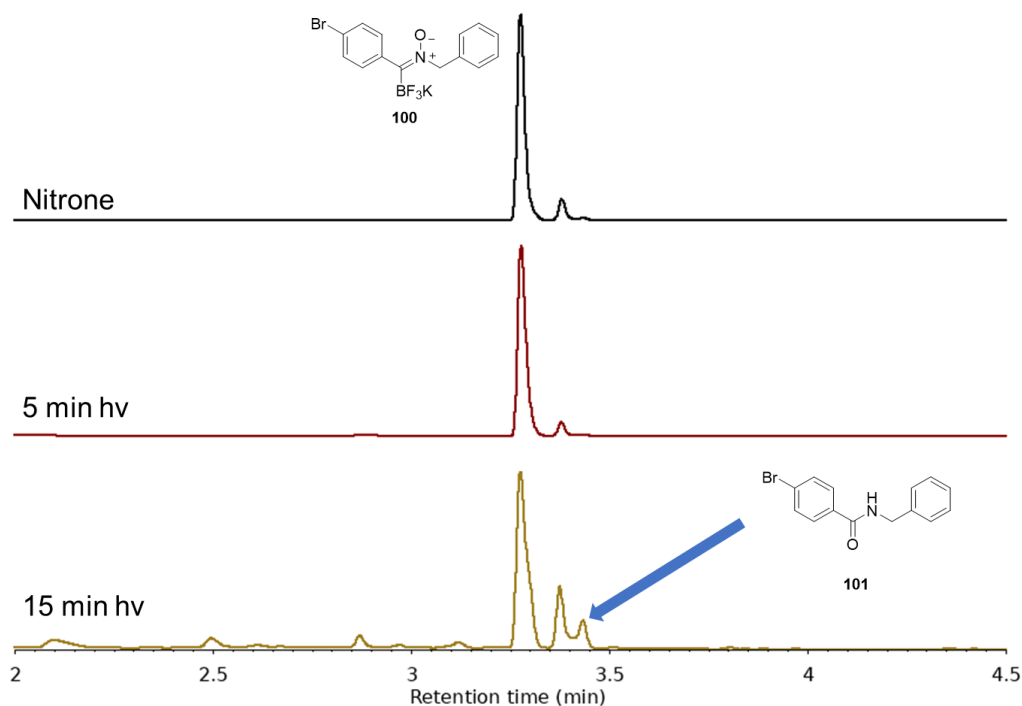


Figure 3. UV chromatogram from the LCMS analysis of p-bromophenyl KAT nitrone (**100**) solution irradiated under 254 nm. Solvent: 1:10 MeOH-H₂O. Concentration: ~ 3mM.

2.2. Spectroscopic properties of KAT nitrone

2.2.1. Infrared spectroscopy

Some distinct bands in the infrared spectrum can be identified for a KAT nitrone. A strong absorption around 1070 cm^{-1} corresponding to the N–O stretching reported for aromatic nitrones¹⁰⁹ was found to overwhelm the B–F stretching patterns, which is the most prominent feature in the IR spectrum of a KAT from 900 cm^{-1} to 1200 cm^{-1} . The band at 1635 cm^{-1} was broadened compared with the KAT and corresponds to the C=N stretching band reported for aromatic nitrones.

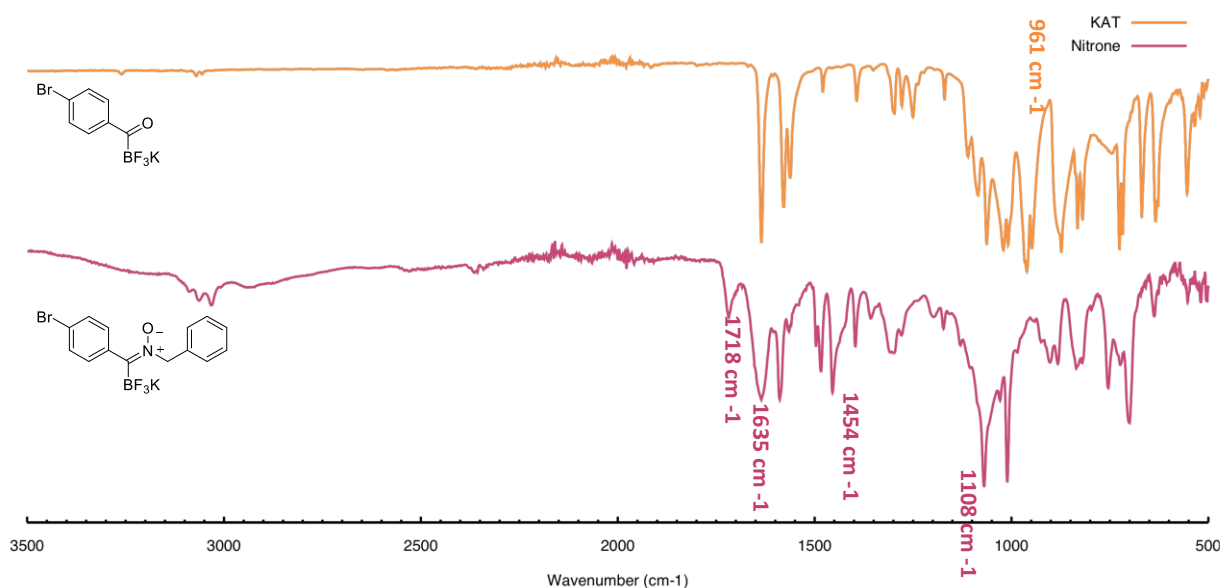


Figure 4. Infrared spectra of p-bromophenyl KAT and its N-benzyl nitron

2.2.2. Nuclear Magnetic spectroscopy

The NMR features of a KAT nitron is demonstrated with p-fluorophenyl KAT-propylphenyl nitron as shown in **Figure 5**. The KAT nitron group was slightly more deshielding than a reference aryl aldonitron¹³⁷ the ¹³C and ¹H nuclei on its N-substituent. The chemical shift of the α -methylene protons on the N-propylphenyl group was 4.17 ppm (CD₃CN), compared to 3.84 ppm (CDCl₃) in the aryl aldonitron reference, and 2.90 ppm (CD₃CN) in N-propylphenyl hydroxylamine before condensation with the KAT. The ¹³C chemical shift (180 ppm) of the C=N group in the KAT nitron was also more downfield than that in the aldonitron (161 ppm). The deshielding power of a KAT nitron group was however lower than that of a KAT group, which contains a carbonyl group with chemical shift 230 ppm. The proton on the phenyl ring ortho to the KAT group also shifted significantly, from 8.06 ppm to 7.38 ppm. The chemical shift difference of the ortho aryl protons and nitrogen α -methylene protons turned out to be useful in determining the composition of a KAT/KAT-nitron/hydroxylamine mixture. The ¹³C peaks suffer from severe broadening due to the B–C quadrupolar coupling, similar to the situation with alkyl trifluoroborates¹³⁸ and cannot be well resolved without particularly long measuring time. For example, a 100 mM sample typically requires ~10000 scans on a 600 MHz spectrometer.

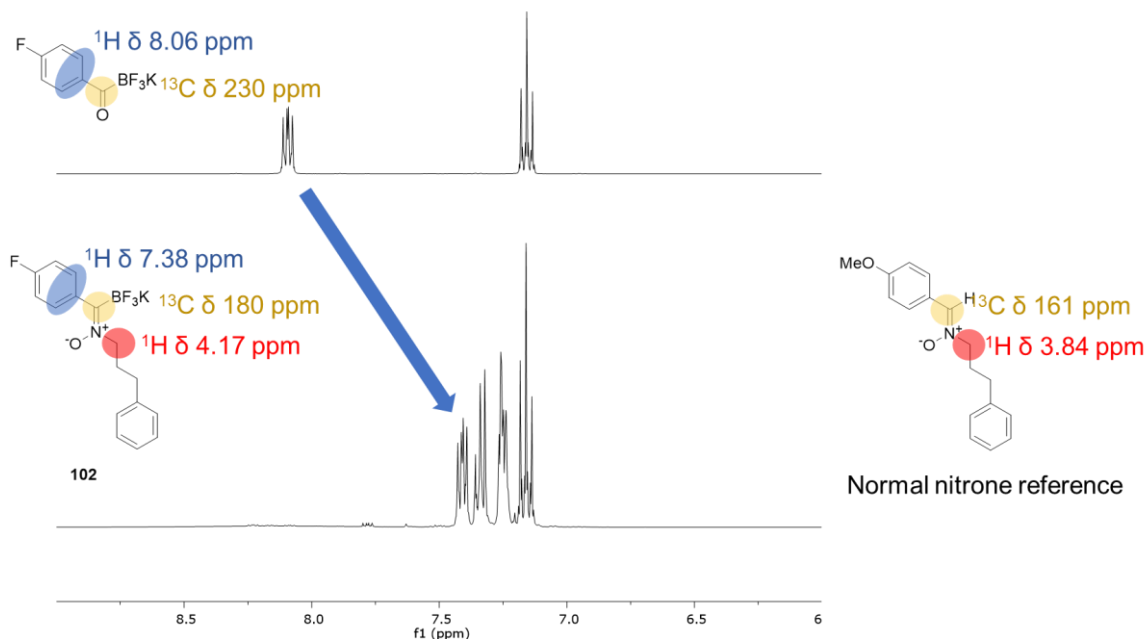


Figure 5. ^1H and ^{13}C NMR characteristics of a KAT nitrone **102**

^{19}F and ^{11}B NMR also give clear indications of a KAT nitrone as shown in **Figure 6**. Both the boron peak and the fluorine peak shifted downfield when a KAT was converted to the nitrone. The B–F coupling constant decreases from about 50 Hz to around 40 Hz. The ^{19}F spectrum was particularly useful to detect residual KAT during KAT nitrone synthesis due to the wide chemical shift spread and lack of interfering peaks compared to ^1H NMR. However, ^{19}F NMR could not give a quantitative measure without modifying the acquisition pulse sequence since the ^{19}F relaxation time of KATs and KAT nitrones were different.

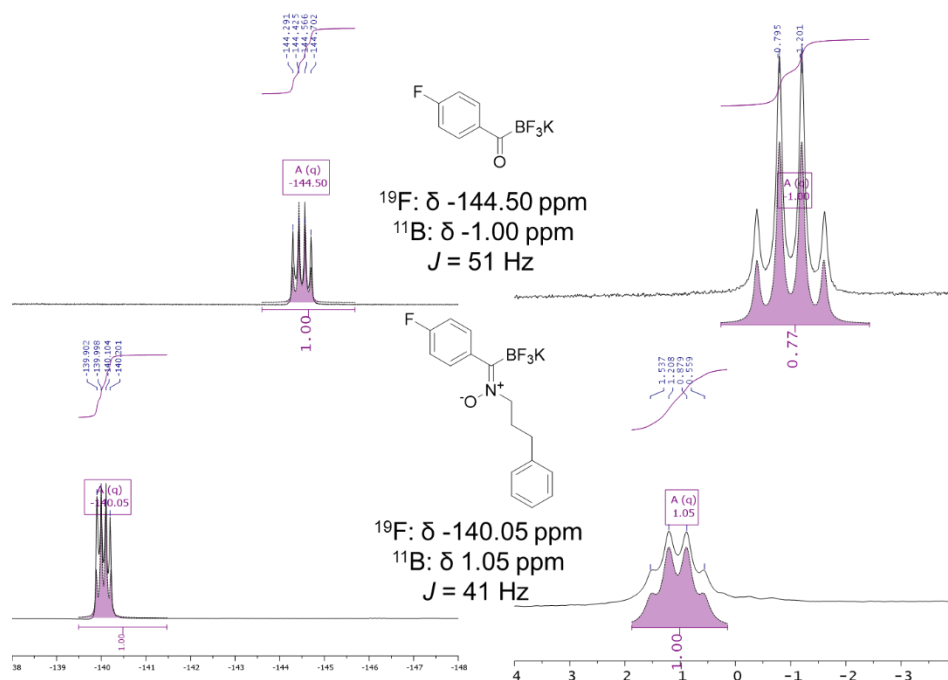


Figure 6. ^{19}F and ^{11}B NMR signature of a KAT nitrone

Cis-trans isomerism was observed during the formation of nitrone **100**. The singlet peak in the ^1H NMR at 5.12 and 4.68 ppm were assigned to the methylene protons from the (Z) and the (E) nitrone, respectively (**Figure 7**). The (Z) nitrone was found to be the more stable isomer in DMSO- d_6 , and the isomerization rate constant measured at 80 °C was found to be around $4.65 \cdot 10^{-6} \text{ M}^{-1}\text{s}^{-1}$ (**Figure 8**).

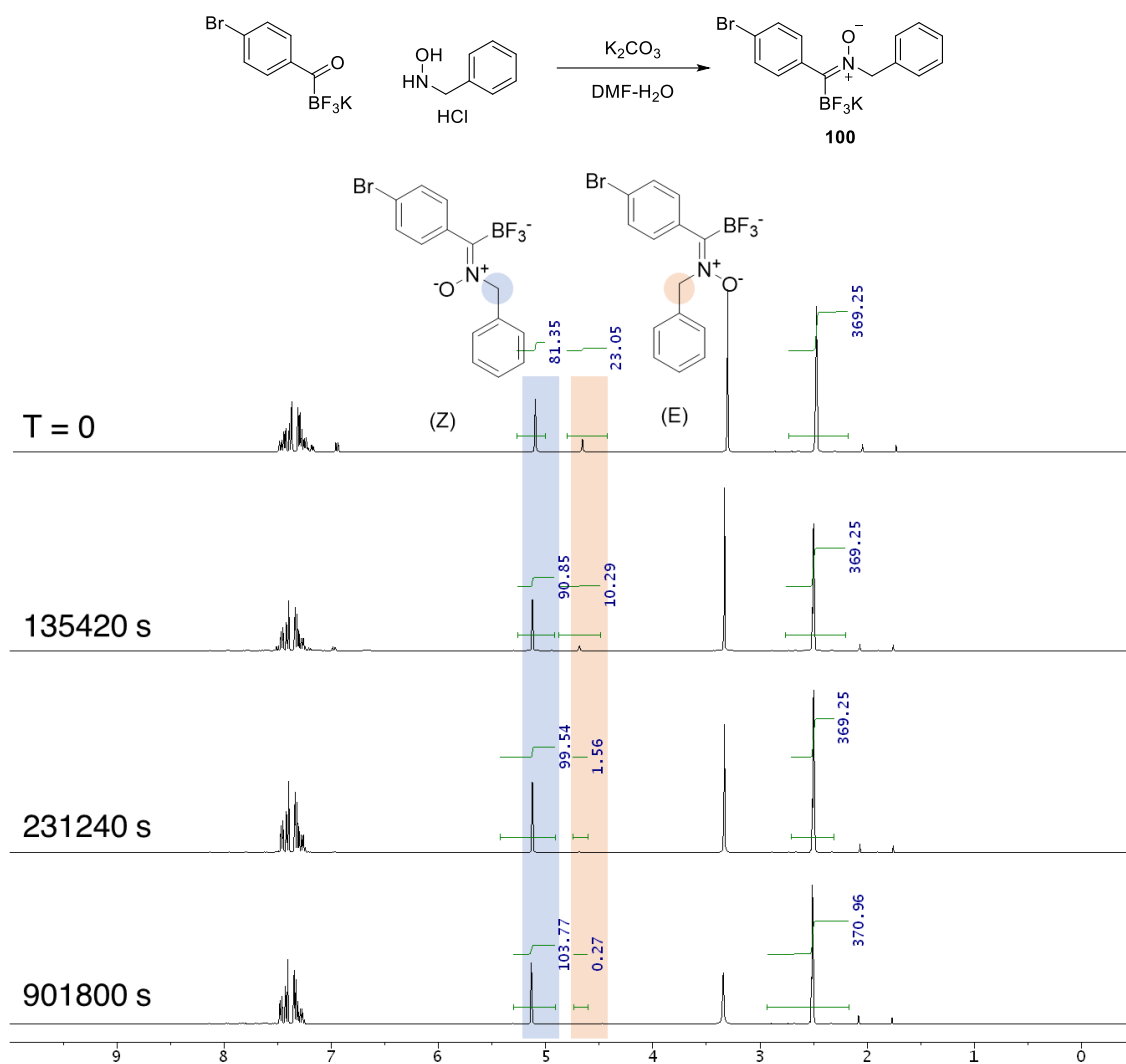


Figure 7. Isomerization of nitrone **100** traced with ^1H NMR in DMSO at 80 C.

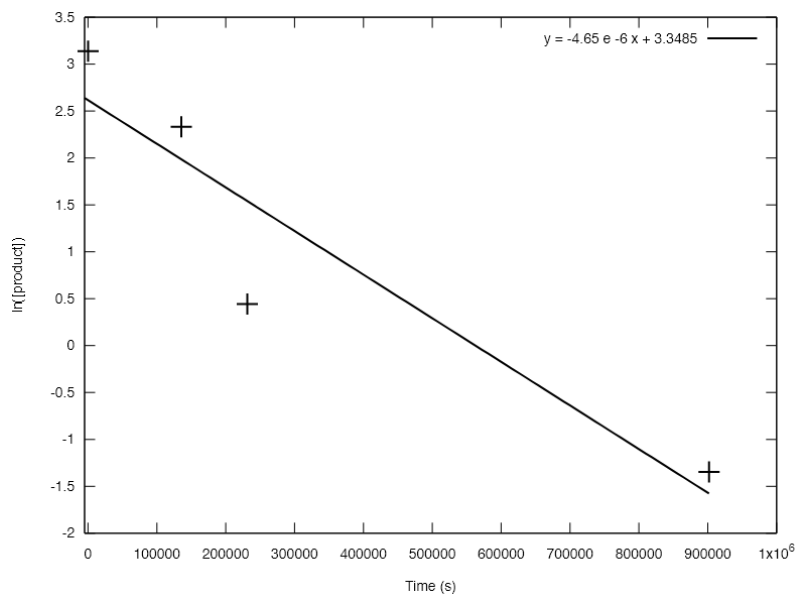


Figure 8. Kinetic plot for the isomerization of nitrone **100**.

2.2.3. UV-Vis spectroscopy

Figure 9 shows the UV absorption spectra of some KATs and their N-benzyl nitrones. The absorption profiles of KAT nitrones varied greatly with the KAT incorporated, but in general a KAT nitrone exhibits a red-shifted tailing absorption from the longest wavelength peak of the KAT. This feature can be used to measure the nitrone content in a mixture with the corresponding KAT, and allowed the kinetic measurements of fast KAT nitrone formation by UV absorption.

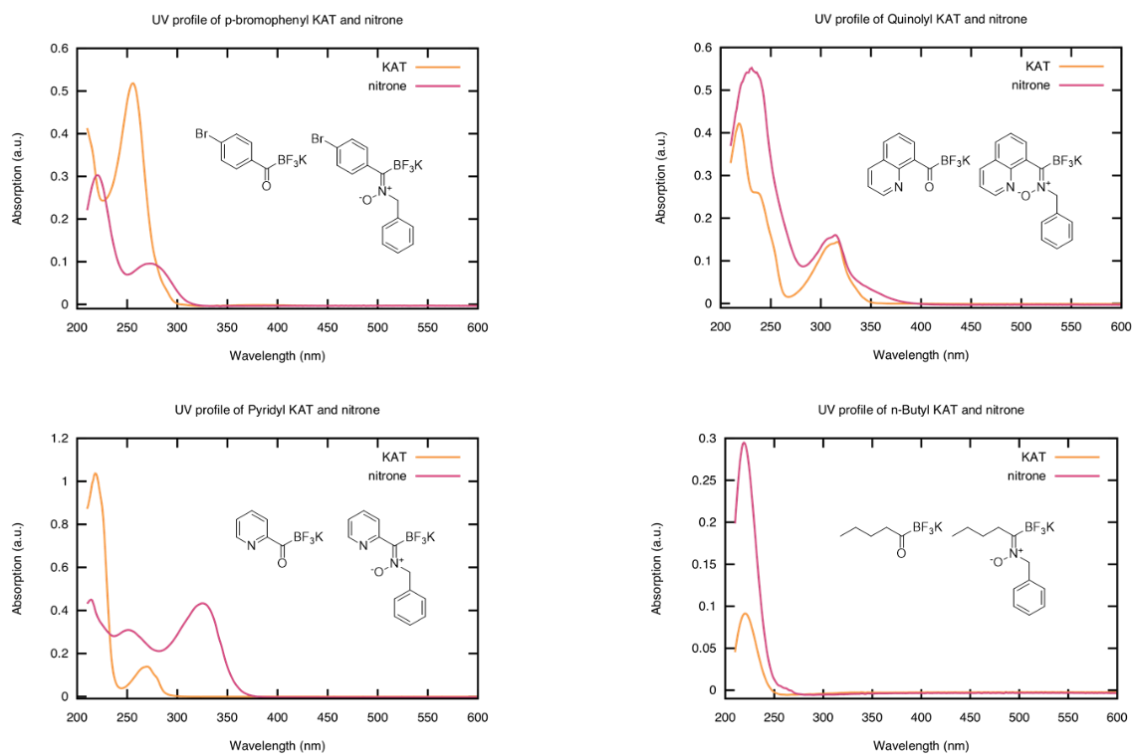


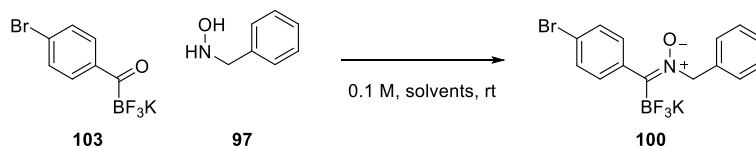
Figure 9. UV absorption spectra of some KATs and their N-benzyl nitrones

2.3. Conditions for KAT-nitrone formation

2.3.1. Solvents

To prepare nitrones from the condensation between KAT and hydroxylamines, the chosen solvent must dissolve the KAT. Most KATs dissolve well only in polar aprotic solvents such as acetone, acetonitrile, DMF, and DMSO. Acetone was the first solvent of choice to extract a KAT from the reaction mixture after being synthesized, but it was not compatible with hydroxylamines due to oxime formation. Acetonitrile was a better choice and was for a long time the standard solvent for KAT nitrone synthesis. Recently however, we found that hydroxylamines were not stable at higher concentrations in acetonitrile.

KAT-nitrones were soluble in all solvents that dissolve KATs, and additionally dissolve well in methanol or methanol-chloroform mixtures. We tried to suspend p-bromophenyl KAT in a MeOH solution of N-benzyl hydroxylamine, to see whether the KAT could be gradually converted to the nitrone which dissolves away, but no nitrone conversion was detected.



Solvent	outcomes
Acetone	Reacts with hydroxylamine 97
CH ₃ CN	Good conversion. Reacts slowly with the hydroxylamine if not quickly consumed.
EtOAc	Did not dissolve 103
THF	Did not dissolve 103 *
H ₂ O	Did not dissolve 103
Methanol	Did not dissolve 103
DMF	Good conversion, difficult to remove. Often co-elutes with the nitrone on silica column
DMSO	Good conversion. Very difficult to remove.
1:1 CH ₃ CN-H ₂ O	Good conversion. Works well for di-, tri- and tetra-KATs

Table 3. Solvent screening for KAT nitrone synthesis with p-bromophenyl KAT **103** and N-benzyl hydroxylamine **97** as model substrates. *: p-tolyl KAT partially dissolves in THF and gave some conversion.

2.3.2. Effect of water

After the preliminary finding that acetonitrile could be a suitable solvent for KAT nitron synthesis, we wished to quantify how fast the nitrones form. A series of kinetic experiments were carried out by mixing KATs and hydroxylamines in deuterated solvents and monitoring the concentration change of KATs, hydroxylamines (HA in Figures), and KAT nitrones (Nitrone in Figures) over time by NMR. A first surprising outcome was that the nitrone formation is faster when performed in an aqueous co-solvent, despite it being a condensation that eliminates a water molecule. **Figure 10** is an example of this effect using p-bromophenyl KAT and N-benzylhydroxylamine. This is an example where a thermodynamic argument (nitrone formation equilibrium is more complete when water was removed) should not be mixed with a kinetic one (nitrone formation is slower when water concentration was low).

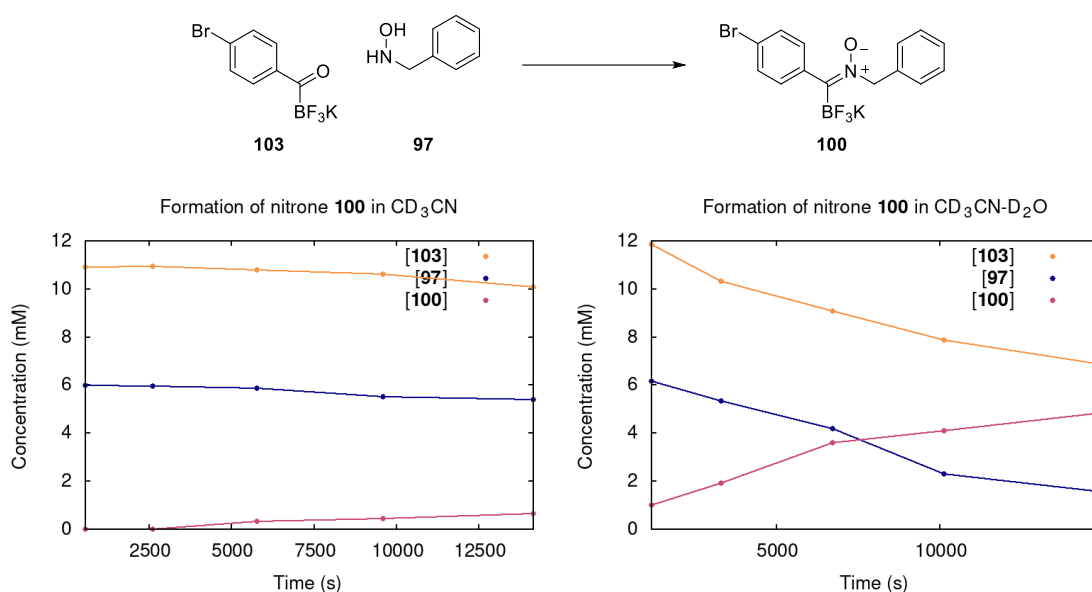


Figure 10. Left: p-Br-phenyl KAT reacting with benzyl hydroxylamine in CD₃CN. Right: Same reaction performed in 1:1 CD₃CN-D₂O

The nitrone formation rate dependency on water content complicated the extraction of rate constant from experiments done in low water content solvents, since the reaction itself produces water. This incurs a self-accelerating effect which could be seen clearly on pyridyl and quinolyl KATs which react faster compared to p-bromophenyl KAT. Their reaction profiles are plotted in **Figure 11**. The reactions were slow for an induction period of three hours, and accelerated afterwards.

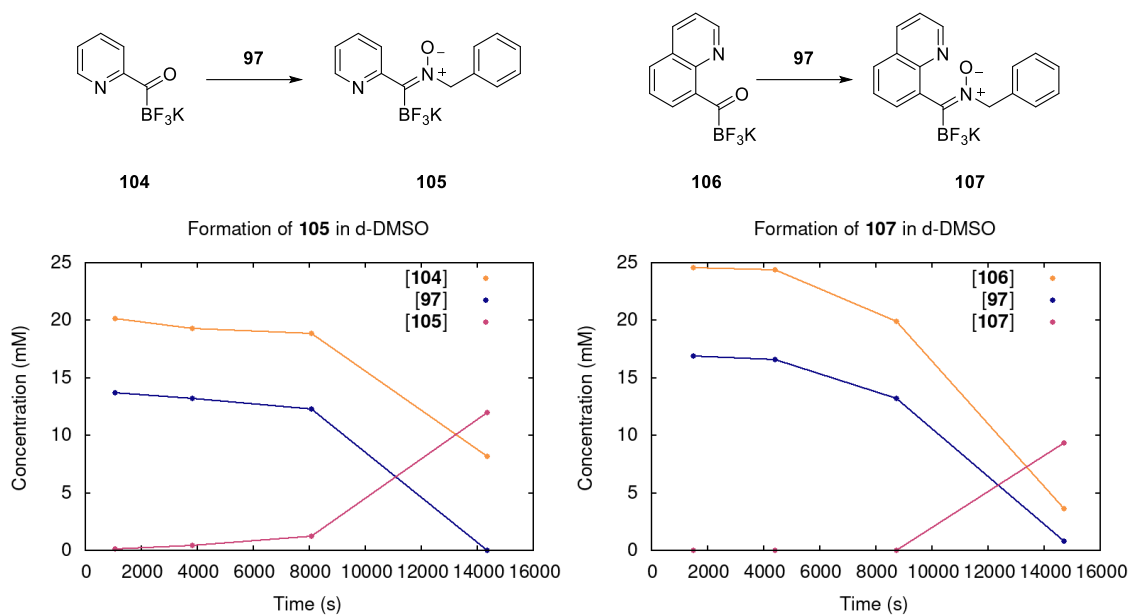


Figure 11. Nitron formation from pyridyl KAT **104** (Left) and quinolyl KAT **106** in DMSO (Right)

When the reactions were performed in 1:1 DMSO-H₂O mixture, the increase in water concentration from the reaction progress became negligible. The reaction profiles return to the expected behavior with faster initial rates that slow down as reactants deplete, as can be seen in the right hand side plot in **Figure 12**, where the nitron formation of n-Butyl KAT was measured.

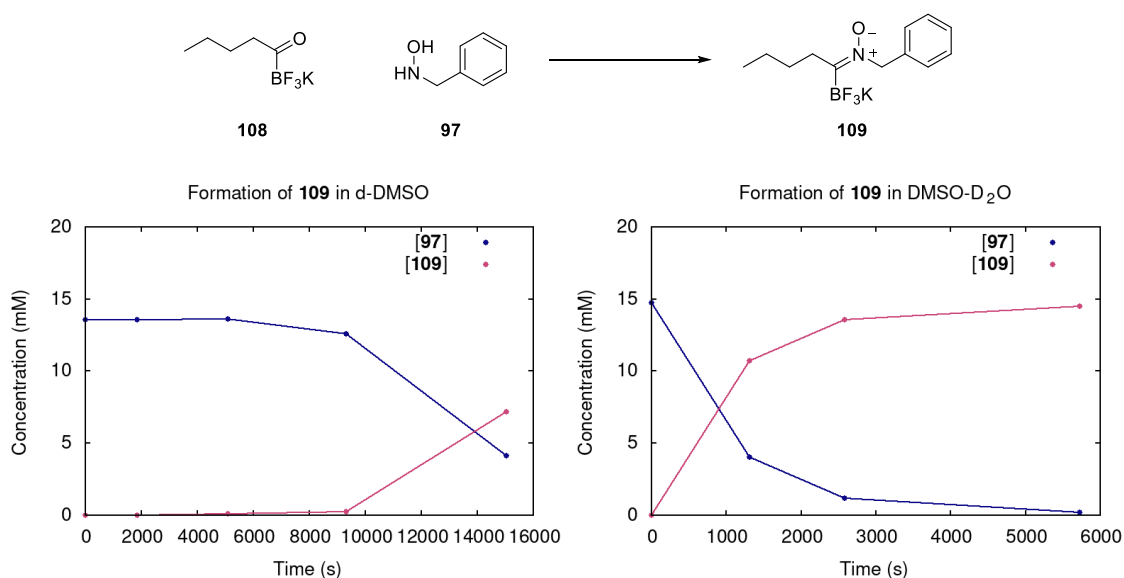
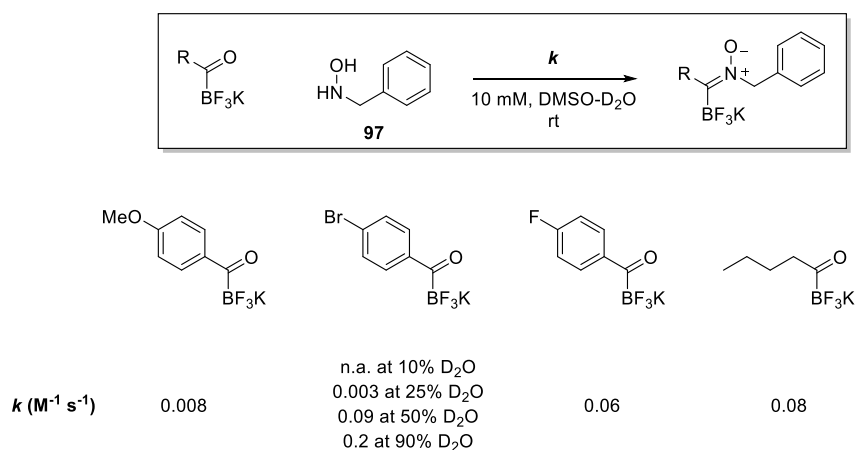


Figure 12. Nitron **109** formation from n-Butyl KAT **108** in DMSO (left) and in 1:1 DMSO-H₂O (right). The KAT concentration was not measured due to overlap with the nitron ¹H signals.

The solvent effect on nitron formation rate was explored further in DMSO, 1:1 DMSO-MeOH and 1:1 DMSO-H₂O with p-bromophenyl KAT and benzyl hydroxylamine. Methanol can also increase the nitron formation rate, albeit to a lesser extent than water. 1:1 DMSO-water mixture was chosen to be the standard reaction media of nitron formation, in which the second order rate constants of some KATs with N-benzyl hydroxylamine were extracted and listed below in **Scheme 28**.



Scheme 28. Nitron formation rate constants in DMSO-D₂O measured with ¹H NMR. The hydroxylamine used was **97**, and the rate constants were second-order.

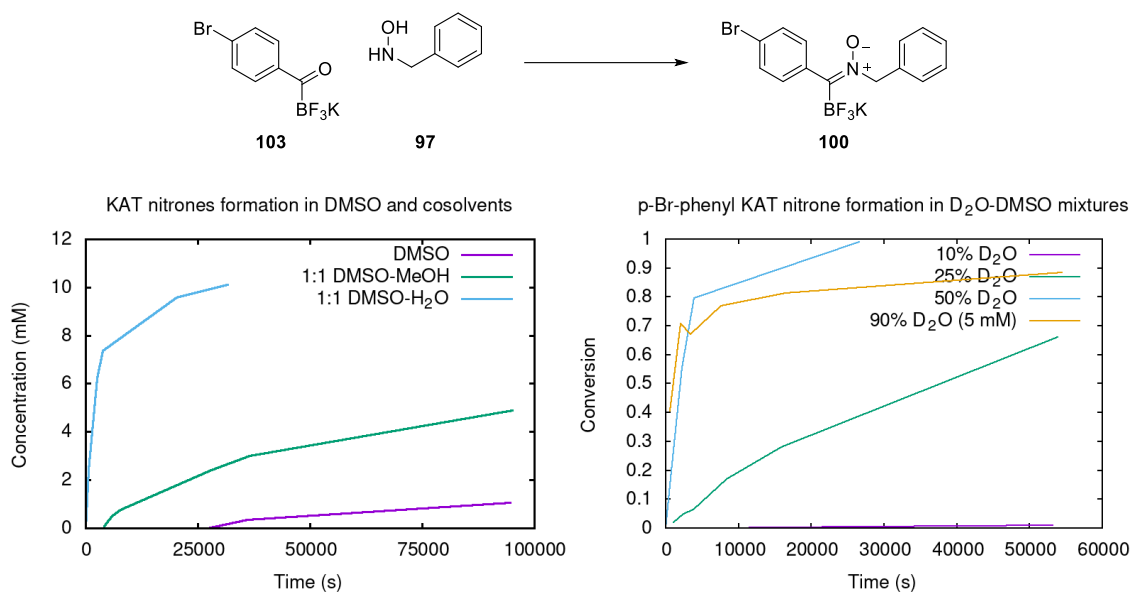


Figure 13. Summary of solvent effect on the formation rate of nitron **100** from p-bromophenyl KAT **103**. The starting concentration of both **103** and **97** were 10 mM for all reactions, except for that performed in 90% D₂O/DMSO, which was too fast to measure with ¹H NMR under 10 mM.

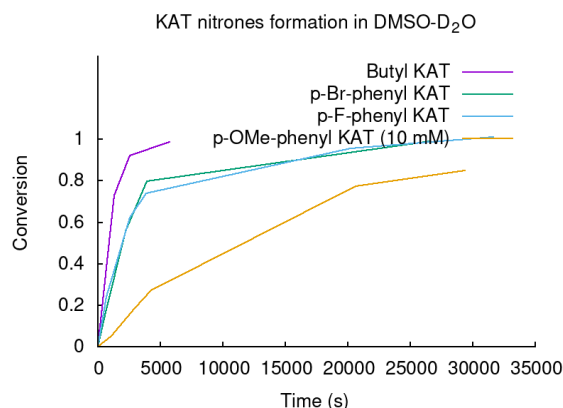


Figure 14. Summary of nitrone formation measured in 1:1 DMSO-H₂O. All reactions were performed under 20 mM initial concentration of KATs and hydroxylamine **97** excepts for the case of p-OMe-phenyl KAT.

The reaction rates of pyridyl KAT **104** and quinolyl KAT **106** nitrone formation in 1:1 DMSO-H₂O were fast. Starting at 10 mM of both the KAT and the hydroxylamine, the reactions ran close to completion within five minutes, making them difficult to be measured by NMR. Fortunately, the UV absorption profile of pyridyl KAT and its nitrone was very different, with a new band at 330 nm arising only from the nitrone (See **Section 2.2**). The nitrone formation rate was measured by UV absorption change where the temporal resolution was higher than NMR. With UV-Vis kinetic measurement we found that pyridyl KAT nitrone formation has a second order rate constant of $\sim 0.59 \text{ M}^{-1}\text{s}^{-1}$ when performed in 1:1 DMSO-H₂O.

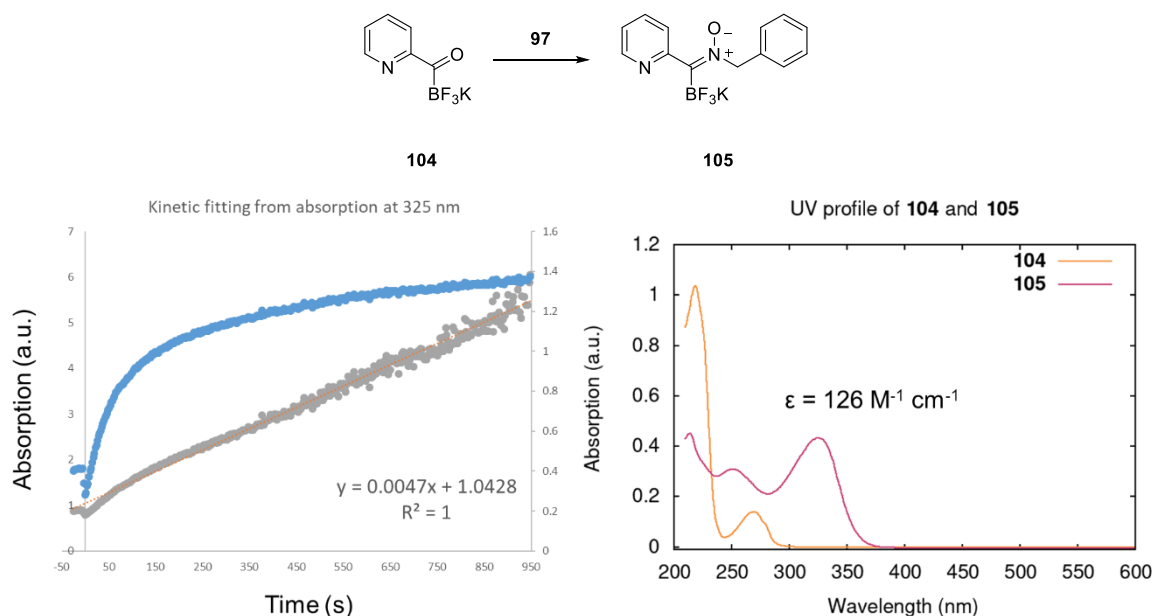
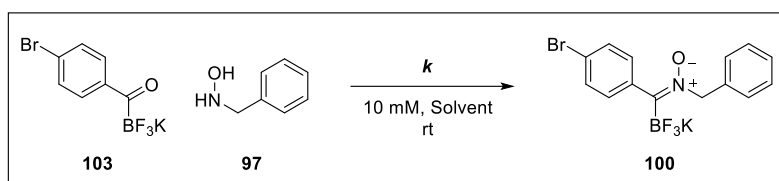


Figure 15. Kinetic measurement of pyridyl KAT nitrone **105** formation in 1:1 DMSO-H₂O.

2.3.3. Acid catalysis

The finding that KAT nitron formation is faster when water or methanol was present led us to suspect that nitron formation is subject to acid catalysis. We then measured the formation rate of nitron **100** under standardized conditions with varying solvent and buffer concentrations. HFIP was chosen as a more acidic alcohol. Potassium acetate buffer at pH 3.8 with concentration from 0.05 M to 0.2 M was added to probe the effect of general acid catalysis. The reaction rate constants were measured by UV-Vis.



Solvent	k_{obs} ($\text{M}^{-1}\text{s}^{-1}$)
1:1 DMSO- H_2O	0.0867
1:1 DMSO-HFIP	0.159
1:1 DMSO-0.05 M AcOK buffer	2.17
1:1 DMSO-0.1 M AcOK buffer	2.88
1:1 DMSO-0.2 M AcOK buffer	3.57

Table 4. 2nd order rate constant of the formation of KAT nitron **100** under various conditions. The solution of **103** and **97** potassium acetate buffer were adjusted to pH 4.8 before starting the reaction.

HFIP, being more acidic than H₂O, accelerated the formation of **100** more than H₂O. Adjusting the pH to 4.8 accelerated the reaction rate even more, to about 20 times faster than that in DMSO-H₂O. The observed rate constant has a slight dependence on the concentration of buffer used, suggesting a general acid catalysis scheme for KAT nitrone formation.

$$k_{obs} = k_0 + k_{AcOH}[AcOH] + \dots$$

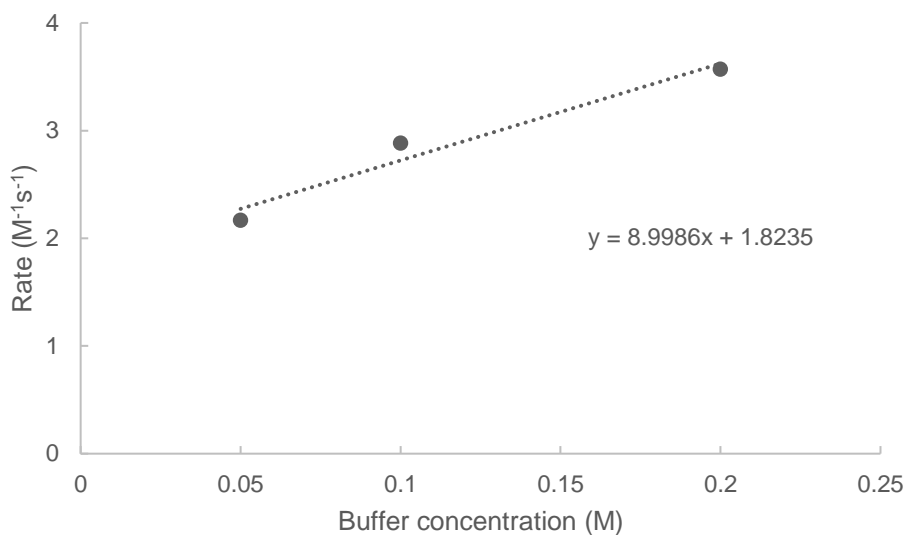


Figure 16. Rate constant of **100** at pH 4.8 plotted against the concentration of buffer in the reaction mixture. k_0 at pH 4.8 can be determined to be 1.82 M⁻¹s⁻¹, and k_{AcOH} was found to be 9.00 M⁻²s⁻¹.

2.3.4. Acetonitrile is not always an innocent solvent

During the kinetic studies a surprising and alarming discovery came from the CD₃CN stock solution of benzyl hydroxylamine **97** used. After two days the concentration of the benzyl hydroxylamine dropped from 160 mM to 120 mM, and large, transparent crystals precipitated from the solution! X-ray crystallography showed that the crystal was an amidoxime adduct¹³⁹ between the hydroxylamine and CD₃CN.

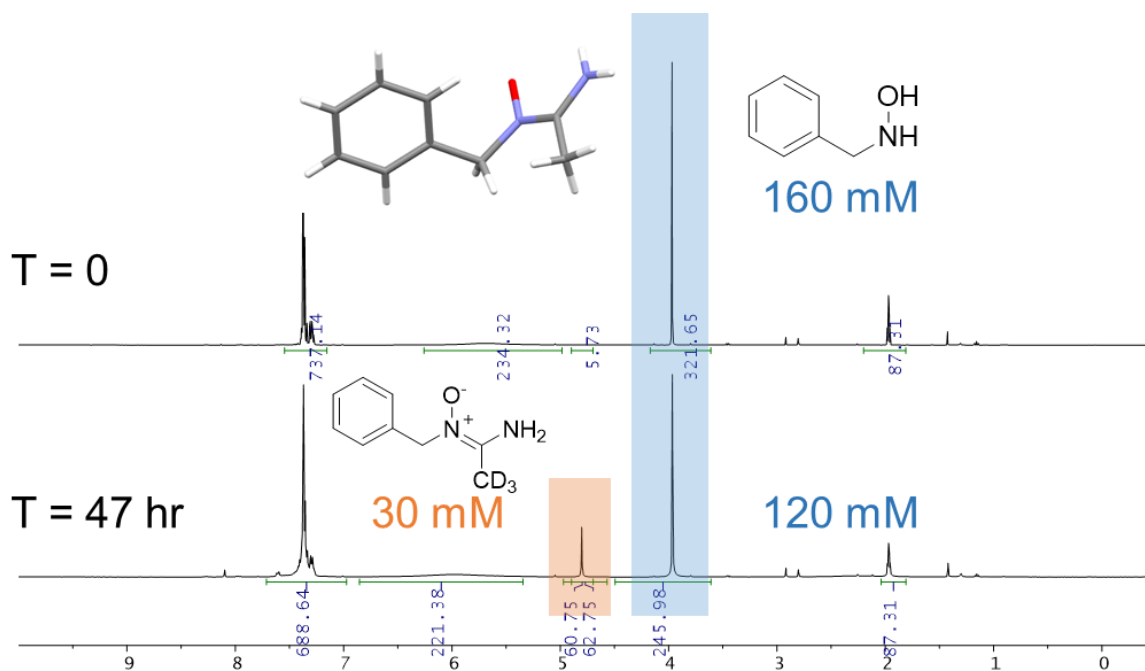


Figure 17. Amidoxime formation in CD₃CN stock solution, evident from the δ 4.8 ppm singlet.

The pseudo 1st-order rate constant of the amidoxime adduct formation is estimated to be about $1.7 \cdot 10^{-6} \text{ s}^{-1}$, assuming the concentration of CD₃CN to be constantly 17 M. This may seem slow, but is a significant competing side reaction when the reaction being studied is a bimolecular event with both reactants at mM concentrations. As shown below in **Figure 18**, the formation of amidoxime is observable even when 1:1 CD₃CN-H₂O was used instead of pure CD₃CN as reaction solvent. Hydrolysis of the amidoxime did not proceed under both acidic and basic conditions, suggesting amidoxime formation to be an irreversible side reaction that greatly impacts nitron formation studies performed in acetonitrile. Luckily, the hydroxylamine was stable in DMSO therefore DMSO-H₂O was chosen to be the standard condition for kinetic measurements described above.

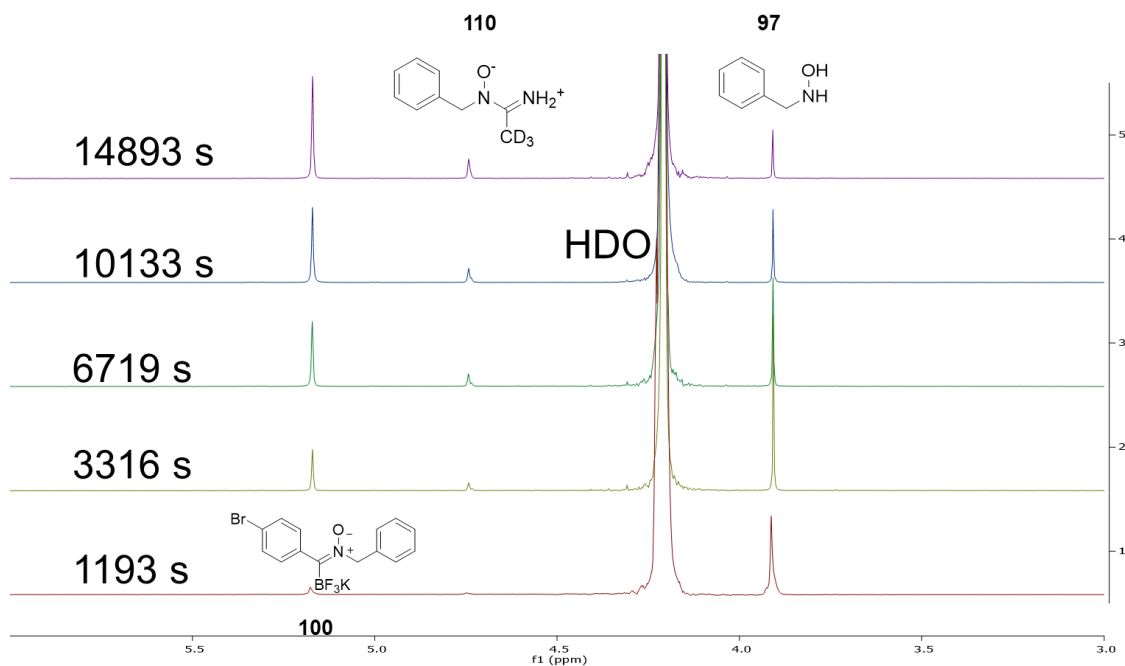
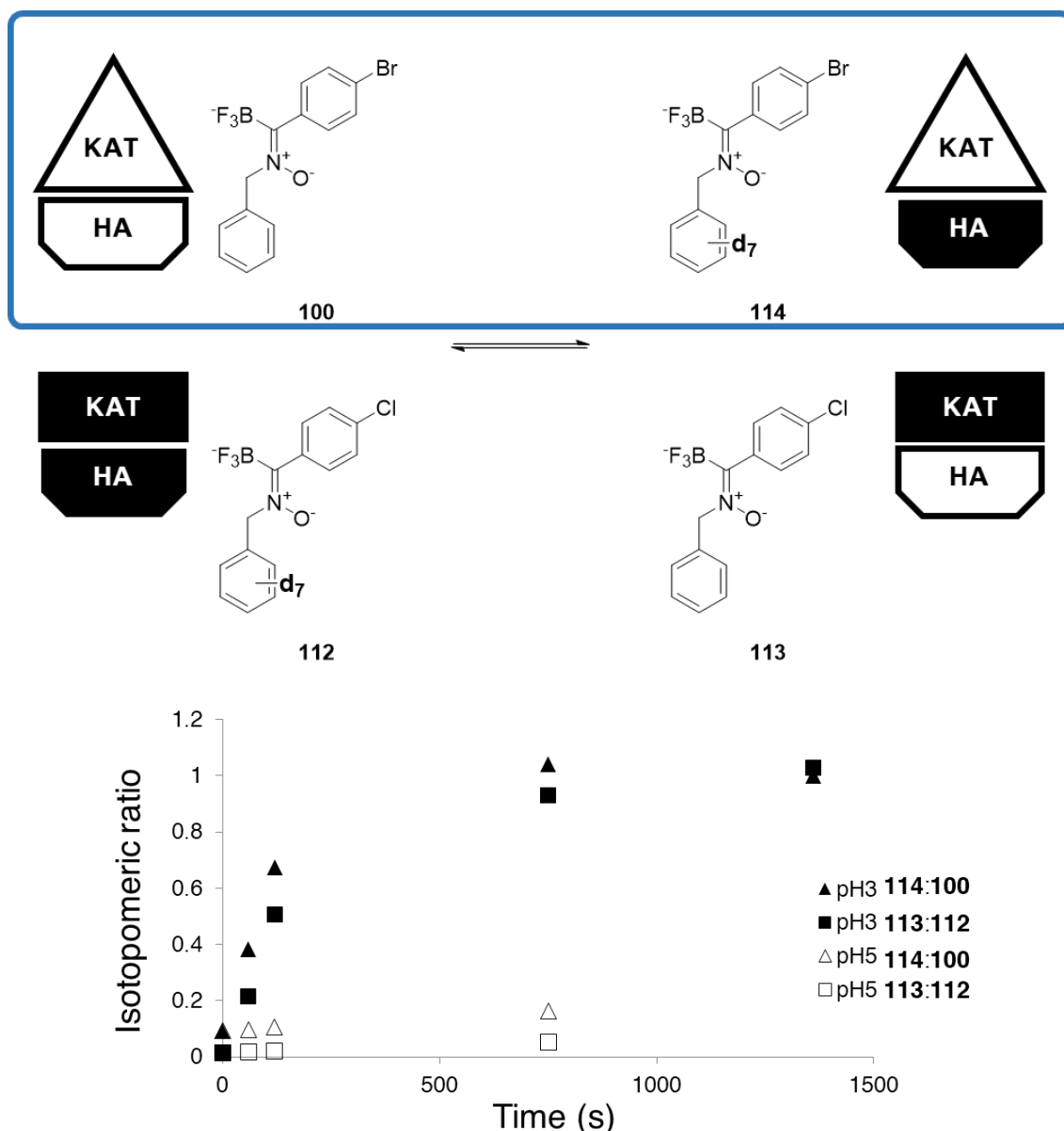


Figure 18. ^1H NMR experiment of p-bromophenyl KAT nitrone **100** formation in 1:1 $\text{CD}_3\text{CN}-\text{H}_2\text{O}$. The amdoxime **110** is clearly forming as in parallel with the nitrone formations as told from the singlet peak around 4.8 ppm.

2.4. Nitrone partner exchange

To probe the exchange of the nitrone partner an isotopomer exchange experiment was performed. Nitrones **100** and **112** were prepared and mixed in a 1:1 fashion and left to exchange partners, producing nitrones **113** and **114**. The hydroxylamine used in **100** was benzyl hydroxylamine, and its isotopically labeled version d7-benzyl hydroxylamine was used in **112**, making the nitrones **100** / **114** a pair of isotopomers, and **112** / **113** another pair of isotopomers. As the KATs and hydroxylamines exchange a statistical mixture will be reached where $[\mathbf{100}]:[\mathbf{114}]$ and $[\mathbf{112}]:[\mathbf{113}]$ approach unity. We assume the ionization yield in LCMS for isotopomers be the same, leading to that ion count ratios of isotopomers from LC-ESI-MS analysis serving as a close estimate of the real ratio between isotopomer concentrations, which is an indicator of the exchange process. The exchange experiment was performed in both pH 5 acetate buffer (50 mM) and pH 3 citrate buffer (50 mM) concentration, with the initial nitrone concentrations being 10 mM each. LCMS analysis was performed after certain time durations and the isotopomer ion count ratios were plotted below in **Scheme 29**.



Scheme 29. Nitroner isotopomer exchange experiment. Isotopomeric ratios were obtained by integration of the mass channel of LCMS data (355 – 359 Da for **100**, 362 – 366 Da for **114**, 318 – 322 Da and 311 – 315 Da for **112** and **113** respectively). The isotopomeric ratio will approach one as the nitrones scramble to a statistical mixture. The equilibration progress at pH 3 were depicted by the solid black data points, and were much faster than that observed at pH 5.

2.5. Nitroner to amide conversion

2.5.1. Identifying a flash acidification condition

A remaining challenge of the KAT nitroner dynamic chemistry is whether it is possible to lock the dynamic nitrones into a static amide bond. **Figure 19** shows a preliminary screen of conditions to transform pyridyl KAT nitroner **105** into the amide **115**. Acidifying with 10% v/v acetic acid after 3 days only gave trace amount of the amide. Treating the nitroner with 20 % $\text{HCl}_{(\text{aq})}$ successfully transformed the nitroner to amide over 40 min, and the conversion can be higher if heated to 60 °C. 20 % $\text{HCl}_{(\text{aq})}$ was also effective in transforming KAT nitrones from

other classes of KATs listed in **Scheme 30**, and was a general condition for KAT nitron fixation.

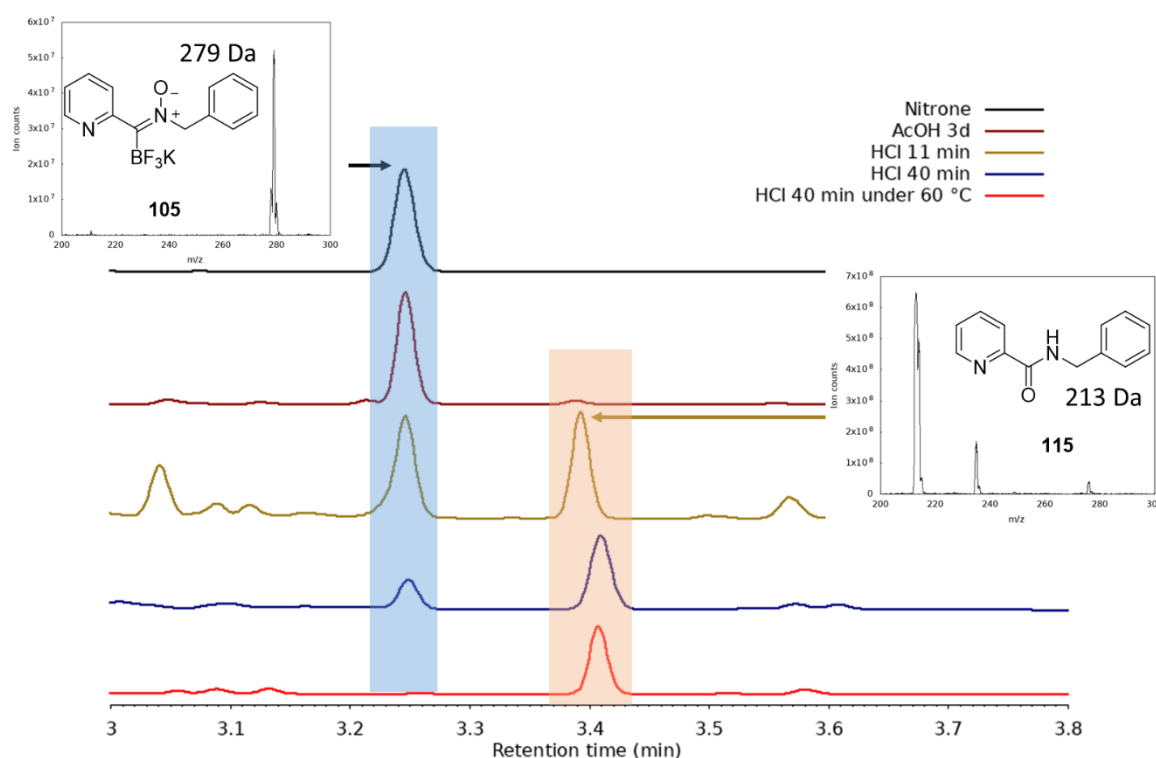
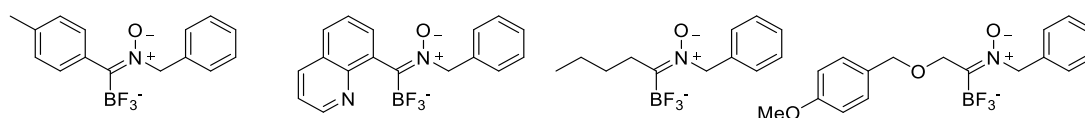
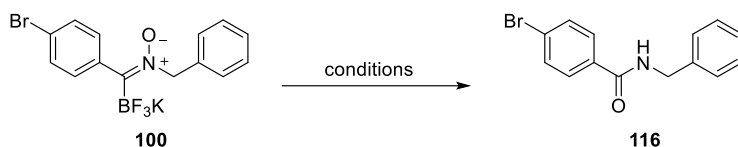


Figure 19. 20% HCl promotes conversion of nitron to amide.



Scheme 30. KAT nitrones that were tested to convert into amide in 2M HCl

Conditions of nitron acidification with weaker acids or HCl with lower concentrations were also screened by LCMS, using p-bromophenyl KAT nitron **100** as a model substrate. **Table 5** summarizes the outcome of subjecting **100** to these conditions. The reactions were carried out in aqueous methanol solution, with the nitron concentration being 3 mM. Under all conditions trace amounts of the amide product can be detected with the mass detector, as shown in the XIC chromatograms 1 ~ 6 in **Figure 20**. The mass of the product amide **116** appears in both the elution time of the nitron and the amide, but their relative heights increase at the amide peak position, as stronger acids are being used. Aqueous hydrochloric acid at 1.2 M also was not strong enough to facilitate the efficient nitron-to-amide conversion. The broad peak at 2.85 min in UV trace was p-bromophenyl KAT, showing that significant KAT nitron hydrolysis under these conditions.



	Conditions	Outcome
1	2 M oxalic acid	Slight conversion
2	0.1 M HATU	n.r.
3	2 M Formic acid	n.r.
4	2 M dichloroacetic acid	n.r.
5	2 M H ₂ SO ₄	n.r.
6	0.6 M HCl	n.r.
7	1.2 M HCl	n.r.
8	2.0 M HCl	> 50%
9	2.0 M HCl, 60 °C	Complete conversion

Table 5. Conditions to convert pBr-phenyl KAT nitrone **100** into amide after 4 hr

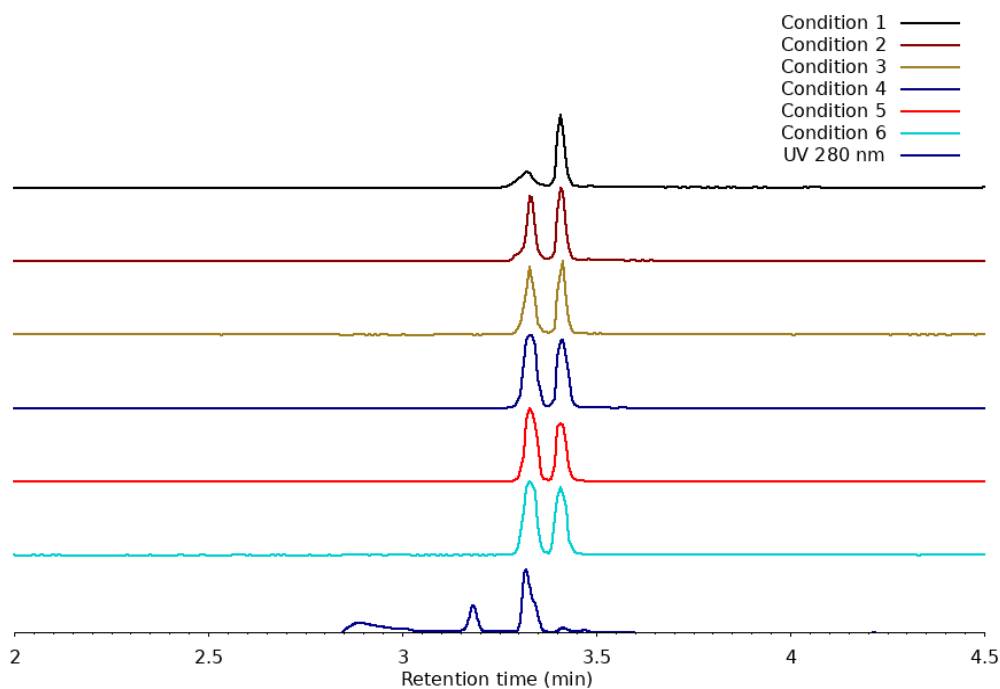
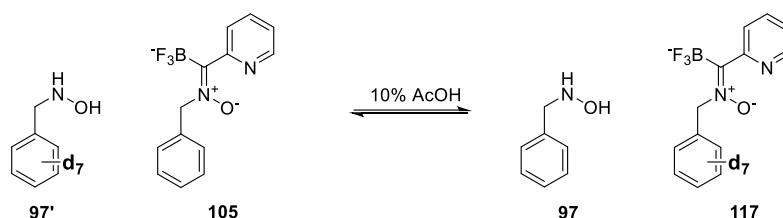


Figure 20. Extracted Ion Chromatograms (XICs) from reaction mixtures of p-Br-phenyl KAT nitrone **100** subjected to various acidifying conditions. The UV chromatogram (the lowest line) was shifted 0.04 min to the later to align the time of arrival difference between the diode array and mass detector. XIC chromatograms collected cations with m/z from 290–293 Da. The UV trace was almost identical under all conditions, and that from condition 6 was taken as an example.

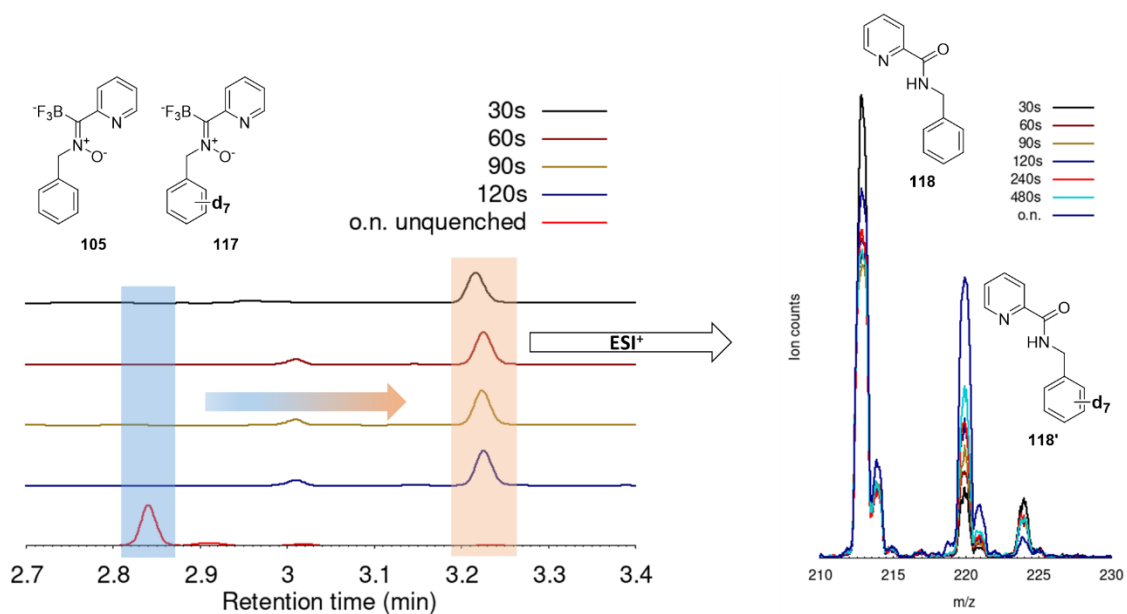
2.5.2. “Snapshot” experiment

The condition to fix the KAT nitron bond into a persistent amide linkage is acidification, which also promotes nitron exchanges shown in **Scheme 29**. We wished to find a stronger acidic condition under which the amide formation can be fast enough to fix the current combination of KATs and hydroxylamines quickly, so that this condition can be used record a “snapshot” of the off-equilibrium system. Nitron **105** was dissolved in 5% DMSO-10% AcOH-H₂O to form a 2 mM solution. To this solution, 1 equiv of d₇-hydroxylamine **97'** was added to exchange with the h₇-hydroxylamine part of **105**. 30s, 60s, 120s, 240s, and 480s after the addition of d₇-hydroxylamine **97'**, a portion of the reaction mixture is mixed with equal volume of 12 M HCl_(aq) to take a “snapshot” of the distribution of nitrones, represented by the ratio of amides [**118**]:[**118'**], which changes over time to approach unity.



Scheme 31. Hydroxylamine exchange for "snapshot" experiment

The results are summarized in **Scheme 32**. LCMS chromatograms from the snapshots indicated complete conversion of nitron to amide within the ~ 2 minute delay between acidification and LCMS injection. The ESI⁺ mass trace extracted from the amide peak indicated a gradual growth of the **118'** abundance, and the decrease of **118**. The reaction mixtures stored overnight underwent minimal amide formation. We were pleased to see that we could use a weak acidic conditions to facilitate the nitron exchange without prematurely fixing the dynamic exchange, and use a strong acidic conditions to quickly freeze the current state of exchange without blurring the snapshot to equilibrium state. This validates KAT nitron exchange to be a dynamic chemistry system.



Scheme 32. LCMS analysis of the acidification snapshots. Chromatograms (left) were monitored at 254 nm. The ESI⁺ ion counts (right) were extracted from the retention time of the amide.

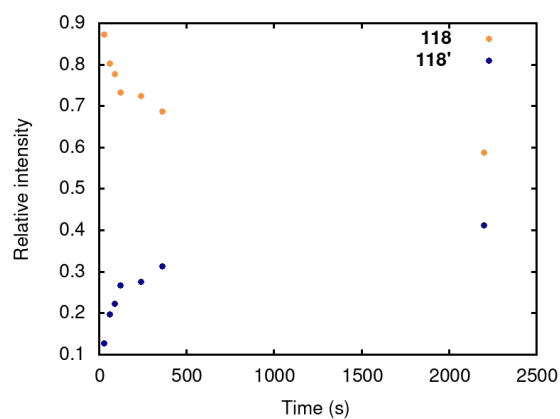
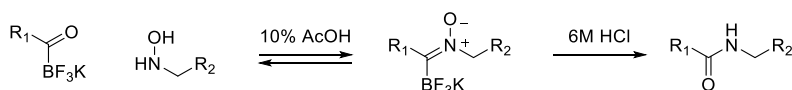


Figure 21. Relative MS intensities from isotomer pair **118** and **118'** converge in the snapshot experiment

2.6. Summary

KAT nitrones were found to be a stable compound that can be formed in aqueous environments from KATs and hydroxylamines. The spectroscopic behavior of KAT nitrones were characterized, so studies on the rate of their formation can be undertaken. The formation rate was found to be higher when the H₂O contents of the solvent mixtures were higher. The KAT nitrone formation rate for KATs were found to be pyridine KATs > butyl KAT > phenyl KATs in 1:1 DMSO-H₂O. CH₃CN was not a suitable solvent for these studies since hydroxylamines were reactive towards CH₃CN.

The KAT-hydroxylamine pair exchange of KAT nitrones was also found to be facile in aqueous solutions. The exchange rate was pH dependent, with the rate being faster at lower pH. Under strongly acidic conditions such as 6 M HCl, a system of KAT nitrones can be converted to the amide, before the KAT hydroxylamine partner exchange reaches equilibrium, rendering this a viable condition to freeze the combinations of KAT nitrone bonds. These findings suggest KAT nitrone to be a fixable dynamic chemical system.



3

KAT-nitrones for covalent organic frameworks (COFs)

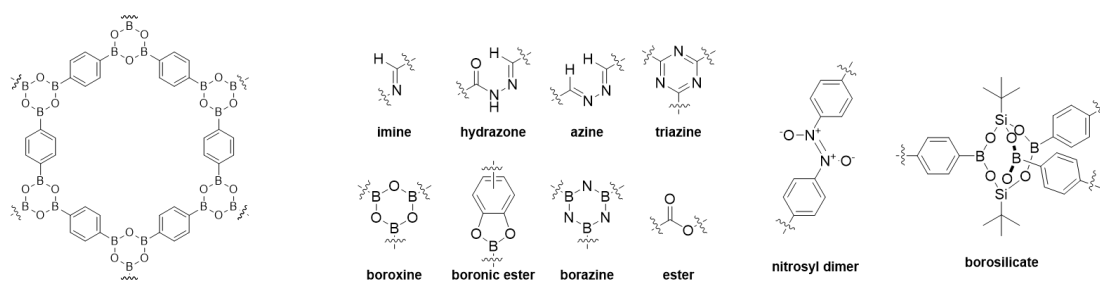
那不就是
星球存在的方式嗎？
幾乎「什麼都沒發生」？
文明與愛情 空間與時間
人的量尺和
星球的量尺
之間的差距
有時大於
「發生」和
「沒有發生」

*Isn't it the way
Of celestial existence?
As if / "nothing happens"?*
Civilization and romance
Space and time
Scale of mankind and
Scale of the planets
The difference in between
Is at times greater than that of
"Happening" and / "Not happening"

羅智成一藍色時期 IV / Chih-Cheng Lo – Blue era IV

3.1. Covalent organic frameworks (COFs)

The first covalent organic frameworks (COFs) were reported by Yaghi et. al in 2005. It was constructed from boronic ester condensation,¹⁴⁰ and since its premiere as a novel crystalline, pore-shape persistent material, novel designs and new applications COFs emerge continuously.¹⁴¹ Similar to other rigid porous materials, such as metal organic frameworks and zeolites, COFs have shown its capabilities in gas storage, separation, and catalyst immobilization due to their shape persistency, high surface area and prominent host-guest interactions. With regards to the rational design of these materials, COFs allow the highest freedom in terms of chemical diversity. Not long after the report of the first COFs, a variety of chemical bonds were employed in COF synthesis including imine,¹⁴² borosilicate,¹⁴³ hydrazone,¹⁴⁴ azine,¹⁴⁵ borazine,¹⁴⁶ ester,¹⁴⁷ and nitrosyl-dimer.¹⁴⁸



The first COF reported

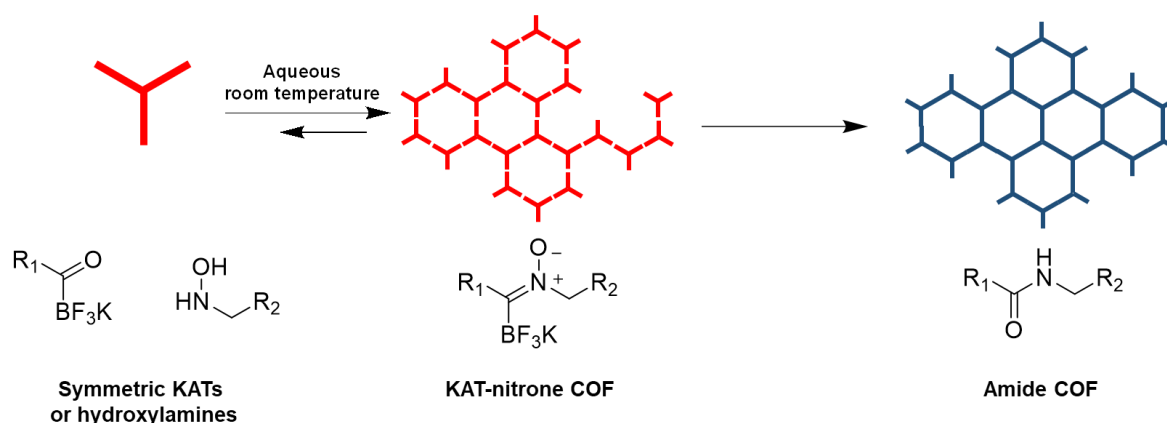
Linkages used for COF construction

Scheme 33. Common chemical linkages used for COF formation

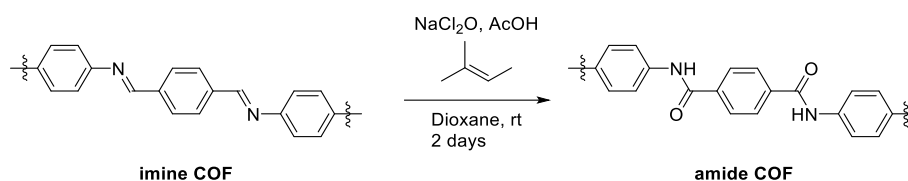
One of the most prominent challenges of COF synthesis is to find conditions to form a highly-ordered crystalline material instead of just an amorphous hyperbranched polymer. Successful COF synthesis conditions often employ heat and strong acid catalysis, posing a restriction on functional groups that can be installed on a building block for COF synthesis. The underlying reason for these harsh COF synthesis conditions is that they enhance reversibility of bond formation, and allow amorphous regions of the material to reorganize and crystallize. This process of annealing an amorphous kinetic product into the final COF has been characterized by Dichtel et. al in a boronic ester COF and a imine COF, where addition of water or end-capping monomers helps to make the COF formation more reversible, to avoid pre-mature precipitation, and results in products with higher crystallinity and surface area.^{98,149,150}

In Chapter 2 we identified that KAT-nitrone formation could be a dynamic chemical linkage which is convertible to static amide bonds. We hypothesized that from carefully designed KATs and hydroxylamines one might be able to build COFs from forming KAT-nitrone bonds.

Furthermore, the KAT-nitrone bond could be later converted by acidification after COF formation, forming a hydrolysis-resistant amide COF that is harder to obtain directly due to the amide bond formation being less reversible. This would enable the synthesis of amide COFs under aqueous and ambient conditions (**Scheme 34**). Triggering chemical bond formation between building blocks after COF assembly has been reported in a few cases.^{87,151} Yaghi et al. reported a similar strategy in 2016, which is shown in in **Scheme 35**.⁸⁷ First an imine linked COF was synthesized, followed by treatment with Pinnick oxidation mixture which oxidized the imine bonds to amide bonds.

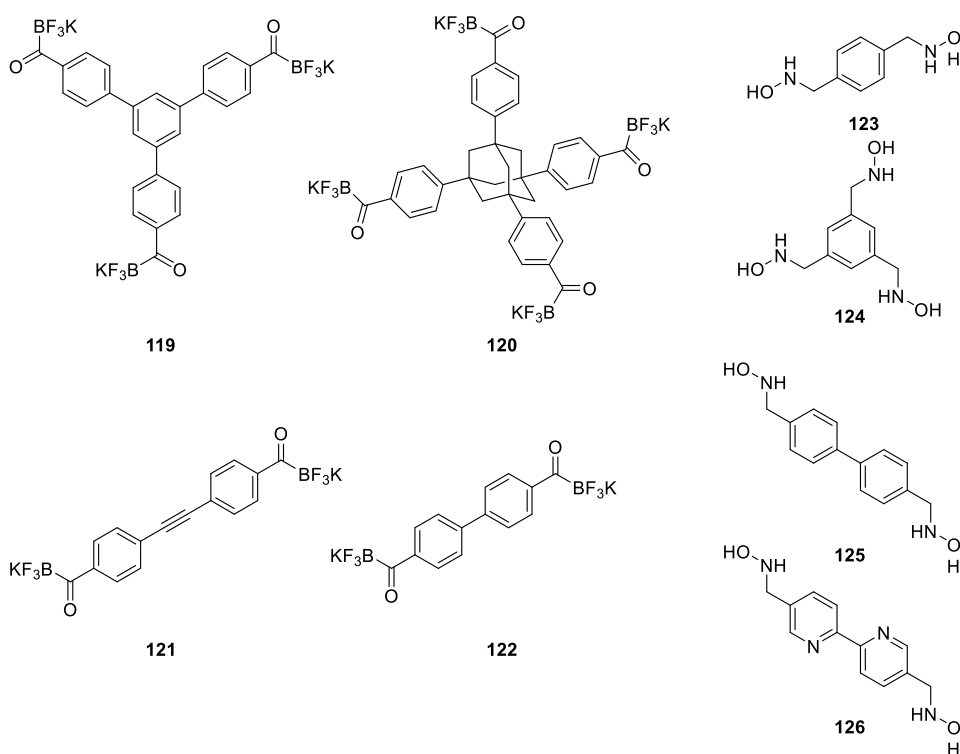


Scheme 34. Proposed concept of dynamic COF construction based on KAT-nitrone formation



Scheme 35. An imine COF was shown to be convertible to amide COF via oxidation by the Yaghi group.⁸⁷

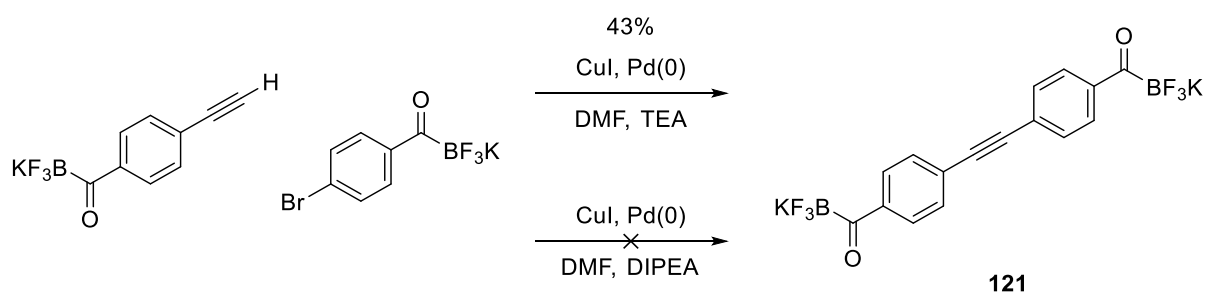
We designed a series of symmetrical KATs **119–122** and hydroxylamines **123–126** with high degree of symmetry hoping that they might assemble in a reversible manner and reorganize into an ordered KAT nitrone framework as depicted in **Scheme 35**. These symmetric di-, tri- and tetra KATs and hydroxylamines were synthesized and the following section reports their synthesis. Although the desired KAT-nitrone COFs were not yet obtained by the time this thesis was written, the findings and lessons learned along the preparation of related KATs and hydroxylamines are none the less of merit and will be summarized in this chapter.



Scheme 36. Symmetric KAT (**119** – **122**) and hydroxylamine (**123** - **126**) building blocks synthesized for attempted COF synthesis.

3.2. Synthesis of multivalent KATs

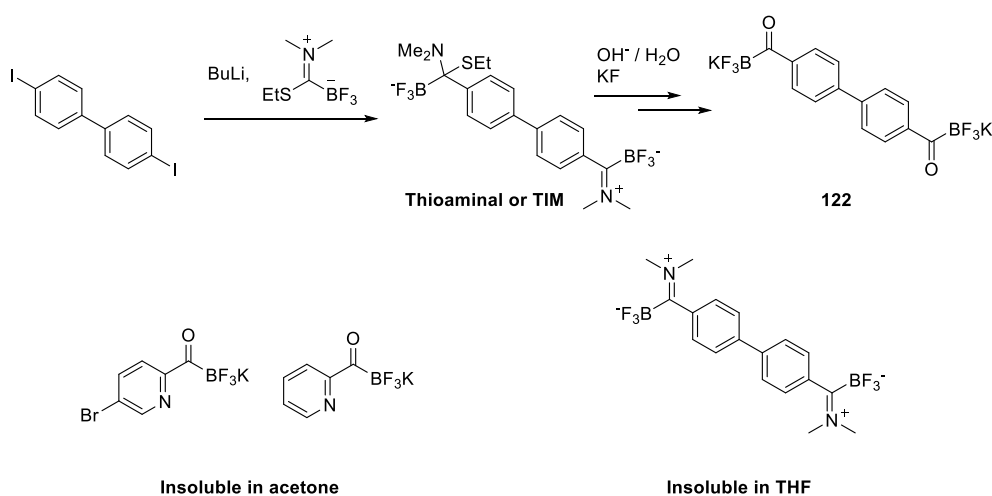
Although 4-arm-PEG tetra KATs were already known²⁸ at the beginning of this research, the synthesis of small molecule multivalent KATs was still non-trivial. **121** was the first small molecule di-KAT synthesized from transition metal catalyzed coupling between two KATs, as shown in **Scheme 37**. During the work-up and purification of this di-KAT, it soon became clear that it did not dissolve in acetone or CH_3CN , but only in DMF or DMSO.



Scheme 37. Sonogashira coupling on KATs to create a di-KAT. Note that using *N,N*-diisopropylamine as the base afforded very low yields. It was found later that secondary amines can form TIMs with the reactant KAT under this condition.

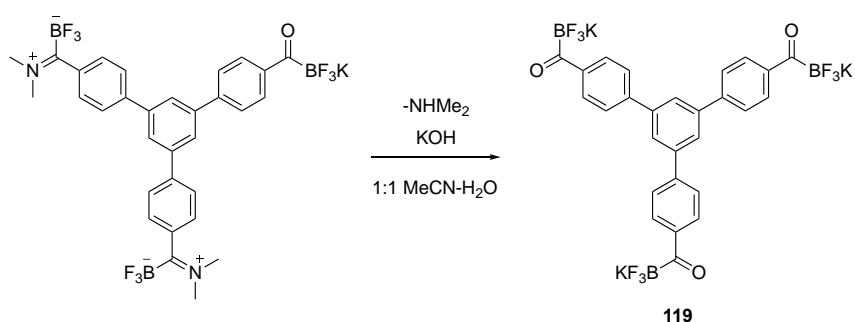
Previous attempts on preparing multivalent KATs mostly adopted the KAT transfer reagent route. The problem was not limited to the product KAT being insoluble in acetone, which has also known precedents such as 2-pyridyl KATs.¹⁷ The key obstacle was the lower

solubility of synthetic intermediates that were expected to be hydrolyzed during work-up procedures. **Scheme 38** describes the synthesis of biphenyl-di-KAT **122**. Diiodobiphenyl was lithiated with *n*BuLi and the resulting aryllithium was trapped in situ by the KAT transfer reagent to form either a tetrahedral thioaminal intermediate, or a TIM by losing an ethanethiol anion. It was found that a mixture of these intermediates was carried over during work up, together with the product di-KAT, and was not hydrolyzed efficiently by the workup mixture of $\text{KF}_{(\text{aq})}/\text{THF}$. The synthesis of this KAT was previously considered unsuccessful¹⁵² earlier, probably due to this inseparable contamination.



Scheme 38. Insolubility of intermediate complicated multivalent KAT synthesis

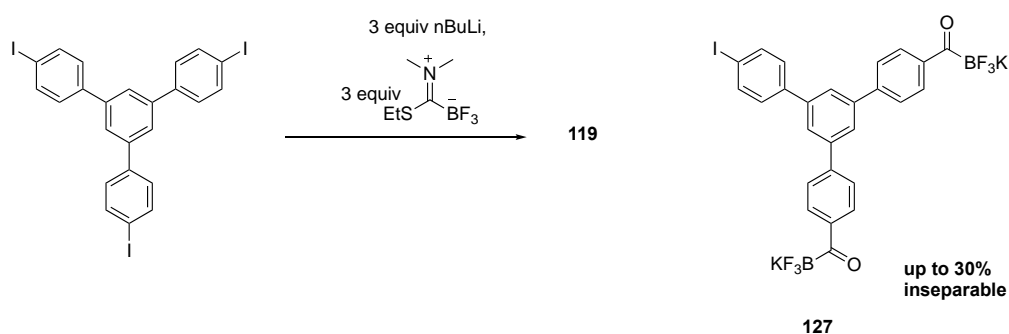
Luckily the mixture of all productive intermediates were soluble in aqueous acetonitrile. With stronger basic condition and prolonged work-up time all the KAT groups can be released to afford a clean product. The progress of the *N,N*-dimethyl TIM hydrolysis could be traced by ^{19}F NMR, or by detecting the generated dimethylamine in the gas outlet with pH paper.



Scheme 39. Stronger TIM hydrolysis condition was needed for multivalent KATs

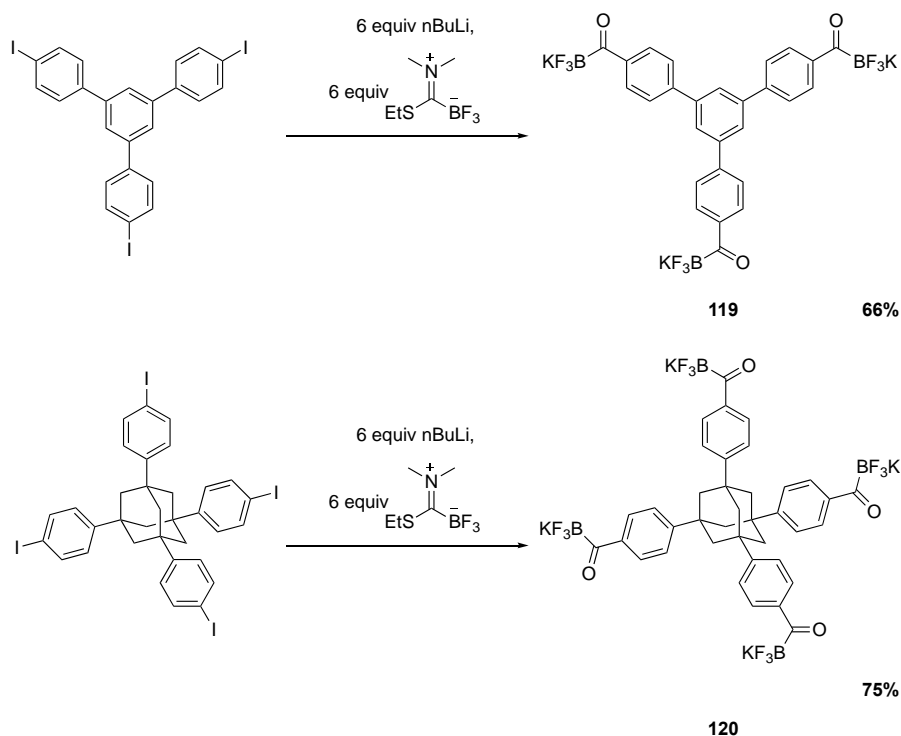
The other obstacle to tris-KAT synthesis was incomplete lithiation, which produces inseparable di-KAT byproducts. This was less severe in the case of mono-KAT or di-KAT synthesis, because the less-KATylated byproduct was either an aryl halide, or a mono-KAT,

which could be easily removed by CH_2Cl_2 or acetone while leaving the product KAT undissolved. This was not the case for the synthesis of triphenylbenzene-tris-KAT **119** or of tetra-KAT **120**. The monoiodo di-KAT **127** has the same solubility behavior as the desired product tris-KAT **119**. We found that 6 equiv of lithiation reagent and KAT reagent were needed to drive the KATylation to completion.



Scheme 40. Incomplete lithiation leads to complex mixtures during the synthesis of KAT **119**.

After optimization of the synthetic and work-up procedure, satisfactory isolation yield and purity can be obtained on KAT **119** and **120**. The lower solubility of these multivalent KAT in organic solvents turned from a curse to a blessing because most impurities can be dissolved away more easily than the KAT of interest, and repetitive precipitation was often a smooth process.



Scheme 41. Optimized synthesis of tris-KAT **119** and tetra-KAT **120**.

3.3. Strong intermolecular association of multivalent KATs

The dramatically lower solubility of multivalent KATs compared to mono-KATs suggests the existence of strong intermolecular interaction in these KATs. Clues from variable-temperature NMR indicated that the KAT groups of multivalent KATs are strongly interacting with each other as shown in **Figure 22**.

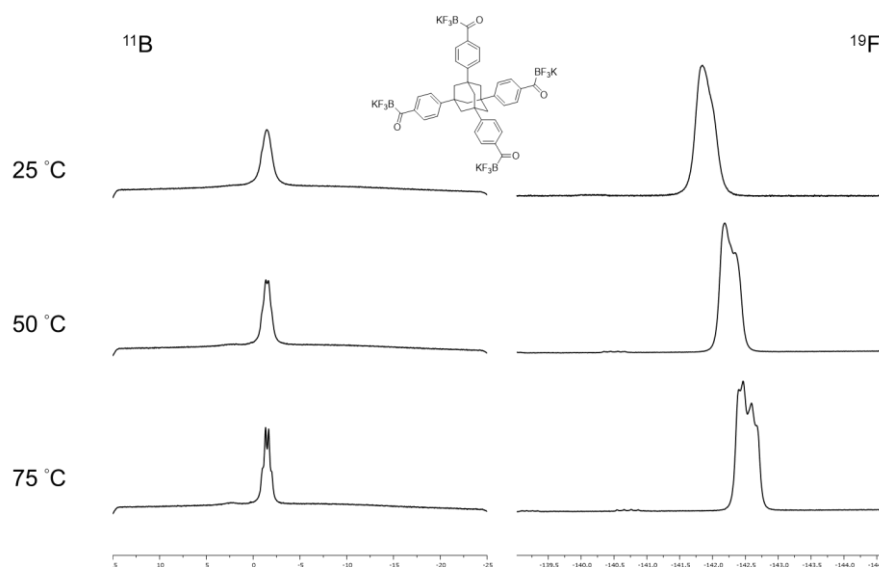


Figure 22. ^{11}B and ^{19}F NMR of KAT **120** in DMSO, recorded at 25 °C, 50 °C and 75 °C. The B–F coupling patterns were usually clearly seen in mono-KATs, but appear as broad singlets for molecules bearing more than one KAT group.

The intermolecular interactions between KAT groups were also visible in the crystal structure of KATs. In most cases the KAT groups will form an ionic cluster, layer or column in the crystal packing. In cases of multivalent KATs, this leads to a porous structure as shown below in **Figure 23**. Tris-KAT **119** crystal grown from evaporating acetone into its saturated DMF solution was shown to co-crystallize with solvents included in the hexagonal pore forming from its KAT-KAT interactions. The pore and ionic aggregate in each layer of the structure stack up to form continuous columns along the *c* axis of the crystal. This assembly is already a sort of metal organic framework (MOF), if we consider potassium to be the metal in this case.

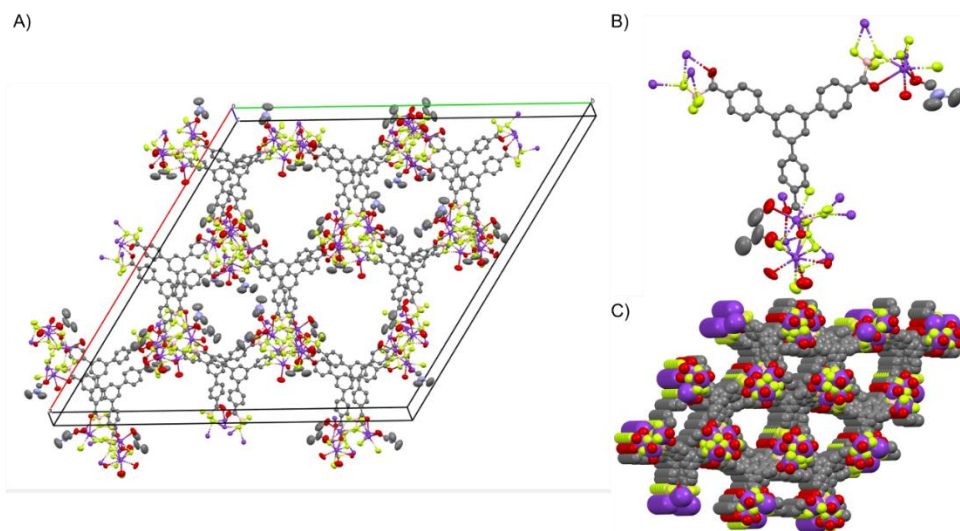


Figure 23. X-ray diffraction structure of a KAT **119** crystal grown from diffusing acetone into its DMF solution. Hydrogens were omitted for clarity. **A:** The unit cell shows that **119** assembled in a way that KAT groups aggregate in ionic clusters and formed hexagonal pores across its trigonal core. **B:** the non-equivalent subunit contains one molecule of **119**, together with one molecule of acetone and DMF each included in the hexagonal pore. The thermal ellipsoids of the included solvent were more diffuse than the KATs. **C:** The space filling model of the same crystal structure, viewed along the *c* axis showing 6 stacked unit cells indicates that layers of the hexagonal assembly stack up along the *c* axis to form long columns of hexagonal pore, aromatic stack, and ionic cluster.

The tetra-KAT crystal structure was also largely determined by its KAT-KAT interactions. The unit cell contains eight equivalent KAT molecules, forming an array of KAT ionic clusters, each with a “coordination number” of eight arising from eight KAT groups, arranged in a body-centered cubic packing. If the substituent on the terminal phenyl rings were a nitro group, the major intermolecular interaction becomes the stacking between nitrophenyl groups leading to a more compact crystal packing (**Figure 24**). From these findings we expect the interaction between KAT or KAT nitrone groups to be a determining factor in molecular assemblies or the crystal engineering of related materials.

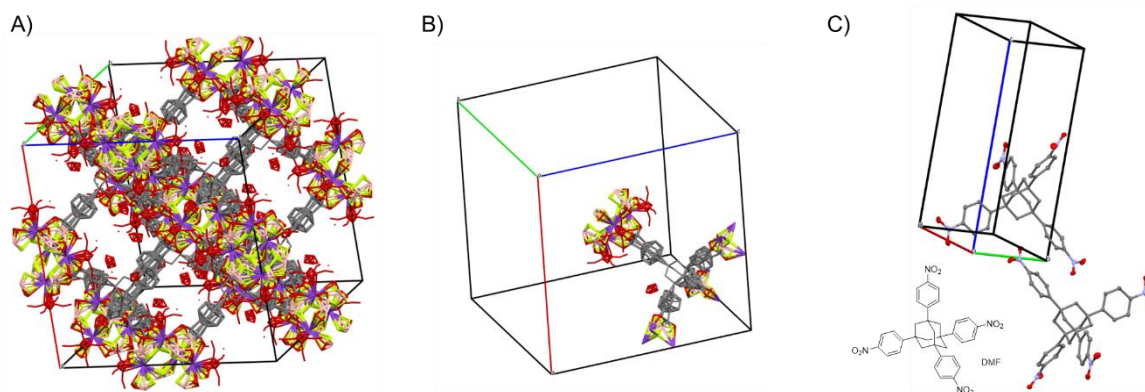


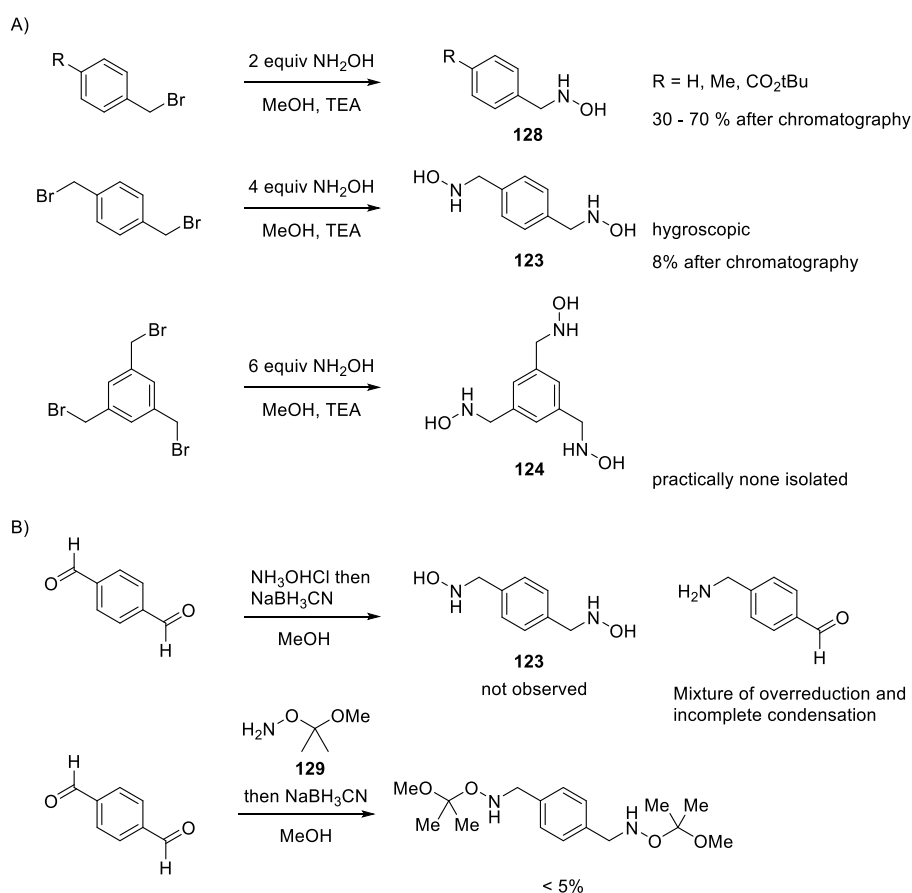
Figure 24. **A:** Crystal structure of tetrahedral tetra-KAT **120** crystal grown from DMF-acetone. **B:** One non-equivalent molecule of **120** lies in each unit cell. Note that the disorder arising from the rotational position of the phenyl rings. **C:** Crystal structure of 1,3,5,7-tetrakis(*p*-nitrophenyl)adamantane grown

from DMF-CH₂Cl₂ for comparison. The clathrate DMF in the structure was omitted for clarity. The nitrophenyl groups between two neighboring molecules interact in a Ph-NO₂ stacked manner.*

* A note-worthy similarity among these multi-KATs and 1,3,5,7-tetrakis(p-nitrophenyl)adamantane is that they all have very low solubilities in most organic solvents, but dissolve rather well in DMF. With no surprise, DMF is also included in all their crystal structures.

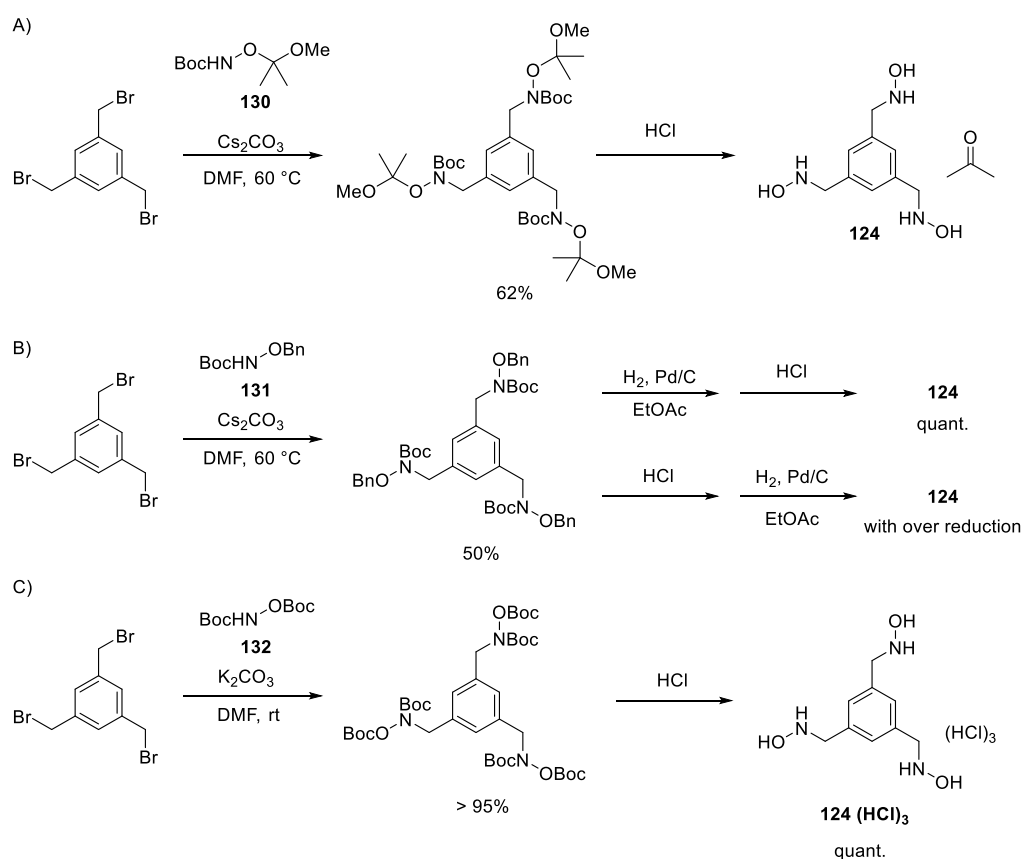
3.4. Synthesis of multivalent hydroxylamines

A protection group strategy is key to successful preparation of multivalent hydroxylamines. At the beginning of this study the N-alkyl hydroxylamines were synthesized either from reductive hydroxyamination or direct replacement of a halide by hydroxylamine. These two methods suffered from several drawbacks when we moved to the synthesis of multivalent hydroxylamines. The first is that the conversion per halide site, which is acceptably high for the synthesis of monohydroxylamine, is not necessarily high enough for multi-hydroxylamine synthesis and could complicate the purification of multi-hydroxylamine mixture. The second was the hydrophilicity of the product multivalent hydroxylamines, which hampered their extraction from the aqueous phase after reaction workup. Direct evaporation of an aqueous work-up mixture would leave ionic impurities behind, however without an aqueous work-up, free-base hydroxylamine will remain in the crude mixture and its evaporation raised safety concerns. A N,O-doubly protected hydroxylamine was needed to solve these synthetic and processing issues.

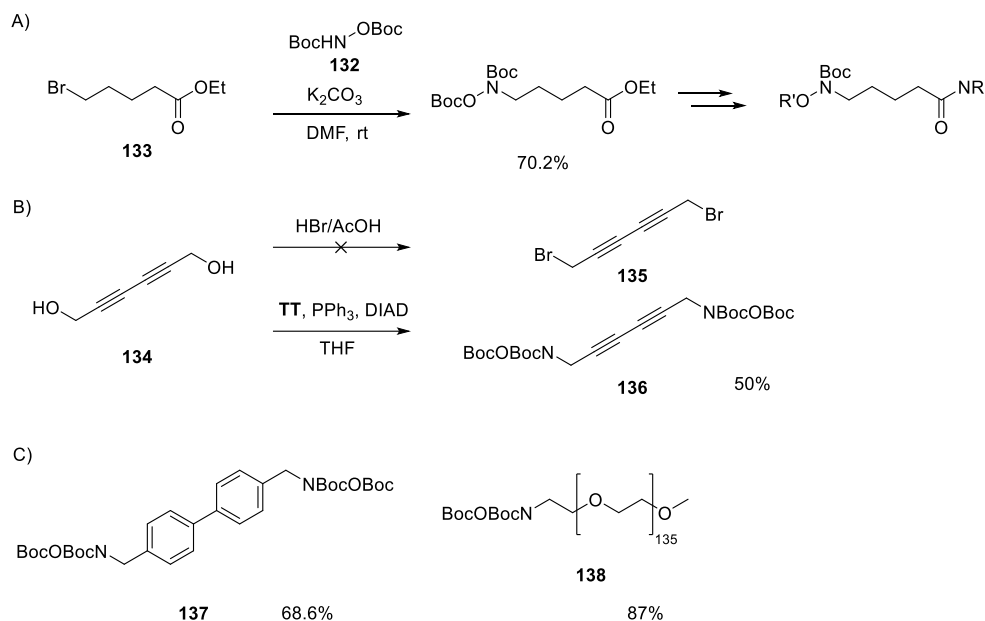


Scheme 42. A: Direct substitution of an alkyl halide with hydroxylamine is satisfactory only for the synthesis of mono-hydroxylamines. **B:** reductive hydroxyamination was also not suitable for bis-hydroxylamine synthesis.

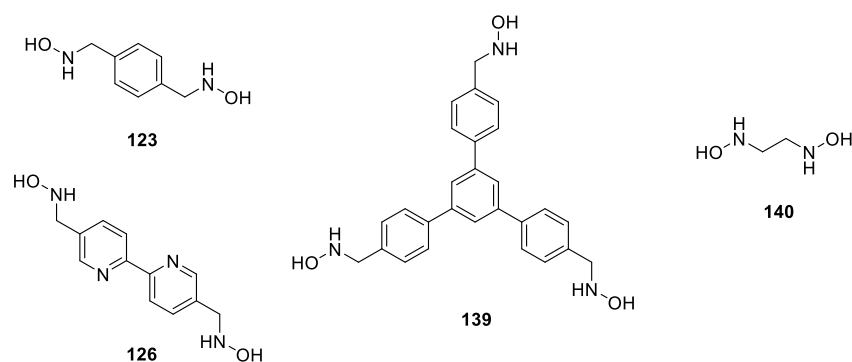
With N-Boc-O-2-methoxy-prop-2-yl protected hydroxylamine **130**, alkyl halides can be smoothly transformed to the triple-doubly protected hydroxylamine which upon acidic deprotection gives **124**. The acetone from the deprotection of the isopropylene acetal reacts with the hydroxylamine formed, so we switched the O-protection group to a benzyl group with reagent **131**. **131** also undergoes smooth substitution with alkyl halides, however the hydrogenation posed a restriction on the deprotection sequence to avoid overreduction of the hydroxylamine to an amine (**Scheme 43B**). Finally the adaptation of O-carbonate carbamate **132**^{153–158} gave the most satisfying results. **132** was found to be more acidic and gave higher conversions under milder conditions compared to what was needed for **130** and **131** (**Scheme 43C**). The higher acidity of **132** also permitted it to serve as a nucleophile in Mitsunobu reactions to convert an alcohol directly to a protected hydroxylamine, where the synthesis of the halide is problematic (**Scheme 44B**). A selected example of multi-hydroxylamine synthesized by **132** was summarized in **Scheme 45**. Among which, hydroxylamine **140** is considered to be the smallest stable bis-hydroxylamine possible was also synthesized from **132** and 1,2-dibromoethane.



Scheme 43. O-carbonate protected hydroxylamines enabled the easy synthesis and purification of multivalent hydroxylamines.



Scheme 44. N-Boc-O-Boc carbamate **132** undergoes substitution and **A**: gives high conversion also with non-benzylic alkyl halides. **B**: and can undergo Mitsunobu reaction. **C**: Yields of hydroxylamine from the corresponding alcohols after Mitsunobu reaction with **132**.



Scheme 45. Bis- and tris-hydroxylamines synthesized from the corresponding alkyl bromides and reagent **132**.

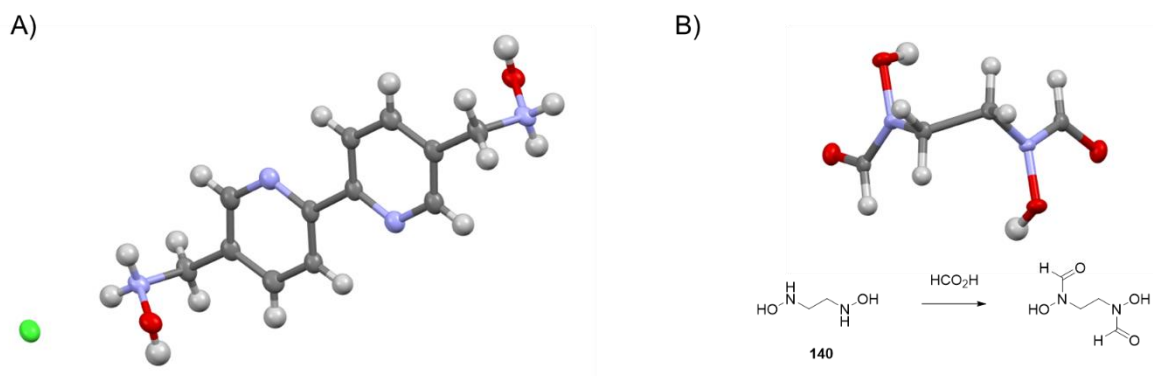


Figure 25. X-ray diffraction structure of **A**: **126** with HCl. **B**: **140** with formic acid gave the corresponding formyl hydroxamic acid

3.5. Attempts on COF formation from KATs and hydroxylamines

3.5.1. Fast formation of the nitrone

With the building block multivalent KATs (**119–122**, **141**) and hydroxylamines (**123–126**) in hand we attempted COF formation by mixing them under various conditions. The nitrone formation occurs rapidly under concentration ranges from 10–100 mM and results in precipitation. The reaction progress can be traced with NMR, in which the observable signals in the solution phase decreased over time as the formed nitrone precipitates, and solid state ^{19}F and ^{13}C NMR indicated the formed solid to contain mainly the nitrone.

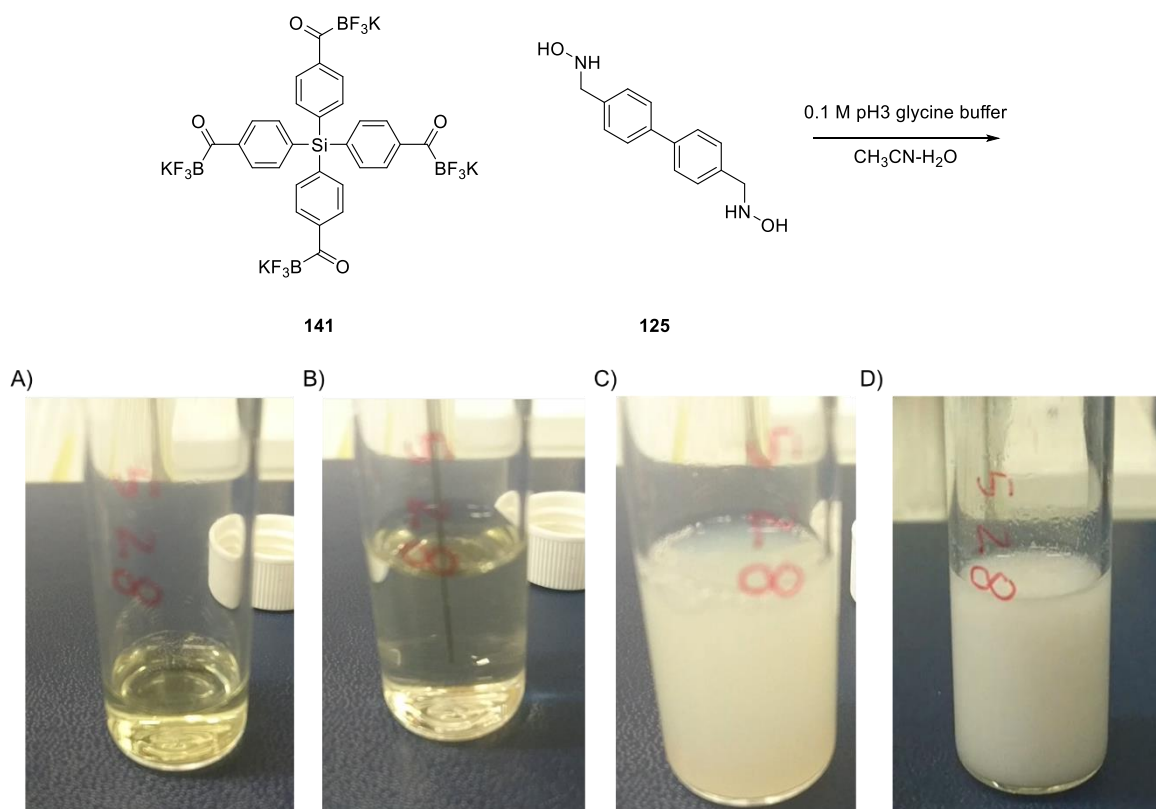


Figure 26. Reaction between KAT **141** (5 mM) and hydroxylamine **142** (10 mM) in 1:1 $\text{CH}_3\text{CN-H}_2\text{O}$ formed precipitates quickly. **A:** The KAT solution **B:** Right after addition the solution of **142** **C:** 1s after **142** addition **D:** 15s after addition.

The solid precipitate was analyzed by powder XRD. As shown in **Figure 27** the peak from KAT **141** ($\sim 7^\circ$) was not found in the diffraction profile of the product precipitate, and peaks at lower angle ($\sim 3^\circ$) suggests the existence of repeating structure of longer range. The sharp peaks around 19° , 31° and 38° arises from potassium fluorosilicate, and their relative intensities increased as the mixture as incubated at pH3 for longer time. We suspect that the aryl silyl group at the center of KAT **141** hydrolyzes, therefore the use of KAT **141** was avoided in further COF formation trials.

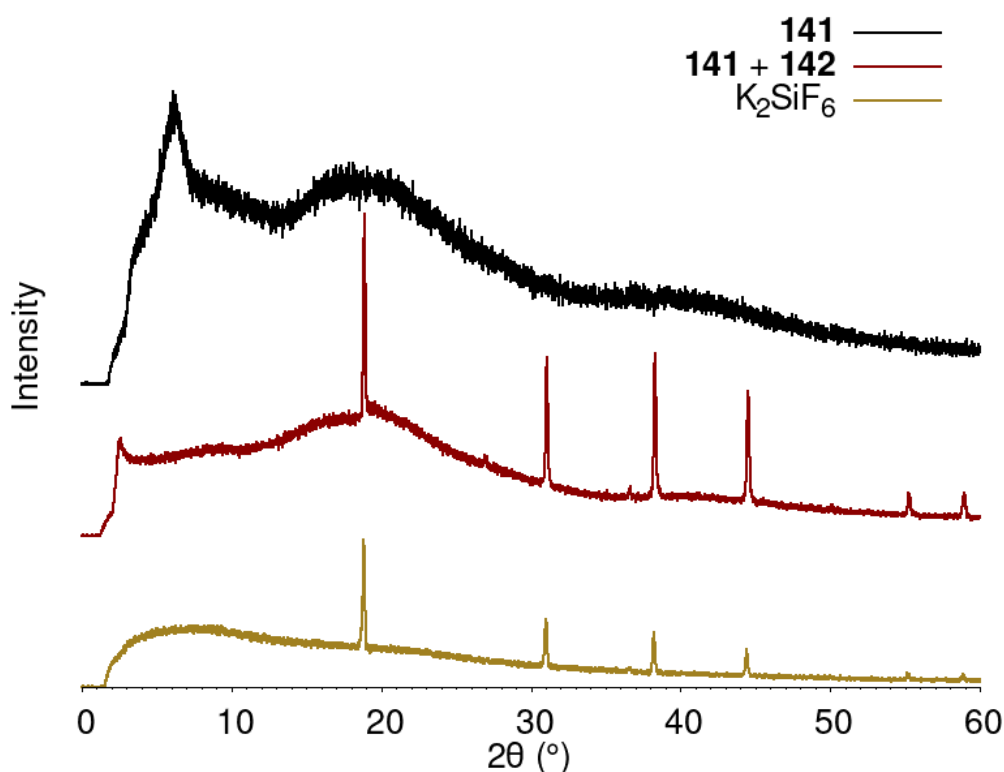


Figure 27. Powder XRD profile of the nitrone product from KAT **141** with hydroxylamine **142**, in comparison with KAT **141** and potassium fluorosilicate. The sharp reflection peaks were attributed from the hexafluorosilicate and rise over reaction time.

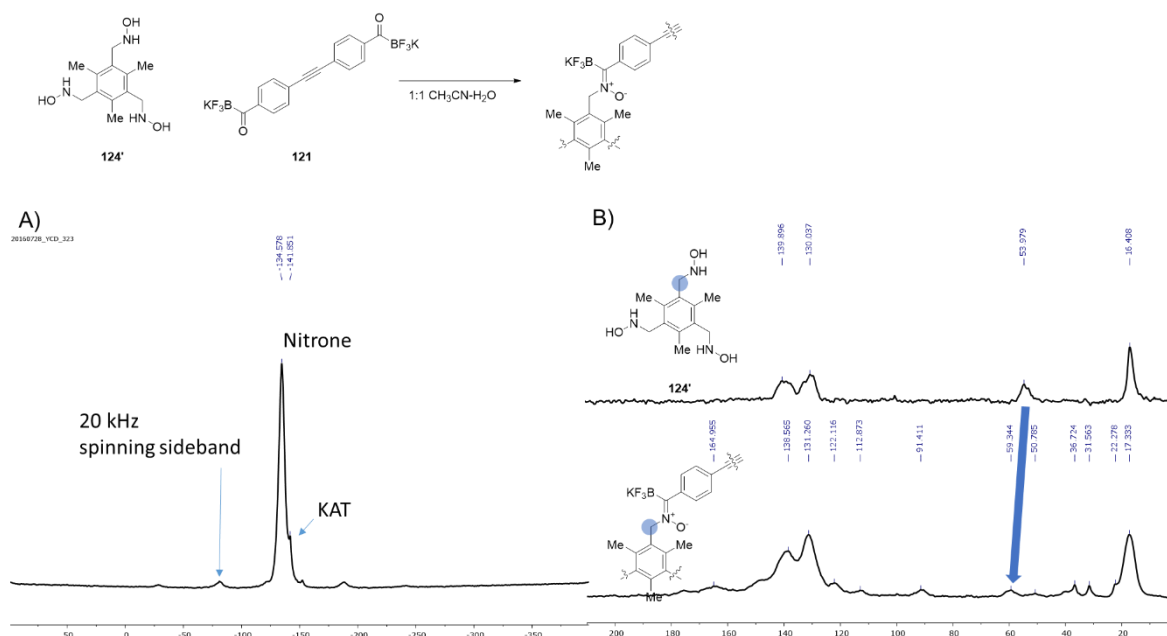


Figure 28. Magic Angle Spinning (MAS) Solid state NMR of insoluble solid formed from hydroxylamine **124'** and di-KAT **121**. **A:** ^{19}F NMR shows that nitrone was the main component (-135 ppm), with a trace amount of remaining KAT (-142 ppm). **B:** ^{13}C NMR shows the shift of the methylene carbon from that of **124'** (54 ppm) to that of the nitrone (60 ppm).

The insoluble precipitate obtained from the reaction of KAT with hydroxylamines can also be analyzed with IR. In an example from the reaction between KAT **119** and hydroxylamine **126**, the characteristic bands of both the KAT and hydroxylamine have disappeared and new bands have been formed.

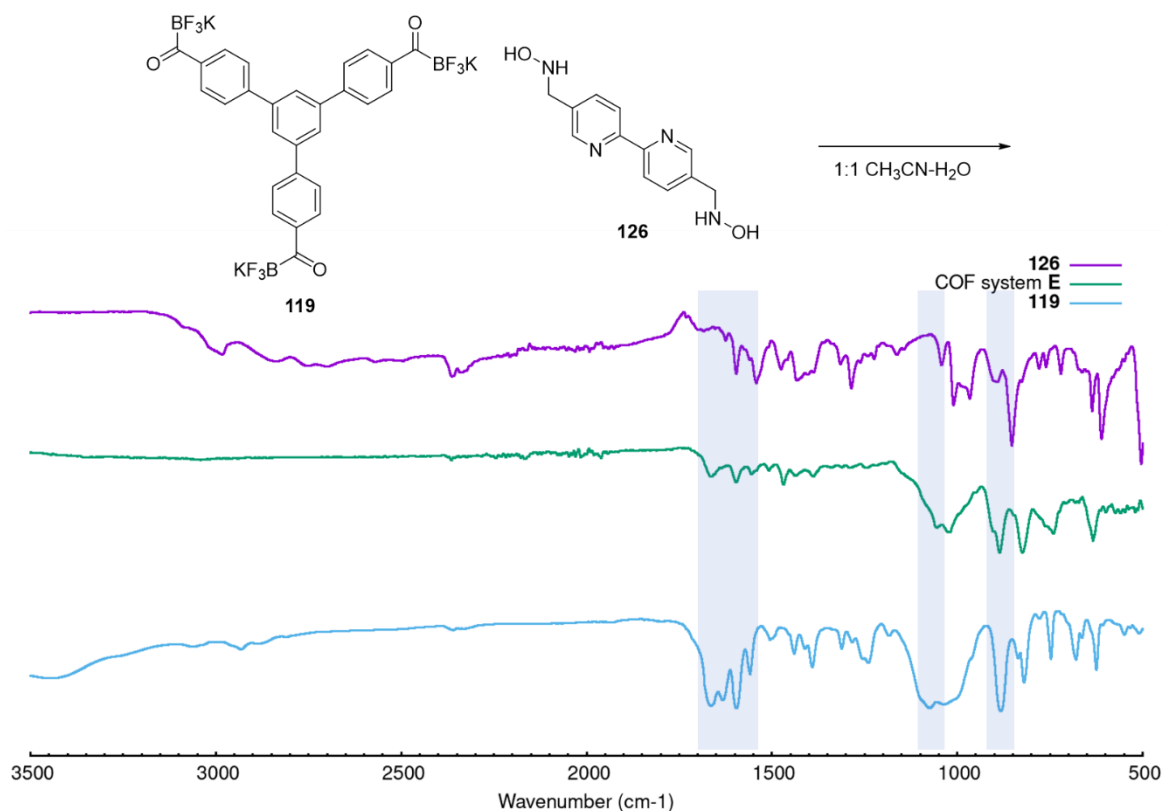


Figure 29. IR spectrum of the precipitated formed from mixing COF **119** and hydroxylamine **126** in 1:1 $\text{CH}_3\text{CN}-\text{H}_2\text{O}$, in comparison of that of **119** and **126**. KAT bands ($1600\text{--}1700\text{ cm}^{-1}$, $900\text{--}1200\text{ cm}^{-1}$) have disappeared and new bands were formed.

3.5.2. Seeking crystallinity with powder XRD

Table 6 listed eight combinations of KAT-hydroxylamine combination, namely **A–H**, that were chosen for the screening of COF formation conditions. Tris-KAT **119** and tetra-KAT **120** were combined with bis-hydroxylamines **123**, **125**, and **126**, while as di-KATs **121** and **122** were combined with tris-hydroxylamine **124**. A variety of solvents, temperatures and acidic/basic conditions (**Table 7**) have been used and powder XRD was used to identify crystallinity of the precipitate formed under such conditions.

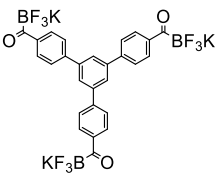
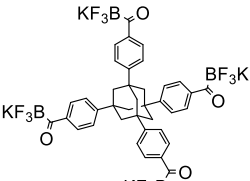
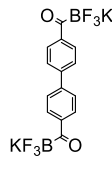
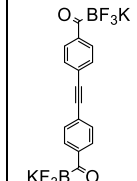
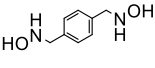
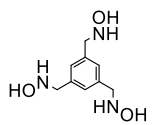
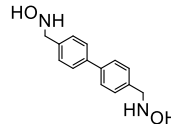
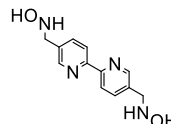
				
	A	B		
			C	D
	E	F		
	G	H		

Table 6. KAT and hydroxylamine combinations used for screening COF forming conditions

From the findings in **Chapter 2**, we are aware that the solvents used must dissolve KAT and hydroxylamine for facile nitron formation. We also wished the nitron exchange to be facile, which would allow the formed material to rearrange into the thermodynamically more stable configuration. The solvents, reaction temperature, and pH values were therefore modulated, and the initial precipitation behavior was recorded. Once the precipitation forms from a COF formation trial, the solid part was collected by centrifugation and dried on vacuum before subjecting to powder XRD analysis. **Table 7** lists some representative conditions that has been tried with combinations **A–H**.

	Combination	Solvent	Temp.	pH/acid/base	Results
1	A	1:1 MeCN-H ₂ O (20 mM)	rt	123 (HCl) ₂ used	Precipitate
2	A	1:1 MeCN-H ₂ O (20 mM)	rt	pH 3.8	Precipitate
3	A	1:1 MeCN-H ₂ O (20 mM)	rt	pH 4.7	Precipitate
4	A	1:1 MeCN-H ₂ O (20 mM)	rt	2 equiv K ₂ CO ₃	Precipitate
5	A	1:1 MeCN-H ₂ O (2.0 mM)	rt	123 (HCl) ₂ used	Turbid solution
6	A	DMF (20 mM)	rt	123 (HCl) ₂ used	Precipitate
7	A	DMF (2.0 mM)	rt	123 (HCl) ₂ used	Turbid solution
8	A	2:2:1 MeCN-H ₂ O-DMF (2.0 mM)	rt	123 (HCl) ₂ used	Turbid solution
9	A	2:2:1 MeCN-H ₂ O-MeOH (60 mM)	rt	pH 4.7	Turbid solution
10	A	DMSO (2.0 mM)	rt / 80 °C	123 (HCl) ₂ used	Clear solution. Turns turbid upon heating.
11	A	80:20:5 mesitylene- dioxane-H ₂ O (2.0 mM)	rt	123 (HCl) ₂ used	Turbid solution
12	A	1:1 mesitylene-DMF	rt / 125 °C	123 (HCl) ₂ used	Clear solution. Turns turbid upon heating.
13	B	DMSO (80 mM)	rt	123 (HCl) ₂ used	Precipitate
14	B	DMSO (80 mM)	rt	2 equiv K ₂ CO ₃	No precipitate
15	B	DMSO (80 mM)	rt	1.25 equiv TEA	Turbid solution
16	B	DMSO (80 mM)	rt	pH 4.7	Turbid solution
17	C	1:1 MeCN-H ₂ O (20 mM)	rt	pH 3.8	Precipitate
18	C	1:1 MeCN-H ₂ O (20 mM)	rt	pH 4.7	No precipitate
19	D	1:1 MeCN-H ₂ O (20 mM)	rt	pH 3.8	No precipitate
20	D	1:1 MeCN-H ₂ O (20 mM)	rt	pH 4.7	No precipitate
21	E	1:1 MeCN-H ₂ O (20 mM)	rt	pH 4.7	Precipitate
22	E	1:1 MeCN-H ₂ O (20 mM)	rt	2 equiv K ₂ CO ₃	Precipitate

23	E	2:2:1 MeCN-H ₂ O-DMF (20 mM)	rt	pH 4.7	Turbid solution
24	E	2:2:1 MeCN-H ₂ O-MeOH (20 mM)	rt	pH 4.7	Turbid solution
25	E	4:1 DMF-H ₂ O (20 mM)	rt	pH 4.7	No precipitate
26	E	4:1 DMF-H ₂ O (60 mM)	rt	pH 4.7	Turbid solution
27	E	5:1 NMP-H ₂ O (20 mM)	rt	pH 4.7	Turbid solution
28	E	2:1 DMF-DIPEA (100 mM)	rt	-	No precipitate
29	E	DMSO (20 mM)	rt	125 (HCl) ₂ used	No precipitate
30	E	DMSO (20 mM)	rt	2 equiv TEA	Turbid solution
31	E	Neat grinding with H ₂ O	rt	2equiv TEA	Not dissolved
32	F	DMSO (20 mM)	90 °C	2 equiv TEA	Turbid solution
33	G	1:1 MeCN-H ₂ O (2 mM)	rt	2 equiv K ₂ CO ₃	No precipitate
34	G	1:1 MeCN-H ₂ O (2 mM)	rt	125 (HCl) ₂ used	Precipitate
35	G	1:1 MeCN-H ₂ O (20 mM)	rt	2 equiv K ₂ CO ₃	Turbid solution
36	G	DMF (20 mM)	rt	2 equiv K ₂ CO ₃	Precipitate
37	G	1:1 MeCN-H ₂ O (20 mM)	rt	pH 7.0 (K ₂ CO ₃)	Turbid solution
38	G	1:1 MeCN-H ₂ O (60 mM)	rt	2 equiv K ₂ CO ₃	Turbid solution
39	G	1:1 DMF-H ₂ O	rt	2 equiv K ₂ CO ₃	Turbid solution
40	H	1:1 MeCN-H ₂ O (2 mM)	rt	2 equiv K ₂ CO ₃	Turbid solution
41	H	1:1 MeCN-H ₂ O (20 mM)	rt	2 equiv K ₂ CO ₃	Turbid solution
42	H	1:1 MeCN-H ₂ O (60 mM)	rt	2 equiv K ₂ CO ₃	Turbid solution

Table 7. Selected results of various KAT-hydroxylamine combinations treated with various conditions. Concentrations and equivalences were calculated basing on the number of nitrones. pH 3.8 was achieved with glycine buffer (0.1 M), and pH 4.7 was achieved with potassium acetate buffer.

The last column of **Table 7** classified the trial outcome into three categories. Right after mixing the reaction components, “No precipitate” denoted that no visible cloudiness could be seen with naked eyes. But in all cases fine suspension particles can be observed by using a laser pointer to illuminate a light path through the solution, which was described as Tyndall effect (**Figure 30A**). A “turbid solution” was used to describe the cases shown in **Figure 30B**.

Examples of “Precipitate” were shown in **Figure 30C**. Regardless of the initial precipitation behavior, all conditions produced solid after standing for 72 hours.

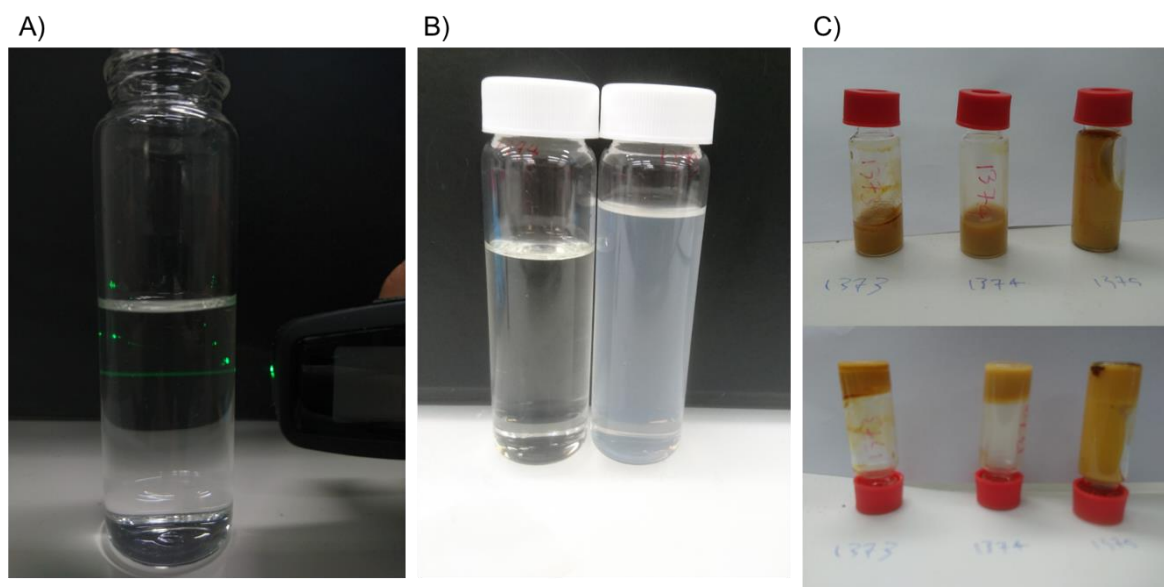


Figure 30. **A:** Particle suspension invisible to bare eyes can be detected with light scattering. **B:** Examples of turbid solution. **C:** Examples of precipitate.

A general trend was found that precipitation was faster, and the solid yield was higher when the reaction media was concentrated and acidic. The addition of dioxane, mesitylene and toluene did not change the outcome significantly and posed a risk of phase separation of the solvent mixture. Polar aprotic solvents such as DMSO, DMF, and NMR tend to delay the precipitation, which was considered beneficial because premature precipitation was considered detrimental to the dynamicity of COF annealing,^{98,159} but the solid yield was lower when these solvents were used.

Powder XRD is the method of choice to detect long-range order in COFs, which is highly correlated to their stability and high surface area as a porous material. The diffraction peak positions for 2D COFs can be estimated from the dimension of the proposed structures with the Bragg condition $2d \sin \theta = n\lambda$. The strongest peaks in reported 2D COFs were always the (100) peak, corresponding to the longest axis of the unit cell. We followed reported procedure to synthesize **BND-TFB-COF** from 1,3,5-triformylbenzene and benzidine and found the XRD pattern to be identical as reported.¹⁶⁰ The (100) peak and a weak interlayer stacking (001) peak can be identified in our measurements. If the desired COF was formed in the trials, we would also expect to observe these two peaks in the positions (2–3° and 15–25° 2 θ) predicted from the proposed structure, as shown in **Figure 31B**.

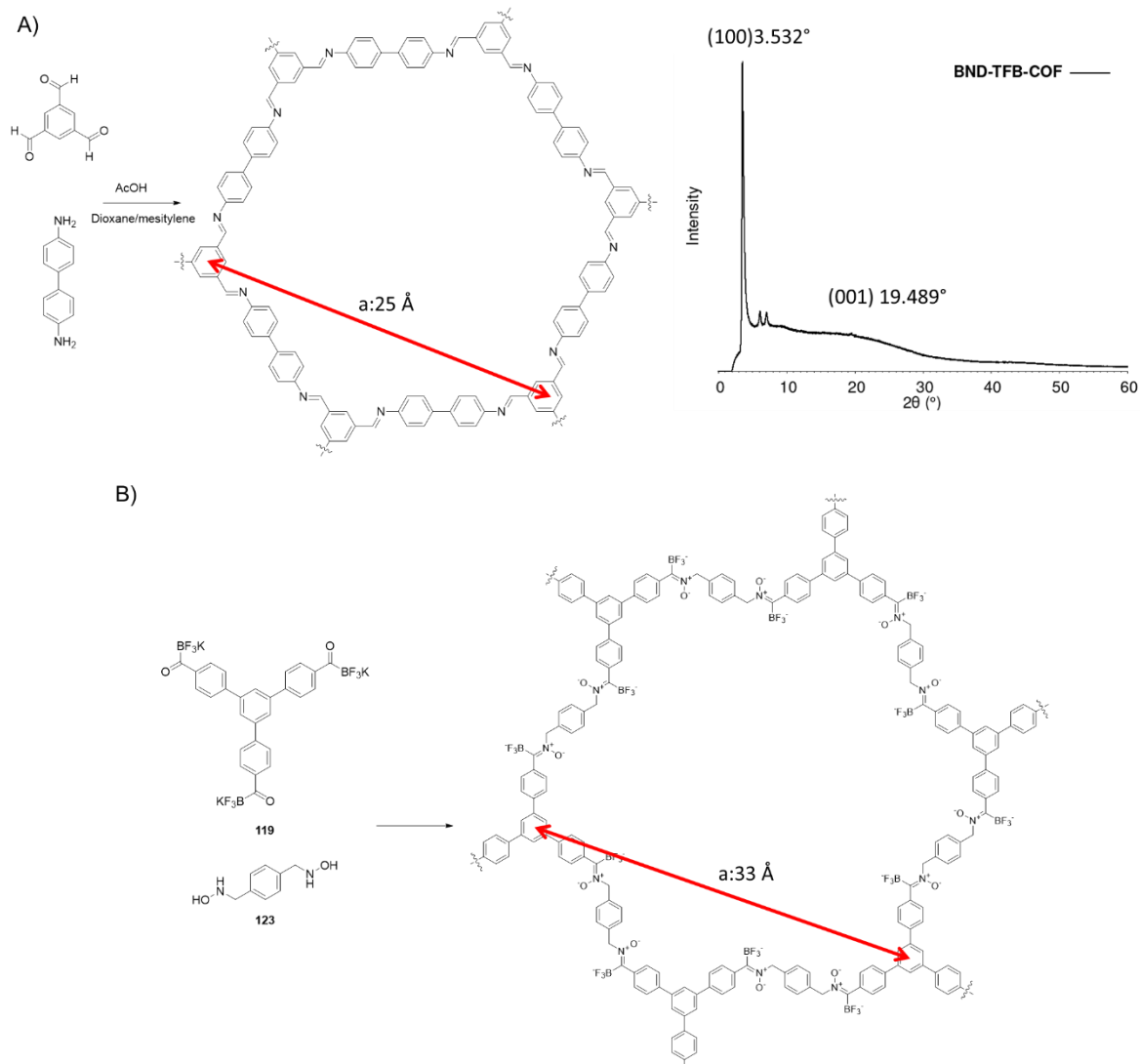


Figure 31. Dimension of COF unit cell determines the position of diffraction peaks. **A:** The unit cell of **BND-TFB-COF**, which was synthesized from benzidine and 1,3,5-triformyl benzene following reported procedure,¹⁶⁰ has a unit cell with $a = 25 \text{ \AA}$, giving the (100) reflection peak at $2\theta = 3.532^\circ$. A faint peak at $2\theta = 19.489^\circ$ corresponds to the interlayer stacking vector (001) 4.5 \AA . **B:** Hypothesized structure of COF system **A**. With the projected a axis to be around 33 \AA , we expect to find a reflection peak around $2\theta = 2.6^\circ$ as the (100) reflection, if the desired COF was formed.

A series of Powder XRD data from the trials with system **E** was shown below in **Figure 32**. No strong peak under $3^\circ 2\theta$ was observed. Only conditions 25 and condition 28 showed a slight bulge in the low angle region of the measurement. Conditions 27, 29 and 30 involving DMSO and NMP gave a broad peak around $20^\circ 2\theta$, indicating that these solvents might be beneficial for the inter-sheet organization of the formed aggregate.

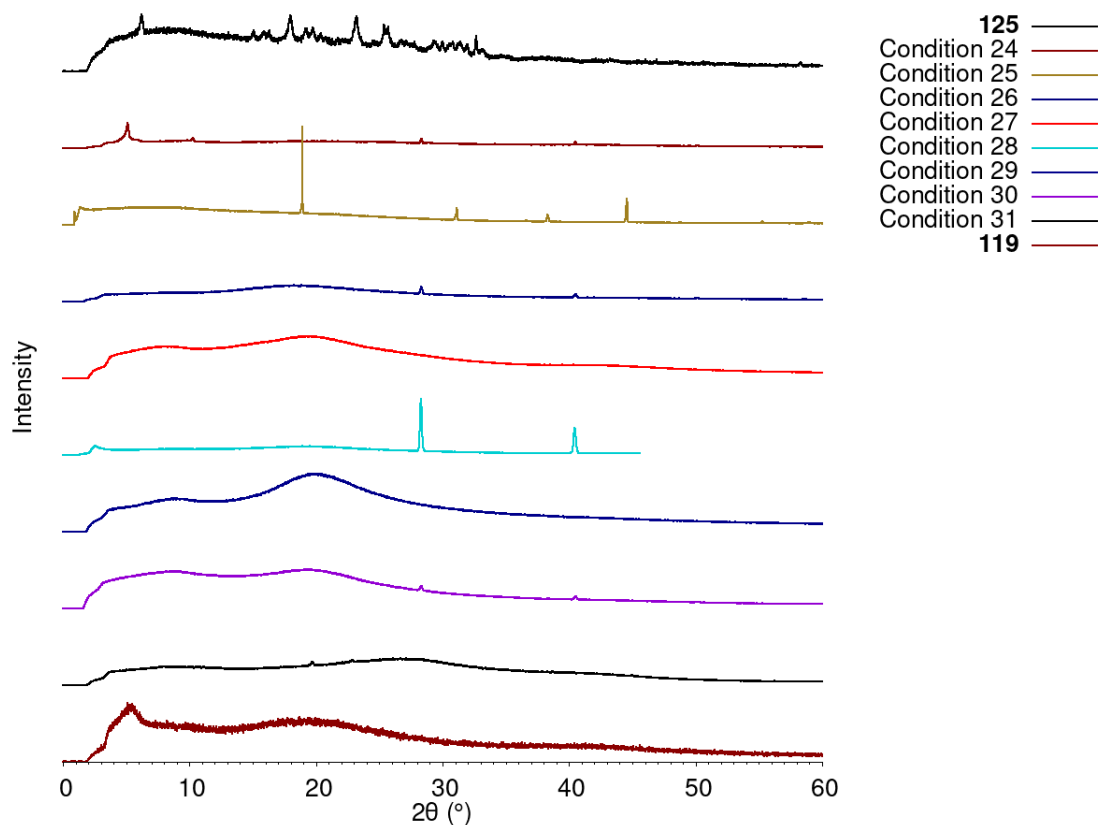


Figure 32. Selected XRD result of system **E** treated with conditions 24–31 in **Table 7**.

The low angle rise in cases 25 and 28 were signatures of nanoparticles, where the reflections arise from not intermolecular order, but inter-particle order. We hypothesize that the ionic nature of KATs and KAT nitrones might produce negatively charged nitrone particles, that repels the approach of KAT building blocks therefore retarding the particle growth beyond a certain limit.

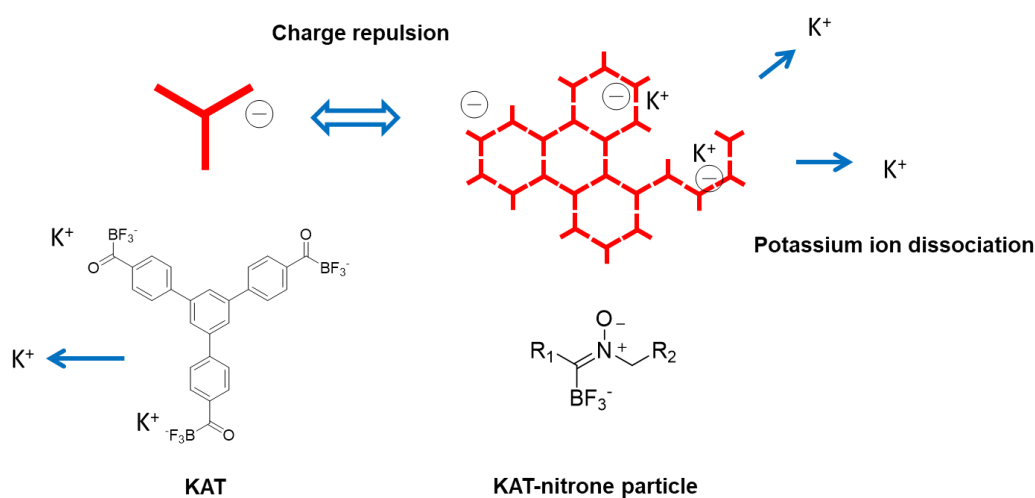


Figure 33. Charge build-up hypothesis. Potassium ion has a higher diffusibility than the formed nitrone network, and will leave behind net negative charges on the KAT-nitron particle.

This theory was supported by the SEM image of COF system **E** under condition 5. The material has a texture similar to sponge, and the particle size was found to be around 10 nm, which could explain the amorphous results obtained from XRD analysis.

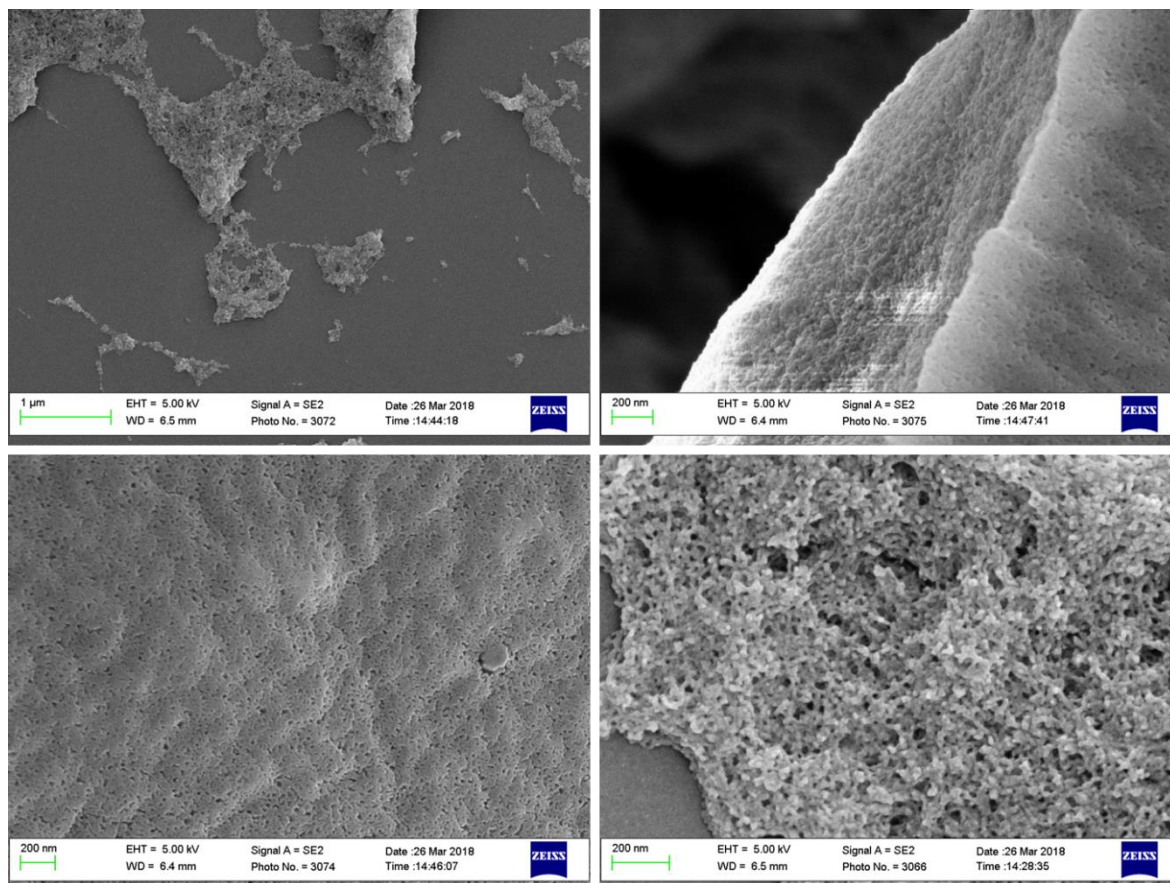


Figure 34. SEM image of the condensation product from system **E**

In attempt to overcome the charge imbalance, bipyridyl bis-hydroxylamine **126** was designed for the formation of COF systems **G** and **H**. Selected powder XRD results were summarized in **Figure 35**.

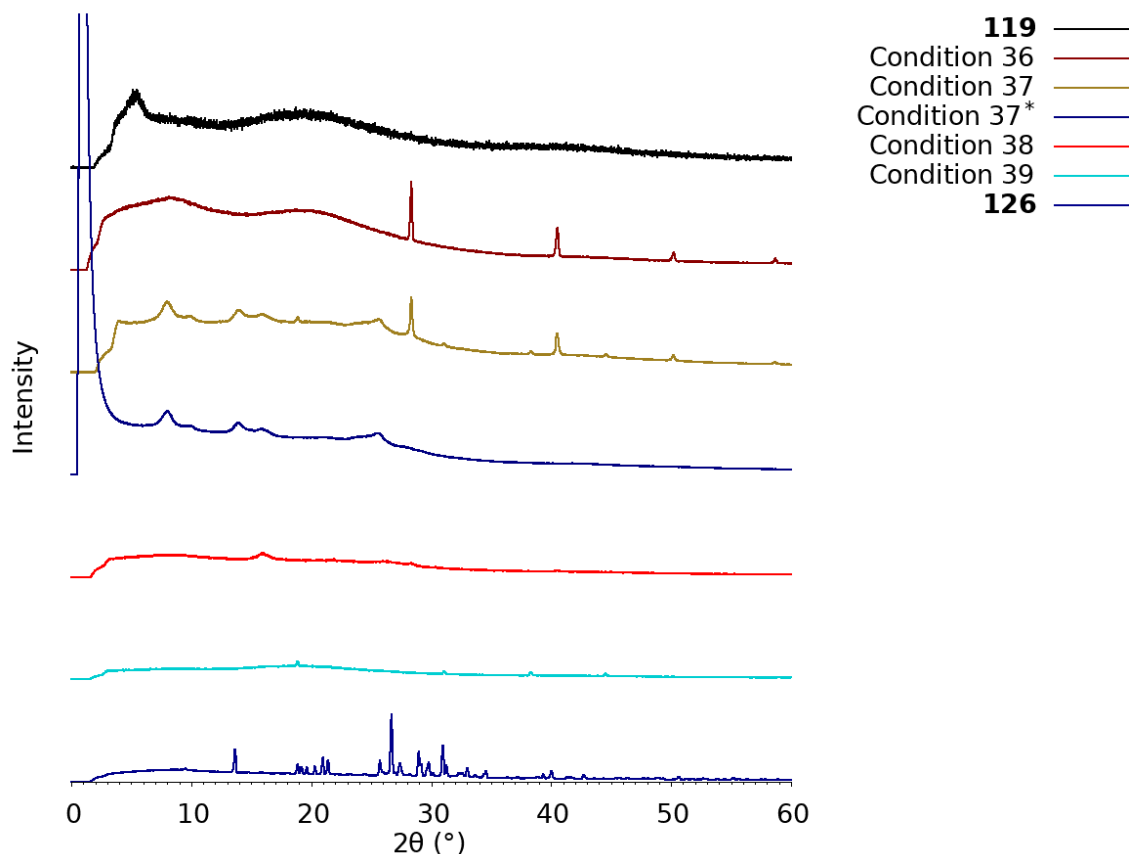


Figure 35. Selected XRD result of system **G** treated with conditions 36–39 in **Table 7**. Conditions 33–35 only gave weakly diffracting materials and the profiles are not shown. *: acidification of the material formed from condition 37.

The powder XRD analysis of material obtained from condition 35, 37 and 38 indicated that system **G** is very sensitive to acid-base equilibrium. The carefully controlled neutral condition 37 gives by far the results most similar to a COF, yet still lacks the signature (100) reflection. Acidification of this material (37* in **Figure 35**) with 6M HCl again gives very strong zero-angle scattering peak, which indicated the formation of nanoparticles.

3.6. Summary and Outlook

Symmetric multivalent KATs and multivalent hydroxylamines were designed with the purpose to apply them in KAT nitrone COF synthesis. Complete lithiation of the aryl halide precursor, as well as a solvent mixture with better solubility for the basic work-up, were both crucial for successful synthesis of multivalent KATs. The lower solubility of multivalent KATs was attributed to strong intermolecular KAT-KAT interactions. The synthesis of multivalent hydroxylamines was improved by adapting N-carbamate-O-carbonate reagent **132**, which is more reactive than other N,O-doubly protected hydroxylamine variants and give cleaner deprotection results. These multivalent KATs and hydroxylamines react quickly and completely in aqueous solvents as predicted, yet the material formed has yet to show the characteristics of a COF.

Unfortunately all attempts so far in synthesizing a COF from a KAT and a hydroxylamine have failed. Mixing a multi-KAT and multi-hydroxylamine immediately generates insoluble precipitate readily under dilute conditions. The materials formed was shown by IR and solid-state NMR to be mainly consisting of KAT-nitrones, however powder X-ray diffraction analysis indicated that there is not much order at the range of ~ 1 nm, which corresponds to most pore diameter of COFs. The particle size formed from KAT-nitrone polymerization was also found to be smaller than most COF particles in SEM analysis, which is consistent with the strong zero-angle scattering signals observed, suggesting that a condition more favorable for particle growth is needed.

Two new key findings (See **Section 0**) regarding KAT-nitrone formation that only arrived recently that could shine a new light on further approaches of KAT-nitrone COF formation. The first is that the presence of water increases the nitrone formation rate, the second is that acetonitrile reacts with N-alkyl hydroxylamines. We originally considered adding water to the reaction mixture as a means to retard KAT nitrone formation, which however would accelerate their formation opposite to our wishes. Also all reaction conditions using acetonitrile should be avoided since the amidoxime formed will irreversibly cap the hydroxylamine building block, forbidding further particle growth.

4

Design and building block synthesis of a KAT-nitrone dynamically linked PROTAC

中級山

Mid-ranged mountains.

Taiwanese mountaineering term, referring to mountain area within altitude 1500 m – 3000 m. The forest physiognomy within this range were complex and made navigation difficult within, at times more dangerous than in higher altitudes. 80% of the mountaineering accidents in Taiwan were reported in mid-range mountains.

4.1. PROTACs

4.1.1. Adapter of an adapter

Proteolysis Targeting Chimeras (PROTACs) degrade proteins by creating a new molecular recognition mode that rewrites the substrate specificity of an E3 ubiquitin ligase.^{161–163} A PROTAC consists of a ligand to the Protein of Interest (POI), an E3 ligase ligand, and an interconnecting linker to bring the E3 ligase together with the POI, which is not a native substrate of that E3 ligase. The ubiquitination machinery is then directed to ubiquitinate the POI, labeling it for proteasomal degradation. Targeted degradation is considered to be a promising therapeutic approach to address protein targets, alternative to their inhibition with synthetic ligands.

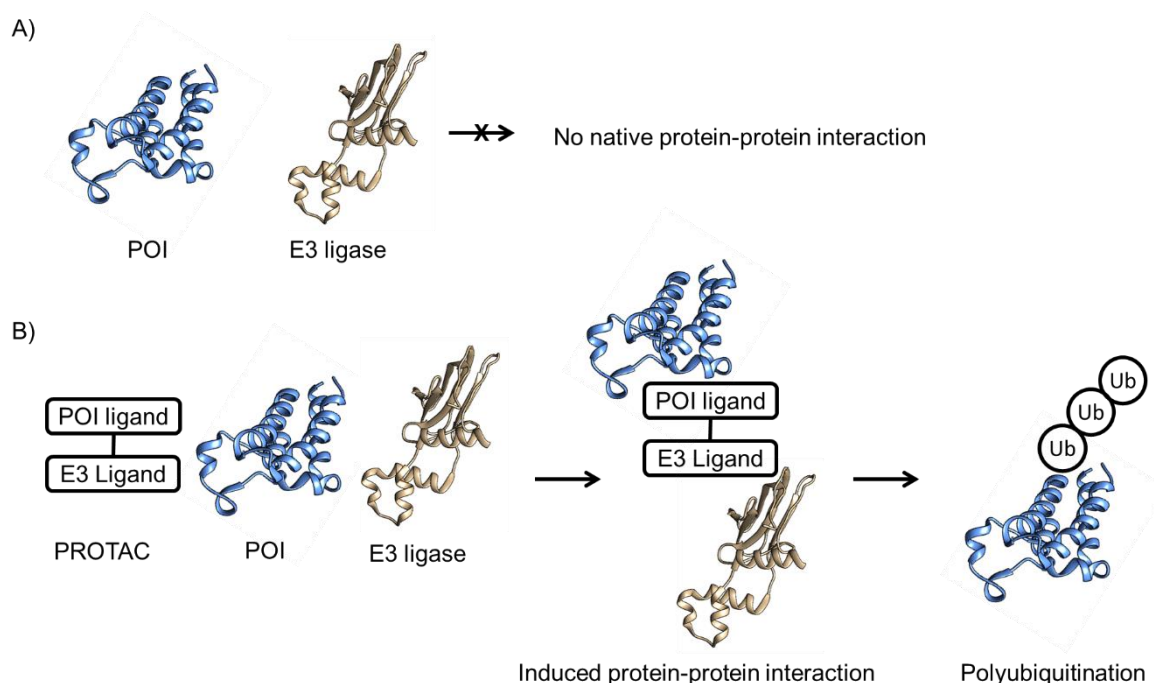
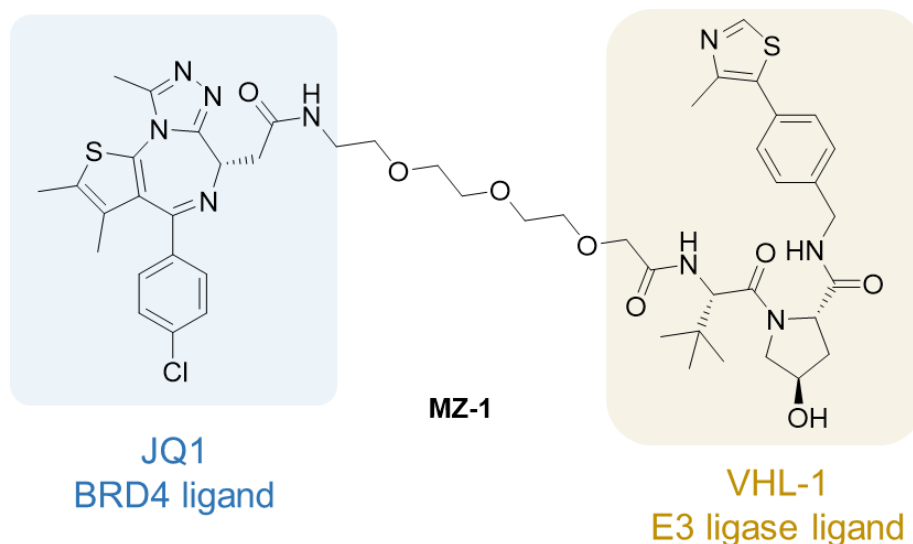


Figure 36. A PROTAC connects a Protein of Interest (POI) and a certain E3 ligase in cases where **A:** No native protein-protein interaction exists and the POI was not degraded. **B:** A new mode of induced protein-protein interaction was turned on by the product, and leads to the polyubiquitination of the POI and its subsequent degradation by the proteasome.

An example PROTAC MZ-1 is shown in **Scheme 46**, which consists a Bromo- and Extra-terminal (BET) protein ligand JQ1,¹⁶⁴ and a von Hippel-Lindau (VHL) E3 ligase ligand, linked by a triethylene glycol linker. BET proteins are a class of proteins involved in regulating cellular proliferation, and their deregulation is correlated to cancer and inflammatory diseases.¹⁶⁵ Among the members of BET proteins, namely BRDT, BRD2, BRD3, and BRD4, the inhibition or silencing of BRD4 was proposed to be a valuable target for inflammatory diseases. However existing BET protein ligands did not exhibit high selectivity across the BET class. PROTAC

MZ-1, on the other hand, was shown to degrade BRD4 selectively over BRD3 and BRD4,¹⁶⁶ showing how the PROTAC strategy may bring new possibilities and to previously unreachable therapeutic targets, by generating new modes of protein-protein interactions.



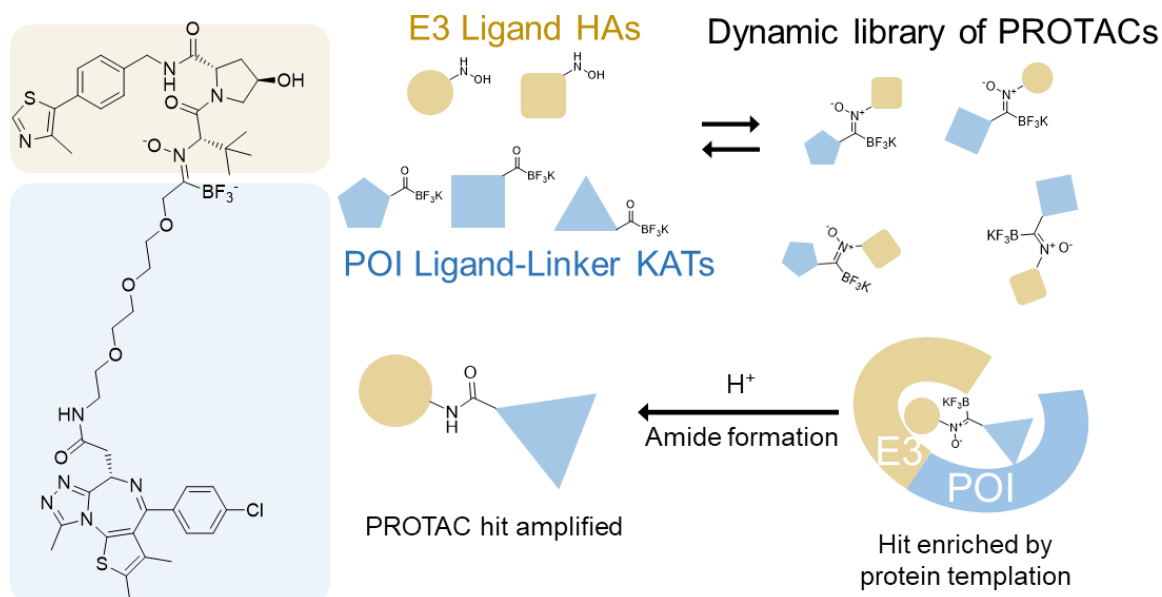
Scheme 47. Example of a PROTAC MZ-1,¹⁶⁶ reported by Ciulli et al. in 2015 to direct the selective degradation of BRD4, a potential drug target for cancer and immunological diseases.

The potency of the PROTAC-generated molecular recognition mode depends nontrivially on the combination of the three components and requires new strategies for their discovery. In the case of MZ-1, the triethylene glycol linker between the E3 ligand and the POI ligand also participates in the binding event.¹⁶⁷ A dynamic combinatorial library would be able to screen these cooperative events that only arise when the PROTAC, the POI, and the E3 ligase are all present. In Chapter 2 we showed an example (**Scheme 16**) where Ciulli et al. have demonstrated that a disulfide linked fragment-based dynamic library can be biased towards a stronger binder when the target protein is used as a molecular template.⁷⁹ In a thiol-disulfide based DCC system, target proteins with cysteine residues may interfere as the required thiol concentration (> 3mM) in such systems can lead to the reduction of disulfide bridges. We consider KAT-nitrone dynamic chemistry to be a better alternative for dynamic library generation, since the reaction between KAT and hydroxylamines does not mutually interfere with thiols or other functional groups on native proteins. In addition, the fixation of KAT-nitrones would give rise to an amide bond, which is abundant in known PROTAC constructs.

4.1.2. KAT-nitrone split MZ-1 design

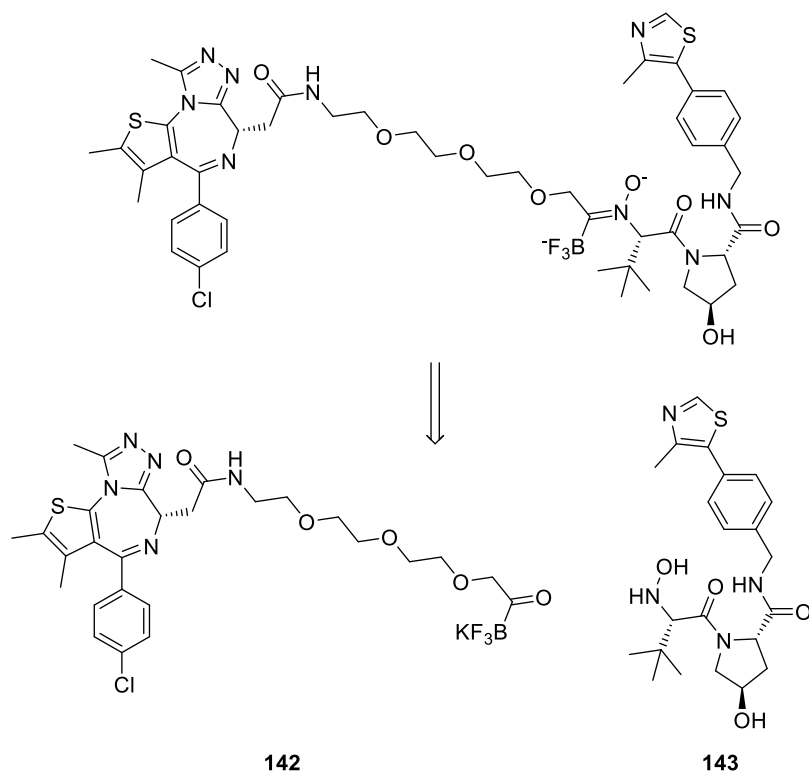
When E3 ligand hydroxylamines (HAs) and POI Ligand-linker KATs are mixed, a dynamic library will be formed over all possible combination of KATs and HAs (**Scheme 48**). When the E3 and the POI proteins were added to this dynamic library, it is expected that a ternary

complex be formed between the E3, the POI and the nitrone with a productive combination that results in high affinity binding. The formation of such ternary complex would shift the equilibrium towards such a nitrone PROTAC hit. This bias in nitrone population could be fixed upon acidification and the hit could be identified by LCMS.



Scheme 48. Dynamic library consisting of KATs and hydroxylamines building blocks

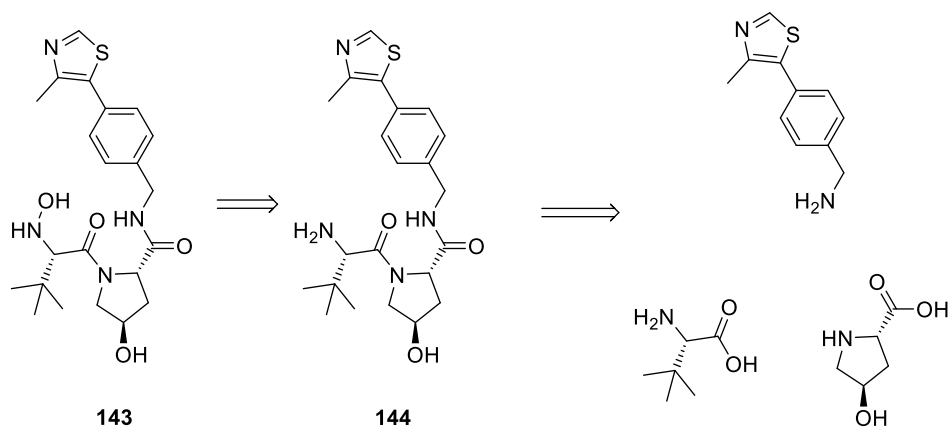
MZ-1 was chosen to be the first proof-of-concept target of this library due to its relatively well understood binding mode with the VHL E3 and the target protein BRD4.¹⁶⁷ Switching one amide bond to a KAT nitrone gives a KAT nitrone linked MZ-1, which can be formed from building blocks **142** and **143**. Their synthesis will be described in the next sections.



Scheme 49. Design of a KAT-nitron split MZ-1 PROTAC and building blocks **142** and **143**.

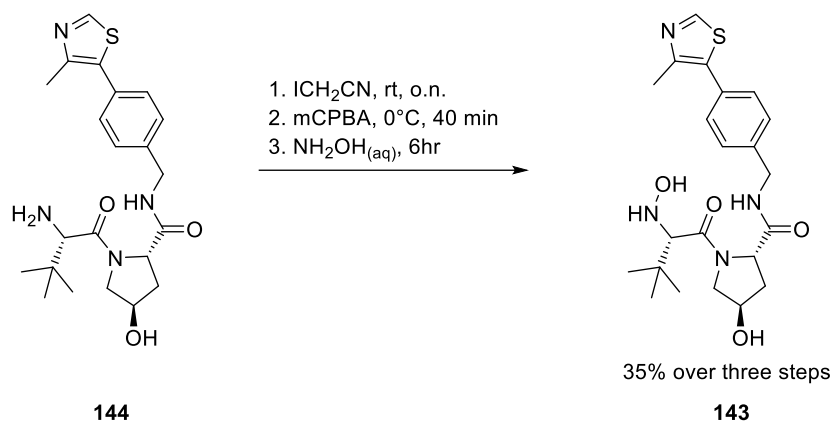
4.2. Synthesis of the VHL hydroxylamine

The synthesis of the VHL hydroxylamine **143** was largely based on the reported synthesis of the VHL-1 amine **144** reported by Crews et al.¹⁶⁸



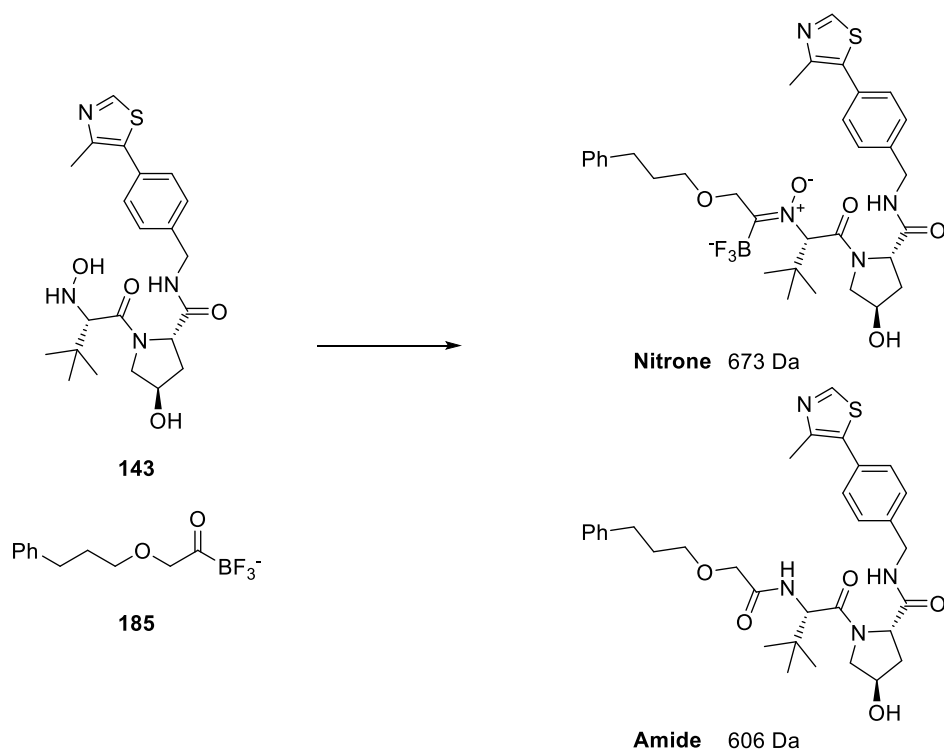
Scheme 50. Retrosynthesis of the VHL ligand hydroxylamine **143** leads to the corresponding amine **144**, which was obtained from two consecutive amide coupling steps.

The conversion of the amine to the hydroxylamine can be done in two steps via Fukuyama's method.¹⁶⁹ The mCPBA oxidation time is crucial for the overall yield, as overoxidation to the oxime occurs over prolonged time or under higher temperature.



Scheme 51. The synthesis of VHL hydroxylamine **143** from the amine precursor **144**.

After synthesis of the VHL hydroxylamine **143**, it was tested with an α -alkoxy KAT **185** and acidified to verify that KAT nitron formation and amide formation could occur with **143** as shown in **Scheme 52**. The LCMS outcomes shows that both the KAT nitron and the amide formed in dilute aqueous conditions. (< 2 mM, 1:1 CH₃CN-H₂O)



Scheme 52. KAT nitron formation test with VHL hydroxylamine **143**.

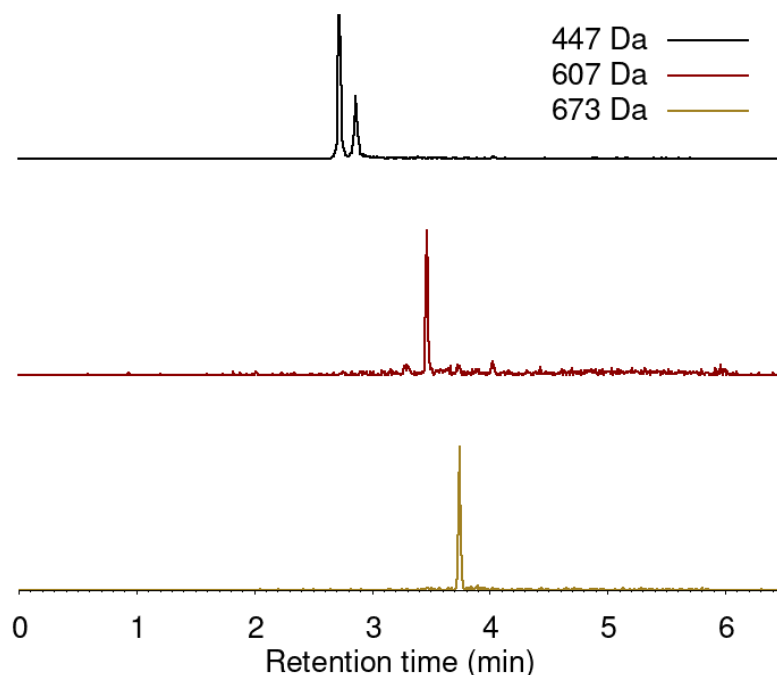
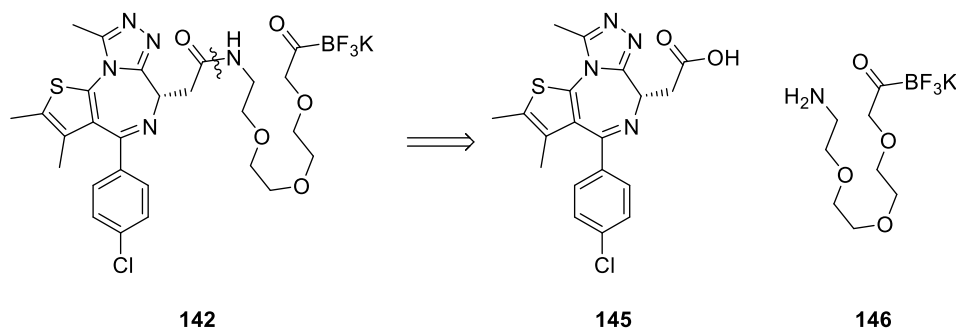


Figure 37. LCMS analysis of nitrone and amide formation between VHL hydroxylamine **143** and KAT **185**. KAT **185** was selected as a model for KAT **142** due to their common α -alkoxy motif. The nitrone was detected at 673 Da (negative), and the amide at 607 Da (positive). Hydroxylamine **143** was detected at 447 Da (positive), and shows a smaller impurity peak which is attributed to the oxime byproduct.

4.3. Synthesis of the JQ1-KAT

4.3.1. Via a final amide coupling with amine-linker KAT

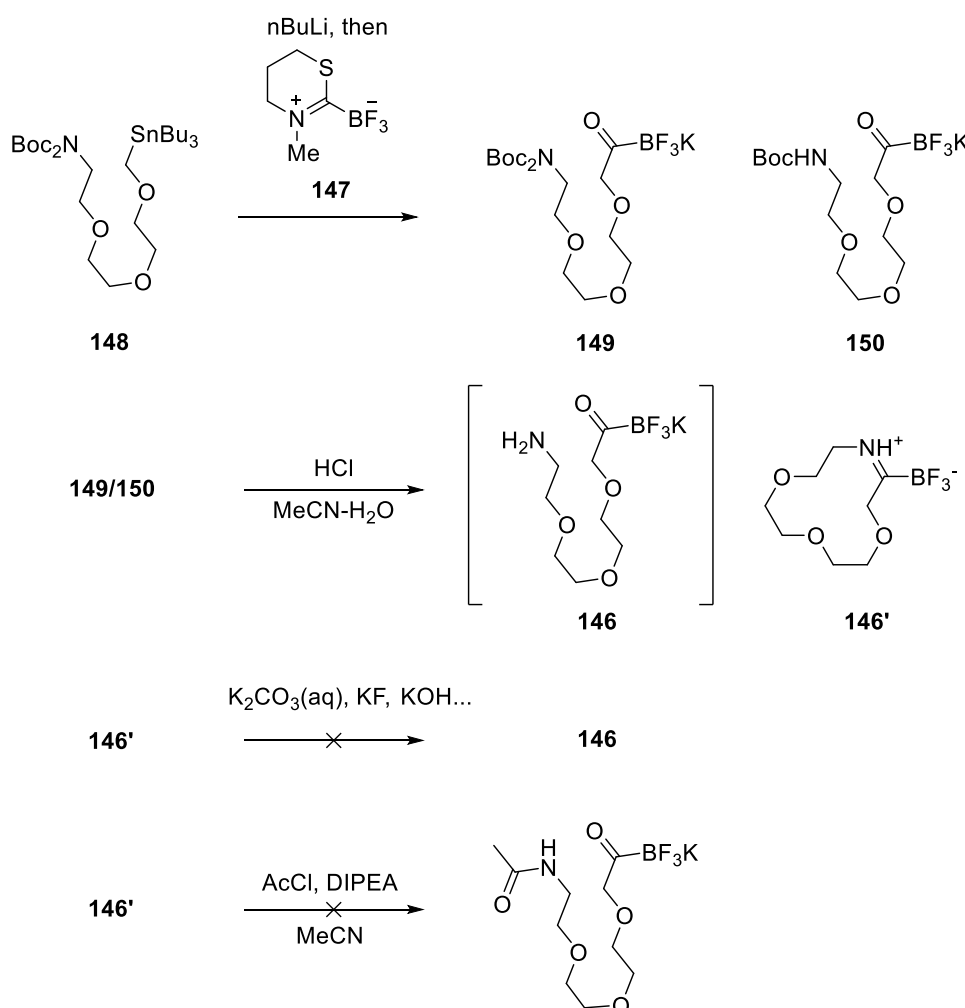
The first attempt to synthesize **142** was to perform an amide bond coupling of JQ1 acid **145** with an triethylene glycol amine KAT **146**.



Scheme 53. A: First retrosynthesis attempt to synthesize KAT **142**

With a new KAT reagent **147** (described in Chapter 5) the Boc protected version of **146** can be prepared from the corresponding stannane **148**. **149** was isolated as a mixture containing **150**, as some of the Boc groups were removed during the basic work-up conditions. Unfortunately KAT **146** could not be isolated, despite the facile Boc deprotection of KAT **149/150**. A newly formed peak in the LCMS chromatogram with 240 Da in the negative ion

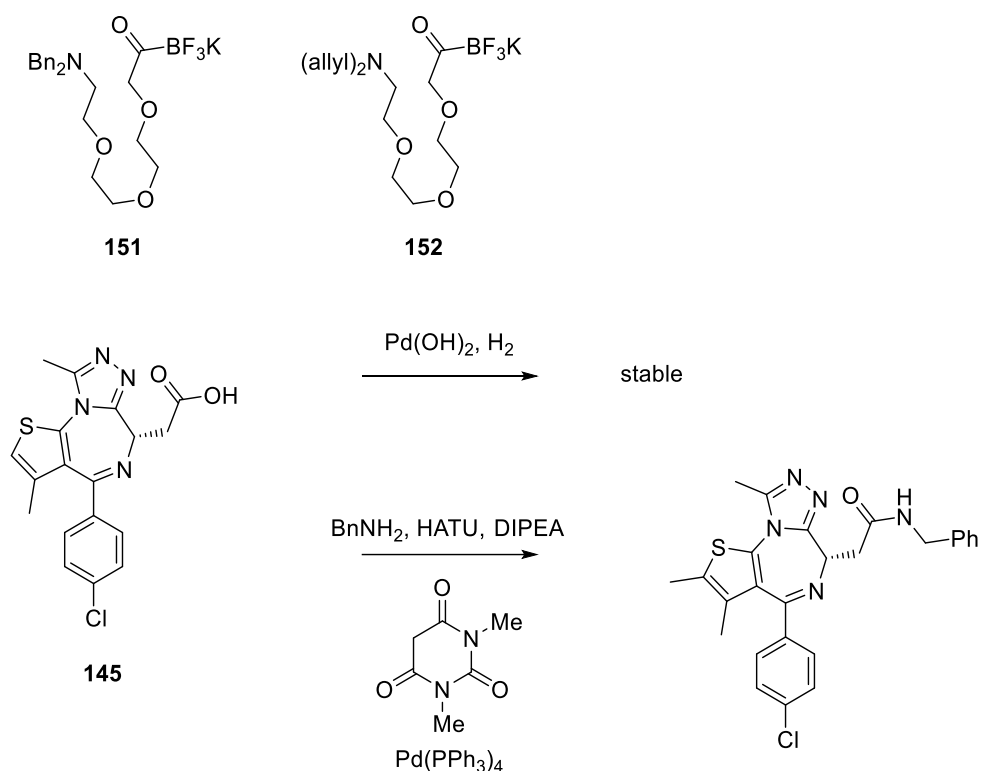
channel was attributed to the cyclic TIM **146'**. Attempts to shorten the Boc deprotection time, or basic hydrolysis of **146** failed to regenerate **146**. **146'** also did not undergo acylation with acetyl chloride, indicating the acylation with activated **144** to be unlikely. Therefore, we sought other nitrogen protecting groups that could be released in non-acidic conditions which would be less likely to facilitate TIM formation. These deprotection conditions should also be compatible with amide bond coupling conditions.



Scheme 54. Attempts on the synthesis of triethylene glycol amine KAT **146** by the cyclic reagent **147**. KAT **146** was not stable and couldn't be a building block for the desired amide across the triethylene glycol linker.

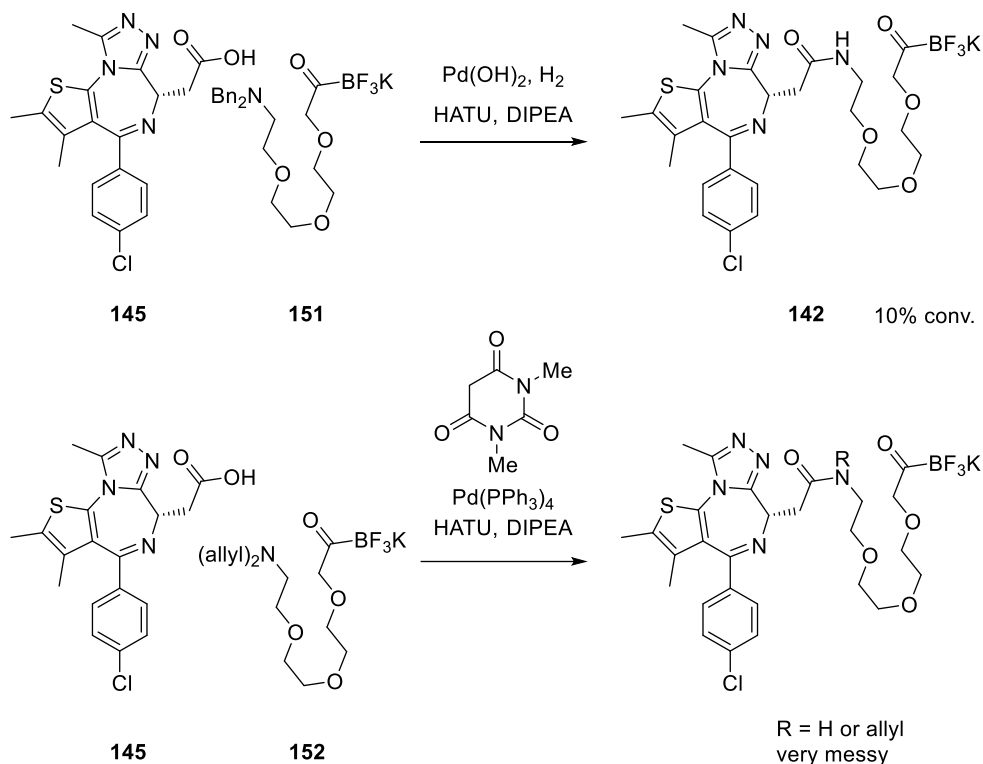
N,N-dibenzyl KAT **151** and N,N-diallyl KAT **152** were prepared through the same route of **148**, from their corresponding stannanes. The primary amine of **151** can be released by catalytic hydrogenation, and that of **152** by Pd(0) catalysis. We wished to perform the amide bond coupling between JQ1 acid **145** with the KAT with in situ amine deprotection therefore the amine deprotection conditions were tested with **145** both for its stability, and the robustness of its amide bond coupling under such conditions. H₂ at 1 atm with Pd(OH)₂

catalysis was identified as a viable hydrogenation condition, and $\text{Pd}(\text{PPh}_3)_4/1,3$ -dimethylbarbituric was found to be compatible with the amide bond coupling conditions.



Scheme 55. KAT **151** and **152** were synthesized and their N-deprotection conditions were tested with JQ1 acid **145**, showing that **145** was stable in the hydrogenative condition for releasing **146**, and that 1,3-dimethylbarbituric did not interfere with amide bond coupling.

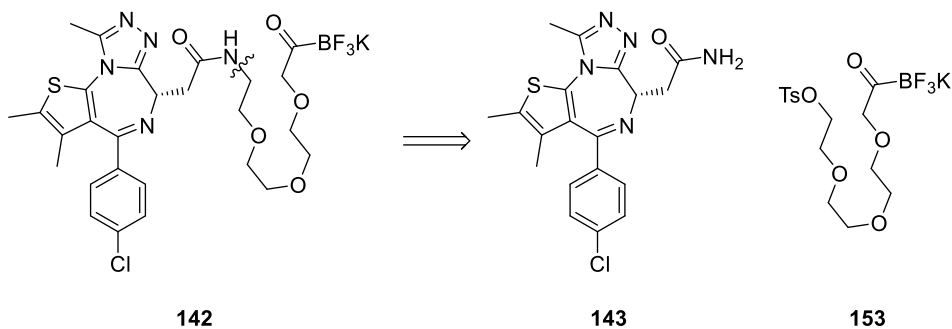
The in situ de-benzylation of KAT **151** in HATU mediated amide bond coupling with **145** gave the desired KAT **142**, although in very low conversion. In situ de-allylation amide coupling of **152** lead to a complex mixture beyond our purification attempt, with significant amount of N-allyl amide that can be observed, and did not convert to N-H amide over time. Both routes were not successful for the preparation of **142**.



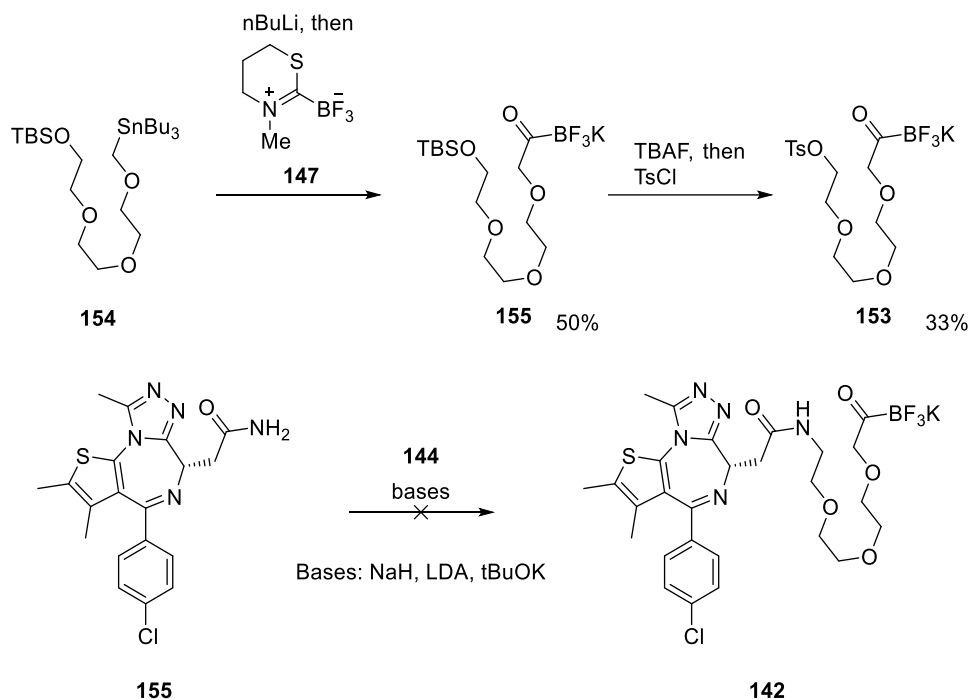
Scheme 56. In situ amine deprotection with JQ1 amide formation

4.3.2. Via alkylative KATylation

Another approach to **142** was the alkylation of primary amide **143** by an alkyl electrophile KAT **153**. **153** was obtained from KAT **155**, which can be synthesized also from the corresponding stannane **154** and reagent **147**.

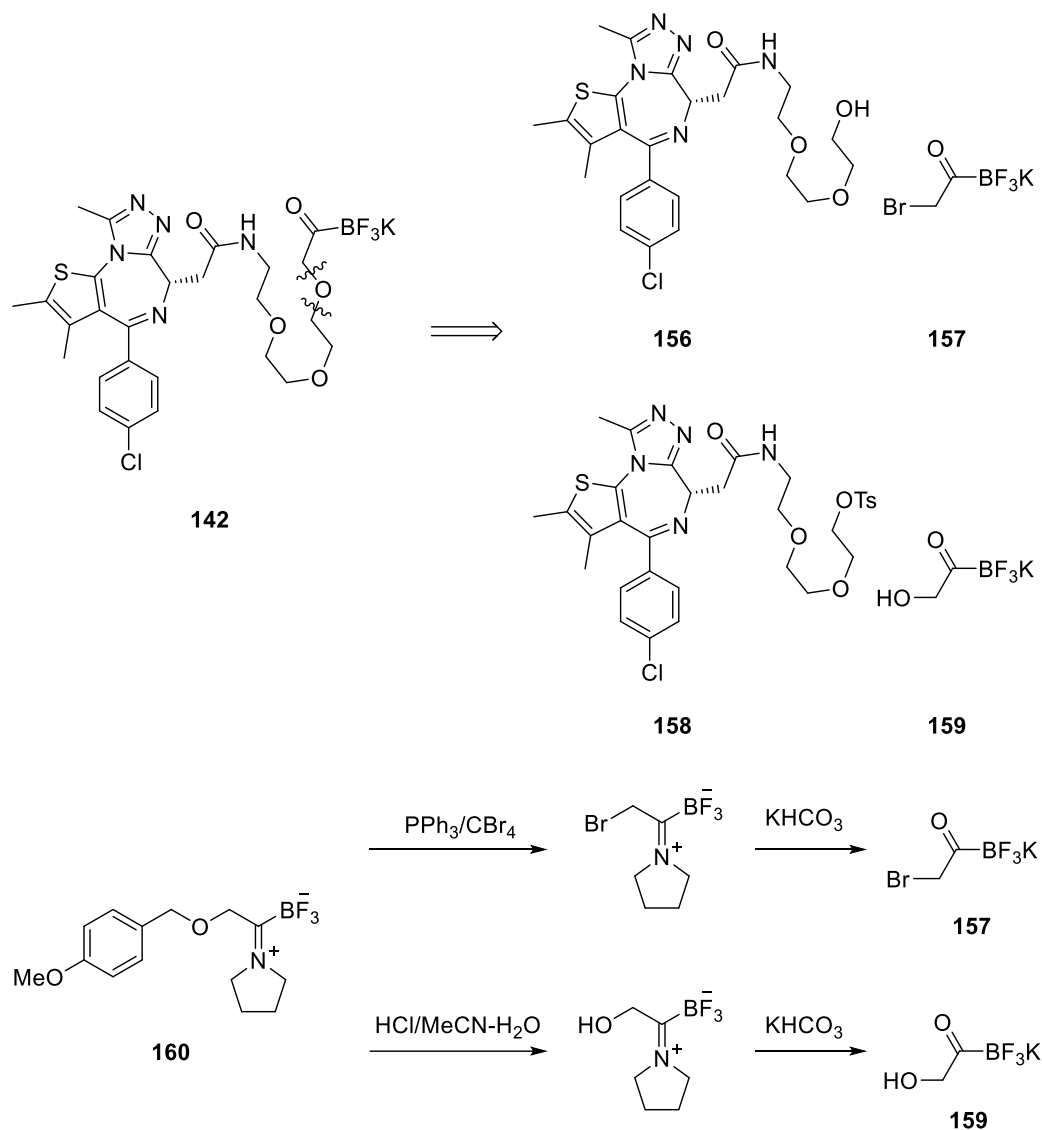


Scheme 57. Retrosynthesis of KAT **142** leading to JQ1 primary amide **143** and electrophilic KAT **153**.



Scheme 58. Synthesis of alkyl electrophile KAT **153** and attempts to the alkylation of amide **155**.

All our attempts at deprotonating amide **155** for alkylation by **153** failed. We observed that **155** was unstable under strongly basic conditions over prolonged time. Two other alkylative approaches tried were summarized below in **Scheme 59**. Both routes still suffer from the same obstacle of JQ1's instability in basic conditions required for amide or alcohol alkylation.



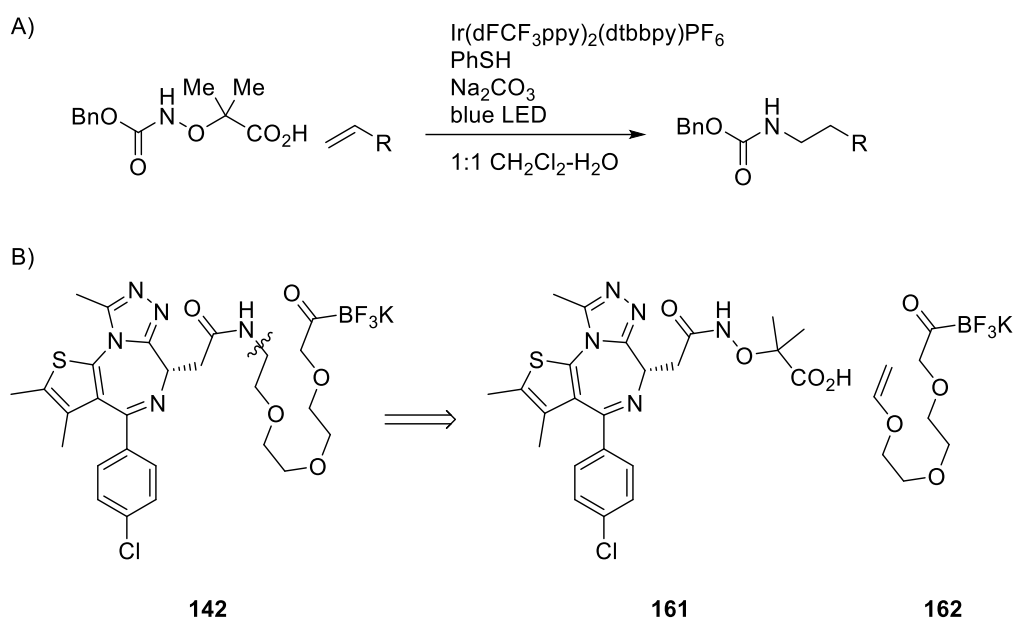
Scheme 59. Alkylative approaches to KAT **142** relying on α -functionalized alkyl electrophile KATs **157** and α -hydroxy KAT **159**. Aside from the instability of **156** and **158** under basic condition, **157** and **159** also could not be isolated yet and has to be generated freshly from TIM **160**.

4.3.3. Via photocatalytic hydroamidation with a JQ1 redox-active hydroxamic acid

During our struggle in the assembly of KAT **142**, an anti-Markovnikov hydroamidation reaction of alkenes reported by the Studer group came to our attention.^{†170} We see this as a

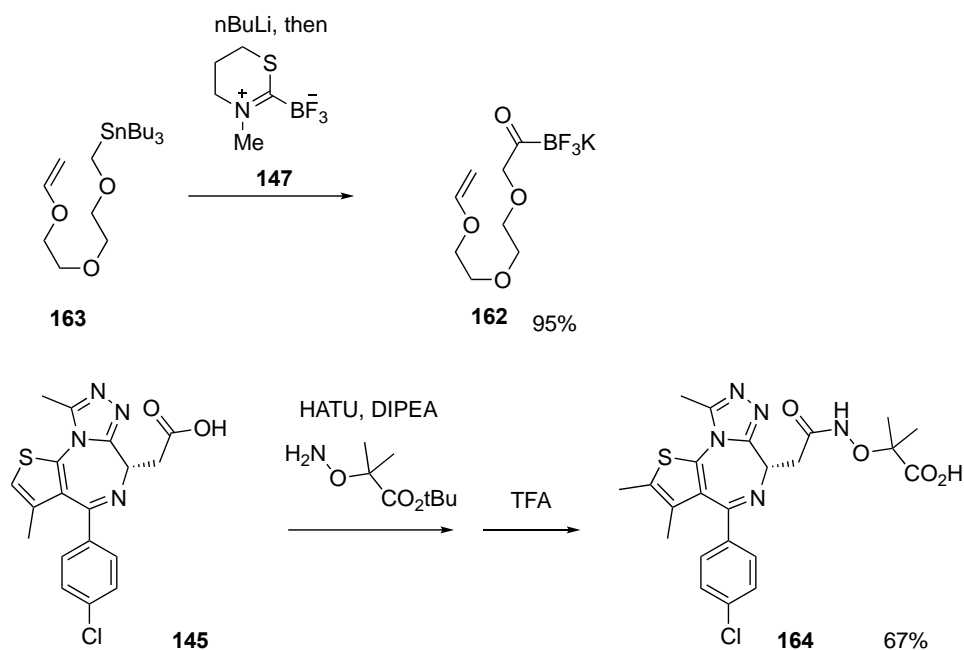
[†] The literature reconnaissance credit goes to former colleague Dr. Yayi Wang. We are also thankful to Yayi for his knowledge in photoredox chemistry and generosity in helping develop these conditions.

candidate route for installing the amide bond in **142**, which did not require strong bases, and could be orthogonal to KAT reactivities.



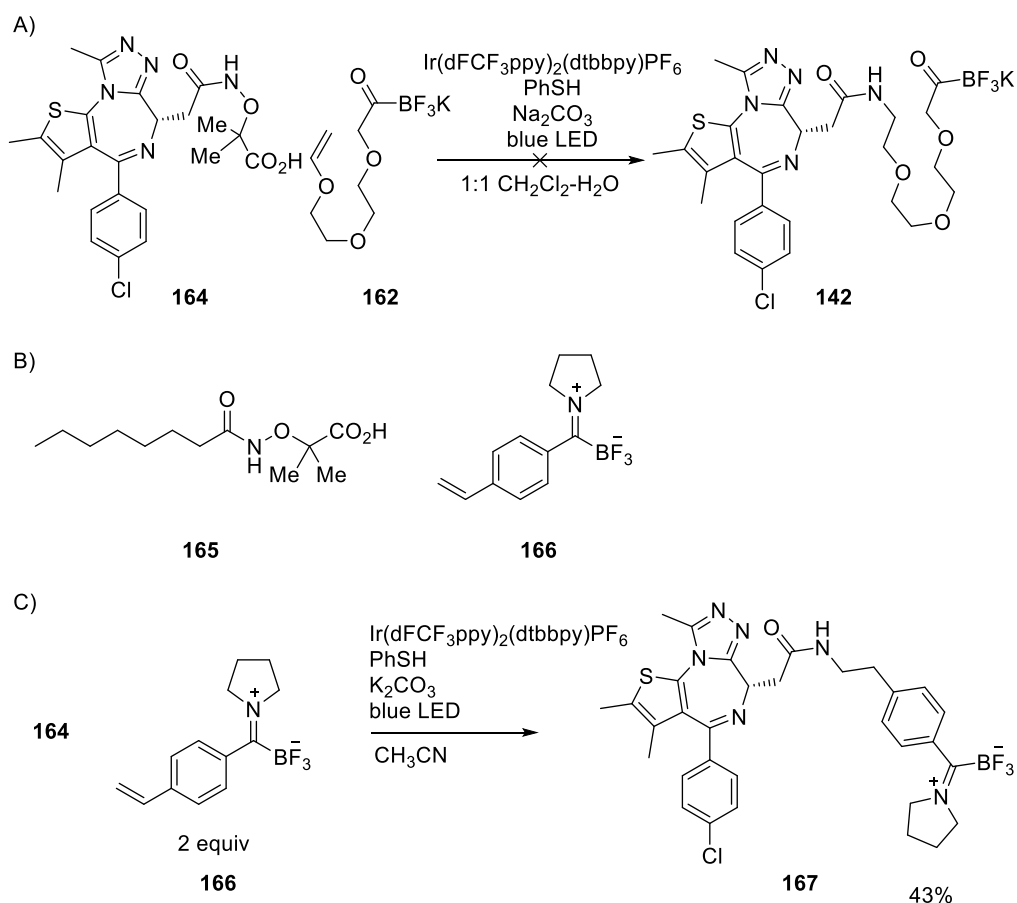
Scheme 60. A: An anti-markovnikov hydroamidation of alkenes that could lead to **B:** A strategy to disconnect the N-C bond between the amide group and triethylene glycol linker in **142**.

We tested if this chemistry was compatible with both JQ1 or KATs and could therefore be used to construct the amide linkage in **142**. The building block olefin KAT **162** was easily synthesized from stannane **163** with reagent **147**, and the required redox active amide in the form of a hydroxamic acid **164** was synthesized from JQ1 acid in two steps with moderate yield.



Scheme 61. Synthesis of olefin KAT **162** from stannane **163**, and redox active hydroxamic acid **164** from JQ1 acid **145**.

Initial screening showed that hydroxamic acid **164** underwent smooth addition to vinyl ethers. An unprotected KAT, however, was not compatible, and the KAT group was converted to an unknown species, according to ^{19}F NMR of the crude mixture (**Scheme 62A**). We soon found that the KAT has to be protected in form of a TIM to survive the photoredox conditions, but the original solvent mixture, aqueous CH_2Cl_2 , hydrolyzes the TIMs back to KATs. A screen of more suitable reaction solvent was conducted using less precious redox-active hydroxamic acid **165** and olefin TIM **166** (**Scheme 62B**). These studies revealed that the reaction works equally well in acetonitrile to form TIM **167** (**Scheme 62C**).



Scheme 62. A: The Ir catalyzed photoredox condition was not compatible with a bare KAT. **B:** Less expensive model substrates used for photoredox condition screening **C:** Revised photoredox hydroamination condition allows the hydroamidation of a TIM in acetonitrile.

The photoredox hydroamidation of olefin TIM **168** gave **169** and its subsequent hydrolysis gave **142**. The presence of KAT **142** is checked by mixing it with hydroxylamine **97** and observing the nitrone formation with LCMS.

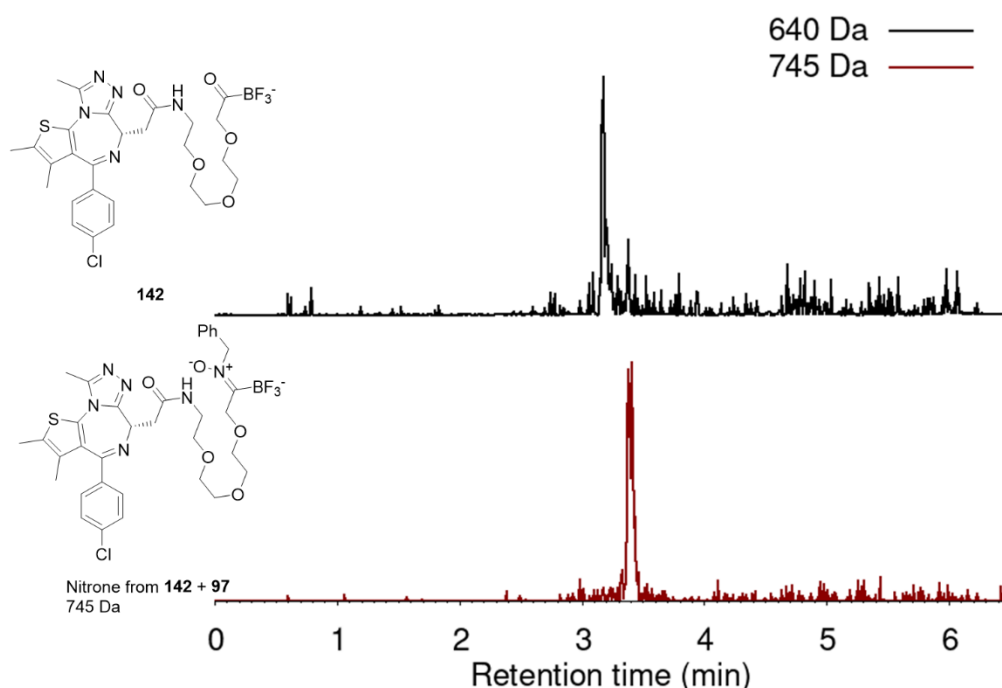
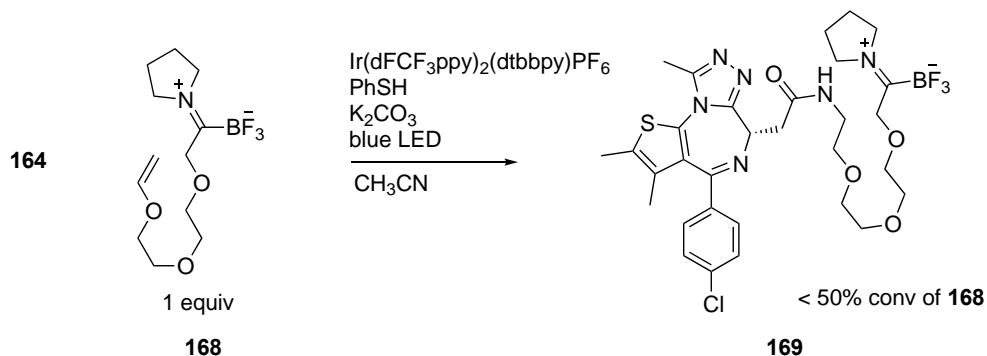


Figure 38. LCMS analysis of mixing KAT **142** with hydroxylamine **97**. Nitronium formation was observed.

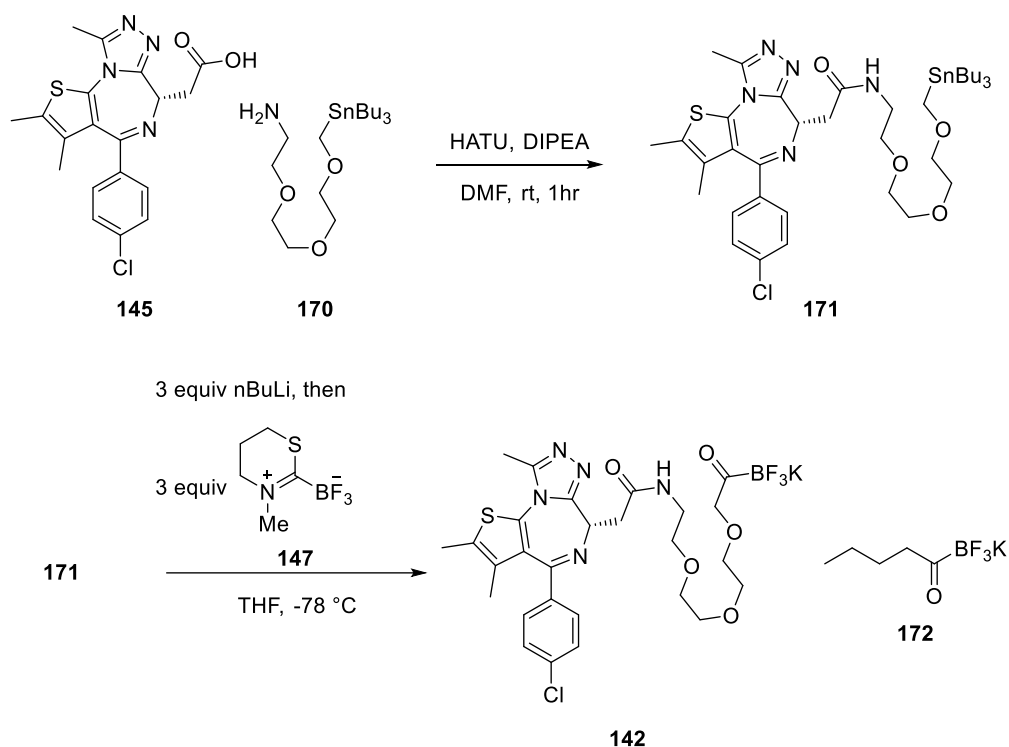
The separation of either **169** or **142** from the reaction mixture turns out to be a difficult and low yielding chromatographic process. The next section will describe the most recent approach to synthesize **142**.



Scheme 63. Synthesis of **169**, the TIM form of **142**, via an iridium-catalyzed photoredox hydroamidation.

4.3.4. Brute-force JQ1-linker lithiation via stannane chemistry

So far the best approach of preparing KAT **142** is via the lithiation or stannane **171** (**Scheme 64**). **171** can be synthesized from JQ1 acid **145** and stannylamine **170**. Lithiation of **171** with 3 equivalents of $n\text{BuLi}$ followed by trapping the formed alkoxythyllithium with 3 equivalents of **147** gives a mixture containing mostly **142** and butyl KAT **172** after work-up. A suitable procedure to isolate **142** in pure form from this mixture needs to be further optimized.



Scheme 64. Synthesis of KAT **142** via lithiation of **171** and reagent **147**.

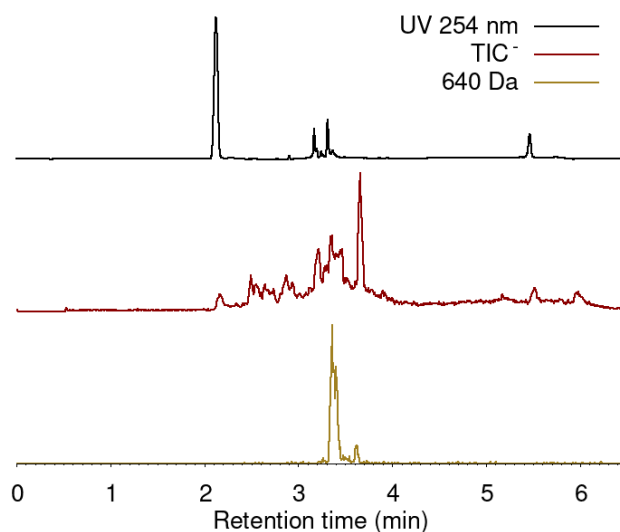
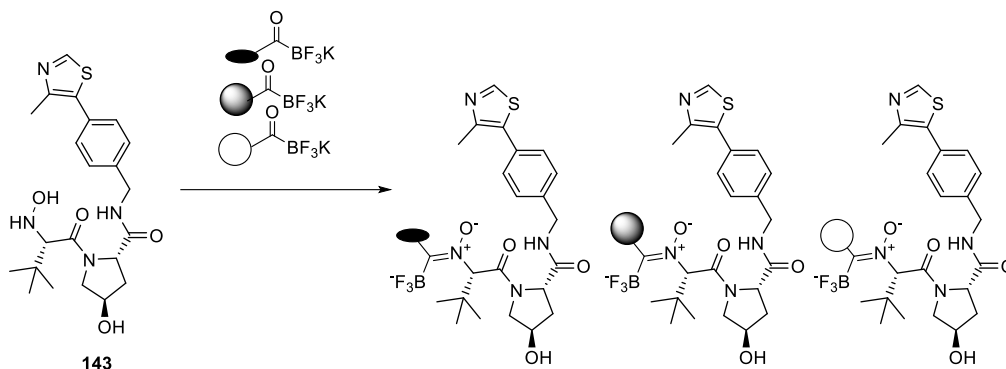


Figure 39. LCMS analysis of reaction mixture of **142** synthesis via stannane **171**.

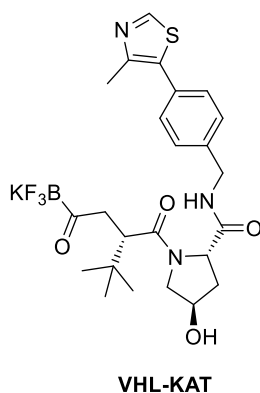
4.4. Summary and Outlook

A VHL E3 Ligand hydroxylamine **143** was successfully synthesized and was shown to under go the “2-step” KAT ligation as described in **Section 1.2**. With this hydroxylamine in hand, we could envisage that a KAT-nitrone dynamic covalent library can be formed with any protein binder with a KAT functional group.



Scheme 65. Other protein binders with a KAT group can be used to form a nitrone library with the E3 hydroxylamines

The attempted synthesis of JQ1-KAT **142**, however, proved to be difficult and is still ongoing. This situation lead us to a proposal that, if KAT synthesis was the bottle neck, it might be more productive to place the KAT group on the VHL ligand, and prepare the variety of protein binders bearing a hydroxylamine. The number of potential protein binders overwhelm that of known E3 ligase ligands, therefore the more synthetic challenging functional group should be placed on the E3 ligases to avoid a KAT synthesis bottleneck on protein ligand KAT syntheses.



Scheme 66. Reversed polarity of disconnecting an amide bond in PROTACs gives a **VHL-KAT**.

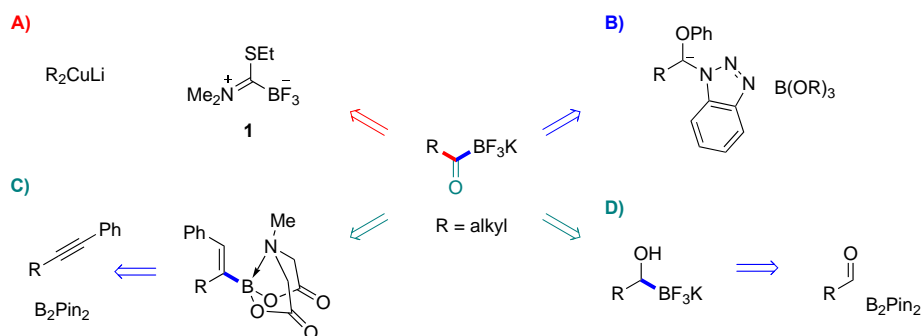
5

Cyclic thiotrifluoroborate iminium reagents for alkyl KAT synthesis

Everything not forbidden is compulsory
-The totalitarian principle

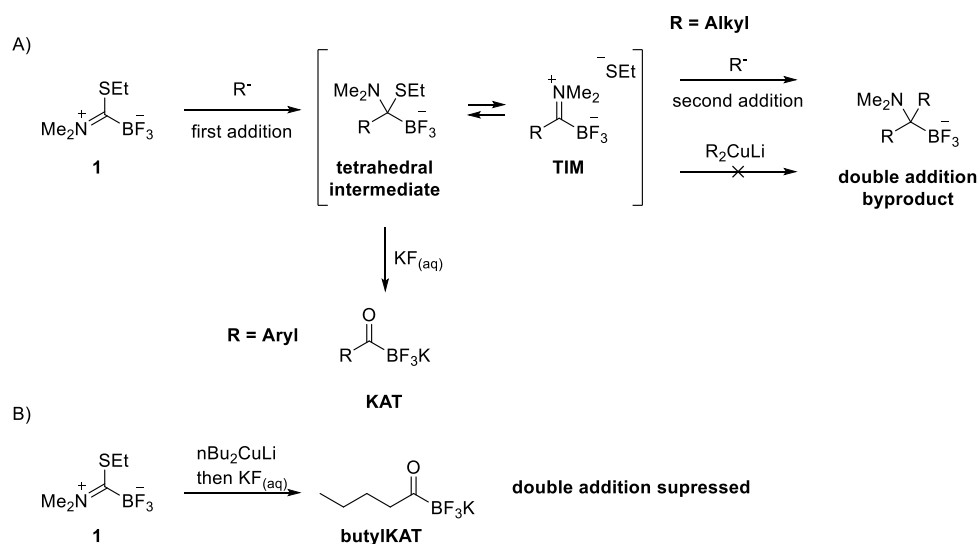
5.1. A need for α -alkoxy KATs, and synthetic routes of alkyl KATs

Four common strategies for the synthesis of alkyl KATs are listed in **Scheme 67**. The first method was reported by our group in 2018, using a dialkyl cuprate to transfer an alkyl group to the KAT transfer reagent **1**,¹⁷ widening the applicable scope of **1** from aryl KATs synthesis to include the synthesis of alkyl KATs (**Scheme 67A**).¹⁷¹ The second strategy involves the trapping of a masked acyl anion in form of Katrizky's benzotriazole N,O-acetal^{172–174} by a trialkyl borate, which was reported in 2012 by our group as the first general route to KAT synthesis (**Scheme 67B**).¹² Two other approaches, developed by the Ito group, construct the C–B bond by copper catalyzed addition of bis(pinacolato)diboron to an aldehyde or an alkyne, and furnishes the KAT carbonyl group by an oxidation of the intermediate after boron addition (**Scheme 67C/D**).^{36,37} The α -hydroxytrifluoroborate or alkenylboronate formed underwent ligand switch on the boron and oxidation to form the KAT group.



Scheme 67. Common strategies used to synthesize alkyl KATs. **A:** Construct of the C–C bond from the addition of dialkyl cuprate to the KAT transfer reagent **1**.¹⁷¹ **B:** Construct the C–B bond from borylation of an acyl anion equivalent.¹² **C:** Construct the carbonyl group by the ozonolysis of an alkenyl MIDA-boronate derived from an alkyne.³⁶ **D:** Construct the carbonyl group by oxidation of an α -trifluoroboryl alcohol, which was synthesized from Cu(I) catalyzed borylation of an aldehyde.³⁷

Reagent **1** enabled the synthesis of a variety of aryl KATs due to the facile and selective nucleophilic addition of aryllithium to **1**.¹⁷ This was not the case when an alkyllithium was used, as the intermediate adduct reacted with another equivalent of alkyllithium to form a double addition byproduct (**Scheme 68A**). An example was shown in **Figure 40**, where LCMS analysis shows that reacting *n*BuLi with **1** gave mostly the double addition product and only trace amounts of *n*-Butyl KAT. To enable the synthesis of an alkyl KAT from the alkyl anion, the reaction environment must favor the first addition step, and disfavor the second addition step, which would consume an extra alkyl anion, as well as destroy the productive mono-adduct intermediate. Converting the carbon nucleophile to a dialkyl cuprate was found to successfully suppress the second addition step and allowed the synthesis of alkyl KATs by **1**.¹⁷¹



Scheme 68. A: KAT reagent **1** undergoes nucleophilic addition with carbanion organometallic reagents to form a tetrahedral intermediate, which forms a KAT after hydrolysis, or undergoes a second addition to form a double addition byproduct. **B:** The second addition of dialkyl cuprates to reagent **1** is suppressed, enabling the synthesis of alkyl KATs with reagent **1**.

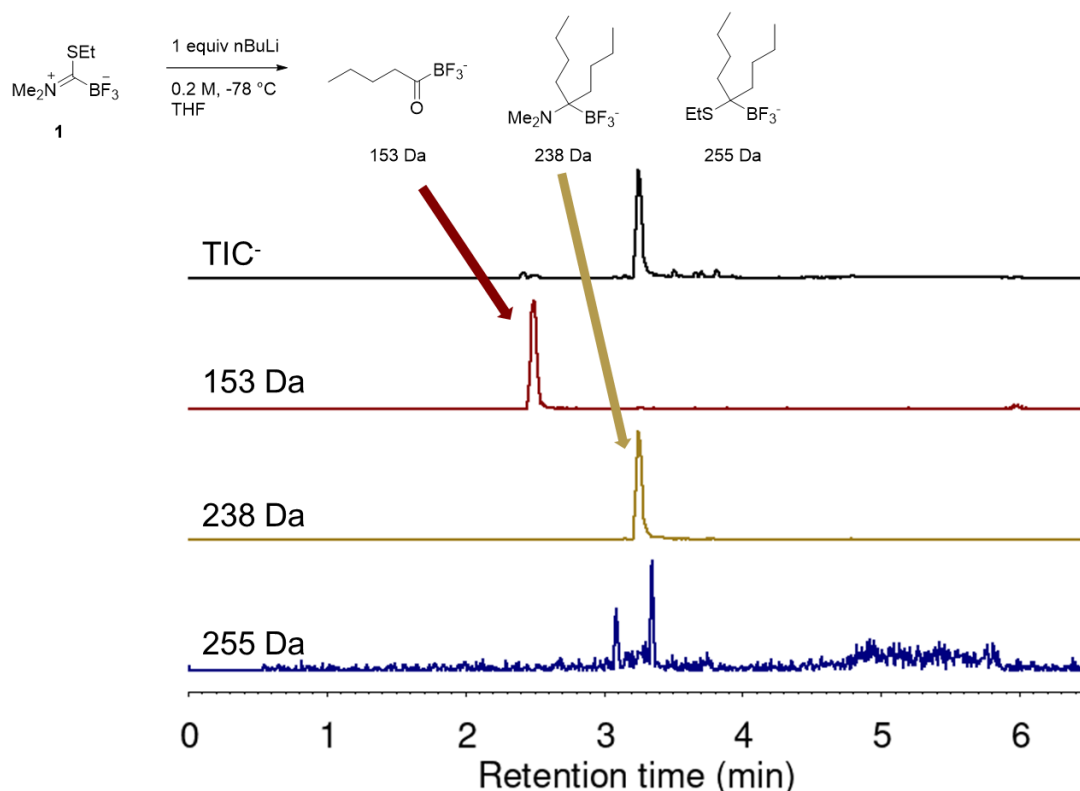
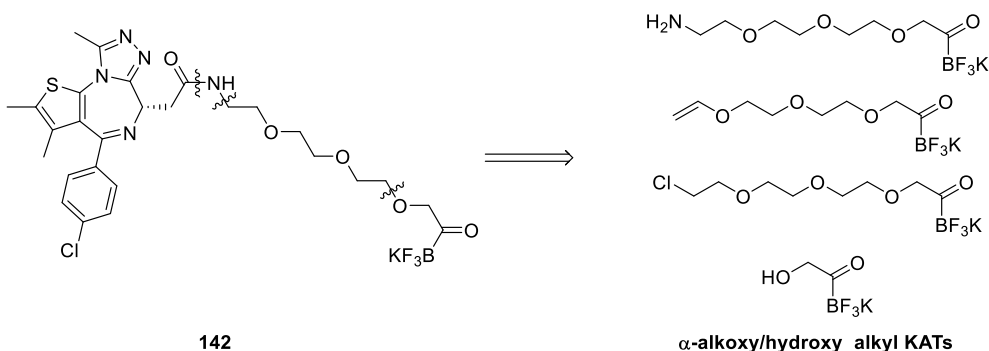


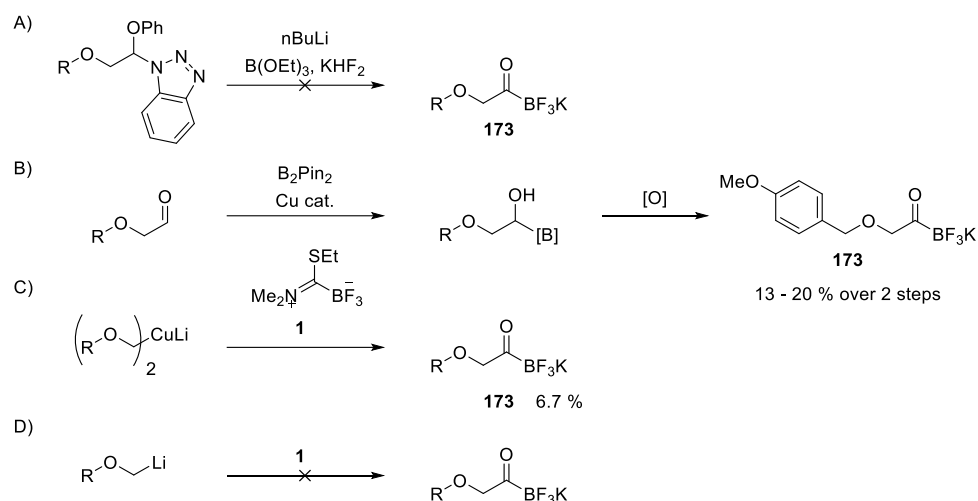
Figure 40. LCMS analysis of the crude mixture after of treating KAT reagent **1** with nBuLi under -78°C . The double addition α -aminotrifluoroborate (238 Da) was found to be the main product in the total ion count (TIC) trace. The amount of butyl KAT (153 Da) formation was negligible.

We encountered KAT **142** as a key building block during the pursuit of a KAT-nitrone split MZ-1 PROTAC described in the Chapter 4. All attempts at the synthesis of **142** required access to a novel class of alkyl KATs that has not been reported before: α -alkoxy KATs.



Scheme 69. α -alkoxyalkyl KATs were needed to construct JQ1-TEG-KAT

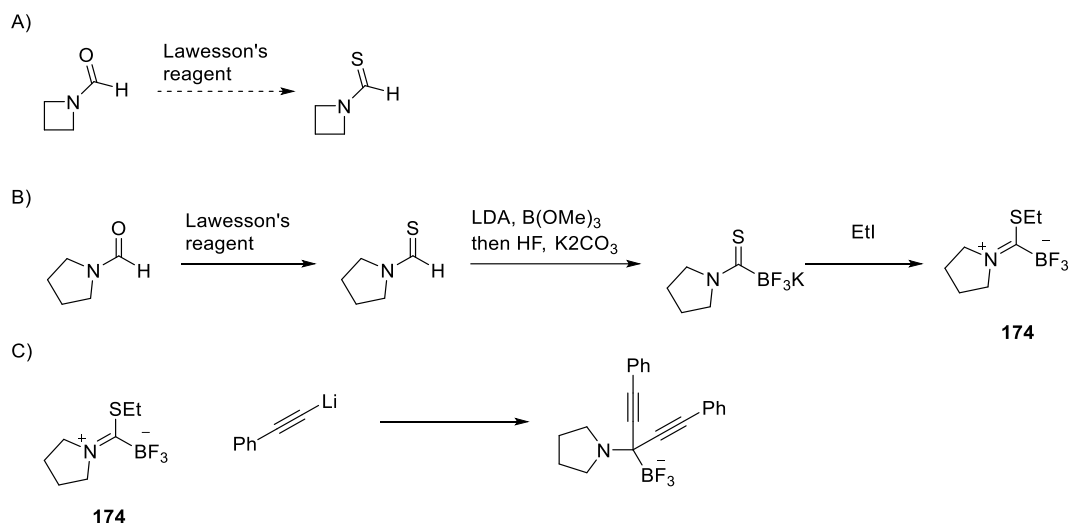
Scheme 70 outlines the outcome of applying known methods of alkyl KAT synthesis to α -alkoxy KATs, using *p*-methoxybenzyloxymethyl KAT **173** as a model target. The benzotriazole N,O-acetal did not stabilize the β -alkoxy anion and was not suitable for boron trapping (**Scheme 70A**). The borylation of *p*-methoxybenzyloxy acetaldehyde with subsequent oxidation gave the desired KAT, but the yield left room for improvement (**Scheme 70B**). The cuperate route also afforded the desired KAT, albeit with low yields (**Scheme 70C**). The reaction between the alkyllithium with reagent **1** gave predominantly the double addition product, and no **173** was isolated, implying that α -alkoxyalkyllithiums also undergo a second addition to reagent **1** readily, as occurs with other alkyllithiums (**Scheme 70D**). We wished to have a KAT reagent that could react with an alkyl nucleophile to form KATs selectively and in higher yields. The path to finding such a reagent, based on **1**, will be described in the rest of this chapter.



Scheme 70. Synthetic attempts towards α -alkoxy KATs. R = p-methoxybenzyl.

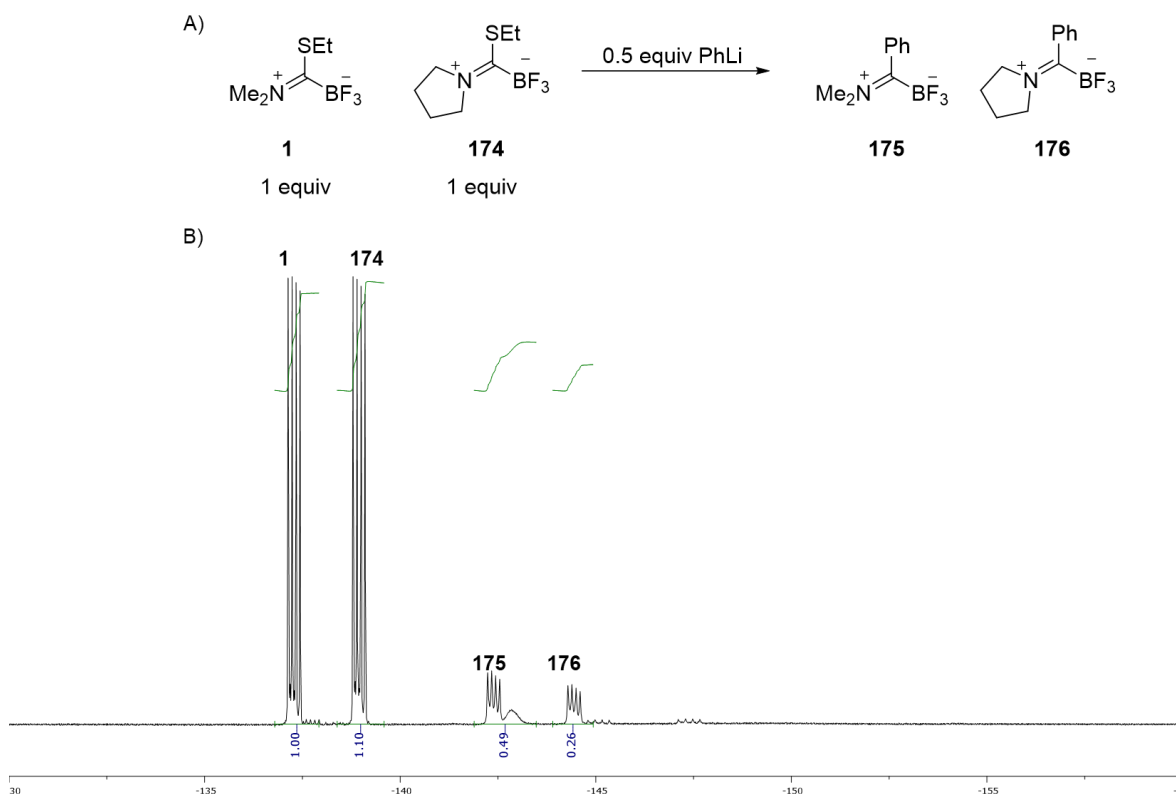
5.2. Pyrrolidine iminiums didn't stabilize the tetrahedral intermediate enough

We sought to design a reagent that favors the first addition step in **Scheme 68A** while preventing the second addition of carbon nucleophiles. This could be achieved if the KAT reagent were more reactive, and the tetrahedral intermediate were more stabilized. We hypothesized that using a cyclic amine fragment in KAT reagents, instead of the dimethylamine in **1**, could favor the pyramidalization of the central carbon atom in KAT reagents. This could destabilize the KAT reagent and favor the formation of a tetrahedral intermediate, possibly enhancing the reactivity of the first nucleophilic addition and retarding the second addition. Azetidine could have a powerful pyramidalization effect, but its thioformamide synthesis was not successful therefore we took a step back to start with the 5-membered ring pyrrolidine. KAT reagent **174** was synthesized from pyrrolidine formamide through the sequence shown in **Scheme 71**.



Scheme 71. A: Azetidine thioformamide synthesis was not successful. **B:** Synthesis of pyrrolidine iminium KAT reagent **174**. **C:** **174** did not prevent double addition of carbanions.

Unfortunately **174** did not prevent double addition of organometallic reagents, even with a weaker carbon nucleophile such as phenylacetylide. Furthermore, a competitive trapping experiment of **1** versus **174** with phenyllithium (**Scheme 72A**) indicated that **1** was slightly more reactive than **174**, nullifying the hypothesis that the pyrrolidine ring could enhance the carbon nucleophile trapping of **174** or prevent a second carbon nucleophile addition.

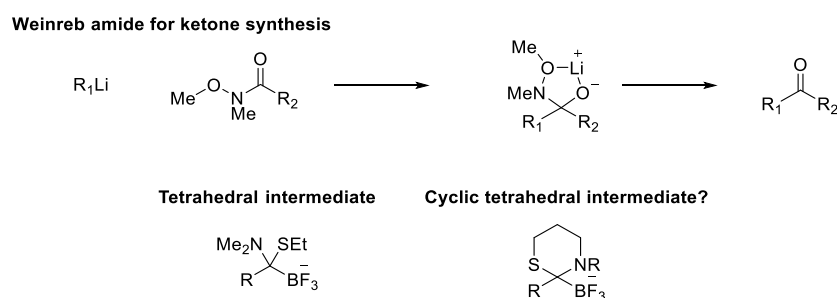


Scheme 72. A: Competitive reaction of KAT reagent **1** and pyrrolidine KAT reagent **174** towards PhLi
B: the ^{19}F NMR of the reaction mixture. From a 1:1 mixture of **1** and **174**, the yield of **175** was higher indicating that **1** to be more reactive.

5.3. A cyclic, N-S tethered reagent that stabilizes the intermediate

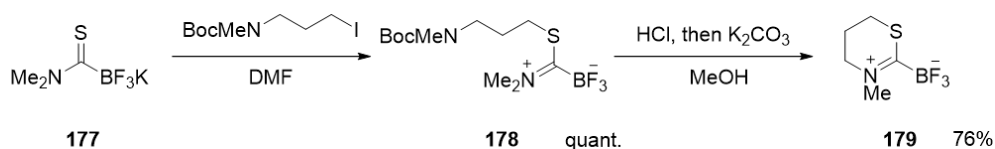
5.3.1. Synthesis, properties and clean single addition

The tetrahedral intermediate needed to resist a second addition. With inspiration from the Weinreb amide, which stabilizes a mono-adduct of organometallics to N-methoxy-N-methyl amides through chelating the metal ion to form a cyclic tetrahedral intermediate, we designed an N-S tethered KAT reagent **179** (**Scheme 73**). **179** was synthesized through the steps shown in **Scheme 74A**. Compound **177**, which was also the precursor of KAT reagent **1**, was alkylated to give **178**. Upon Boc deprotection and neutralization, **178** cyclized spontaneously to expel a molecule of N,N-dimethylamine and formed reagent **179**.

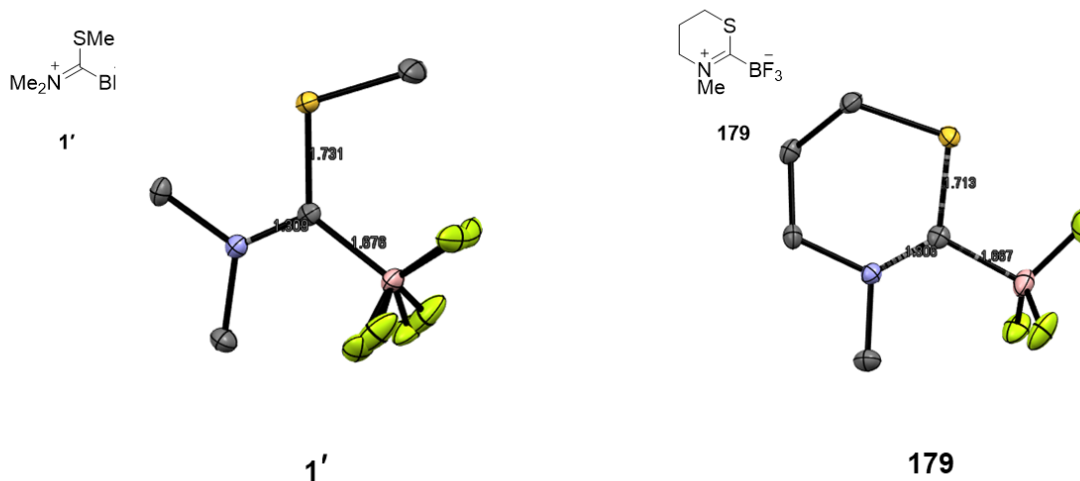


Scheme 73. Inspiration from Weinreb's ketone synthesis¹⁷⁵ lead the design of a new KAT reagents

A)



B)

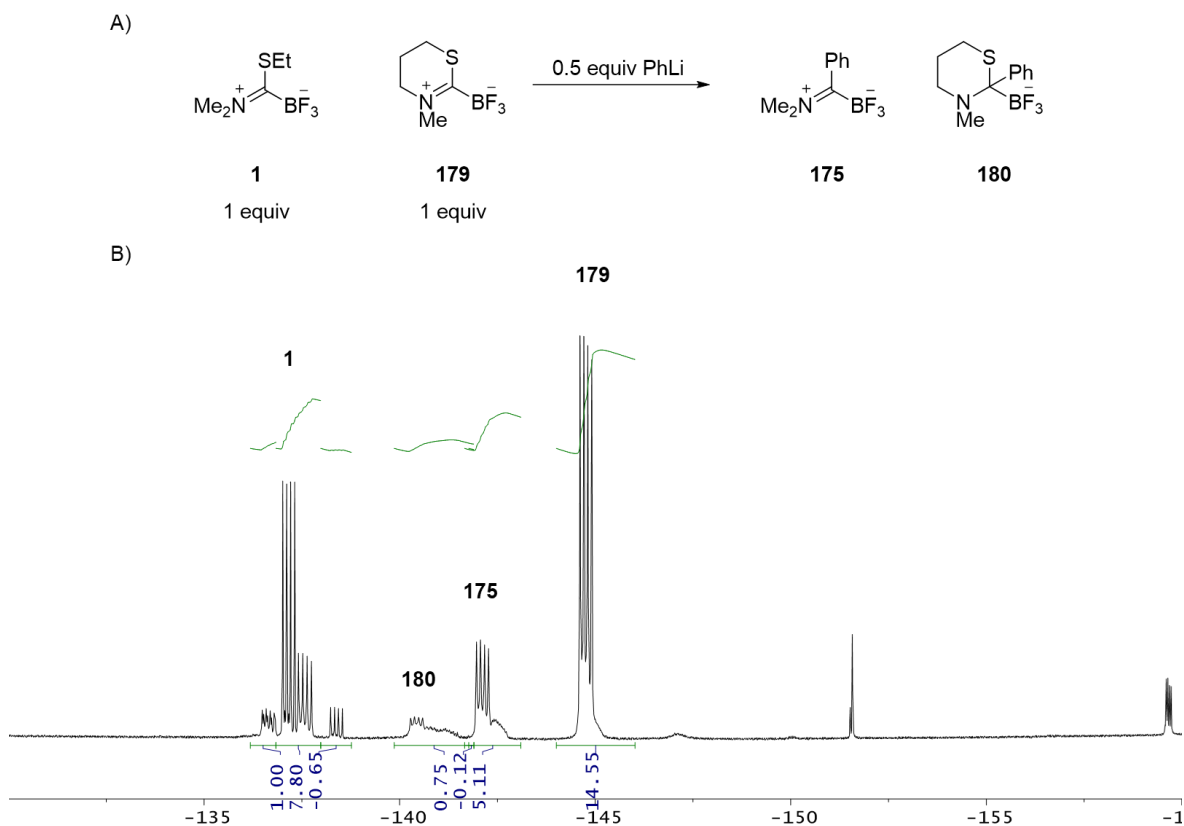


Scheme 74. A: Synthesis of N-S tethered cyclic KAT reagent **179** **B:** and the X-ray diffraction structure in comparison with **1'**, which had a methylthiol group in place of the ethylthiol in **1**.¹⁷ The geometry around the central carbon of **179** was almost identical to that in **1'**.

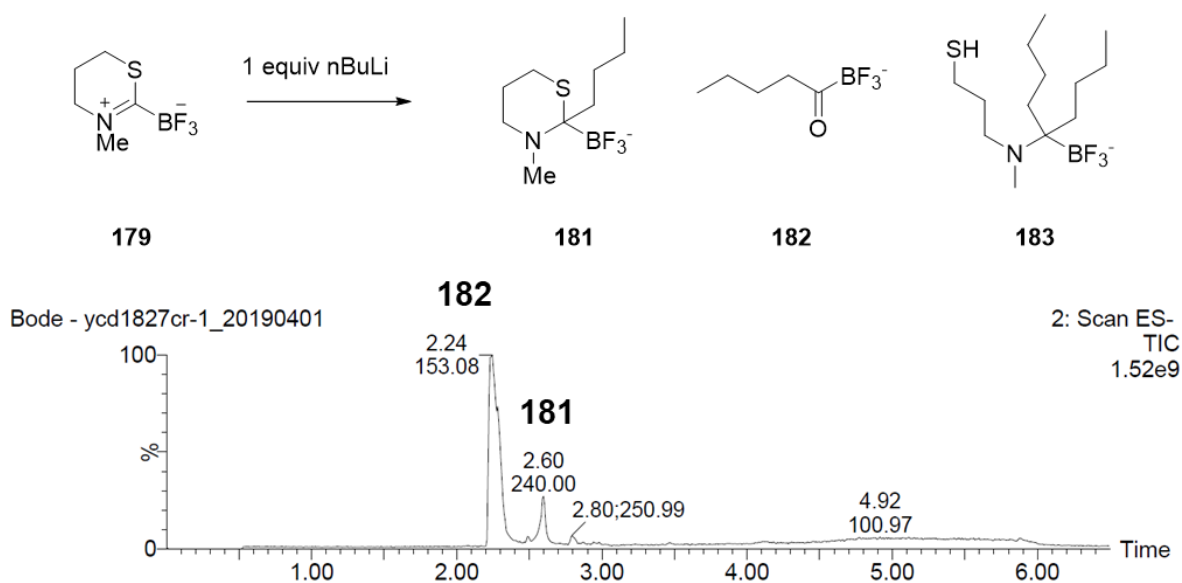
Reagent **179** was isolated as a crystalline white solid which was odorless upon long term storage, unlike **1**, which was odorless fresh after synthesis but soon emits the smell of ethanethiol in a few hours due to slight amount of hydrolysis. The fact **179** being odorless could either be attributed to its higher hydrolytic stability, or to the nonvolatility of its hydrolysis product, 3-methylaminothiol. Either way, the odor nuisance of **1** during storage or use was not a problem for **179**. **179** was also found to have a higher melting point and lower solubility in organic solvents (mp 112.6–113.5 °C, < 0.15 M solubility in THF at 23 °C) than **1** (mp 45 °C, > 1M solubility in THF at 23 °C).

Although competitive trapping of **179** versus **1** showed that reagent **1** was more reactive towards phenyllithium, **179** was found to give cleanly the single addition product when one equivalent of butyllithium was added at –78 °C, according to LCMS analysis. This suggested that **179** favors the mono-addition product by stabilizing the tetrahedral intermediate against nucleophilic attack. Reagent **179** was treated with 1.65 equiv of nBuLi and still gave predominantly the single addition intermediate, and afford the resulting n-butyl KAT with 83%

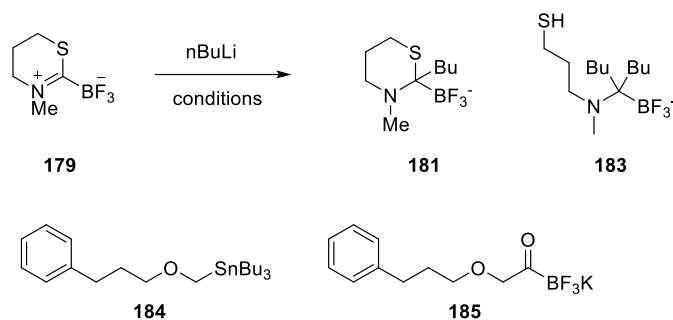
isolated yield. The reaction temperature however, must be kept below -40°C , otherwise only the double addition product **183** was observed in the LCMS analysis of the reaction mixture.



Scheme 75. A: Competitive reaction of KAT reagent **1** and cyclic KAT reagent **179** towards PhLi. **B:** the ^{19}F NMR of the reaction mixture. From a 1:1 mixture of **1** and **179**, the consumption of **1** was higher than that of **179**, indicating **1** to be more reactive.



Scheme 76. Reaction between **179** and nBuLi



	Conditions	Outcome
1	1 equiv $n\text{BuLi}$, $-78\text{ }^\circ\text{C}$	Mono-addition 181
2	1 equiv $n\text{BuLi}$, rt	Double addition 183
3	1 equiv $n\text{BuLi}$, $0\text{ }^\circ\text{C}$	181 + 183
4	1 equiv $n\text{BuLi}$, $-40\text{ }^\circ\text{C}$	181
5	1.65 equiv $n\text{BuLi}$, $-78\text{ }^\circ\text{C}$	181 , 83% KAT 182 isolated
6	1 equiv 184 , followed by adding $n\text{BuLi}$ at $-78\text{ }^\circ\text{C}$	185

Table 8. Reaction outcome of cyclic reagent **179** under various conditions

5.3.2. Extraordinary stability of the KAT thioaminal after single addition

The tetrahedral adduct from reagent **179** was exceptionally stable. **186** was isolated as an example. It eventually hydrolyzes when dissolved in the LCMS solvent 1:1 MeCN- H_2O , but the process is slow enough to give a well-formed peak when the sample was prepared in 1:1 MeCN-MeOH instead. This gave an illusion that the hydrolytic workup procedure for KAT synthesis from reagent **179** was a trivial task since the hydrolysis occurs spontaneously without additional reagent. It turned out the challenge was the removal of solvent: since the hydrolysis product 3-methylaminopropanethiol was not volatile, concentration of the hydrolyzed reaction mixture will facilitate the condensation between the aminothiols and the KAT, reversing the intended hydrolysis.

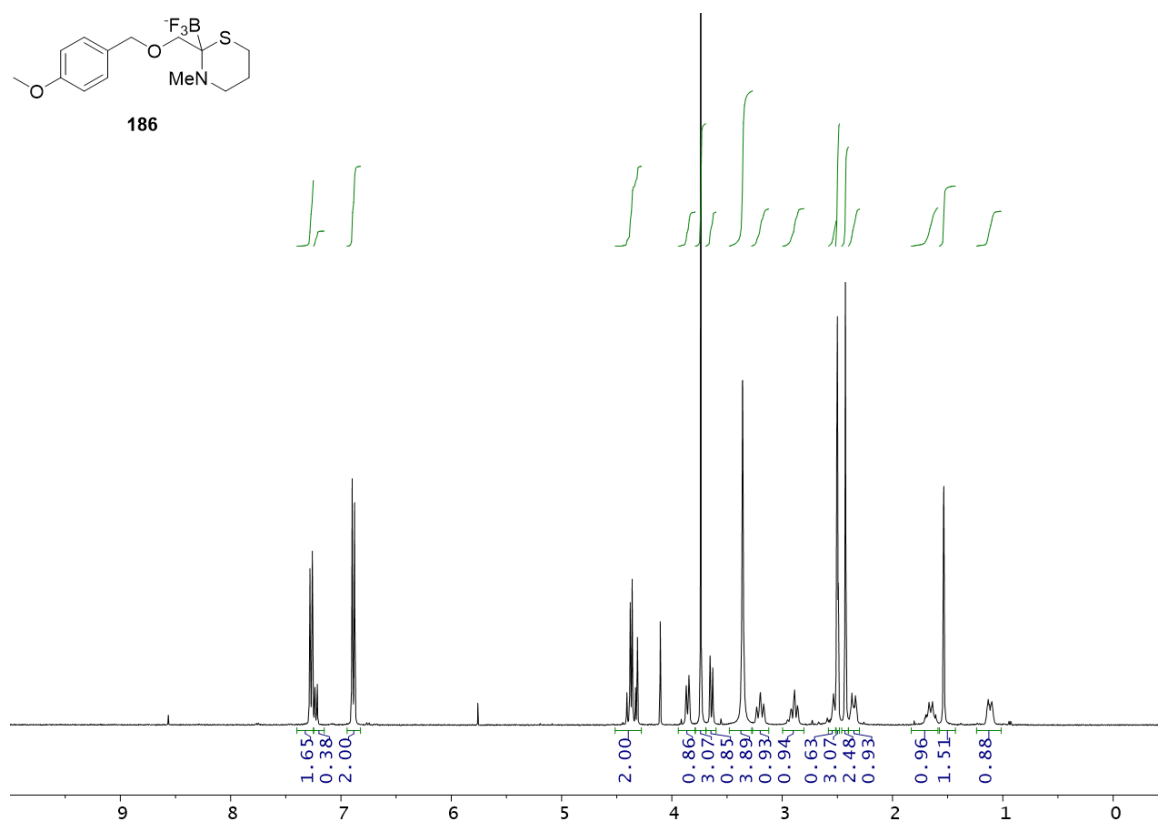
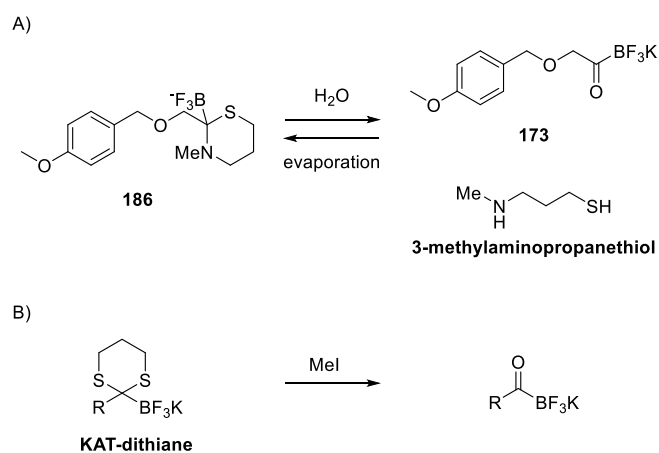
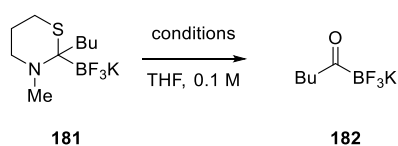


Figure 41. ^1H NMR spectrum of tetrahedral intermediate **186**. The NMR spectrum was not well resolved in solvents other than DMSO and gives very broad peaks in acetone- d_6 , CD_3CN and CD_3OD .



Scheme 77. A: Hydrolysis of intermediate **186** to form KAT **173** was spontaneous in dilute aqueous solutions (cf **Scheme 76** LCMS chromatogram, where the peak of KAT **182** was dominant over peak of the tetrahedral intermediate **181**). However, upon evaporation in intention to isolate the KAT, the 3-methylaminothiol adds back onto the KAT. **B:** A similar hydrolysis could also be in action for KAT-dithiane hydrolysis.

A series of work-up conditions were tested to prevent the thioaminal from re-forming during solvent removal. In the end we found it necessary to use an aminothiols trapping reagent. Both formaldehyde and acetaldehyde successfully trapped the aminothiols and liberated the KAT for further purification. We have previously seen that KAT synthesis through the borylation of dithiane was also troubled at the step of removing the 1,3-propanethiol from the dithiane, and required the addition of methyl iodide.¹⁷⁶ A similar reversible hydrolysis could be the common problem.



	Conditions	Outcome
1	KF _(aq) 6.5M 10% v/v	N.R.
2	KHF _{2(aq)} satd. 10 % v/v	N.R.
3	HF _(aq) 48%, 10 % v/v	N.R.
4	K ₂ CO _{3(aq)} satd., 20% v/v	N.R.
5	KOH _(aq) 6M, 20% v/v	N.R.
7	CH ₂ O _(aq) 35%, 20% v/v	182 + slow decomposition
8	CH ₂ O _(aq) 35%, 5% v/v	Mixture of 181 and 182
9	CH ₂ O _(aq) 35%, 20% v/v, KF _(aq) 6.5 M 10% v/v	182 , slowly forms a byproduct
10	Acetaldehyde 20% v/v, KF _(aq) 6.5 M 10% v/v	182 , complete in 4 hr

Table 9. Conditions screening for the hydrolysis of intermediate **181** to KAT **182**. A **181** solution formed from treating **179** with nBuLi was added the reagents listed and stirred vigorously overnight before being evaporated and analyzed by LCMS using non-aqueous MeOH-CH₃CN to prepare the injection sample.

Upon prolonged treatment with formaldehyde, α -alkoxy KATs formed byproducts that have yet to be identified (**Figure 42**). Treatment with acetaldehyde did not give rise to this byproduct and was chosen to be the standard aminothiols trapping agent. The final work-up procedure to accompany the use of reagent **179** with alkyllithiums is as follows: 1 mL of the reaction mixture was quenched with 0.1 mL of 6.5 M KF_(aq) followed by 0.2 mL acetaldehyde. The quenched reaction mixture was left to stir vigorously overnight before evaporation. The byproduct 3-methyl-1-thia-3-azacyclohexane could be washed away with Et₂O, in which most KATs were insoluble.

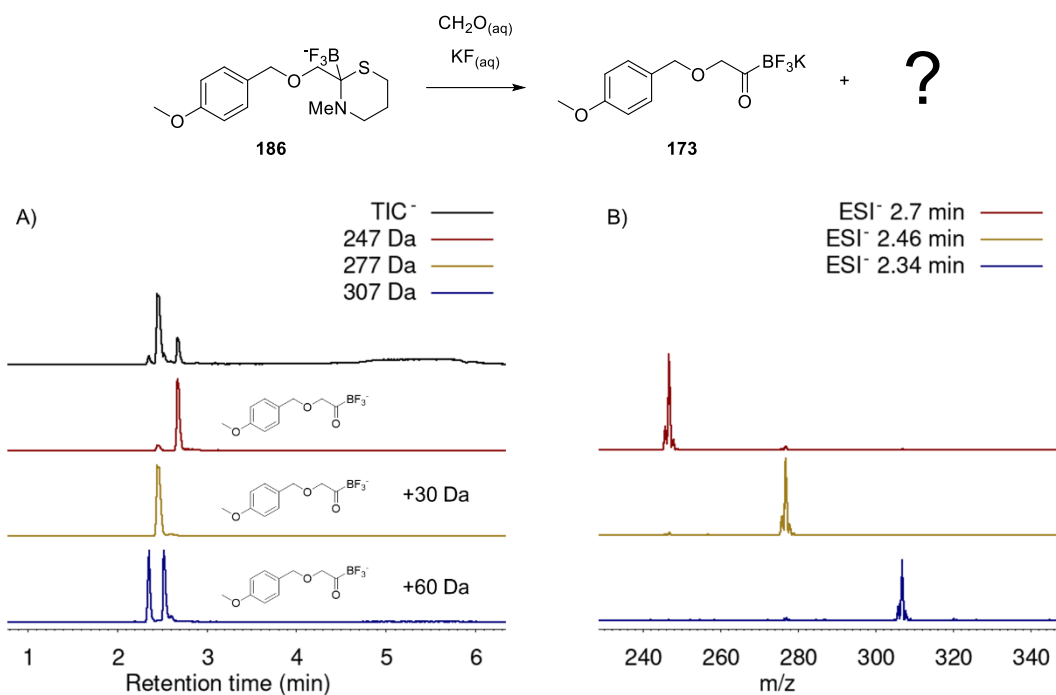
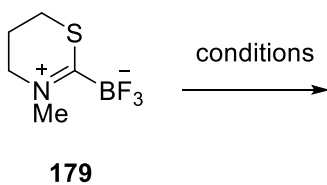


Figure 42. Byproduct formation from intermediate **186** when treated with formaldehyde for prolonged time. **186** shows up at retention time 2.7 min, with $m/z = 247$ Da. Peaks with 277 Da appear at 2.46 min, and 307 Da appear at 2.34 min. Only α -alkoxy KATs exhibit this behavior.

5.3.3. Reactivity towards other organometallics or radical sources

Reagents and conditions under which **179** was treated with and gave no conversion was summarized below in **Table 10**. We hoped that the ability of reagent **179** to stabilize the tetrahedral adduct will allow it to react with other organometallic reagents and form KATs, under harsher conditions where reagent **1** only gives a mixture containing double addition products (entries 1–6). We were also constantly interested in the possibility of generating KATs from alkyl radicals (entries 8–9). Unfortunately, reagent **179** only reacted with alkyllithiums so far.

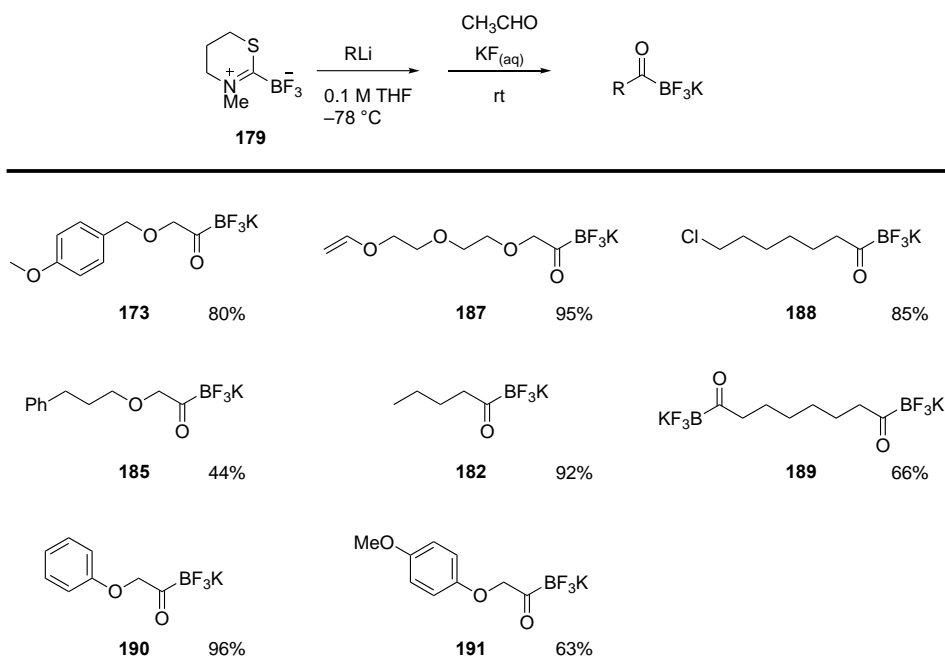


	Conditions	Outcome
1	iPrMgCl, THF, -78°C	N.R.
2	iPrMgCl, THF, rt	Trace amount of double addition.
3	EtMgBr, -78 °C	N.R.
4	ZnEt ₂ neat, rt	N.R.
5	ZnEt ₂ , ZnCl ₂ , rt	N.R.
6	Allyl iodide, In(0)	N.R.
7	MeLi, -78°C	Mono-addition
8	Benzoyl peroxide, CD ₃ Cl	N.R.
9	Benzoyl peroxide, PhMe, reflux	N.R.

Table 10. Miscellaneous reaction conditions used to activate reagent **179**

5.3.4. Alkyl di-KATs, potential α -leaving group KATs, and JQ1-TEG-KAT

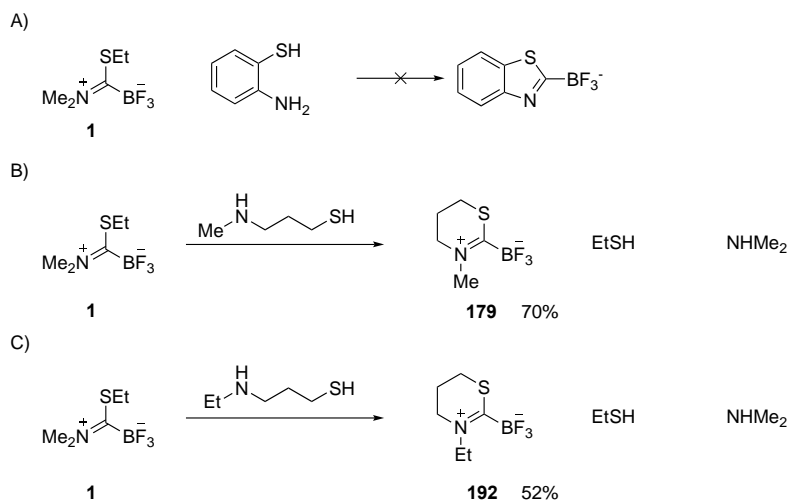
The ability of **179** to directly trap an alkyllithium and form the corresponding KAT has enabled the synthesis of some KATs that were otherwise hard to obtain. These include α -alkoxy, α -phenoxy and alkyl di-KATs as listed below.



Scheme 78. Scope of KATs synthesized from reagent **179**.

5.4. Alternative synthesis of **179** and its more soluble N-ethyl variant

We have previously tried to substitute the amine and thiols of **1**, by reacting **1** directly with thioaniline (**Scheme 79A**), but did not obtain the desired product.¹⁵² We were pleased to find that, on the contrary, reaction between **1** and N-methylaminopropanthiol gave **179** smoothly. This gave an expedient alternate synthesis of **179**, since reagent **1** is now commercially available, and is purchased by our group in decagram quantities. The yield of **179** from this amine-thiol substitution route is comparable with the original procedure described in section 5.3. An N-ethyl variant can also be prepared through the same strategy with N-ethylaminopropanethiol. The N-ethyl variant **192** was more soluble in organic solvents and dissolves up to 0.2 M in THF at -78°C , whereas **179** dissolves no more than 0.05 M in THF under room temperature. The handling and usage of **192** was therefore less problematic since it is easier to transfer and prepare a homogenous reaction mixture. The yield of KAT synthesis with **192** was essentially the same with that obtained from **179**.

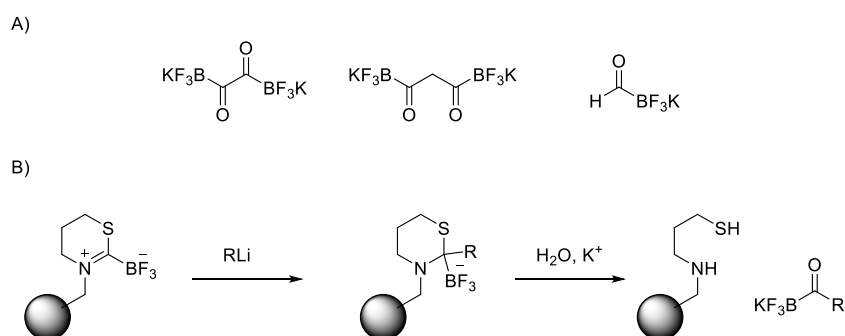


Scheme 79. Alternative synthesis of reagent **179** and **192** from commercially available **1**.

5.5. Summary

A class of N–S tethered cyclic KAT reagent, **179** and **192** was designed to avoid the double addition problem of alkyl KAT synthesis and enabled access to α -alkoxy KATs in satisfying yields. With alkyllithiums, these reagents form a cyclic thioaminal structure which stabilized the intermediate during KAT synthesis, and required a modified work-up procedure that traps the thioamine byproduct, to release the KAT.

It would be interesting to see if some minimalistic KATs and di-KATs might also be accessible from reagent **179** in the future, from alkyldilithium addition, hydride reduction or single electron reduction (**Scheme 80B**). The N-alkyl may also serve as a handle to place the aminothiol part of the KAT reagent on a solid support (**Scheme 80B**), which will greatly simplify the workup and purification of KAT synthesis.



Scheme 80. Further possible developments basing on reagent **179**

6

Brief journey with other KATs

This chapter aims to summarize some other findings in KAT chemistry that could not be developed into independent chapters.

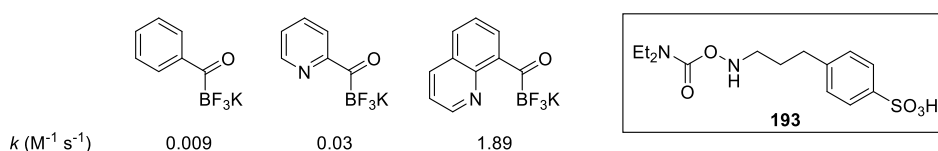
請硬朗地戰鬥去罷。至於我，這失敗的一生，也該有個結束。
Do fight on gallantly. As for me, my lifelong failure, should now end.

陳映真·山路 / YingZhen Chen – Mountain Road

6.1. The role of a proton donor neighbor on KAT ligation rates

6.1.1. Basicity of pyridine and quinoline KATs

During the investigation of KAT ligation rate we discovered that a nearby protonation site can enhance KAT ligation rate drastically.³⁵ **Scheme 81** shows a representative collection of KAT ligation rate constants measured in aqueous CH₃CN buffered at pH 7.4. Quinoline KAT was found to ligate 60 times faster than pyridine KAT under these conditions. This was contradictory to our first instinct, which says that pyridines (pK_a 5.2) should be more basic than quinolines (pK_a 4.9) and serve as a more populated intramolecular proton donor at pH 7.4. We performed acid-base titrations to help decipher this seemingly inverted trend of KAT ligation rates and KAT basicity. To our surprise, we found quinoline KAT to be one pK_a unit more basic than pyridine KAT in aqueous CH₃CN, as shown in **Figure 43**. In the crystal structure the KAT group was found to be interacting with the proton, possibly contributing to the observed, unexpectedly higher basicity (**Figure 44**).



Scheme 81. KAT ligation rate constants of phenyl, 2-pyridyl, and 8-quinolyl KATs with hydroxylamine **193** in aqueous acetonitrile at pH 7.4.

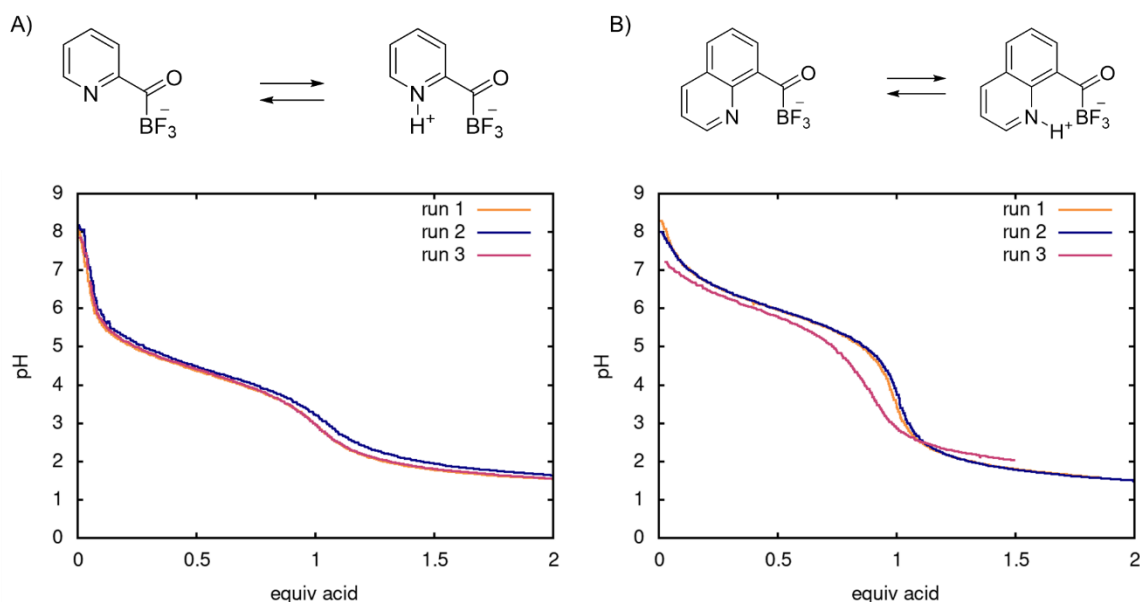
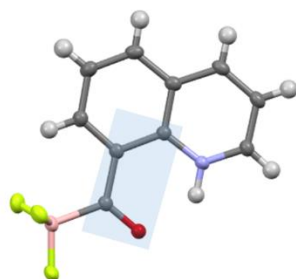


Figure 43. Acid titration curve shows that **A)** pyridine KAT has a conjugate acid pK_a of 4.41 and **B)** quinoline KAT to that of 5.89. The titration was performed in 1:1 CH₃CN-H₂O, with concentration 0.1 M.

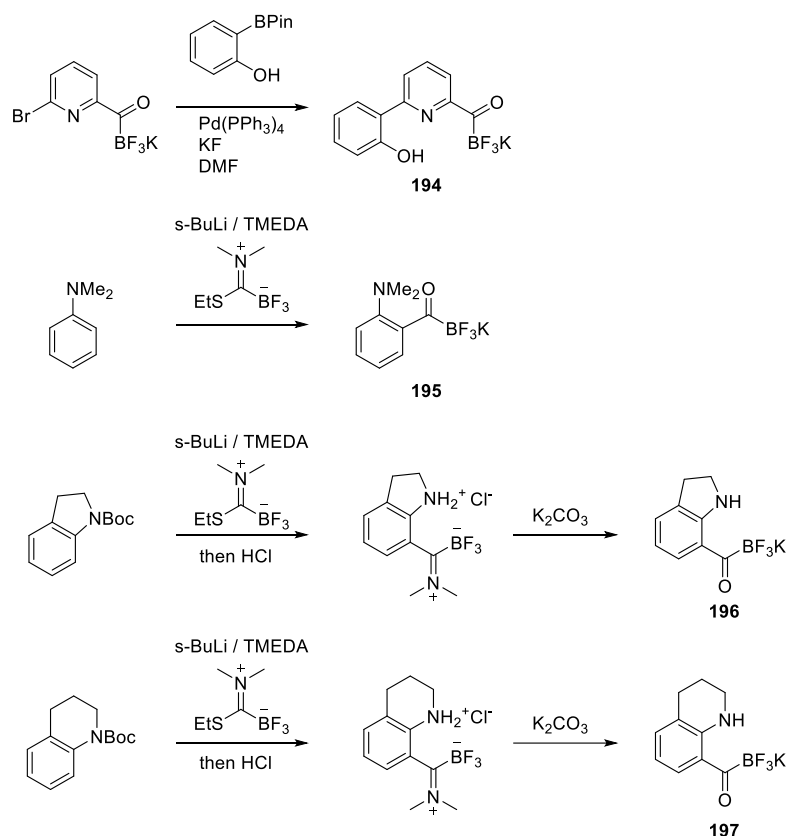


O-C-C-C dihedral angle: -6.48°

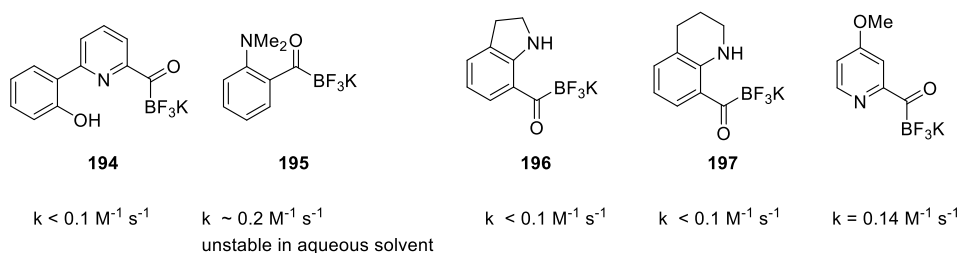
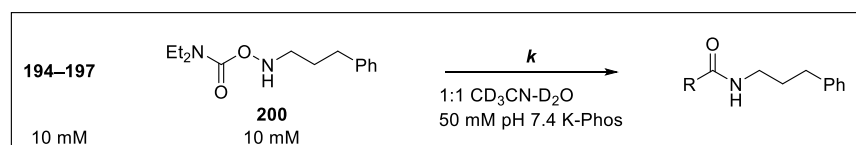
Figure 44. X-ray diffraction structure of quinoline KAT crystallized with 2 equiv of HCl. The proton is in interaction with both the quinoline nitrogen and the KAT carbonyl. The KAT group was fixed in a coplanar conformation with the quinoline ring.

6.1.2. Synthesis of KATs bearing proton donors

With the hypothesis that a nearby proton could accelerate the rate of KAT ligation, we went on to synthesize KATs with built-in proton donor, like **194** with a hydroxyphenyl group, or with a sp^3 hybridized nitrogen heteroatom like **195**, **196**, and **197**. **194** was synthesized through a Suzuki coupling of 6-bromo-pyridyl-2-KAT and 2-hydroxyphenyl boronic acid pinacol ester. KATs **195**, **196**, and **197** were synthesized through lithiation guided by the nitrogen or the tert-butyl carbamate group (**Scheme 82**). None of these KATs ligated significantly faster than known pyridyl KATs. The fastest among them was **195**, with a second order rate constant of $\sim 0.2 \text{ M}^{-1}\text{s}^{-1}$, but it proved to be unstable in aqueous solution (**Scheme 83**). The N,N-dimethyl TIM intermediates in the synthesis of **196** and **197** were remarkably stable towards hydrolysis and additional bases were required to obtain the KAT. The X-ray diffraction structure of **194** and the N,N-dimethylamino TIM of **196** were depicted in **Figure 45**.



Scheme 82. Synthesis of KATs **194–197** with proton donors in proximity.



Scheme 83. The KAT ligation 2nd order rate constants of KATs **194 – 197** reacting with hydroxylamine **200**. Rate constants were measured in 1:1 CD₃CN-D₂O 50 mM potassium phosphate buffer at pH 7.4. The rate constant of 4-methoxy-2-pyridyl KAT ligating with **200** was shown as a reference.

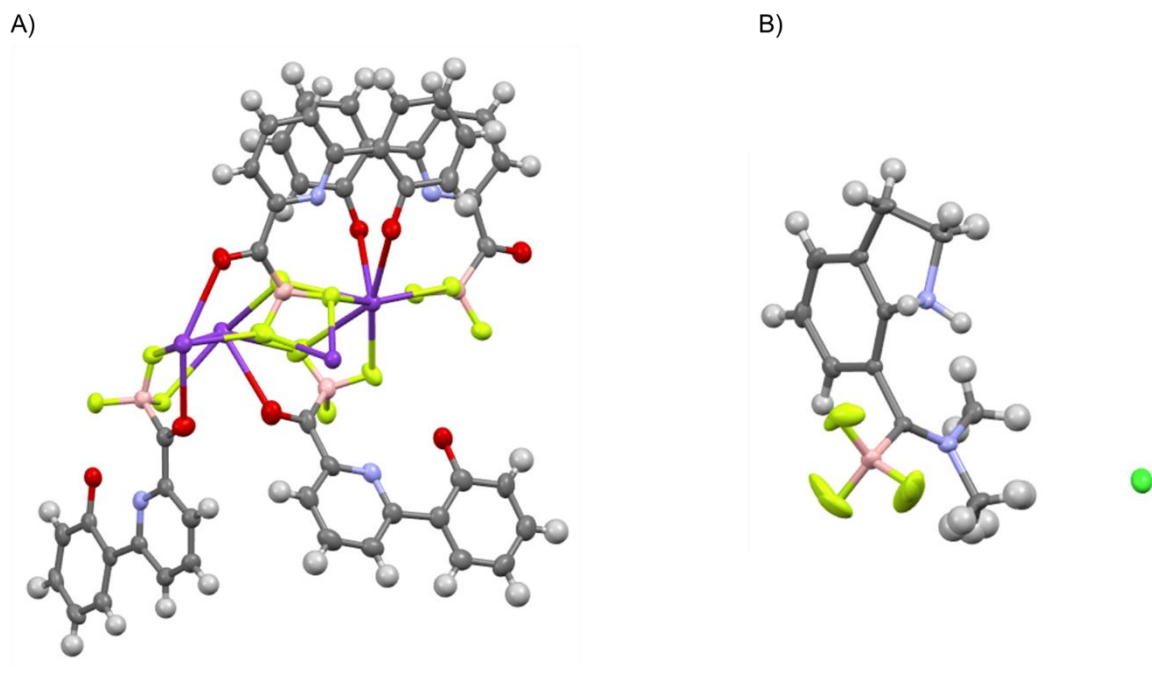


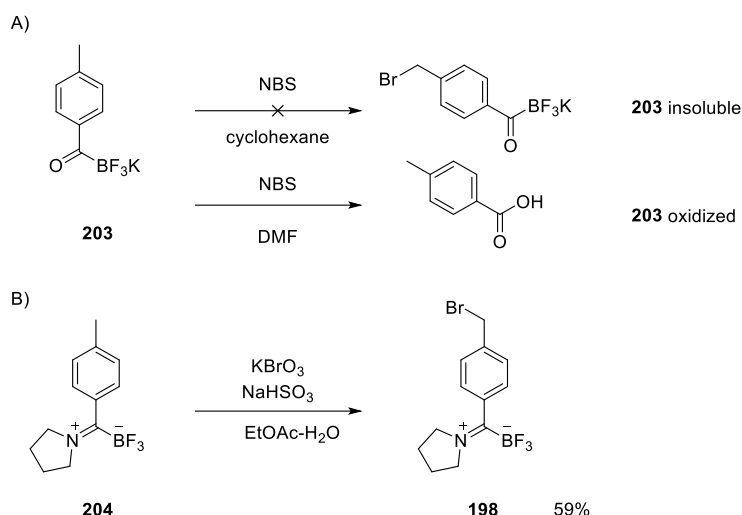
Figure 45. X-ray diffraction crystal structure of **A) KAT 194** and **B) N,N-dimethyl TIM of KAT 196 with HCl**

6.2. Synthesis of KATs and hydroxylamines for incorporation in polymers

This section describes the synthesis of bromomethyl KATs and styryl KATs, which were the preliminary studies paving way to the incorporation of KATs to polymer building blocks.³⁴

6.2.1. Bromomethylphenyl KATs

Installing an electrophilic handle on a KAT is essential for countless potential applications of KATs, unfortunately a naive bromination of a p-methylbenzoyl KAT **203** did not result in the desired benzyl bromide. Conditions for radical bromination did not employ solvents that could dissolve KATs, while bromination reagents such as NBS oxidize the KAT functional group in polar aprotic solvents that dissolve KATs. Fortunately, we found that TIM **204** could be brominated, in a biphasic condition that generates bromine radical by gradual reduction of potassium bromate,¹⁷⁷ to give the bromomethyl TIM **198**. It was later found that the benzylic position of **204** can also be selectively brominated by NBS in acetonitrile.¹⁷⁸ The TIM acts both as a solubilizing group and a protection group for KATs in this context.

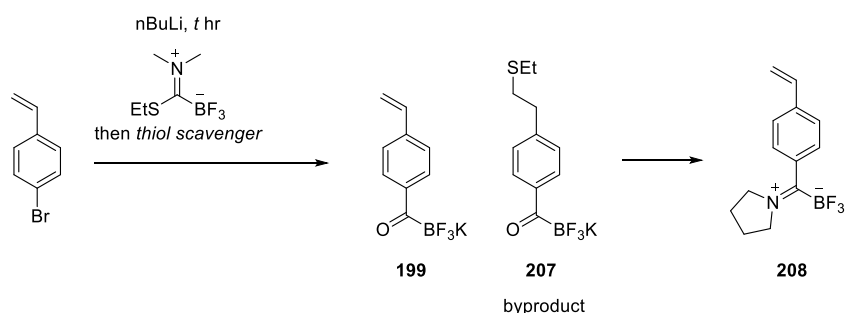


Scheme 84. A: Bromination at benzylic position on KATs is difficult but **B:** can occur on TIMs

6.2.2. KATs with polymerizable groups

Some of the works in this section were done with the help of Maria Reichenbach during her semester project in the Bode group.

We set out to design a KAT that could be incorporated in a polymer, for example, polystyrene. A logical polystyrene monomer with a KAT group would be KAT **199**, or its pyrrolidine TIM form **208**. The synthesis of styryl KAT **199** from the KAT reagent route required extensive modification from the general procedure. Lithiation of p-bromostyrene required longer time at $-78\text{ }^{\circ}\text{C}$, and a thiol scavenger was necessary to prevent the ethylthiol work-up product from adding to the styryl double bond. Methyl vinyl ketone was found to be suitable for this purpose. The product KAT **199** can be converted to a pyrrolidine TIM for chromatographic purification or ATRP polymerization.



Scheme 85. The synthesis of styryl KAT by the KAT reagent suffers from a thiol adduct byproduct that was generated during work-up.

Lithiation duration	Thiol scavenger	Outcome
0 (in situ lithiation)	-	Styryl bromide mostly remained Forming 207
2 hr	-	Less styryl bromide remaining Forming 207
3.5 hr	AgNO ₃	Lithiation complete 207 formation reduced Crude mixture polymerized
3.5 hr	Methyl vinyl ketone	Mostly 199 . 65% yield.

Table 11. Condition optimization for the synthesis of styryl KAT **199**.

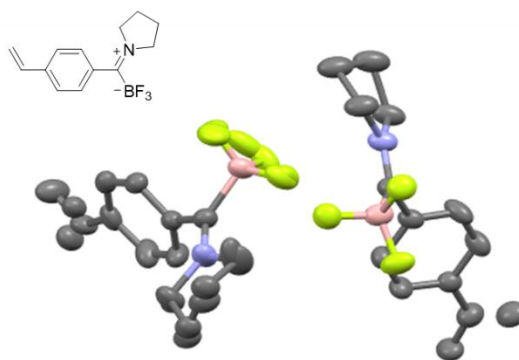
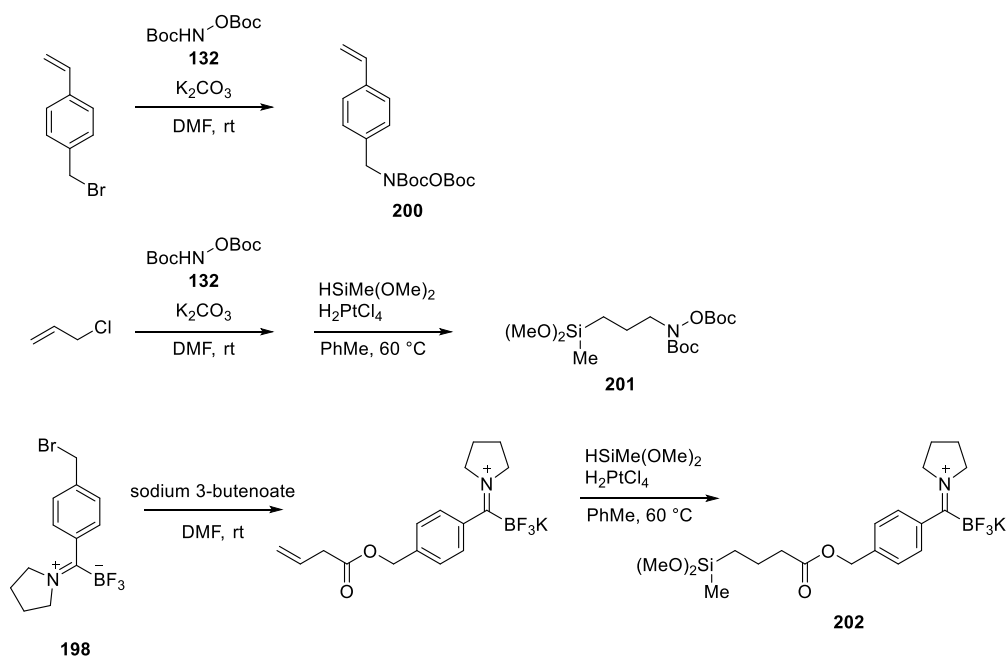


Figure 46. Crystal structure of the TIM **208**. The terminal vinyl carbon position is in disorder.

A hydroxylamine **200** for polystyrene incorporation was also synthesized. Hydroxylamine **201** and TIM **202** bearing a methyldimethoxysilyl group at the terminal were also synthesized as possible PDMS monomers with the sequence shown in **Scheme 86**.



Scheme 86. Other KAT and hydroxylamine derivatives synthesized with polymerizable group in this project.

7

Experimental section

... mia chimica impastata di puzze, scoppi e piccolo misteri futili

– Potassio, Il Systema Periodico, Primo Levi

7.1. Synthetic procedures and characterization of compounds

7.1.1. General Procedural information

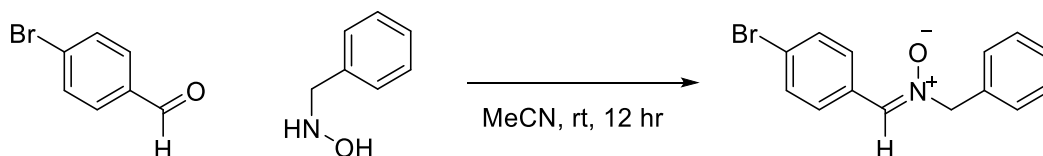
All reactions were carried out in over-dried glassware and were stirred with Teflon-coated magnetic stir bars unless specified otherwise. Air- or moisture-sensitive reactions were conducted in dry glassware sealed with a rubber septum under nitrogen atmosphere. Thin layer chromatography (TLC) was performed on glass backed plates pre-coated with silica gel (Merck, Silica Gel 60 F254) which were visualized by fluorescence quenching under UV light or by staining with KMnO_4 solutions. Flash column chromatography was performed on Silicycle Silica Flash F60 (230–400 Mesh) using a forced flow of air at 0.4 bar. Internal volume (V_{int}) of flash silica columns were measured by the volume of solvent taken up during column packing. Eluent ratios were recorded in volume-volume ratios. Cyclohexane, CH_2Cl_2 , and EtOAc were distilled before use. THF for reactions involving organometallic reagents were distilled from Na-fluorenone ketyl before use. N,N-diisopropylamine was distilled from CaH_2 and stored under N_2 before use. LC-MS was performed either on a Dionex UltiMate 3000 RSLC connected to a Surveyor MSQ Plus mass spectrometer, or on a Waters H-class Acuity HPLC connected to a SQ detector 2. Some KAT reagent **1** was provided by Eli Lilly through a collaboration, and was purified by column chromatography (CHCl_3) before use. Synthetic reagents were not purified unless stated in the procedure.

7.1.2. Synthesis of nitrones and amidoxime in Chapter 2

General procedure for the preparation of a KAT nitrone

The KAT (0.2 mmol) and the hydroxylamine hydrochloride (0.2 mmol) were dissolved in 2 mL 1:1 DMF- H_2O and stirred at room temperature. The reaction progress was monitored by LCMS analysis of a portion of the reaction mixture, diluted 200 fold with 1:1 CH_3CN -MeOH. After the desired reaction time the solvent was either evaporated or removed by N_2 purge. Purification was carried out by chromatography on silica, or precipitation from Et_2O .

Preparation of nitrone from N-benzyl hydroxylamine and benzaldehyde

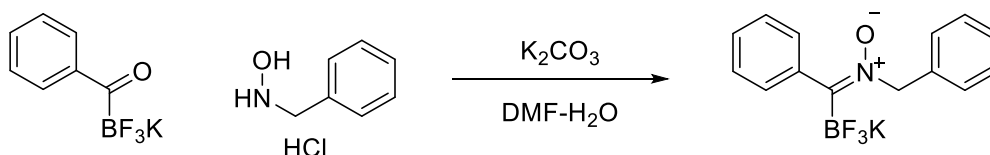


N-benzylhydroxylamine (42.5 mg, 345 μmol , 1.0 equiv) and 4-bromobenzaldehyde (102.4 mg, 553 μmol , 1.6 equiv) were dissolved in CH_3CN (1.5 mL) and stirred for 12 hr at 23 $^\circ\text{C}$, after which TLC and ^1H NMR indicated consumption of the hydroxylamine. The solvent was evaporated and the residue was chromatographed on silica (Eluent: 1/3 EtOAc/Cy) to give a

white solid as the product (12.2mg, 42.0 μmol , 12.2%). The spectroscopic signals were in agreement with previous reports.¹⁷⁹

$^1\text{H NMR}$ (400 MHz, CDCl_3): δ [ppm] = 8.09 (d, J = 8.7 Hz, 2H), 7.52 (d, J = 8.7 Hz, 2H), 7.49–7.38 (m, 5H), 7.35 (s, 1H), 5.04 (s, 2H); **$^{13}\text{C NMR}$** (100 MHz, CDCl_3): δ [ppm] = 133.26, 133.09, 131.83, 130.03, 129.44, 129.42, 129.26, 129.18, 124.41, 71.56.

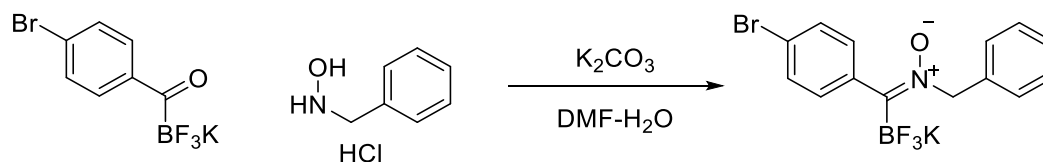
Nitrone from N-benzyl hydroxylamine and phenyl KAT



Phenyl KAT (50.0 mg, 236 μmol , 1 equiv), N-benzylhydroxylamine hydrochloride (38.2 mg, 239 μmol , 1.01 equiv), and K_2CO_3 (16.4 mg, 119 μmol , 0.50 equiv) were dissolved in 2 mL 1:1 DMF- H_2O and stirred at 23 $^\circ\text{C}$ for 12 hr before the solvents were evaporated. The residue was chromatographed on a silica column packed in 1:1 cyclohexane-acetone. Chromatography: V_{int} 25 mL, eluents: 20 mL 1:1 cyclohexane:acetone, 100 mL 2:1 cyclohexane:acetone into fractions 1–12, among which fractions 3–6 contained the product, and was evaporated to give the nitrone as a clear oil.

$^1\text{H NMR}$ (400 MHz, CD_3OD): δ [ppm] = 7.67 – 7.52 (m, 2H), 7.49 – 7.25 (m, 8H), 5.39 (s, 2H); **$^{19}\text{F NMR}$** (377 MHz, CD_3OD): δ [ppm] = -140.60 (q, J = 38.4 Hz); **$^{11}\text{B NMR}$** (128 MHz, CD_3OD) δ 0.26 (q, J = 38.9 Hz); **IR** (v/cm^{-1} , neat ATR): 3069, 3036, 1658, 1459, 1297, 1055, 1032, 922, 905, 886, 751, 701; **HRMS(ESI)**: calcd for $\text{C}_{14}\text{H}_{12}\text{BF}_3\text{NOK}$ (M-K): 278.0970, found 278.0972.

Nitrone (100) from N-benzyl hydroxylamine and phenyl KAT

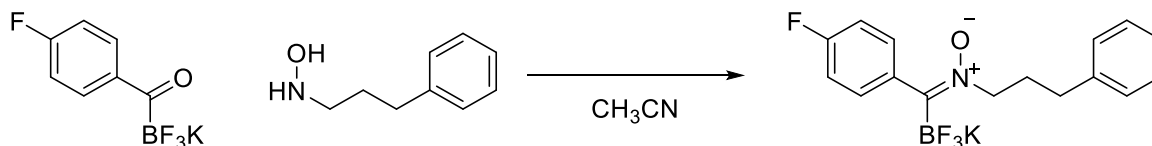


p-Bromophenyl KAT (89 mg, 307 μmol , 1 equiv), N-benzylhydroxylamine hydrochloride (51.3 mg, 321 μmol , 1.05 equiv), and K_2CO_3 (23.5 mg, 170 μmol , 0.55 equiv) were dissolved in 3 mL 1:1 DMF- H_2O . The yellow color of the KAT in solution vanishes in ~ 2 min. The reaction mixture was stirred at 23 $^\circ\text{C}$ for 12 hr before being evaporated. The residue was chromatographed on a silica column packed in 1:1 cyclohexane-acetone. **Chromatography:** V_{int} 23.5 mL, eluents: 29 mL 1:1 cyclohexane:acetone, 100 mL 2:1 cyclohexane:acetone into

fractions 1–12, among which fractions 7–12 contained the product and was evaporated to give **100** as a clear oil.

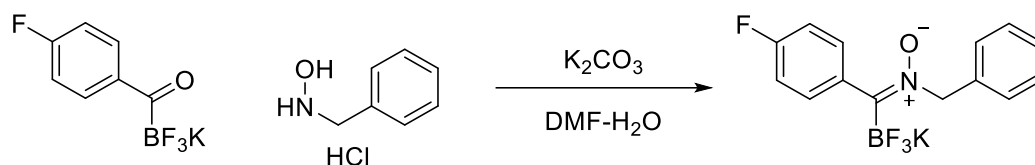
¹H NMR (400 MHz, DMSO-d₆): δ [ppm] = 7.49 – 7.45 (m, 2H), 7.43 – 7.39 (m, 2H), 7.37 – 7.31 (m, 4H), 7.27 (M, 1H), 5.13 (s, 2H). **¹³C NMR** (150 MHz, DMSO-d₆): δ [ppm] = 154.97 (br), 138.80, 137.34, 131.80, 129.92, 129.17, 128.28, 127.52, 119.29, 65.62 (q, J = 3.4 Hz). **¹⁹F NMR** (376 MHz, DMSO-d₆): δ [ppm] = -133.79 (br, s); **¹¹B NMR** (128 MHz, DMSO-d₆): δ [ppm] = 1.60 (br, s); **IR** (ν/cm⁻¹, ATR/CD₃OD dried film): 3110, 3088, 3063, 3032, 3008, 2966, 2941, 2847, 1718, 1635, 1589, 1565, 1540, 1483, 1454, 1396, 1357, 1300, 1279, 1244, 1197, 1172, 1130, 1104, 1069, 1029, 1010, 985, 924, 902, 882, 864, 835, 796, 754, 723, 700, 672, 637, 552, 519; **HRMS**(ESI): calcd for C₁₄H₁₁BBrF₃NOK (M-K⁻): 356.0075, found 356.0076. **Elemental analysis**: Calc 42.46% C, 2.80%H, 3.54% N, found 42.45% C, 2.73%H, 3.82%N.

KAT Nitron (102) from N-propylphenyl hydroxylamine and p-fluorophenyl KAT



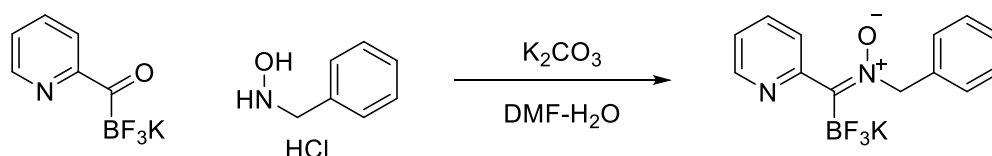
p-fluorophenyl KAT (198.8 mg, 864.3 μmol, 1 equiv) and N-(3-phenylpropyl)-hydroxylamine (263 mg, 1.74 mmol, 2.01 equiv) were dissolved CH₃CN (2 mL) and left to stand overnight. The solvent was evaporated and the residue was chromatographed on silica. The residue was chromatographed on a silica column (Φ 2.5 cm, l 11.5 cm) packed in 10:90:1 MeOH-CHCl₃-Et₃N. Chromatography: V_{int} 50 mL, eluents: 50 mL 10:90:1 MeOH-CHCl₃-Et₃N, 100 mL 14:90 MeOH-CHCl₃ into fractions 1–27, among which fractions 9–25 contained the product.

¹H NMR (400 MHz, CD₃CN): δ [ppm] = δ 7.42 – 7.34 (m, 2H), 7.34 – 7.27 (m, 2H), 7.25 – 7.18 (m, 3H), 7.13 (t, J = 9.0 Hz, 2H), 4.19 – 4.09 (m, 2H), 2.75 – 2.61 (m, 2H), 2.23 – 2.07 (m, 2H); **¹³C NMR** (100 MHz, CD₃CN) δ [ppm] = 181.75 – 177.08 (m)_z, 165.07, 162.61, 142.16, 131.76(d, J = 3.3 Hz), 131.21 (d, J = 8.6 Hz), 129.41 (d, J = 3.4 Hz), 127.08, 118.38, 115.75, 115.53, 60.89 (q, J = 3.4 Hz), 33.19, 30.21; **¹⁹F NMR** (377 MHz, CD₃CN) : δ [ppm] = -140.05 (q, J = 37.0 Hz); **¹¹B NMR** (128 MHz, CD₃CN) : δ [ppm] = -1.00 (q, J = 52.8 Hz); **IR** (ν/cm⁻¹, KBr pellet): 3419 (br), 3220(br), 3027, 2962, 2929, 2864, 1664, 1636, 1605, 1566, 1502, 1455, 1412, 1241, 1158, 1112, 1079, 1063, 1020, 993, 956, 827, 745, 698, 598; **HRMS**(ESI): calcd for calcd for C₁₆H₁₅BF₄NOK (M-K⁻): 324.1191, found 324.1188.

Nitrone (111) from N-Benzyl hydroxylamine with p-fluorophenyl KAT

p-fluorophenyl KAT was used, following the procedure for nitrone **102** to obtain nitrone **111** as a white powder (73.2%, mp 227.7-231.7 dec).

¹H NMR (400 MHz, DMSO-d₆) δ 7.49 – 7.41 (m, 4H), 7.37 – 7.24 (m, 3H), 7.03 (m, 2H), 5.12 (s, 2H, major isomer CH₂), 4.66 (m, 0.2H, minor isomer CH₂). **¹³C NMR** (151 MHz, DMSO-d₆) δ 160.87 (d, J = 242.5 Hz), 155.07 (br, s), 137.47, 135.66 (d, J = 3.2 Hz), 131.66 (d, J = 7.7 Hz), 129.17, 128.27, 127.49, 115.25 (d, J = 21.3 Hz, minor isomer), 113.68 (d, J = 20.9 Hz, major isomer), 65.58 (d, J = 3.4 Hz, major isomer), 64.55 (s, minor isomer). **¹⁹F NMR** (377 MHz, DMSO-d₆) δ -133.23 (major isomer), -138.23 (minor isomer). **¹¹B NMR** (128 MHz, DMSO-d₆) δ 0.24 – -2.32 (m). **IR** (ATR, cm⁻¹): 3072, 3046, 2960, 1604, 1552, 1506, 1454, 1401, 1282, 1214, 1155, 1131, 1091, 1041, 1012, 979, 939, 907, 884, 857, 833, 804, 781, 749, 707, 665, 638, 612, 586, 536, 514. **HRMS** (ESI): calcd for C₁₄H₁₁BF₄NO (M-K⁻): 296.0875, found: 296.0878

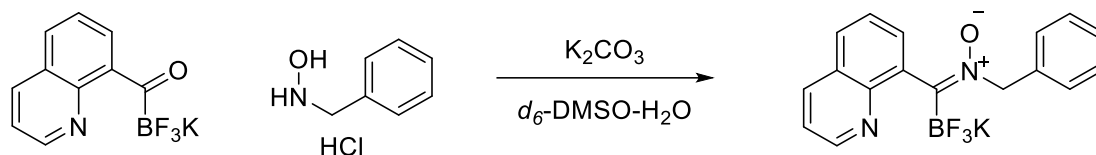
Nitrone (105) from N-Benzyl hydroxylamine with Pyridyl KAT

Pyridyl KAT (8.1 mg, 38 μmol, 1 equiv) and N-benzylhydroxylamine hydrochloride (23.7 mg, 148.5 μmol, 3.9 equiv), and K₂CO₃ (9.7 mg, 70 μmol, 1.85 equiv) were dissolved in 2 mL 1:1 DMF-H₂O and evaporated immediately. The mixture was dried under vacuum overnight before being dissolved in 4 mL 10% MeOH/CHCl₃ and filtered with 5 μm PVDF filter. The filtrate was evaporated down to 1 mL, precipitated with 15 mL Et₂O. The precipitated was collected by centrifugation (7500 rpm, 20 min), and reprecipitated twice more before being dried under vacuum overnight to give the product as an oil (7 mg, 22 μmol, 58%).

¹H NMR (600 MHz, DMSO-d₆): δ [ppm] = 8.47 (ddd, J = 4.8, 1.7, 0.9 Hz, 1H), 7.64 (td, J = 7.7, 1.9 Hz, 1H), 7.58 – 7.45 (m, 2H), 7.39 – 7.33 (m, 2H), 7.32 – 7.28 (m, 1H), 7.18 – 7.10 (m, 2H), 5.13 (s, 2H); **¹³C NMR**: (151 MHz, DMSO-d₆): δ [ppm] = 158.83, 156.46 (br, s), 148.16, 136.55, 134.91, 128.89, 127.82, 127.14, 123.24, 120.86, 64.83; **¹⁹F NMR** (377 MHz, DMSO-d₆): δ [ppm] = -134.81 (s); **¹¹B NMR** (128 MHz, DMSO-d₆): δ [ppm] = 0.86 (s); **IR** (ATR, cm⁻¹

¹): 3096, 3068, 3032, 1586, 1536, 1427, 1191, 1124, 1087, 1040, 1010, 983, 958, 909, 887, 781, 750, 721, 694, 679, 632, 618, 546; **HRMS** (ESI): calcd for C₁₃H₁₂BF₃N₂OK (M-K⁻): 279.0922, found: 279.0929.

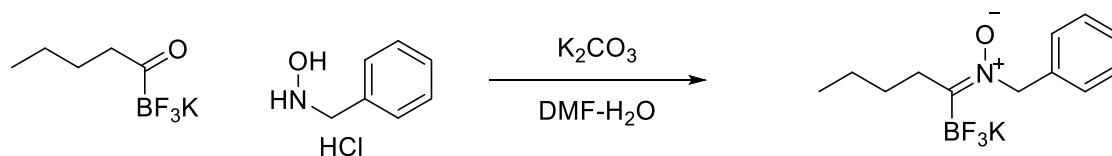
Nitrone (107) from N-Benzyl hydroxylamine with Quinolyl KAT



Quinoline KAT (10.1 mg, 38.4 μ mol, 1 equiv), N-benzylhydroxylamine hydrochloride (15.8mg, 99 μ mol, 2.58 equiv), and was dissolved in 1:1 DMF-H₂O (1 mL) and evaporated. The residue was dried in vacuum, dissolved in 1:10 MeOH-CHCl₃ and filtered. After three times reprecipitation with Et₂O (8 mL), the product was obtained as a hygroscopic wax (9 mg, 24.4 μ mol, 63.5%)

¹H NMR (400 MHz, DMSO-d₆) δ [ppm] = 8.86 (dd, J = 4.1, 1.8 Hz, 1H), 8.28 (dd, J = 8.3, 1.8 Hz, 1H), 7.78 (dd, J = 8.2, 1.5 Hz, 1H), 7.69 – 7.63 (m, 2H), 7.52 (dd, J = 8.1, 7.0 Hz, 1H), 7.46 (dd, J = 8.2, 4.1 Hz, 1H), 7.41 – 7.21 (m, 4H), 5.31 (d, J = 13.1 Hz, 1H), 5.19 (d, J = 13.1 Hz, 1H); **¹³C NMR** (151 MHz, DMSO) δ 157.75, 149.12, 145.80, 140.81, 137.32, 135.66, 128.54, 127.66, 127.11, 126.64, 125.86, 125.63, 120.65, 113.18 (d, J = 20.9 Hz), 64.60 (d, J = 2.9 Hz); **¹⁹F NMR** (376 MHz, DMSO-d₆) δ -135.55. **¹¹B NMR** (128 MHz, DMSO-d₆) δ 1.77; **IR** (ATR, neat): 3062, 3035, 2972, 1662, 1595, 1553, 1497, 1454, 1388, 1366, 1314, 1281, 1259, 1230, 1197, 1157, 1131, 1108, 1039, 1010, 921, 894, 829, 799, 743, 709, 663, 618, 587, 541, 516; **HRMS** (ESI): calcd for C₁₇H₁₃BF₃N₂OK (M-K⁻): 329.1079, found: 329.1083.

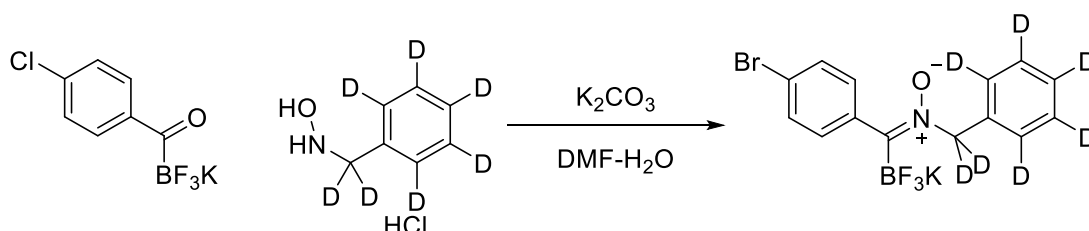
KAT nitrone formation in NMR sample without isolation of the nitrone Nitrone (99) from N-Benzyl hydroxylamine with Butyl KAT



A solution of butyl KAT in DMSO-d₆ (61.4 mM, 195.5 μ L, 1 equiv) was mixed with a solution of N-benzylhydroxylamine (DMSO-d₆, 351.3 mM, 22.2 μ L, 0.650 equiv), DMSO-d₆ (82.3 μ L), and D₂O (300 μ L). The conversion of the hydroxylamine was > 66% after 20 min, and complete after 70 min according to ¹H NMR monitoring. **¹H NMR** (400 MHz, 1:1 DMSO-d₆-D₂O): δ [ppm] = 7.38 – 7.12 (m, 5H), 4.90 (s, 2H), 2.29 (td, J = 7.7, 4.6 Hz, 2H), 1.37 – 1.20 (m, 4H), 0.85 – 0.60 (m, 3H). **¹⁹F NMR** (377 MHz, 1:1 DMSO-d₆-D₂O) : δ [ppm] = -135.55

(br); **IR** (ATR, neat): 2957, 2931, 2871, 1653, 1636, 1604, 1568, 1497, 1465, 1455, 1418, 1404, 1378, 1361, 1320, 1308, 1296, 1263, 1241, 1196, 1159, 1106, 1077, 1015, 936, 881, 837, 810, 780, 754, 733, 720, 697, 673, 660, 646, 630, 619, 606, 593, 577, 564, 547, 536, 524, 511; **HRMS**(ESI): calcd for $C_{12}H_{16}BF_3NOK$ (M-K⁻): 258.1283, found: 258.1285.

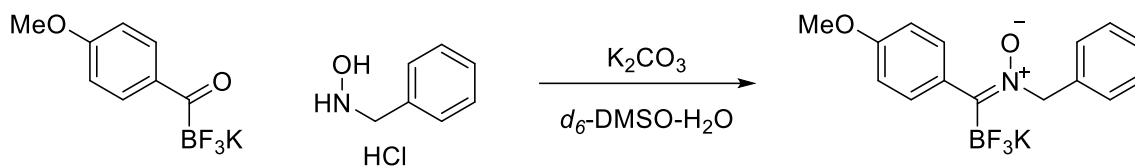
Nitrone (112) from d7-N-Benzyl hydroxylamine with p-chlorophenyl KAT



p-chlorophenyl KAT and d7-N-benzylhydroxylamine hydrochloride was used, following the procedure for nitrone **102** to obtain nitrone **112** as a white powder.

¹H NMR (400 MHz, DMSO-*d*₆) δ 7.43 (d, *J* = 8.4 Hz, 2H), 7.29 (d, *J* = 8.6 Hz, 2H); **¹³C NMR** (151 MHz, DMSO-*d*₆) δ 155.00, 138.36, 137.07, 131.47, 130.67, 129.92, 129.09 – 128.56 (m), 128.05 – 127.52 (m), 126.97, 65.30 – 64.51 (m); **¹⁹F NMR** (377 MHz, DMSO-*d*₆) δ -133.83 (br), -139.44 (minor isomer). **¹¹B NMR** (128 MHz, DMSO-*d*₆) δ 0.69 – -2.62 (m); **IR** (ATR, neat): 3092, 1666, 1595, 1550, 1488, 1396, 1329, 1299, 1280, 1225, 1176, 1133, 1113, 1081, 1042, 1007, 970, 941, 913, 899, 843, 821, 798, 777, 728, 710, 657, 636, 623, 601, 582, 549, 509; **HRMS** (ESI⁺): calcd for $C_{14}H_4BCIF_3NOD_7$: 319.1019, found 319.1019.

Nitrone (109) from N-Benzyl hydroxylamine with p-methoxyphenyl KAT



A solution of p-methoxyphenyl KAT in DMSO-*d*₆ (54.2 mM, 161.36 μL, 1 equiv) was mixed with a solution of N-benzylhydroxylamine (DMSO-*d*₆, 351.3 mM, 17.1 μL, 0.687 equiv), DMSO-*d*₆ (121.7 μL), and D₂O (300 μL). **H NMR** (400 MHz, 1:1 DMSO-*d*₆-D₂O) : δ [ppm] = 7.40 – 7.34 (m, 2H), 7.34 – 7.26 (m, 3H), 7.24 – 7.16 (m, 2H), 6.85 – 6.80 (m, 2H), 5.08 (s, 2H), 3.69 (s, 3H); **¹³C NMR** (151 MHz, DMSO-*d*₆): δ 155.61, 137.77, 131.62, 131.19, 129.15, 128.52, 128.18, 127.33, 113.72, 112.24, 65.52 (q, *J* = 3.5 Hz); **¹⁹F NMR** (377 MHz, 1:1 DMSO-*d*₆-D₂O) : δ [ppm] = -134.44; **IR** (ATR, neat): 3295, 3087, 3035, 2963, 1739, 1605, 1573, 1542, 1510, 1456, 1304, 1275, 1247, 1172, 1117, 1098, 1019, 972, 939, 907, 885, 838, 793, 733,

704, 665, 640, 618, 589, 553, 516; **HRMS** (ESI): calcd for $C_{15}H_{14}BF_3NO_2K$ (M-K⁻): 308.1075, found: 308.1081.

Formation of amidoxime byproduct (110) from N-benzyl hydroxylamine



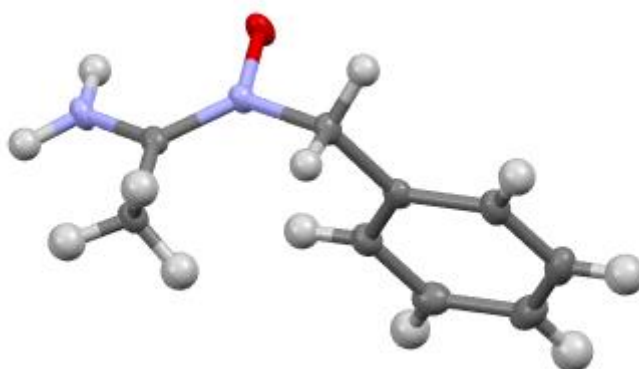
N-benzylhydroxylamine was dissolved in CD_3CN to make a solution of concentration 160 mM, which was measured by 1H NMR using the residual CHD_2CN peak as the internal standard. After 47 hours, the concentration of the hydroxylamine dropped to 120 mM and the aldoxime concentration was 30 mM. Transparent crystals precipitated from the NMR sample and was collected as the product. The crystal was collected and submitted for x-ray crystallography.

The CH_3 -isotopomer was synthesized with the same procedure, using CH_3CN instead of CD_3CN . Its crystal structure was identical with the deuterated isotopomer.



1H NMR (400 MHz, $DMSO-d_6$) δ 7.32 (d, $J = 4.1$ Hz, 1H), 7.31 – 7.21 (m, 0H), 6.55 (s, 1H), 4.72 (s, 1H), 2.07 (s, 1H). **^{13}C NMR** (126 MHz, $DMSO-d_6$) δ 144.03, 136.78, 128.17, 127.58, 127.11, 57.59, 14.53. **IR** (ATR, cm^{-1}): 3172, 3113, 3086, 3061, 3028, 2906, 2856, 1657, 1604, 1495, 1453, 1432, 1377, 1351, 1142, 1076, 1027, 971, 933, 906, 870, 841, 792, 728, 695, 663, 628, 601, 575, 532. **HRMS** (ESI): calcd for $C_9H_{13}N_2O_1$ (M+H⁺): 165.1022, found 165.1023

Crystal Data for $C_9H_{12}N_2O$ (M = 164.21 g/mol): monoclinic, space group $P2_1/c$ (no. 14), $a = 13.9395(2)$ Å, $b = 5.65960(10)$ Å, $c = 10.8937(2)$ Å, $\beta = 101.410(2)^\circ$, $V = 842.44(3)$ Å³, $Z = 4$, $T = 100.0(1)$ K, $\mu(Cu\ K\alpha) = 0.697$ mm⁻¹, $D_{calc} = 1.295$ g/cm³, 17354 reflections measured ($6.468^\circ \leq 2\theta \leq 160.726^\circ$), 1826 unique ($R_{int} = 0.0470$, $R_{sigma} = 0.0222$) which were used in all calculations. The final R_1 was 0.0362 ($I > 2\sigma(I)$) and wR_2 was 0.0943 (all data).

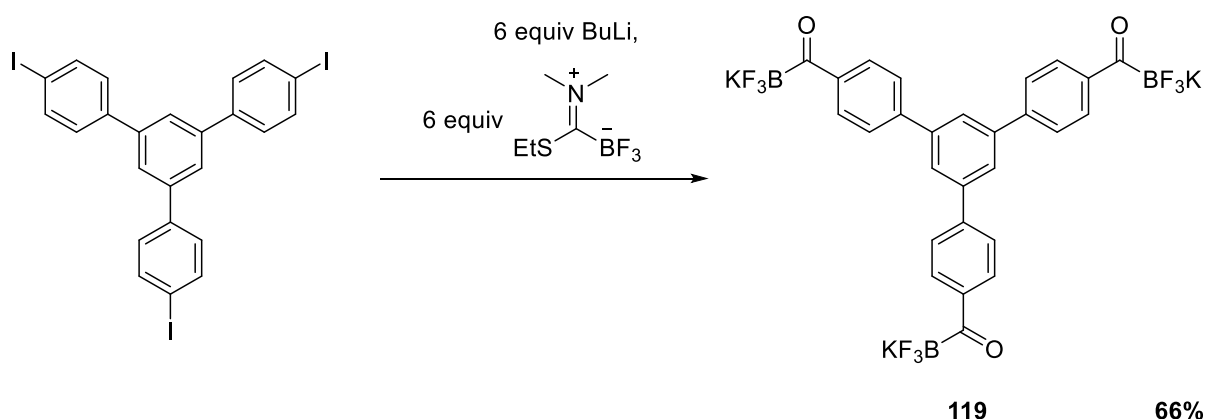


7.1.3. Synthesis of multivalent KATs in Chapter 3

General procedure for synthesis of multivalent KATs with reagent 1

The corresponding aryl iodide and reagent 1 (1.5–2 equiv per iodide) were dissolved in THF to make a 0.02 M solution and cooled to $-78\text{ }^{\circ}\text{C}$ using an acetone-dry ice bath. During the cooling process the iodide may precipitate. *n*BuLi (1.6 M in hexanes, 1.5–2 equiv per iodide) was added over 1 hr to give a clear yellow solution. The reaction mixture was stirred for one hour at $-78\text{ }^{\circ}\text{C}$, after which $\text{KF}_{(\text{aq})}$ (6.5 M, 8 equiv per iodide) was added to the reaction mixture which was stirred overnight at $23\text{ }^{\circ}\text{C}$ to give a milky white suspension. The suspension was diluted with equal volume of CH_2Cl_2 and stirred for 10 min and the solid portion was collected by filtration. The solid was washed with H_2O and CH_2Cl_2 before being dried in vacuum or azeotropically dried with toluene. The dried product was dissolved in DMF and precipitated with acetone to remove the mono-KAT byproduct.

Synthesis of 119

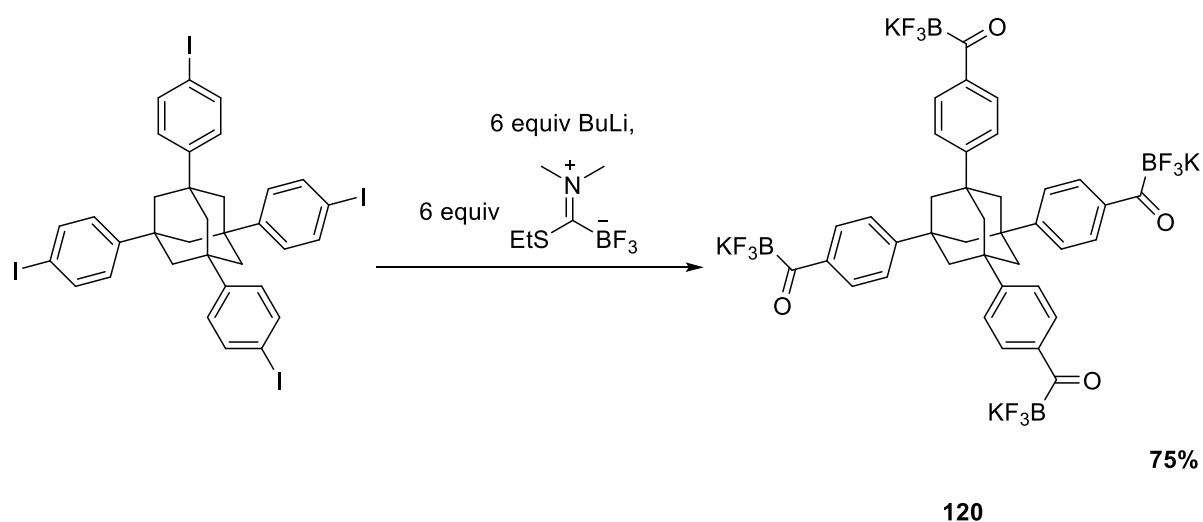


Following the general procedure, 1055.7 mg (1.54 mmol, 1 equiv) of using 1,3,5-tris(4-iodophenyl)benzene and 6 equiv of reagent 1 were dissolved in THF (46.2 mL) and *n*BuLi was added. **119** was isolated after two times precipitation with acetone (14 mL) as a pale yellow powder (719.8 mg, 1.02 mmol, 66.2% mp $220\text{ }^{\circ}\text{C}$ dec)

The starting material was synthesized with the procedure reported by Shekouhy et al. from 4-iodoacetophenone using $B(HSO_4)_3$ as a catalyst.¹⁸⁰

1H NMR (400 MHz, DMSO- d_6) δ 8.04 (d, J = 8.1 Hz, 1H), 7.98 (s, 0H), 7.91 (d, J = 8.4 Hz, 1H); **^{13}C NMR** (151 MHz, DMSO) δ 232.49 (br), 141.97, 141.23, 140.19, 128.36, 126.60, 124.78; **^{19}F NMR** (377 MHz, DMSO) δ -141.57; **^{11}B NMR** (160 MHz, DMSO- d_6) δ 0.65 (q, J = 18.3 Hz), -0.80; **IR** (ν/cm^{-1} , KBr): 3070, 3029, 2958, 2932, 2963, 2934, 2880, 1708, 1666, 1637, 1598, 1559, 1391, 1242, 1072, 1036, 1007, 884, 819; **HRMS** (MALDI/DCTB): calcd for $C_{27}H_{15}B_3F_9K_3O_3$ (M-K⁻): 669.04363 found: 669.04414.

Synthesis of 120



The starting material 1,3,5,7-Tetrakis-(4-iodophenyl)adamantane was synthesized from adamantane according to the procedure reported by Keana et al.¹⁸¹

Following the general procedure, 1284.1 mg (1.600 mmol) of 1,3,5,7-Tetrakis-(4-iodophenyl)adamantane were dissolved in THF (46.2 mL) and 6 equiv of reagent **1** were dissolved in THF (46.2 mL) and *n*BuLi was added. **120** was isolated after two times precipitation with acetone (14 mL) as a pale yellow powder (995.78 mg, 1.02 mmol, 75.3% mp 250 °C dec).

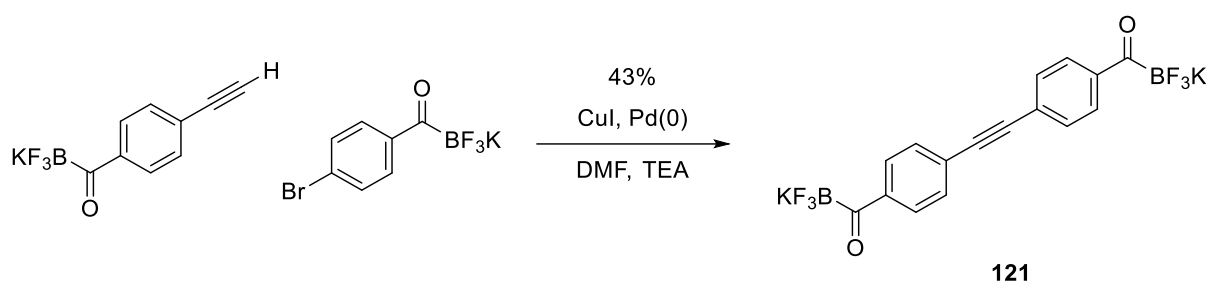
1H NMR (500 MHz, Acetone- d_6) δ 7.90 (d, J = 8.3 Hz, 8H), 7.58 (d, J = 8.6 Hz, 8H), 2.14 (s, 12H); **^{13}C NMR** (151 MHz, DMSO) δ 232.57, 152.24, 139.30, 127.83, 127.81, 124.62, 124.59, 46.22, 14.08; **^{19}F NMR** (376 MHz, DMSO- d_6) δ -141.94; **^{11}B NMR** (160 MHz, Acetone- d_6) δ -1.49; **IR** (ν/cm^{-1} , KBr): 3618, 3555, 3454, 3085, 3070, 2932, 2899, 2854, 1631, 1597, 1561, 1512, 1477, 1445, 1405, 1357, 1320, 1294, 1258, 1191, 1079, 1032, 879, 843, 814, 781, 747, 714, 682, 664, 626, 604, 553, 542, 528, 502, 486, 458, 447, 432, 416, 387, 377,

358; **HRMS**: still screening for ionization conditions; **Elemental analysis**: Calc 46.75% C, 2.89%H, 4.43%B, 23.35%F, 6.56%O, found 46.95% C, 3.37%H, 20.6%F, 7.58%O.

Synthesis of d16 version of 120

The synthesis was identical to that of **120**. The starting material was prepared from 1,3,5,7-tetrabromoadamantane and benzene-d6 following the procedure the procedure reported by Keana et al.¹⁸¹

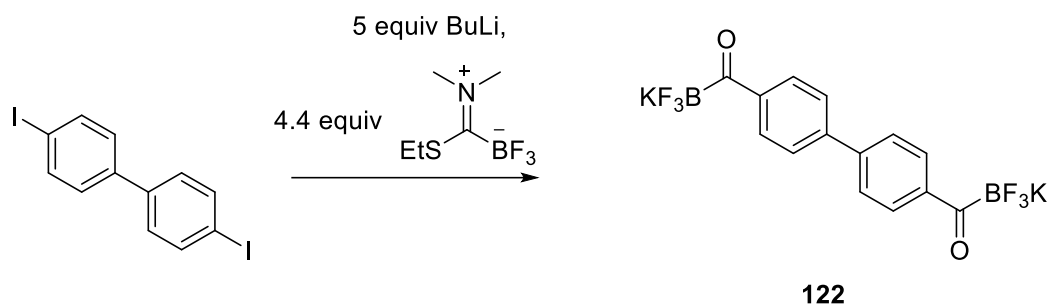
Synthesis of 121



p-bromophenyl KAT (220.0 mg, 756.2 μmol , 1 equiv), p-ethynylphenyl KAT (214.2 mg, 907.5 μmol , 1.2 equiv), CuI (7.2mg, 37.8 μmol , 0.05 equiv), and Pd(PPh₃)₄ (17 mg, 15 μmol , 0.02 equiv) were dissolved in DMF (10 mL, dry) and TEA (5 mL, distilled) and stirred in a vial at 80 °C overnight. The solvent was evaporated and the residue was dispersed in 1 mL DMF, precipitated with 20 mL acetone, re-dissolved and precipitated with 5 mL H₂O before being dried on vacuum to give **121** as a brownish yellow solid (143.6 mg, 321.9 μmol , 42.6%, mp 137 °C dec)

¹H NMR (300 MHz, DMSO-d₆) δ 7.93 (d, J = 8.1 Hz, 2H), 7.59 (d, J = 8.2 Hz, 2H); **¹³C NMR** (101 MHz, DMSO) δ 162.78, 131.54, 128.45, 124.70, 91.29, 65.38; **¹⁹F NMR** (282 MHz, DMSO-d₆) δ -141.63; **¹¹B NMR** (128 MHz, DMSO-d₆) δ -0.54 (q, J = 54 Hz); IR (v/cm⁻¹, KBr): 3431, 3264, 3159, 2967, 2903, 2835, 2755, 2722, 2633, 2534, 2474, 2414, 2080, 1965, 1637, 1597, 1466, 1399, 1305, 1181, 1151, 1086, 1024, 973, 884, 835, 803, 772, 741, 705, 672, 611, 533, 500, 468, 436, 380; **HRMS** (ESI): calcd for C₁₆H₈B₂F₆O₂K₂ (M-2K²⁺): 184.0313, found: 184.0315.

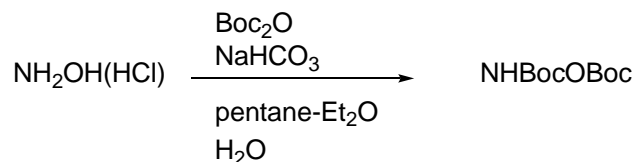
Synthesis of 122



Following the general procedure, 4,4'-diiodobiphenyl, 4.4 equiv of **1** and 5 equiv nBuLi were used. Precipitation from acetone gave the product as a yellow powder (mp 220 °C dec).

$^1\text{H NMR}$ (400 MHz, DMSO- d_6) δ 8.00 (d, $J = 8.2$ Hz, 4H), 7.73 (d, $J = 8.4$ Hz, 4H). $^{19}\text{F NMR}$ (376 MHz, DMSO- d_6) δ -141.64 (d, $J = 75.1$ Hz); $^{11}\text{B NMR}$ (128 MHz, DMSO- d_6) δ -0.26; $^{13}\text{C NMR}$ (126 MHz, DMSO) δ 142.28, 140.68, 128.89, 126.78; IR (v/cm $^{-1}$, ATR/neat): 3292, 1738, 1684, 1653, 1631, 1598, 1551, 1517, 1394, 1364, 1313, 1251, 1199, 1145, 1108, 1086, 1055, 1005, 975, 948, 915, 877, 859, 825, 792, 755, 728, 675, 645, 626; **HRMS** (ESI): calcd for $\text{C}_{14}\text{H}_8\text{B}_2\text{F}_6\text{O}_2\text{K}_2$ ($M - 2\text{K}^+$): 172.0313, found 172.0313.

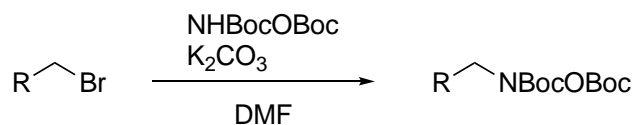
7.1.4. Synthesis of hydroxylamines with 132



Hydroxylamine hydrochloride (33.6 g, 484 mmol, 1 equiv) was dissolved in water (300 mL) and added slowly sodium bicarbonate (85.7 g, 1.02 mol, 2.1 equiv) Boc_2O (216.5 g, 992.0 mmol, 2.05 equiv) was dissolved in 300 mL of 5:1 pentane- Et_2O and added dropwise over 2 hours. The mixture was stirred for 5 hours before the two phases were separated. The organic layer was collected and washed with water (200 mL * 3) and dried over MgSO_4 before being evaporated to a thick liquid which solidifies upon standing. The solid was broken up and washed with pentane, collected by filtration and dried in vacuum to give the product as a white powder (86.2 g, 370 mmol, 76.4% mp 69.3–69.8 °C). The spectroscopic characteristic was identical to published reports.¹⁵⁸

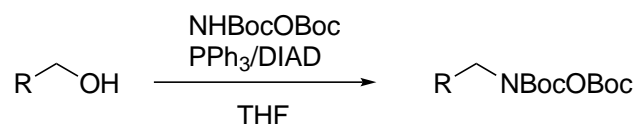
Elemental analysis: Calc. 51.49%C, 8.21%H, 6.00%N, 34.29%O. Found: 51.59%C, 8.08%H, 5.93%N, 34.14%O.

General Procedure A: Synthesis of N-Boc-O-Boc doubly protected hydroxylamines from alkyl halides with **132**



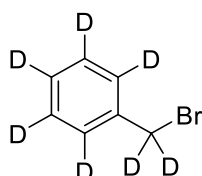
A solution of **132** (1.1 equiv per alkyl halide, 0.5 M) in dry DMF was prepared and K_2CO_3 (1.5 equiv per alkyl halide) was added. The solution was stirred vigorously for 5 min, after which the alkyl halide was added. With benzyl bromides, the temperature will rise significantly. The mixture was stirred vigorously overnight before being poured into water and extracted with EtOAc. The EtOAc layer was washed with water to remove DMF before being dried over MgSO_4 and evaporation to give the product.

General Procedure B: Synthesis of N-Boc-O-Boc doubly protected hydroxylamines by Mitsunobu reaction from primary alcohols and **132**



Triphenylphosphine (1.5 equiv per alcohol) was dissolved in THF to make a 0.45 M solution, and DIAD (1.5 equiv per alcohol) was added dropwise under 0 °C. After stirring at 0 °C for 10 min a white suspension formed. A THF solution of **132** (0.33 M, 1.1 equiv) and the alcohol (0.3M, 1 equiv) was added to the white suspension, after which the mixture was allowed to stir while returning to rt. The white suspension gradually dissolved and the reaction progress was monitored by TLC or LCMS. After the desired reaction time the mixture was added saturated $\text{NH}_4\text{Cl}_{(\text{aq})}$ and treated with an equal amount of EtOAc before being washed with H_2O . The organic layer was dried over MgSO_4 , evaporated, and dispersed in 1:9 EtOAc-cyclohexane before being filtered through a silica plug to remove most of the triphenylphosphine oxide byproduct. The filtrate was evaporated and chromatographed on silica to give the product as a clear oil or white solid.

Synthesis of d7-benzyl bromide

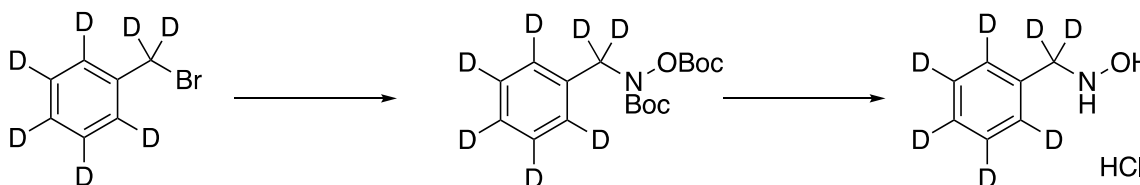


A biphasic system of d₈-toluene (2.00 mL, 1.91 g, 19.0 mmol) in EtOAc (40 mL, ~0.5 M) and aqueous solution of sodium bromate (5.75 g, 38.1 mmol, ~2 M) was stirred vigorously in a 250 mL round bottom flask. A solution of sodium bisulfite (3.962 g, 38.1 mmol) in water (40

mL, ~1M) was added dropwise from a syringe over 30 min. After 10 min the reaction mixture warms up and was therefore cooled by an ice bath. The biphasic mixture was stirred for 2 additional hours under rt after the end of bisulfite addition. After TLC indicated complete conversion, quenching of excess bromine was performed with adding saturated sodium thiosulfate solution under 0 °C (indicated by the color of bromine fading away). The organic layer of the resulting slightly yellow mixture was collected and the aqueous layer was extracted with EtOAc (50 mL x 2) and the combined organic layer was dried over MgSO₄ before being concentrated on a rotary evaporator (> 200 mbar) to afford a crude mixture containing EtOAc (~4.5g). The crude mixture was directly used for the next step without further purification.

Note: The product is a strong lachrymatory agent. ¹H NMR cannot give an estimate to the purity of the crude product.

Synthesis of d7-benzyl hydroxylamine

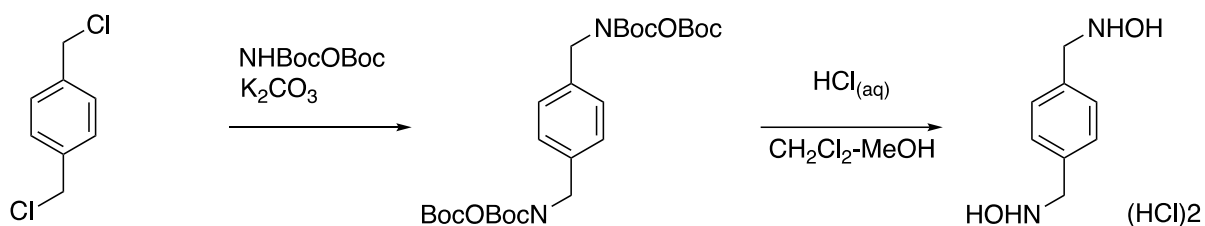


Following General procedure A using benzyl bromide-d7 (132.8 mg, 745.7 μmol), after chromatography (eluent 5% EtOAc/cyclohexane) N-d7-Benzyl-N-Boc-O-Boc hydroxylamine was obtained as a clear oil that solidifies upon standing (112.1 mg, 336.5 μmol, 45%, mp 55.7–58.2 °C)

¹H NMR (400 MHz, CDCl₃) δ 1.48 (s, 9H), 1.46 (s, 9H); ¹³C NMR (101 MHz, CDCl₃) δ 154.99, 152.26, 84.86, 82.72, 28.27, 27.69; HRMS (ESI⁺) calcd for C₁₇H₁₈D₇NO₅ [M+Na⁺]: 353.2064, found 353.2061

N-d7-Benzyl-N-Boc-O-Boc hydroxylamine (150.5 mg, 455.5 μmol, 1 equiv) was dissolved in 1:1 CH₂Cl₂:MeOH (5 mL) and added HCl_(aq) (12M, 1.0 mL, 12 mmol, 26 equiv) and the bubbling solution was stirred vigorously for 4 hours before being blown dry with a nitrogen flow and dried under vacuum to give d7-benzylhydroxylamine hydrochloride as a white powder (74.4 mg, 446.6 μmol, 98%, mp 140 °C dec). HRMS (ESI⁺): calcd for C₇H₃N₁O₁D₇: 131.1196, found 131.1194.

Synthesis of 123

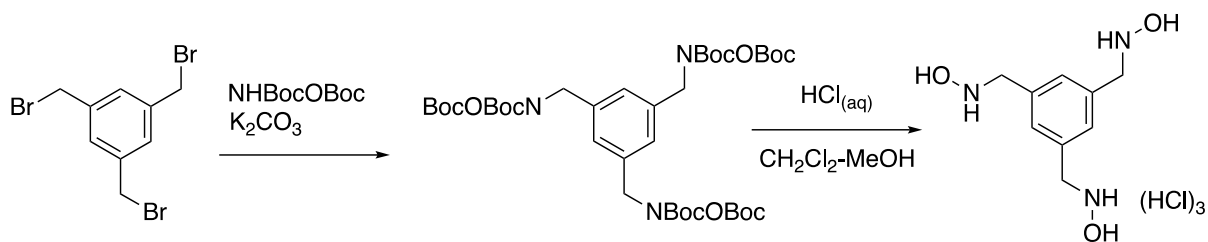


Following General Procedure A, 5.6233 g of 1,4-bis(chloromethyl)benzene (32.123 mmol) was used. After chromatography (eluent: 5% EtOAc-cyclohexane → 20% EtOAc-cyclohexane) the tetra-Boc-protected bis-hydroxylamine was obtained as a white wax like solid (16.7879 g, 29.5216 mmol, 91.9%, mp 92.3–94.6 °C).

¹H NMR (400 MHz, CDCl₃) δ 7.30 (s, 4H), 4.74 (s, 4H), 1.48 (s, 18H), 1.46 (s, 18H); ¹³C NMR (126 MHz, CDCl₃) δ 154.82, 152.12, 135.20, 128.30, 84.75, 82.60, 53.72, 28.12, 27.56; ; IR (ν/cm⁻¹, ATR/neat): 3254, 3138, 3088, 3064, 3035, 2966, 2928, 2910, 2871, 2817, 1806, 1766, 1732, 1509, 1495, 1467, 1452, 1423, 1403, 1387, 1365, 1349, 1323, 1269, 1207, 1180, 1158, 1091, 1069, 1036, 1021, 1005, 931, 913, 866, 839, 795, 778, 754, 695, 665, 650, 619, 603, 587, 557, 530, 515, 502; HRMS (ESI⁺) calcd for C₂₈H₄₄N₂O₁₀[M+NH₄⁺]: 566.3225, found 566.3229.

The tetra-Boc protected hydroxylamine (2.5034 g, 4.4022 mmol, 1 equiv) was dissolved in 1:1 CH₂Cl₂:MeOH (20 mL) and added HCl_(aq) (12M, 10.0 mL, 120 mmol, 27.3 equiv) and the bubbling solution was stirred vigorously overnight before being blown dry with a nitrogen flow, and washed with Et₂O (15 mL * 3) before being dried under vacuum to give 1,4-bis(hydroxyaminomethyl)benzene dihydrochloride as a white powder (1000.9 mg, 4.1512 mmol, 94.3%, mp 165 °C dec)

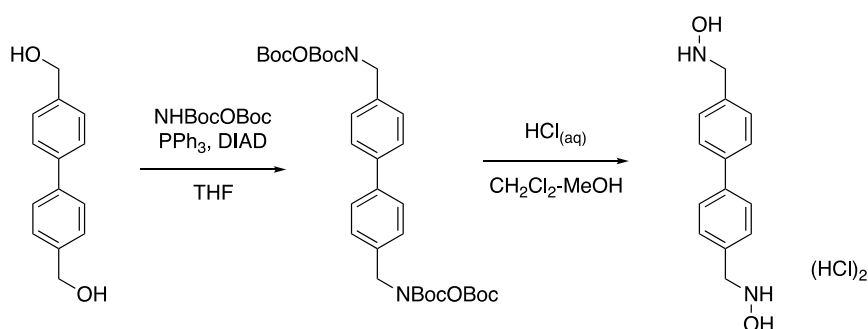
¹H NMR (400 MHz, DMSO-d₆) δ 11.87 (s, 4H), 10.99 (s, 2H), 7.55 (s, 4H), 4.32 (s, 4H); ¹³C NMR (126 MHz, DMSO) δ 130.83, 130.80, 53.27; ; IR (ν/cm⁻¹, KBr): 3006.6, 2980, 2931, 2909, 2883, 2871, 2858, 2791, 2775, 2759, 2738, 2727, 1783, 1716, 1474, 1455, 1432, 1394, 1370, 1347, 1317, 1275, 1257, 1230, 1149, 1113, 1096, 1040, 857, 840, 763, 751.

Synthesis of **124**

Following General procedure A, using 1,3,5-tris(bromomethyl)benzene (2.2153 g, 6.2074 mmol), after chromatography (eluent: 10% EtOAc-cyclohexane → 50% EtOAc), the hexa-Boc protected **124** was obtained as a waxy solid (4.8200 g, 5.9218 mmol, 95.4%).

The hexa-Boc protected tris-hydroxylamine (3.6503 g, 2.9711 mmol, 1 equiv) was dissolved in 1:2 CH₂Cl₂-MeOH (50 mL). HCl_(aq) (12 M, 15.0 mL, 180 mmol, 60.6 equiv) was added and the bubbling reaction mixture was stirred overnight before being blown dry with a nitrogen flow to give a white solid. The solid was washed with CH₂Cl₂ (15 mL * 2) and dried in vacuum to give 1,3,5-tris(hydroxyaminomethyl)benzene as a white powder (939.3 mg, 2.912 mmol, 98.0%, mp 143 °C dec)

¹H NMR (400 MHz, Methanol-d₄) δ 7.84 (s, 3H), 4.53 (s, 6H); ¹³C NMR (101 MHz, MeOD) δ 135.87, 131.97, 55.24; IR (ν/cm⁻¹, KBr): 3424, 3263, 3061, 2973, 2937, 2878, 2802, 2738, 2677, 2491, 1637, 1471, 1433, 1397, 1169, 1082, 997, 805, 699, 630, 511, 464, 417; HRMS(ESI): calcd for C₃₉H₆₃N₃O₁₅ (M+Na⁺): 836.4151, found: 836.4146.

Synthesis of **125**

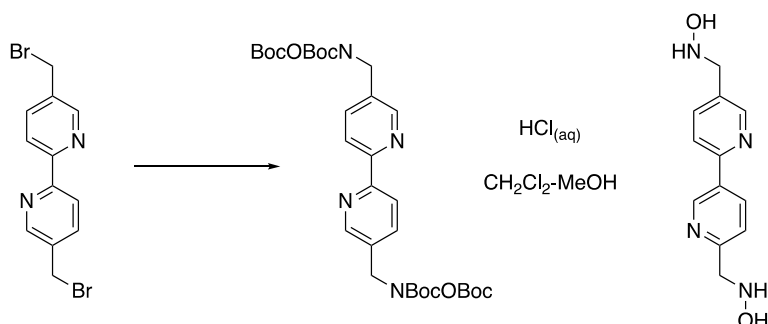
Following General Procedure B, using 4,4'-bis(hydroxymethyl)biphenyl (3.2033 g, 14.950 mmol, 1 equiv), after chromatography (eluent: 2% EtOAc-cyclohexane → 10% EtOAc-cyclohexane), the tetra-Boc protected bis-hydroxylamine was obtained as a white solid (6.6125 g, 10.256 mmol, 68.6%).

¹H NMR (400 MHz, CDCl₃) δ 7.54 (d, J = 8.3 Hz, 4H), 7.40 (d, J = 8.3 Hz, 4H), 4.79 (s, 4H), 1.50 (s, 22H), 1.46 (s, 18H); **¹³C NMR** (101 MHz, CDCl₃) δ 154.99, 152.26, 140.38, 134.96, 128.86, 127.26, 84.95, 82.82, 77.48, 77.16, 76.84, 53.90, 28.29, 27.70; **IR** (v/cm-1, KBr): 3295, 3052, 3027, 2980, 2934, 2824, 1783, 1718, 1608, 1579, 1560, 1500, 1477, 1456, 1429, 1394, 1370, 1347, 1318, 1274, 1256, 1232, 1149, 1116, 1096, 1042, 1006, 957, 937, 898, 855, 839, 806, 780, 762, 737, 696, 678; **HRMS** (ESI): calcd for: C₃₄H₄₈N₂O₁₀ (M + Na): 667.3201, found: 667.3201.

The tetra-Boc hydroxylamine (4.5002 g, 6.9796 mmol, 1 equiv) was dissolved in 1:1 CH₂Cl₂-MeOH (20 mL). HCl (aq) (12 M, 10.0 mL, 120 mmol, 17.2 equiv) was added and the bubbling reaction mixture was stirred overnight before being blown dry with a nitrogen flow to give a white solid. The solid dried in vacuum to give 4,4'-bis(hydroxyamino)biphenyl as a white powder (2.0725 g, 6.540 mmol, 93.7%, mp 152 °C dec)

¹H NMR (400 MHz, DMSO-d₆) δ 11.67 (s, 4H), 10.93 (s, 2H), 7.87 – 7.70 (m, 4H), 7.71 – 7.54 (m, 4H), 4.37 (s, 4H); **IR** (v/cm-1, KBr): 3340, 3285, 3143, 3028, 2918, 2851, 2765, 1764, 1659, 1609, 1462, 1402, 1252, 1118, 867

Synthesis of 126



Following General procedure A, using 4,4-bis(bromomethyl)-2,2'-bipyridyl (1231.7 mg, 3.6012 mmol), the tetra-Boc protected hydroxylamine was obtained without chromatography as a white solid (1814.1 mg, 2.805 mmol, 77.9%).

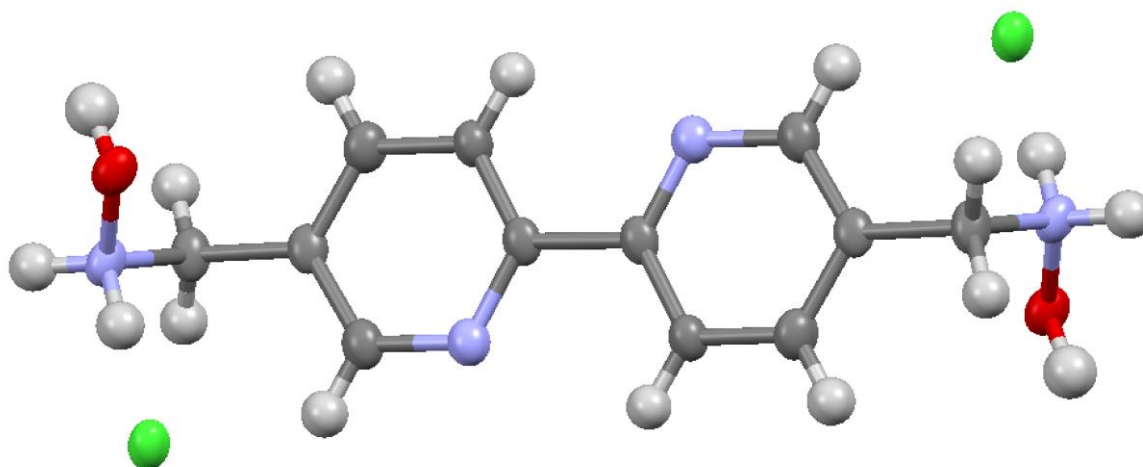
¹H NMR (400 MHz, CDCl₃) δ 8.62 (dd, J = 2.3, 0.8 Hz, 2H), 8.36 (dd, J = 8.1, 0.8 Hz, 2H), 7.83 (dd, J = 8.2, 2.3 Hz, 2H), 4.81 (s, 4H), 1.49 (s, 18H), 1.46 (s, 18H); **¹³C NMR** (101 MHz, CDCl₃) δ 155.61, 154.90, 152.14, 149.36, 137.19, 131.54, 120.97, 85.25, 83.23, 51.76, 28.25, 27.69; **IR** (v/cm-1, ATR/neat): 2980, 2935, 2361, 2338, 1783, 1720, 1469, 1430, 1393, 1370, 1344, 1277, 1240, 1149, 1097, 839, 748, 486, 470, 423, 399, 382, 367; **HRMS** (ESI) calcd for C₃₂H₄₆N₄O₁₀ (M + H): 647.3287, found: 647.3284.

Experimental section

The tetra-Boc hydroxylamine (503.2 mg, 778.1 μmol) was dissolved in 1:1 CH_2Cl_2 -MeOH (10 mL). $\text{HCl}_{(\text{aq})}$ (12 M, 2.0 mL, 24 mmol, 30 equiv) was added and the bubbling reaction mixture was stirred overnight before being blown dry with a nitrogen flow to give a white solid. The solid dried in vacuum to give 4,4'-bis(hydroxyamino)biphenyl dihydrochloride as a white powder (246.4 mg, 770.2 μmol , 98.9%, mp 132 $^\circ\text{C}$ dec)

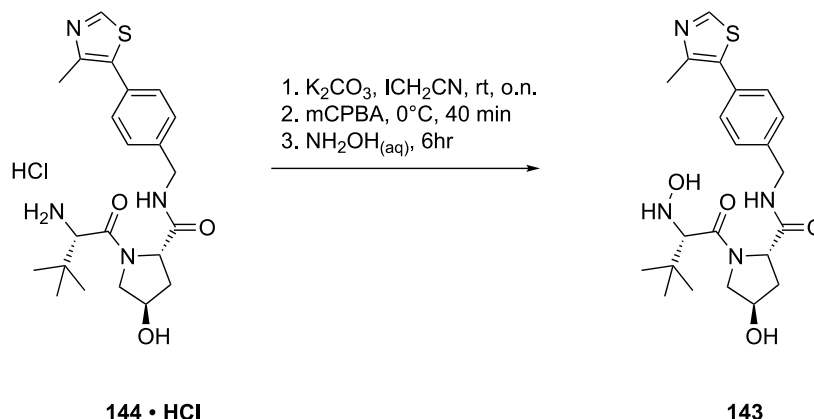
$^1\text{H NMR}$ (400 MHz, DMSO-d_6) δ 12.17 (s, 4H), 9.13 – 8.87 (m, 2H), 8.55 (d, $J = 8.2$ Hz, 2H), 8.31 (d, $J = 8.3$ Hz, 2H), 4.50 (s, 4H); $^{13}\text{C NMR}$ (101 MHz, DMSO-d_6) δ 152.30, 150.48, 141.90, 128.02, 121.35, 50.43; **IR** (v/cm^{-1} , ATR/neat): 3272, 2993, 2950, 2842, 2360, 2340, 1697, 1670, 1635, 1558, 1507, 1472, 1416, 1373, 1100, 999.

Crystal Data for $\text{C}_{12}\text{H}_{16}\text{Cl}_2\text{N}_4\text{O}_2$ ($M = 319.19$ g/mol): triclinic, space group P-1 (no. 2), $a = 4.4130(2)$ \AA , $b = 6.0197(3)$ \AA , $c = 13.6277(7)$ \AA , $\alpha = 97.603(5)^\circ$, $\beta = 91.114(4)^\circ$, $\gamma = 106.256(4)^\circ$, $V = 343.88(3)$ \AA^3 , $Z = 1$, $T = 100.0(1)$ K, $\mu(\text{CuK}\alpha) = 4.324$ mm^{-1} , $D_{\text{calc}} = 1.541$ g/cm^3 , 2542 reflections measured ($6.556^\circ \leq 2\theta \leq 163.11^\circ$), 2542 unique ($R_{\text{int}} = ?$, $R_{\text{sigma}} = 0.0231$) which were used in all calculations. The final R_1 was 0.0754 ($I > 2\sigma(I)$) and wR_2 was 0.2036 (all data).



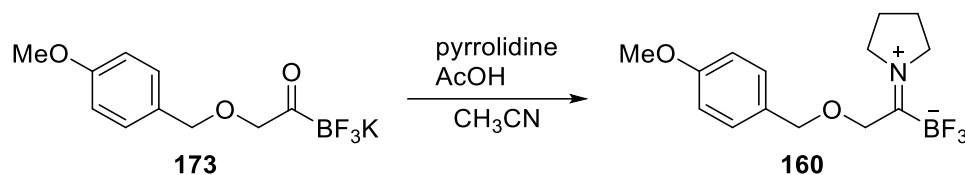
7.1.5. Synthesis of MZ-1 PROTAC fragments used in Chapter 4

Synthesis of VHL hydroxylamine (143)



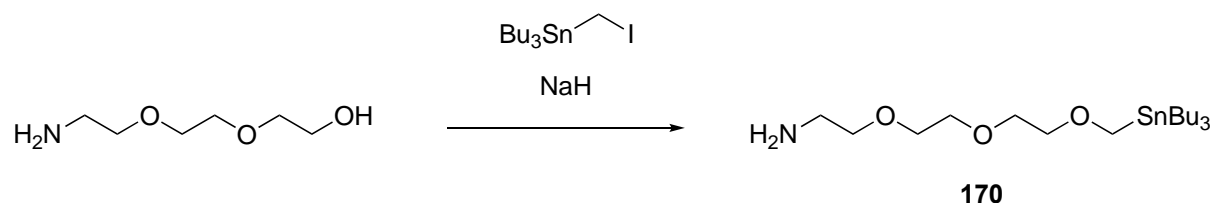
A solution of **144** (934.1 mg, 2.000 mol, 1 equiv) and iodoacetonitrile (173.8 μ L, 400.7 mg, 2.400 mmol, 1.2 equiv) in CH_3CN (20 mL) was prepared and K_2CO_3 (276.4 mg, 2.000, 1.000 equiv) was added and the mixture was stirred overnight. The mixture was diluted with CH_2Cl_2 (200 mL), washed with $\text{NaHCO}_3(\text{aq})$ and H_2O before being dried over Na_2SO_4 and evaporated. The residue was dissolved in CH_2Cl_2 (100 mL) and stirred in a ice bath for 10 min before adding mCPBA (75%, 1.012 g, 4.400 mol, 2.2 equiv). The mixture was stirred for another 40 min at 0 °C before $\text{NH}_2\text{OH}(\text{aq})$ (50%, 16.9 M, 10 mL, 169 mmol, 84 equiv) was added. The ice bath was removed, and the mixture was stirred vigorously for 6 hr while a white precipitate formed. The mixture was filtered through celite, washed with H_2O (30 mL * 4), dried over Na_2SO_4 and evaporated. Purification with reversed phase HPLC (column: YMC C18 (20 mm I.D. \times 250 mm) column, flow rate: 10 mL/min, eluent: 20–80% CH_3CN - H_2O with 0.1% HCO_2H) followed by evaporation gave the product hydroxylamine as a formate salt (327.1 mg, 664.0 μ mol, 33.2%)

$^1\text{H NMR}$ (400 MHz, CD_3CN) δ 8.74 (s, 1H), 8.05 (s, 1H), 7.41 (s, 4H), 7.35 – 7.26 (m, 1H), 4.55 (t, $J = 7.9$ Hz, 1H), 4.51 – 4.41 (m, 2H), 4.31 (dd, $J = 15.5, 5.6$ Hz, 1H), 3.65 (d, $J = 3.4$ Hz, 2H), 3.51 (s, 1H), 2.46 (s, 3H), 2.11 (td, $J = 7.8, 7.4, 3.8$ Hz, 2H), 0.93 (s, 9H); $^{13}\text{C NMR}$ (101 MHz, CD_3CN) δ 174.32, 172.91, 163.09, 151.70, 149.32, 140.28, 132.42, 131.42, 130.07, 128.68, 71.92, 70.80, 60.22, 57.01, 43.19, 38.22, 34.94, 27.34, 16.38; **HRMS** (ESI): calcd for $\text{C}_{21}\text{H}_{31}\text{N}_4\text{O}_4\text{S}$ ($\text{M}+\text{H}^+$): 447.2061, found 447.2056.

PMBOCH₂KAT TIM (160)

KAT **173** (55.0 mg, 192 μmol , 1 equiv) was dissolved in CH_3CN (2 mL). Pyrrolidine (24.04 μL , 20.48 mg, 288.0 μmol , 1.5 equiv) followed by AcOH (16.49 μL , 17.30 mg, 288.0 μmol , 1.5 equiv) were added and the mixture was stirred for 30 min before being evaporated and chromatographed on silica (1:3 acetone-cyclohexane \rightarrow 2:1 acetone-cyclohexane) gave the product as a colorless oil (48.6 mg, 161 μmol , 56%).

¹H NMR (500 MHz, CDCl_3) δ 7.25 – 7.16 (m, 2H), 6.89 (m, 2H), 4.66 (m, 2H), 4.47 (s, 2H), 4.24 – 4.17 (m, 2H), 4.04 (t, $J = 7.0$ Hz, 2H), 3.81 (s, 3H), 2.10 – 1.92 (m, 4H); **¹³C NMR** (151 MHz, CDCl_3) δ 204.85–203.04, 159.81, 129.91, 128.78, 114.16, 73.82, 70.58, 57.07 (q, $J = 3.0$ Hz), 55.44, 55.41, 24.86, 24.03; **¹⁹F NMR** (377 MHz, CDCl_3) δ -147.74 (dd, $J = 40$ Hz); **¹¹B NMR** (160 MHz, CDCl_3) δ -0.62 (q, $J = 40.8$ Hz); **IR** (ATR, neat, cm^{-1}): 2980, 2953, 2927, 2899, 2874, 1729, 1701, 1650, 1591, 1565, 1529, 1487, 1451, 1419, 1398, 1367, 1334, 1298, 1258, 1235, 1214, 1171, 1141, 1109, 1089, 1069, 1042, 1013, 984, 963, 914, 894, 842, 804, 760, 731, 693, 666, 644, 608 ; **HRMS** (ESI): calcd for $\text{C}_{14}\text{H}_{19}\text{BF}_3\text{NO}_2$ ($\text{M}+\text{Na}^+$): 324.1353, found 324.1353.

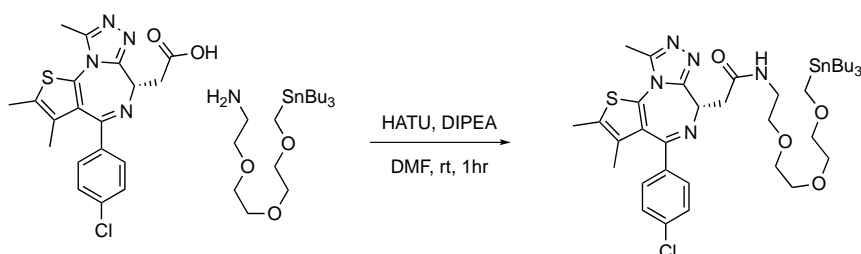
Synthesis of 170

2-[2-(2-Aminoethoxy)ethoxy]ethanol (200 μL , 215 mg, 1.44 mmol, 1 equiv) was added to a THF (10 mL, distilled) suspension of NaH (60%, 66.6 mg, 1.66 mmol, 1.15 equiv) and stirred for 30 min before iodomethyltributylstannane (310.3 μL , 620.6 mg, 1.440 equiv) was added. The mixture turned from a yellow solution to a white milky suspension 3 minutes after stannane addition. The mixture was stirred overnight at rt before being added satd $\text{NaCl}_{(\text{aq})}$ (6 mL), diluted with EtOAc (15 mL), washed with water (5 mL * 2), dried over Na_2SO_4 and evaporated. The residue was chromatographed on a silica column packed in cyclohexane. Chromatography: V_{int} : 59 mL, eluents: 60 mL cyclohexane, 100 mL 2% EtOAc-cyclohexane into fractions 1–9, 100 mL 5% EtOAc-cyclohexane into fractions 9–17, 100 mL 10% EtOAc-cyclohexane into fractions 17–26, among which fractions 16–20 contained the product.

Evaporation of the fractions gave the product as a slightly yellow oil (499.5mg, 1.104 mmol, 76.7%).

¹H NMR (400 MHz, CDCl₃) δ 3.78 (s, 2H), 3.67 – 3.57 (m, 8H), 3.54 – 3.42 (m, 2H), 3.05 – 2.90 (m, 2H), 1.64 – 1.41 (m, 6H), 1.37 – 1.21 (m, 6H), 0.89 (m, 16H); **¹³C NMR** (126 MHz, CDCl₃) δ 74.87, 70.77, 70.55, 70.46, 62.70, 29.27, 27.47, 13.88, 9.23, 9.19, 9.17; **IR**(ATR, neat, cm⁻¹): 3571, 3530, 3476, 3434, 3393, 3344, 3148, 3107, 3056, 2890, 2830, 1681, 1642, 1599, 1496, 1421, 1337, 1286, 1241, 1167, 1064, 1011, 955, 922, 863, 820, 749, 686, 637, 553, 506; **HRMS** (ESI): calcd for C₁₉H₄₃NO₃Sn(M+H⁺): 454.2341 found: 454.2336.

Synthesis of 171



A solution of **145** (128.1 mg, 319.5 μmol, 1 equiv) and **170** (142.3 mg, 314.6 μmol, 0.98 equiv) in DMF (5 mL, dry) was prepared. DIPEA (173.0 μL, 129.3 mg, 1.000 mmol, 3.131 equiv) was added and the mixture was stirred at 23 °C for 5 min before HATU (245.0 mg, 644.3 μmol, 2.017 equiv) was added. The mixture was stirred for an additional hour before being poured into saturated NaCl(aq) (20 mL) and extracted with CHCl₃ (10 mL * 3). The combined organic layers were evaporated and chromatographed on a silica column packed in CHCl₃. Chromatography: V_{int}: 65 ml, eluent: 85 mL CHCl₃, 100 mL 2% MeOH-CHCl₃ into fractions 1–8, 100 mL 3% MeOH-CHCl₃ into fractions 8–16, 200 mL 4% MeOH-CHCl₃ into fractions 17–33, among which fractions 21–23 contained the product. Evaporation of the fractions gave **171** as a bright yellow oil (220.7 mg, 264.3 μmol, 84%).

¹H NMR (400 MHz, CDCl₃) δ 7.44 – 7.36 (m, 2H), 7.31 (d, J = 8.8 Hz, 2H), 6.80 (t, J = 5.4 Hz, 1H), 4.64 (dd, J = 7.3, 6.6 Hz, 1H), 3.76 (s, 2H), 3.71 – 3.57 (m, 7H), 3.57 – 3.46 (m, 5H), 2.65 (s, 3H), 2.38 (s, 3H), 1.65 (s, 3H), 1.52 – 1.41 (m, 6H), 1.35 – 1.20 (m, 6H), 0.98 – 0.76 (m, 15H); **¹³C NMR** (126 MHz, CDCl₃) δ 170.63, 163.90, 155.76, 149.92, 136.83, 136.77, 132.29, 131.00, 130.82, 130.55, 129.95, 128.78, 74.85, 70.74, 70.58, 70.57, 69.91, 62.65, 54.47, 39.53, 39.27, 38.70, 29.20, 27.40, 19.68, 14.50, 13.82, 13.18, 11.93, 9.13. ; **IR** (ν/cm⁻¹, ATR/CDCl₃ dried film): 3300, 2953, 2920, 2868, 1725, 1665, 1590, 1551, 1530, 1486, 1454, 1416, 1399, 1376, 1350, 1311, 1277, 1247, 1214, 1184, 1124, 1088, 1042, 1013, 985, 960,

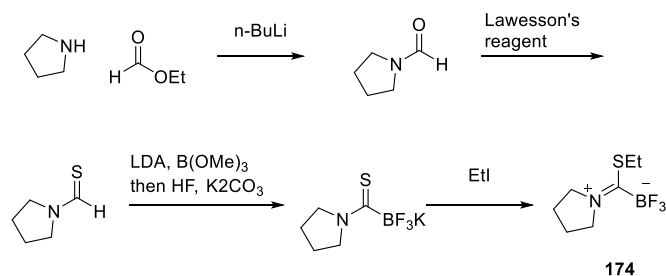
928, 892, 861, 839, 804, 771, 730, 688, 664, 593; **HRMS** (ESI): calcd for $C_{38}H_{58}ClN_5O_4SSn$ (M+Na): 858.2812 found: 858.2827:

7.1.6. Synthesis of KAT reagents in Chapter 5

Revised large scale synthesis of (177)

LDA solution in THF was prepared by dissolving N,N-diisopropylamine (29.3 mL, 21.15 g, 209.03 mmol, 1.1 equiv) in THF (400 mL) and adding nBuLi (125 mL, 1.6 M/hexanes, 200 mmol, 1.05 equiv) under $-10\text{ }^{\circ}\text{C}$ salt-ice bath temperature, over 3 minutes. After the addition of nBuLi, the reaction mixture was cooled in a LN_2 -acetone bath for 1 hr to give a viscous suspension. Triethyl borate (35.6 mL, 30.5 g, 209.03 mmol, 1.1 equiv) was added dropwise to the LDA suspension dropwise over 10 min, during which time it solidifies when coming into contact with the cold reaction mixture. Immediately after the addition of triethyl borate, dimethyl thioformamide (16.943 g, 190.03 mmol, 1 equiv) was diluted with 10 mL THF and added to the mixture over 1 hr. The mixture became a non-viscous, bright yellow solution after half of the dimethyl thioformamide was added. After the end of thioformamide addition the reaction mixture was allowed to stir for 15 min before being warmed to $-78\text{ }^{\circ}\text{C}$ with a dry ice-acetone bath and stirred for another 10 min. 48% $\text{HF}_{(\text{aq})}$ (39.5 mL, 28 M, 1140.2 mmol, 6 equiv) was added and the mixture was stirred vigorously while returning to room temperature overnight to give a bright yellow cloudy solution. This solution was cooled to $0\text{ }^{\circ}\text{C}$ and slowly added K_2CO_3 (118 g, 853.8 mmol, 4.5 equiv) and diluted with CH_2Cl_2 (400 mL) to give a suspension. The suspension was stirred for 30 min before the solid was collected with filtration, washed with CH_2Cl_2 (200 mL * 3) and dried under vacuum to give a free flowing white powder. This powder was extracted with dry DMF (200 mL * 3), and the combined DMF filtrate was evaporated to give a solid, which was washed with Et_2O (100 mL * 2) to remove residual DMF to give **177** as a microcrystalline white powder (26.625 g, 136.5 mmol, 71.8%). The spectroscopic characteristic was identical to previous reports.¹⁷ NMR measurement with an internal standard indicated purity > 95%.

Synthesis of reagent (174)



Pyrrolidine (2.00 mL, 1.70 g, 24.0 mmol, 1.05 equiv) was dissolved in 100 mL Et_2O and stirred in a salt-ice bath at $-5\text{ }^{\circ}\text{C}$ for 10 min before nBuLi (14.26 mL, 22.8 mmol, 1.00 equiv)

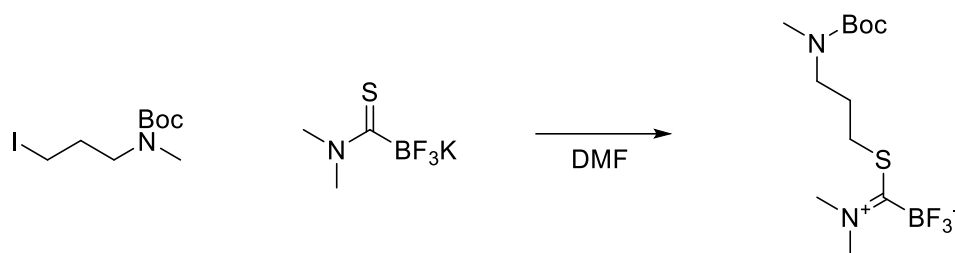
was added over 4 min and stirred for an additional 30 min. Ethyl formate (3.67 mL, 3.38 g, 45.6 mmol, 2 equiv) was added in one portion and the mixture was left to stir overnight and return to rt. Quenching with acetic acid (1.43 mL, 1.5 g, 25 mmol, 1.1 equiv) formed a gel-like white precipitate in the reaction mixture that disperses in 2 min. The reaction mixture was added sodium bicarbonate (2 g), filtered through celite, evaporated to give pyrrolidine formamide containing EtOAc (0.29 mol %) that was used directly in the next step.

Pyrrolidine formamide (2.97 g, 30 mmol) was dissolved in toluene (30 mL) and Lawessons reagent (6.07 g, 15 mmol, 0.5 equiv) was added. The mixture was stirred at 100 °C for 90 min before being filtered through a silica plug and evaporated. The residue after evaporation was chromatographed on a silica column packed with 1:4 EtOAc-Cy. Chromatography: V_{int} 60 mL, eluents: 90 mL 1:4 EtOAc-Cy, 250 mL 1:4 EtOAc-Cy into fractions 1–33, among which fractions 14–30 contained the product. Evaporation of the fractions gave pyrrolidine thioformamide as a clear liquid (2.87 g, 24.9 mmol, 79%). Caution: residual Lawessons reagent decomposes on silica gel and released gas.

An LDA solution in THF (0.5M, 50 mL, 25 mmol, 1 equiv) was freshly prepared from N,N-diisopropylamine and nBuLi and cooled in LN₂-acetone bath for 20 min before adding triethyl borate (4.66 mL, 4.0 g, 27.4 mmol, 1.1 equiv). Pyrrolidine thioformamide (2.864 g, 24.9 mmol, 1 equiv) was added with 2 mL THF over 30 min and the reaction mixture was stirred for an addition hour while warming to –78 °C. HF_(aq) (5.17 mL, 48%, 23M, 149.4 mmol, 6 equiv) was added and the reaction mixture turned red, and then pink-orange. The reaction mixture was stirred overnight before being added K₂CO₃ (15.5 g) and CH₂Cl₂ (100 mL) to form a precipitate that was collect by filtration. The solid was washed with CH₂Cl₂ (20 mL * 2) before being dried in vacuum to give a white powder. The white powder was dispersed in acetone (75 mL) and added ethyl iodide (2.5 mL, 4.875g, 31.3 mmol, 1.25 equiv). The reaction mixture was evaporated after being stirred at 23 °C overnight. Extraction of the remaining solid with CH₂Cl₂ gave **174** as a pale yellow solid (2.507 g, 11.9 mmol, 47.6%, mp 63.2-65.1 °C)

¹H NMR (400 MHz, CDCl₃) δ 4.17 (t, J = 6.7 Hz, 2H), 3.58 (m, 4H), 2.21 – 2.00 (m, 4H), 1.39 (t, J = 7.5 Hz, 3H); **¹³C NMR** (101 MHz, CDCl₃) δ 56.89, 54.34, 28.82, 25.68, 24.43, 14.76; **¹⁹F NMR** (376 MHz, CDCl₃) δ -138.98 (dd, J = 76.7, 38.4 Hz); **¹¹B NMR** (128 MHz, CDCl₃) δ -0.16 (q, J = 38.5 Hz). **IR** (v/cm-1, ATR/heat): 2960, 2938, 2877, 1552, 1457, 1439, 1386, 1339, 1304, 1256, 1230, 1179, 1151, 1121, 1105, 1072, 1040, 1031, 1019, 974, 930, 889, 870, 854, 823, 782, 738, 726, 701, 673, 643, 624, 594, 576, 561, 555, 538, 528, 515, 503; **HRMS** (ESI): calcd for C₇H₁₃BF₃NS (M + NH₄⁺): 229.1152, found: 229.1149.

Synthesis of (178)

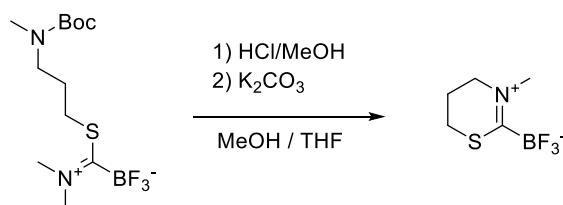


Potassium N,N-dimethylthiocarbamoyl trifluoroborate (7.499 g, 38.45 mmol, 1.25 equiv) was dispersed in 60 mL dry DMF under N_2 . tert-butyl N,N-(3-iodopropyl)methylcarbamate (9.200 g, 30.75 mmol, 1.0 equiv) was added and the mixture was stirred under rt for 17 h. The full consumption of the iodide was checked by TLC (10% MeOH/ $CHCl_3$) before solvent was removed in vacuo (45 °C, < 1 mbar) to give a white slurry or solid. The white mass was dispersed in ~ 100 mL CH_2Cl_2 and filtered through a celite pad to remove KI. The filtrate was evaporated before chromatography on silica to give **178** as a sticky colorless liquid with cloudy suspension (10.2 g, quant). The oily product was pure enough for the next step, and contained only residual $CHCl_3$ as the observed impurity. Chromatography was performed for elemental analysis and melting point measurement.

Chromatography condition: Column volume (cv) ~ 110 mL packed with $CHCl_3$. Elution sequence: $CHCl_3$ 1 cv, 5% MeOH/ $CHCl_3$ 2cv, 10% MeOH/ $CHCl_3$ 2 cv. Pure product resides in fractions after 1 ~ 3.66 cv and were evaporated to give S-(3-(N,N-tert-butoxycarbonylmethyl)-prop-1-yl)-trifluoroborate dimethyliminium as a transparent sticky liquid that solidifies upon standing (5.726 g, 56.7%, mp 46–51 °C)

1H NMR (400 MHz, $CDCl_3$) : δ [ppm] = 3.72 (s, 3H), 3.51 (t, J = 7.4 Hz, 2H), 3.37 (s, 3H), 3.31 (t, J = 6.9 Hz, 2H), 2.84 (s, 3H), 2.15 – 1.81 (m, 2H), 1.44 (s, 9H); ^{13}C NMR (125 MHz, $CDCl_3$) : δ [ppm] = 214.02– 211.79 (m), 155.77, 79.76, 48.37, 47.85, 47.29, 45.56, 34.30, 31.90, 28.51. ^{19}F NMR (377 MHz, $CDCl_3$) δ -137.01 (q, J = 37.6 Hz); ^{11}B NMR (128 MHz, $CDCl_3$) δ -0.16 (q, J = 37.9 Hz); **Elemental analysis**: Calc 43.92% C, 7.37%H, 8.54%N, 17.37%F, 9.77%S, found 44.03% C, 7.53%H, 8.50% N, 13.60%F, 9.65%S.

Synthesis of (179)

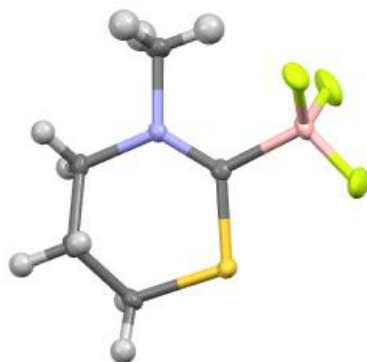


S-(3-(N,N-tert-butoxycarbonylmethyl)-prop-1-yl)-trifluoroborate dimethyliminium (**178**) (4.201g, 12.8 mmol) was added HCl solution in MeOH (1.25 M, > 9 eq, 115.2 mmol, 92.2 mL) under 0 °C and the mixture was stirred overnight under N₂. TLC indicated full consumption of starting material.

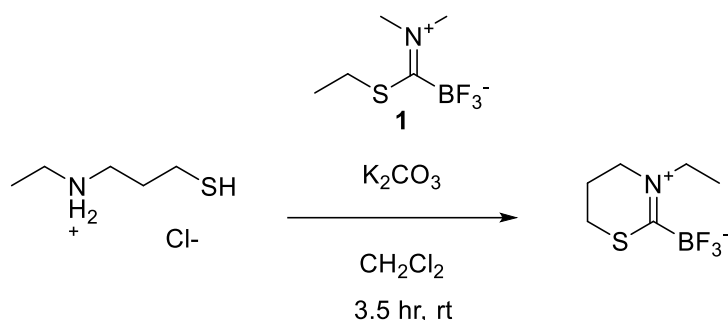
THF (20 mL) was added to the overnight reaction mixture from the previous step. K₂CO₃ (15.9 g, 115.2 mol, 9 equiv) was added slowly to the mixture at rt while the resulting white suspension was stirred vigorously. 15 min later the mixture was mildly warm. The mixture was stirred for another 15 min and the color turns slightly pink. TLC (1:1 acetone-Cy) indicated full conversion. The reaction mixture was further treated with 30 mL of THF before filtered through a celite plug. The slightly yellow filtrate was concentrated in vacuo then washed with 50 mL pentane to give a crude product. The crude product was dissolved in ~ 100 mL CHCl₃, filtered through silica plug, evaporated and then triturated again with pentane to give **179** as a crystalline white powder (1.782 g, 9.74 mmol, 76.1% mp 112.6–113.5 °C)

¹H NMR (600 MHz, CDCl₃) δ 3.57 – 3.50 (m, 5H), 2.94 – 2.84 (m, 2H), 2.48 – 2.20 (m, 2H); ¹³C NMR (151 MHz, CDCl₃) δ 203.51– 200.93(m), 51.41, 47.84, 24.29, 20.13. ¹⁹F NMR (376 MHz, CDCl₃) δ -144.71 (q, J = 37.8 Hz). ¹¹B NMR (128 MHz, CDCl₃) δ -0.07 (q, J = 37.7 Hz); ¹H NMR (400 MHz, CD₃CN) δ 3.53 (d, J = 5.5 Hz, 5H), 2.96 – 2.80 (m, 2H), 2.21 – 2.06 (m, 2H); ¹⁹F NMR (376 MHz, CD₃CN) δ -144.13 (dd, J = 75.6, 37.9 Hz); ¹¹B NMR (128 MHz, CD₃CN) δ -0.69 (q, J = 37.9 Hz); IR (ν/cm⁻¹, ATR/heat): 2998, 2974, 2953, 2873, 1616, 1590, 1454, 1432, 1356, 1292, 1213, 1196, 1175, 1117, 1067, 1037, 1004, 975, 898, 807, 765, 724, 687, 640, 617, 595, 561, 541, 502; HRMS (ESI): calcd for C₅H₉BF₃NS (M+Na⁺) 206.0394 found: 206.0392.

Crystal Data for C₅H₉BF₃NS (M = 183.00 g/mol): monoclinic, space group P2₁/n (no. 14), a = 5.85390(10) Å, b = 9.94400(10) Å, c = 13.51710(10) Å, β = 101.2970(10)°, V = 771.601(17) Å³, Z = 4, T = 100.0(1) K, μ(CuKα) = 3.698 mm⁻¹, D_{calc} = 1.575 g/cm³, 15410 reflections measured (11.124° ≤ 2θ ≤ 159.266°), 1671 unique (R_{int} = 0.0286, R_{sigma} = 0.0127) which were used in all calculations. The final R₁ was 0.0279 (I > 2σ(I)) and wR₂ was 0.0737 (all data).



Synthesis of reagent (192)



N-ethyl-3-mercaptopropan-1-aminium chloride (390 mg, 2.5 mmol, 1.04 equiv) was dissolved in MeOH (5 mL) added K_2CO_3 (353.6 mg, 2.56 mmol, 1.07 equiv) was added and stirred for 15 min at 23 °C to give a slightly pink suspension. A solution of KAT reagent **1** (445.5 mg, 2.4 mmol, 1 equiv) in CH_2Cl_2 (5 mL) was added. Within 7 minutes the suspension turned orange. After 30 min TLC (1:1 acetone-cyclohexane) indicated the consumption of **1**. The reaction mixture was stirred for 3 additional hours before being dried under nitrogen flow in a fumehood to give a white solid overnight. (Note: strongly repulsive smell and possible allergenicity of EtSH, a bleach gas outlet trap is recommended)

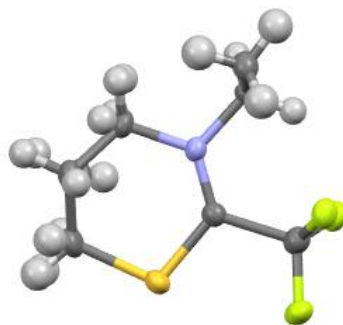
The reaction mixture was dissolved in acetone and chromatographed on a silica column packed in 4:1 cyclohexane-acetone to give the product as white crystalline solid (244.7 mg, 1.24 mmol, 51.7%, mp 94.3–96.0 °C)

Chromatography: V_{int} 47 mL, eluents: 56.5 mL 4:1 cyclohexane:acetone, 100 mL 4:1 cyclohexane:acetone into fractions 1–11, 100 mL 7:3 cyclohexane:acetone into fractions 11–22, 100 mL 4:6 cyclohexane:acetone into fractions 22–33, 100 mL 1:1 cyclohexane:acetone into fractions 34–45, among which fractions 27–42 contained the product.

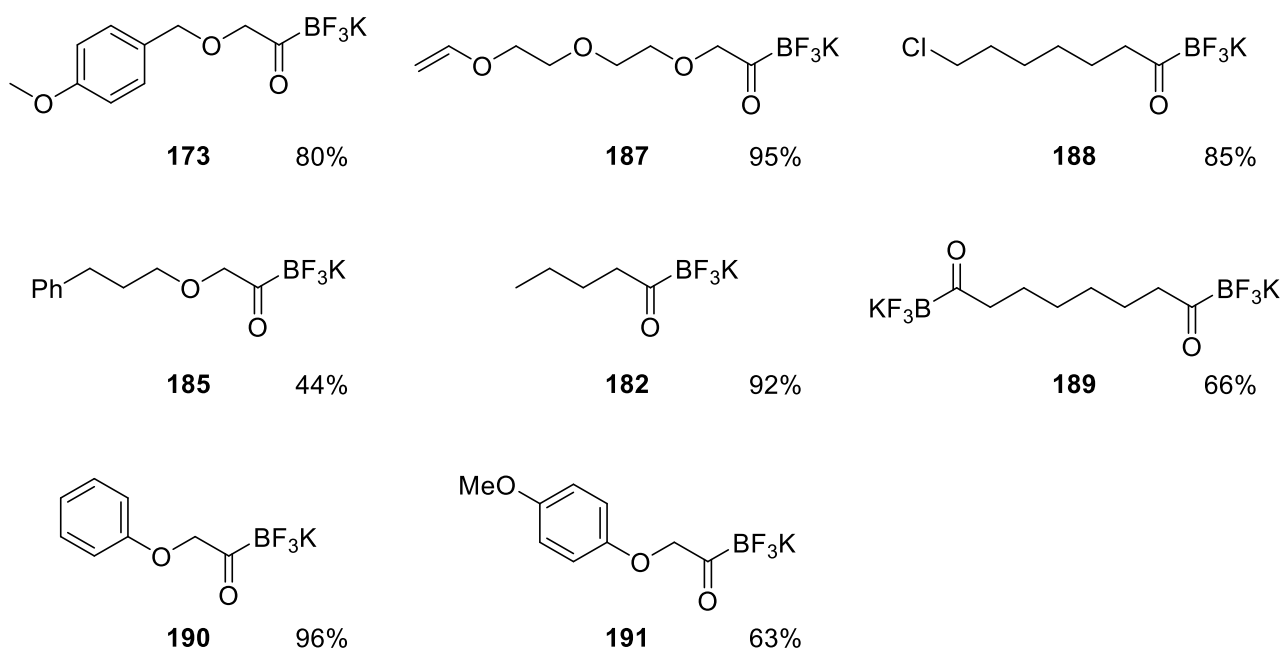
$^1\text{H NMR}$ (600 MHz, CDCl_3) δ 3.98 (q, $J = 7.2$ Hz, 2H), 3.62 – 3.48 (m, 2H), 3.01 – 2.79 (m, 2H), 2.55 – 2.16 (m, 2H), 1.38 (t, $J = 7.2$ Hz, 3H); $^{13}\text{C NMR}$ (151 MHz, CDCl_3) δ 202.87–

200.28, 56.12, 48.63, 25.09, 20.30, 13.35; **^{19}F NMR** (377 MHz, CDCl_3) δ -144.22 (dd, $J = 75.6$, 37.6 Hz); **^{11}B NMR** (128 MHz, CDCl_3) δ -0.59 (q, $J = 37.7$ Hz); **IR** (ATR/heat): 3043, 2998, 2974, 2947, 2884, 2859, 1577, 1478, 1464, 1450, 1438, 1382, 1367, 1349, 1296, 1284, 1267, 1247, 1199, 1188, 1164, 1153, 1101, 1086, 1051, 1016, 988, 942, 902, 884, 853, 815, 786, 716, 701, 680, 661, 641, 623, 591, 563, 539, 525, 511; **HRMS** (ESI⁺): calcd for $\text{C}_6\text{H}_{11}\text{BF}_3\text{NS}$ (M+Na): 220.0551, found: 220.0551;

Crystal Data for $\text{C}_7\text{H}_{11}\text{F}_3\text{NS}$ ($M = 198.23$ g/mol): monoclinic, space group Cc (no. 9), $a = 6.9755(2)$ Å, $b = 12.6444(3)$ Å, $c = 9.9407(3)$ Å, $\beta = 99.851(3)^\circ$, $V = 863.85(4)$ Å³, $Z = 4$, $T = 100.0(1)$ K, $\mu(\text{Cu K}\alpha) = 3.368$ mm⁻¹, $D_{\text{calc}} = 1.524$ g/cm³, 8627 reflections measured ($14.008^\circ \leq 2\theta \leq 159.874^\circ$), 1765 unique ($R_{\text{int}} = 0.0733$, $R_{\text{sigma}} = 0.0367$) which were used in all calculations. The final R_1 was 0.0560 ($I > 2\sigma(I)$) and wR_2 was 0.1514 (all data).



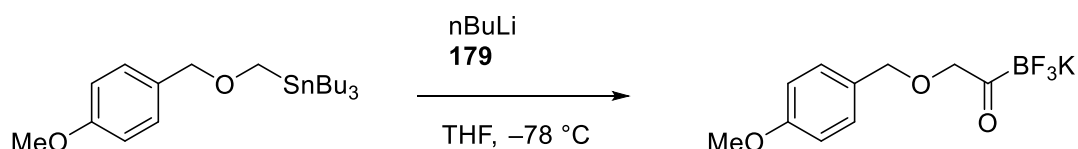
7.1.7. Synthesis of KATs with reagent (179)



General procedure C for KAT synthesis with reagent (179)

A solution of the alkyllithium was prepared in THF (0.05 M) and stirred at $-78\text{ }^{\circ}\text{C}$ for 10 min before reagent solid **179** (1 equiv) was added to the reaction mixture, which was stirred for another hour while allowed to return to rt. Acetaldehyde (20% v/v or 4 mL/mmol reactant) and $\text{KF}_{(\text{aq})}$ (6.5M, 10% v/v or 2 mL/mmol) was added and the reaction mixture was stirred vigorously overnight before being evaporated. The residue was washed with Et_2O and CH_2Cl_2 , and dried under vacuum before being extracted with acetone or DMF, depending on the solubility of the product KAT. The filtrate was evaporated again to give the product as a pale yellow or white solid. If DMF was used, the final filtrate was evaporated to a small volume and the product was collected by reprecipitation in Et_2O .

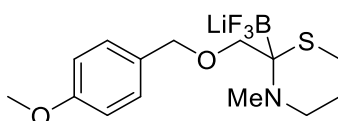
Synthesis of (173)



4-methoxybenzyloxymethyl tributylstannane (225.2 mg, 510.4 μmol , 1 equiv) was dissolved in THF (10 mL, distilled) and nBuLi (1.6 M, 319.0 μL , 1 equiv) was added at $-78\text{ }^{\circ}\text{C}$ and stirred for 5 min to prepare the alkyllithium solution that was applied General Procedure C to obtain **173** as a white solid (116.3 mg, 406.5 μmol , 79.6%). **173** was not soluble in acetone and CH_3CN , and soluble in DMF, DMSO and aqueous CH_3CN .

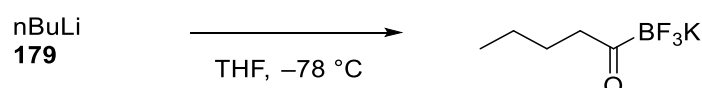
¹H NMR (600 MHz, DMSO-d₆) δ 7.23 (dt, J = 9.0, 0.6 Hz, 2H), 6.89 (d, J = 8.7 Hz, 2H), 4.32 (s, 2H), 4.11 (s, 2H), 3.74 (s, 3H); **¹³C NMR** (151 MHz, DMSO) δ 240.66, 159.04, 131.10, 129.66, 113.97, 77.84, 71.80, 55.48; **¹⁹F NMR** (377 MHz, DMSO-d₆) δ -146.94; **¹¹B NMR** (128 MHz, DMSO-d₆) δ -1.82; **IR** (ATR, neat): 2936, 2871, 2846, 2790, 1723, 1669, 1603, 1494, 1453, 1431, 1403; **HRMS**: calcd for C₁₀H₁₁BF₃O₃K (M-K⁺): 247.0761, found 247.0756.

If the reaction mixture was evaporated without performing the acetaldehyde workup, **186** was obtained as a brown solid.

**186**

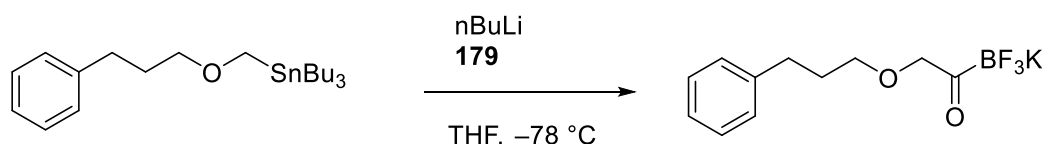
¹H NMR (400 MHz, DMSO-d₆) δ 7.27 (d, J = 8.6 Hz, 2H), 6.89 (d, J = 8.7 Hz, 2H), 4.47 – 4.31 (m, 2H), 3.86 (d, J = 9.7 Hz, 1H), 3.74 (s, 3H), 3.70 – 3.62 (m, 1H), 3.20 (t, J = 12.7 Hz, 1H), 2.89 (t, J = 12.0 Hz, 1H), 2.54 (s, 1H), 2.43 (s, 3H), 2.35 (dd, J = 12.4, 4.2 Hz, 1H), 1.65 (q, J = 11.9 Hz, 1H), 1.21 – 1.07 (m, 1H); **¹³C NMR** (151 MHz, DMSO) δ 158.26, 131.22, 128.79, 113.34, 74.68, 71.69, 65.66, 54.88, 48.36, 38.50, 24.06, 17.16; **¹⁹F NMR** (376 MHz, DMSO-d₆) δ -140.96; **¹¹B NMR** (160 MHz, DMSO-d₆) δ 2.51; **HRMS** (ESI): calcd for C₁₄H₂₀BF₃NO₂SK (M – K) 334.1265, found 334.1271.

Synthesis of (182)



Following General Procedure C, nBuLi (1.6 M, 500 μL, 800 μmol, 1 equiv) was added to a suspension of **179** (146.4 mg, 800 μmol, 1 equiv) in THF (20 mL). n-Butyl KAT was obtained as a white flaky solid (104.02 mg, 736.0 μmol, 92.0%). The analytical data for this KAT was reported before.¹⁷¹

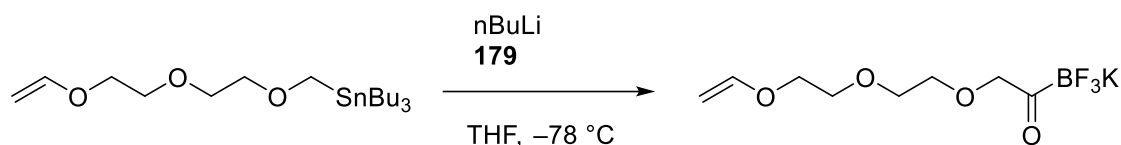
Synthesis of (185)



Using 3-phenylpropyltrimethylstannane (200 μL, 215.2 mg, 489.9 μmol, 1 equiv), following the procedure used for the synthesis of compound **173**, **185** was obtained as a white wax (61.8 mg, 218 μmol, 44.4%). **185** was soluble in acetone, and sparingly soluble in THF.

¹H NMR (400 MHz, DMSO-d₆) δ 7.51 – 6.90 (m, 5H), 4.09 (s, 2H), 3.32 – 3.25 (m, 2H), 2.66 – 2.56 (m, 2H), 1.81 – 1.68 (m, 2H); **¹³C NMR** (151 MHz, DMSO) δ 240.35, 141.96, 128.27, 128.22, 125.61, 78.36, 69.53, 31.76, 31.22; **¹⁹F NMR** (377 MHz, DMSO-d₆) δ -146.91; **¹¹B NMR** (128 MHz, DMSO-d₆) δ -0.99 – -3.42 (m); **IR** (ν/cm⁻¹, ATR/heat): 3085, 3057, 3028, 2936, 2871, 2846, 2790, 1723, 1669, 1603, 1494, 1453, 1431, 1403, 1360, 1333, 1285, 1235, 1164, 1118, 1082, 1048, 1002, 921, 873, 821, 793, 751, 717, 695, 660, 637, 607, 583, 558, 526; **HRMS** (ESI): calcd for C₁₁H₁₃BF₃O₂K (M-K⁻): 245.0968, found 245.0969.

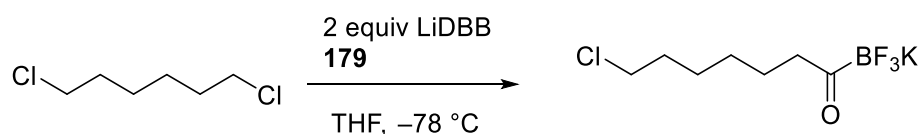
Synthesis of (187)



2-(2-(2-vinyloxy)-ethoxy)ethoxymethyl tributylstannane (500 μL, 560.7 mg, 1.29 mmol, 1.0 equiv) was dissolved in 10 mL THF and cooled to -78 °C and stirred for 20 min before nBuLi (850 uL, 1.6 M, 1.36 mmol, 1.05 equiv) was added over 2 min. The reaction mixture was stirred for 25 min before **179** (236.1 mg, 1.29 mmol, 1.0 equiv) was added. After 45 min the mixture turned from a suspension to a clear solution and was stirred for an additional 30 min before KF_(aq) (6.5M, 1.5 mL) and acetaldehyde (2 mL) was added. The mixture was stirred overnight before being evaporated and precipitated in 1:1 pentane-Et₂O to give a yellow oil that solidifies to a yellow wax upon standing (345.2 mg, 1.23 mmol, 95.3%, mp 46.2–49.9 °C).

¹H NMR (600 MHz, DMSO-d₆) δ 6.50 (dd, J = 14.3, 6.8 Hz, 1H), 4.19 (dd, J = 14.3, 1.8 Hz, 1H), 4.13 (s, 2H), 3.97 (dd, J = 6.7, 1.8 Hz, 1H), 3.82 – 3.75 (m, 2H), 3.65 – 3.58 (m, 2H), 3.54 – 3.48 (m, 2H), 3.47 – 3.40 (m, 2H); **¹³C NMR** (151 MHz, DMSO-d₆) δ 240.29, 151.84, 86.89, 78.61, 69.84, 69.49, 68.73, 67.22; **¹⁹F NMR** (377 MHz, CD₃CN) δ -150.47 (d, J = 39.3 Hz); **¹¹B NMR** (128 MHz, CD₃CN) δ 3.66; **IR** (ATR/heat): 2927, 2901, 2869, 2836, 1662, 1639, 1622, 1579, 1453, 1426, 1403, 1382, 1348, 1321, 1288, 1249, 1191, 1162, 1132, 1097, 1063, 1024, 978, 917, 891, 828, 773, 704, 634, 590, 561, 534; **HRMS** (ESI): calcd for C₈H₁₃BF₃O₄K (M – K): 241.0864, found 241.0859.

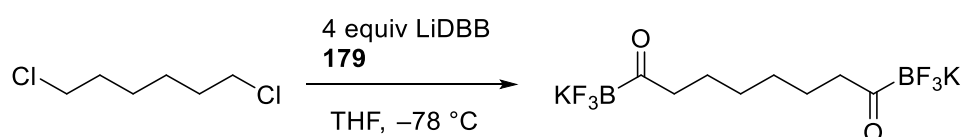
Synthesis of (188)



To a solution of lithium di-tert-butylbiphenyl (LiDBB) in THF (2.60 mL, 0.2M, 521 μmol , 2.2 equiv) at $-78\text{ }^{\circ}\text{C}$, 1,6-dichlorohexane (34.3 μL , 36.7 mg, 237 μmol , 1.0 equiv) was added. The solution turns purple immediately and was stirred for 30 min before **179** (95.3 mg, 521 μmol , 2.2 equiv) was added in THF (4 mL) over 2 min. The purple color faded after 2 mL of the **179** solution was added. The reaction mixture was stirred overnight at rt. $\text{KF}_{(\text{aq})}$ (200 μL , 6.5 M) and acetaldehyde (400 μL) was added and the mixture was stirred for 2 hr before being evaporated. After extraction with acetone (2 mL) and reprecipitated in Et_2O , **188** was obtained as a pale yellow solid (51.1 mg, 201 μmol , 84.8%, mp $115\text{ }^{\circ}\text{C}$ dec).

$^1\text{H NMR}$ (400 MHz, CD_3CN) δ 3.57 (t, $J = 6.8$ Hz, 2H), 2.35 (t, $J = 7.3$ Hz, 2H), 1.80 – 1.66 (m, 2H), 1.50 – 1.35 (m, 4H), 1.31 – 1.20 (m, 2H); $^{13}\text{C NMR}$ (126 MHz, CD_3CN) δ 46.28, 33.36, 31.55, 29.69, 27.58, 23.19. (the carbonyl signal was not resolved); $^{19}\text{F NMR}$ (376 MHz, CD_3CN) δ -150.35 (dd, $J = 108.1, 52.0$ Hz); $^{11}\text{B NMR}$ (128 MHz, CD_3CN) δ 0.37 – -2.43 (m) IR (v/cm^{-1} , ATR/neat): 2931, 2858, 1711, 1661, 1590, 1463, 1444, 1431, 1405, 1362, 1311, 1267, 1222, 1154, 1111, 1070, 992, 978, 929, 864, 853, 839, 822, 810, 774, 746, 723, 693, 649, 633, 608, 587, 554, 529; HRMS (ESI): calcd for $\text{C}_7\text{H}_{12}\text{BCIF}_3\text{OK}$ ($\text{M} - \text{K}$): 215.0627, found 215.0627.

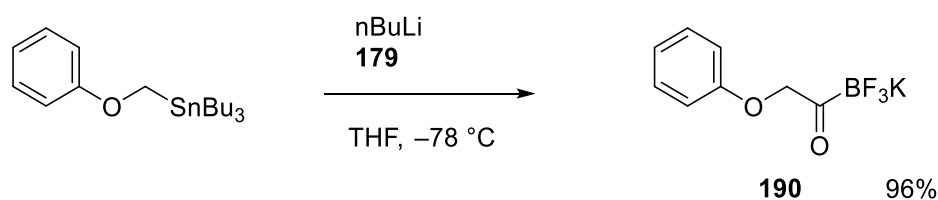
Synthesis of (189)



Following the same procedure for the synthesis of **188**, using 4.4 equiv of LiDBB (5.0 mL, 0.2 M, 1.0 mmol, 4.4 equiv), 1,6-dichlorohexane (32.9 μL , 35.2 mg, 227 μmol , 1 equiv) and **179** (91.5 mg, 500 μmol , 2.2 equiv), after treatment with $\text{KF}_{(\text{aq})}$ and acetaldehyde, evaporation of solvents gave a white solid. The solid was washed with CH_2Cl_2 , redissolved in DMF (3 mL) and reprecipitated in acetone (15 mL) to give **189** as a white solid (53.3 mg, 151 μmol , 66.3%, mp $160\text{ }^{\circ}\text{C}$ dec). **189** was insoluble in acetone and CH_3CN .

$^1\text{H NMR}$ (600 MHz, DMSO-d_6) δ 2.21 (m, 4H), 1.33 – 1.25 (m, 4H), 1.13 – 1.07 (m, 4H); $^{13}\text{C NMR}$ (151 MHz, DMSO) δ 245.72, 44.23, 29.43, 22.20; $^{19}\text{F NMR}$ (376 MHz, DMSO-d_6) δ -147.44 (m); $^{11}\text{B NMR}$ (128 MHz, DMSO-d_6) δ -1.29 (q, $J = 57.6$ Hz); IR (v/cm^{-1} , ATR/neat): 2937, 2924, 2900, 2878, 2846, 1669, 1406, 1368, 1324, 1229, 1184, 1154, 1120, 1101, 1054, 1021, 1003, 975, 926, 822, 776, 761, 721, 706, 677, 661, 650, 631, 591, 580, 554, 536, 509; HRMS (ESI) calcd for $\text{C}_8\text{H}_{12}\text{B}_2\text{F}_6\text{O}_2\text{K}_2$ ($\text{M} - 2\text{K}^{2-}$): 276.0939, found: 276.0935.

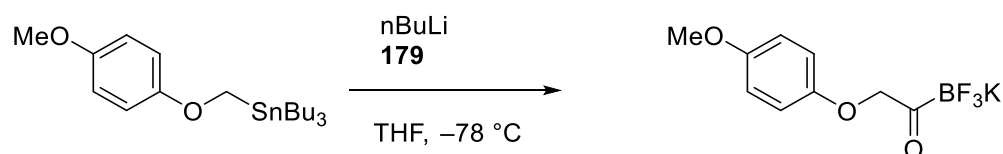
Synthesis of (190)



Following General Procedure C using phenoxymethyltributylstannane (235.3 mg, 592.4 μmol , 1 equiv), after extraction with DMF (4 mL) and precipitation in Et_2O (15 mL), **190** was obtained as a white solid (137.6 mg, 568.5 μmol , 96.0%, mp $143\text{ }^{\circ}\text{C}$ dec)

$^1\text{H NMR}$ (400 MHz, $\text{CD}_3\text{CN-D}_2\text{O}$) δ 7.31 – 7.17 (m, 2H), 6.98 – 6.86 (m, 1H), 6.84 – 6.74 (m, 2H), 4.86 (s, 2H); $^{13}\text{C NMR}$ (151 MHz, $\text{CD}_3\text{CN-D}_2\text{O}$) δ 241.64, 158.87, 130.51, 121.95, 115.38, 75.93; $^{19}\text{F NMR}$ (376 MHz, $\text{CD}_3\text{CN-D}_2\text{O}$) δ -151.60 (dd, $J = 48\text{ Hz}$); $^{11}\text{B NMR}$ (128 MHz, $\text{CD}_3\text{CN-D}_2\text{O}$) δ -4.23 (q, $J = 53\text{ Hz}$); **IR**(ATR, neat): 3344, 1681, 1599, 1496, 1482, 1421, 1337, 1287, 1241, 1191, 1167, 1095, 1064, 1037, 1011, 995, 956, 922, 883, 863, 820, 749, 686, 655, 637, 613, 575, 553, 506; **HRMS** (ESI) calcd. for $\text{C}_8\text{H}_7\text{BF}_3\text{O}_2\text{K}$ ($M - \text{K}$): 203.0947, found 203.0945.

Synthesis of (191)

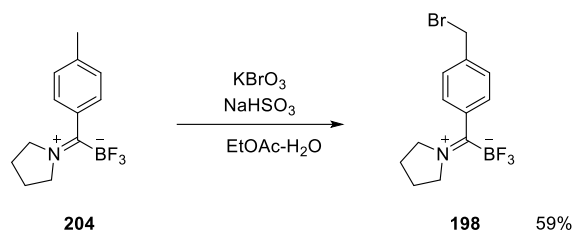


Following General Procedure C using p-methoxyphenoxymethyltributylstannane (452 mg, 1.06 mmol, 1.0 equiv), after extraction with DMF (15 mL) the filtrate was evaporated and chromatographed on silica (1:1 acetone-cyclohexane) to give a brown solid (181.7 mg, 667.8 μmol , 63.1%, mp $105\text{ }^{\circ}\text{C}$ dec)

$^1\text{H NMR}$ (600 MHz, CD_3CN) δ 6.95 – 6.64 (m, 4H), 4.81 (s, 2H), 3.71 (s, 4H); $^{13}\text{C NMR}$ (151 MHz, CD_3CN) δ 242.86, 154.94, 153.47, 116.67, 115.44, 76.83, 56.21; $^{19}\text{F NMR}$ (377 MHz, CD_3CN) δ -151.21 – -153.83 (m); $^{11}\text{B NMR}$ (128 MHz, CD_3CN) δ -1.77 (q, $J = 52.5, 47.7\text{ Hz}$); **IR**: (ATR, neat, cm^{-1}) 3056, 2890, 1642, 1599, 1496, 1421, 1337, 1286, 1241, 1167, 1064, 1011, 955, 922, 863, 820, 749, 686, 637; **HRMS** (ESI): calcd for $\text{C}_9\text{H}_9\text{BF}_3\text{O}_3\text{K}$ ($M - \text{K}$): 233.0602, found 233.0606.

7.1.8. Synthesis of Compounds in Chapter 6

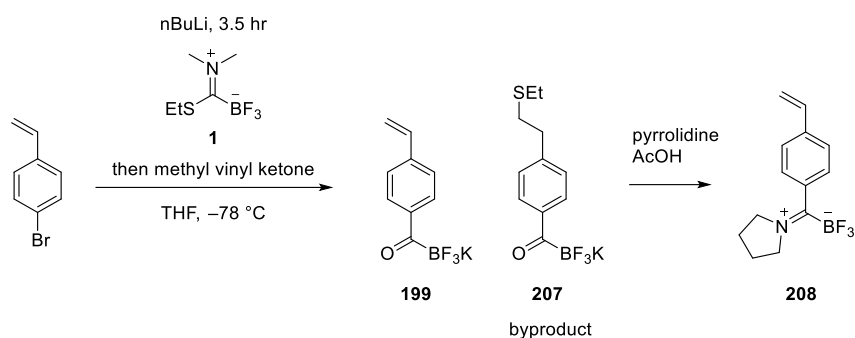
Synthesis of (198)



p-methylphenyl pyrrolidine TIM (230.8 mg, 957.4 μmol , 1 equiv) was dissolved in 1 mL EtOAc and mixed with $\text{KBrO}_3(\text{aq})$ (2 M, 1 mL) and the resulting biphasic mixture was stirred vigorously. An aqueous solution of NaHSO_3 (1 M, 2 mL) was added dropwise into the mixture, during which heat evolved and the color turns red after the addition of each drops before fading slowly. The addition lasted 2 min, after which the mixture was allowed to stir for another 20 min before the organic layer was collected, washed with NaHSO_3 until colorless, evaporated, and chromatographed on a silica column packed in 4:1:1 Cy-EtOAc- CH_2Cl_2 .

Chromatography: V_{int} 35 mL, eluents: 55 mL 4:1:1 cyclohexane-EtOAc- CH_2Cl_2 , 180 mL 2:1:1 EtOAc- CH_2Cl_2 into fractions 1–16, among which fractions 13–21 contained the product. After evaporation of the fractions the product was obtained as a white solid (179.5 mg, 561 μmol , 58.6%, mp 145°C dec)

$^1\text{H NMR}$ (400 MHz, CDCl_3) δ 7.50 – 7.38 (m, 2H), 7.31 – 7.22 (m, 2H), 4.47 (s, 2H), 4.40 – 4.28 (m, 2H), 3.73 – 3.56 (m, 2H), 2.24 – 2.07 (m, 2H), 2.05 – 1.88 (m, 2H); **$^{13}\text{C NMR}$** (126 MHz, CDCl_3) δ 205.96– 203.00 (m), 139.79, 137.08, 129.25, 125.76, 55.84, 55.73 (q, $J = 3.2$ Hz), 32.53, 24.33, 24.01; **$^{19}\text{F NMR}$** (376 MHz, CDCl_3) δ -143.88 (q, $J = 39$ Hz); **$^{11}\text{B NMR}$** (128 MHz, CDCl_3) δ -0.36 (q, $J = 40.1$ Hz); **IR** (v/cm^{-1} , ATR/neat): 3029, 2997, 1633, 1074, 1044, 1014, 970, 890, 819, 628, 606; **HRMS** (ESI): calcd for $\text{C}_{12}\text{H}_{14}\text{BBrF}_3\text{N}$ ($\text{M} + \text{NH}_4$): 337.0695, found 337.0697.

Synthesis of styryl KAT (**199**) and its pyrrolidine TIM (**208**)

p-Bromostyrene (980 mg, 4.91 mmol, 1.00 equiv) was dissolved in THF (50 mL) and stirred at $-78\text{ }^{\circ}\text{C}$. nBuLi (3.2 mL, 1.6 M, 5.1 mmol, 1.04 equiv) was added dropwise. The solution immediately turns yellow was stirred for 3.5 h. KAT reagent **1** (1.000 g, 5.40 mmol, 1.1 equiv) was added and the mixture was stirred for an additional 30 min at $-78\text{ }^{\circ}\text{C}$ before being quenched with methyl vinyl ketone (1.3 mL) and $\text{KF}_{(\text{aq})}$ (6 mL, 6.5 M). The quenched mixture was stirred at rt for 15 min before being evaporated and dried under vacuum, after which the product was extracted with acetone (20 mL) and reprecipitated in Et_2O (150 mL * 2) to give a pale yellow powder containing KAT **199** (893.8 mg, purity 85% (NMR), 3.19 mmol, 65%)

¹H NMR (400 MHz, CD_3CN) δ 8.01 (dq, $J = 8.0, 0.6\text{ Hz}$, 2H), 7.56 – 7.49 (m, 2H), 6.82 (ddt, $J = 17.7, 10.9, 0.5\text{ Hz}$, 1H), 5.90 (dd, $J = 17.7, 1.0\text{ Hz}$, 1H), 5.35 (dd, $J = 10.9, 0.9\text{ Hz}$, 1H); **¹³C NMR** (126 MHz, CD_3CN) δ 141.06, 137.58, 129.40, 126.77 (d), 116.38, 115.86; **¹⁹F NMR** (376 MHz, CD_3CN) δ -144.44 (q, $J = 52\text{ Hz}$); **¹¹B NMR** (128 MHz, CD_3CN) δ -0.99 (q, $J = 53.9\text{ Hz}$); **HRMS** (ESI): calcd for $\text{C}_9\text{H}_7\text{BF}_3\text{OK}$ ($M - K$): 199.0548, found 199.0549.

KAT **199** (140 mg, 588 μmol , 1.0 equiv) and pyrrolidine hydrochloride (69.0 mg, 647 μmol , 1.1 equiv) were dissolved in DMF (3 mL) left to stir for 1h before being evaporated and chromatographed on silica (eluent: 2:1:1 cyclohexane-EtOAc- CH_2Cl_2) to give **208** as a white solid (122 mg, 482 μmol , 82%, mp 105.4–107.7 $^{\circ}\text{C}$).

¹H NMR (500 MHz, CDCl_3) δ 7.54 – 7.39 (m, 1H), 7.38 – 7.14 (m, 1H), 6.70 (dd, $J = 17.6, 10.9\text{ Hz}$, 1H), 5.81 (dd, $J = 17.6, 0.8\text{ Hz}$, 1H), 5.34 (dd, $J = 10.9, 0.7\text{ Hz}$, 1H), 4.47 – 4.32 (m, 1H), 3.69 (t, $J = 7.2\text{ Hz}$, 1H), 2.21 – 2.05 (m, 1H), 2.03 – 1.91 (m, 1H); **¹³C NMR** (151 MHz, CDCl_3) δ 206.54–203.97 (m), 139.74, 136.29, 135.91, 126.36, 126.12, 116.22, 55.82, 55.67 (d, $J = 3.3\text{ Hz}$), 24.43, 24.22; **¹⁹F NMR** (377 MHz, CDCl_3) δ -144.34 (q, $J = 40\text{ Hz}$); **¹¹B NMR** (160 MHz, CDCl_3) δ -0.30 (q, $J = 40.1\text{ Hz}$); **IR** (ATR, neat): 2980, 2953, 2927, 1729, 1701, 1681, 1591, 1565, 1555, 1529, 1487, 1451, 1433, 1419, 1398, 1380, 1367, 1298, 1258, 1171,

1141, 1109, 1089, 1042, 1013, 963, 914, 894, 842, 804, 731, 644, 608; **HRMS** (ESI): calcd for C₁₃H₁₅BF₃N (M+Na) 276.1144 found: 276.1146.

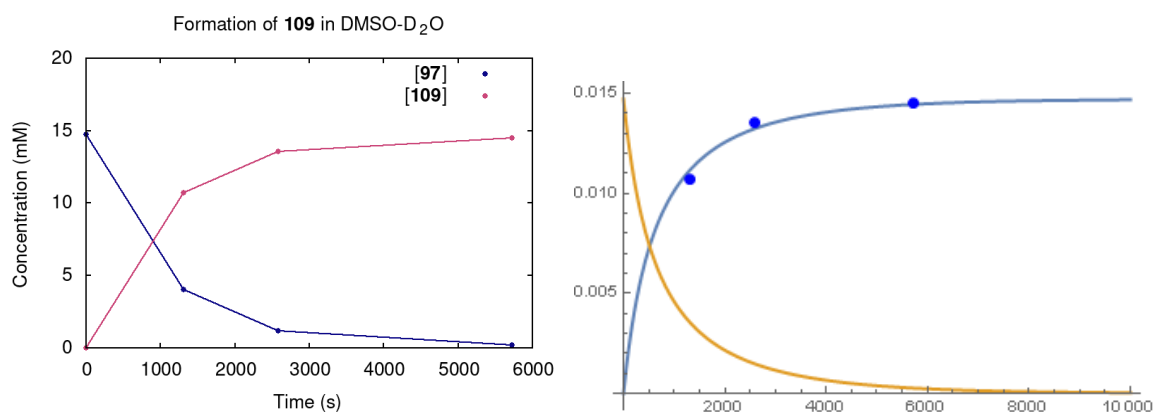
7.2. Nitron exchange experiments

7.2.1. Nitron partner exchange In Section 2.4

Nitrones **111** and **112** were synthesized from the corresponding KATs and hydroxylamines and chromatographed before preparing stock solutions of 40 mM in CD₃CN. The intensity of the residual proton solvent peak (CHD₂CN) was pre-determined using mesitylene as an internal standard for the batch of CD₃CN used. The integration of nitron ¹H peaks versus the residual solvent peak intensity was used to determine the concentration of the nitron solutions. To the stock solution, appropriate amounts of CH₃CN and H₂O were added to make a solution of 1:1 CH₃CN(+CD₃CN)-H₂O, containing 20 mM of either nitron **111** or **112**. An equal volume of these two solutions were mixed to form the nitron exchange reaction mixture, with both nitrones having starting concentration of 10 mM.

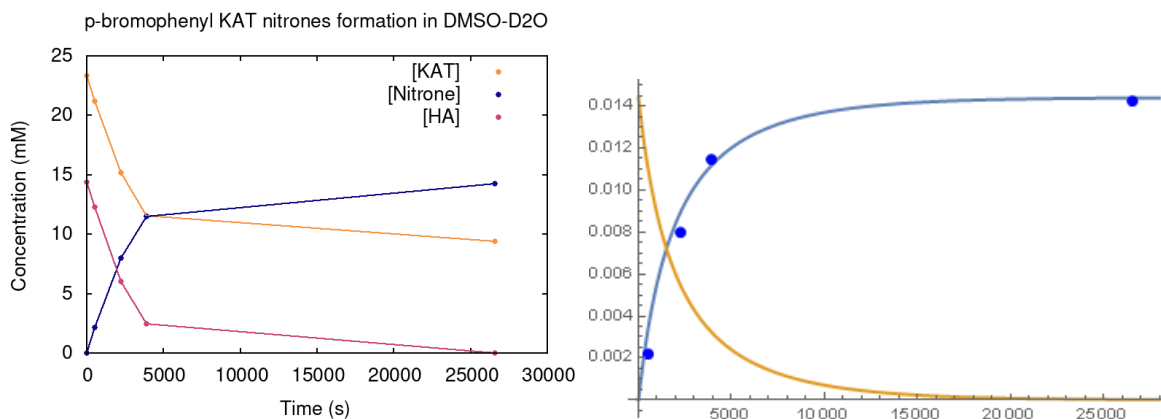
7.3. Kinetic measurement results of KAT nitron formation

7.3.1. Butyl, p-F-phenyl and p-OMe-phenyl KAT in 1:1 DMSO-H₂O

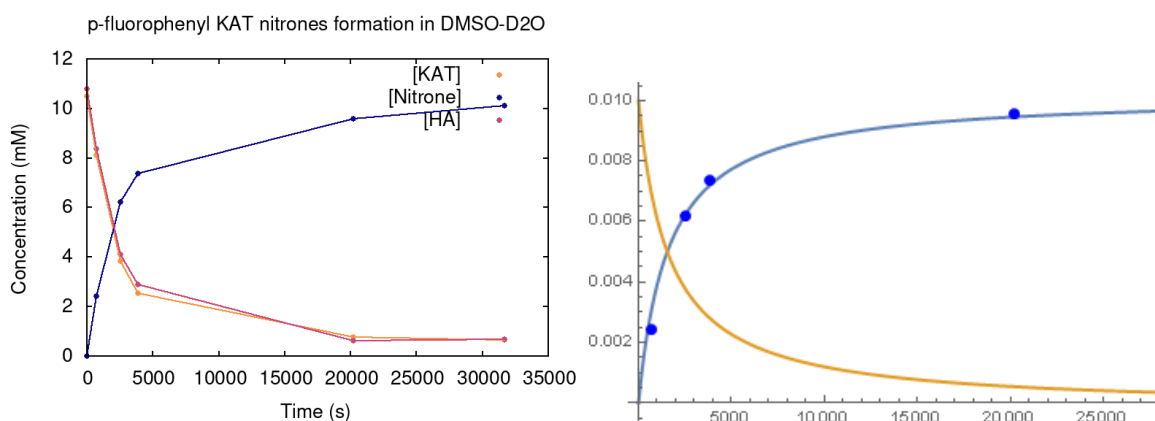


Butyl KAT + **97**: $k = 0.0822 \text{ M}^{-1}\text{s}^{-1}$. Left: collected data. Right: model fitting.

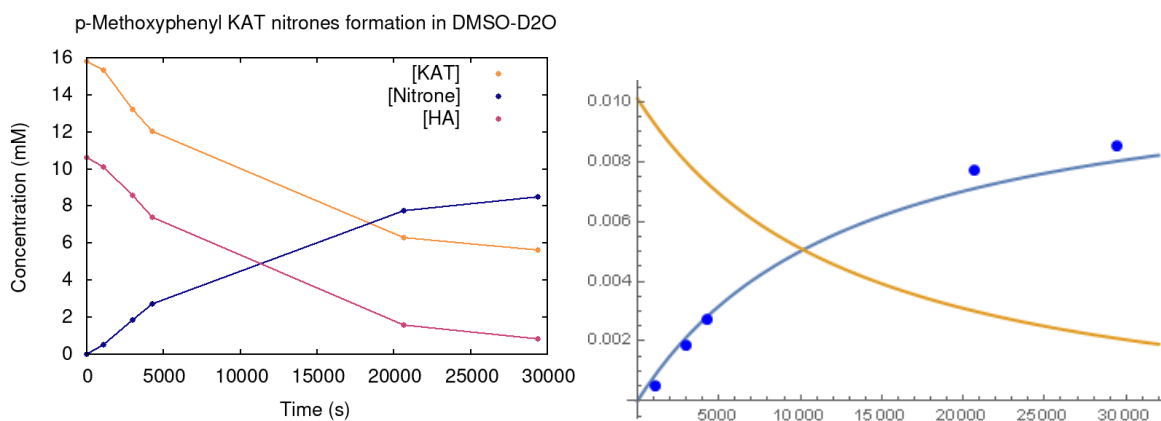
Experimental section



p-Bromophenyl KAT + **97**: $k = 0.0246 \text{ M}^{-1}\text{s}^{-1}$. Left: collected data. Right: model fitting.

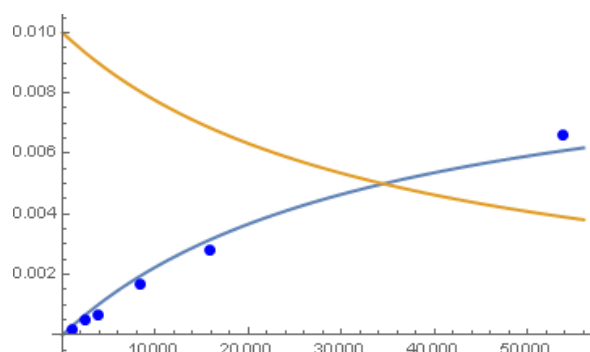


p-Fluorophenyl KAT + **97**: $k = 0.0602 \text{ M}^{-1}\text{s}^{-1}$. Left: collected data. Right: model fitting.

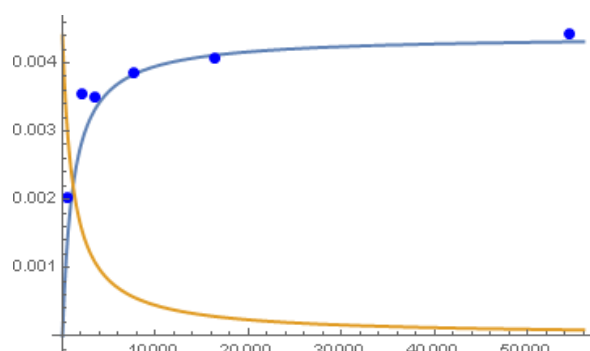


p-methoxyphenyl KAT + **97**: $k = 0.0085 \text{ M}^{-1}\text{s}^{-1}$. Left: collected data. Right: model fitting.

7.3.2. Nitron 100 formation from p-Br-phenyl KAT and hydroxylamine 97 at various water concentration



25% D₂O: $k \sim 0.003 \text{ M}^{-1}\text{s}^{-1}$

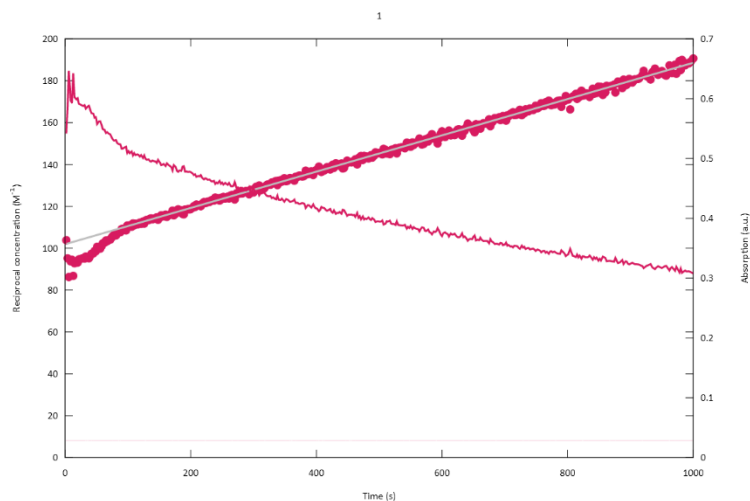


90% H₂O: $k \sim 0.2 \text{ M}^{-1}\text{s}^{-1}$

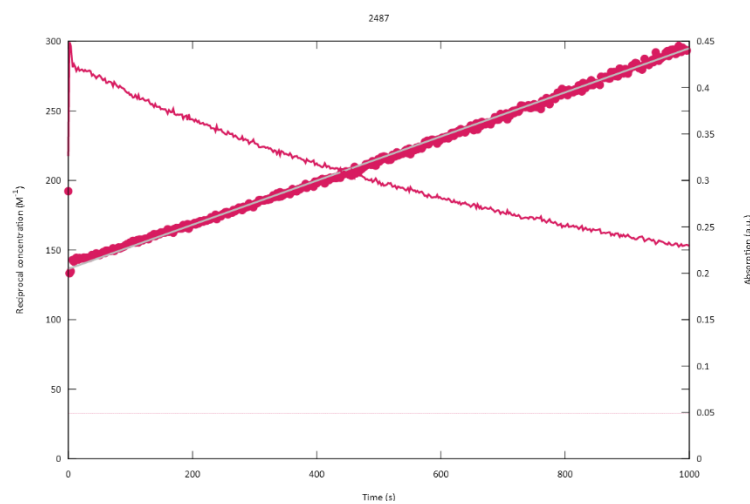
7.3.3. UV-Vis data of KAT nitron 100 formation from p-bromophenyl KAT

UV-Vis absorption was collected from 375–385 nm and a time course was plotted. The extinction coefficient of p-bromophenyl KAT over this range was determined to be 53.309 cm^{-1} .

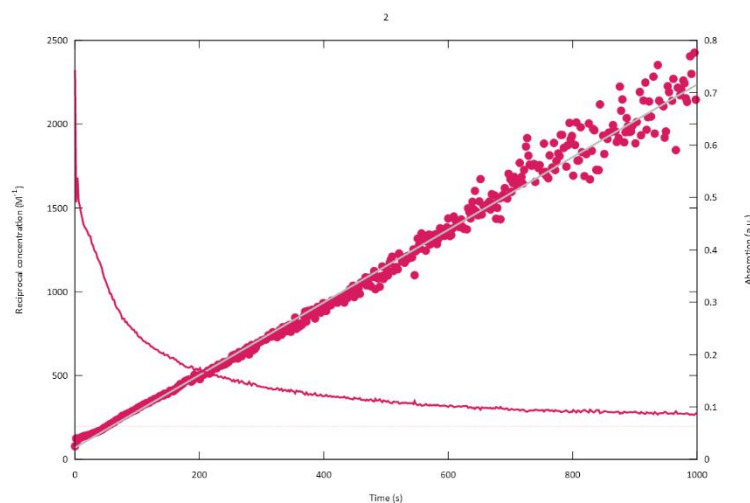
Experimental section



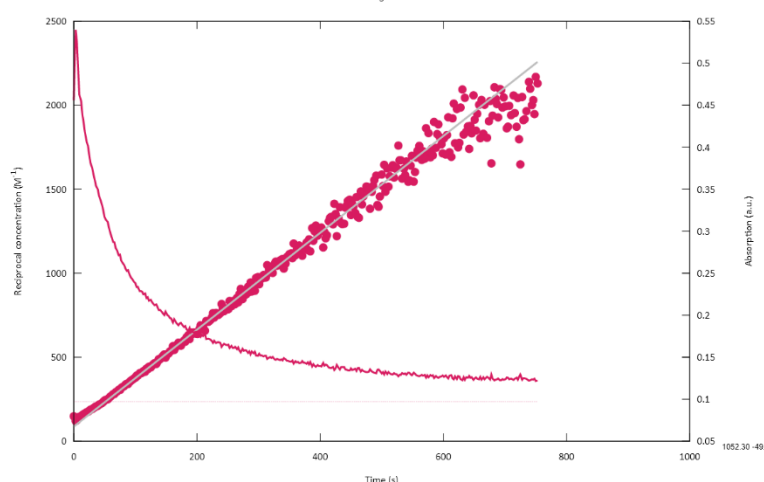
Condition: 1:1 DMSO-H₂O. Curve: absorption value. Dots: reciprocal concentration. Gray line: linear regression.



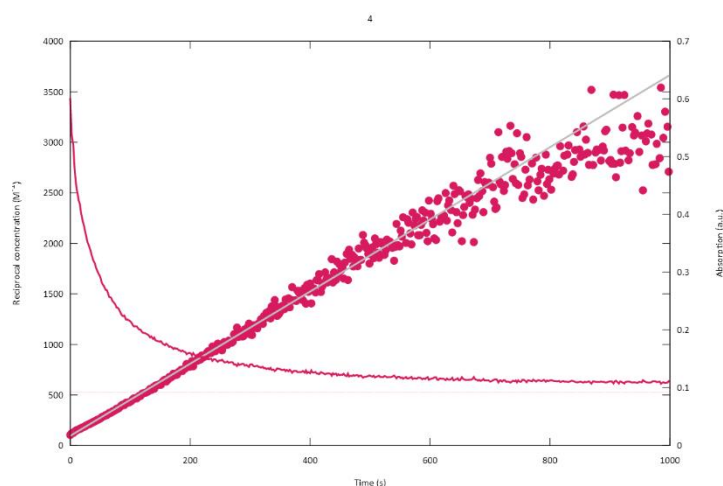
Condition: 1:1 DMSO-HFIP. Curve: absorption value. Dots: reciprocal concentration. Gray line: linear regression.



Condition: 1:1 DMSO-H₂O with 0.05 M AcOK buffer. Curve: absorption value. Dots: reciprocal concentration. Gray line: linear regression.



Condition: 1:1 DMSO- H_2O with 0.1 M AcOK buffer. Curve: absorption value. Dots: reciprocal concentration. Gray line: linear regression.

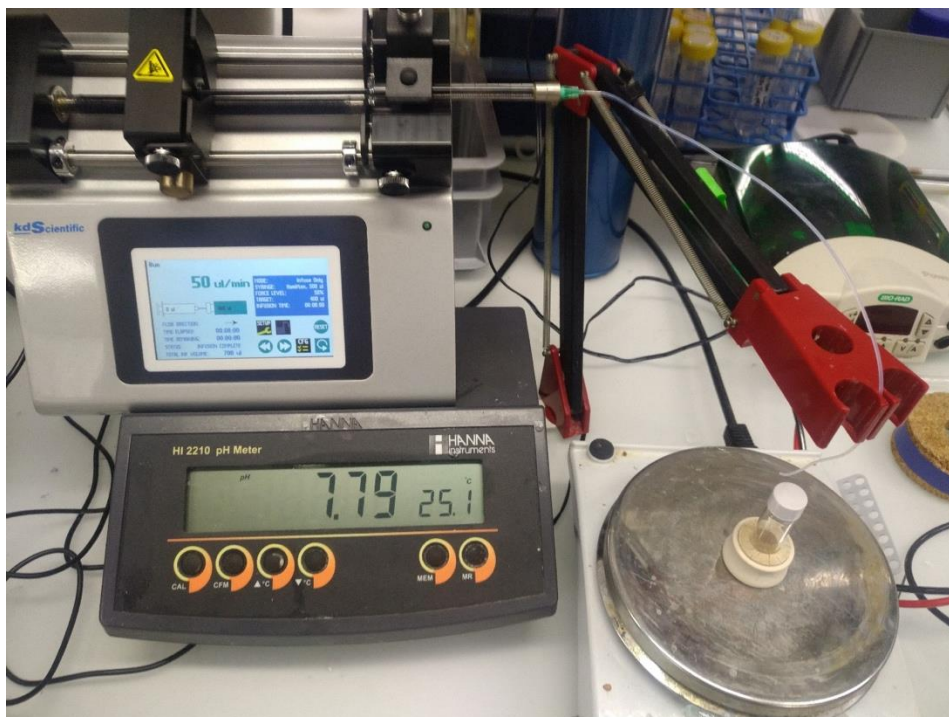


Condition: 1:1 DMSO- H_2O with 0.2 M AcOK buffer. Curve: absorption. Dots: reciprocal concentration. Gray line: linear regression.

7.4. Acid-Base titration of pyridine and quinoline KATs

The titration was performed in 1:1 CH_3CN-H_2O solvents with HCl (0.1 M). pH was measured by HANNA HI 2210 pH Meter, and volume of the titrant was controlled by a syringe pump. The data was extracted from a video of the titration process. Image frames were captured using ffmpeg, Optical Character Recognition (OCR) were performed with tesseract for the syringe pump screen, and ssocr was used to read the pH meter seven segment display. The temporal resolution of data acquisition was around 1 second. A Ruby script was written to automate the process and is public available at:

https://github.com/gnezd/ad_hoc_titrator



7.5. LC-MS and IR raw data processing scripts

The LCMS chromatograms and spectra were plotted from the Waters SQD raw data directly, with a customized Ruby script, which is publicly available at:

https://github.com/gnezd/SQD_data_parse

The IR raw data were extracted from the JASCO jws file also with a customized Ruby script which is available at:

https://github.com/gnezd/Jasco_jws

8

References

References

- (1) Burg, A. B.; Schlesinger, H. I. Hydrides of Boron. VII. Evidence of the Transitory Existence of Borine (BH₃): Borine Carbonyl and Borine Trimethylamine. *J. Am. Chem. Soc.* **1937**, 59, 780–787.
- (2) Brown, H. C. Boranes in Organic Chemistry. In *Advances in Organometallic Chemistry*; 1973; Vol. 11, pp 1–20.
- (3) Cowan, R. D. The Infra- Red Spectrum of Borine Carbonyl and a Normal Coordinate Analysis of Axial WXYZ 3 Molecules. *J. Chem. Phys.* **1950**, 18, 1101–1107.
- (4) Bethke, G. W.; Wilson, M. K. Vibrational Spectrum of Borine Carbonyl. *J. Chem. Phys.* **1957**, 26, 1118–1130.
- (5) Hillman, M. E. D. The Carbonylation of Organoboranes. I. The Carbonylation of Trialkylboranes. A Novel Synthesis of Trialkylcarbinols. *J. Am. Chem. Soc.* **1962**, 84, 4715–4720.
- (6) Hillman, M. E. D. The Carbonylation of Organoboranes. II. The Carbonylation of Trialkylboranes in the Presence of Glycols. *J. Am. Chem. Soc.* **1963**, 85, 982–984.
- (7) Brown, H. C.; Rathke, M. W. Reaction Of Carbon Monoxide At Atmospheric Pressure With Trialkylboranes In The Presence Of Water. Synthesis Of Dialkyl Ketones Via Hydroboration. *J. Am. Chem. Soc.* **1967**, 89, 2738–2740.
- (8) Brown, H. C.; Rathke, M. W. Reaction of Carbon Monoxide at Atmospheric Pressure with Trialkylboranes. Synthesis of Trialkylcarbinols via Hydroboration. *J. Am. Chem. Soc.* **1967**, 89, 2737–2738.
- (9) Yamashita, M.; Suzuki, Y.; Segawa, Y.; Nozaki, K. Synthesis, Structure of Borylmagnesium, and Its Reaction with Benzaldehyde to Form Benzoylborane. *J. Am. Chem. Soc.* **2007**, 129, 9570–9571.
- (10) Wu, D.; Taguchi, J.; Tanriver, M.; Bode, J. W. Synthesis of Acylboron Compounds. *Angew. Chem., Int. Ed.* **2020**, 59, 16847–16858.
- (11) He, Z.; Trinchera, P.; Adachi, S.; St. Denis, J. D.; Yudin, A. K. Oxidative Geminal Functionalization of Organoboron Compounds. *Angew. Chem., Int. Ed.* **2012**, 51, 11092–11096.
- (12) Dumas, A. M.; Bode, J. W. Synthesis of Acyltrifluoroborates. *Org. Lett.* **2012**, 14, 2138–2141.
- (13) Molander, G. A.; Raushel, J.; Ellis, N. M. Synthesis of an Acyltrifluoroborate and Its Fusion with Azides To Form Amides. *J. Org. Chem.* **2010**, 75, 4304–4306.
- (14) Dumas, A. M.; Molander, G. a.; Bode, J. W. Amide-Forming Ligation of Acyltrifluoroborates and Hydroxylamines in Water. *Angew. Chem., Int. Ed.* **2012**, 51, 5683–5686.
- (15) Noda, H.; Erős, G.; Bode, J. W. Rapid Ligations with Equimolar Reactants in Water with the Potassium Acyltrifluoroborate (KAT) Amide Formation. *J. Am. Chem. Soc.* **2014**, 135, 5611–5614.
- (16) Schuhmacher, A.; Ryan, S. J.; Bode, J. W. Catalytic Synthesis of Potassium Acyltrifluoroborates (KATs) from Boronic Acids and the Thioimidate KAT Transfer Reagent. *Angew. Chem., Int. Ed.* **2020**, 1–6.
- (17) Erős, G.; Kushida, Y.; Bode, J. W. A Reagent for the One-Step Preparation of Potassium Acyltrifluoroborates (KATs) from Aryl- and Heteroarylhalides. *Angew. Chem., Int. Ed.* **2014**, 53, 7604–7607.

-
- (18) Galvez, A. O.; Schaack, C. P.; Noda, H.; Bode, J. W. Chemoselective Acylation of Primary Amines and Amides with Potassium Acyltrifluoroborates under Acidic Conditions. *J. Am. Chem. Soc.* **2017**, *139*, 1826–1829.
- (19) Saxon, E.; Armstrong, J. I.; Bertozzi, C. R. A “Traceless” Staudinger Ligation for the Chemoselective Synthesis of Amide Bonds. *Org. Lett.* **2000**, *2*, 2141–2143.
- (20) Dawson, P.; Muir, T.; Clark-Lewis, I.; Kent, S. Synthesis of Proteins by Native Chemical Ligation. *Science* **1994**, *266*, 776–779.
- (21) Noda, H.; Bode, J. W. Synthesis and Chemoselective Ligations of MIDA Acylboronates with O-Me Hydroxylamines. *Chem. Sci.* **2014**, *5*, 4328–4332.
- (22) Noda, H.; Bode, J. W. Synthesis and Reactivities of Monofluoro Acylboronates in Chemoselective Amide Bond Forming Ligation with Hydroxylamines. *Org. Biomol. Chem.* **2016**, *14*, 16–20.
- (23) Noda, H.; Bode, J. W. Synthesis of Chemically and Configurationally Stable Monofluoro Acylboronates: Effect of Ligand Structure on Their Formation, Properties, and Reactivities. *J. Am. Chem. Soc.* **2015**, *137*, 3958–3966.
- (24) Noda, H. Synthesis and Reactivities of Monofluoro Acylboronates in Chemoselective Amide Bond Forming Ligation with Hydroxylamines, ETH Doctoral thesis, 2015.
- (25) Osuna Gálvez, A.; Bode, J. W. Traceless Templated Amide-Forming Ligations. *J. Am. Chem. Soc.* **2019**, *141*, 8721–8726.
- (26) Liu, S. M.; Mazunin, D.; Pattabiraman, V. R.; Bode, J. W. Synthesis of Bifunctional Potassium Acyltrifluoroborates. *Org. Lett.* **2016**, *18*, 5336–5339.
- (27) Schauenburg, D.; Osuna Gálvez, A.; Bode, J. W. Covalently Functionalized Amide Cross-Linked Hydrogels from Primary Amines and Polyethylene Glycol Acyltrifluoroborates (PEG-KATs). *J. Mater. Chem. B* **2018**, *6*, 4775–4782.
- (28) Mazunin, D. Formation and Functionalization of Hydrogels with the Potassium Acyltrifluoroborate (KAT) Ligation; ETH Doctoral Thesis: Zürich, 2016.
- (29) Mazunin, D.; Brogiere, N.; Zenobi-Wong, M.; Bode, J. W. Synthesis of Biocompatible PEG Hydrogels by PH-Sensitive Potassium Acyltrifluoroborate (KAT) Amide Ligations. *ACS Biomater. Sci. Eng.* **2015**, *1*, 456–462.
- (30) Mazunin, D.; Bode, J. W. Potassium Acyltrifluoroborate (KAT) Ligations Are Orthogonal to Thiol-Michael and SPAAC Reactions: Covalent Dual Immobilization of Proteins onto Synthetic PEG Hydrogels. *Helv. Chim. Acta* **2017**, *100*.
- (31) Song, H.; Wu, D.; Mazunin, D.; Liu, S. M.; Sato, Y.; Brogiere, N.; Zenobi-Wong, M.; Bode, J. W. Post-Assembly Photomasking of Potassium Acyltrifluoroborates (KATs) for Two-Photon 3D Patterning of PEG-Hydrogels. *Helv. Chim. Acta* **2020**, *103*.
- (32) White, C. J.; Bode, J. W. PEGylation and Dimerization of Expressed Proteins under Near Equimolar Conditions with Potassium 2-Pyridyl Acyltrifluoroborates. *ACS Cent. Sci.* **2018**, *4*, 197–206.
- (33) Chiotellis, A.; Ahmed, H.; Betzel, T.; Tanriver, M.; White, C. J.; Song, H.; Da Ros, S.; Schibli, R.; Bode, J. W.; Ametamey, S. M. Chemoselective ¹⁸F-Incorporation into Pyridyl Acyltrifluoroborates for Rapid Radiolabelling of Peptides and Proteins at Room Temperature. *Chem. Commun. (Cambridge, U. K.)* **2020**, *56*, 723–726.
- (34) Schauenburg, D.; Divandari, M.; Neumann, K.; Spiegel, C. A.; Hackett, T.; Dzeng, Y.;
-

- Spencer, N. D.; Bode, J. W. Synthesis of Polymers Containing Potassium Acyltrifluoroborates (KATs) and Post- polymerization Ligation and Conjugation. *Angew. Chem., Int. Ed.* **2020**, *59*, 14656–14663.
- (35) Tanriver, M.; Dzeng, Y.-C.; Da Ros, S.; Bode, J. W. Manuscript in Preparation; 2021.
- (36) Taguchi, J.; Ikeda, T.; Takahashi, R.; Sasaki, I.; Ogasawara, Y.; Dairi, T.; Kato, N.; Yamamoto, Y.; Bode, J. W.; Ito, H. Synthesis of Acylborons by Ozonolysis of Alkenylboronates: Preparation of an Enantioenriched Amino Acid Acylboronate. *Angew. Chem., Int. Ed.* **2017**, *56*, 13847–13851.
- (37) Taguchi, J.; Takeuchi, T.; Takahashi, R.; Masero, F.; Ito, H. Concise Synthesis of Potassium Acyltrifluoroborates from Aldehydes through Copper(I)- Catalyzed Borylation/Oxidation. *Angew. Chem., Int. Ed.* **2019**, *58*, 7299–7303.
- (38) Jackl, M. K.; Schuhmacher, A.; Shiro, T.; Bode, J. W. Synthesis of N, N-Alkylated α -Tertiary Amines by Coupling of α -Aminoalkyltrifluoroborates and Grignard Reagents. *Org. Lett.* **2018**, *20*, 4044–4047.
- (39) Shiro, T.; Schuhmacher, A.; Jackl, M. K.; Bode, J. W. Facile Synthesis of α -Aminoboronic Acids from Amines and Potassium Acyltrifluoroborates (KATs) via Trifluoroborate-Iminiums (TIMs). *Chem. Sci.* **2018**, *9*, 5191–5196.
- (40) Schuhmacher, A.; Shiro, T.; Ryan, S. J.; Bode, J. W. Synthesis of Secondary and Tertiary Amides without Coupling Agents from Amines and Potassium Acyltrifluoroborates (KATs). *Chem. Sci.* **2020**, *11*, 7609–7614.
- (41) Bode, J. W.; Fox, R. M.; Baucom, K. D. Chemoselective Amide Ligations by Decarboxylative Condensations Of N-Alkylhydroxylamines and α -Ketoacids. *Angew. Chem., Int. Ed.* **2006**, *45*, 1248–1252.
- (42) Ju, L.; Lippert, A. R.; Bode, J. W. Stereoretentive Synthesis and Chemoselective Amide-Forming Ligations of C-Terminal Peptide α -Ketoacids. *J. Am. Chem. Soc.* **2008**, *130*, 4253–4255.
- (43) Pusterla, I.; Bode, J. W. The Mechanism of the α -Ketoacid-Hydroxylamine Amide-Forming Ligation. *Angew. Chem., Int. Ed.* **2012**, *51*, 513–516.
- (44) Rohrbacher, F.; Wucherpfennig, T. G.; Bode, J. W. Chemical Protein Synthesis with the KAHA Ligation; 2014; pp 1–31.
- (45) Bode, J. W. Chemical Protein Synthesis with the α -Ketoacid–Hydroxylamine Ligation. *Acc. Chem. Res.* **2017**, *50*, 2104–2115.
- (46) Pusterla, I.; Bode, J. W. The Mechanism of the α -Ketoacid-Hydroxylamine Amide-Forming Ligation. *Angew. Chem., Int. Ed.* **2012**, *51*, 513–516.
- (47) Dumas, A. M. Unpublished Results; 2012.
- (48) Stankiewicz, J.; Eckardt, L. H. Chembiogenesis 2005 and Systems Chemistry Workshop. *Angew. Chem., Int. Ed.* **2006**, *45*, 342–344.
- (49) Ludlow, R. F.; Otto, S. Systems Chemistry. *Chem. Soc. Rev.* **2008**, *37*, 101–108.
- (50) Corbett, P. T.; Leclaire, J.; Vial, L.; West, K. R.; Wietor, J.-L.; Sanders, J. K. M.; Otto, S. Dynamic Combinatorial Chemistry. *Chem. Rev.* **2006**, *106*, 3652–3711.
- (51) Ladame, S. Dynamic Combinatorial Chemistry: On the Road to Fulfilling the Promise. *Org. Biomol. Chem.* **2008**, *6*, 219–226.
- (52) Lehn, J.-M. Dynamic Combinatorial Chemistry and Virtual Combinatorial Libraries. In

- Essays in Contemporary Chemistry; Verlag Helvetica Chimica Acta: Zürich, 2007; pp 307–326.
- (53) Mondal, M.; Hirsch, A. K. H. Dynamic Combinatorial Chemistry: A Tool to Facilitate the Identification of Inhibitors for Protein Targets. *Chem. Soc. Rev.* **2015**, 44, 2455–2488.
- (54) Herrmann, A. Dynamic Combinatorial/Covalent Chemistry: A Tool to Read, Generate and Modulate the Bioactivity of Compounds and Compound Mixtures. *Chem. Soc. Rev.* **2014**, 43, 1899–1933.
- (55) Cougnon, F. B. L.; Sanders, J. K. M. Evolution of Dynamic Combinatorial Chemistry. *Acc. Chem. Res.* **2012**, 45, 2211–2221.
- (56) Otto, S. *Dynamic Combinatorial Chemistry*; Reek, J. N. H., Otto, S., Eds.; Wiley, 2010.
- (57) Hunt, R. A. R.; Otto, S. Dynamic Combinatorial Libraries: New Opportunities in Systems Chemistry. *Chem. Commun. (Cambridge, U. K.)* **2011**, 47, 847–858.
- (58) Herrmann, A. Dynamic Mixtures and Combinatorial Libraries: Imines as Probes for Molecular Evolution at the Interface between Chemistry and Biology. *Org. Biomol. Chem.* **2009**, 7, 3195–3204.
- (59) Li, J.; Nowak, P.; Otto, S. Dynamic Combinatorial Libraries: From Exploring Molecular Recognition to Systems Chemistry. *J. Am. Chem. Soc.* **2013**, 135, 9222–9239.
- (60) Jin, Y.; Yu, C.; Denman, R. J.; Zhang, W. Recent Advances in Dynamic Covalent Chemistry. *Chem. Soc. Rev.* **2013**, 42, 6634.
- (61) Ro, S.; Rowan, S. J.; Pease, A. R.; Cram, D. J.; Stoddart, J. F. Dynamic Hemicarcerands and Hemicarceplexes. *Org. Lett.* **2000**, 2, 2411–2414.
- (62) Jin, Y.; Wang, Q.; Taynton, P.; Zhang, W. Dynamic Covalent Chemistry Approaches toward Macrocycles, Molecular Cages, and Polymers. *Acc. Chem. Res.* **2014**, 47, 1575–1586.
- (63) Rowan, S. J.; Cantrill, S. J.; Cousins, G. R. L.; Sanders, J. K. M.; Stoddart, J. F. Dynamic Covalent Chemistry. *Angew. Chem., Int. Ed.* **2002**, 41, 898–952.
- (64) Jin, Y.; Wang, Q.; Taynton, P.; Zhang, W. Dynamic Covalent Chemistry Approaches toward Macrocycles, Molecular Cages, and Polymers. *Acc. Chem. Res.* **2014**.
- (65) Jiang, W.; Schäfer, A.; Mohr, P. C.; Schalley, C. A. Monitoring Self-Sorting by Electrospray Ionization Mass Spectrometry: Formation Intermediates and Error-Correction during the Self-Assembly of Multiply Threaded Pseudorotaxanes. *J. Am. Chem. Soc.* **2010**, 132, 2309–2320.
- (66) Ludlow, R. F.; Otto, S. Two-Vial, LC–MS Identification of Ephedrine Receptors from a Solution-Phase Dynamic Combinatorial Library of over 9000 Components. *J. Am. Chem. Soc.* **2008**, 130, 12218–12219.
- (67) Ciesielski, A.; El Garah, M.; Haar, S.; Kovaříček, P.; Lehn, J. M.; Samorì, P. Dynamic Covalent Chemistry of Bisimines at the Solid/Liquid Interface Monitored by Scanning Tunneling Microscopy. *Nat. Chem.* **2014**, 6.
- (68) Lehn, J.-M. From Supramolecular Chemistry towards Constitutional Dynamic Chemistry and Adaptive Chemistry. *Chem. Soc. Rev.* **2007**, 36, 151–160.
- (69) Belowich, M. E.; Stoddart, J. F. Dynamic Imine Chemistry. *Chem. Soc. Rev.* **2012**, 41, 2003–2024.

References

- (70) Minkenberg, C. B.; Florusse, L.; Eelkema, R.; Koper, G. J. M.; Van Esch, J. H. Triggered Self-Assembly of Simple Dynamic Covalent Surfactants. *J. Am. Chem. Soc.* **2009**, *131*, 11274–11275.
- (71) Black, S. P.; Sanders, J. K. M.; Stefankiewicz, A. R. Disulfide Exchange: Exposing Supramolecular Reactivity through Dynamic Covalent Chemistry. *Chem. Soc. Rev.* **2014**, *43*, 1861–1872.
- (72) Lehn, J.-M. From Supramolecular Chemistry towards Constitutional Dynamic Chemistry and Adaptive Chemistry. *Chem. Soc. Rev.* **2007**, *36*, 151–160.
- (73) Wang, J.; Chen, X.; Cui, W.; Yi, S. PH-Responsive Vesicles from Supra-Amphiphiles Based on Dynamic Imine Bond. *Colloids Surf., A* **2015**, *484*, 28–36.
- (74) Sarma, R. J.; Otto, S.; Nitschke, J. R. Disulfides, Imines, and Metal Coordination within a Single System: Interplay between Three Dynamic Equilibria. *Chem. - Eur. J.* **2007**, *13*, 9542–9546.
- (75) Vantomme, G.; Jiang, S.; Lehn, J. M. Adaptation in Constitutional Dynamic Libraries and Networks, Switching between Orthogonal Metalloselection and Photoselection Processes. *J. Am. Chem. Soc.* **2014**, *136*, 9509–9518.
- (76) Su, X.; Aprahamian, I. Hydrazone-Based Switches, Metallo-Assemblies and Sensors. *Chem. Soc. Rev.* **2014**, *43*, 1963–1981.
- (77) Haney, C. M.; Horne, W. S. Dynamic Covalent Side-Chain Cross-Links via Intermolecular Oxime or Hydrazone Formation from Bifunctional Peptides and Simple Organic Linkers. *J. Pept. Sci.* **2014**, *20*, 108–114.
- (78) Turega, S. M.; Lorenz, C.; Sadownik, J. W.; Philp, D. Target-Driven Selection in a Dynamic Nitrene Library. *Chem. Commun. (Cambridge, U. K.)* **2008**, No. 34, 4076–4078.
- (79) Scott, D. E.; Dawes, G. J.; Ando, M.; Abell, C.; Ciulli, A. A Fragment-Based Approach to Probing Adenosine Recognition Sites by Using Dynamic Combinatorial Chemistry. *ChemBioChem* **2009**, *10*, 2772–2779.
- (80) Cougnon, F. B. L.; Au-Yeung, H. Y.; Pantok, G. D.; Sanders, J. K. M. Exploring the Formation Pathways of Donor–Acceptor Catenanes in Aqueous Dynamic Combinatorial Libraries. *J. Am. Chem. Soc.* **2011**, *133*, 3198–3207.
- (81) Otsuka, H.; Nagano, S.; Kobashi, Y.; Maeda, T.; Takahara, A. A Dynamic Covalent Polymer Driven by Disulfide Metathesis under Photoirradiation. *Chem. Commun. (Cambridge, U. K.)* **2010**, *46*, 1150–1152.
- (82) Ji, S.; Cao, W.; Yu, Y.; Xu, H. Dynamic Diselenide Bonds: Exchange Reaction Induced by Visible Light without Catalysis. *Angew. Chem., Int. Ed.* **2014**, *53*, 6781–6785.
- (83) Tamaki, K.; Ishigami, A.; Tanaka, Y.; Yamanaka, M.; Kobayashi, K. Self-Assembled Boronic Ester Cavitand Capsules with Various Bis(Catechol) Linkers: Cavity-Expanded and Chiral Capsules. *Chem. - Eur. J.* **2015**, *21*, 13714–13722.
- (84) Wang, Q.; Zhang, C.; Noll, B. C.; Long, H.; Jin, Y.; Zhang, W. A Tetrameric Cage with D_{2h} Symmetry through Alkyne Metathesis. *Angew. Chem., Int. Ed.* **2014**, *53*, 10663–10667.
- (85) Monfette, S.; Fogg, D. E. Equilibrium Ring-Closing Metathesis. *Chem. Rev.* **2009**, *109*, 3783–3816.
- (86) Xu, J. F.; Chen, Y. Z.; Wu, L. Z.; Tung, C. H.; Yang, Q. Z. Dynamic Covalent Bond

- Based on Reversible Photo [4 + 4] Cycloaddition of Anthracene for Construction of Double-Dynamic Polymers. *Org. Lett.* **2013**, 15, 6148–6151.
- (87) Waller, P. J.; Lyle, S. J.; Osborn Popp, T. M.; Diercks, C. S.; Reimer, J. A.; Yaghi, O. M. Chemical Conversion of Linkages in Covalent Organic Frameworks. *J. Am. Chem. Soc.* **2016**, 138, 15519–15522.
- (88) Erguven, H.; Keyzer, E. N.; Arndtsen, B. A. A Versatile Approach to Dynamic Amide Bond Formation with Imine Nucleophiles. *Chem. - Eur. J.* **2020**, 26, 5709–5716.
- (89) Ruff, Y.; Garavini, V.; Giuseppone, N. Reversible Native Chemical Ligation: A Facile Access to Dynamic Covalent Peptides. *J. Am. Chem. Soc.* **2014**, 136, 6333–6339.
- (90) Stephenson, N. A.; Zhu, J.; Gellman, S. H.; Stahl, S. S. Catalytic Transamidation Reactions Compatible with Tertiary Amide Metathesis under Ambient Conditions. *J. Am. Chem. Soc.* **2009**, 131, 10003–10008.
- (91) Pappas, C. G.; Shafi, R.; Sasselli, I. R.; Siccardi, H.; Wang, T.; Narang, V.; Abzalimov, R.; Wijerathne, N.; Ulijn, R. V. Dynamic Peptide Libraries for the Discovery of Supramolecular Nanomaterials. *Nat. Nanotechnol.* **2016**, 11, 960–967.
- (92) Lippert, A. R.; Naganawa, A.; Keleshian, V. L.; Bode, J. W. Synthesis of Phototrappable Shape-Shifting Molecules for Adaptive Guest Binding. *J. Am. Chem. Soc.* **2010**, 132, 15790–15799.
- (93) He, M.; Bode, J. W. Racemization as a Stereochemical Measure of Dynamics and Robustness in Shape-Shifting Organic Molecules. *Proc. Natl. Acad. Sci.* **2011**, 108, 14752–14756.
- (94) Teichert, J. F.; Mazunin, D.; Bode, J. W. Chemical Sensing of Polyols with Shapeshifting Boronic Acids As a Self-Contained Sensor Array. *J. Am. Chem. Soc.* **2013**, 135, 11314–11321.
- (95) Otto, S. Exploring and Exploiting Molecular Recognition Using Covalent Chemistry under Thermodynamic Control. *J. Mater. Chem.* **2005**, 15, 3357.
- (96) Denissen, W.; Winne, J. M.; Du Prez, F. E. Vitrimers: Permanent Organic Networks with Glass-like Fluidity. *Chem. Sci.* **2015**, 7, 30–38.
- (97) Christensen, P. R.; Scheuermann, A. M.; Loeffler, K. E.; Helms, B. A. Closed-Loop Recycling of Plastics Enabled by Dynamic Covalent Diketoenamine Bonds. *Nat. Chem.* **2019**, 11, 442–448.
- (98) Smith, B. J.; Overholts, A. C.; Hwang, N.; Dichtel, W. R. Insight into the Crystallization of Amorphous Imine-Linked Polymer Networks to 2D Covalent Organic Frameworks. *Chem. Commun. (Cambridge, U. K.)* **2016**, 52, 3690–3693.
- (99) Feriante, C.; Evans, A. M.; Jhulki, S.; Castano, I.; Strauss, M. J.; Barlow, S.; Dichtel, W. R.; Marder, S. R. New Mechanistic Insights into the Formation of Imine-Linked Two-Dimensional Covalent Organic Frameworks. *J. Am. Chem. Soc.* **2020**, 142, 18637–18644.
- (100) Pfeiffer, P. Lichtchemische Synthese von Indolderivaten. *Liebigs Ann. Chem.* **1916**, 411, 72–158.
- (101) Miescher, K. Nitrone Und Nitrene., ETH Doctoral Thesis, 1918.
- (102) Staudinger, H.; Miescher, K. Über Nitrone Und Nitrene. *Helv. Chim. Acta* **1919**, 2, 554–582.

References

- (103) Smith, L. I. Aliphatic Diazo Compounds, Nitrones, and Structurally Analogous Compounds. Systems Capable of Undergoing 1,3-Additions. *Chem. Rev.* **1938**, 23, 193–285.
- (104) Exner, O. A New Synthesis of N-Methylketoximes. *Collect. Czech. Chem. Commun.* **1951**, 16, 258–267.
- (105) Hamer, J.; Macaluso, A. Nitrones. *Chem. Rev.* **1964**, 64, 473–495.
- (106) Delpierre, G. R.; Lamchen, M. Nitrones. *Q. Rev. Chem. Soc.* **1965**, 19, 329.
- (107) Tufariello, J. J. Alkaloids from Nitrones. *Acc. Chem. Res.* **1979**, 12, 396–403.
- (108) Confalone, P. N.; Huie, E. M. The [3 + 2] Nitron-Olefin Cycloaddition Reaction. In *Organic Reactions*; John Wiley & Sons, Inc.: Hoboken, NJ, USA, 1988; Vol. 36, pp 1–173.
- (109) Breuer, E. Nitrones and Nitronic Acid Derivatives: Their Structure and Their Roles in Synthesis. In *Nitrones, Nitronates and Nitroxides (1989)*; John Wiley & Sons, Inc.: Chichester, UK, 1989; pp 139–244.
- (110) Gothelf, K. V.; Jørgensen, K. A. Asymmetric 1,3-Dipolar Cycloaddition Reactions. *Chem. Rev.* **1998**, 98, 863–910.
- (111) Belen'kii, L. I.; Grigor'ev, I. A.; Ioffe, L. S. Nitrile Oxides, Nitrones, and Nitronates in Organic Synthesis; Feuer, H., Ed.; John Wiley & Sons, Inc.: Hoboken, NJ, USA, 2007.
- (112) Kolis, S. P.; Hansen, M. M.; Arslantas, E.; Brändli, L.; Buser, J.; DeBaillie, A. C.; Frederick, A. L.; Hoard, D. W.; Hollister, A.; Huber, D.; et al. Synthesis of BACE Inhibitor LY2886721. Part I. An Asymmetric Nitron Cycloaddition Strategy. *Org. Process Res. Dev.* **2015**, 19, 1203–1213.
- (113) Reidl, T. W.; Son, J.; Wink, D. J.; Anderson, L. L. Facile Synthesis of Azetidine Nitrones and Diastereoselective Conversion into Densely Substituted Azetidines. *Angew. Chem., Int. Ed.* **2017**, 56, 11579–11583.
- (114) Lisnyak, V. G.; Lynch-Colameta, T.; Snyder, S. A. Mannich-Type Reactions of Cyclic Nitrones: Effective Methods for the Enantioselective Synthesis of Piperidine-Containing Alkaloids. *Angew. Chem., Int. Ed.* **2018**, 57, 15162–15166.
- (115) Murahashi, S.-I.; Imada, Y. Synthesis and Transformations of Nitrones for Organic Synthesis. *Chem. Rev.* **2019**, 119, 4684–4716.
- (116) Sukhorukov, A. Y. C–H Reactivity of the A-Position in Nitrones and Nitronates. *Adv. Synth. Catal.* **2020**, 362, 724–754.
- (117) Murahashi, S. I.; Mitsui, H.; Shiota, T.; Tsuda, T.; Watanabe, S. Tungstate-Catalyzed Oxidation of Secondary Amines to Nitrones. α -Substitution of Secondary Amines via Nitrones. *J. Org. Chem.* **1990**, 55, 1736–1744.
- (118) Goti, A.; De Sarlo, F.; Romani, M. Highly Efficient and Mild Synthesis of Nitrones by Catalytic Oxidation of Hydroxylamines with Tetra-*n*-Propylammonium Perruthenate. *Tetrahedron Lett.* **1994**, 35, 6571–6574.
- (119) Cardona, F.; Bonanni, M.; Soldaini, G.; Goti, A. One-Pot Synthesis of Nitrones from Primary Amines and Aldehydes Catalyzed by Methyltrioxorhenium. *ChemSusChem* **2008**, 1, 327–332.
- (120) Publication, A. Transformation of Primary Amines To N-Monoalkylhydroxylamines: N-Hydroxy-(S)-1-Phenylethylamine Oxalate. *Org. Synth.* **2003**, 80, 207.

- (121) Berthet, M.; Cheviet, T.; Dujardin, G.; Parrot, I.; Martinez, J. Isoxazolidine: A Privileged Scaffold for Organic and Medicinal Chemistry. *Chem. Rev.* **2016**, *116*, 15235–15283.
- (122) Brandi, A.; Cardona, F.; Cicchi, S.; Cordero, F. M.; Goti, A. Stereocontrolled Cyclic Nitrono Cycloaddition Strategy for the Synthesis of Pyrrolizidine and Indolizidine Alkaloids. *Chem. - Eur. J.* **2009**, *15*, 7808–7821.
- (123) Supranovich, V. I.; Levin, V. V.; Struchkova, M. I.; Dilman, A. D. Photocatalytic Reductive Fluoroalkylation of Nitrones. *Org. Lett.* **2018**, *20*, 840–843.
- (124) Lees, K. R.; Zivin, J. A.; Ashwood, T.; Davalos, A.; Davis, S. M.; Diener, H.; Grotta, J.; Lyden, P.; Shuaib, A.; Hårdemark, H.; et al. NXY-059 for Acute Ischemic Stroke. *N. Engl. J. Med.* **2006**, *354*, 588–600.
- (125) Green, A. R.; Ashwood, T.; Odergren, T.; Jackson, D. M. Nitrones as Neuroprotective Agents in Cerebral Ischemia, with Particular Reference to NXY-059. *Pharmacol. Ther.* **2003**, *100*, 195–214.
- (126) Xu, C.-P.; Huang, P.-Q.; Py, S. SmI₂-Mediated Coupling of Nitrones and Tert-Butanesulfinyl Imines with Allenates: Synthesis of β -Methylenyl- γ -Lactams and Tetramic Acids. *Org. Lett.* **2012**, *14*, 2034–2037.
- (127) Masson, G.; Cividino, P.; Py, S.; Vallée, Y. SmI₂-Induced Umpolung of the C=N Bond: First Reductive Conjugate Addition of Nitrones to α,β -Unsaturated Esters. *Angew. Chemie* **2003**, *115*, 2367–2370.
- (128) Prikhod'ko, A.; Walter, O.; Zevaco, T. A.; Garcia-Rodriguez, J.; Mouhtady, O.; Py, S. Synthesis of α -Amino Acids through Samarium(II) Iodide Promoted Reductive Coupling of Nitrones with CO₂. *Eur. J. Org. Chem.* **2012**, *2012*, 3742–3746.
- (129) Imada, Y.; Okita, C.; Maeda, H.; Kishimoto, M.; Sugano, Y.; Kaneshiro, H.; Nishida, Y.; Kawamorita, S.; Komiya, N.; Naota, T. Ring-Expanding Metathesis Oligomerization of Cyclic Nitrones. *Eur. J. Org. Chem.* **2014**, *2014*, 5670–5674.
- (130) Andrade, M. M.; Barros, M. T.; Pinto, R. C. Exploiting Microwave-Assisted Neat Procedures: Synthesis of N-Aryl and N-Alkyl nitrones and Their Cycloaddition En Route for Isoxazolidines. *Tetrahedron* **2008**, *64*, 10521–10530.
- (131) Colacino, E.; Nun, P.; Colacino, F. M.; Martinez, J.; Lamaty, F. Solvent-Free Synthesis of Nitrones in a Ball-Mill. *Tetrahedron* **2008**, *64*, 5569–5576.
- (132) Chiang, Y.-L.; Russak, J. A.; Carrillo, N.; Bode, J. W. Synthesis of Enantiomerically Pure Isoxazolidine Monomers for the Preparation of β 3 -Oligopeptides by Iterative α -Keto Acid-Hydroxylamine (KAHA) Ligations. *Helv. Chim. Acta* **2012**, *95*, 2481–2501.
- (133) Yu, S.; Ishida, H.; Juarez-Garcia, M. E.; Bode, J. W. Unified Synthesis of Enantiopure B₂h, B₃h and B_{2,3}-Amino Acids. *Chem. Sci.* **2010**, *1*, 637.
- (134) Frey, W.; Baskakova, A.; Menzel, A.; Jäger, V. Crystal Structure of 2,3-O-Cyclohexylidene-D-Glyceraldehyde N-Benzyl nitrono, C₁₆H₂₁NO₃. *Zeitschrift für Krist. - New Cryst. Struct.* **2010**, *225*, 245–246.
- (135) Merino, P.; Anoro, S.; Cerrada, E.; Laguna, M.; Moreno, A.; Tejero, T. Crystal and Molecular Structures of N-Benzyl-C-(2-Pyridyl) Nitrono and Its ZnBr₂ Complex. A Study of Their Reactivity. *Molecules* **2001**, *6*, 208–220.
- (136) Zhang, Y.; Blackman, M. L.; Leduc, A. B.; Jamison, T. F. Peptide Fragment Coupling Using a Continuous-Flow Photochemical Rearrangement of Nitrones. *Angew. Chem., Int. Ed.* **2013**, *52*, 4251–4255.

- (137) Xing, D.; Xu, X.; Yang, L. Highly Chemoselective Rearrangement of 3-Aryloxaziridines to Nitrones or Amides. *Synthesis* **2009**, 2009, 3399–3404.
- (138) Oliveira, R. A.; Silva, R. O.; Molander, G. A.; Menezes, P. H. ^1H , ^{13}C , ^{19}F and ^{11}B NMR Spectral Reference Data of Some Potassium Organotrifluoroborates. *Magn. Reson. Chem.* **2009**, 47, 873–878.
- (139) Naidu, B. N.; Sorenson, M. E. Facile One-Pot Synthesis of 2,3,5-Substituted 1,2,4-Oxadiazolines from Nitriles in Aqueous Solution. *Org. Lett.* **2005**, 7, 1391–1393.
- (140) Ockwig, N. W.; Cote, A. P.; Keeffe, M. O.; Matzger, A. J.; Yaghi, O. M. Porous, Crystalline, Covalent Organic Frameworks. *Science* **2005**, 310, 1166–1170.
- (141) Geng, K.; He, T.; Liu, R.; Dalapati, S.; Tan, K. T.; Li, Z.; Tao, S.; Gong, Y.; Jiang, Q.; Jiang, D. Covalent Organic Frameworks: Design, Synthesis, and Functions. *Chem. Rev.* **2020**, 120, 8814–8933.
- (142) Matsumoto, M.; Dasari, R. R.; Ji, W.; Feriante, C. H.; Parker, T. C.; Marder, S. R.; Dichtel, W. R. Rapid, Low Temperature Formation of Imine-Linked Covalent Organic Frameworks Catalyzed by Metal Triflates. *J. Am. Chem. Soc.* **2017**, 139, 4999–5002.
- (143) Hunt, J. R.; Doonan, C. J.; LeVangie, J. D.; Côté, A. P.; Yaghi, O. M. Reticular Synthesis of Covalent Organic Borosilicate Frameworks. *J. Am. Chem. Soc.* **2008**, 130, 11872–11873.
- (144) Zhu, Y.; Wan, S.; Jin, Y.; Zhang, W. Desymmetrized Vertex Design for the Synthesis of Covalent Organic Frameworks with Periodically Heterogeneous Pore Structures. *J. Am. Chem. Soc.* **2015**, 137, 13772–13775.
- (145) Dalapati, S.; Jin, S.; Gao, J.; Xu, Y.; Nagai, A.; Jiang, D. An Azine-Linked Covalent Organic Framework. *J. Am. Chem. Soc.* **2013**, 135, 17310–17313.
- (146) Jackson, K. T.; Reich, T. E.; El-Kaderi, H. M. Targeted Synthesis of a Porous Borazine-Linked Covalent Organic Framework. *Chem. Commun. (Cambridge, U. K.)* **2012**, 48, 8823.
- (147) Zhao, C.; Lyu, H.; Ji, Z.; Zhu, C.; Yaghi, O. M. Ester-Linked Crystalline Covalent Organic Frameworks. *J. Am. Chem. Soc.* **2020**, 142, 14450–14454.
- (148) Beaudoin, D.; Maris, T.; Wuest, J. D. Constructing Monocrystalline Covalent Organic Networks by Polymerization. *Nat. Chem.* **2013**, 5, 830–834.
- (149) Smith, B. J.; Hwang, N.; Chavez, A. D.; Novotney, J. L.; Dichtel, W. R. Growth Rates and Water Stability of 2D Boronate Ester Covalent Organic Frameworks. *Chem. Commun. (Cambridge, U. K.)* **2015**, 51, 7532–7535.
- (150) Duncan, N. C.; Hay, B. P.; Hagaman, E. W.; Custelcean, R. Thermodynamic, Kinetic, and Structural Factors in the Synthesis of Imine-Linked Dynamic Covalent Frameworks. *Tetrahedron* **2012**, 68, 53–64.
- (151) Huang, N.; Ding, X.; Kim, J.; Ihee, H.; Jiang, D. A Photoresponsive Smart Covalent Organic Framework. *Angew. Chem., Int. Ed.* **2015**, 54, 8704–8707.
- (152) Erös, G. Unpublished Results. 2014.
- (153) Carpino, L. A.; Giza, C. A.; Carpino, B. A. O-Acylhydroxylamines. I. Synthesis of O-Benzoylhydroxylamine 1. *J. Am. Chem. Soc.* **1959**, 81, 955–957.
- (154) Staszak, M. A.; Doecke, C. W. The Use of N,O-Bis(Tert-Butoxycarbonyl)-Hydroxylamine in the Synthesis of N-Hydroxylamines and Hydroxamic Acids. *Tetrahedron Lett.* **1994**, 35, 6021–6024.
-

-
- (155) Blart, E.; Geneêt, J. P.; Safi, M.; Savignac, M.; Sinou, D. Palladium(O)-Catalyzed Substitution of Allylic Substrates in an Aqueous-Organic Medium. *Tetrahedron* **1994**, *50*, 505–514.
- (156) Knight, D. W.; Leese, M. P. A Survey of Suitable Protecting Groups for the Synthesis of Hydroxylamines by Mitsunobu Reactions. *Tetrahedron Lett.* **2001**, *42*, 2593–2595.
- (157) Meadows, M. K.; Roesner, E. K.; Lynch, V. M.; James, T. D.; Anslyn, E. V. Boronic Acid Mediated Coupling of Catechols and N-Hydroxylamines: A Bioorthogonal Reaction to Label Peptides. *Org. Lett.* **2017**, *19*, 3179–3182.
- (158) Staszak, M. A.; Doecke, C. W. A Facile Synthesis of N,O-Bis(Tert-Butoxycarbonyl)-Hydroxylamine. *Tetrahedron Lett.* **1993**, *34*, 7043–7044.
- (159) Smith, B. J.; Dichtel, W. R. Mechanistic Studies of Two-Dimensional Covalent Organic Frameworks Rapidly Polymerized from Initially Homogenous Conditions. *J. Am. Chem. Soc.* **2014**, *136*, 8783–8789.
- (160) Vitaku, E.; Dichtel, W. R. Synthesis of 2D Imine-Linked Covalent Organic Frameworks through Formal Transimination Reactions. *J. Am. Chem. Soc.* **2017**, *139*, 12911–12914.
- (161) Pettersson, M.; Crews, C. M. PROteolysis TARgeting Chimeras (PROTACs) — Past, Present and Future. *Drug Discov. Today Technol.* **2019**, *31*, 15–27.
- (162) Bondeson, D. P.; Mares, A.; Smith, I. E. D.; Ko, E.; Campos, S.; Miah, A. H.; Mulholland, K. E.; Routly, N.; Buckley, D. L.; Gustafson, J. L.; et al. Catalytic in Vivo Protein Knockdown by Small-Molecule PROTACs. *Nat. Chem. Biol.* **2015**, *11*, 611–617.
- (163) Burslem, G. M.; Smith, B. E.; Lai, A. C.; Jaime-Figueroa, S.; McQuaid, D. C.; Bondeson, D. P.; Toure, M.; Dong, H.; Qian, Y.; Wang, J.; et al. The Advantages of Targeted Protein Degradation Over Inhibition: An RTK Case Study. *Cell Chem. Biol.* **2018**, *25*, 67-77.e3.
- (164) Filippakopoulos, P.; Qi, J.; Picaud, S.; Shen, Y.; Smith, W. B.; Fedorov, O.; Morse, E. M.; Keates, T.; Hickman, T. T.; Felletar, I.; et al. Selective Inhibition of BET Bromodomains. *Nature* **2010**, *468*, 1067–1073.
- (165) Taniguchi, Y. The Bromodomain and Extra-Terminal Domain (BET) Family: Functional Anatomy of BET Paralogous Proteins. *Int. J. Mol. Sci.* **2016**, *17*, 1849.
- (166) Zengerle, M.; Chan, K.-H.; Ciulli, A. Selective Small Molecule Induced Degradation of the BET Bromodomain Protein BRD4. *ACS Chem. Biol.* **2015**, *10*, 1770–1777.
- (167) Gadd, M. S.; Testa, A.; Lucas, X.; Chan, K. H.; Chen, W.; Lamont, D. J.; Zengerle, M.; Ciulli, A. Structural Basis of PROTAC Cooperative Recognition for Selective Protein Degradation. *Nat. Chem. Biol.* **2017**, *13*, 514–521.
- (168) Buckley, D. L.; Gustafson, J. L.; Van Molle, I.; Roth, A. G.; Tae, H. S.; Gareiss, P. C.; Jorgensen, W. L.; Ciulli, A.; Crews, C. M. Small-Molecule Inhibitors of the Interaction between the E3 Ligase VHL and HIF1 α . *Angew. Chem., Int. Ed.* **2012**, *51*, 11463–11467.
- (169) Tokuyama, H.; Kuboyama, T.; Amano, A.; Yamashita, T.; Fukuyama, T. A Novel Transformation of Primary Amines to N-Monoalkylhydroxylamines. *Synthesis* **2000**, No. 9, 1299–1304.
- (170) Jiang, H.; Studer, A. Anti-Markovnikov Radical Hydro- and Deuteroamidation of Unactivated Alkenes. *Chem. – A Eur. J.* **2019**, *25*, 7105–7109.
-

References

- (171) Liu, S. M.; Wu, D.; Bode, J. W. One-Step Synthesis of Aliphatic Potassium Acyltrifluoroborates (KATs) from Organocuprates. *Org. Lett.* **2018**, 20, 2378–2381.
- (172) Katritzky, A. R.; Lan, X.; Yang, J. Z.; Denisko, O. V. Properties and Synthetic Utility of N-Substituted Benzotriazoles. *Chem. Rev.* **1998**, 98, 409–548.
- (173) Katritzky, A. R.; Kirichenko, K. Acyl Anion Synthons: Benzotriazole Stabilized Compared to Classical. *ARKIVOC* (Gainesville, FL, U. S.) **2006**, 2006, 119–151.
- (174) Katritzky, A. R.; Lang, H.; Wang, Z.; Zhang, Z.; Song, H. Benzotriazole-Mediated Conversions of Aromatic and Heteroaromatic Aldehydes to Functionalized Ketones. *J. Org. Chem.* **1995**, 60, 7619–7624.
- (175) Nahm, S.; Weinreb, S. M. N-Methoxy-n-Methylamides as Effective Acylating Agents. *Tetrahedron Lett.* **1981**, 22, 3815–3818.
- (176) Liu, S. M. Efforts toward the Synthesis of Potassium Acyltrifluoroborates, ETH Doctoral Thesis, Zürich, 2018.
- (177) Kikuchi, D.; Sakaguchi, S.; Ishii, Y. An Alternative Method for the Selective Bromination of Alkylbenzenes Using NaBrO₃/NaHSO₃ Reagent. *J. Org. Chem.* **1998**, 63, 6023–6026.
- (178) Gálvez, A. O. Unpublished Results. **2018**.
- (179) Reeves, J. T.; Lorenc, C.; Camara, K.; Li, Z.; Lee, H.; Busacca, C. A.; Senanayake, C. H. Carbamoyl Anion Addition to Nitrones. *J. Org. Chem.* **2014**, 79, 5895–5902.
- (180) Safaei, H. R.; Davoodi, M.; Shekouhy, M. Highly Efficient Synthesis of Substituted Benzenes in the Presence of B(HSO₄)₃ as a New and Reusable Catalyst Under Solvent-Free Conditions. *Synth. Commun.* **2013**, 43, 2178–2190.
- (181) Li, Q.; Rukavishnikov, A. V.; Petukhov, P. A.; Zaikova, T. O.; Keana, J. F. W. Nanoscale 1,3,5,7-Tetrasubstituted Adamantanes and p-Substituted Tetraphenyl-Methanes for AFM Applications. *Org. Lett.* **2002**, 4, 3631–3634.

9

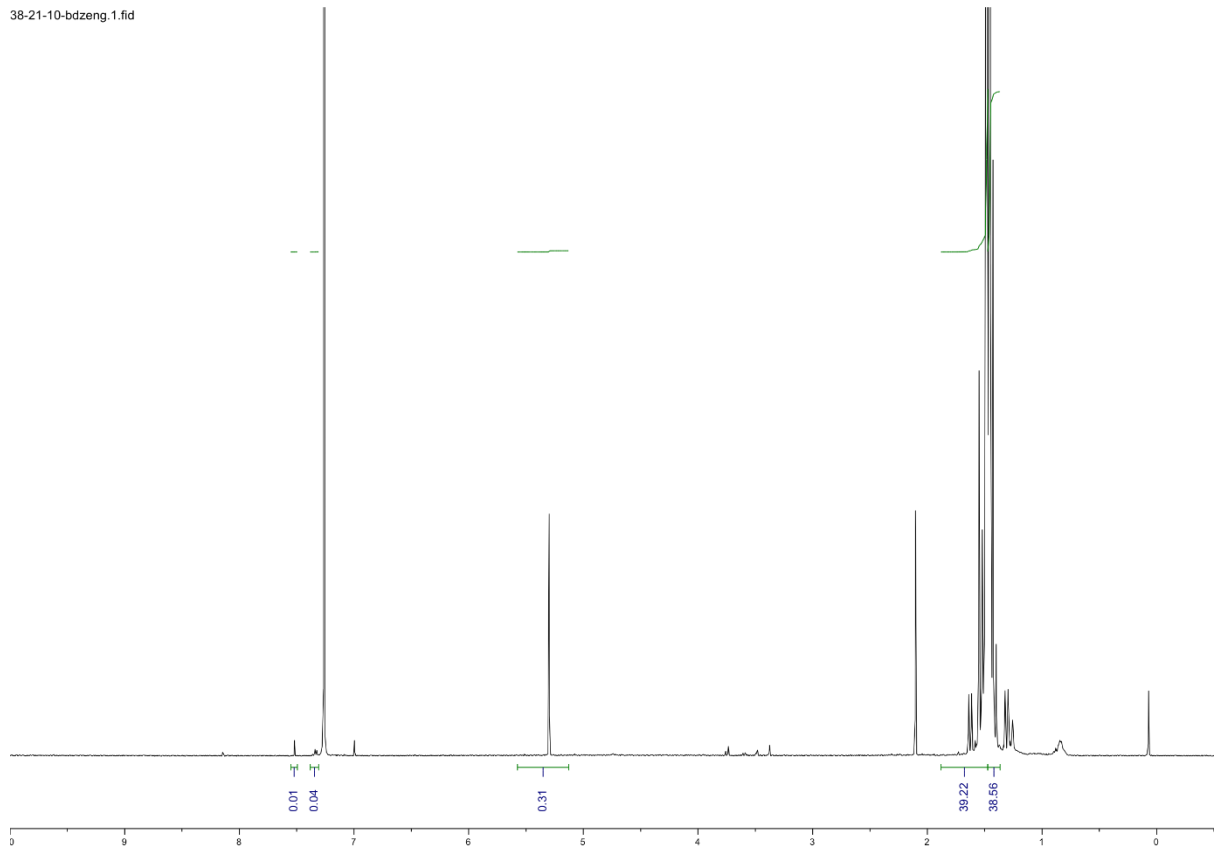
NMR Spectra

NMR Spectra

Compound 97-d7

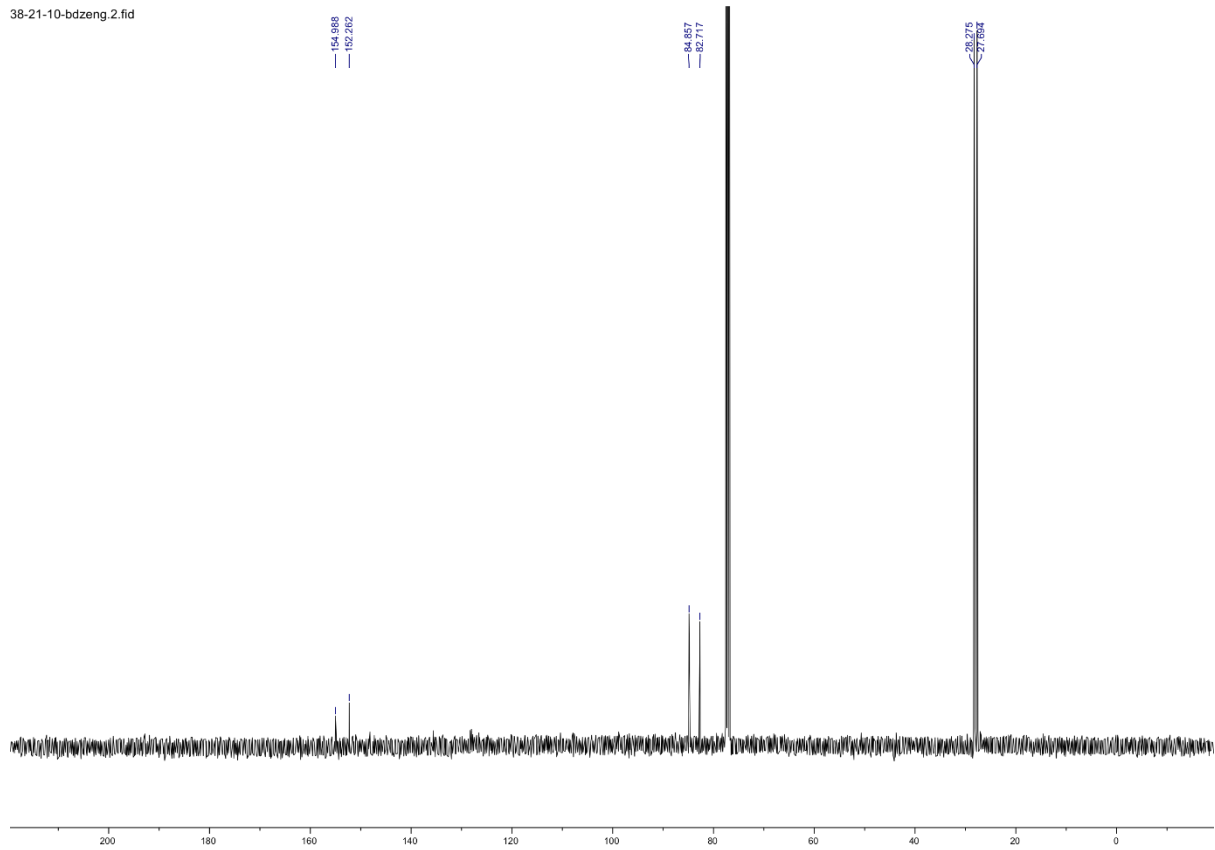
^1H 400 MHz

38-21-10-bdzenq.1.fid



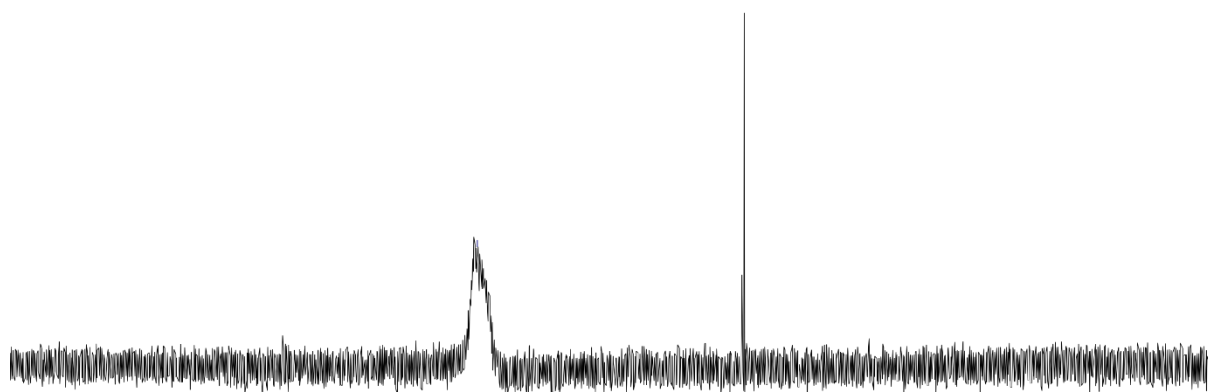
^{13}C 100 MHz

38-21-10-bdzenq.2.fid



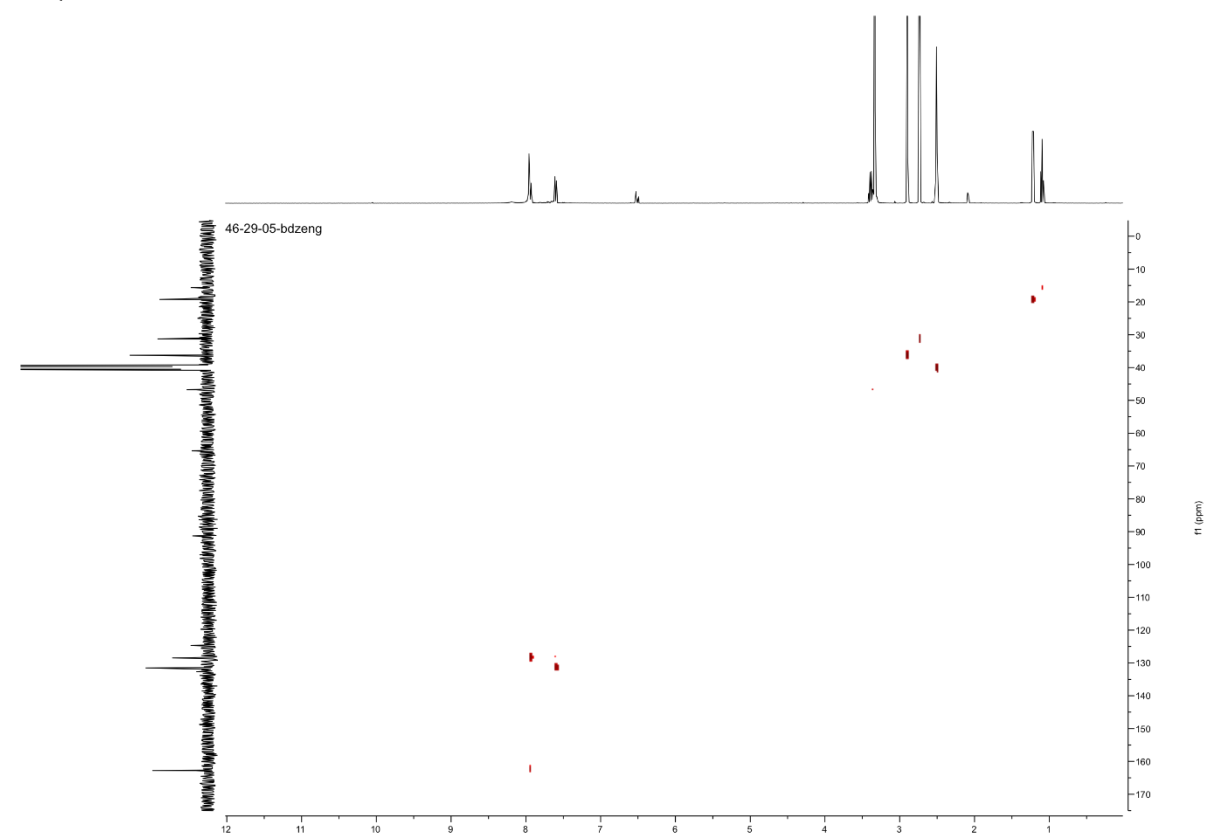
282MHz 19F-NMR

-141.615



30 -135 -140 -145 -150 -155 -1

HSQC 400MHz



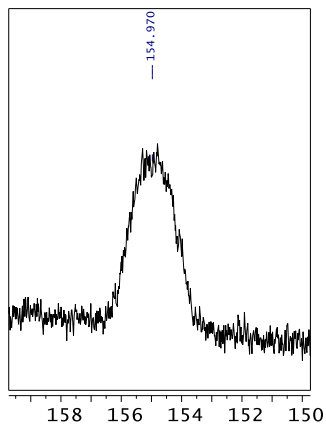
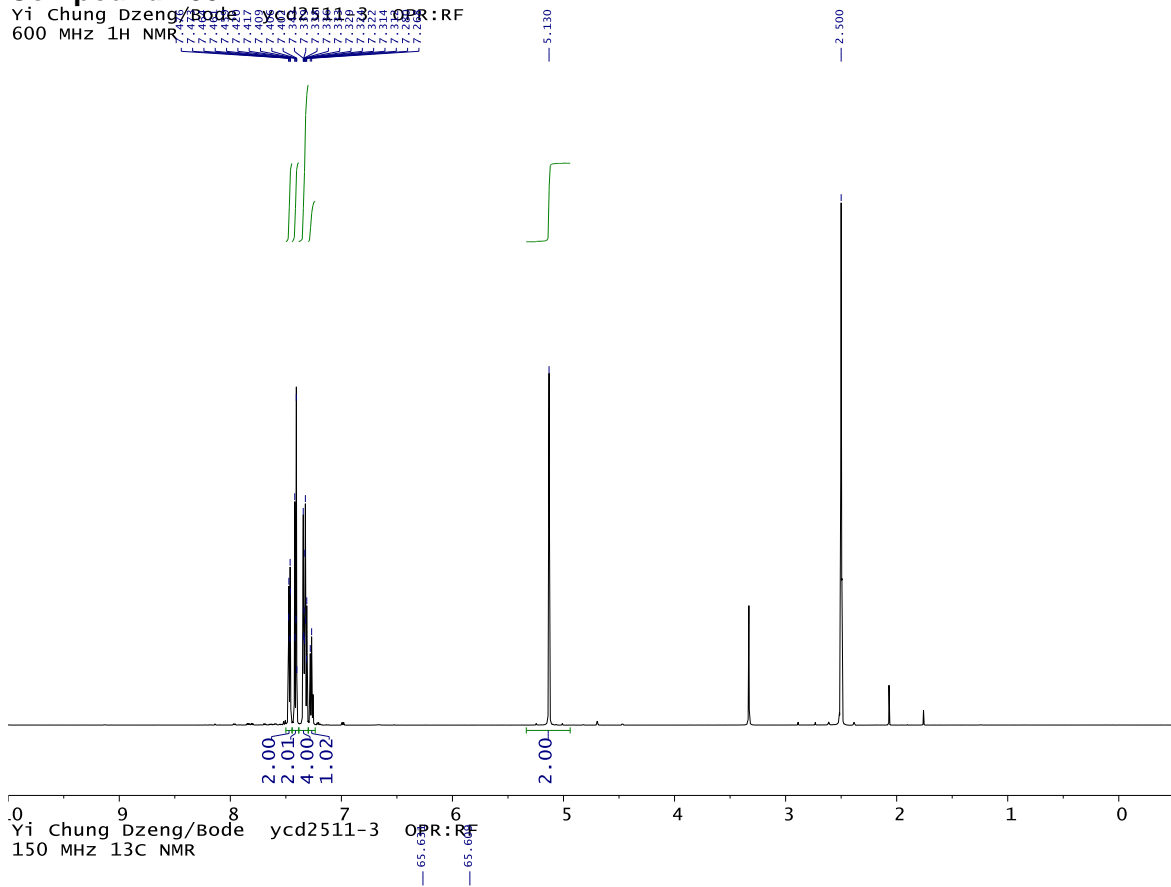
46-29-05-bdzensg

f1 (ppm)

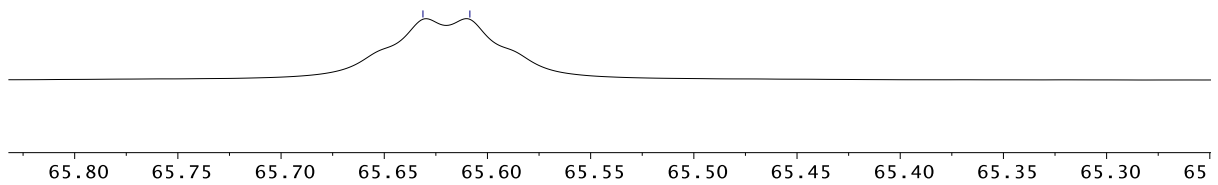
NMR Spectra

Compound 100

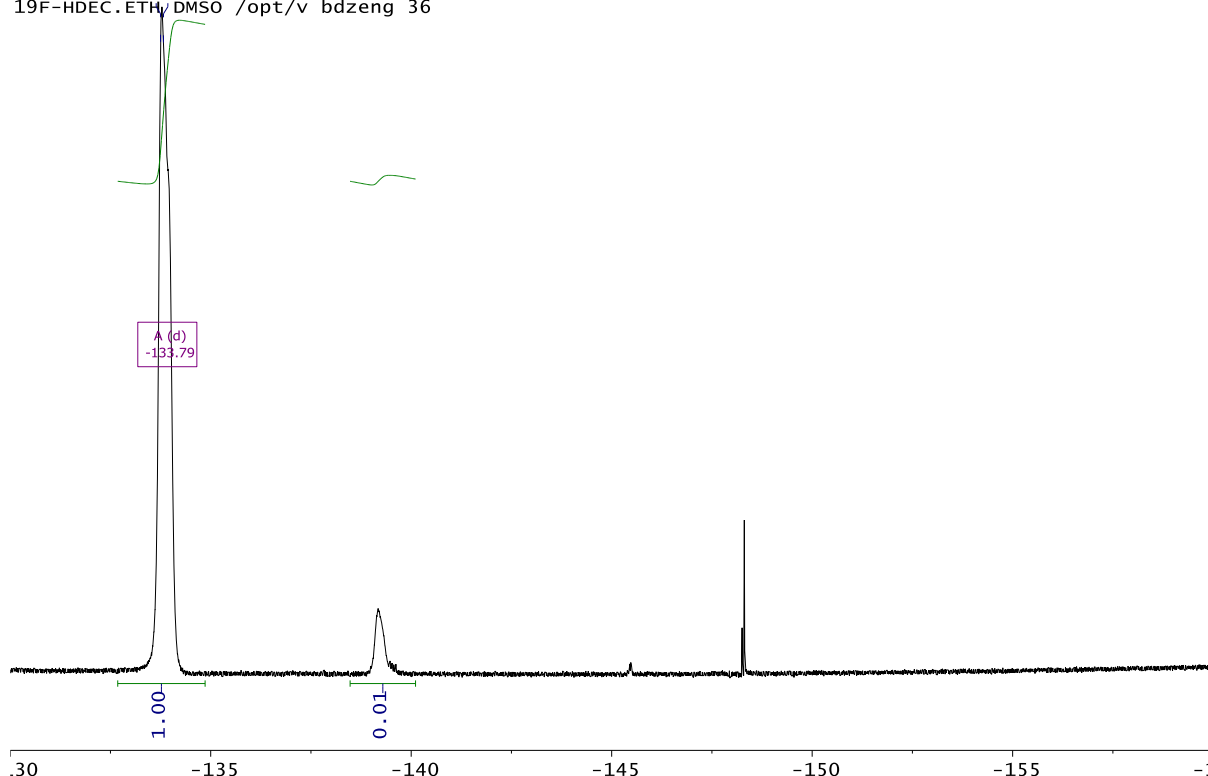
Yi Chung Dzeng/Bode ycd2511-3 OPR:RF
600 MHz 1H NMR



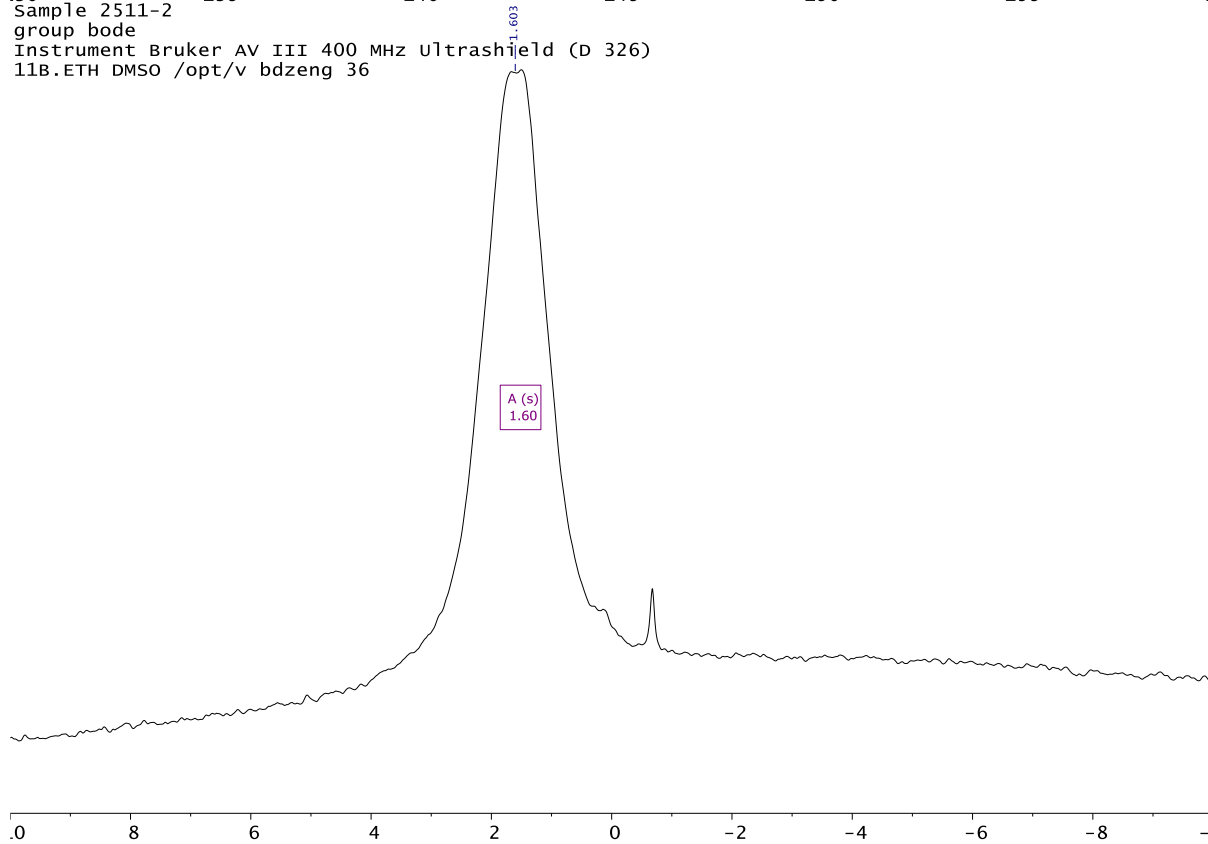
B (q)
65.62



Sample 2511-2
 group bode
 Instrument Bruker AV III 400 MHz Ultrashield (D 326)
 19F-HDEC.ETH/DMSO /opt/v bdzeng 36



Sample 2511-2
 group bode
 Instrument Bruker AV III 400 MHz Ultrashield (D 326)
 11B.ETH DMSO /opt/v bdzeng 36

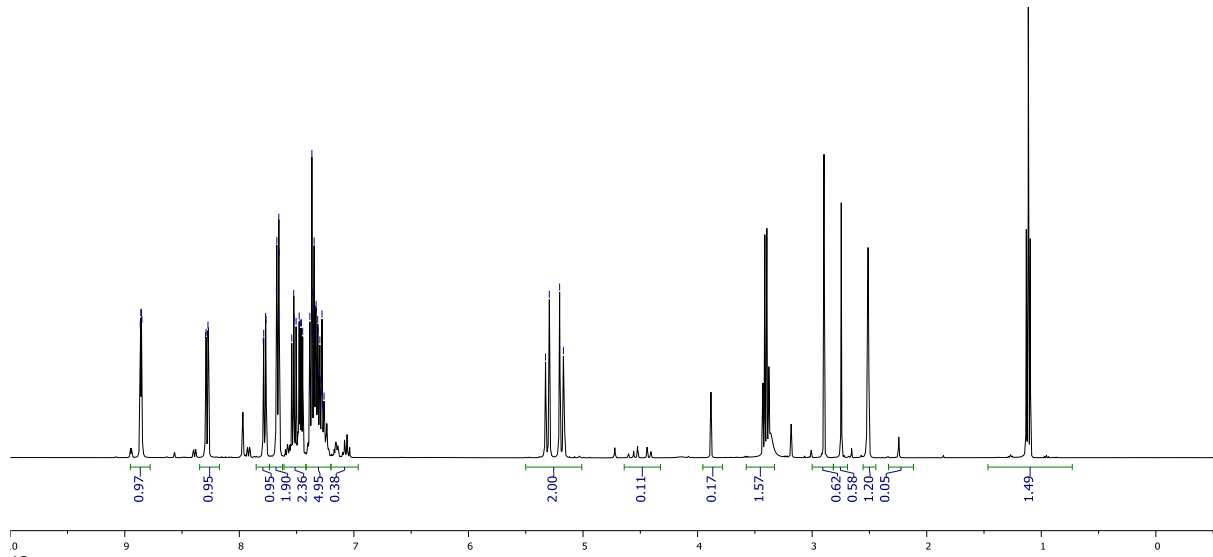
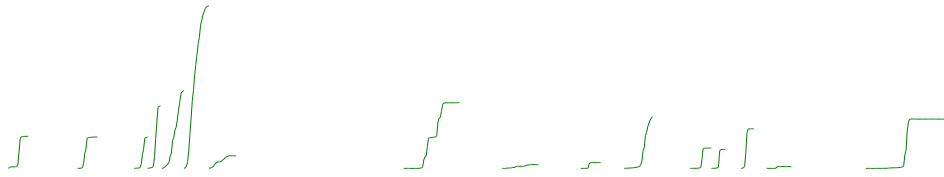


NMR Spectra

Compound 107

¹H NMR 400 MHz

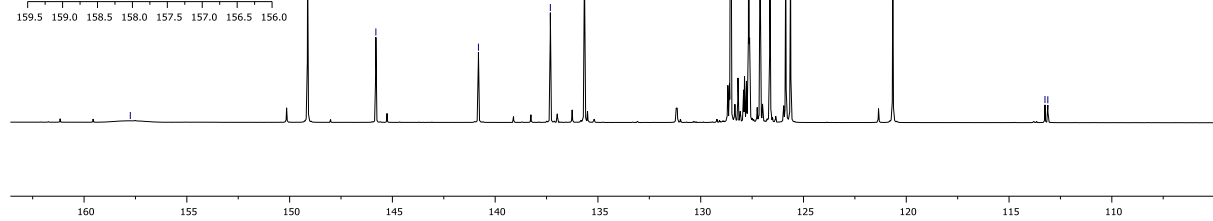
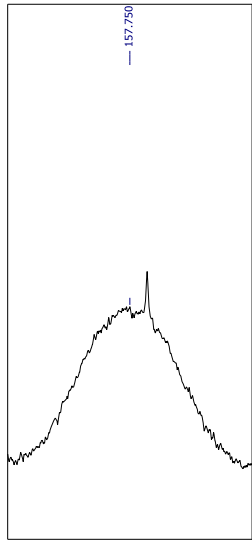
210912-0555-1.fid
8.166, 8.164, 8.162, 8.160, 8.158, 8.156, 8.154, 8.152, 8.150, 8.148, 8.146, 8.144, 8.142, 8.140, 8.138, 8.136, 8.134, 8.132, 8.130, 8.128, 8.126, 8.124, 8.122, 8.120, 8.118, 8.116, 8.114, 8.112, 8.110, 8.108, 8.106, 8.104, 8.102, 8.100, 7.770, 7.767, 7.764, 7.761, 7.677, 7.659, 7.656, 7.653, 7.543, 7.525, 7.522, 7.478, 7.467, 7.457, 7.447, 7.387, 7.385, 7.380, 7.380, 7.383, 7.351, 7.347, 7.334, 7.330, 7.316, 7.311, 7.302, 7.297, 7.294, 7.284, 7.279, 7.273, 7.264, 7.264, 5.327, 5.294, 5.204, 5.171



¹³C NMR 150 MHz

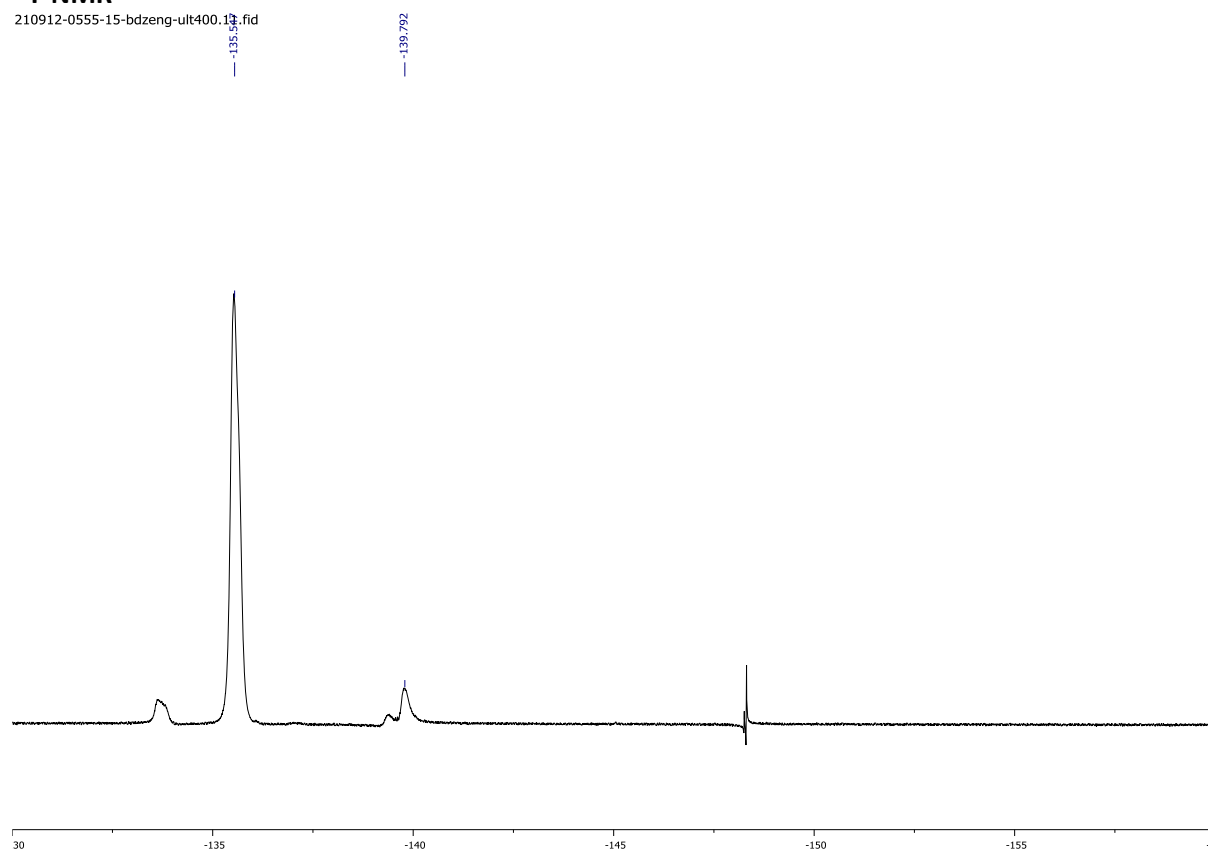
H4570.2.fid

157.750, 149.124, 145.803, 140.814, 137.315, 135.657, 128.543, 127.643, 127.110, 126.635, 125.864, 125.630, 120.654, 113.252, 113.114

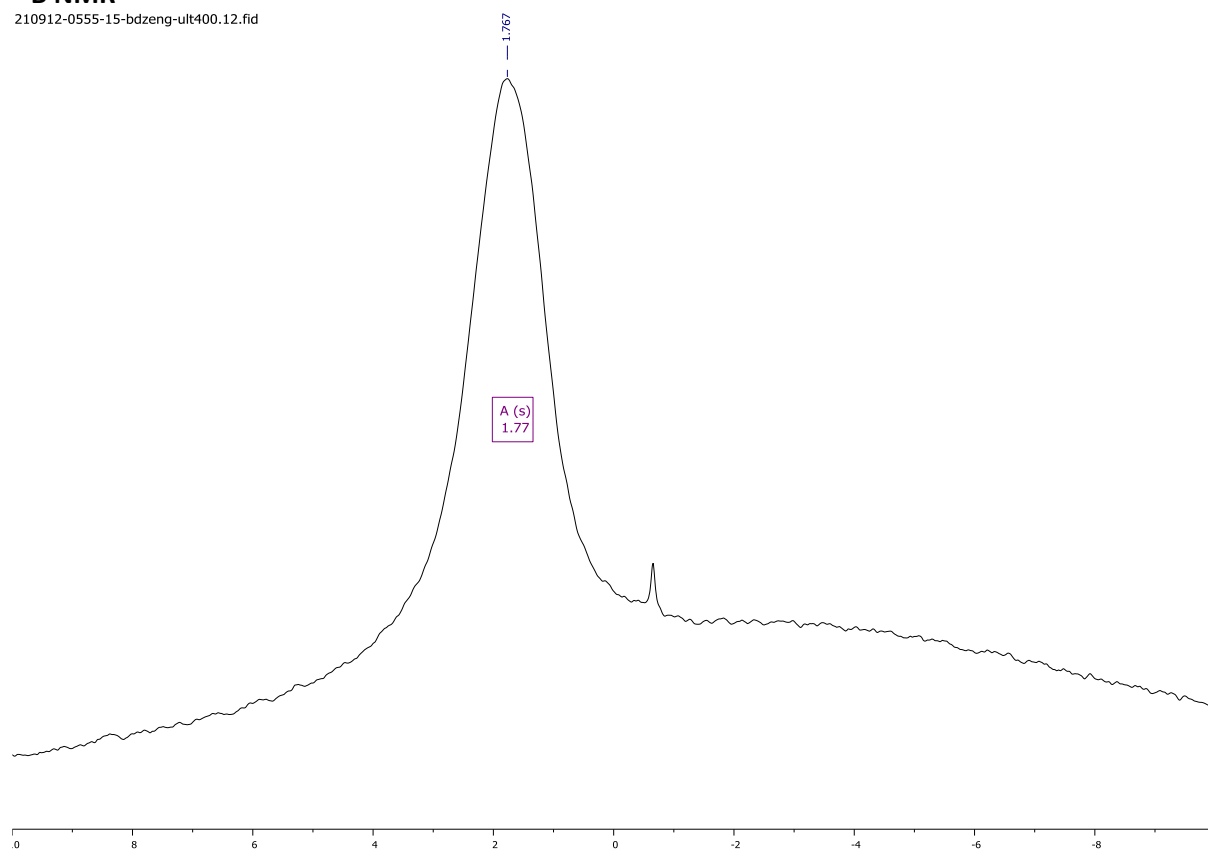


^{19}F NMR

210912-0555-15-bdzeng-ult400.12.fid

 **^{11}B NMR**

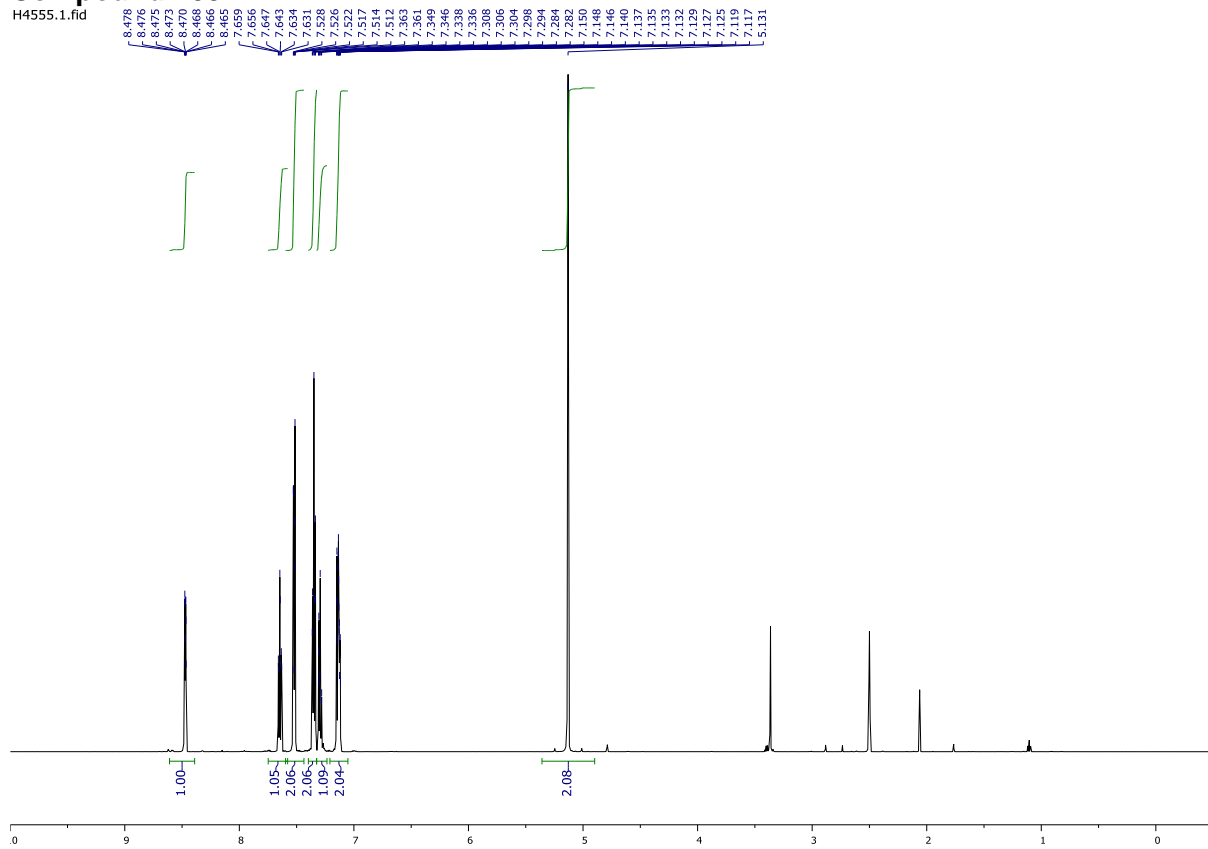
210912-0555-15-bdzeng-ult400.12.fid



NMR Spectra

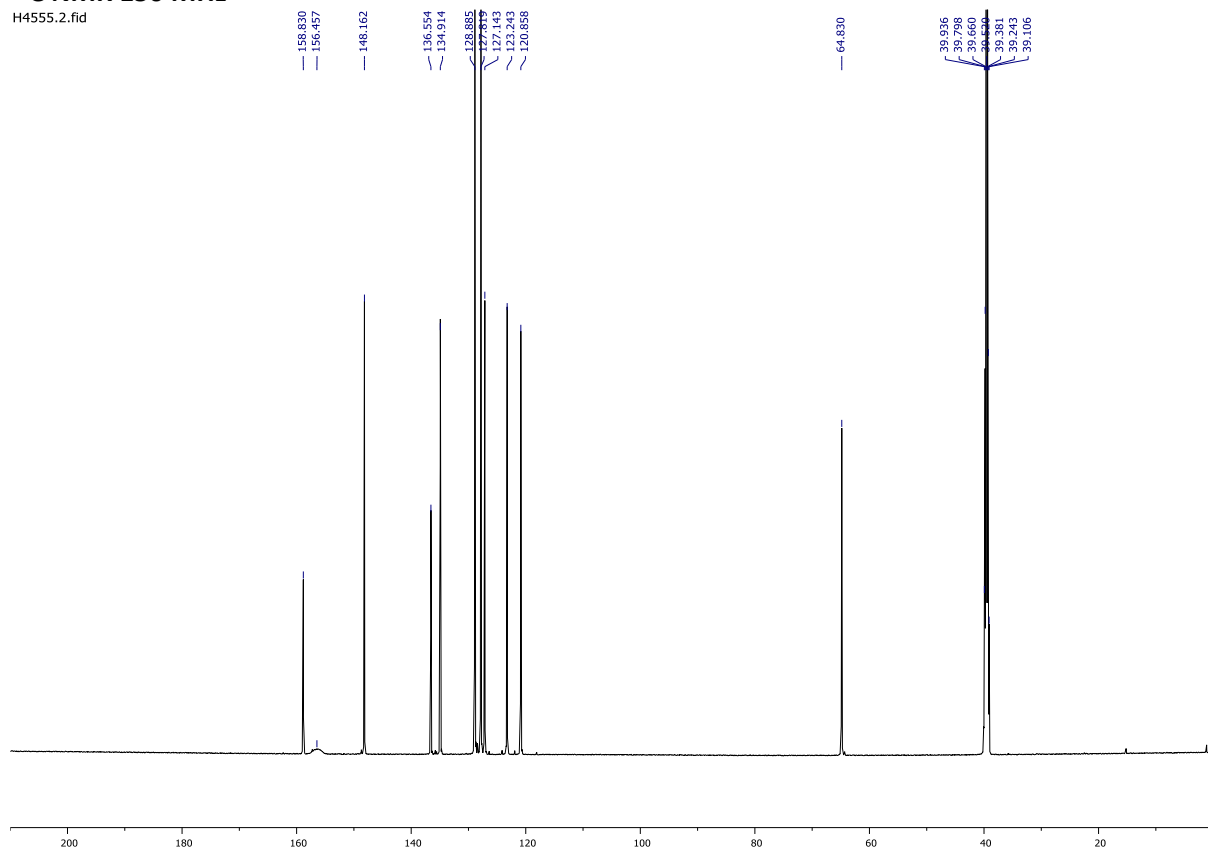
Compound 105

H4555.1.fid

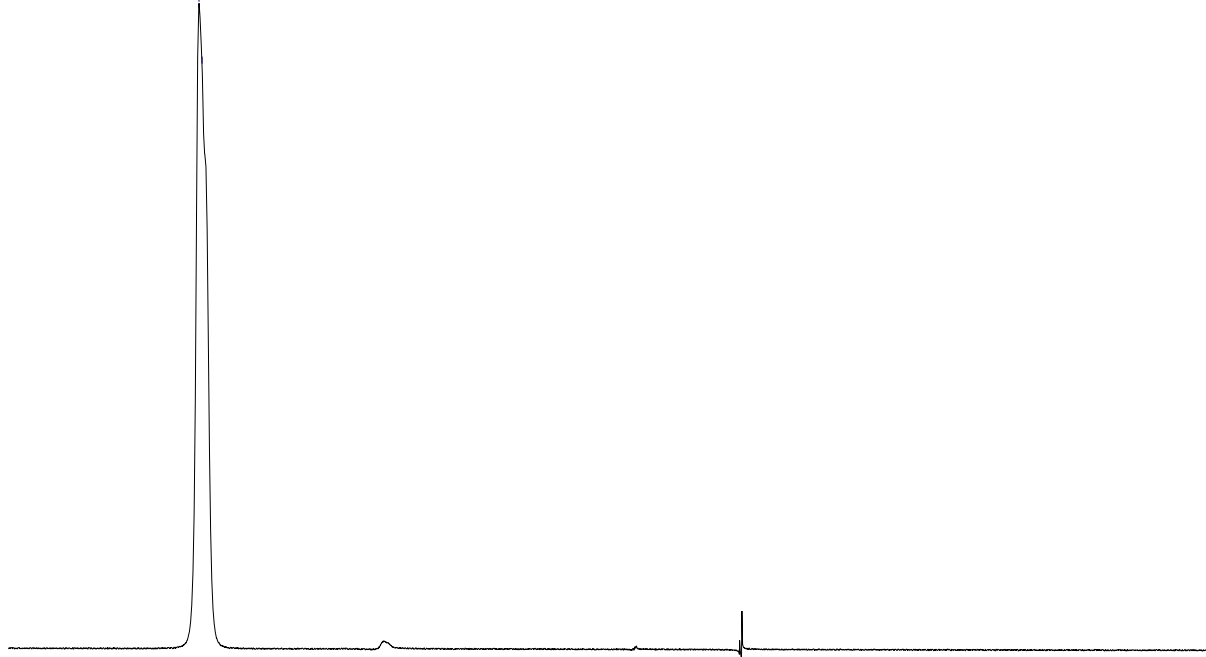


¹³C NMR 150 MHz

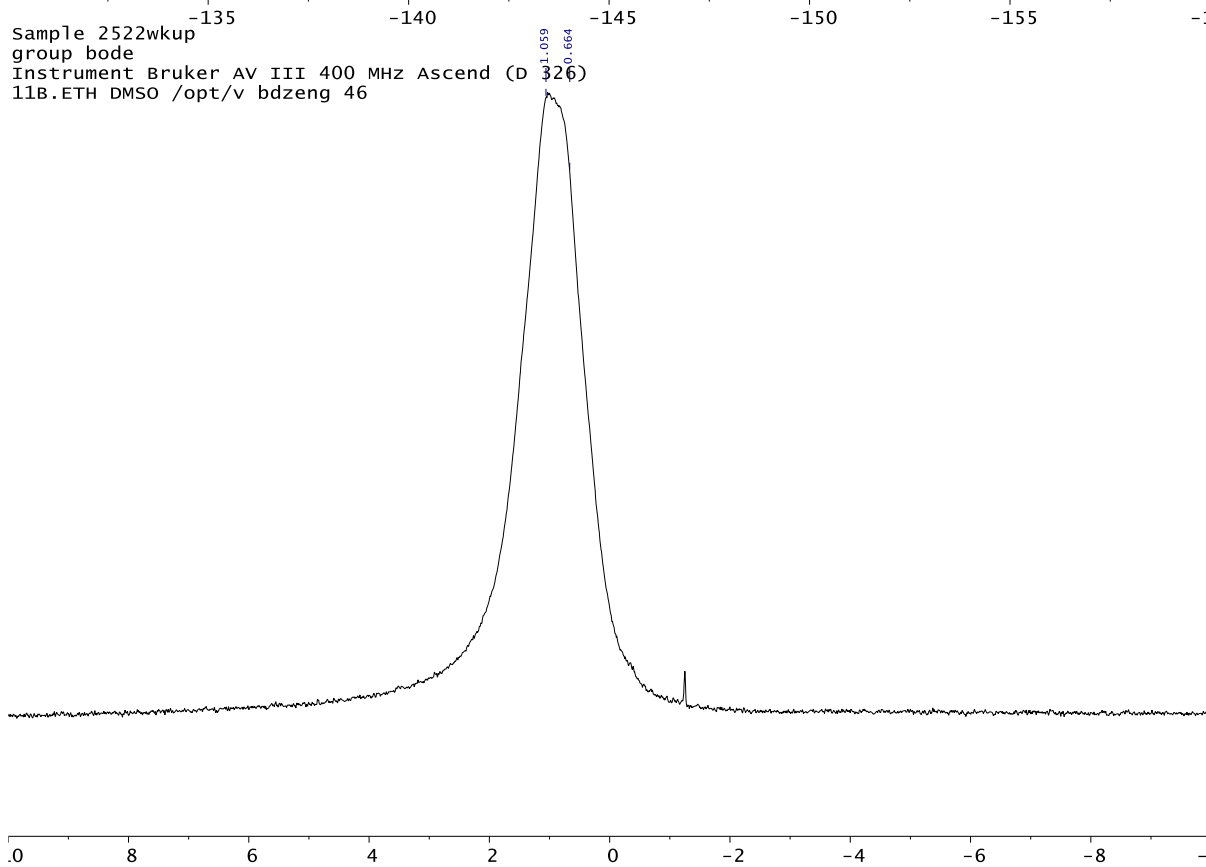
H4555.2.fid



Sample 2522wkup
 group bode
 Instrument Bruker AV III 400 MHz Ascend (D 326)
 19F-HDEC DMSO /opt/v bdzeng 46



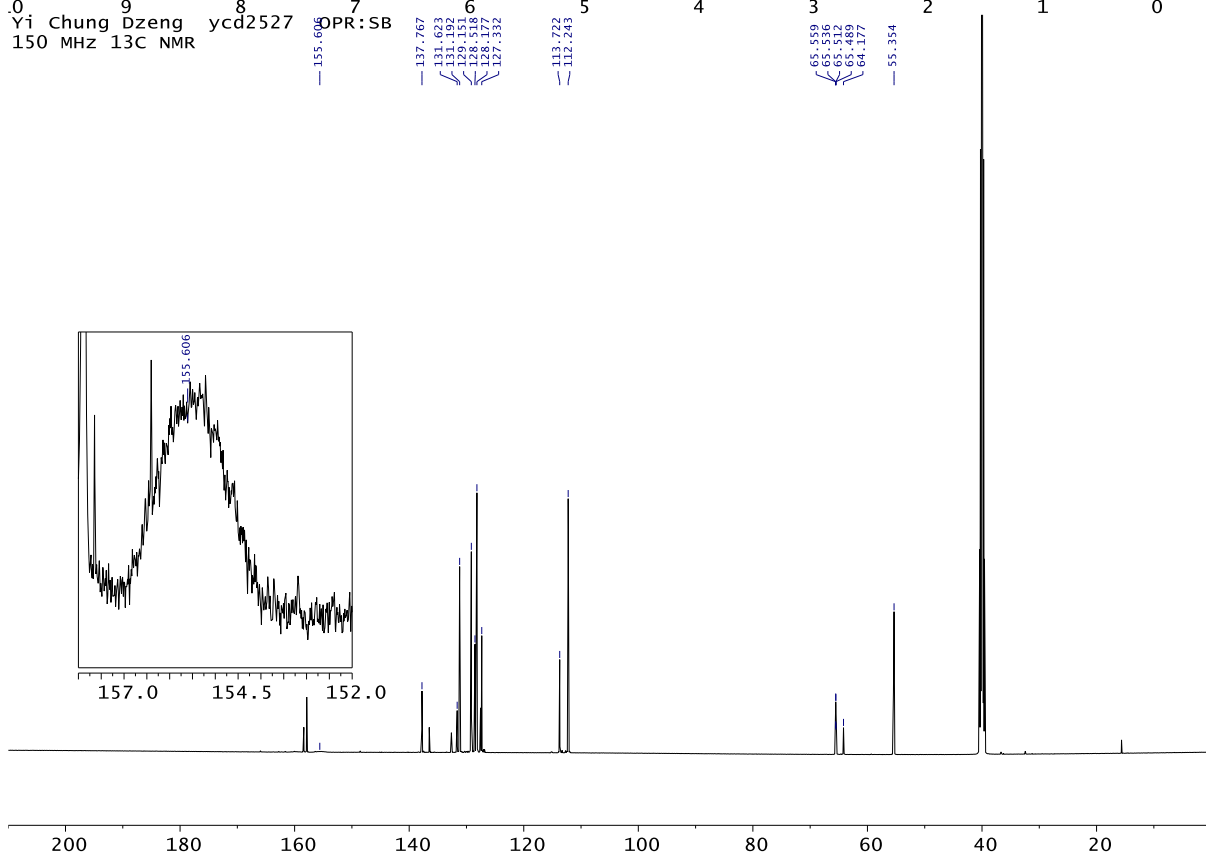
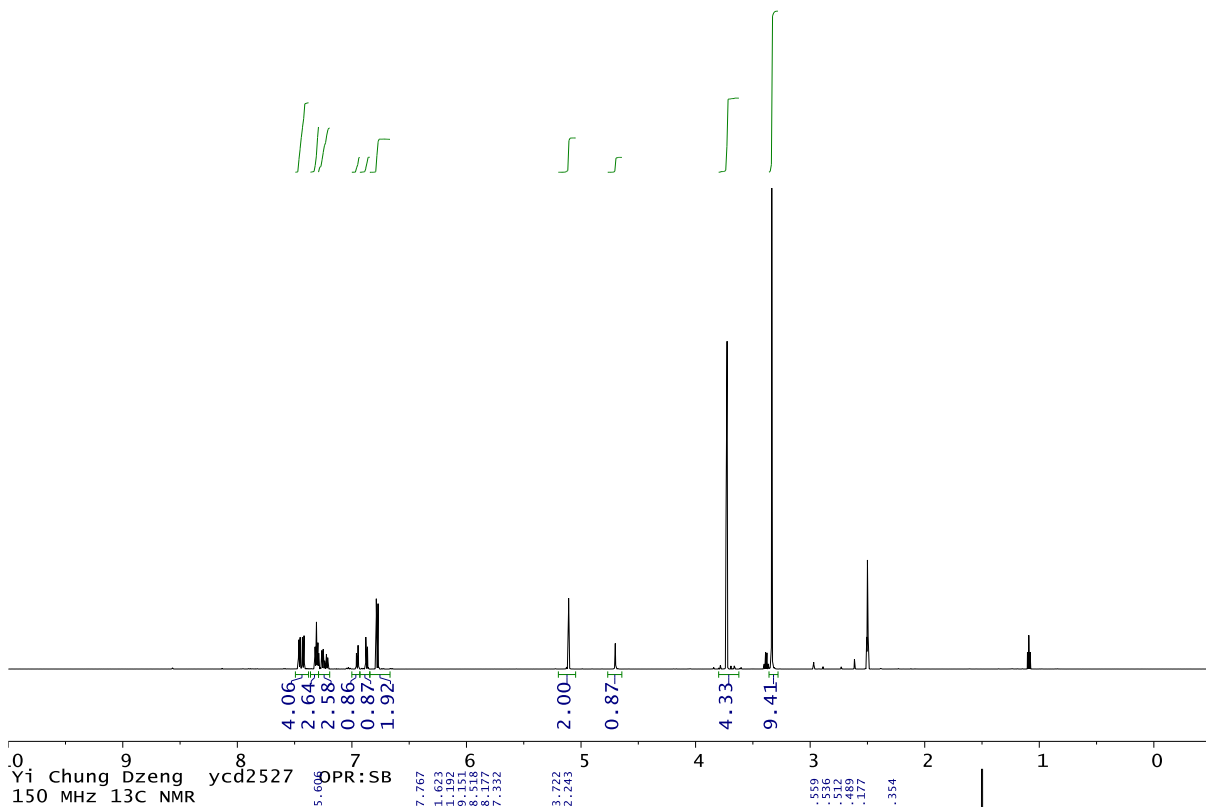
Sample 2522wkup
 group bode
 Instrument Bruker AV III 400 MHz Ascend (D 326)
 11B.ETH DMSO /opt/v bdzeng 46



NMR Spectra

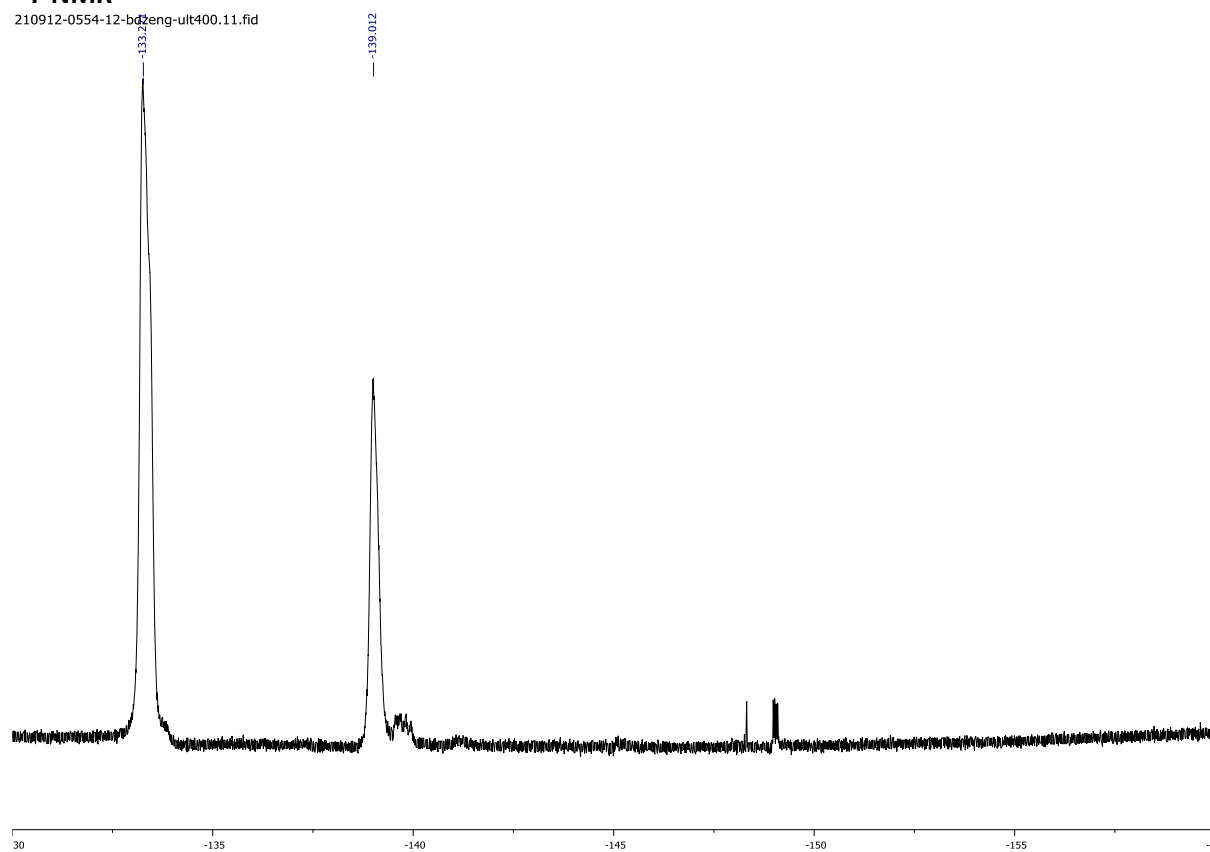
Compound 109

Yi Chung Dzeng ycd2527 OPR:SB
600 MHz ¹H NMR

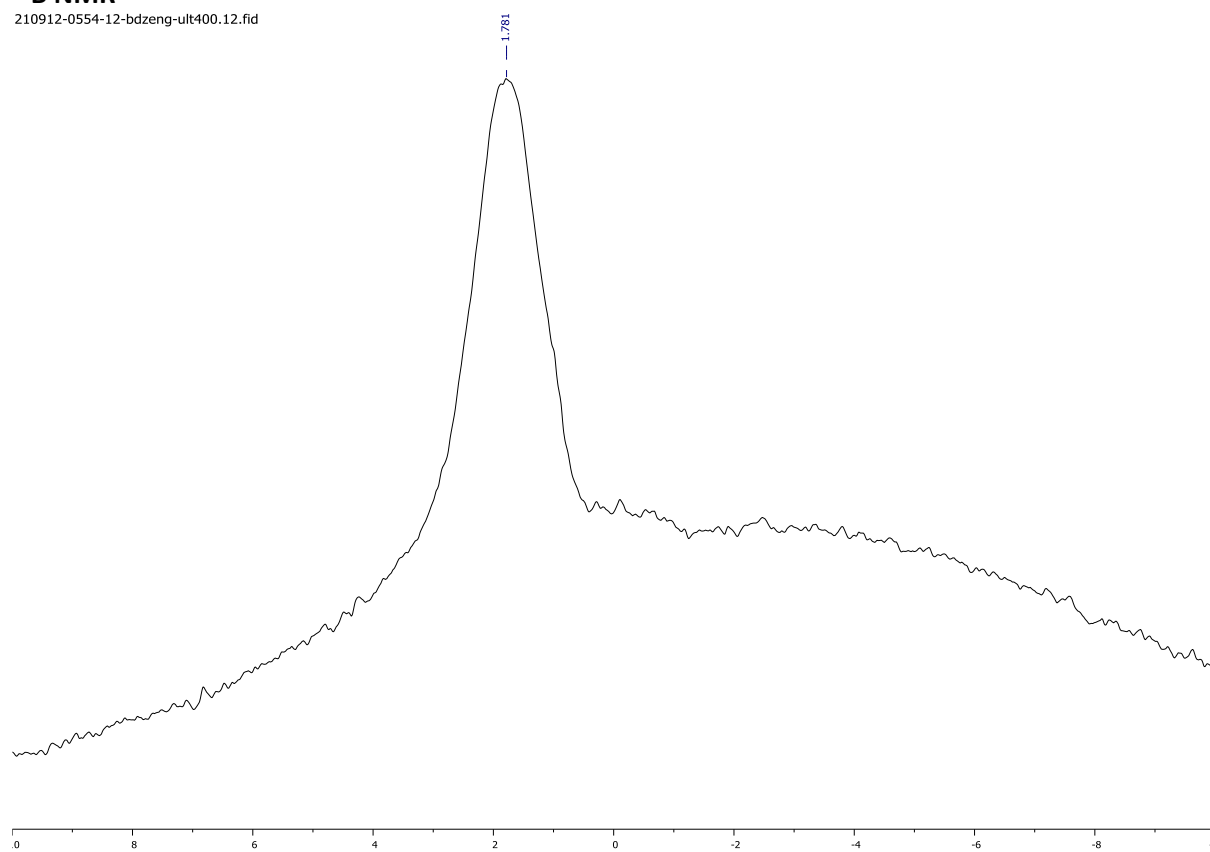


^{19}F NMR

210912-0554-12-bdzen-ult400.11.fid

 **^{11}B NMR**

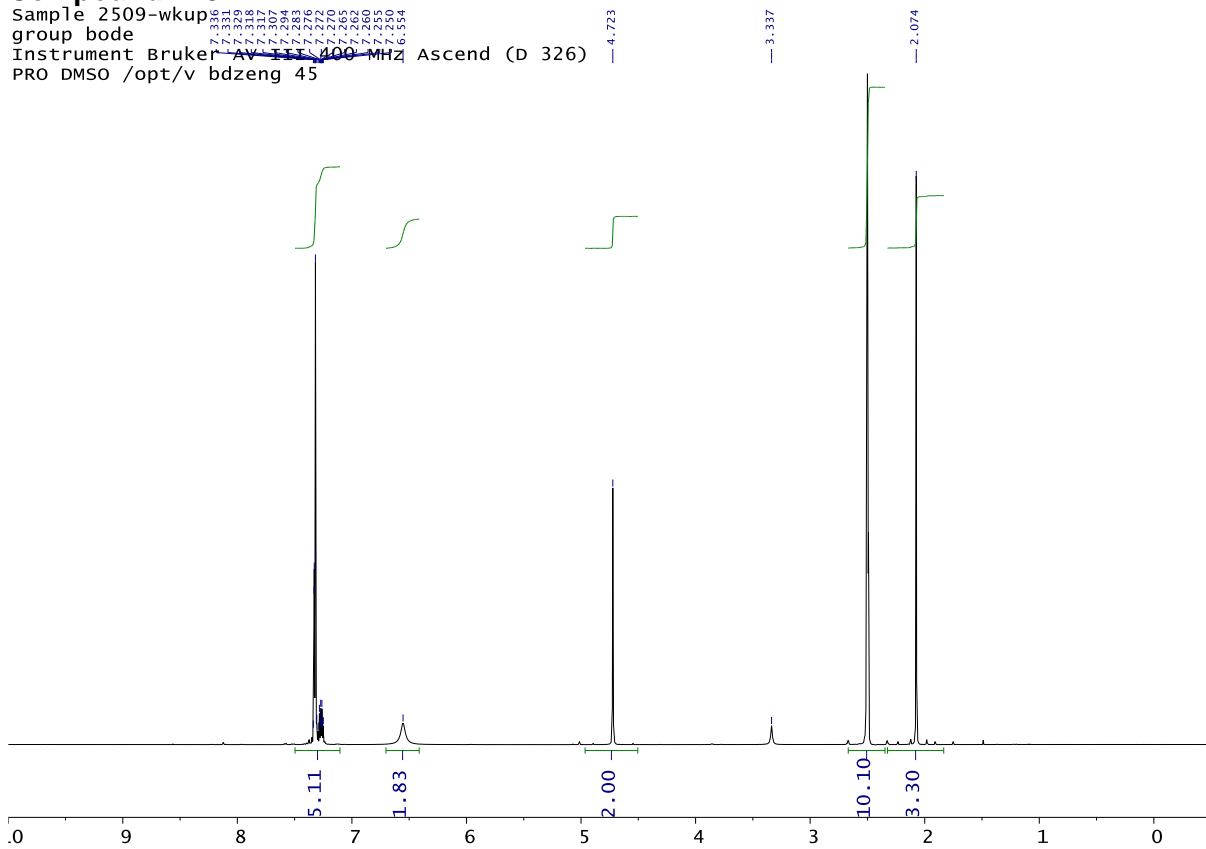
210912-0554-12-bdzen-ult400.12.fid



NMR Spectra

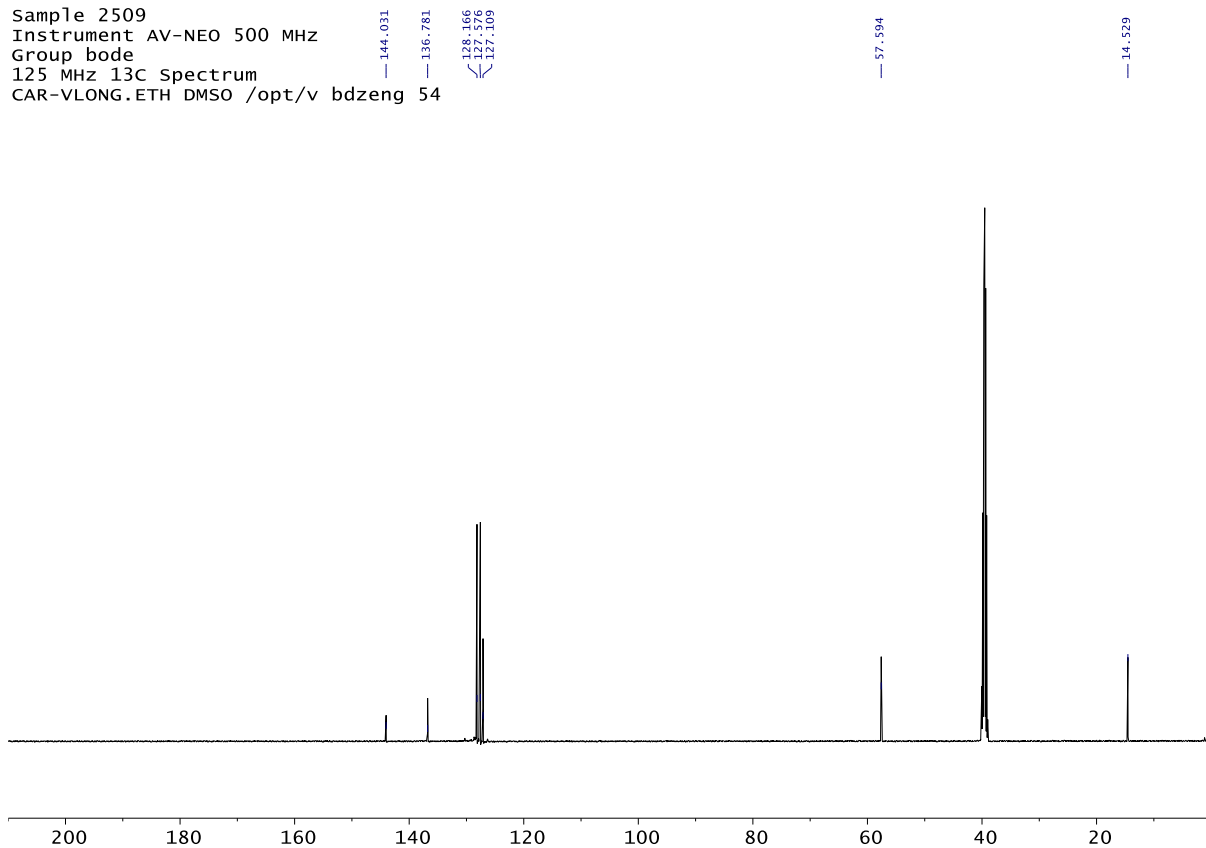
Compound 110

Sample 2509-wkup
group bode
Instrument Bruker AV-400 400 MHz Ascend (D 326)
PRO DMSO /opt/v bdzeng 45



¹³C NMR 125 MHz

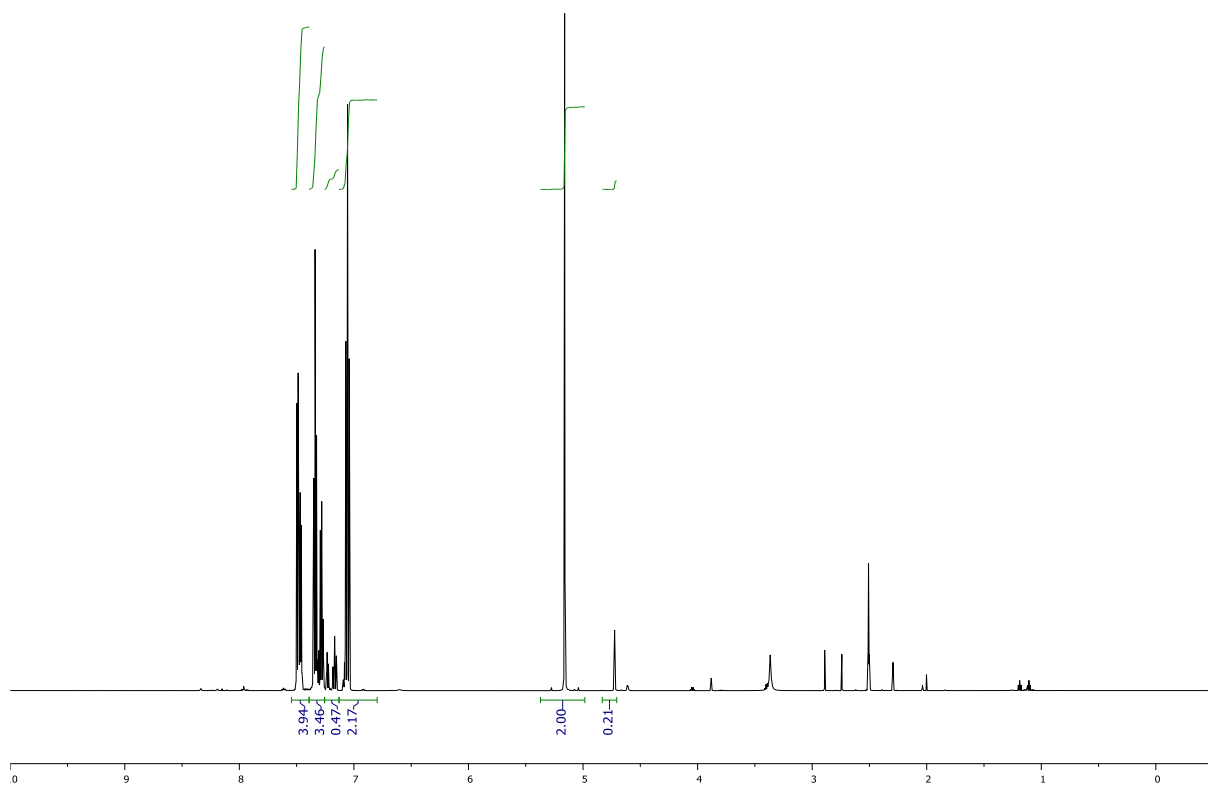
Sample 2509
Instrument AV-NEO 500 MHz
Group bode
125 MHz ¹³C Spectrum
CAR-VLONG.ETH DMSO /opt/v bdzeng 54



Compound 111

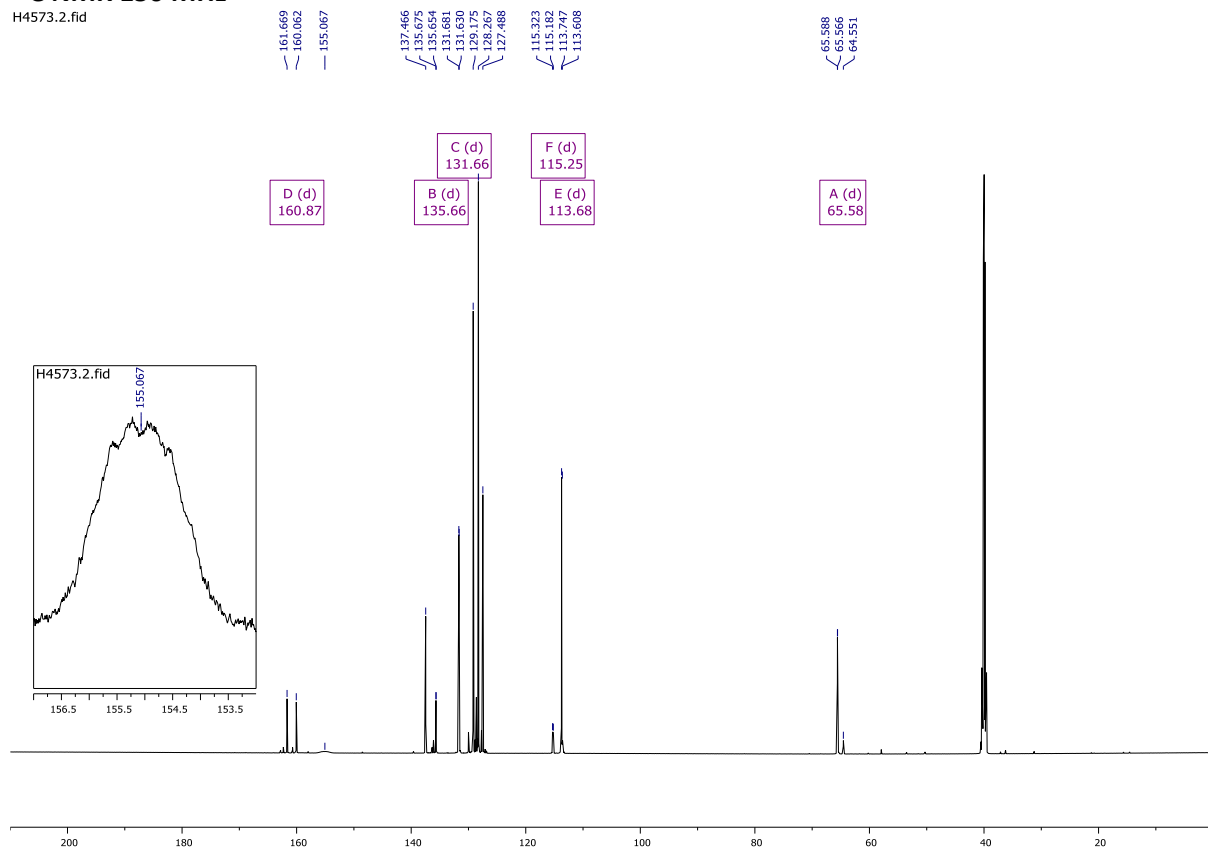
¹H NMR 600 MHz

H4573.1.fid



¹³C NMR 150 MHz

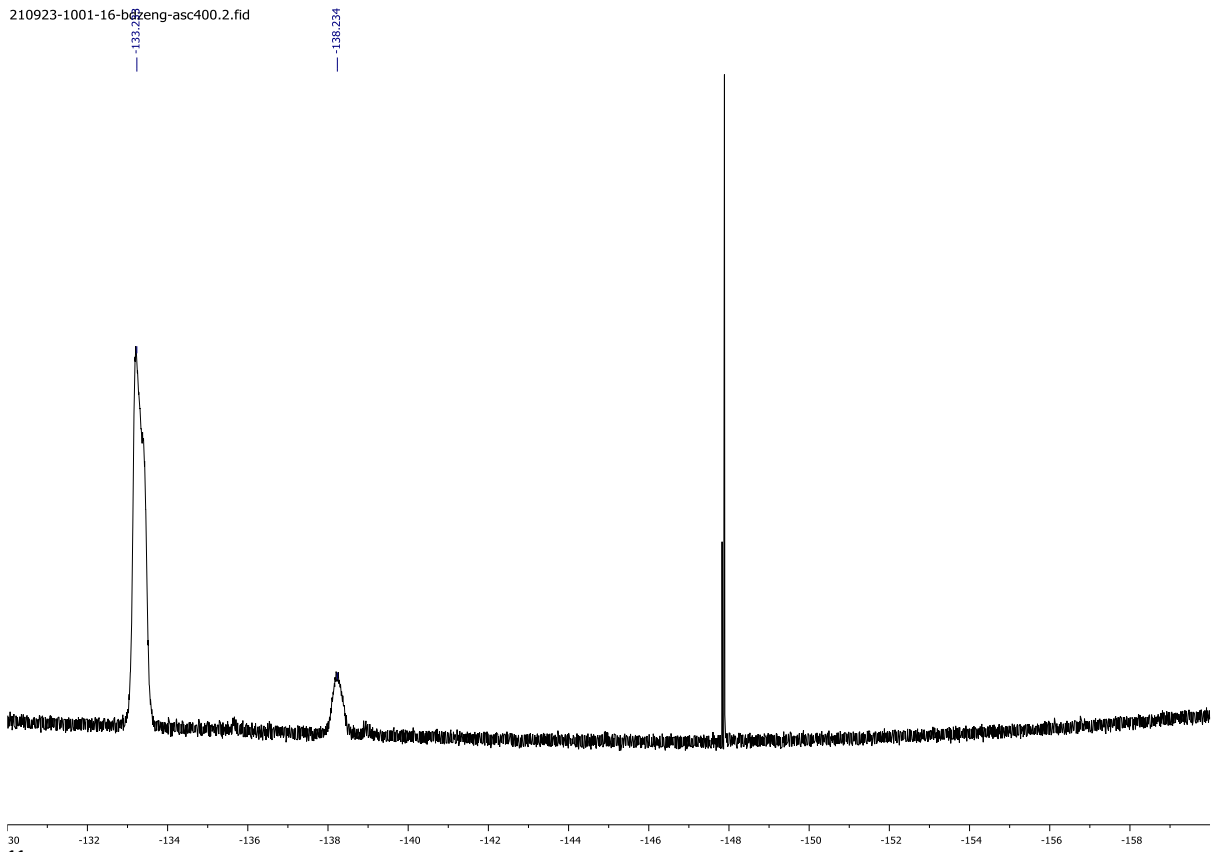
H4573.2.fid



¹⁹F NMR

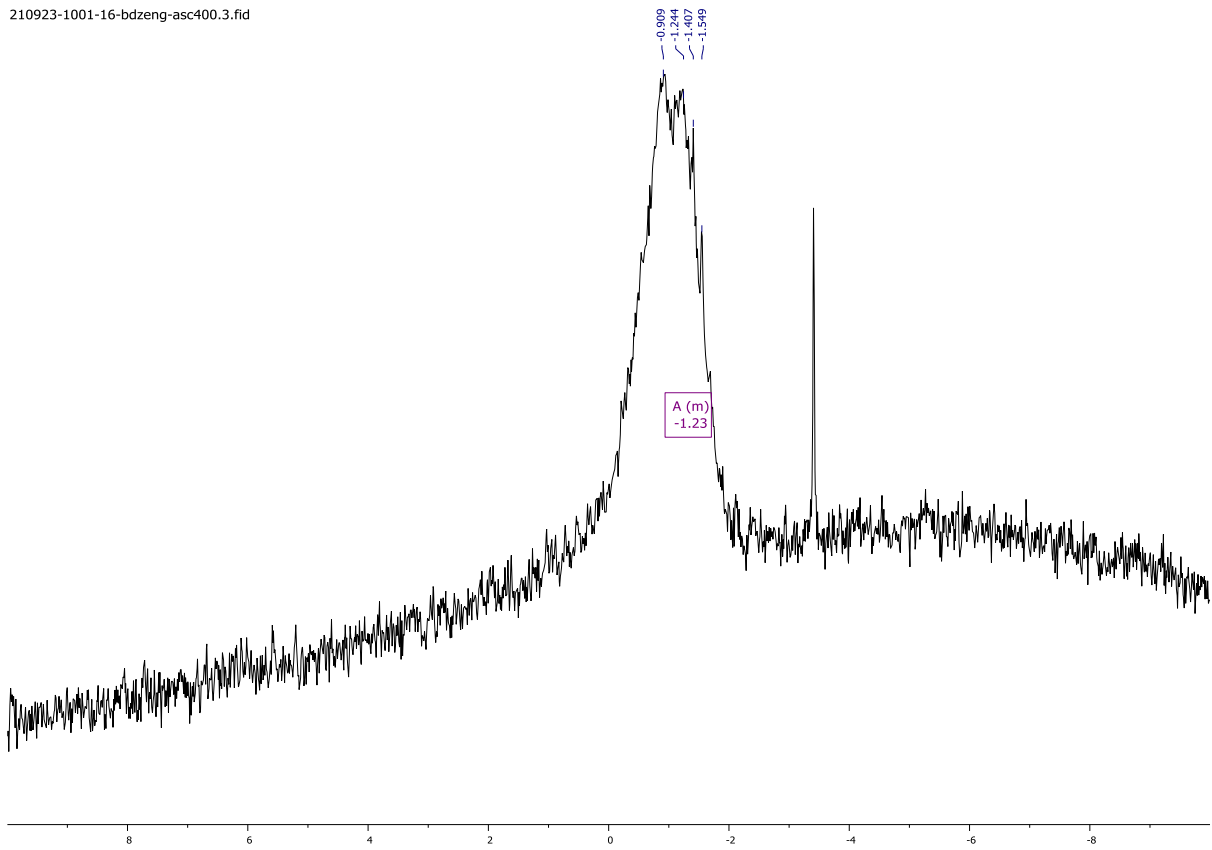
NMR Spectra

210923-1001-16-bdzeneng-asc400.2.fid



^{11}B NMR

210923-1001-16-bdzeneng-asc400.3.fid

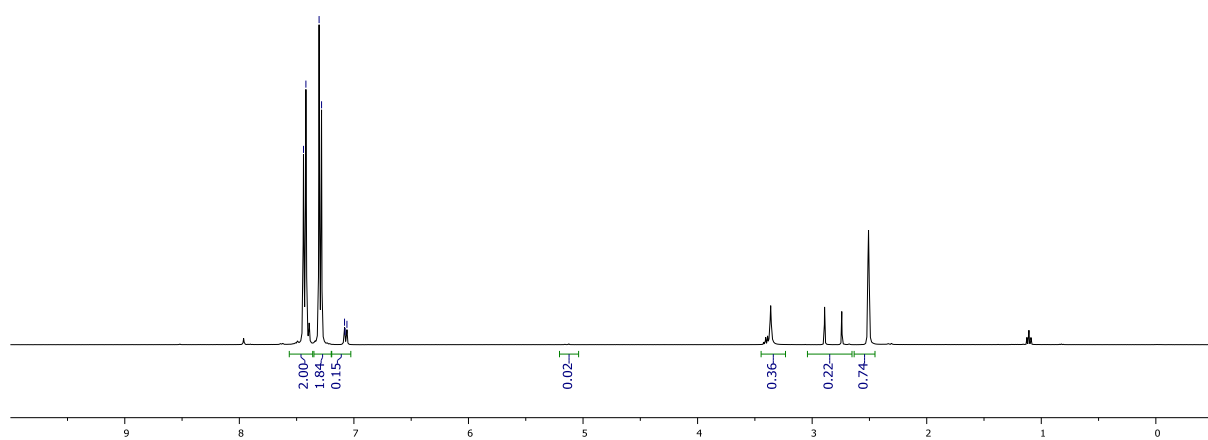


Compound 112

¹H NMR 400 MHz

210911-1713-25-bdzen-g-asc400.1.fid

7.440
7.439
7.282
7.082
7.077
7.061

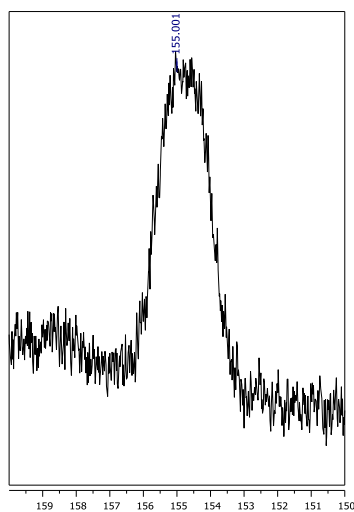


¹³C NMR 150 MHz

H4569.2.fid

155.001
138.359
137.070
131.474
130.673
129.919
129.787
128.627
127.910
127.751
127.591
126.970

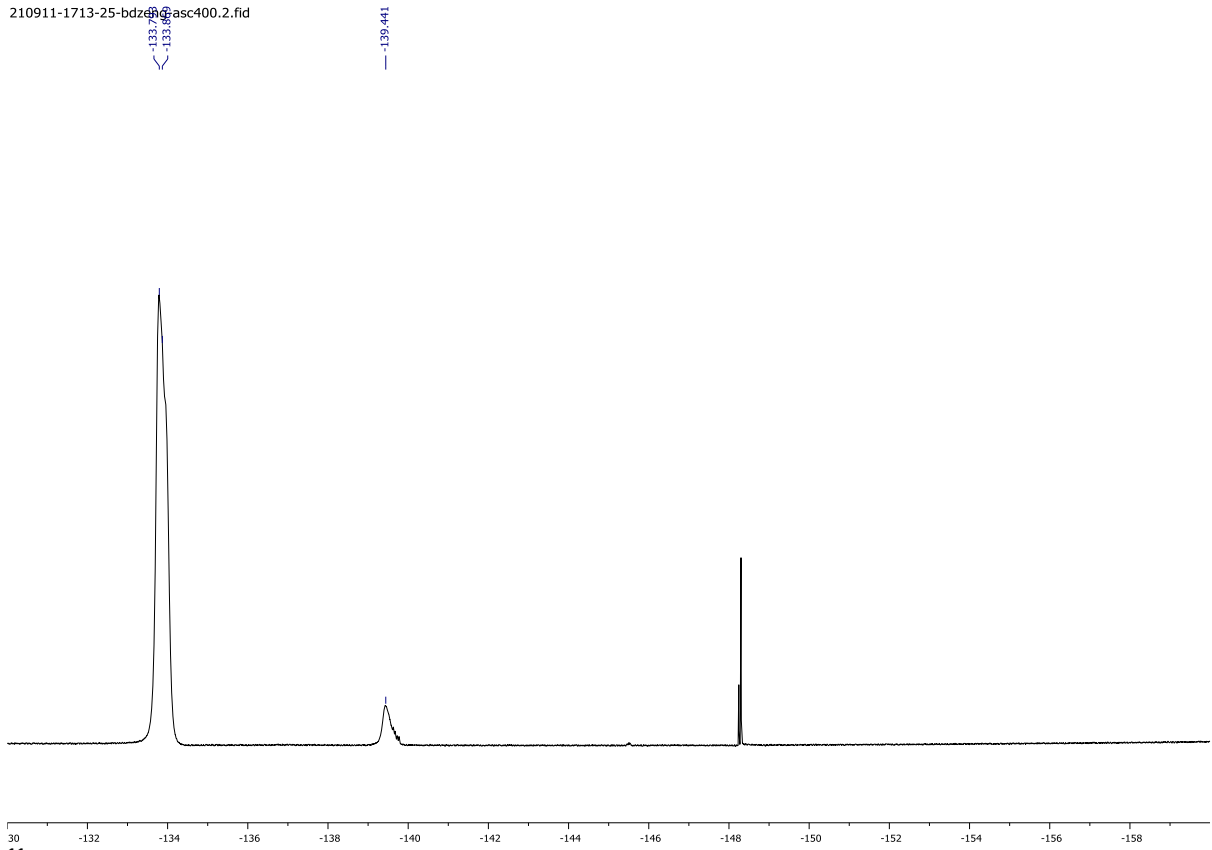
65.233
64.949
64.676



¹⁹F NMR

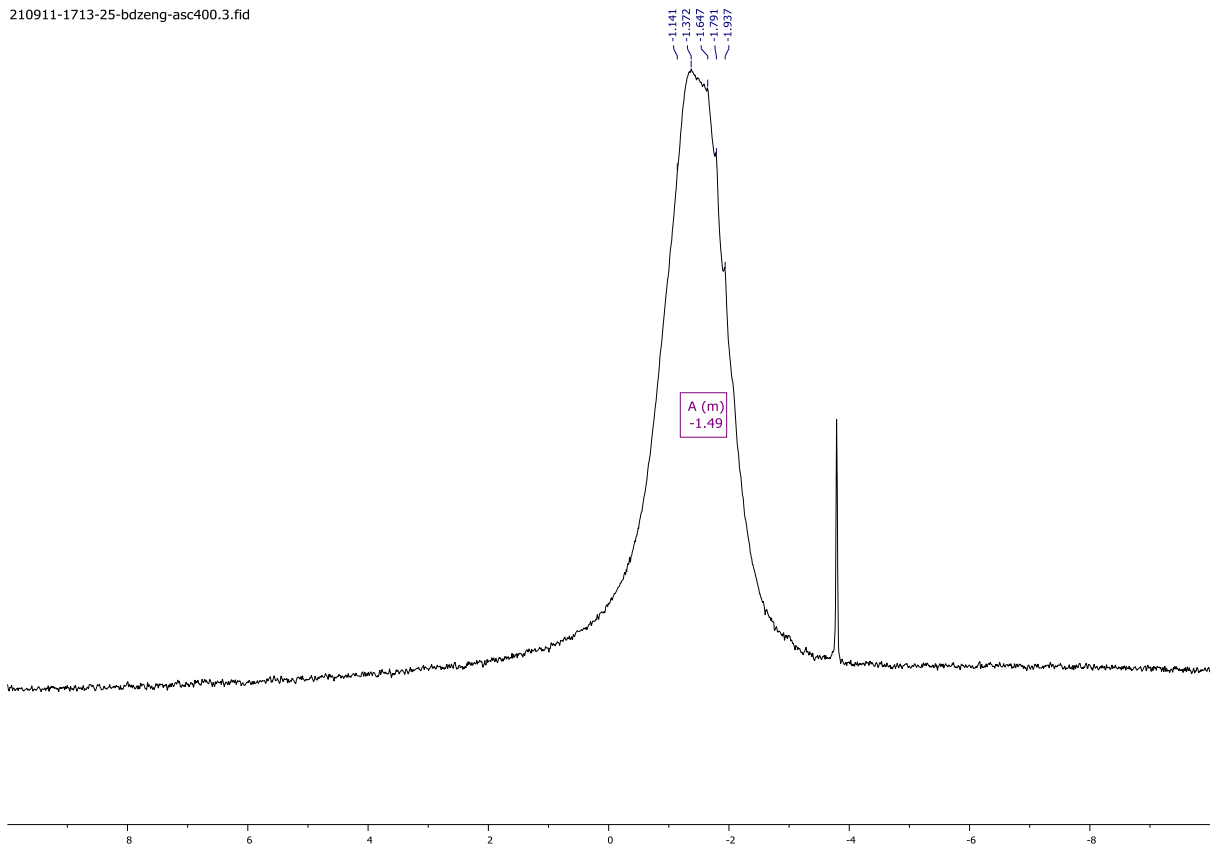
NMR Spectra

210911-1713-25-bdzen-asc400.2.fid



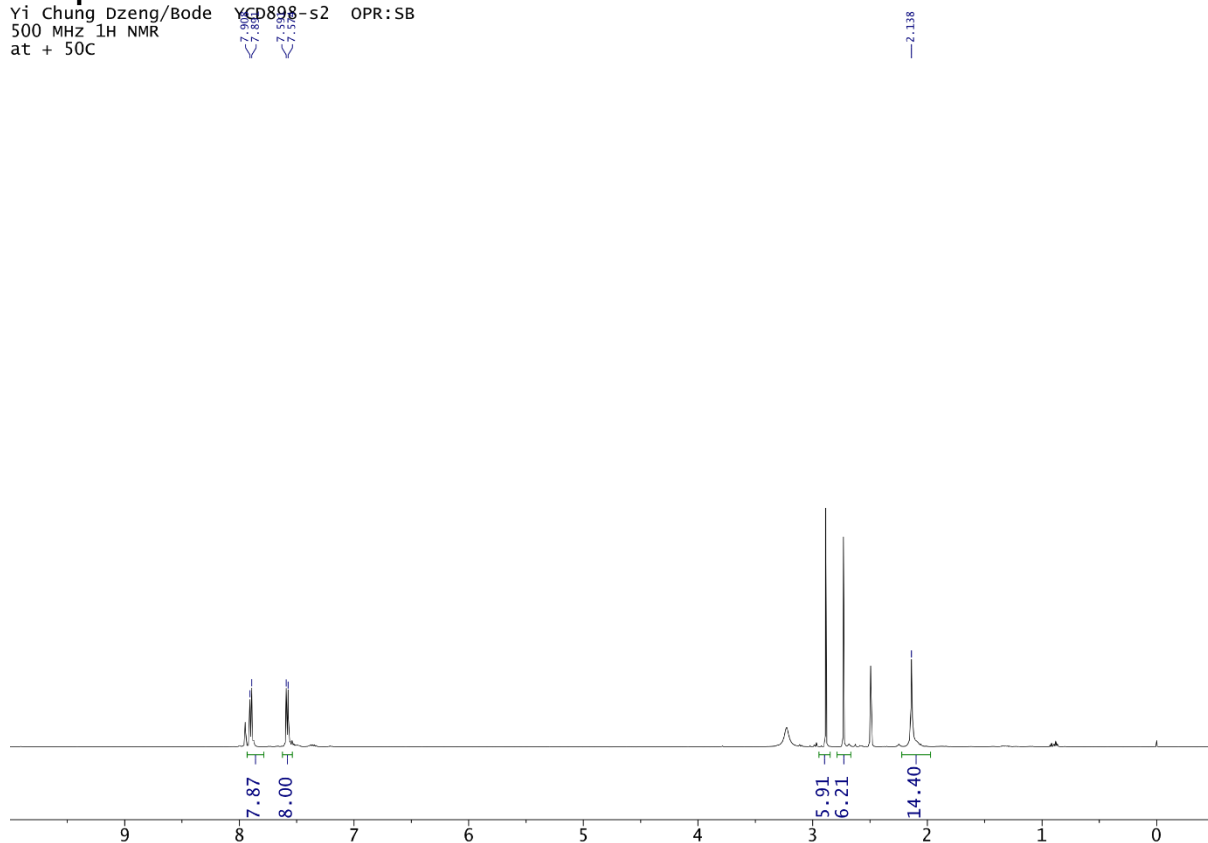
¹¹B NMR

210911-1713-25-bdzen-asc400.3.fid



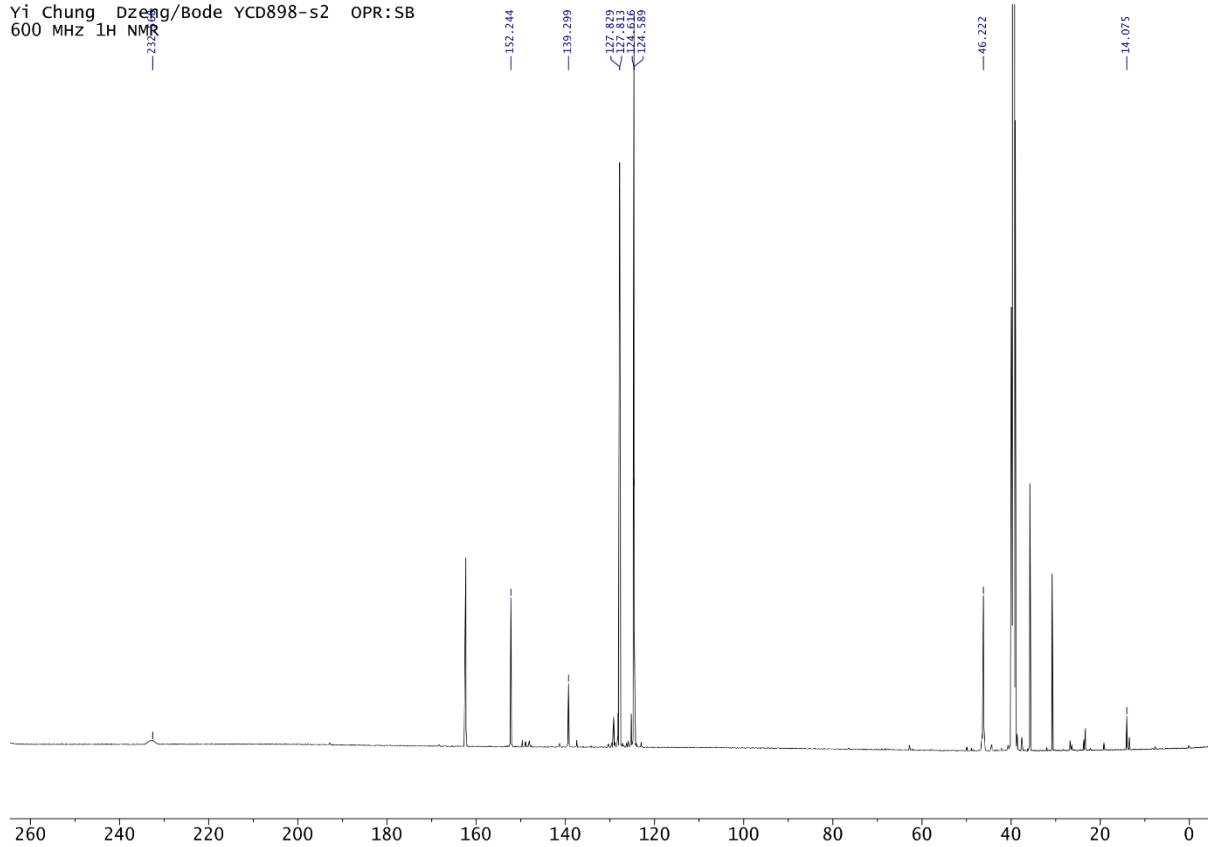
Compound 120

Yi Chung Dzeng/Bode YCD898-s2 OPR:SB
 500 MHz ¹H NMR
 at + 50C



¹³C NMR 150 MHz

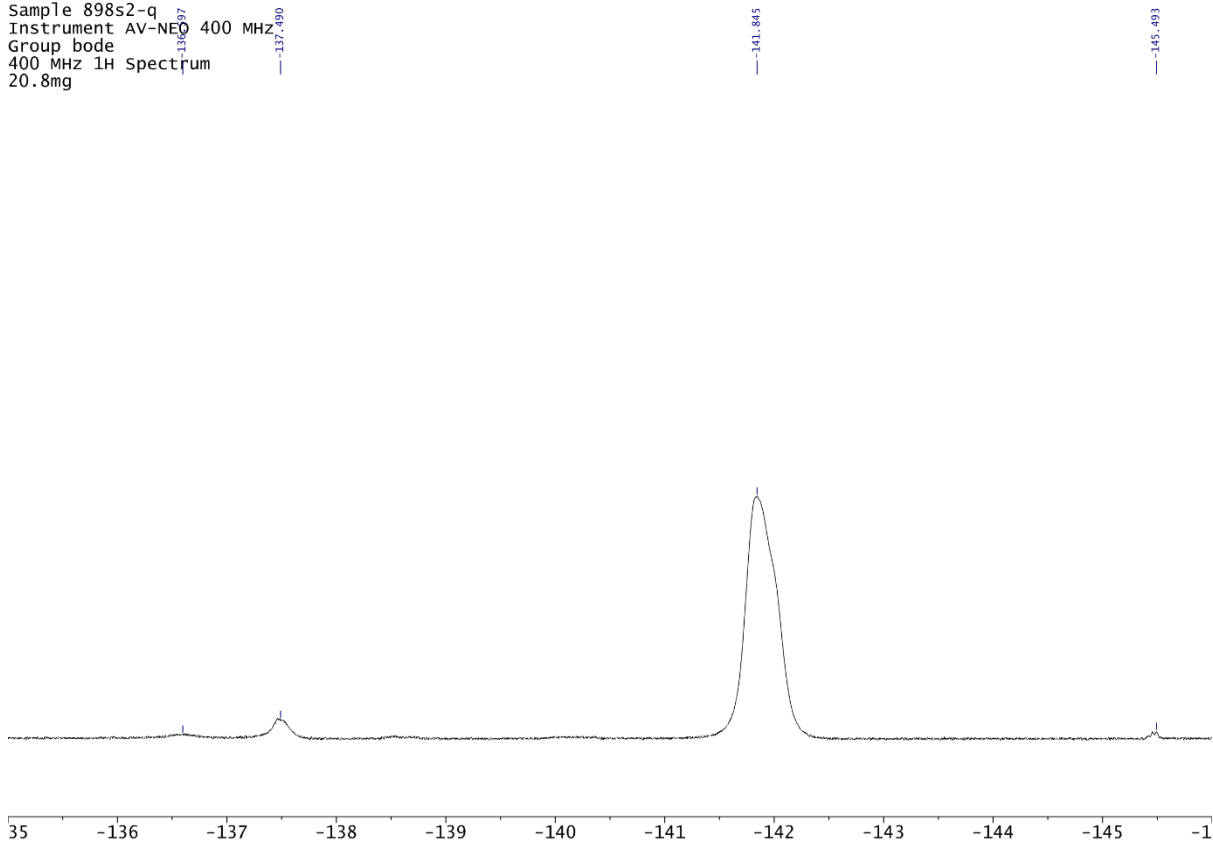
Yi Chung Dzeng/Bode YCD898-s2 OPR:SB
 600 MHz ¹H NMR



NMR Spectra

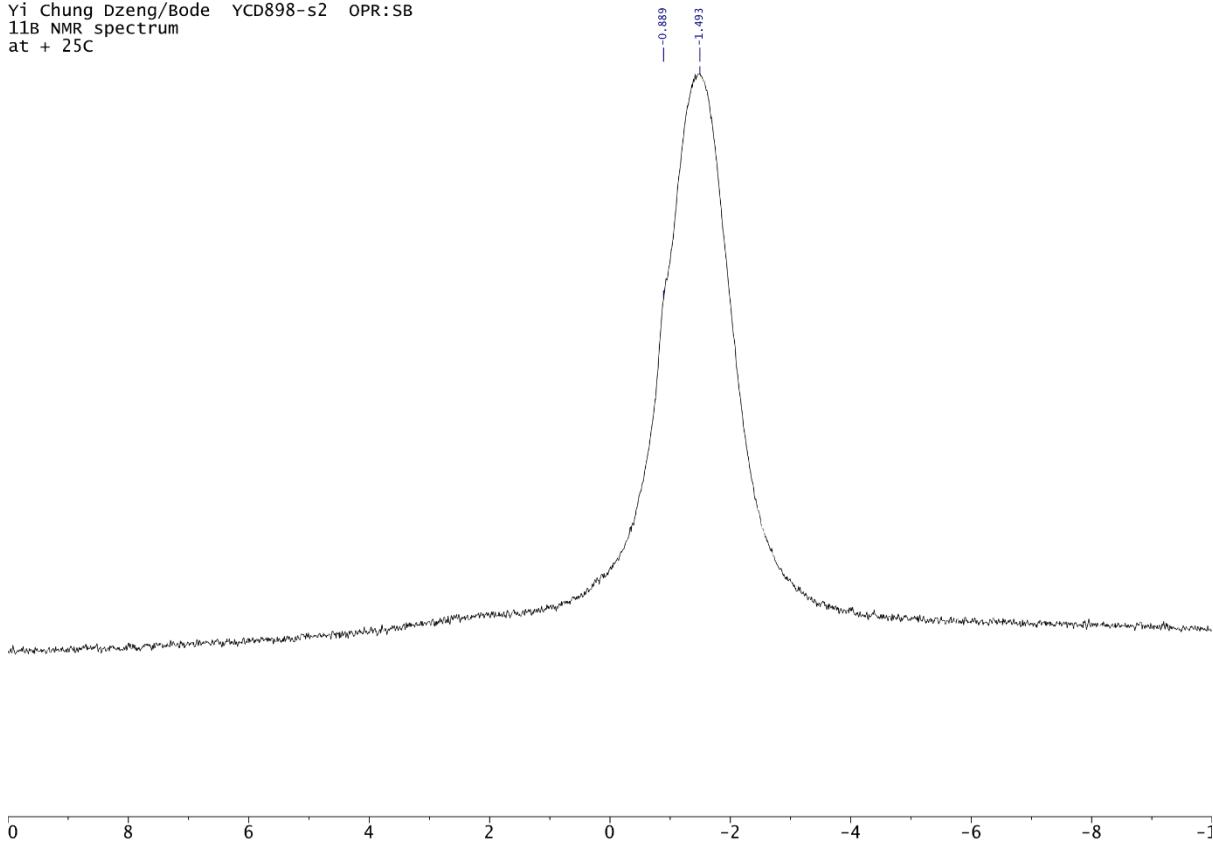
¹⁹F NMR

Sample 898s2-q
Instrument AV-NEO 400 MHz
Group bode
400 MHz 1H spectrum
20.8mg

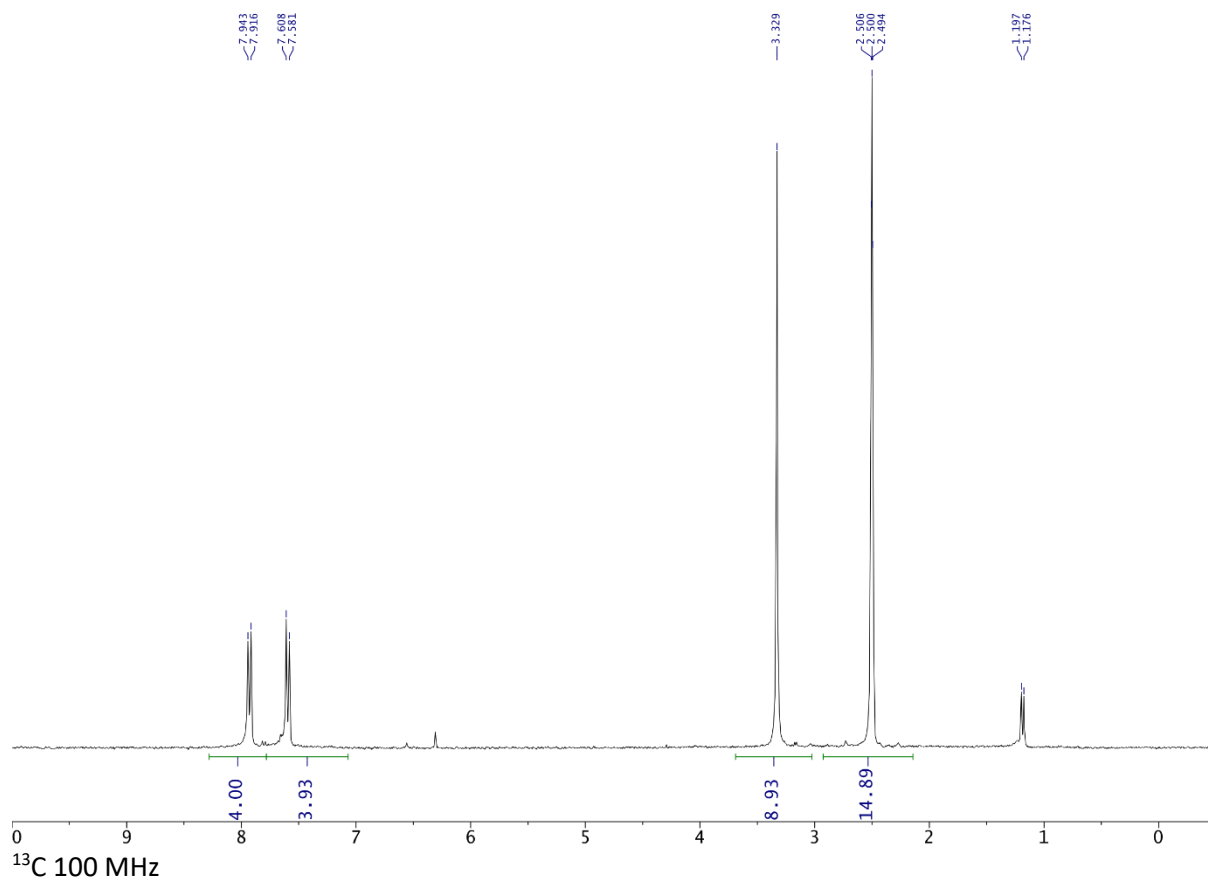


¹¹B 128 MHz

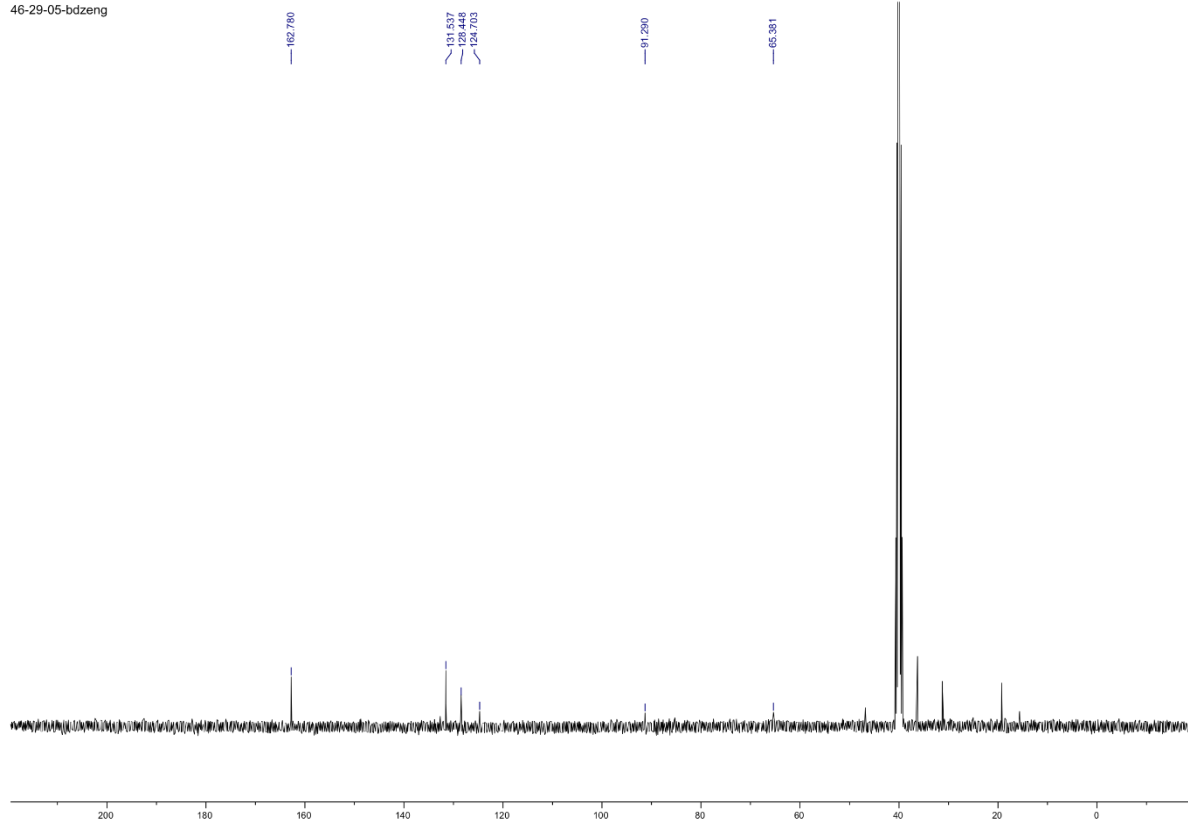
Yi Chung Dzeng/Bode YCD898-s2 OPR:SB
11B NMR spectrum
at + 25C



Compound 121

 ^1H 400 MHz ^{13}C 100 MHz

46-29-05-bdzenq



NMR Spectra

^{11}B 128 MHz

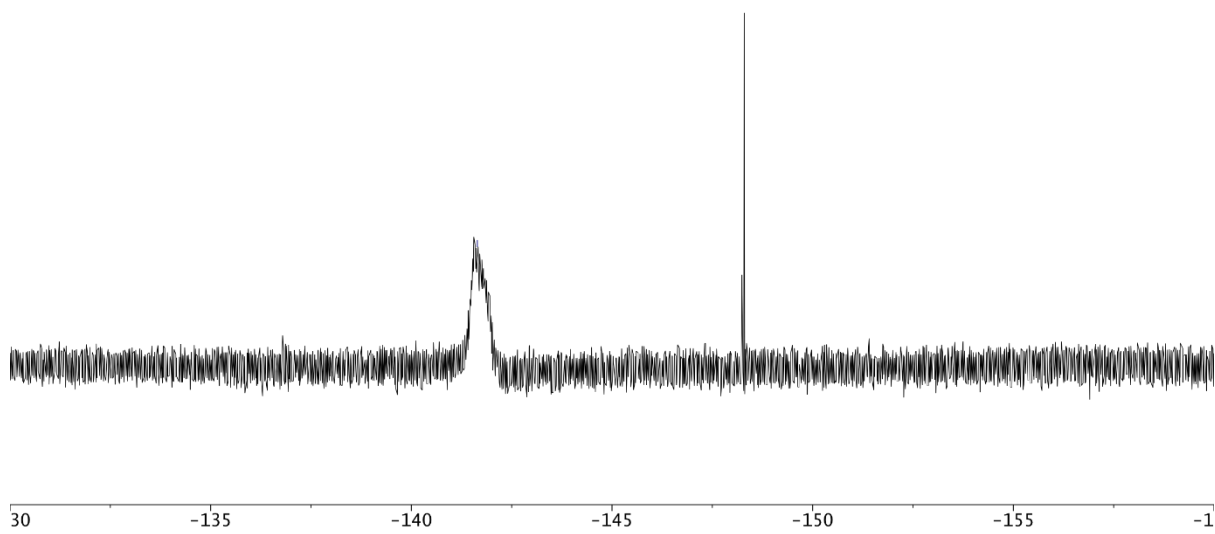
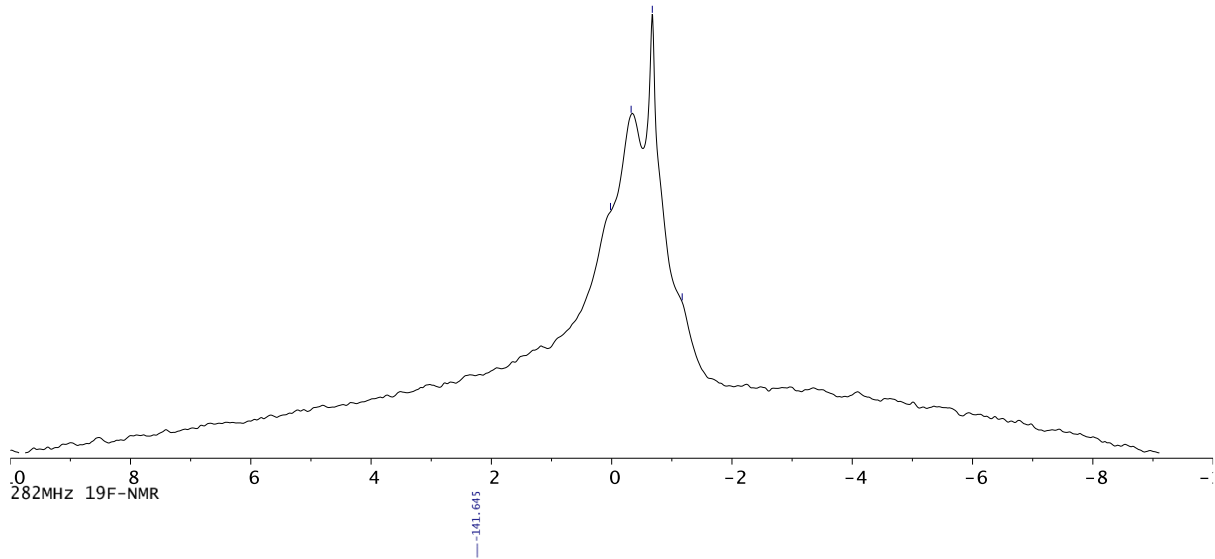
Sample 2483L1

group bode

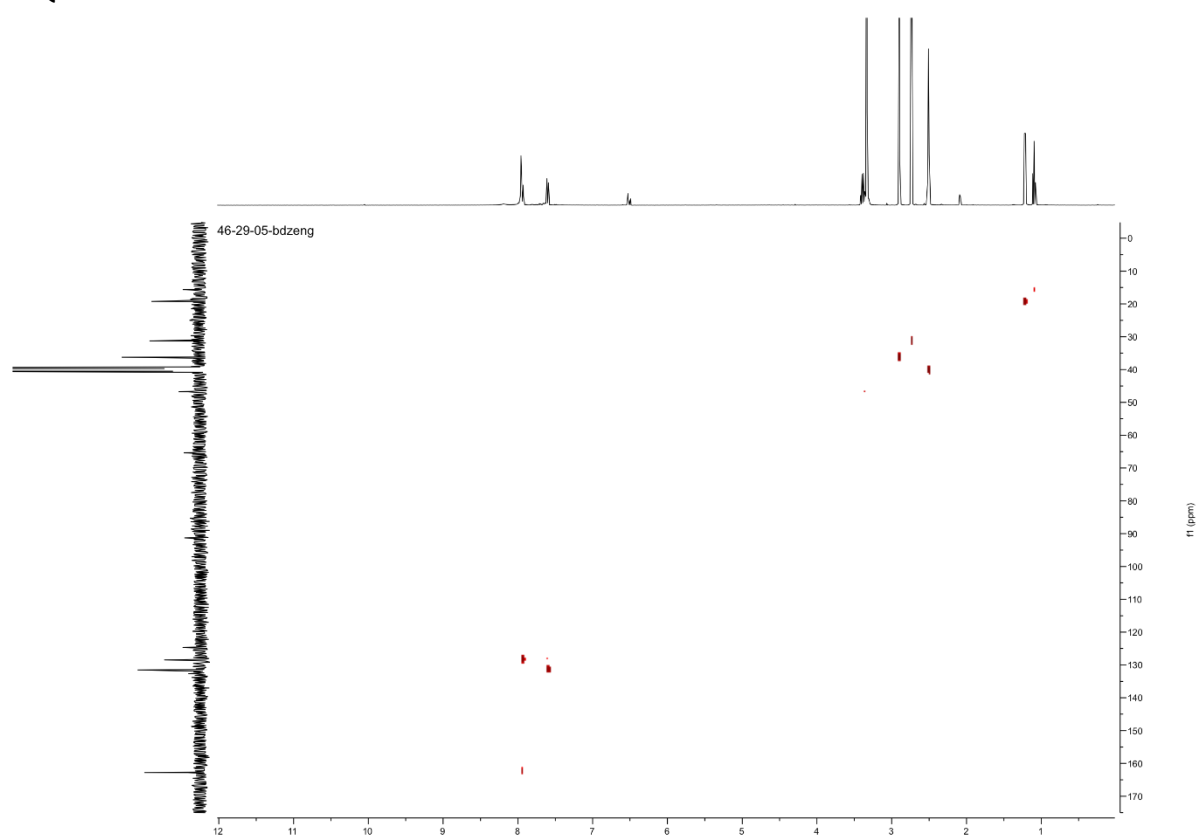
Instrument Bruker AV III 400 MHz Ultrashield (D 326)

11B.ETH DMSO /opt/v bdzeng 16

0.020
0.273
0.676
-1.173



HSQC 400 MHz



NMR Spectra

Compound 122

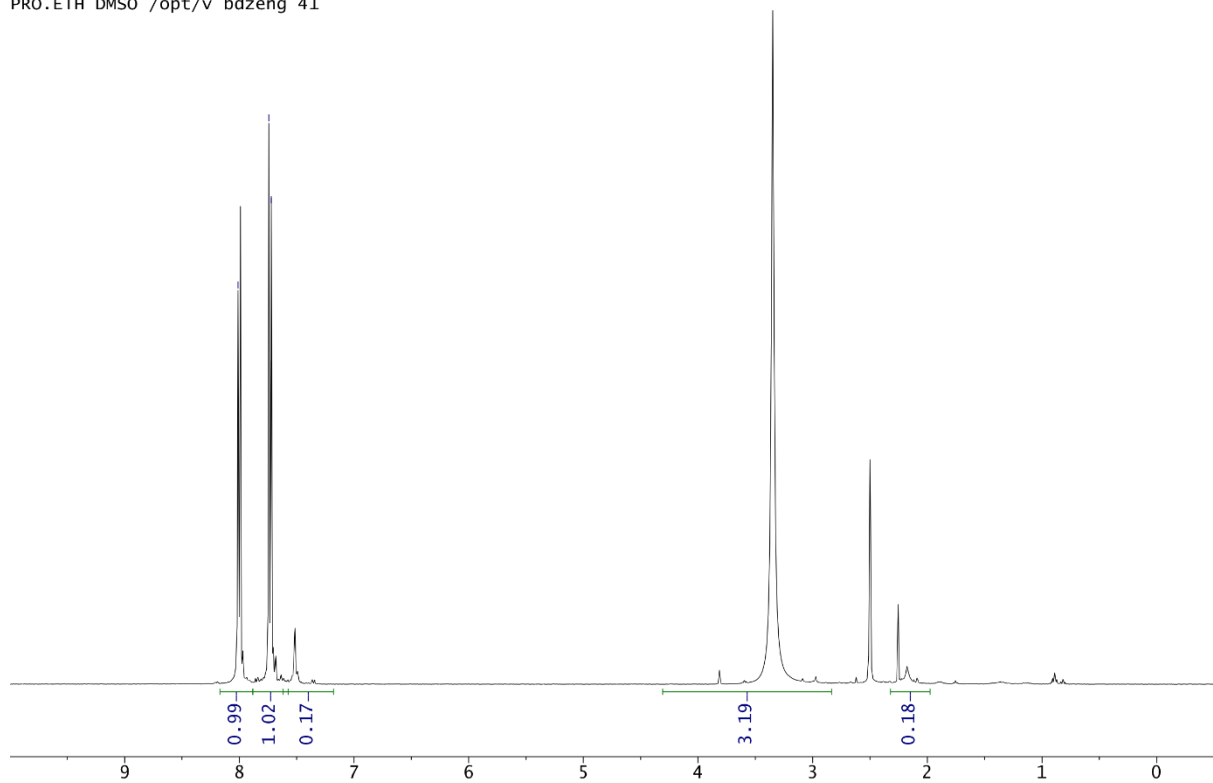
¹H 400 MHz

Sample 1k87-qc

group bode

Instrument Bruker AV III 400 MHz Ultrashield (D 326)

PRO.ETH DMSO /opt/v bdzeng 41



¹³C 100 MHz

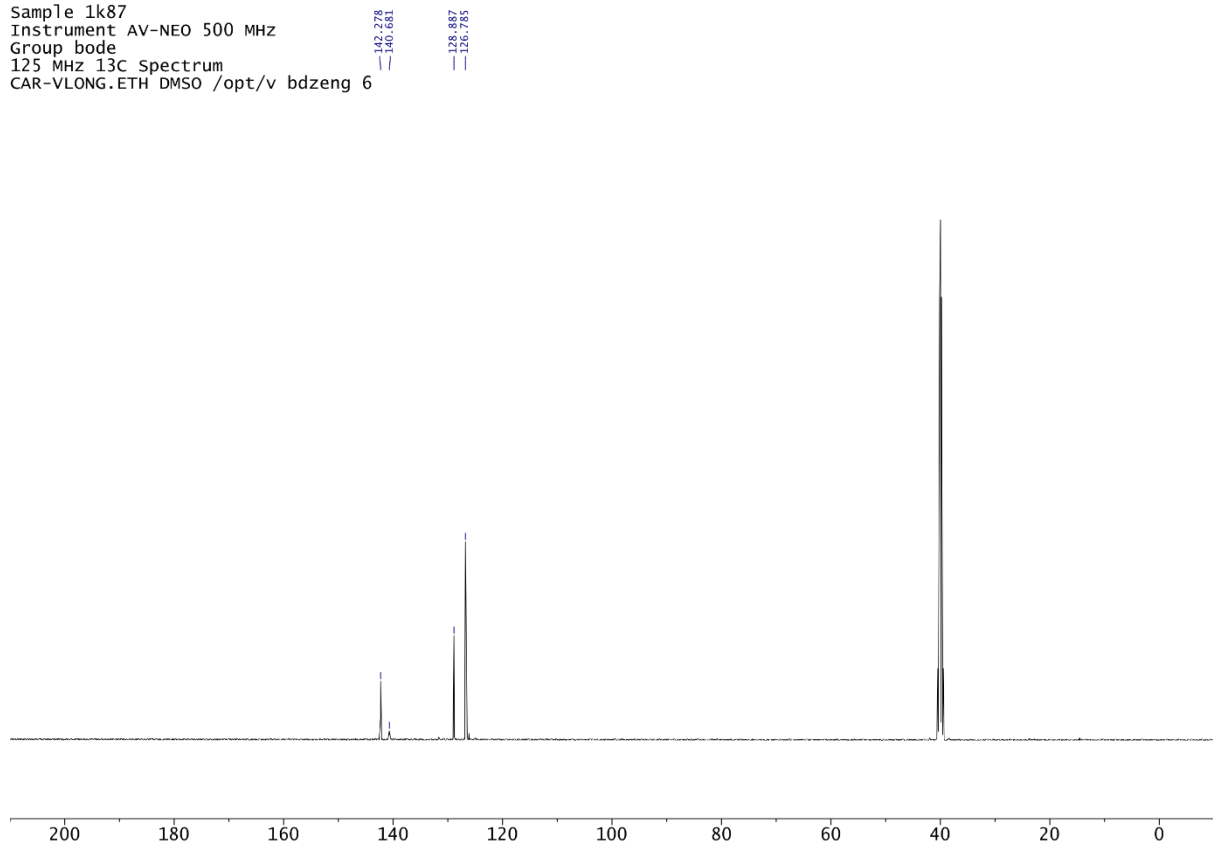
Sample 1k87

Instrument AV-NEO 500 MHz

Group bode

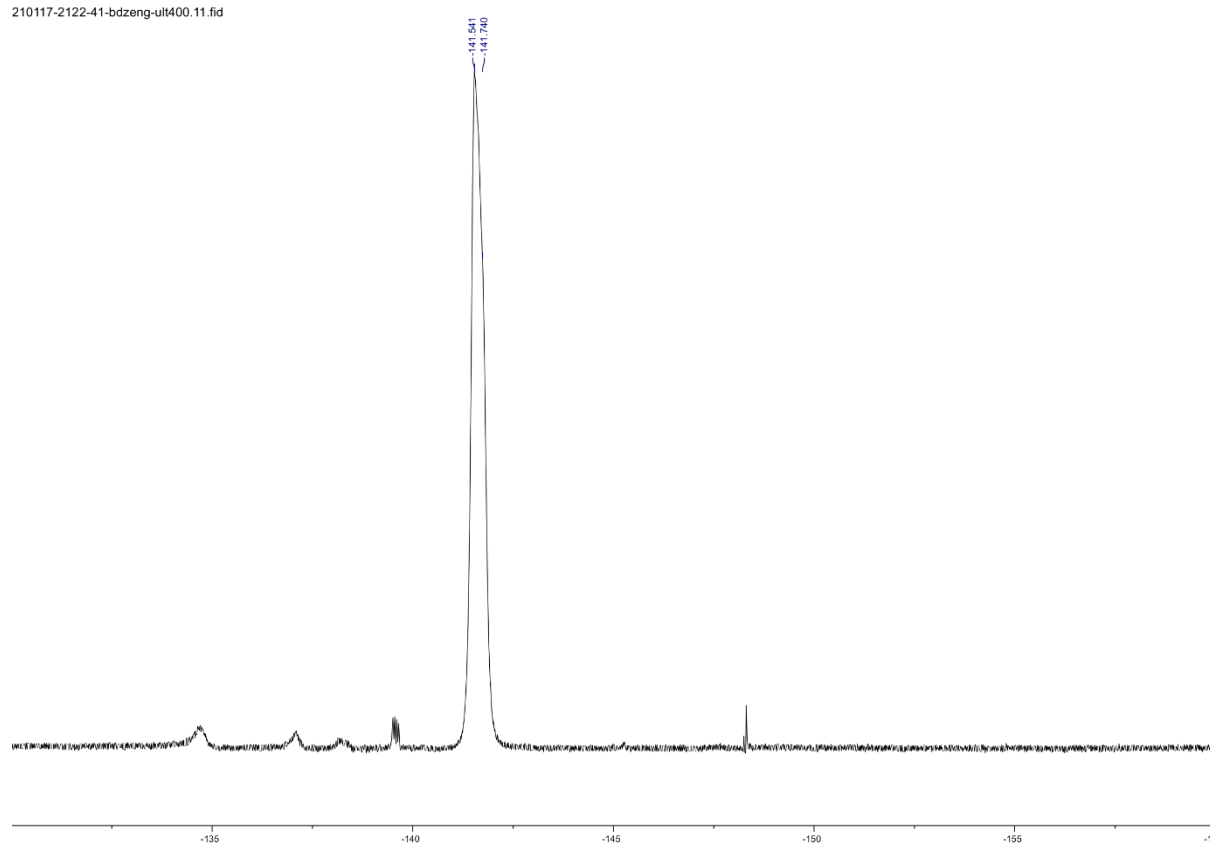
125 MHz ¹³C Spectrum

CAR-VLONG.ETH DMSO /opt/v bdzeng 6

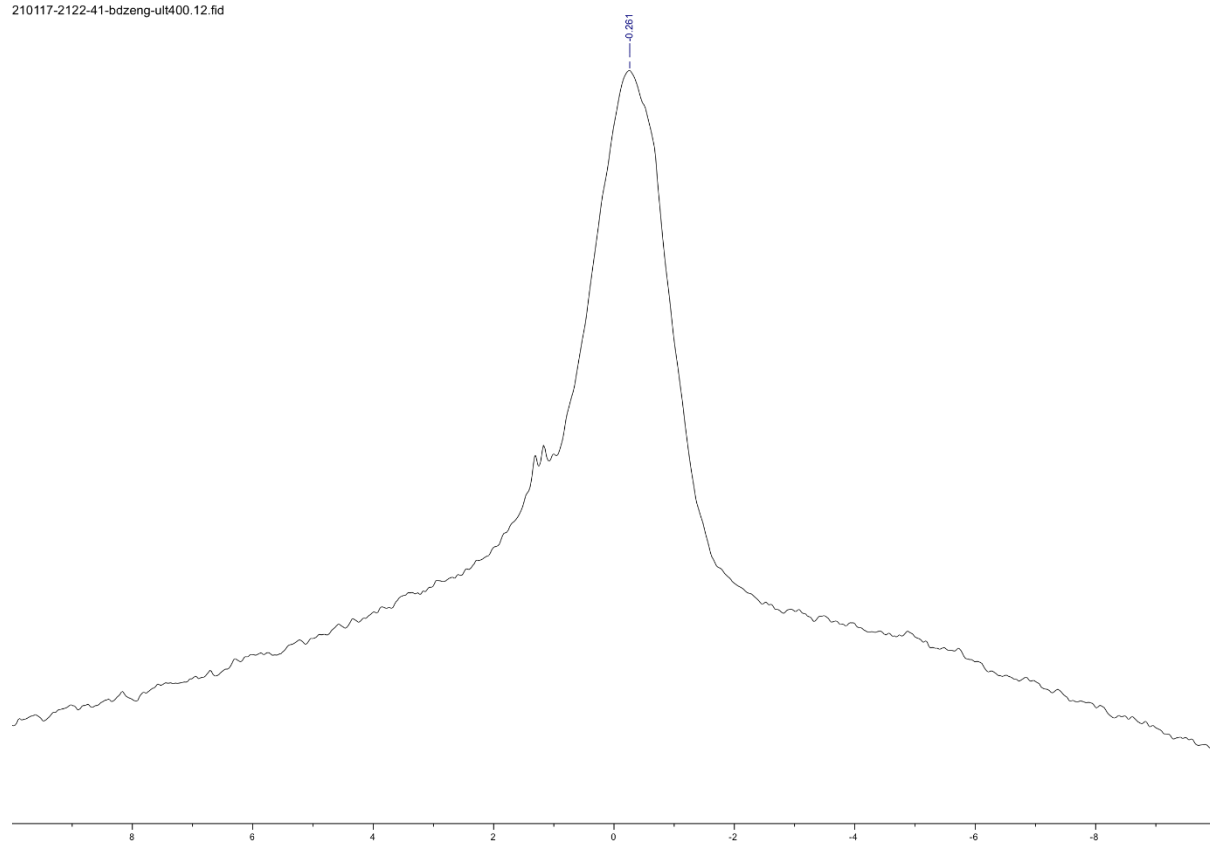


^{19}F 376 MHz

210117-2122-41-bdzeng-ult400.11.fid

 ^{11}B 128 MHz

210117-2122-41-bdzeng-ult400.12.fid



NMR Spectra

Compound 123-Boc4

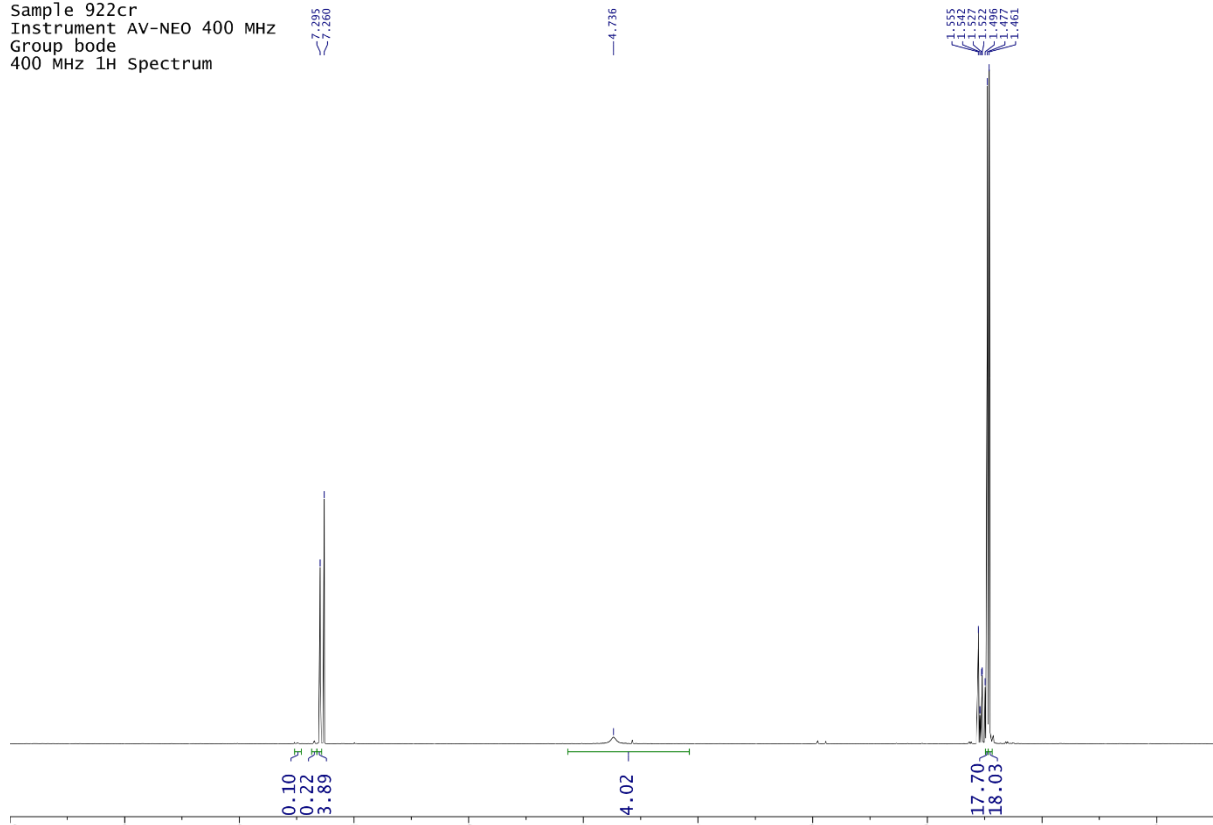
^1H 400 MHz

Sample 922cr

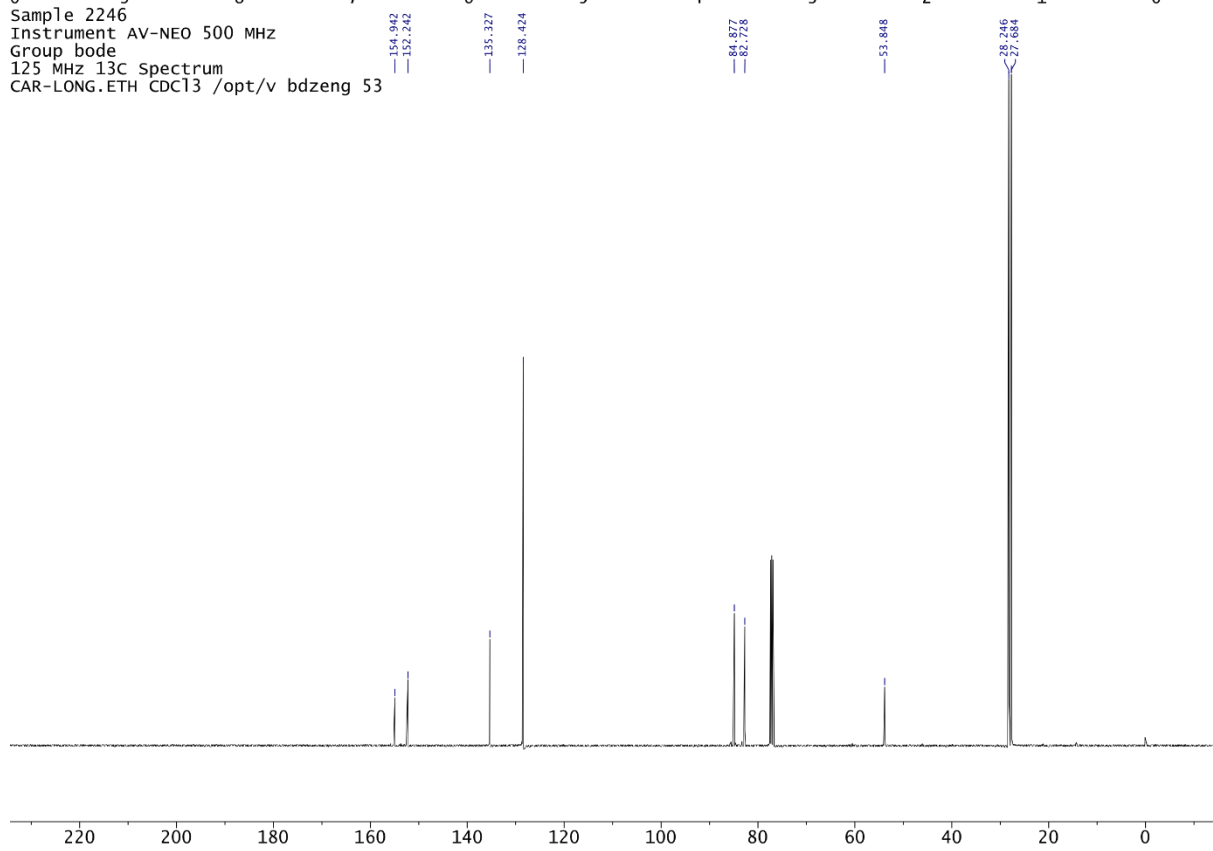
Instrument AV-NEO 400 MHz

Group bode

400 MHz ^1H Spectrum

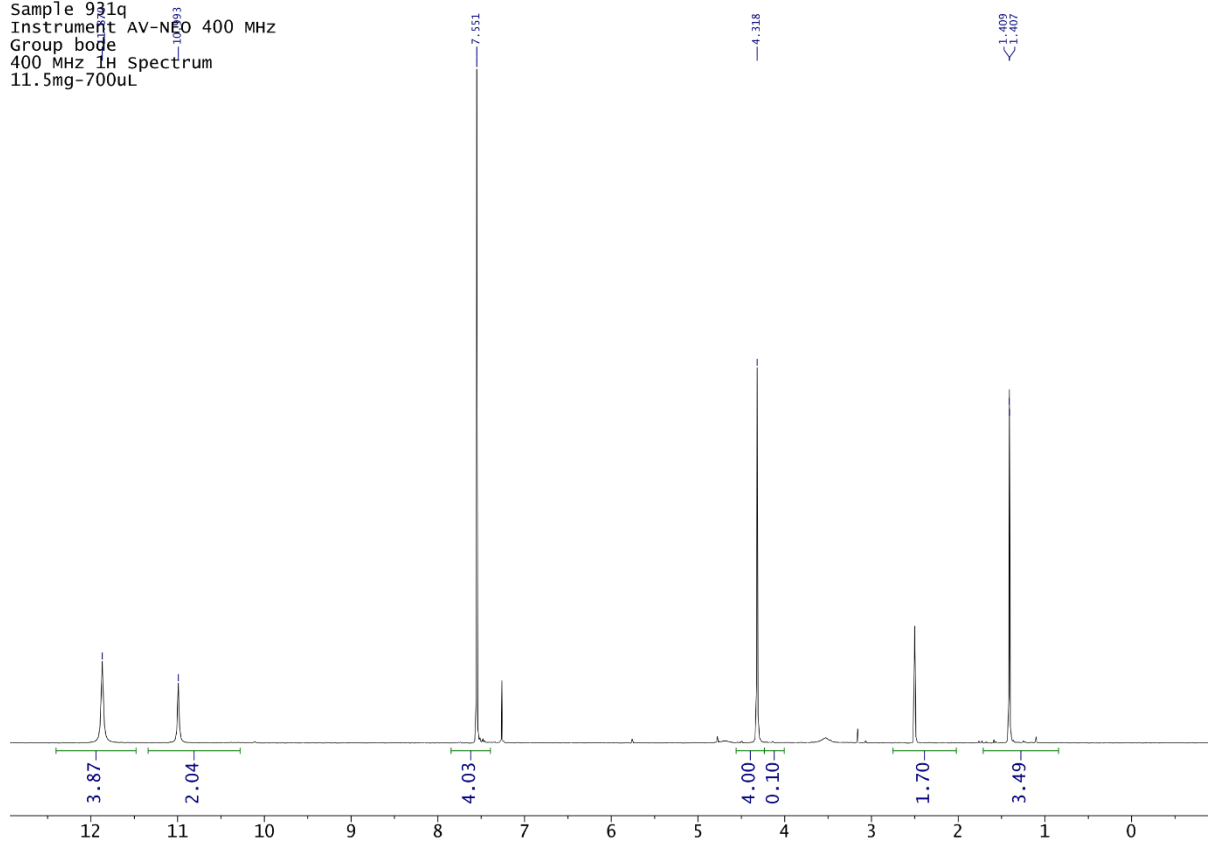


Sample 2246
Instrument AV-NEO 500 MHz
Group bode
125 MHz ^{13}C Spectrum
CAR-LONG.ETH CDCl₃ /opt/v bdzeng 53

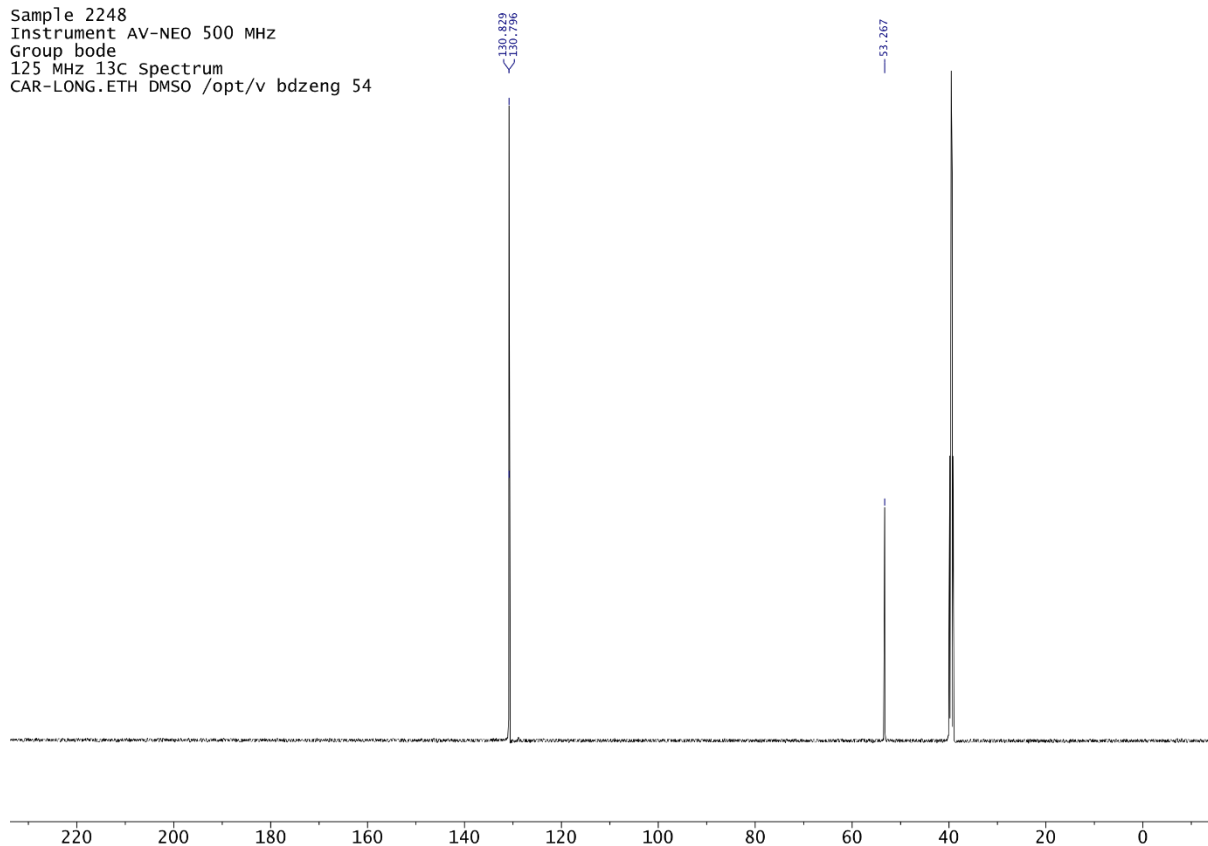


Compound 123

¹H 400 MHz
 Sample 931q
 Instrument AV-NEO 400 MHz
 Group bode
 400 MHz 1H spectrum
 11.5mg-700uL



Sample 2248
 Instrument AV-NEO 500 MHz
 Group bode
 125 MHz ¹³C spectrum
 CAR-LONG.ETH DMSO /opt/v bdzeng 54

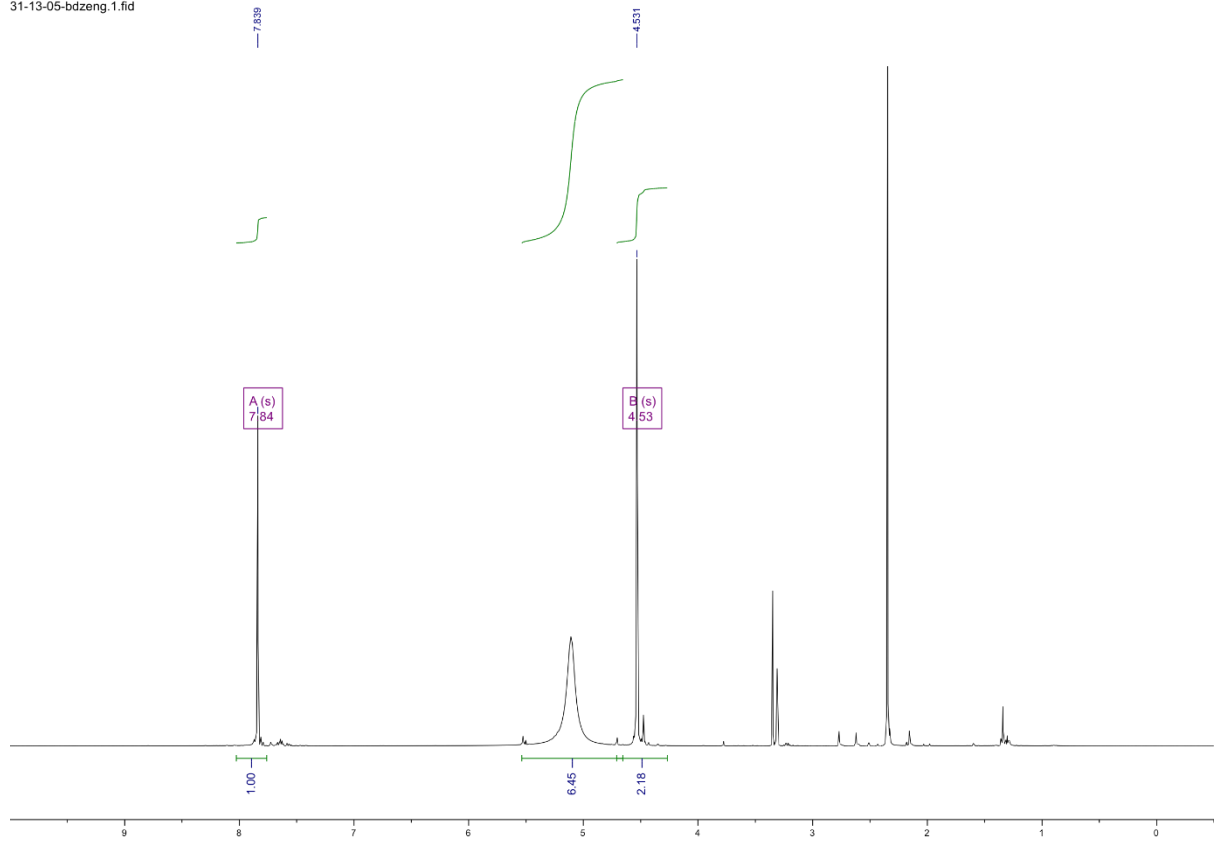


NMR Spectra

Compound 124

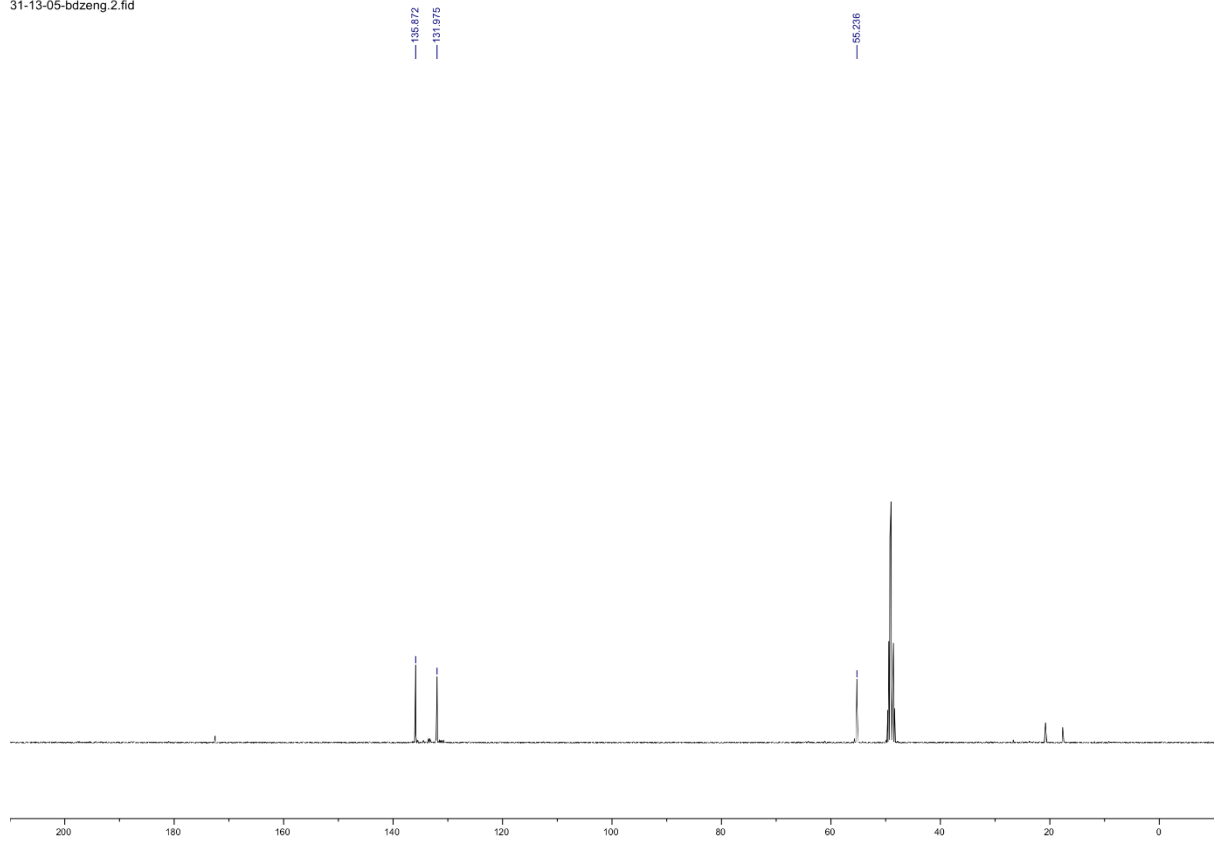
^1H 400 MHz

31-13-05-bdzeng.1.fid

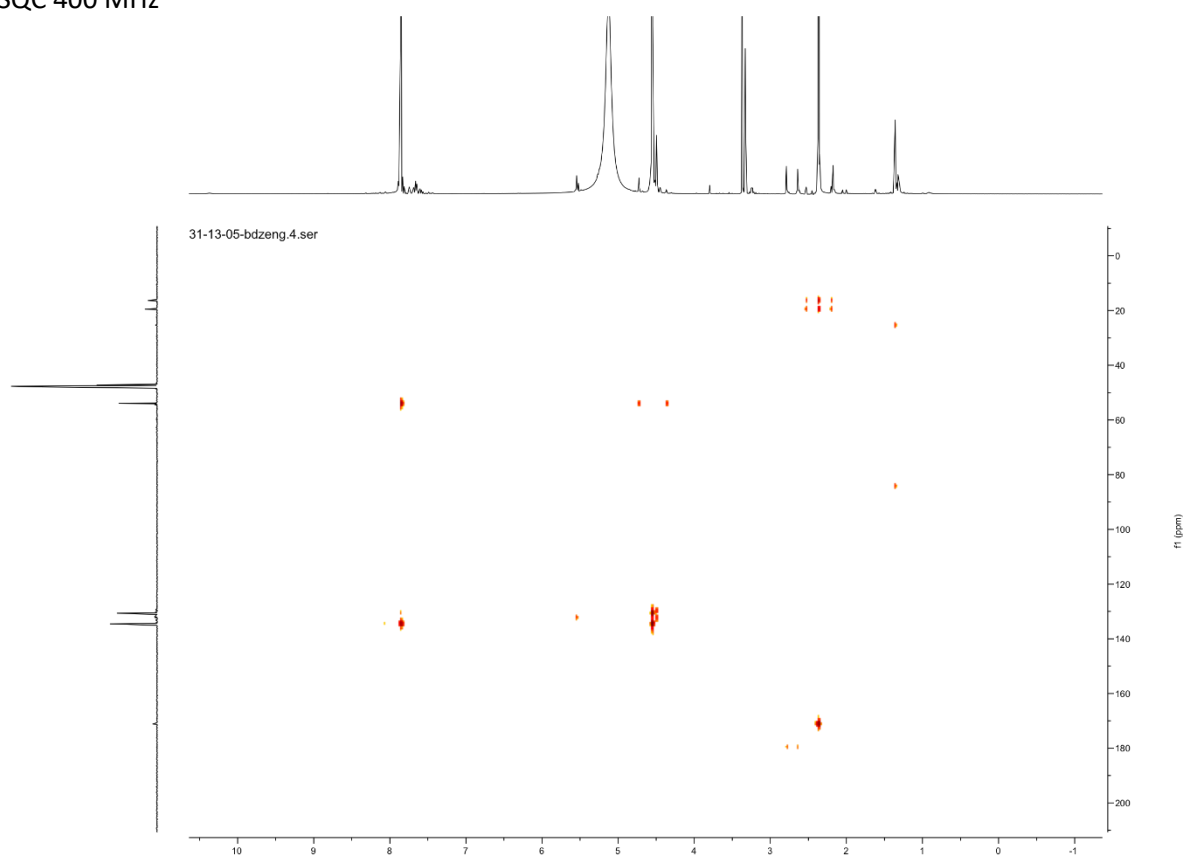


^{13}C 100 MHz

31-13-05-bdzeng.2.fid



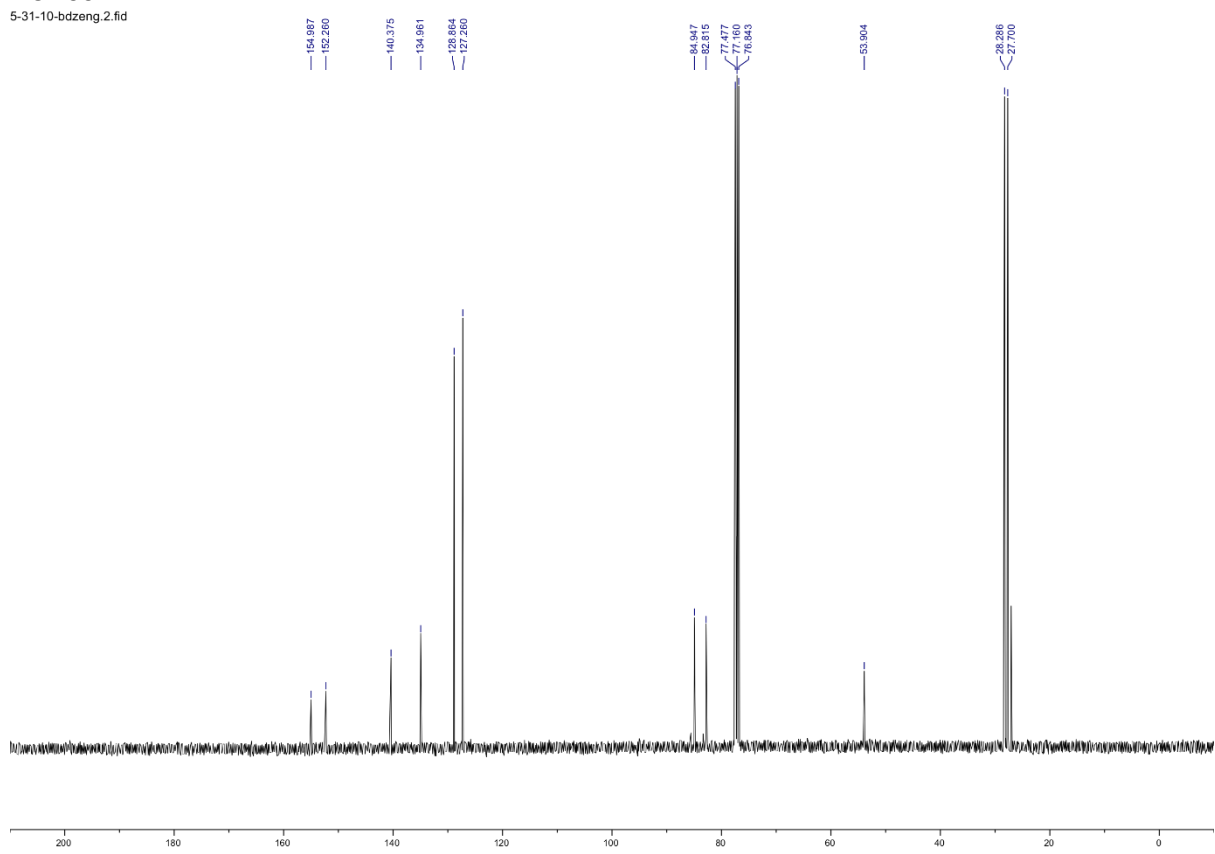
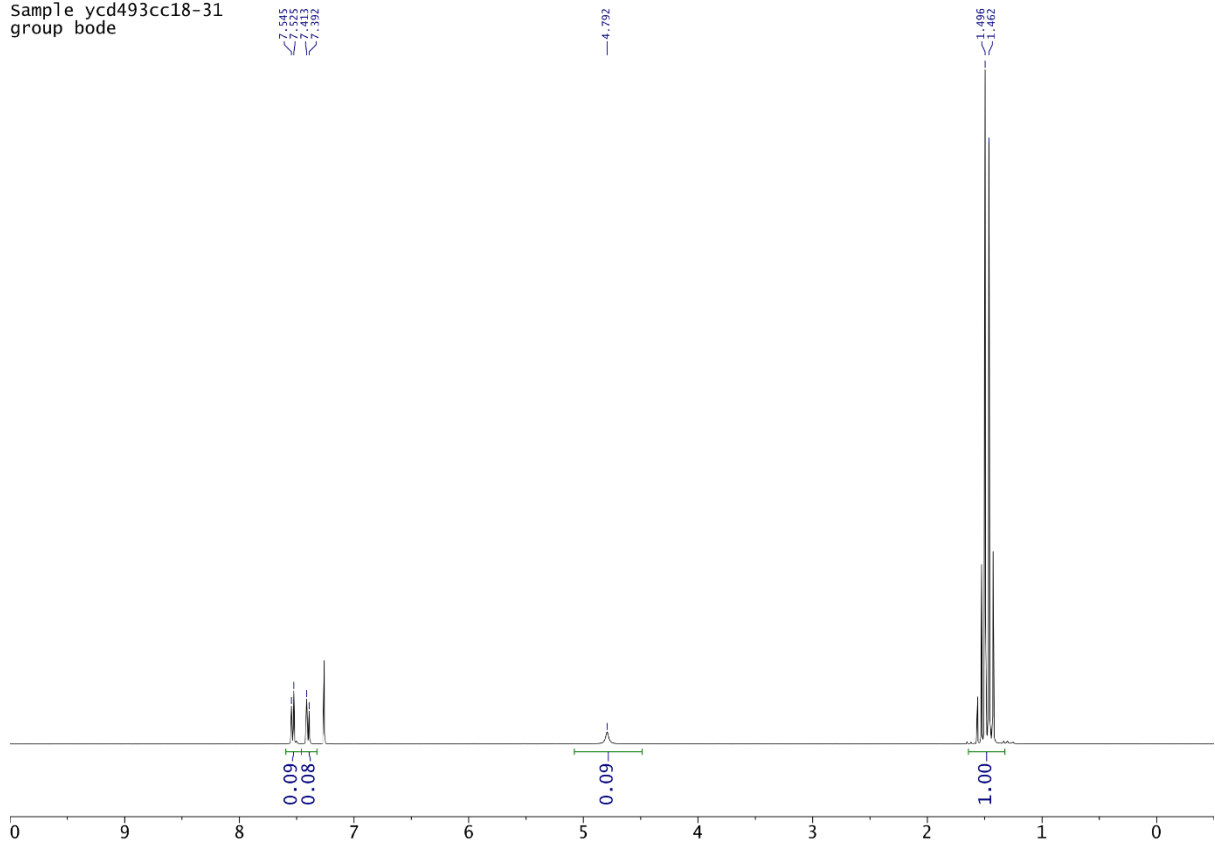
HSQC 400 MHz



NMR Spectra

Compound 125-Boc₄

¹H 400 MHz
sample ycd493cc18-31
group bode



Compound 125 ^1H 400 MHz

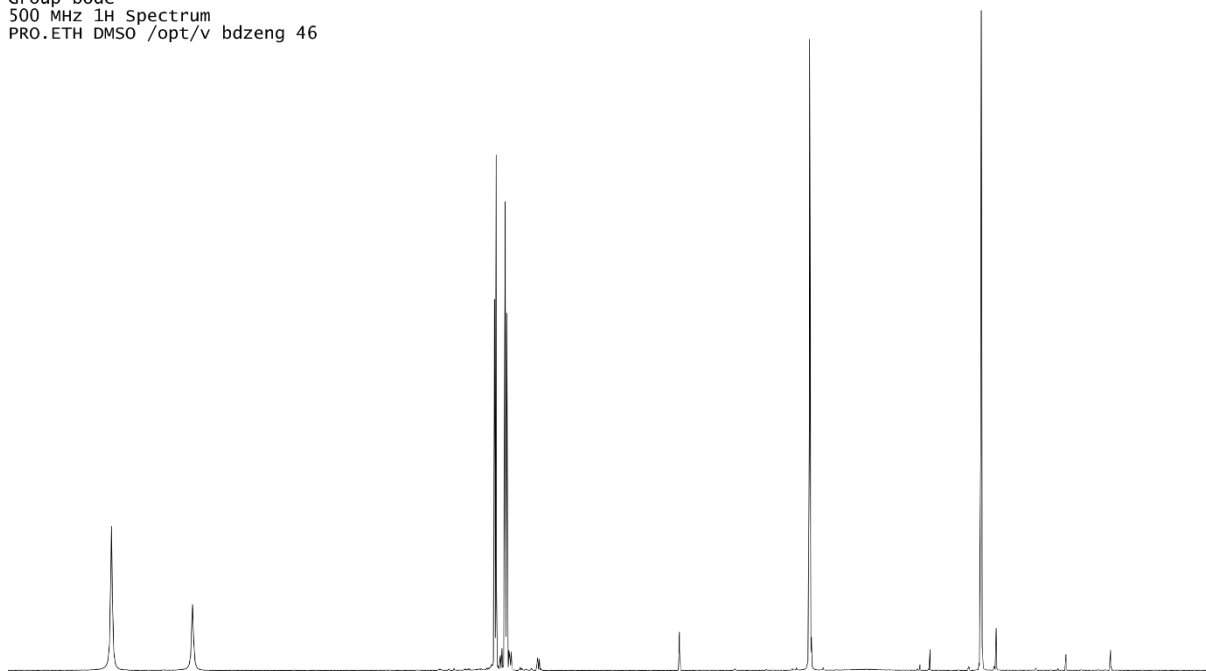
Sample 1621-s1

Instrument AV-NEO 500 MHz

Group bode

500 MHz ^1H Spectrum

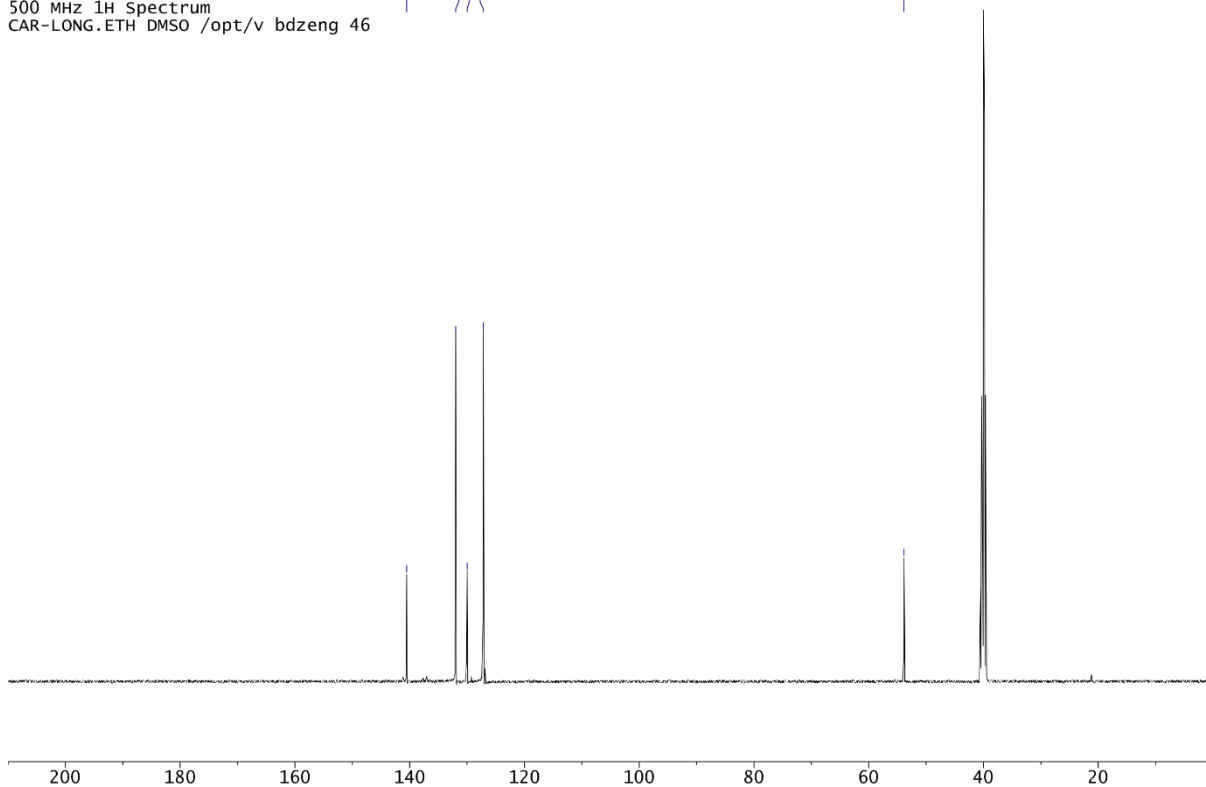
PRO.ETH DMSO /opt/v bdzeng 46



3 12 11 10 9 8 7 6 5 4 3 2 1 0

Sample 1621-s1
Instrument AV-NEO 500 MHz
Group bode
500 MHz ^1H Spectrum
CAR-LONG.ETH DMSO /opt/v bdzeng 46

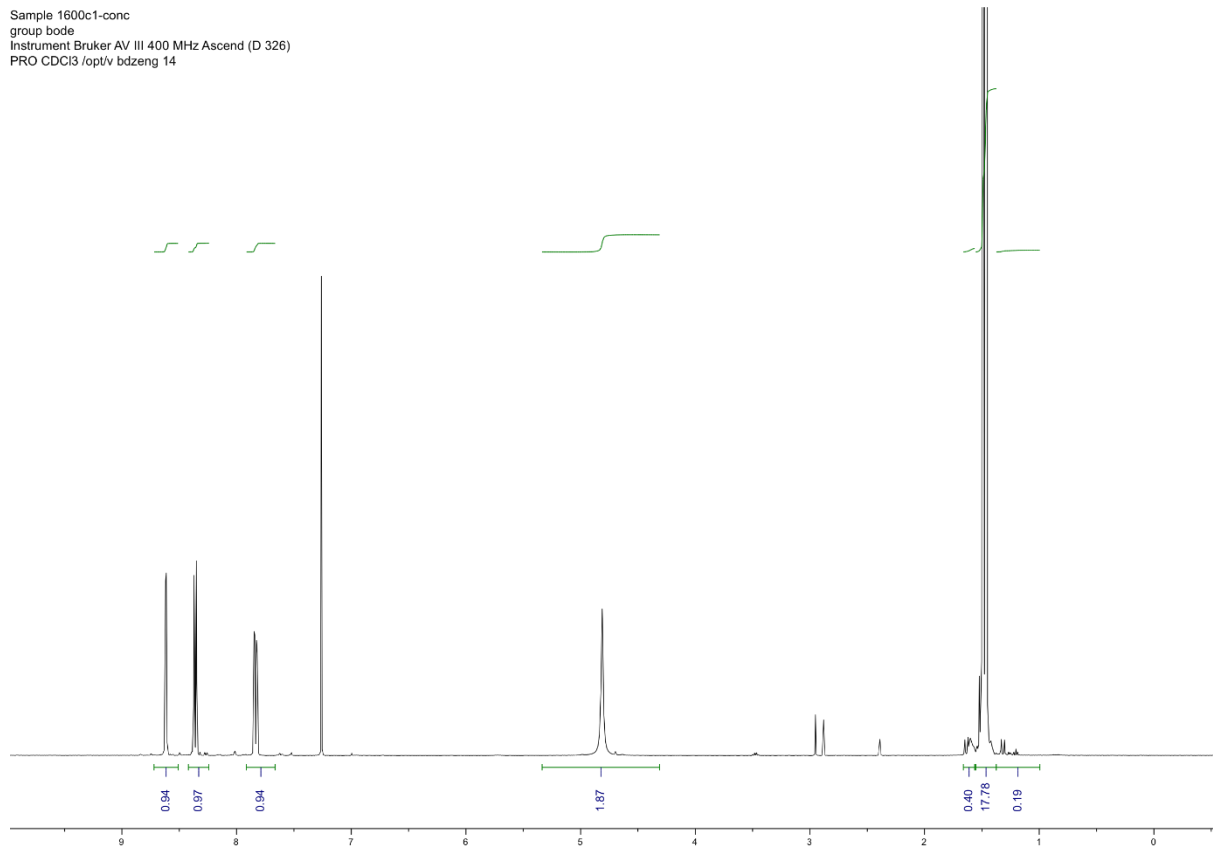
140.514
131.981
127.184
53.836



Compound 126-Boc₄

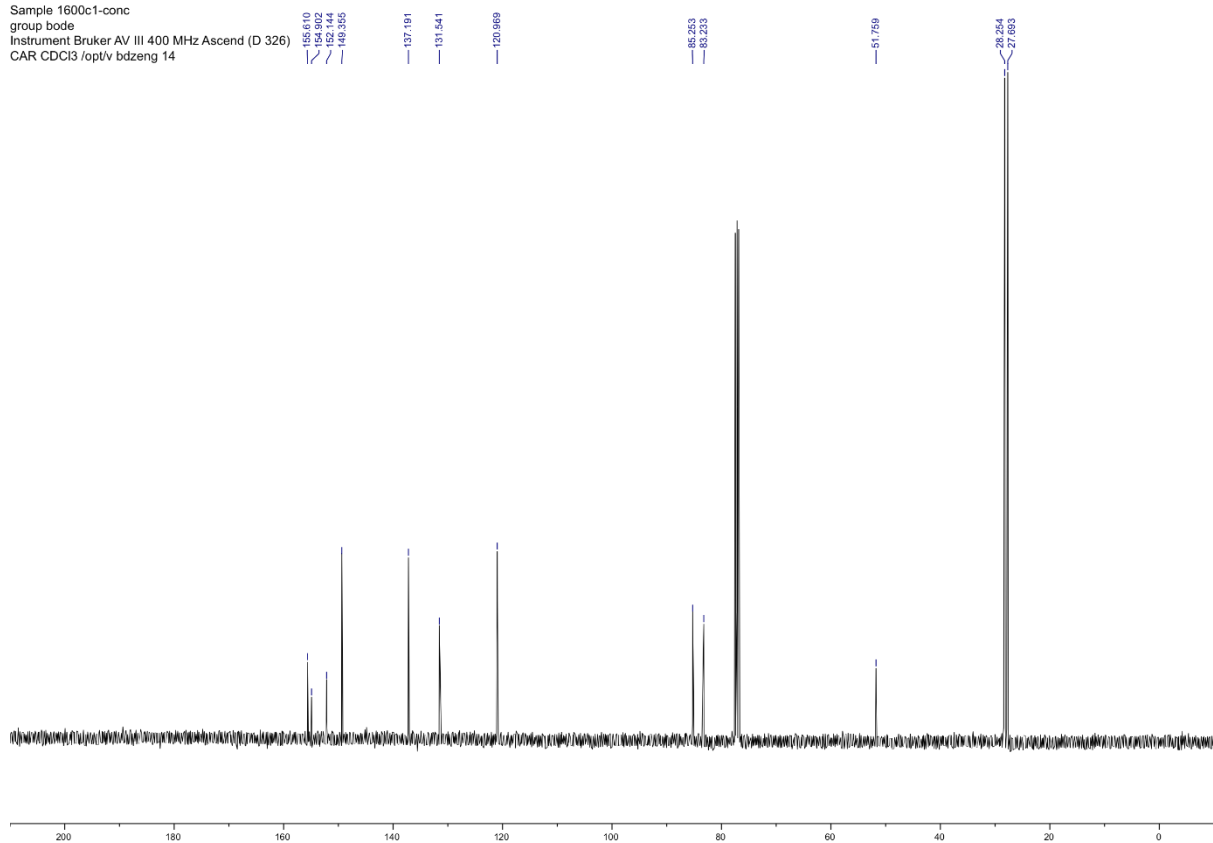
¹H 400 MHz

Sample 1600c1-conc
 group bode
 Instrument Bruker AV III 400 MHz Ascend (D 326)
 PRO CDCl₃ /opt/v bdzeng 14



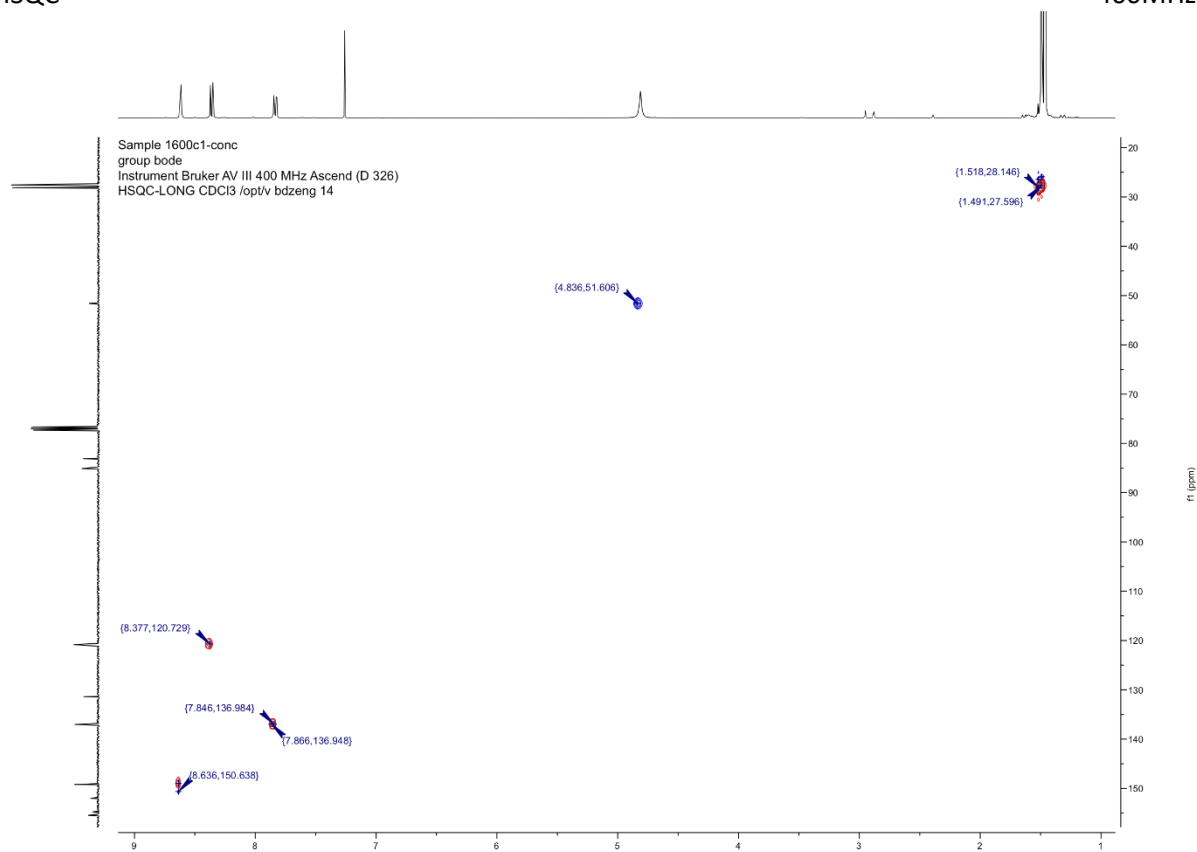
¹³C 100 MHz

Sample 1600c1-conc
 group bode
 Instrument Bruker AV III 400 MHz Ascend (D 326)
 CAR CDCl₃ /opt/v bdzeng 14

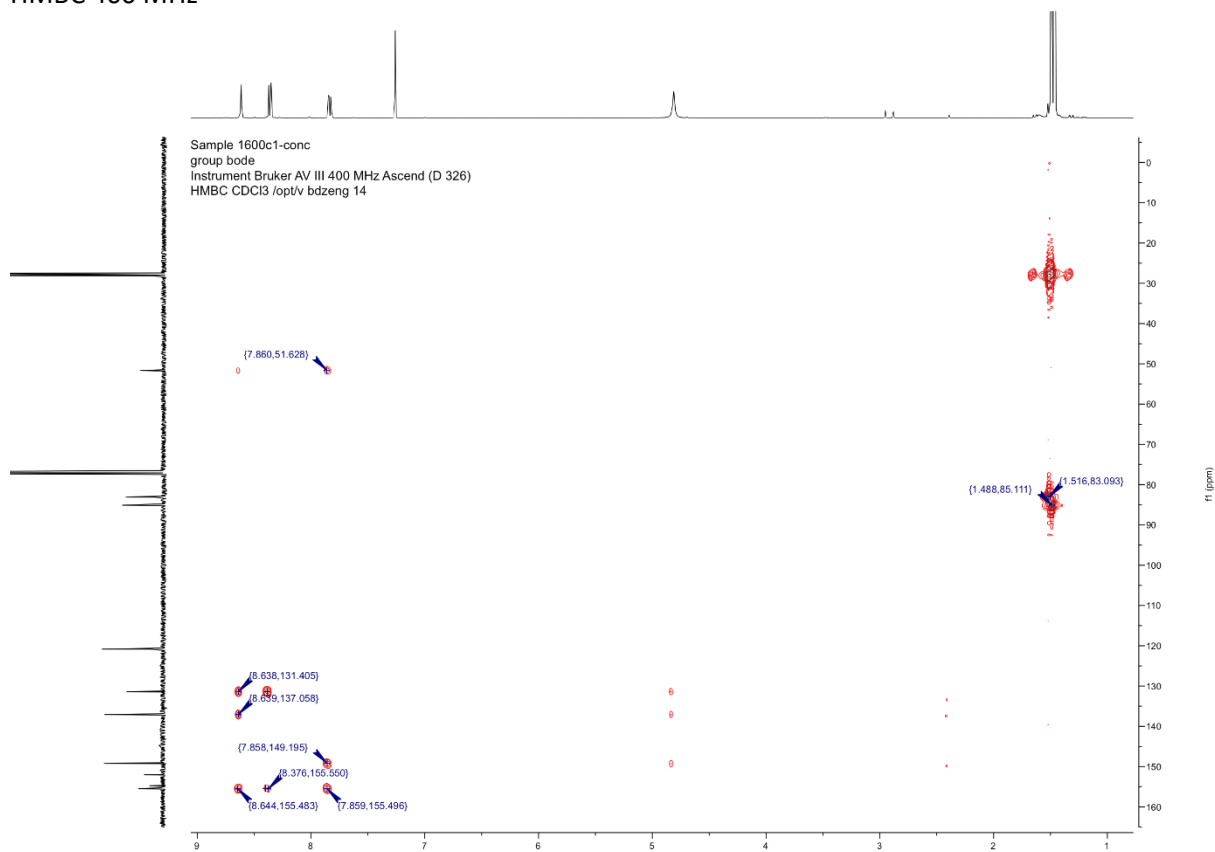


HSQC

400MHz



HMBC 400 MHz



NMR Spectra

Compound 126

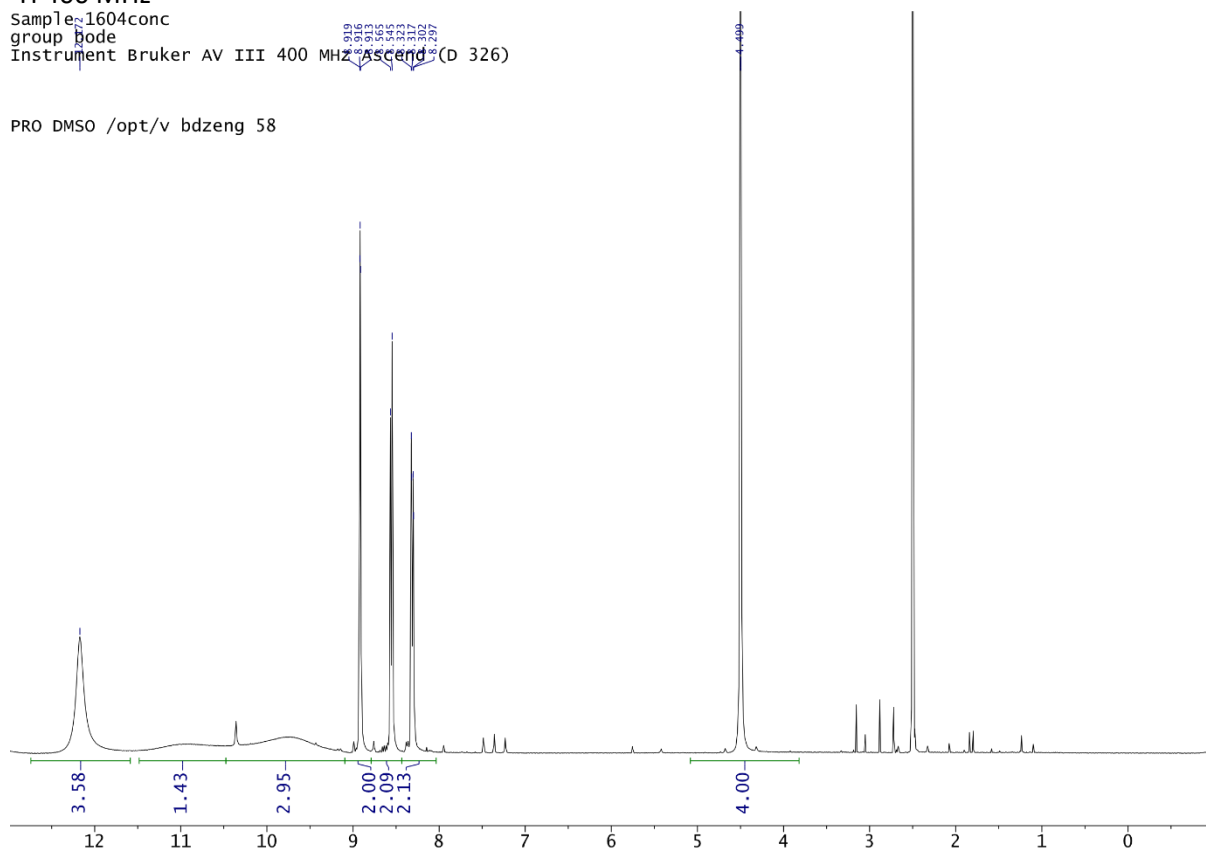
^1H 400 MHz

Sample 1604conc

group bode

Instrument Bruker AV III 400 MHz Ascend (D 326)

PRO DMSO /opt/v bdzeng 58



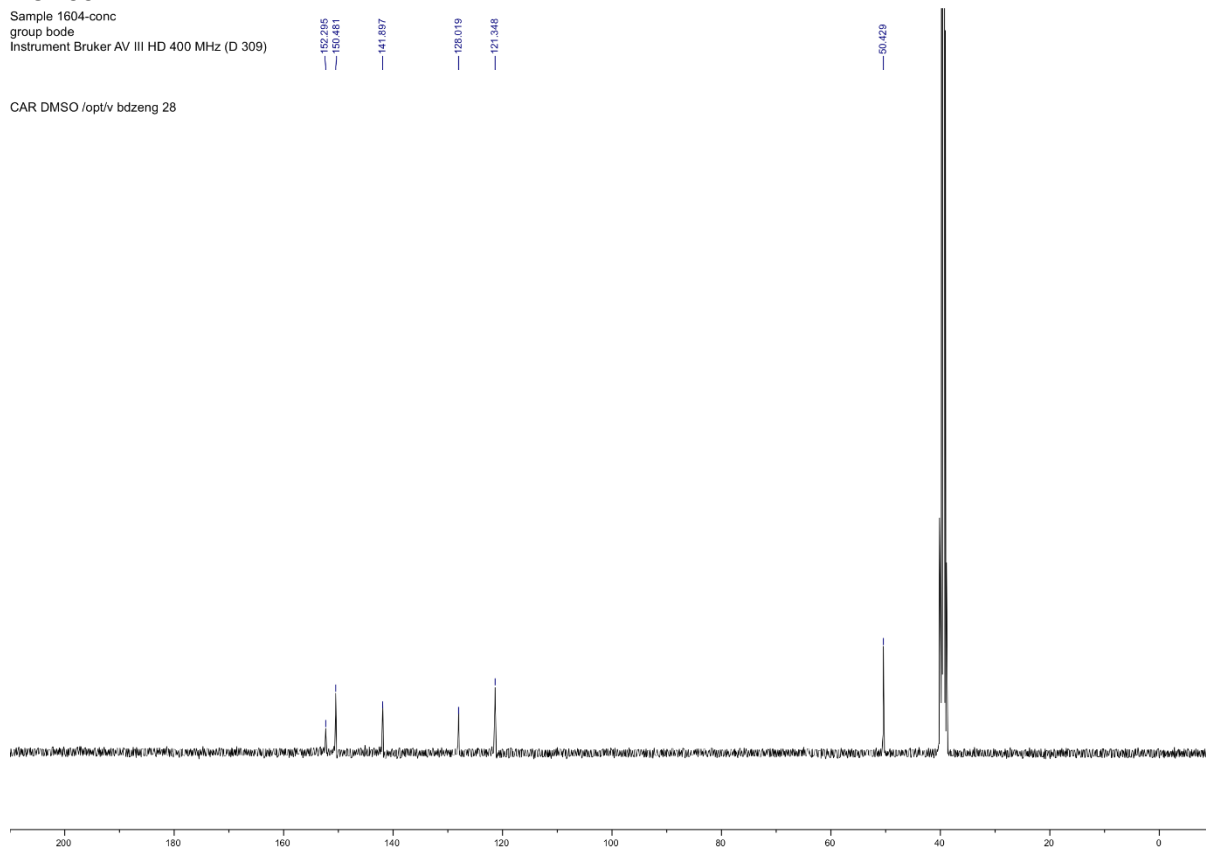
^{13}C 100 MHz

Sample 1604-conc

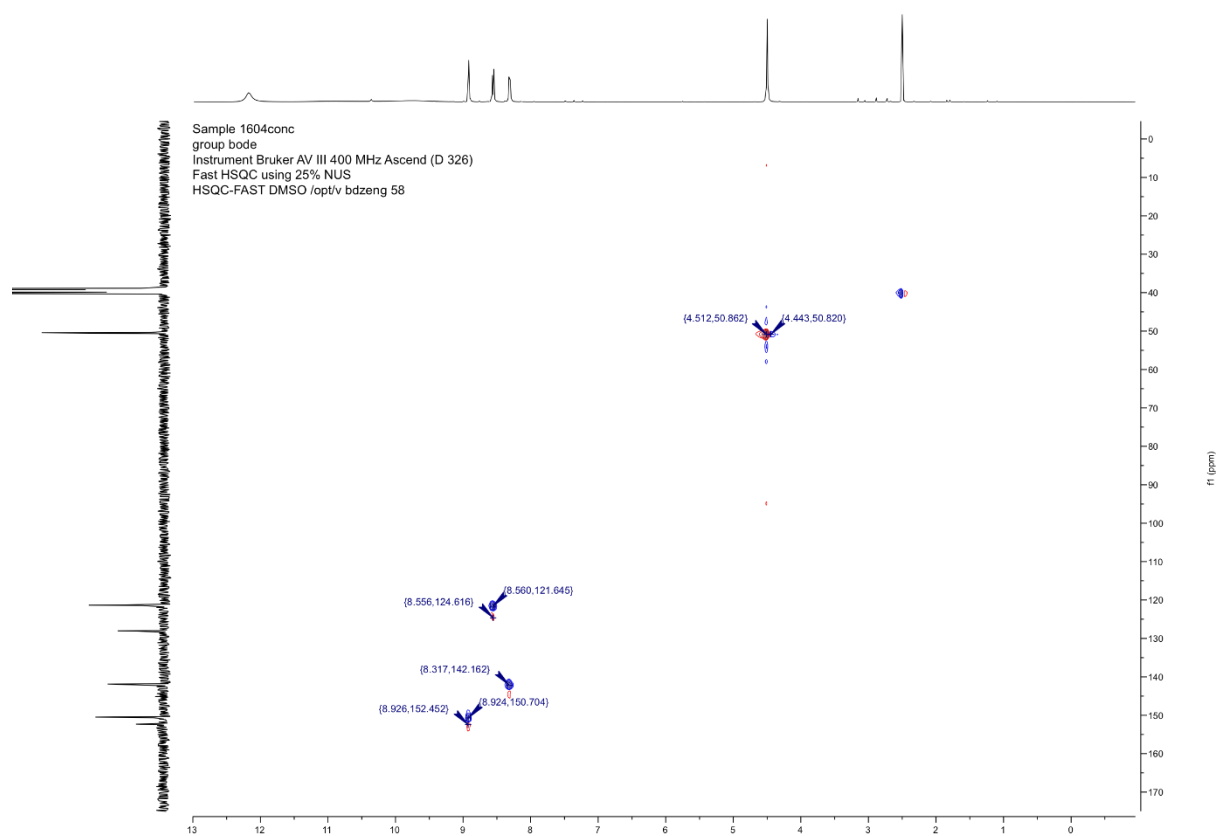
group bode

Instrument Bruker AV III HD 400 MHz (D 309)

CAR DMSO /opt/v bdzeng 28



HSQC 400 MHz

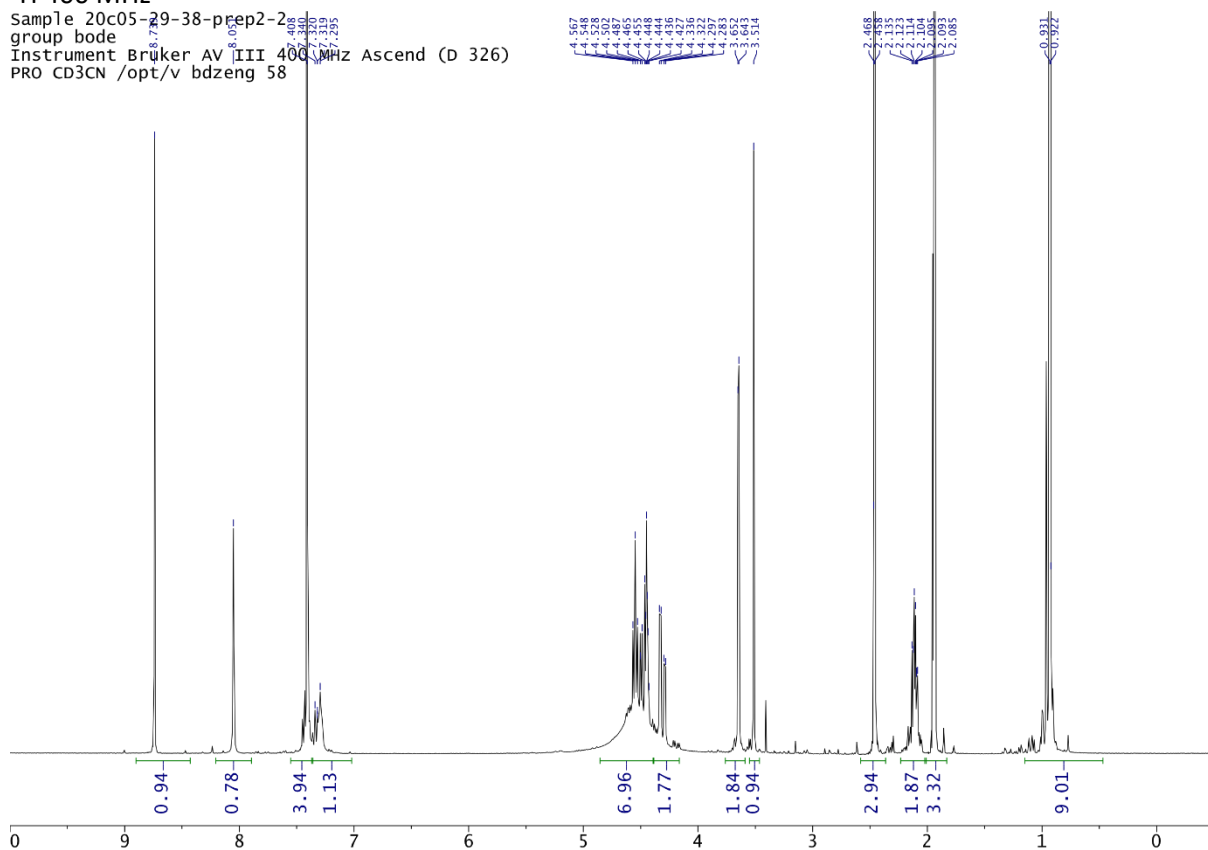


NMR Spectra

Compound 143

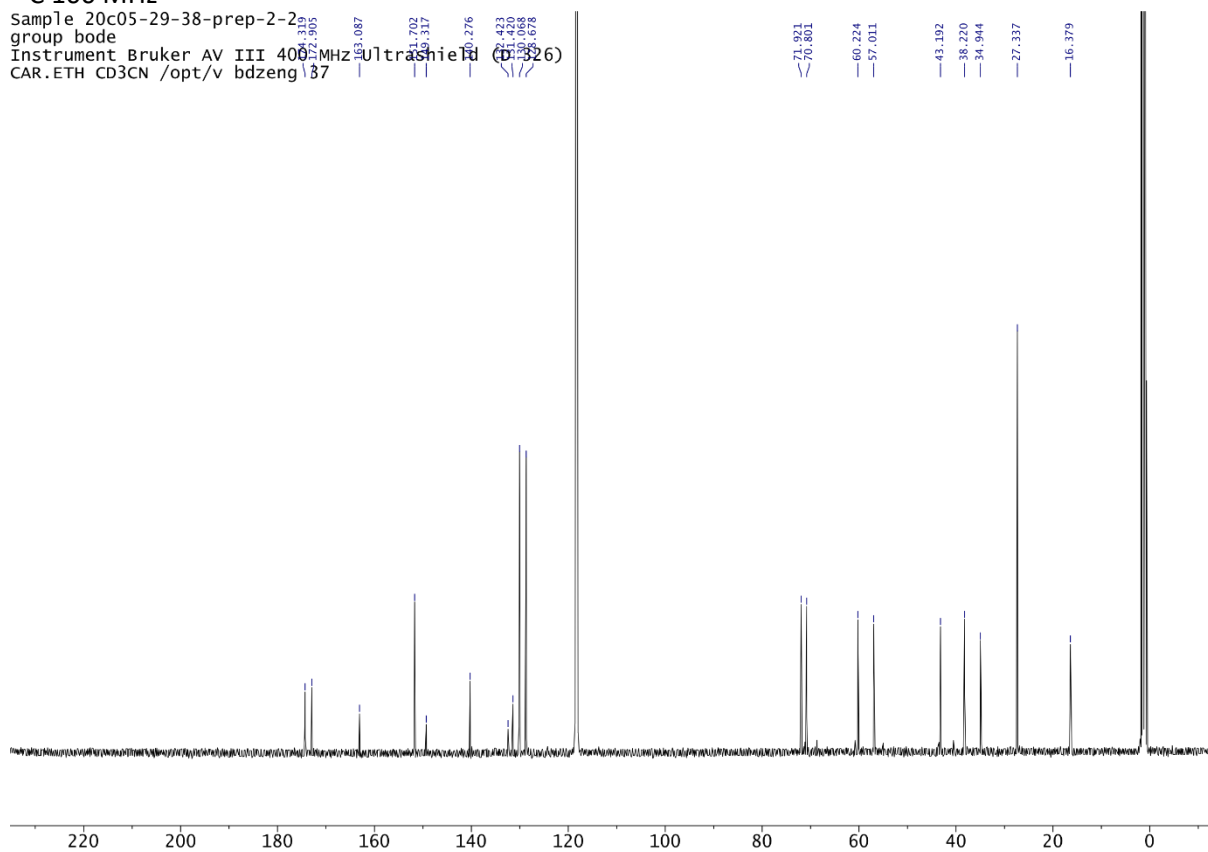
¹H 400 MHz

Sample 20c05-29-38-prep2-2
group bode
Instrument Bruker AV III 400 MHz Ascend (D 326)
PRO CD3CN /opt/v bdzeng 58

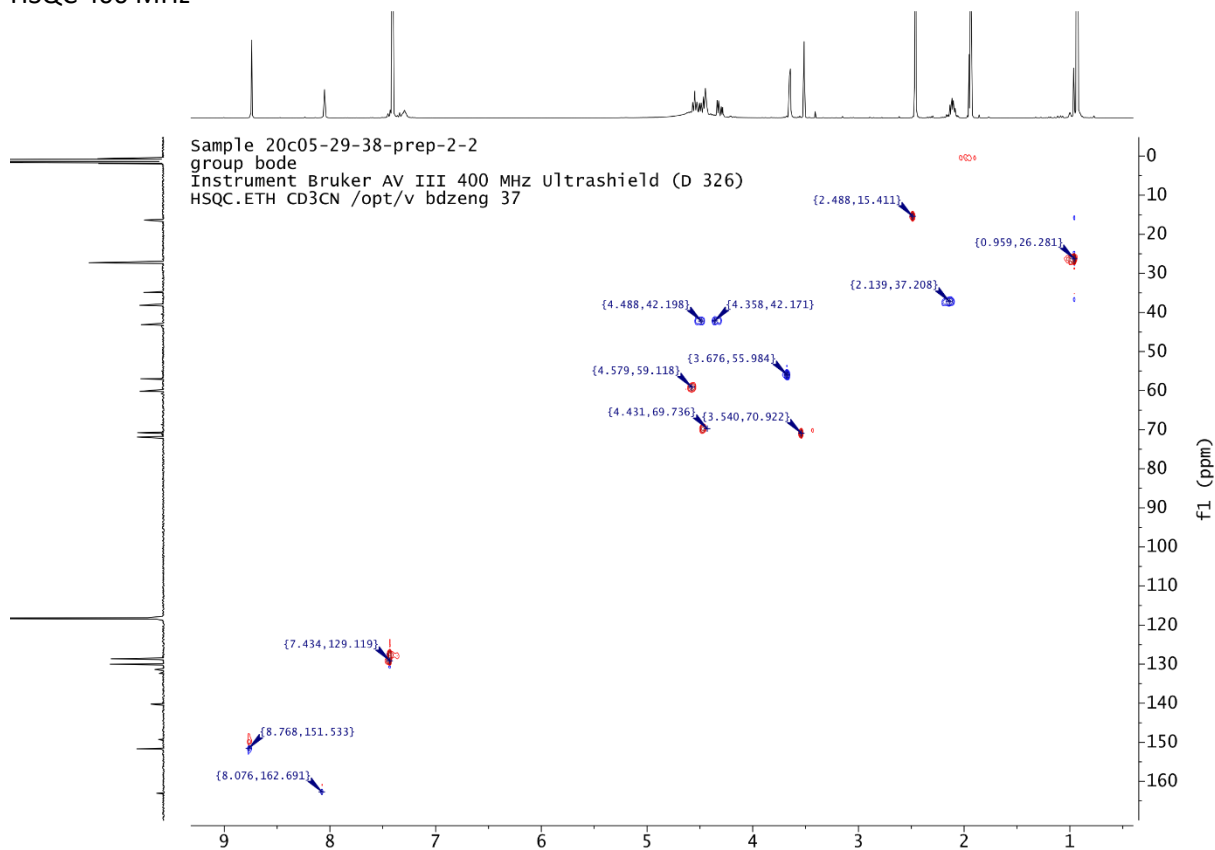


¹³C 100 MHz

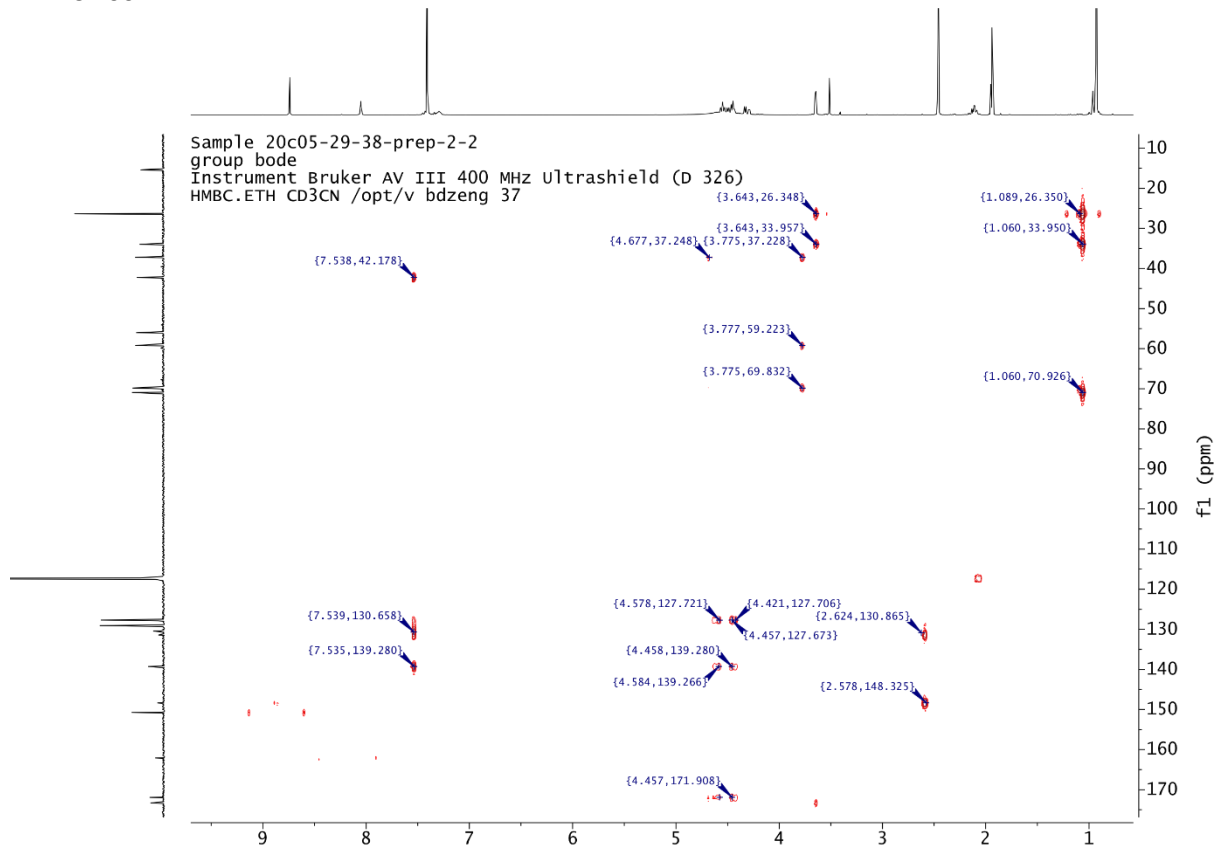
Sample 20c05-29-38-prep2-2
group bode
Instrument Bruker AV III 400 MHz Ultrashield (D 326)
CAR.ETH CD3CN /opt/v bdzeng 37



HSQC 400 MHz



HMBC 400 MHz

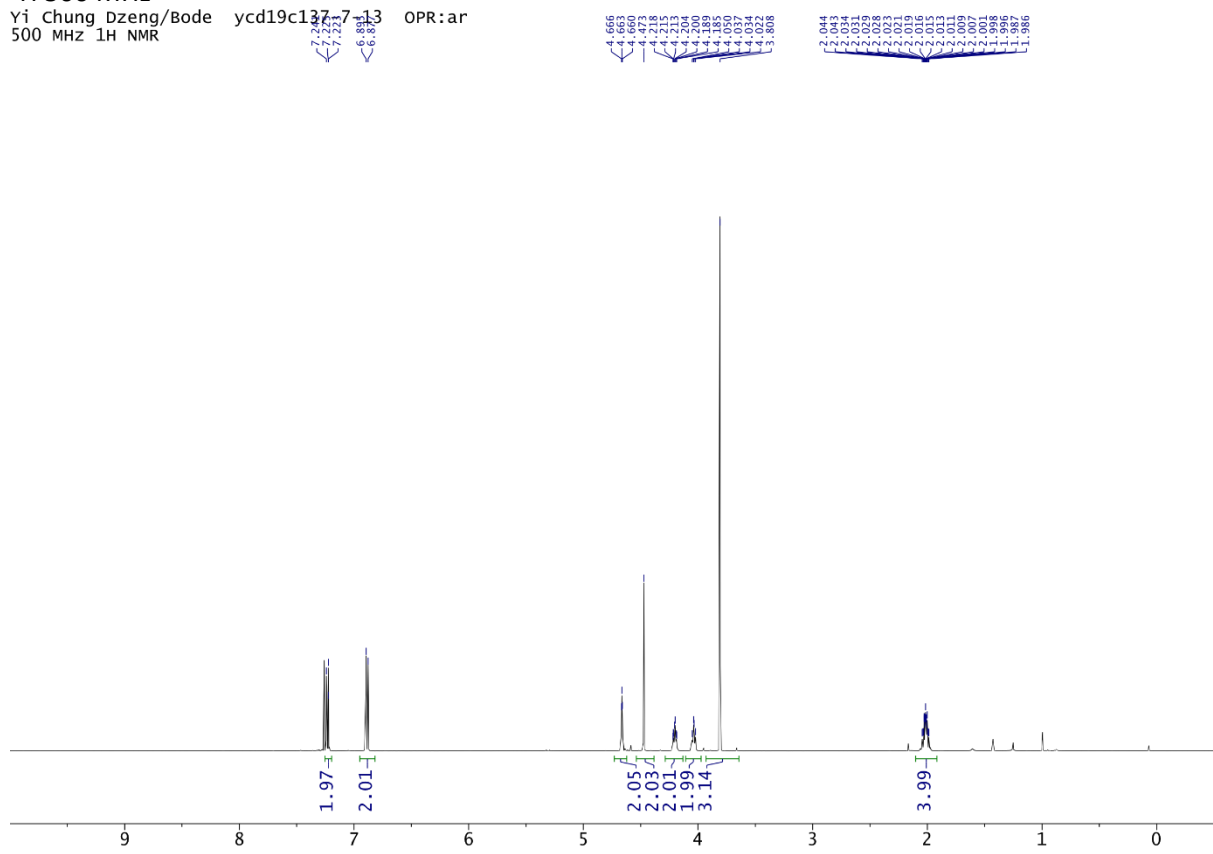


NMR Spectra

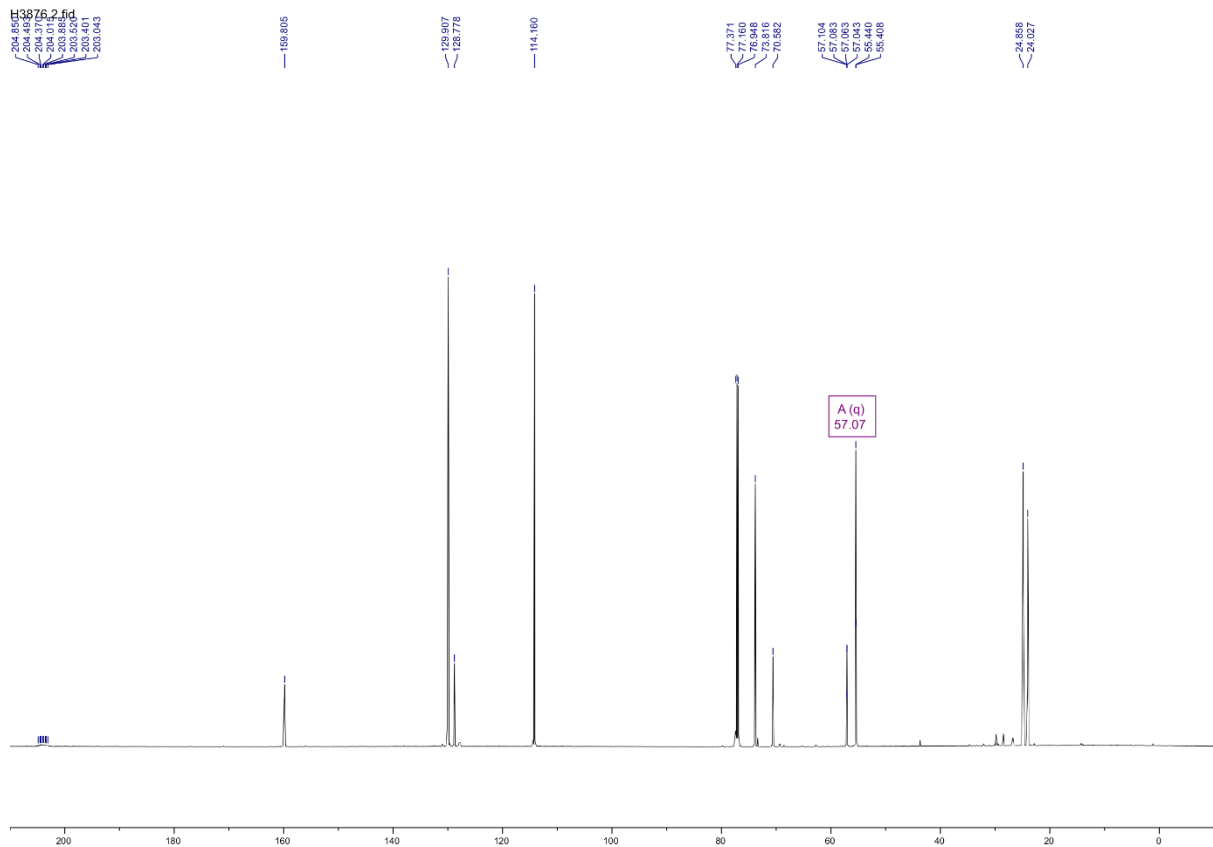
Compound 160

^1H 500 MHz

Yi Chung Dzeng/Bode ycd19c137-7-13 OPR:ar
500 MHz ^1H NMR

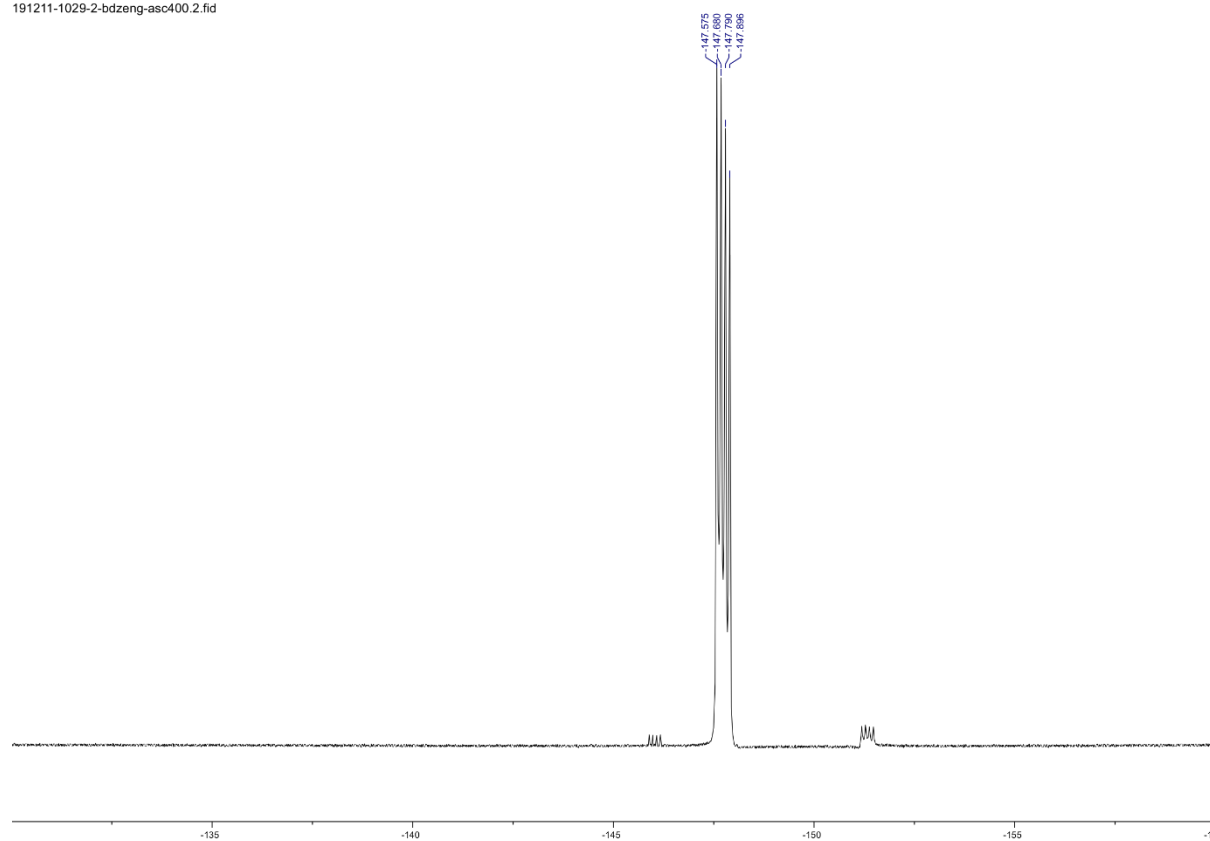


^{13}C 125 MHz



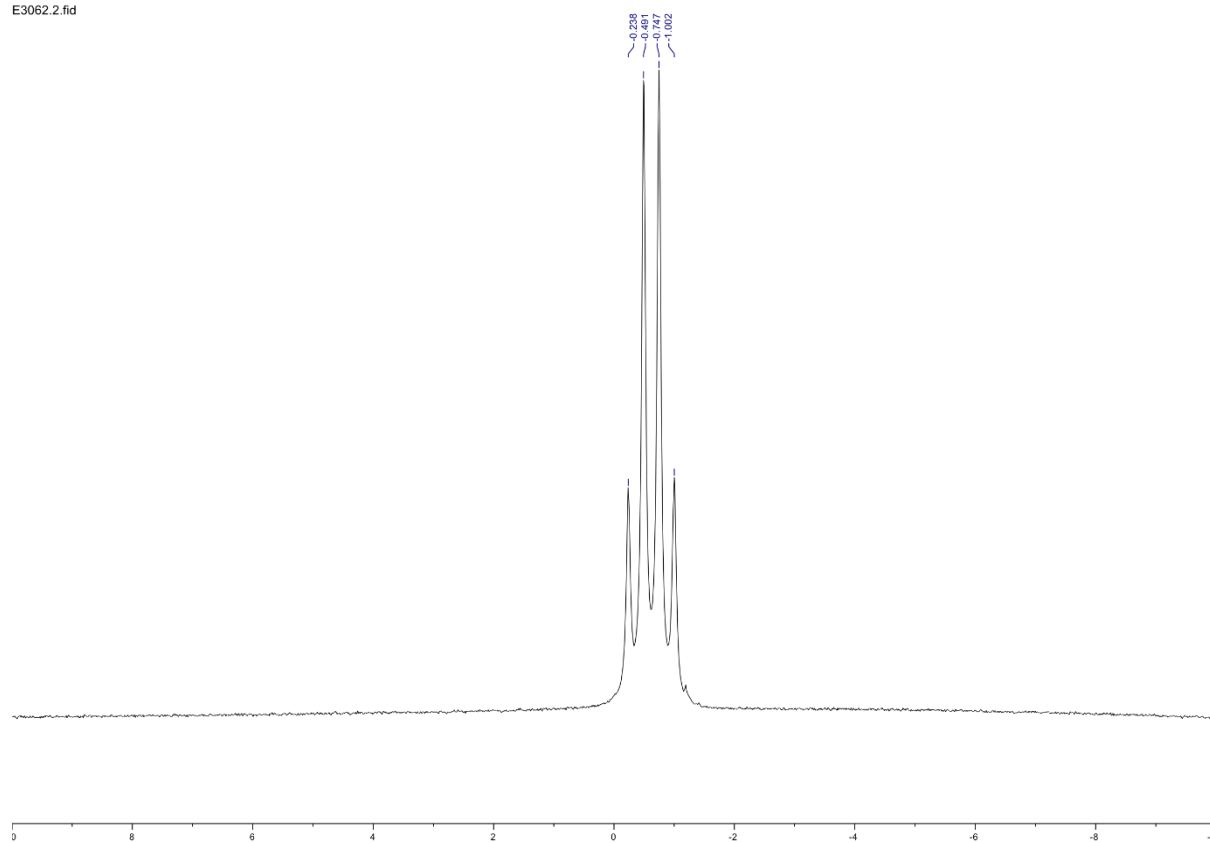
^{19}F 377 MHz

191211-1029-2-bdzeng-asc400.2.fid

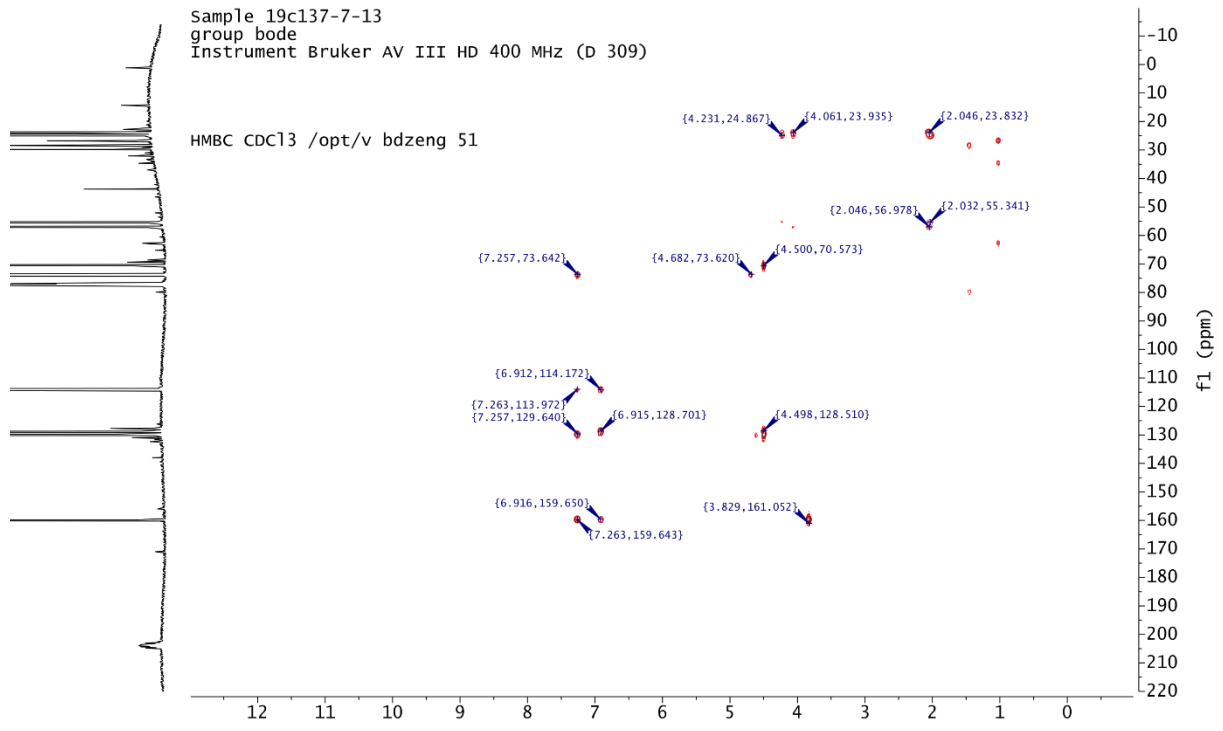
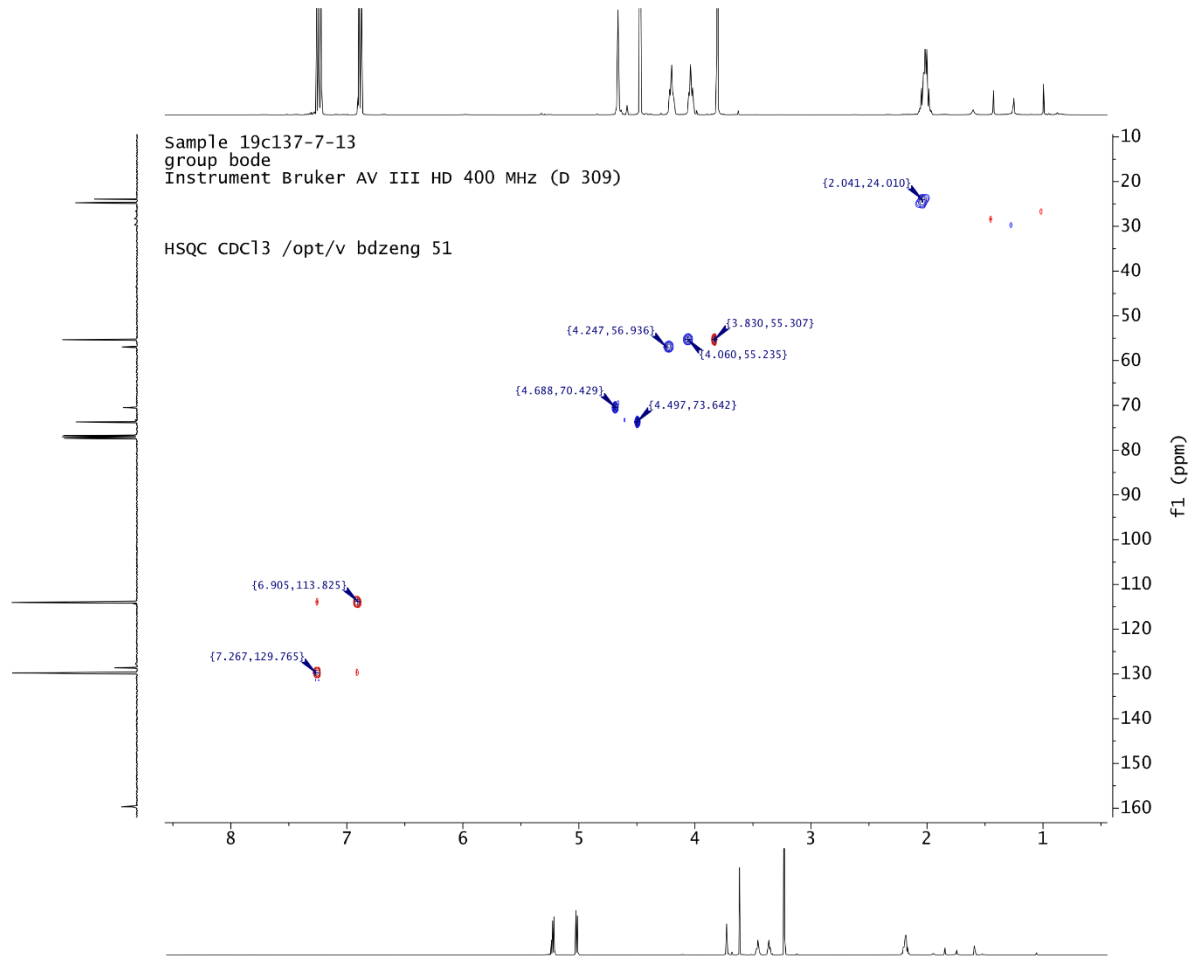


^{11}B 160 MHz

E3062.2.fid



NMR Spectra



Compound 170

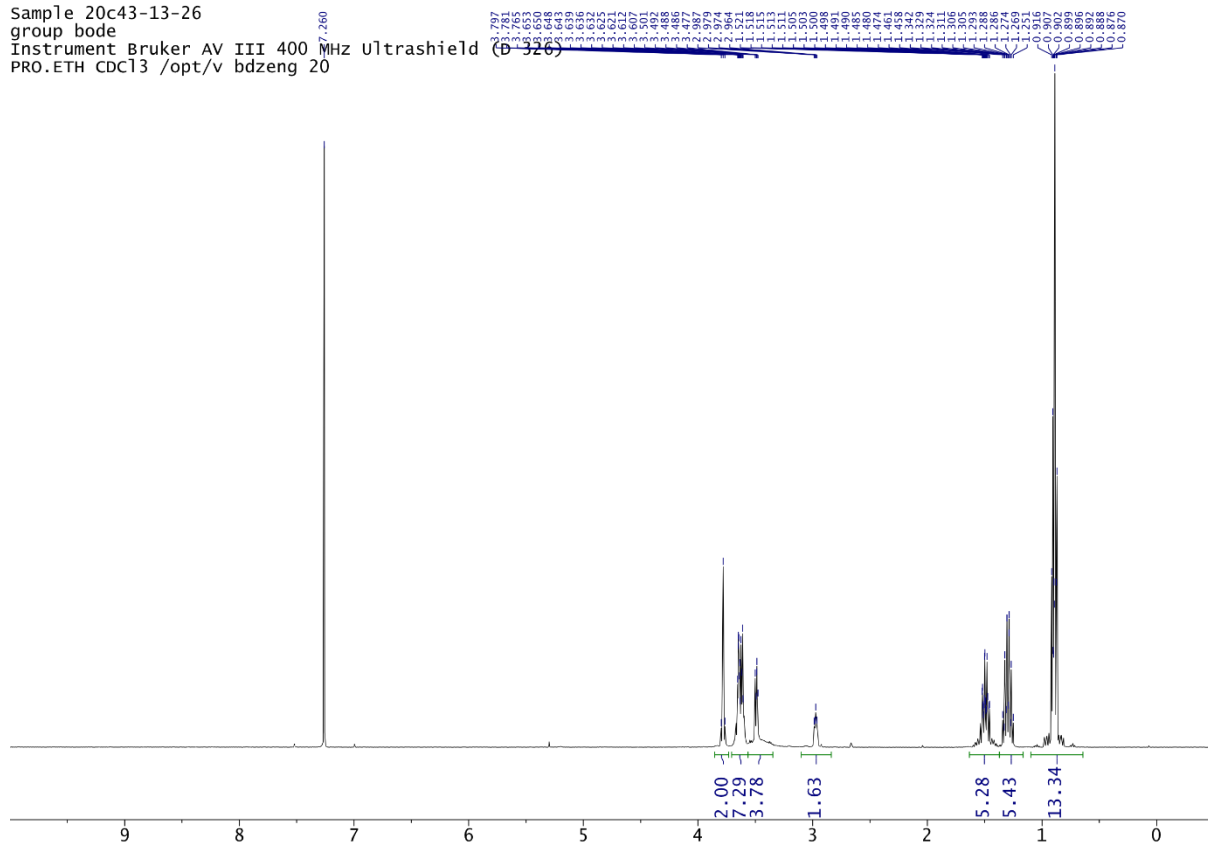
¹H 400 MHz

Sample 20c43-13-26

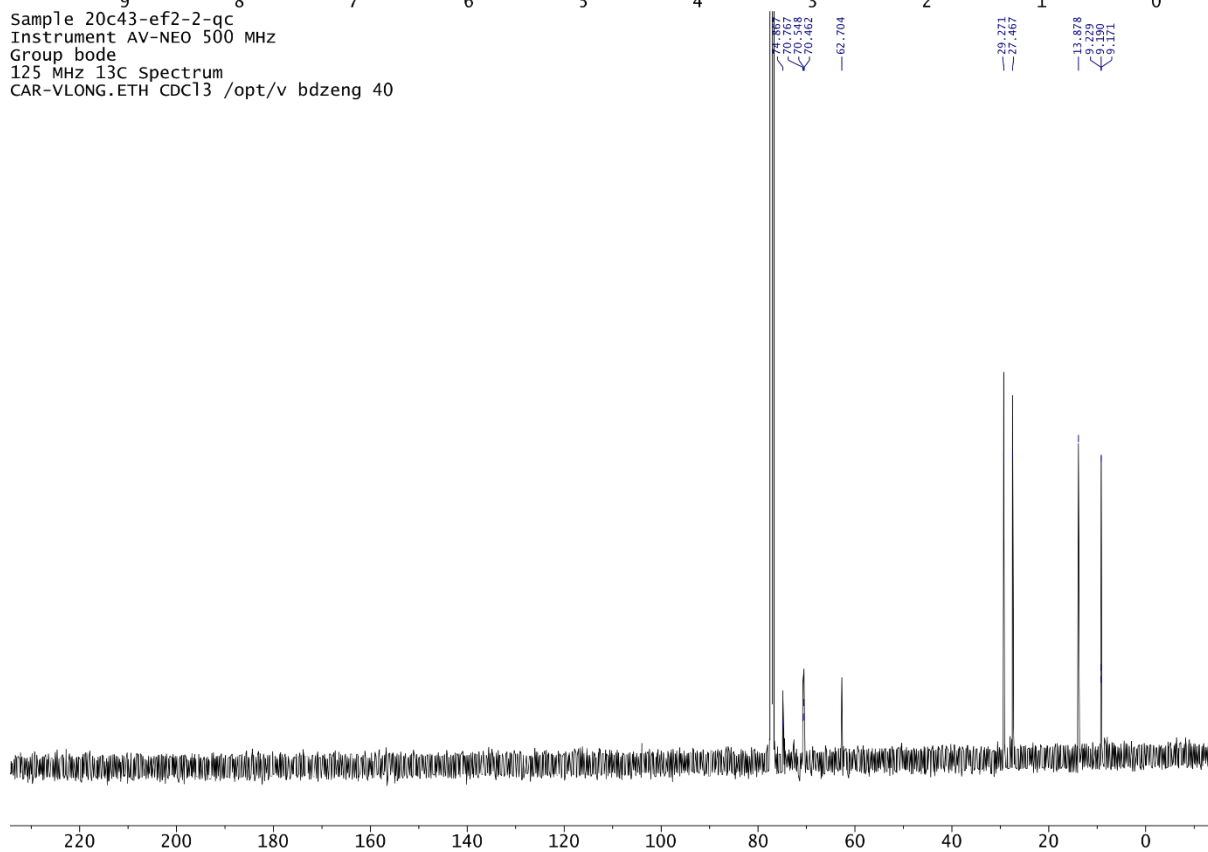
group bode

Instrument Bruker AV III 400 MHz Ultrashield (D-326)

PRO.ETH CDC13 /opt/v bdzeng 20



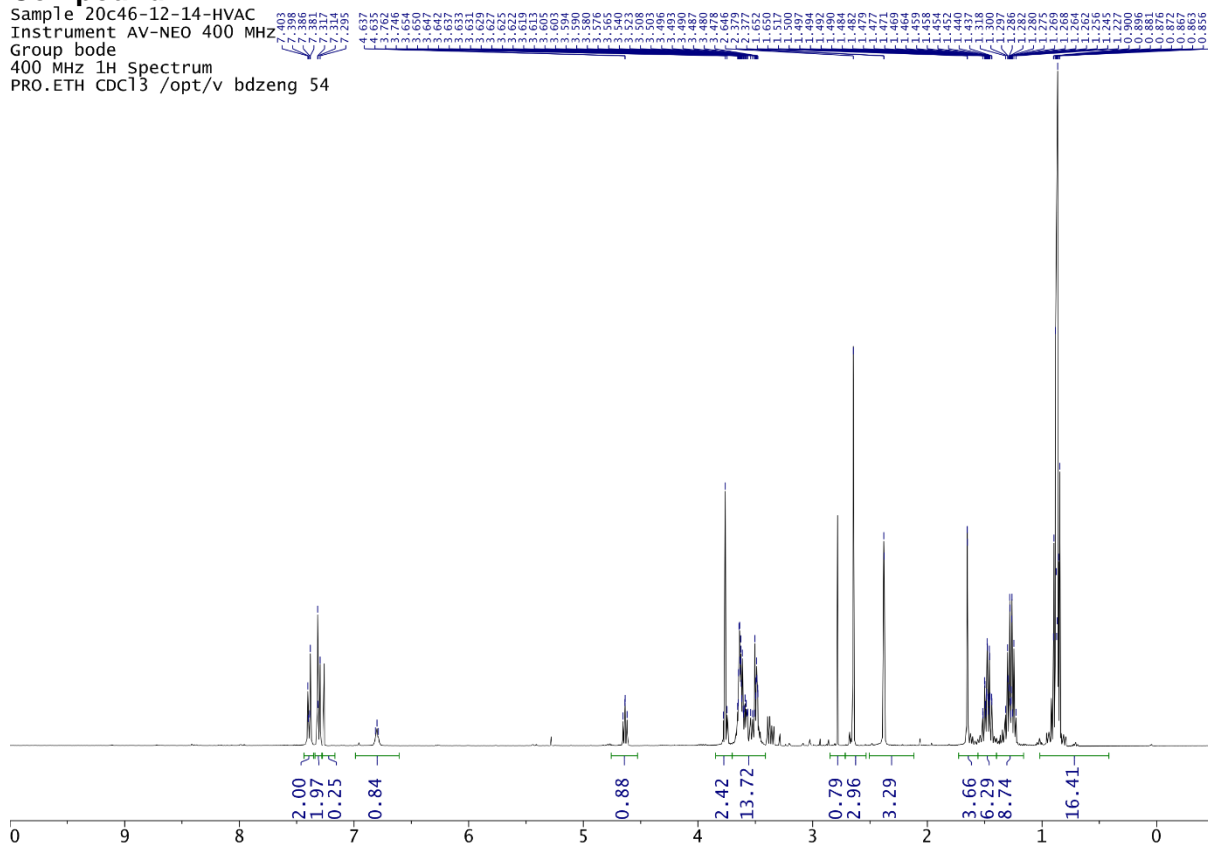
Sample 20c43-ef2-2-qc
 Instrument AV-NEO 500 MHz
 Group bode
 125 MHz ¹³C Spectrum
 CAR-VLONG.ETH CDC13 /opt/v bdzeng 40



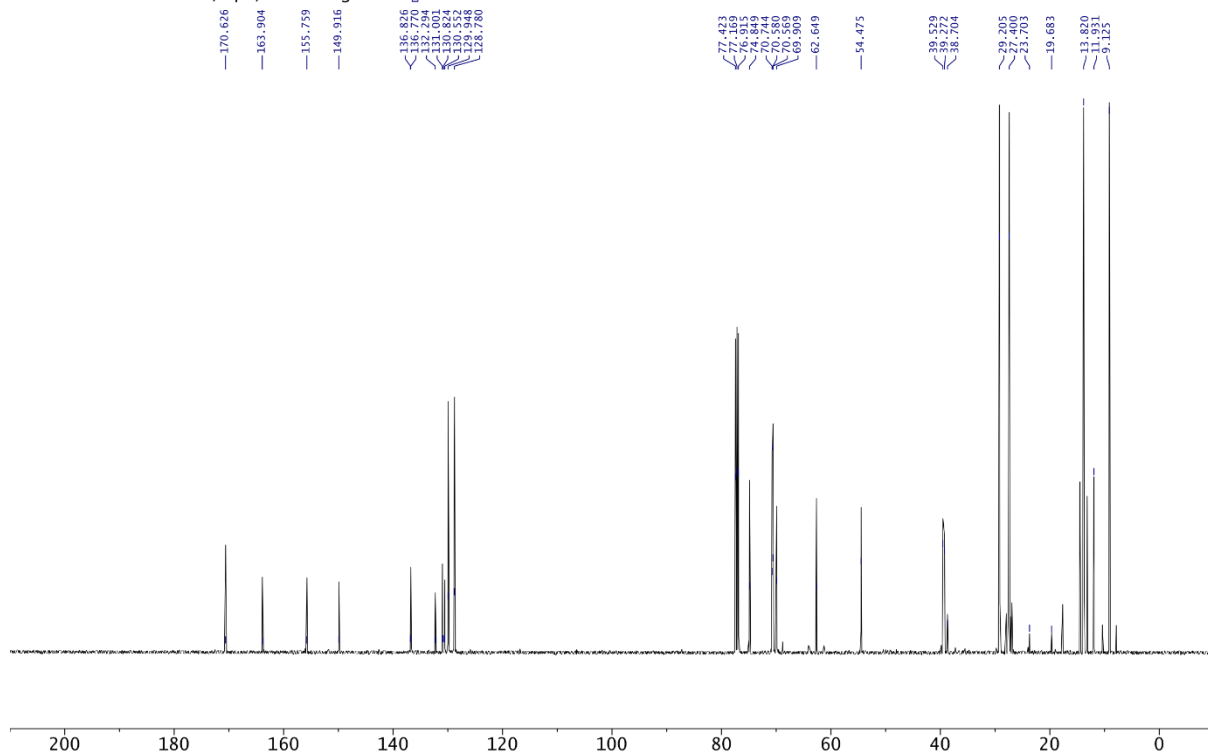
NMR Spectra

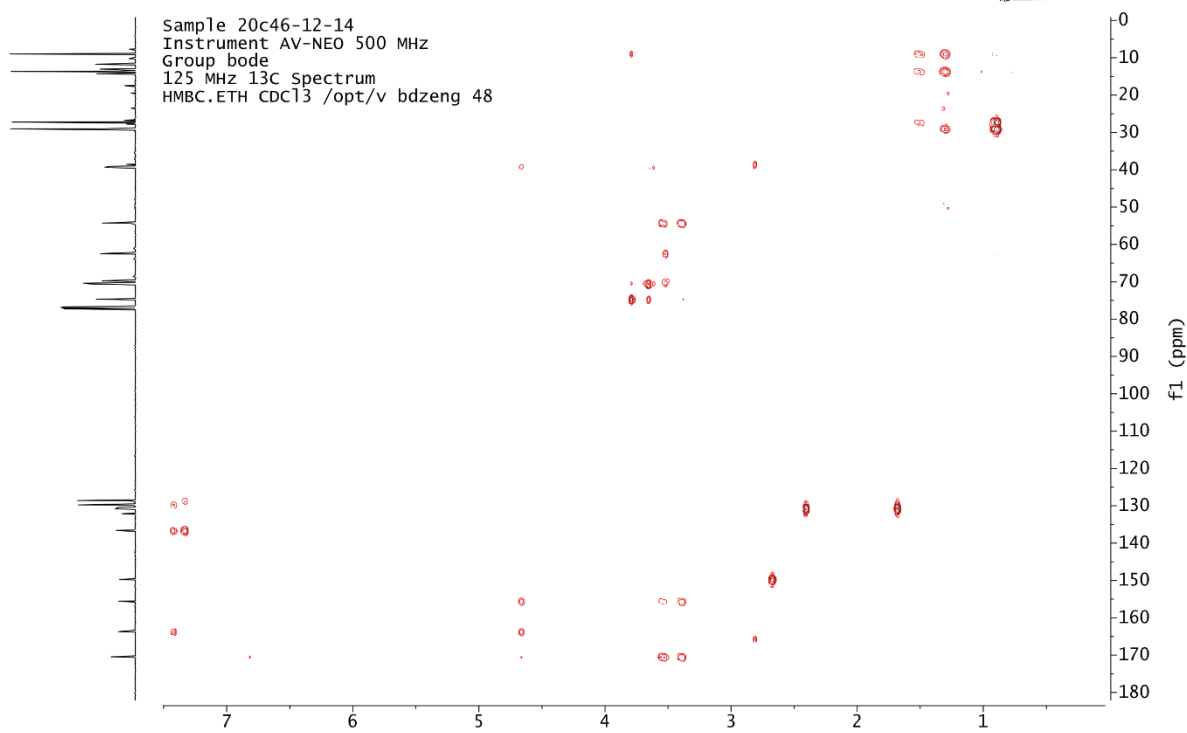
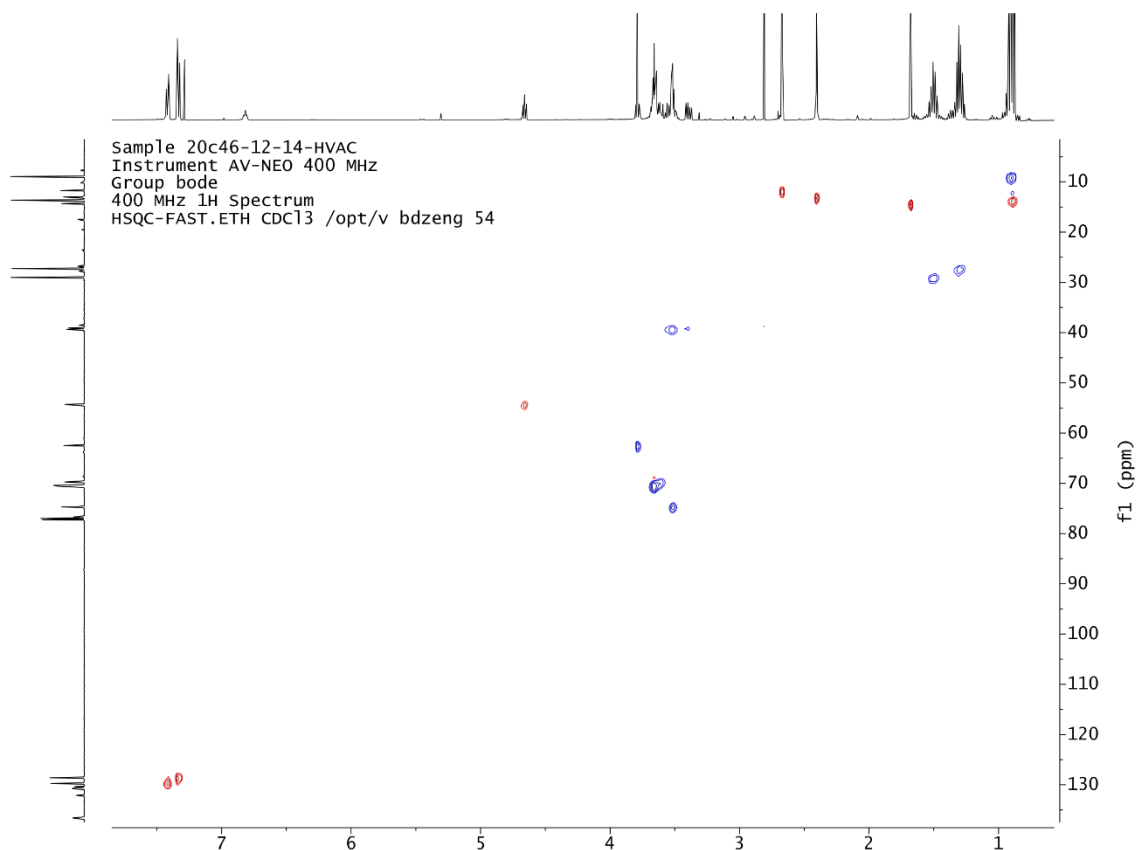
Compound 171

Sample 20c46-12-14-HVAC
 Instrument AV-NEO 400 MHz
 Group bode
 400 MHz 1H Spectrum
 PRO.ETH CDC13 /opt/v bdzeng 54



Sample 20c46-12-14
 Instrument AV-NEO 500 MHz
 Group bode
 125 MHz 13C Spectrum
 CAR-LONG.ETH CDC13 /opt/v bdzeng 48





NMR Spectra

Compound 174

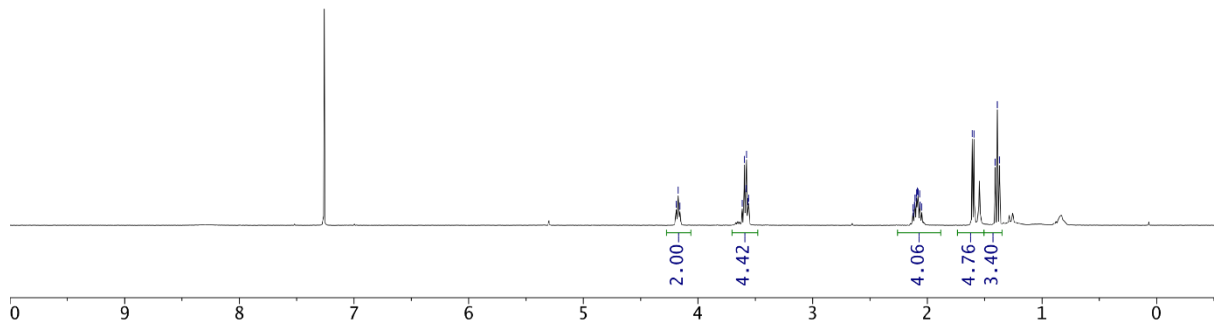
^1H 400 MHz

sample ycd853comb

group bode

PRO CDC13 /opt/v bdzeng 4

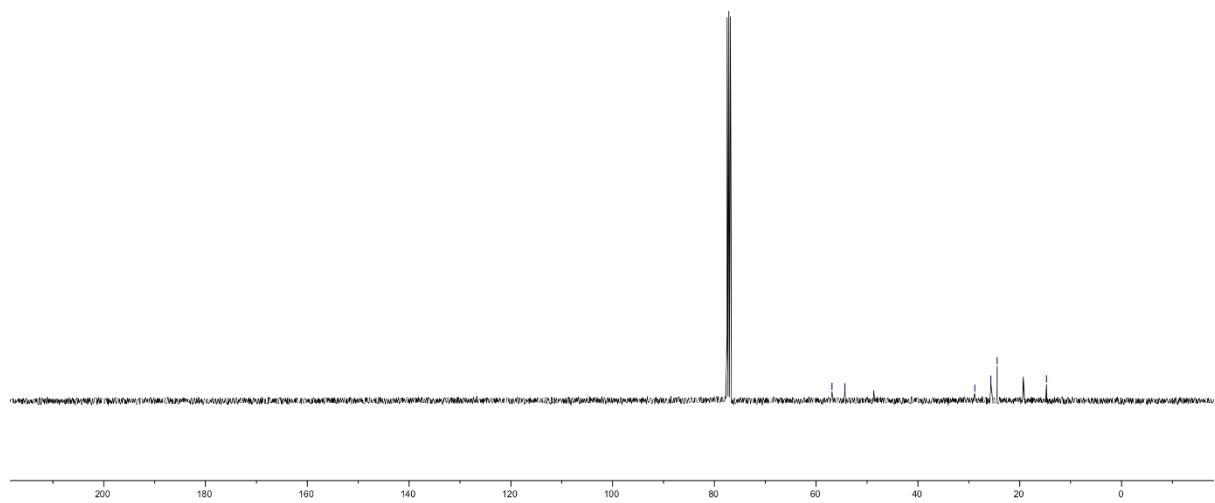
4.291
4.152
3.614
3.595
3.577
3.564
3.558
2.126
2.122
2.107
2.097
2.087
2.079
2.065
2.049
1.993
1.408
1.370



^{13}C 100 MHz

170624-1621-22-bdzeng-avn400.2.fid

56.887
54.343
28.823
25.676
24.435
14.757



^{19}F 376 MHz

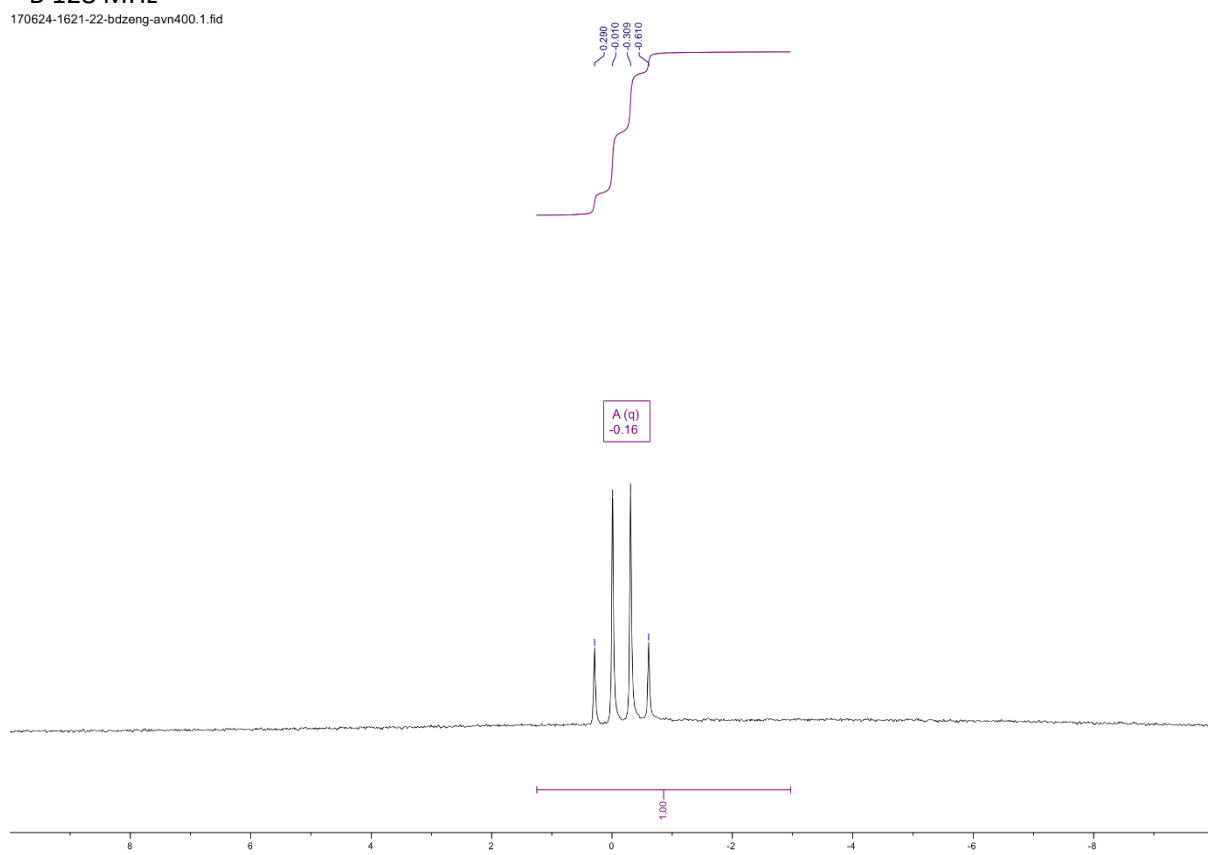
Sample ycd853comb
group bode
F19_full_dec CDC13 /opt/v bdzeng



30 -135 -140 -145 -150 -155 -1

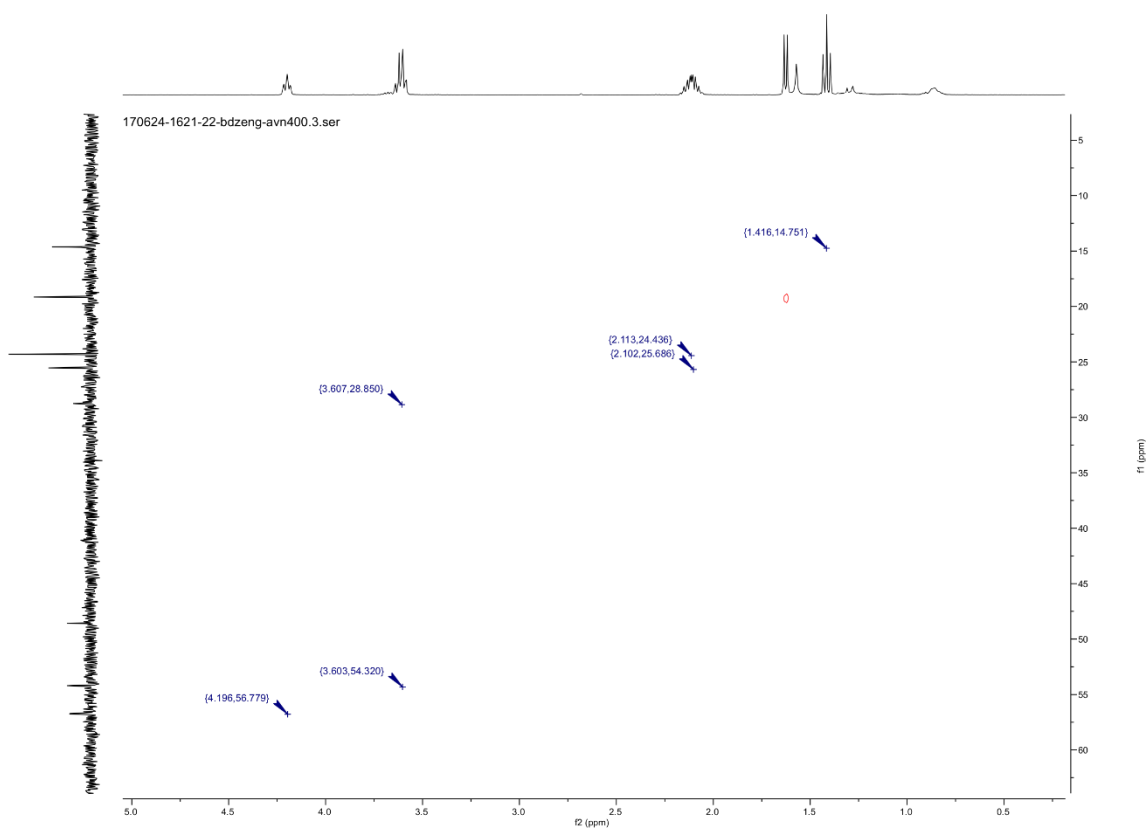
^{11}B 128 MHz

170624-1621-22-bdzeng-avn400.1.fid



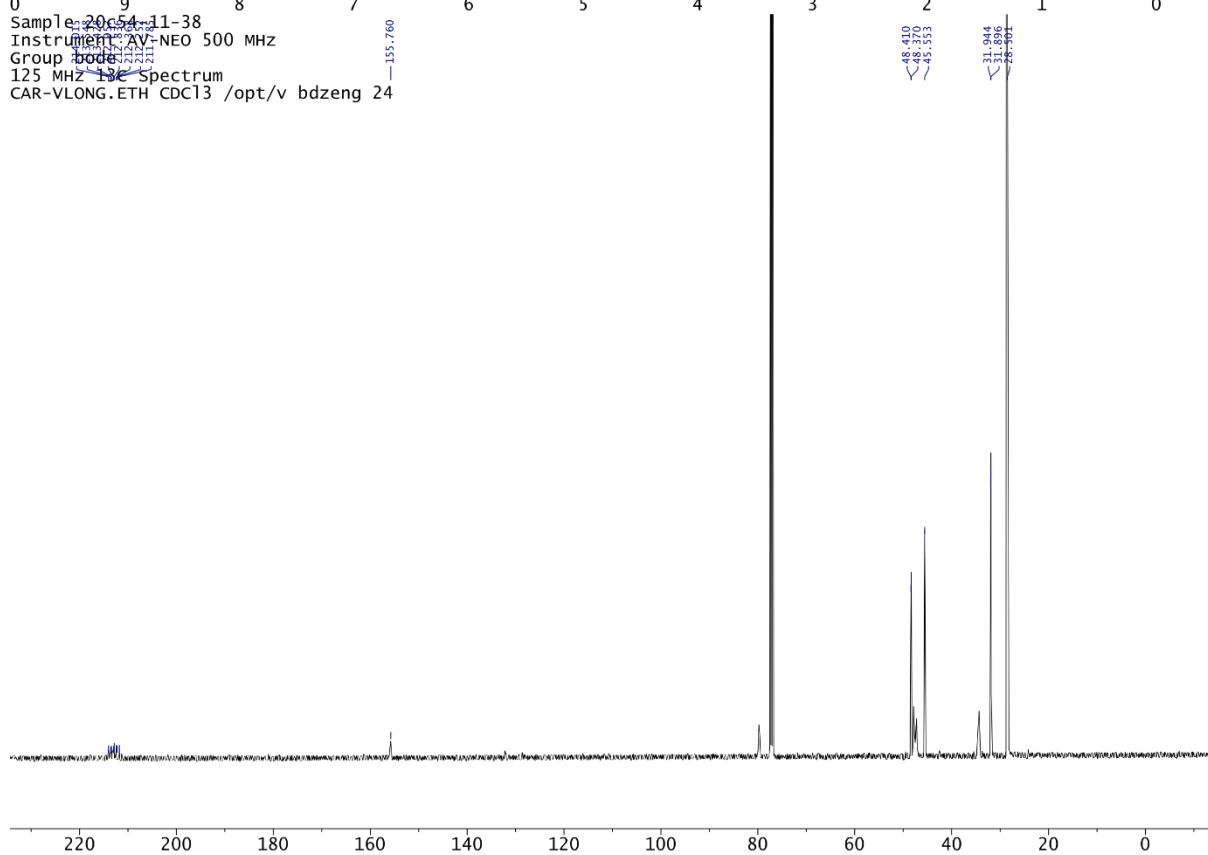
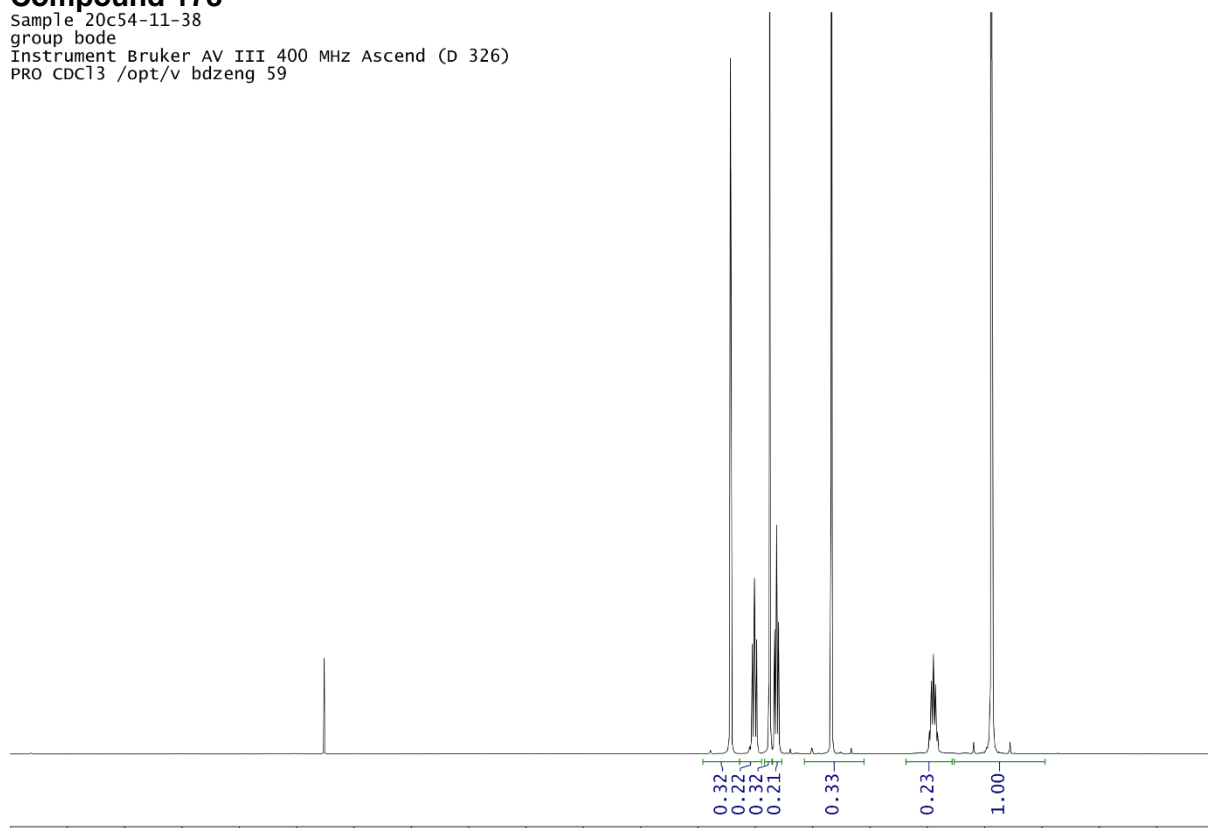
NMR Spectra

HSQC 400MHz



Compound 178

Sample 20c54-11-38
 group bode
 Instrument Bruker AV III 400 MHz Ascend (D 326)
 PRO CDC13 /opt/v bdzeng 59



Sample 20c54-11-38
 Instrument AV-NEO 500 MHz
 Group bode
 125 MHz 13C Spectrum
 CAR-VLONG.ETH CDC13 /opt/v bdzeng 24

NMR Spectra

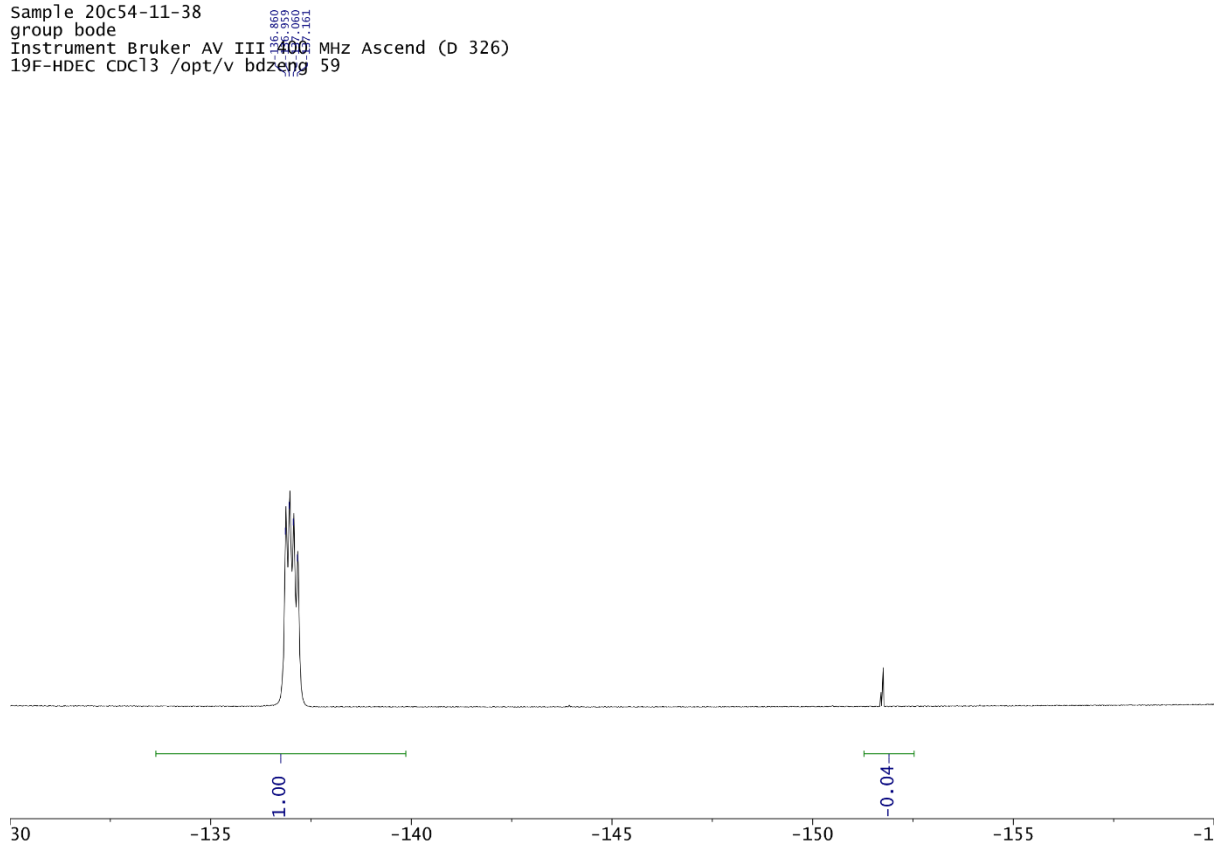
¹⁹F 377 MHz

Sample 20c54-11-38

group bode

Instrument Bruker AV III 400 MHz Ascend (D 326)

19F-HDEC CDC13 /opt/v bdzeng 59



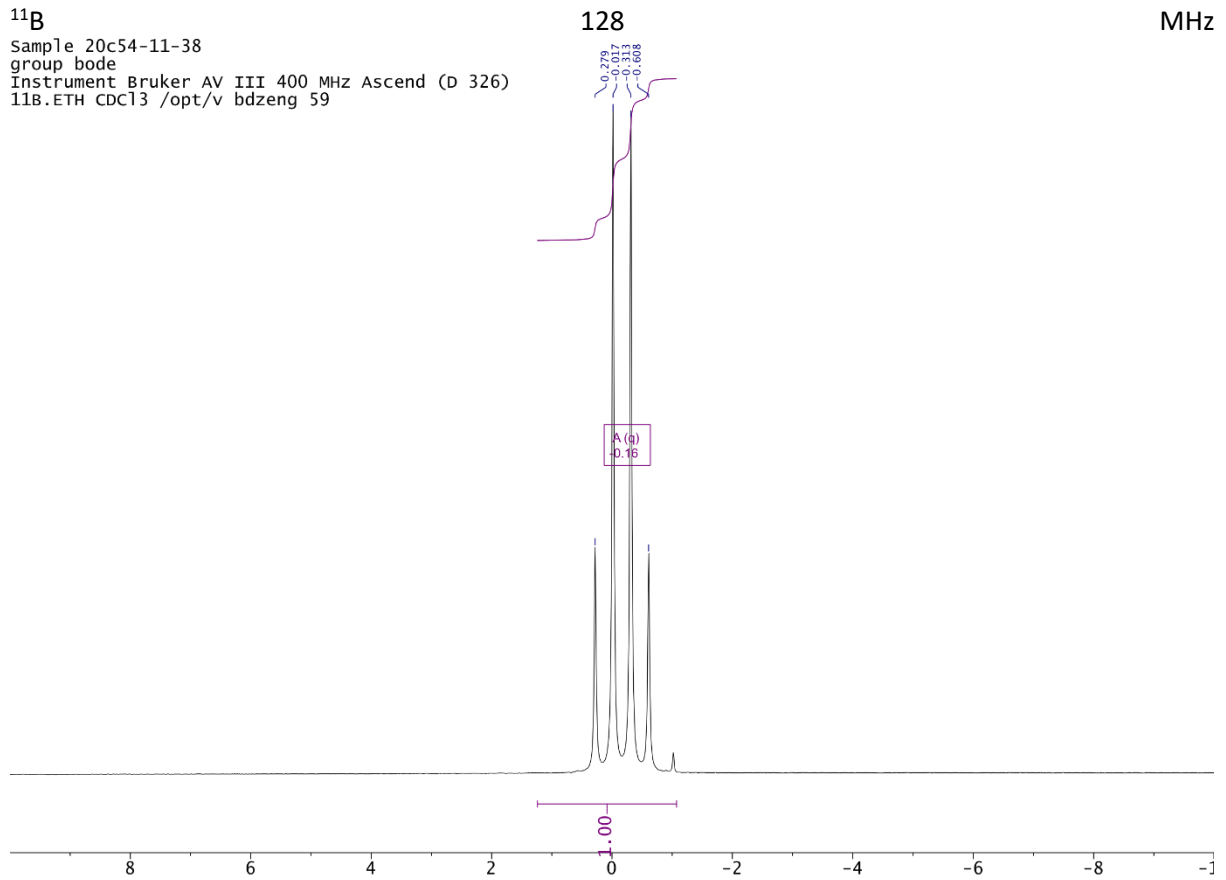
¹¹B

Sample 20c54-11-38

group bode

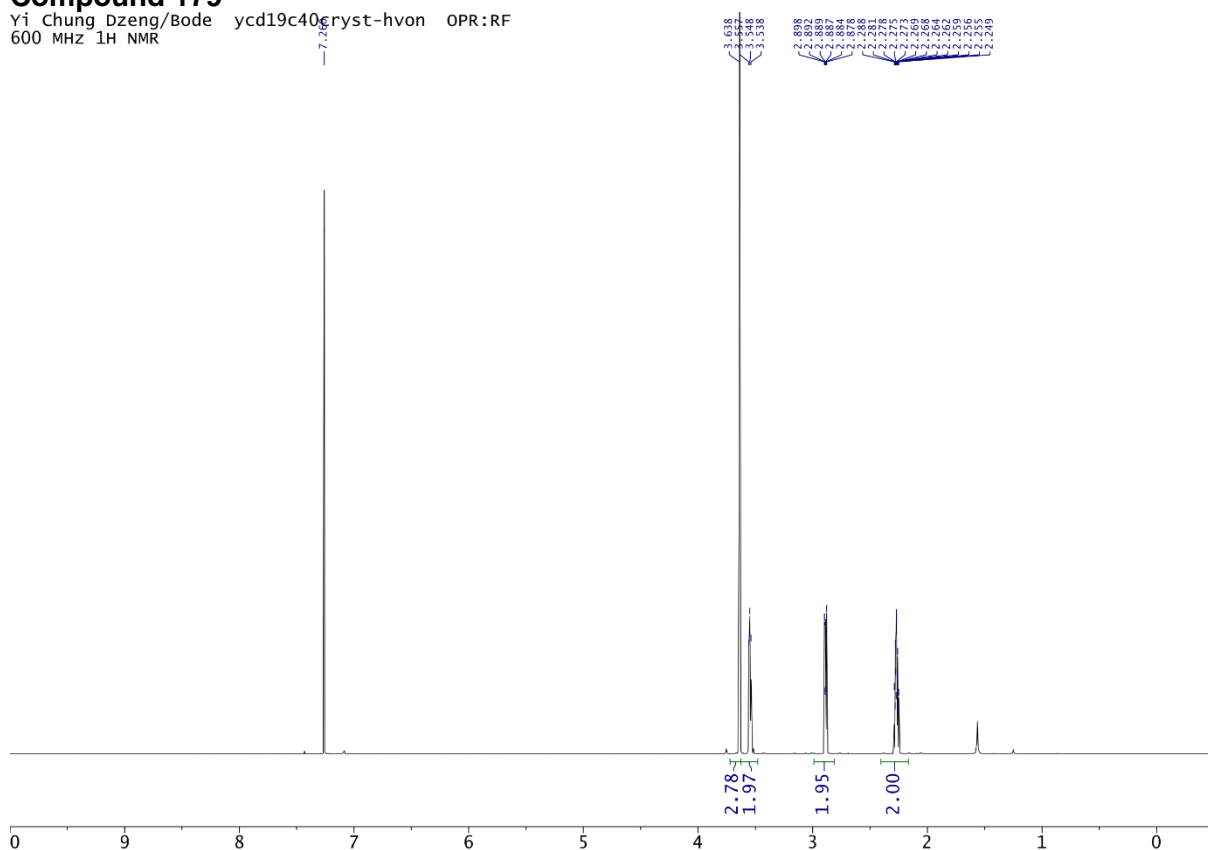
Instrument Bruker AV III 400 MHz Ascend (D 326)

11B.ETH CDC13 /opt/v bdzeng 59

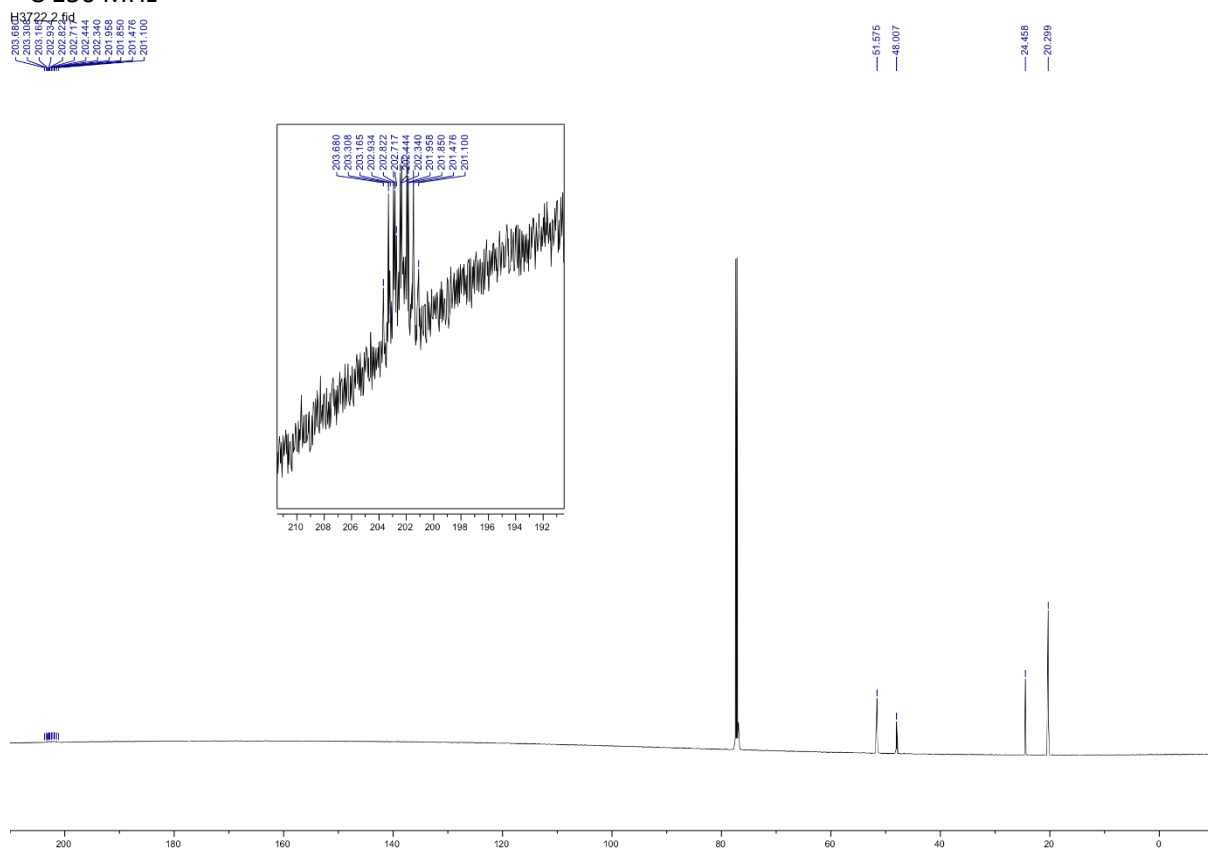


Compound 179

Yi Chung Dzeng/Bode ycd19c40cryst-hvon OPR:RF
600 MHz ¹H NMR



¹³C 150 MHz



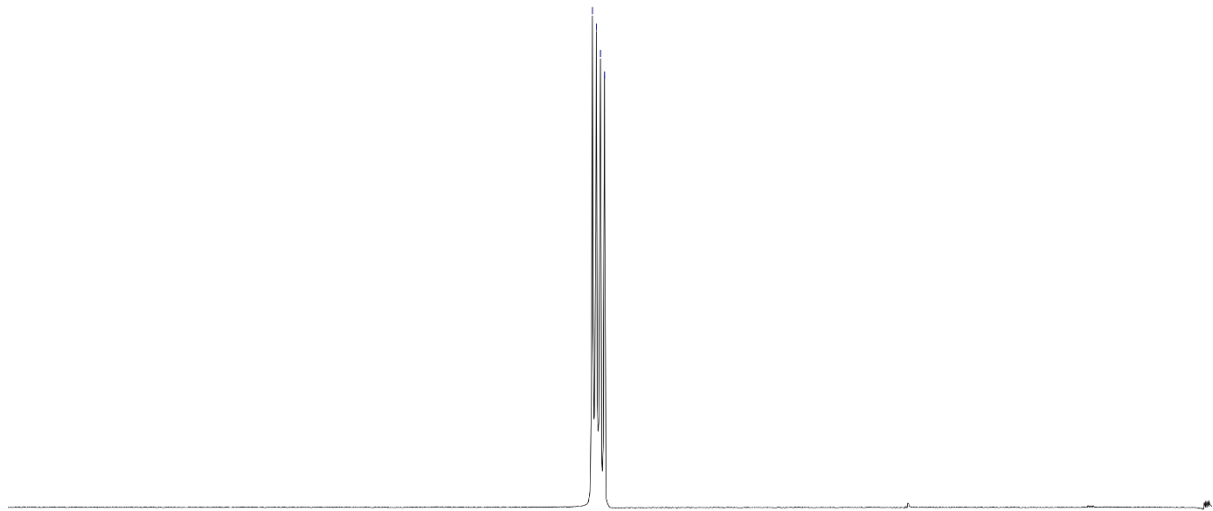
NMR Spectra

^{19}F 376 MHz

Sample 17c20-cryst
group bode
Instrument Bruker AV III 400 MHz Ultrashield (D 326)
F19CPD

144.862
144.862
144.763
144.864

F19_full_dec CDCl₃ /opt/v bdzeng 31

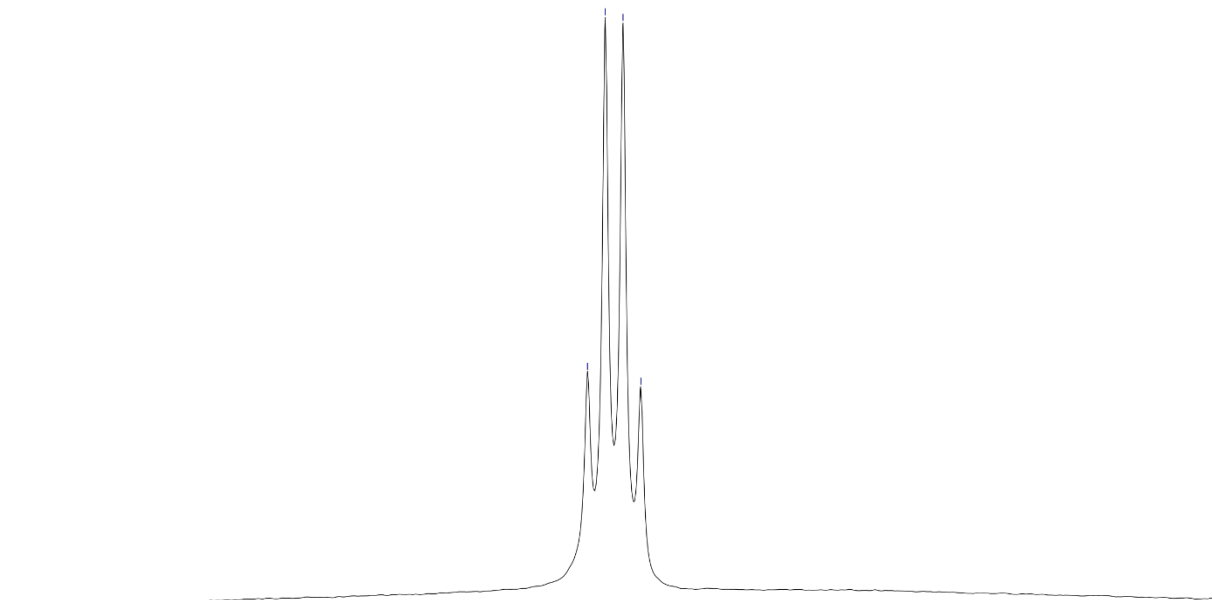


^{11}B 128 MHz

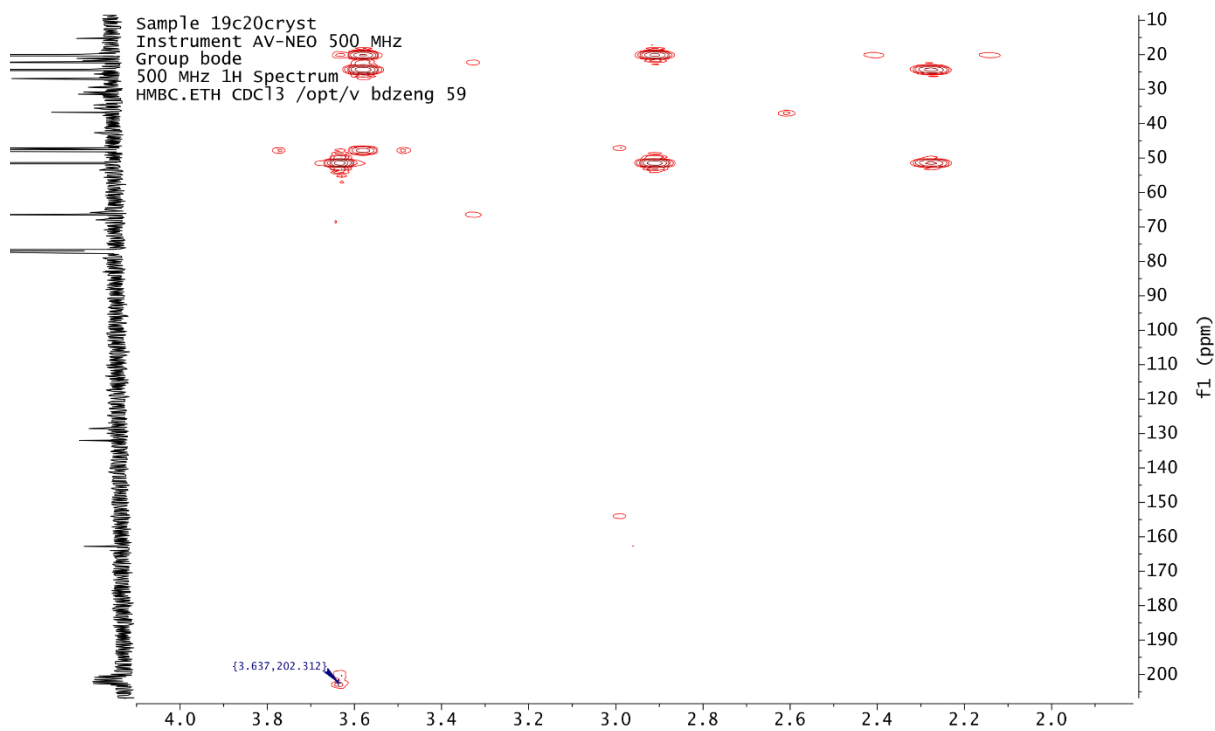
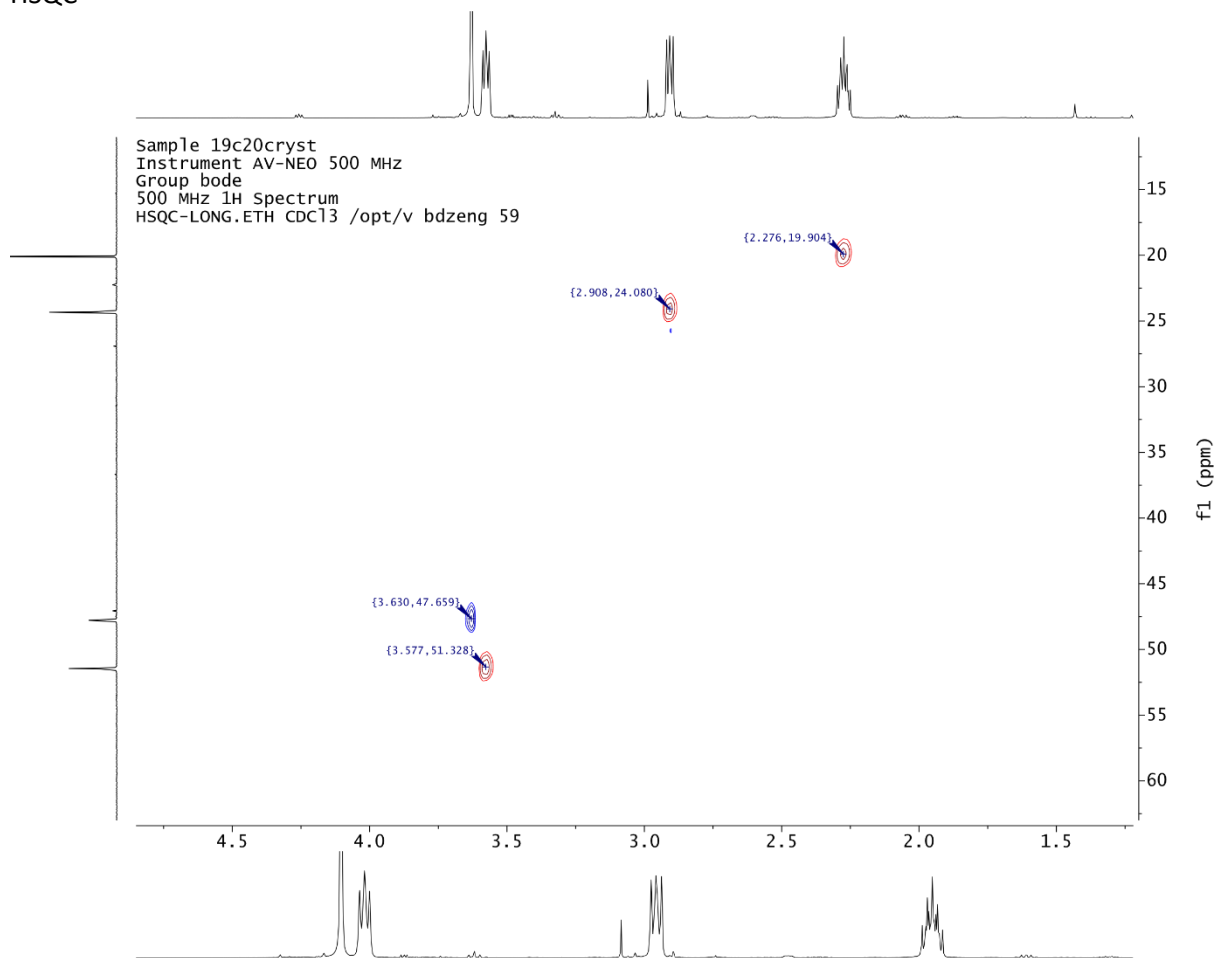
Sample 17c20-cryst
group bode
Instrument Bruker AV III 400 MHz Ultrashield (D 326)

0.784
0.889
-0.217
-0.312

B11 spectrum
11B.ETH CDCl₃ /opt/v bdzeng 31



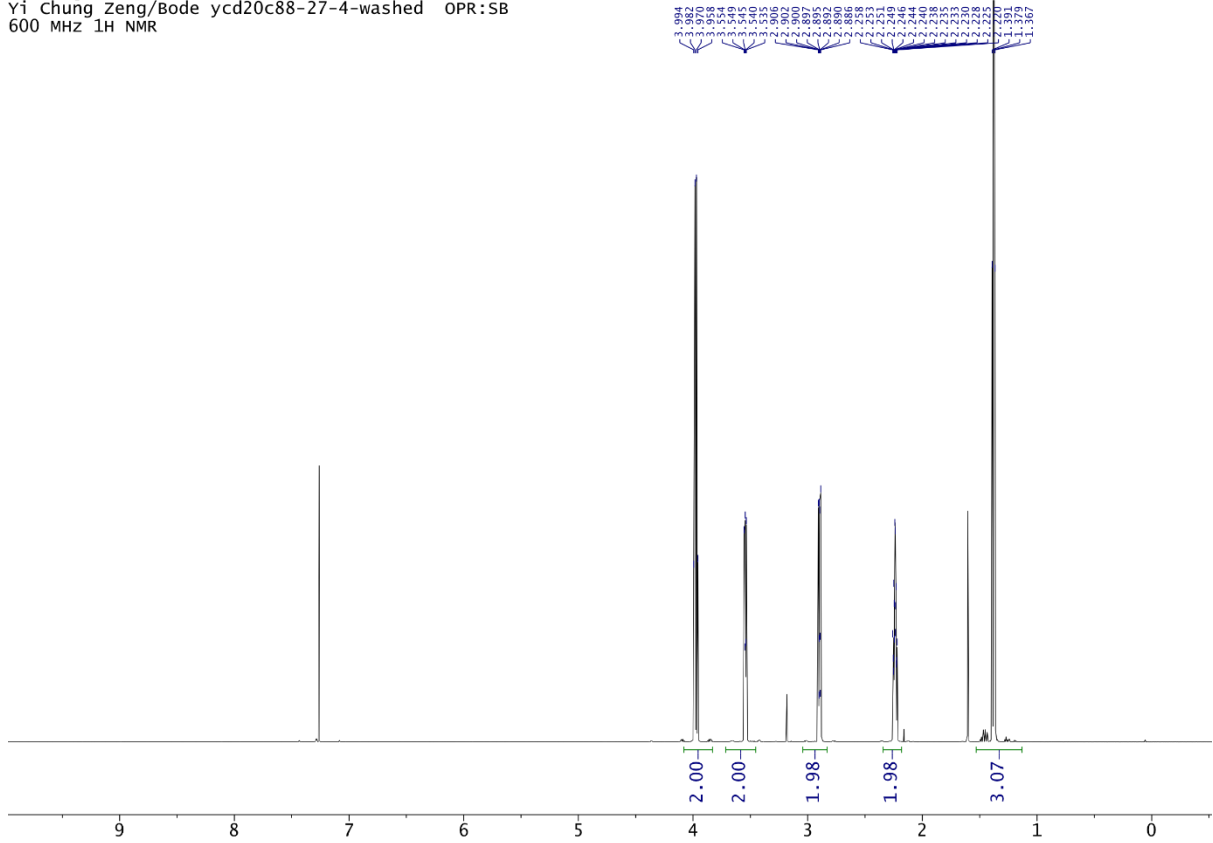
HSQC



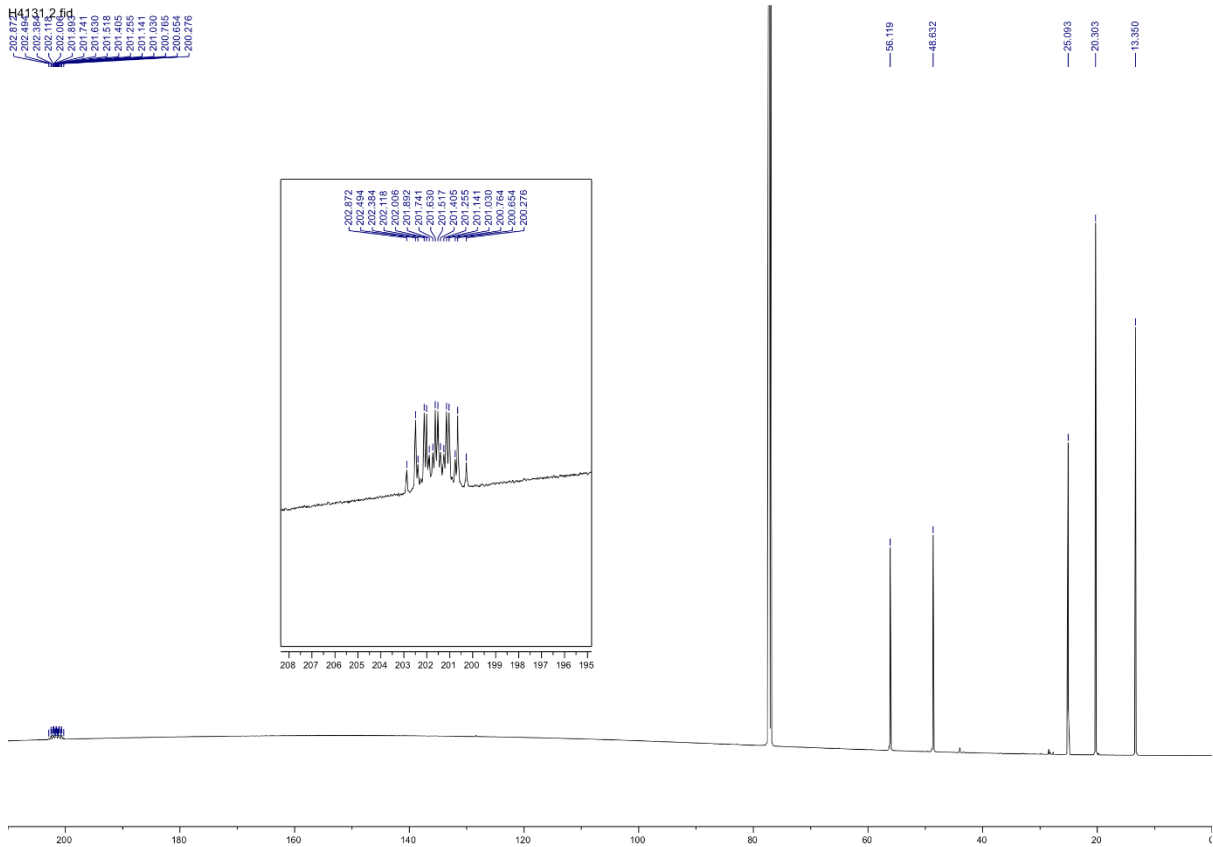
NMR Spectra

Compound 192

Yi Chung Zeng/Bode ycd20c88-27-4-washed OPR:SB
600 MHz ¹H NMR

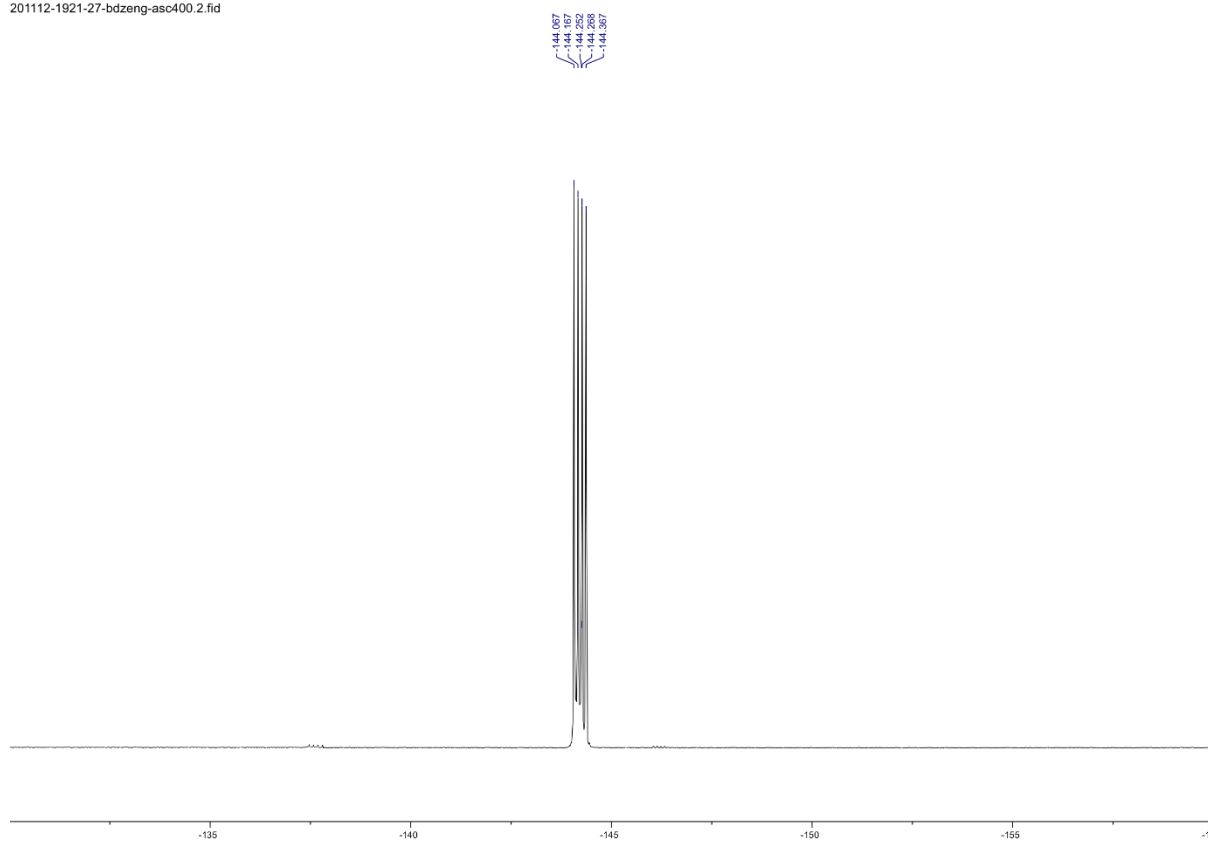


¹³C 150 MHz



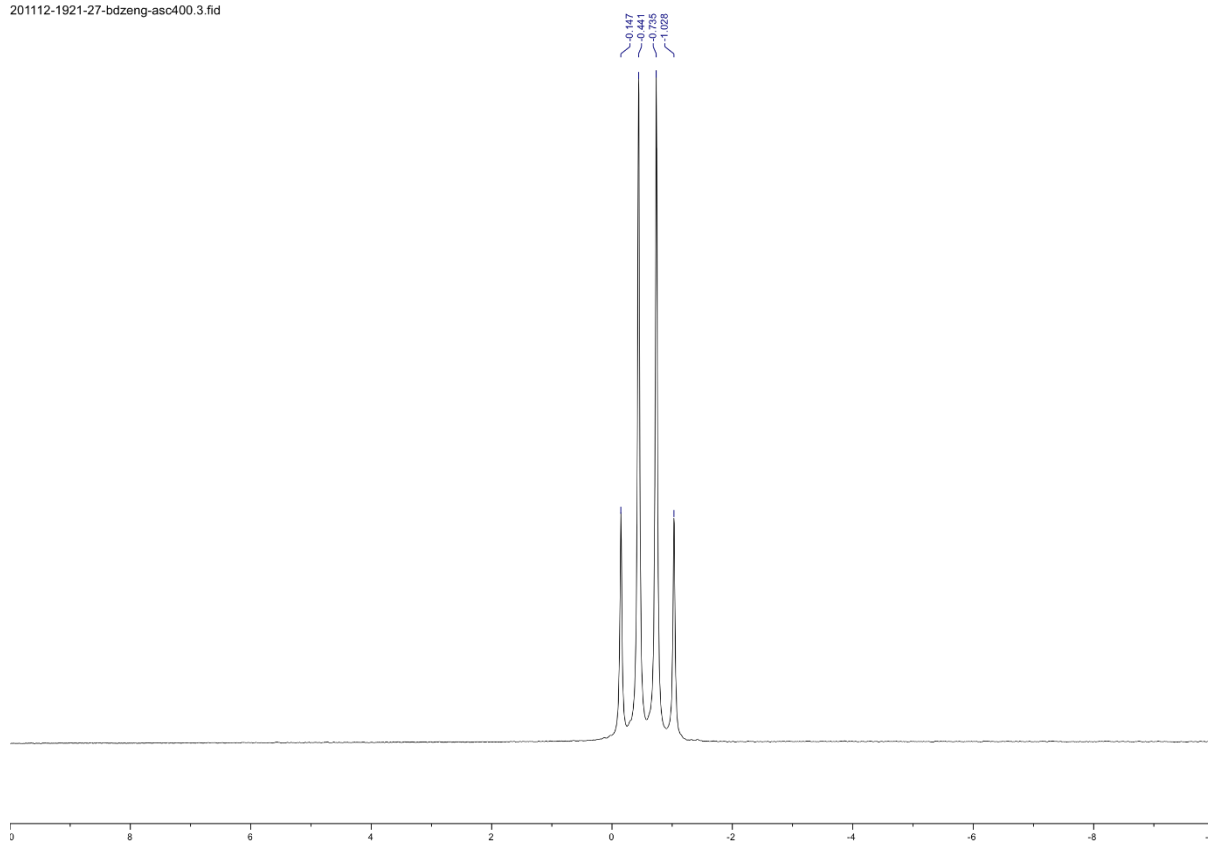
¹⁹F 377 MHz

201112-1921-27-bdzeng-asc400.2.fid

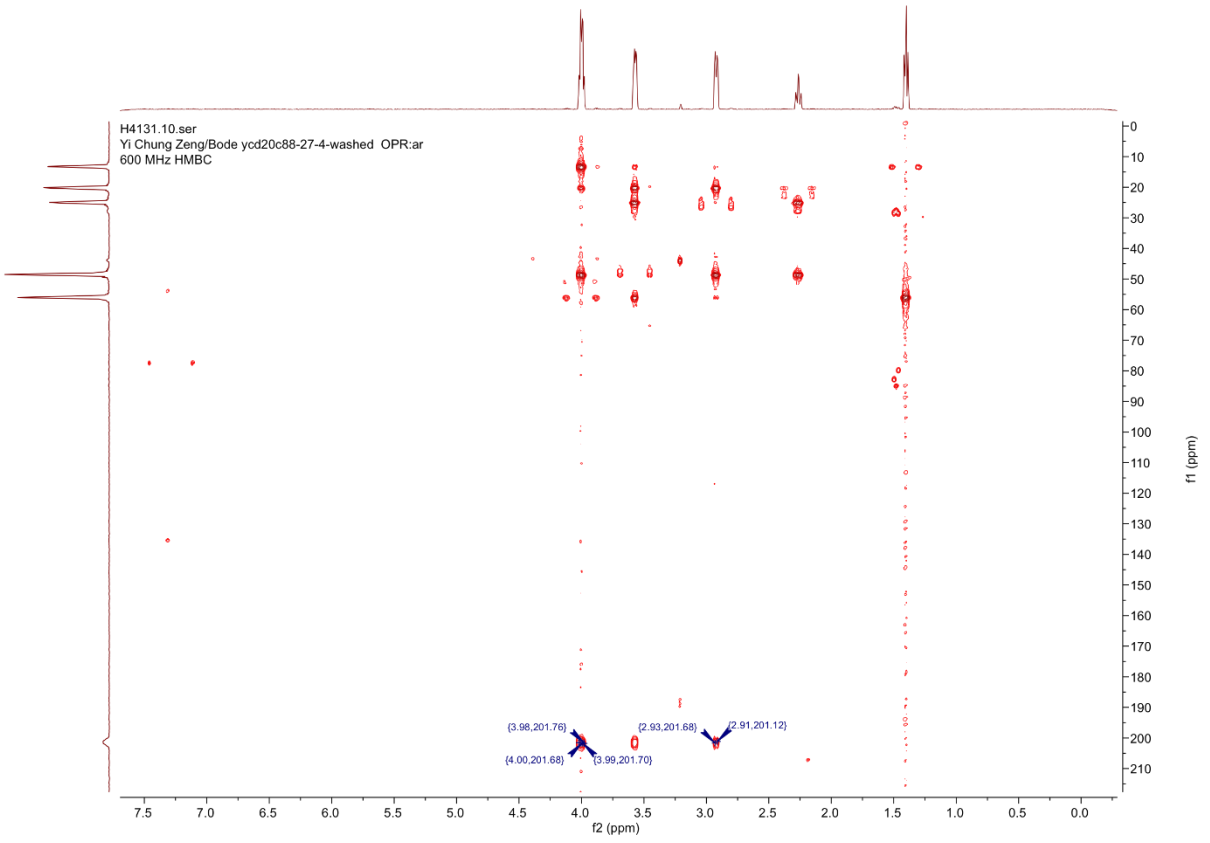


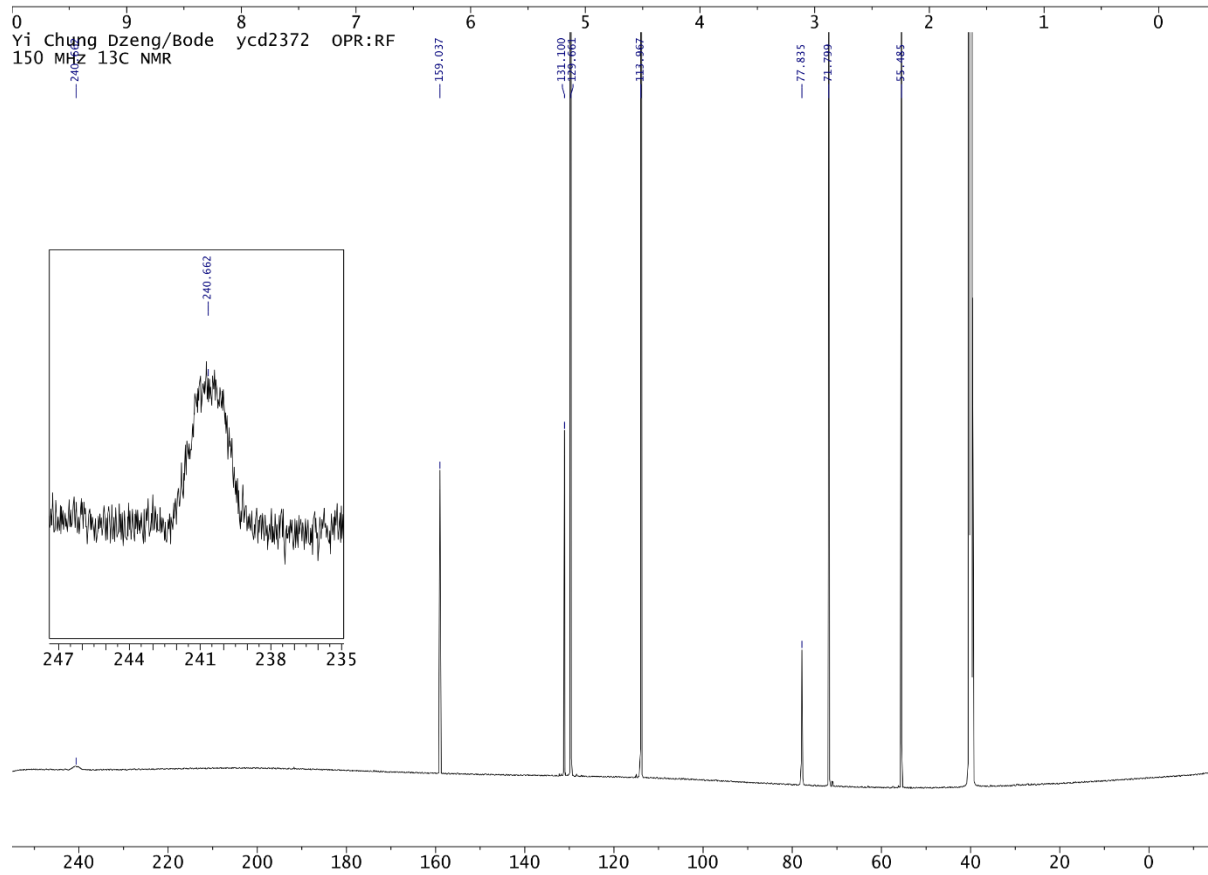
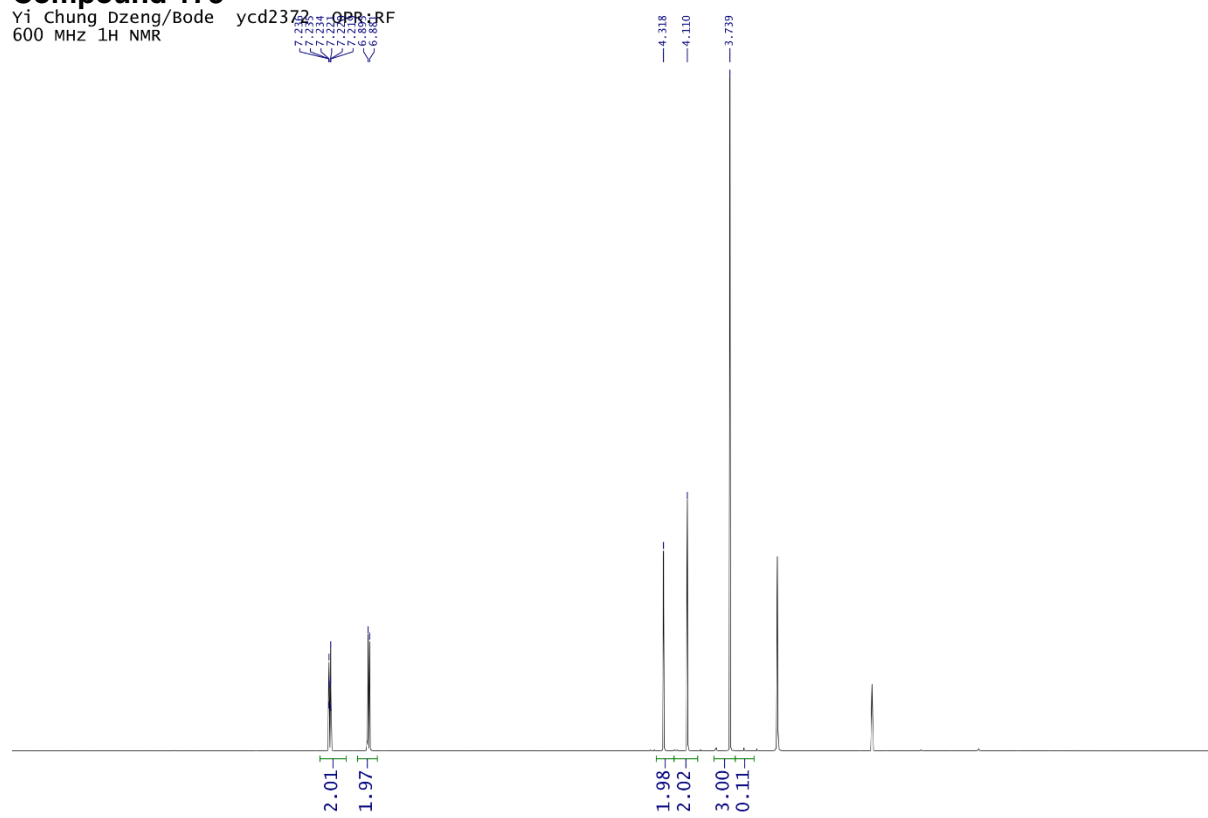
^{11}B 128 MHz

201112-1921-27-bdzeng-asc400.3.fid



NMR Spectra

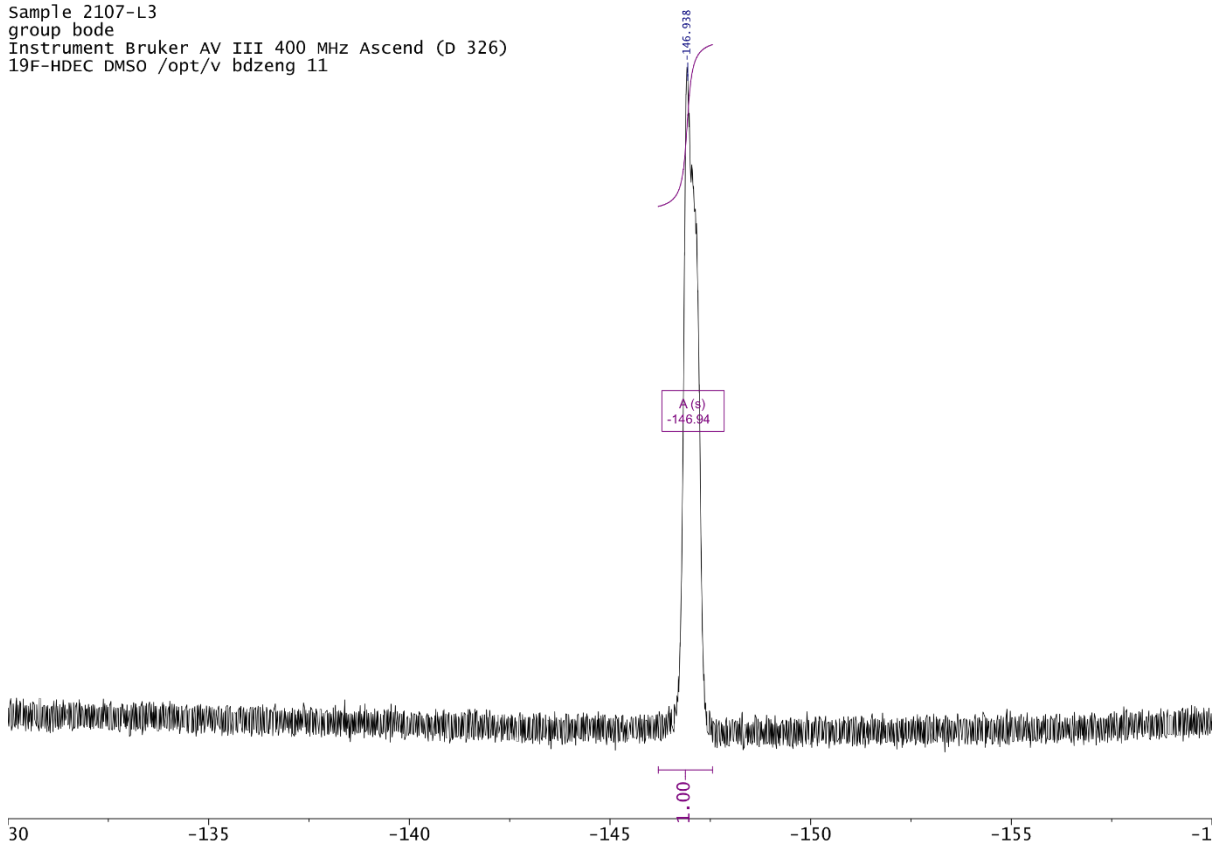


Compound 173Yi Chung Dzeng/Bode ycd2372 OPR:RF
600 MHz 1H NMR

NMR Spectra

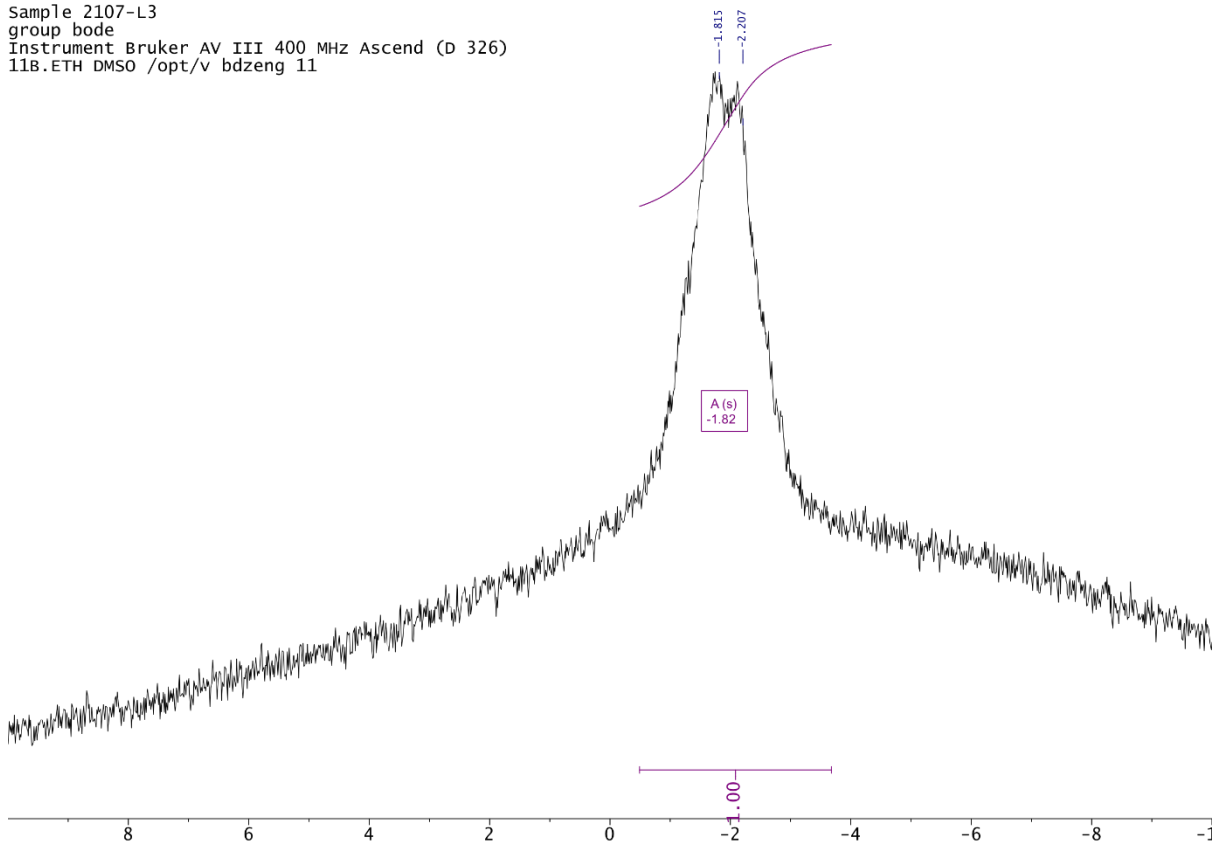
^{19}F 377 MHz

Sample 2107-L3
group bode
Instrument Bruker AV III 400 MHz Ascend (D 326)
19F-HDEC DMSO /opt/v bdzeng 11



^{11}B 128 MHz

Sample 2107-L3
group bode
Instrument Bruker AV III 400 MHz Ascend (D 326)
11B.ETH DMSO /opt/v bdzeng 11



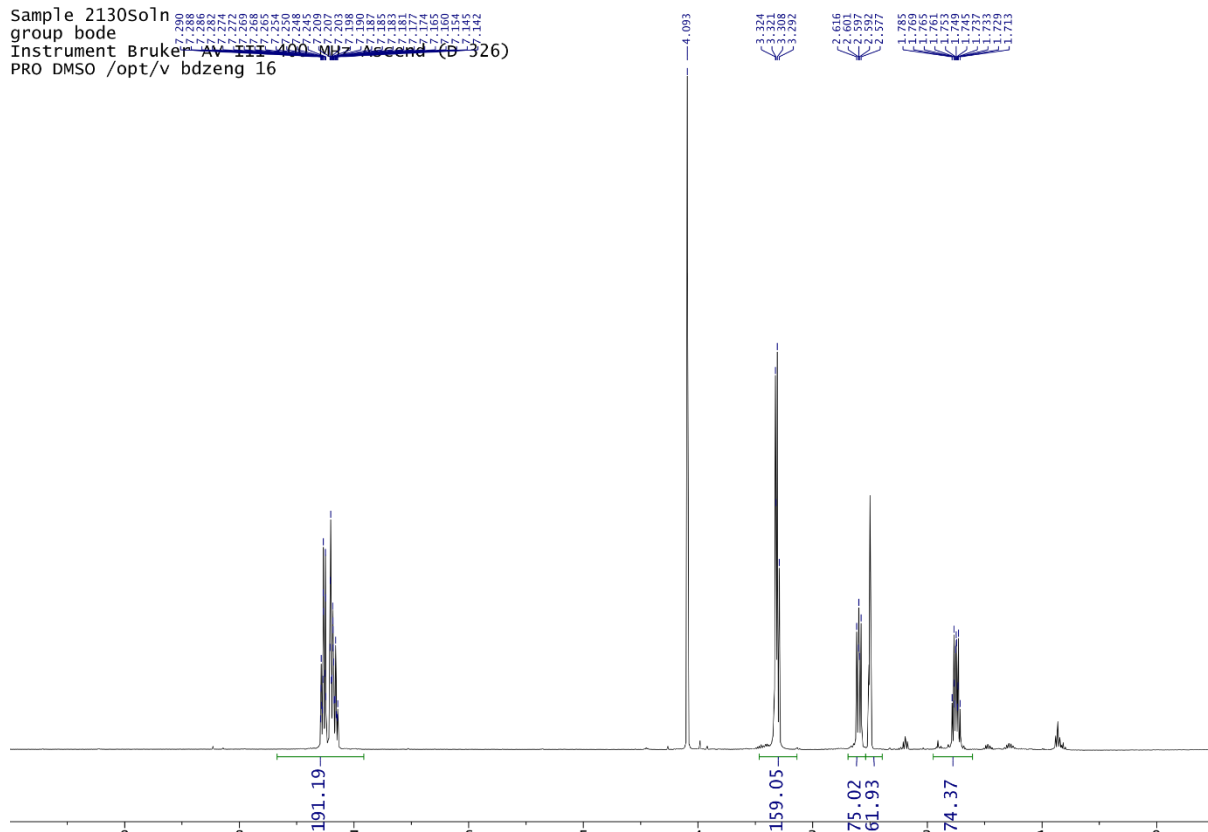
Compound 185

¹H 400 MHz

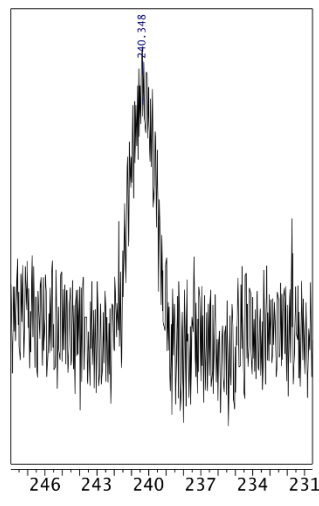
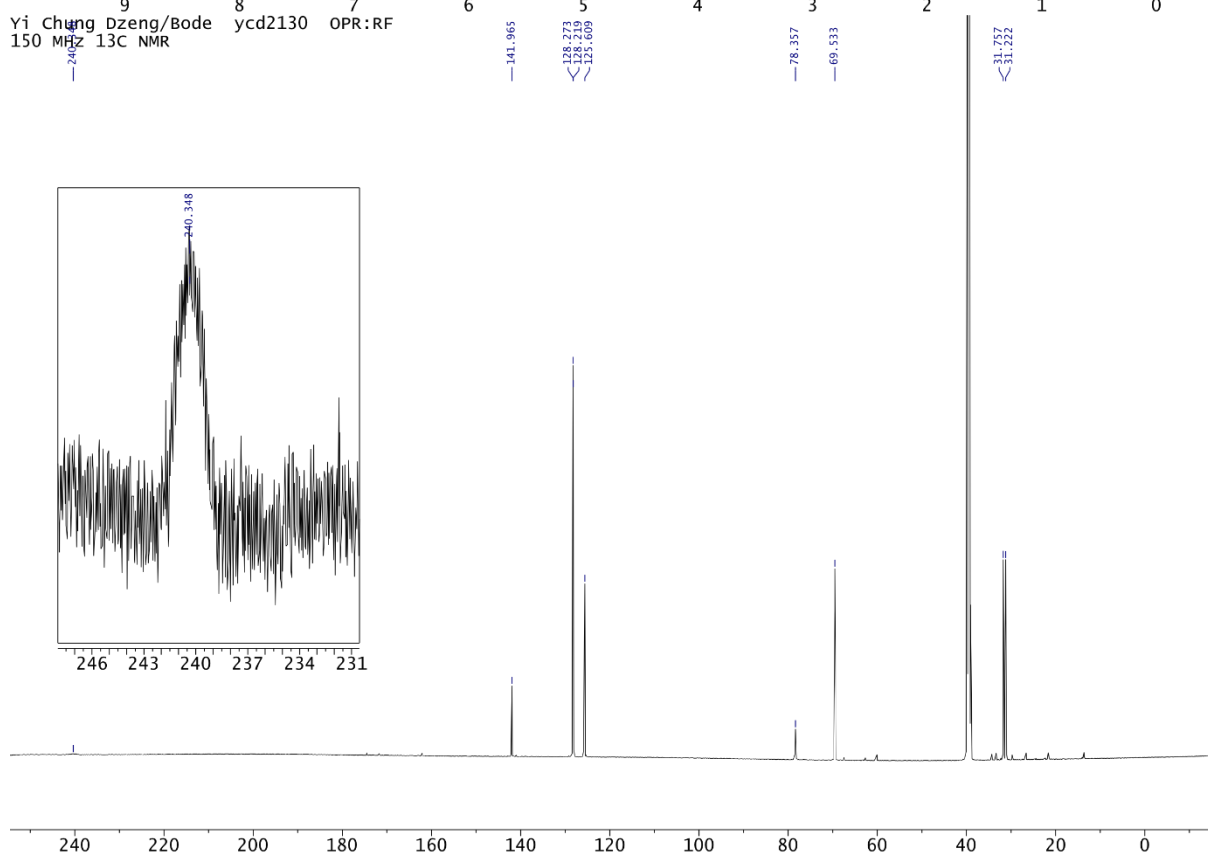
Sample 2130soln

group bode

Instrument Bruker AV 400 MHz Ascend (b-326)
 PRO DMSO /opt/v bdzeng 16



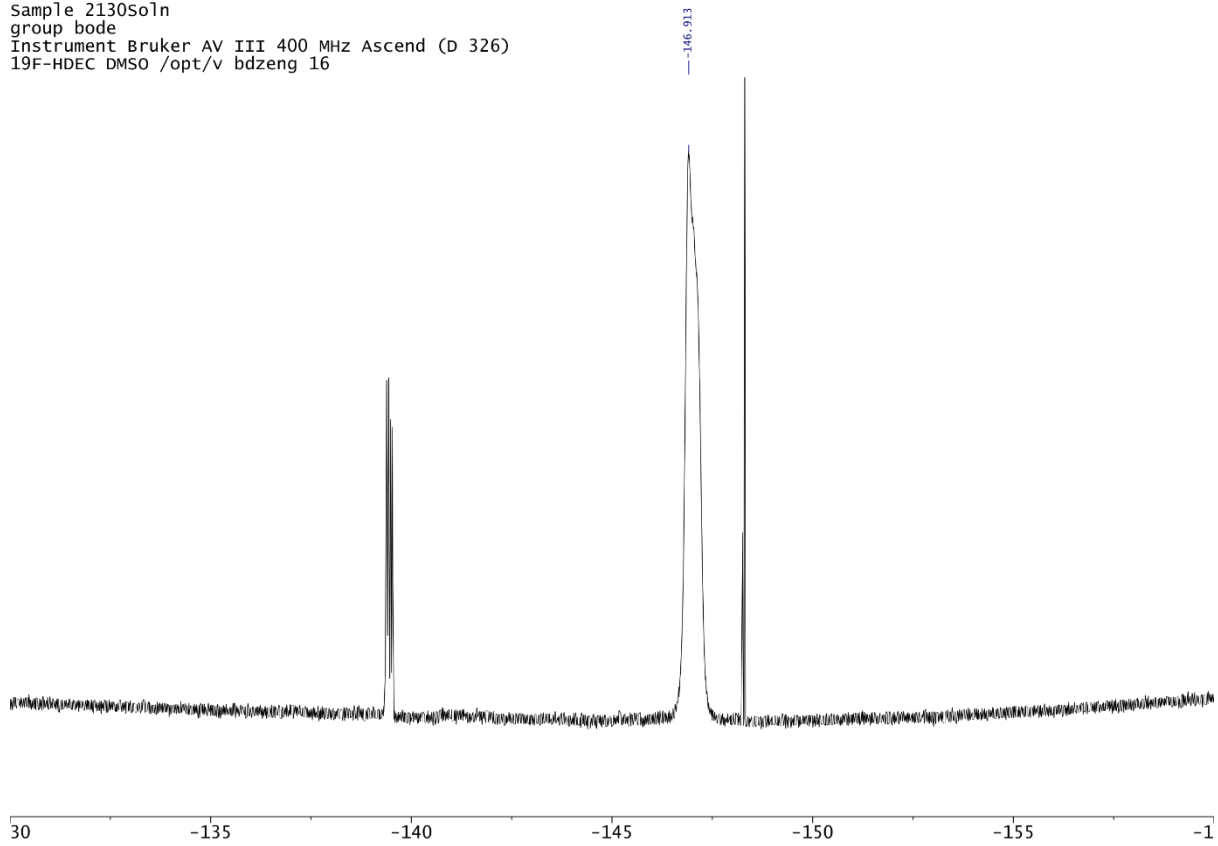
Yi Chung Dzung/Bode ycd2130 OPR:RF
 150 MHz 13C NMR



NMR Spectra

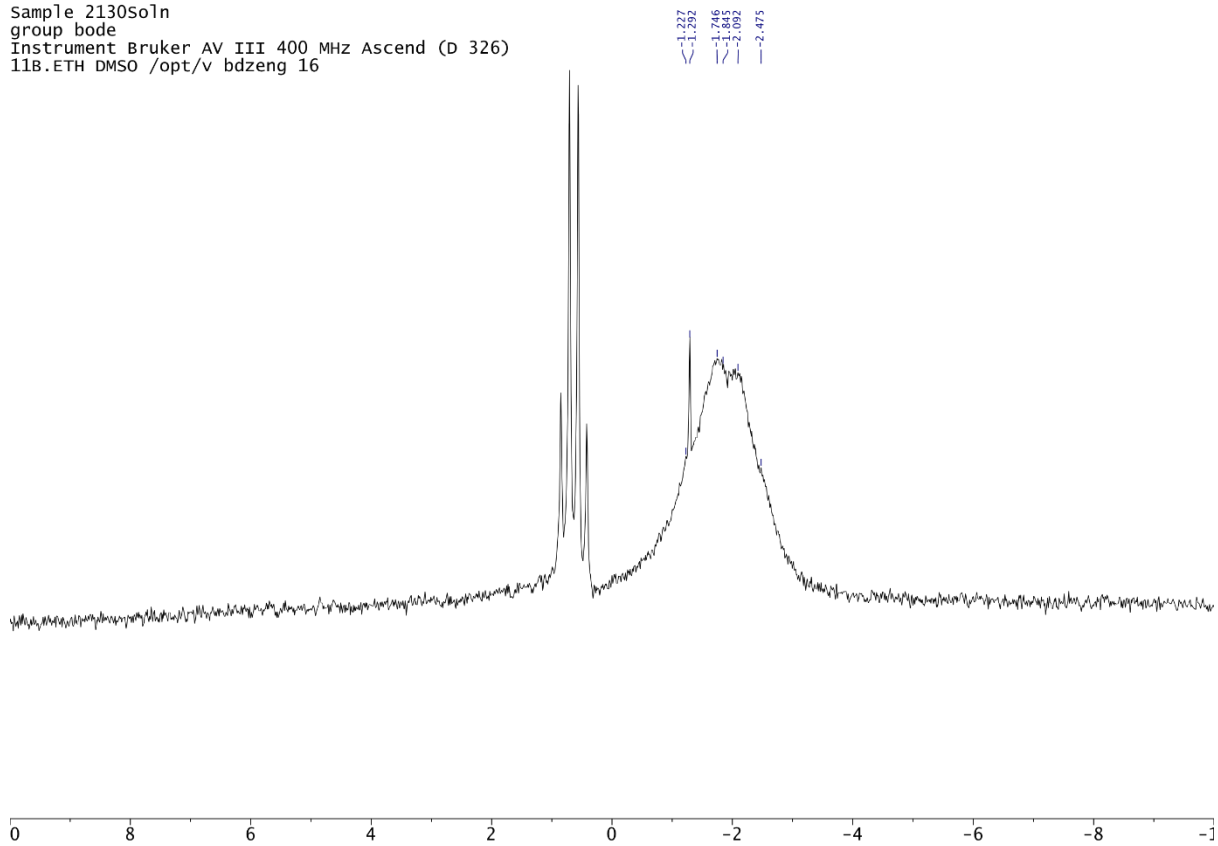
^{19}F 377 MHz

Sample 2130soln
group bode
Instrument Bruker AV III 400 MHz Ascend (D 326)
19F-HDEC DMSO /opt/v bdzeng 16



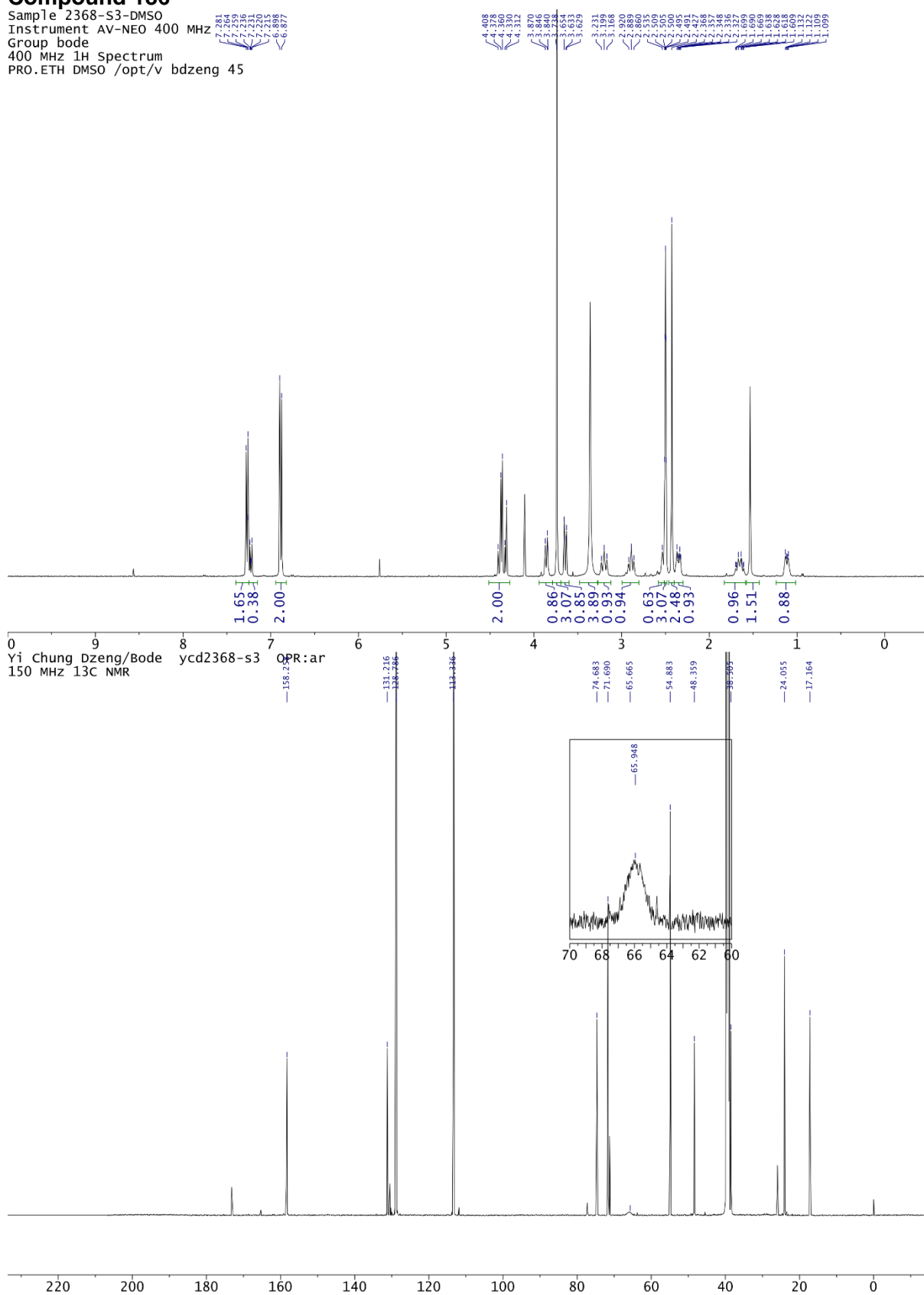
^{11}B 128 MHz

Sample 2130soln
group bode
Instrument Bruker AV III 400 MHz Ascend (D 326)
11B.ETH DMSO /opt/v bdzeng 16



Compound 186

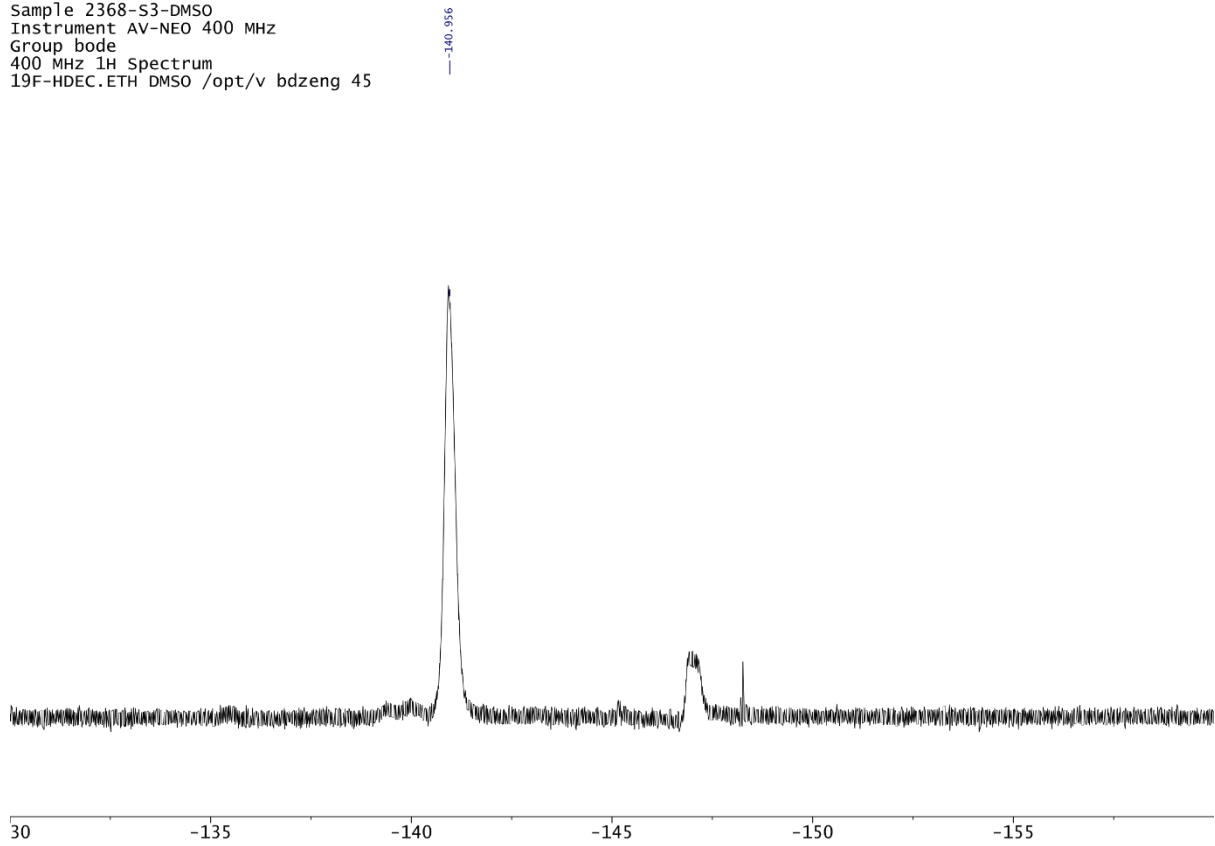
Sample 2368-S3-DMSO
 Instrument AV-NEO 400 MHz
 Group bode
 400 MHz 1H Spectrum
 PRO.ETH DMSO /opt/v bdzeng 45



NMR Spectra

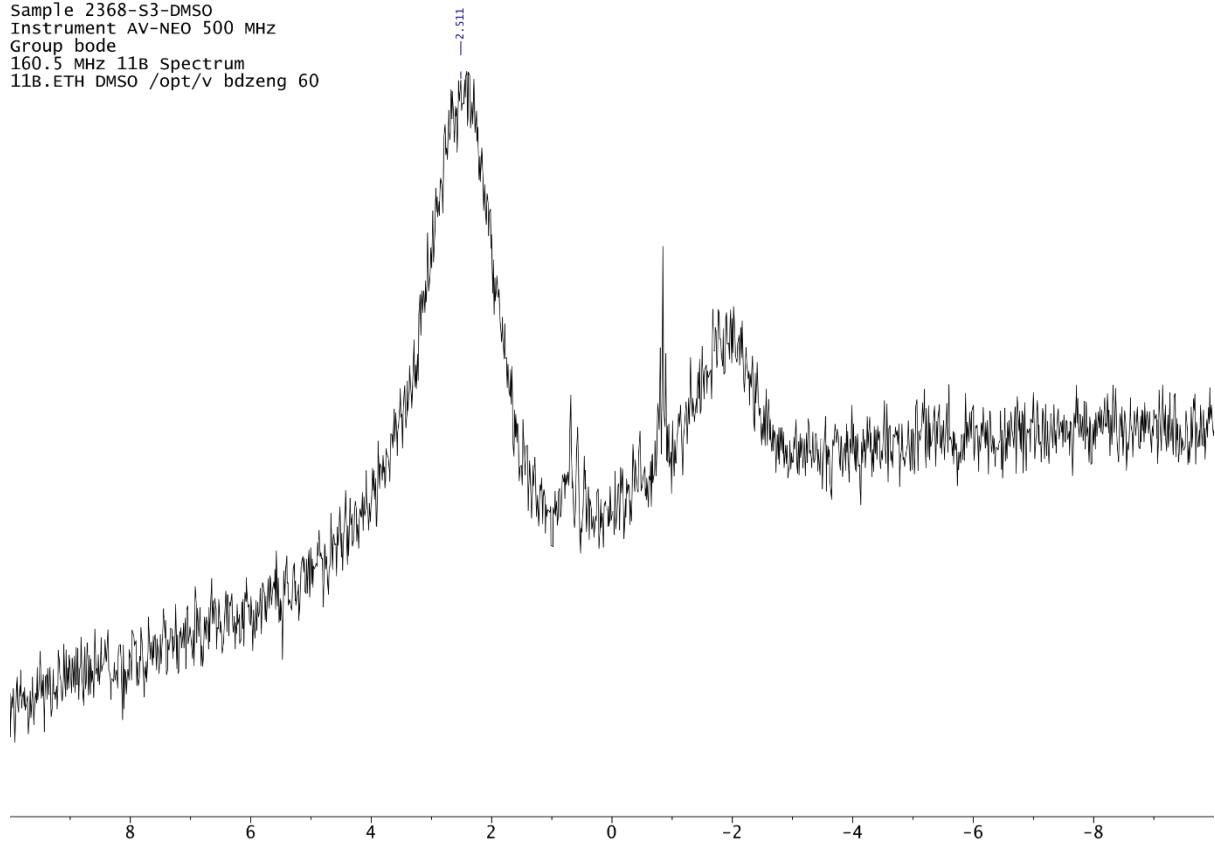
^{19}F 376 MHz

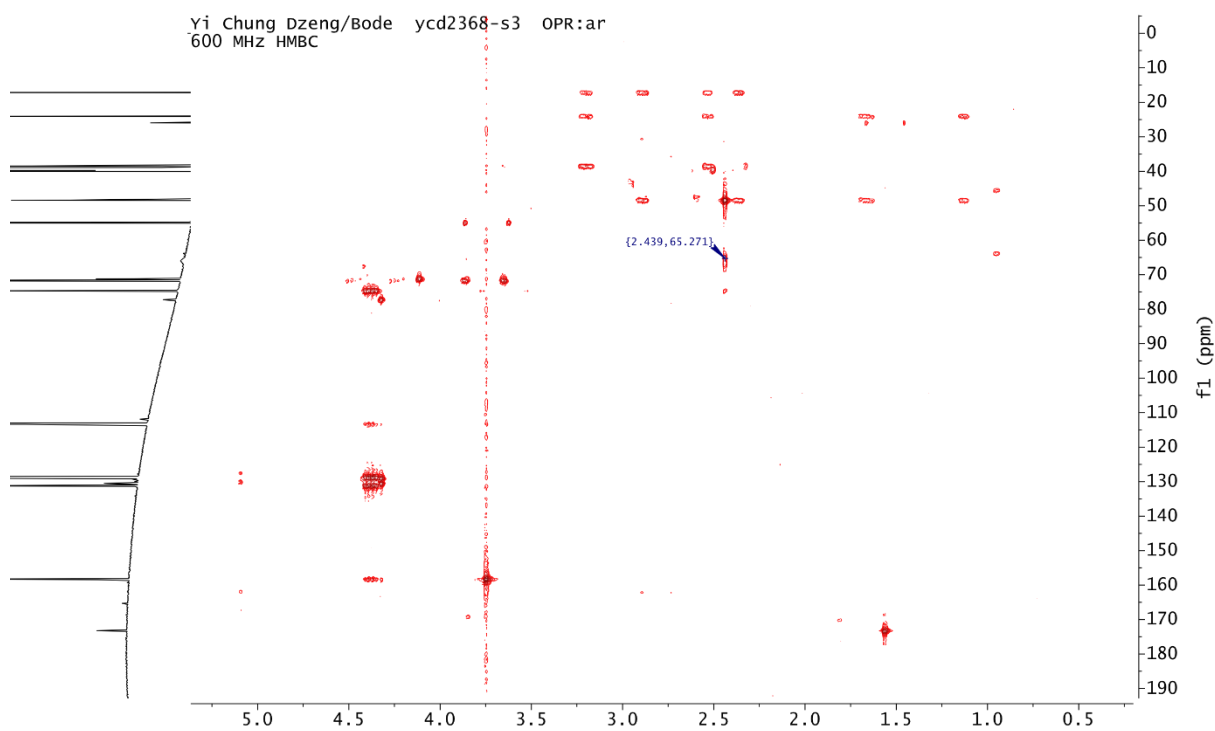
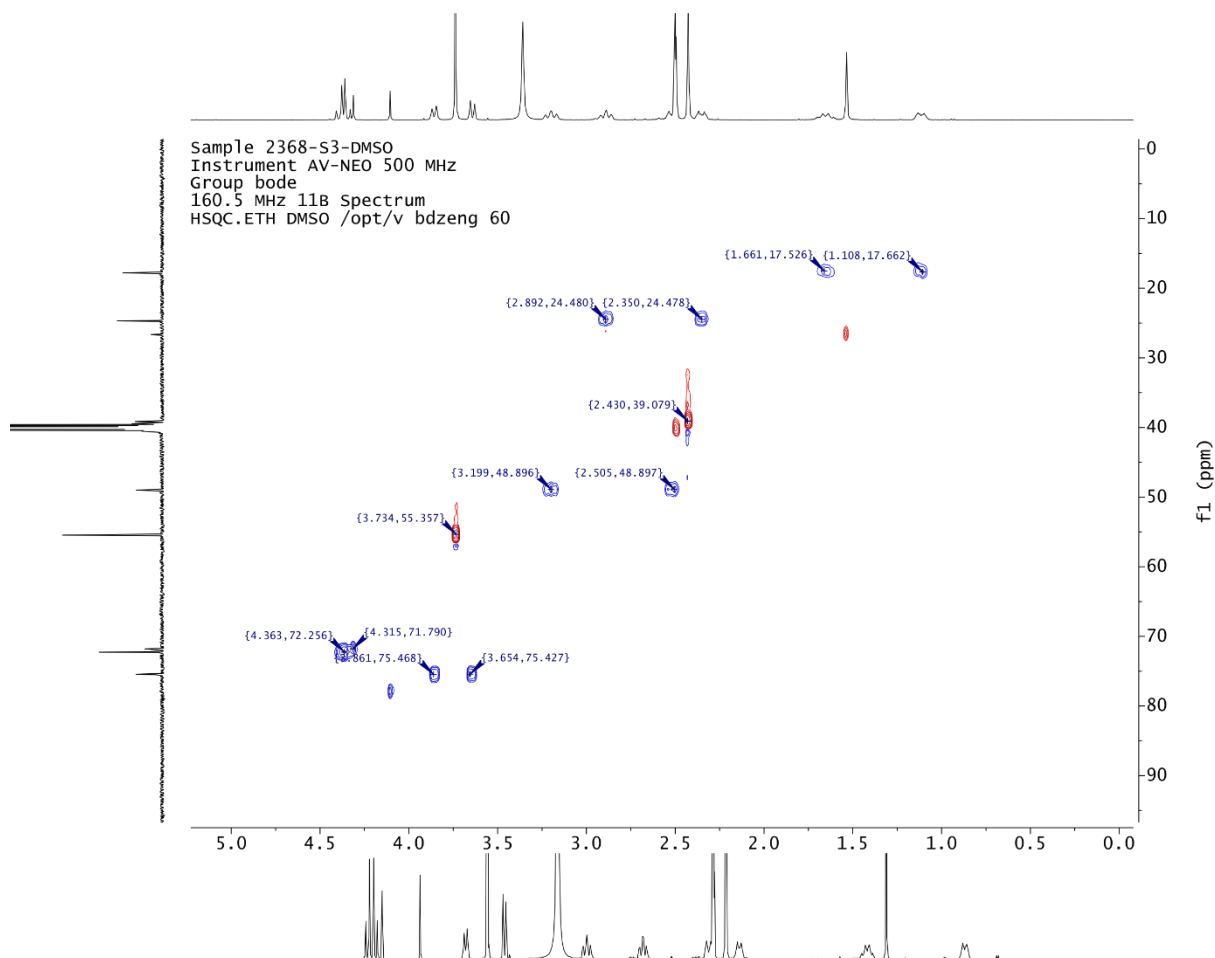
Sample 2368-S3-DMSO
Instrument AV-NEO 400 MHz
Group bode
400 MHz ^1H Spectrum
19F-HDEC.ETH DMSO /opt/v bdzeng 45



^{11}B 128 MHz

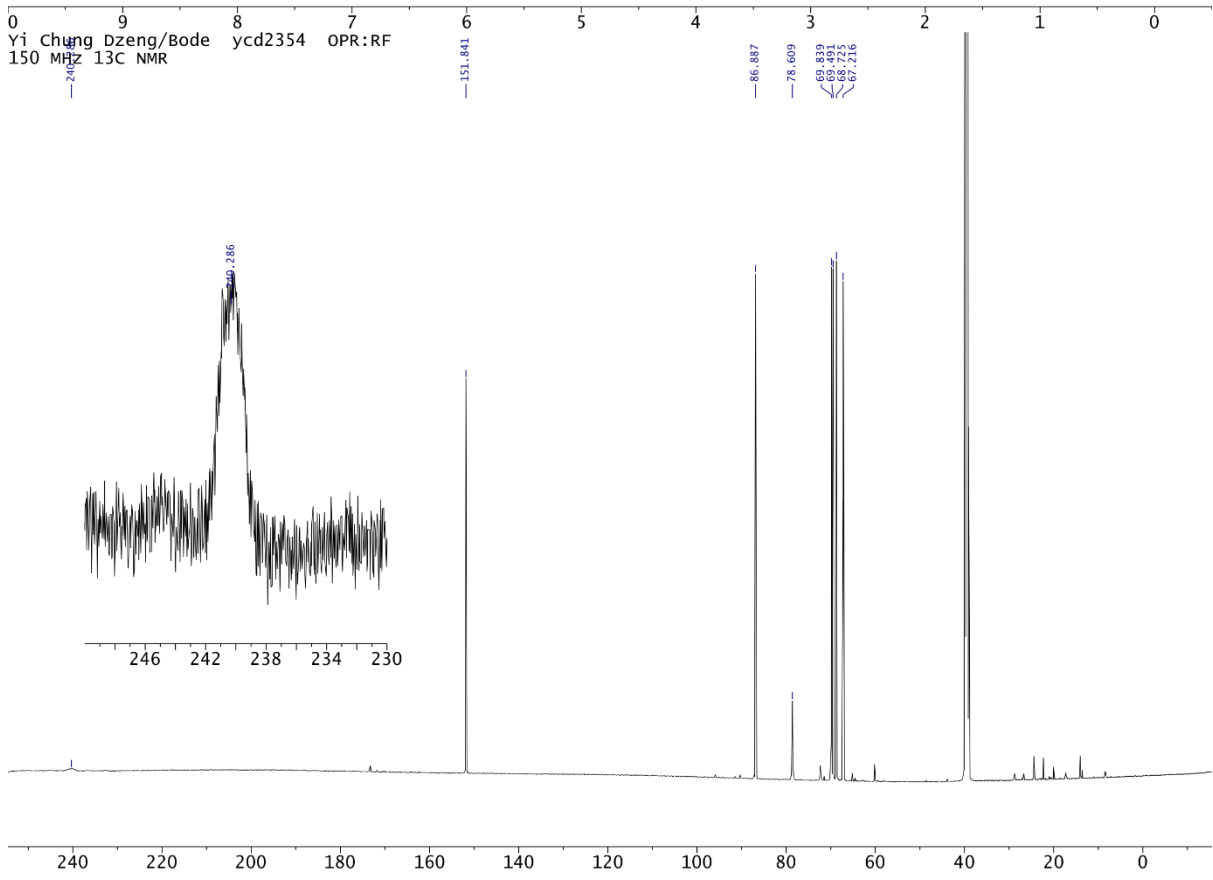
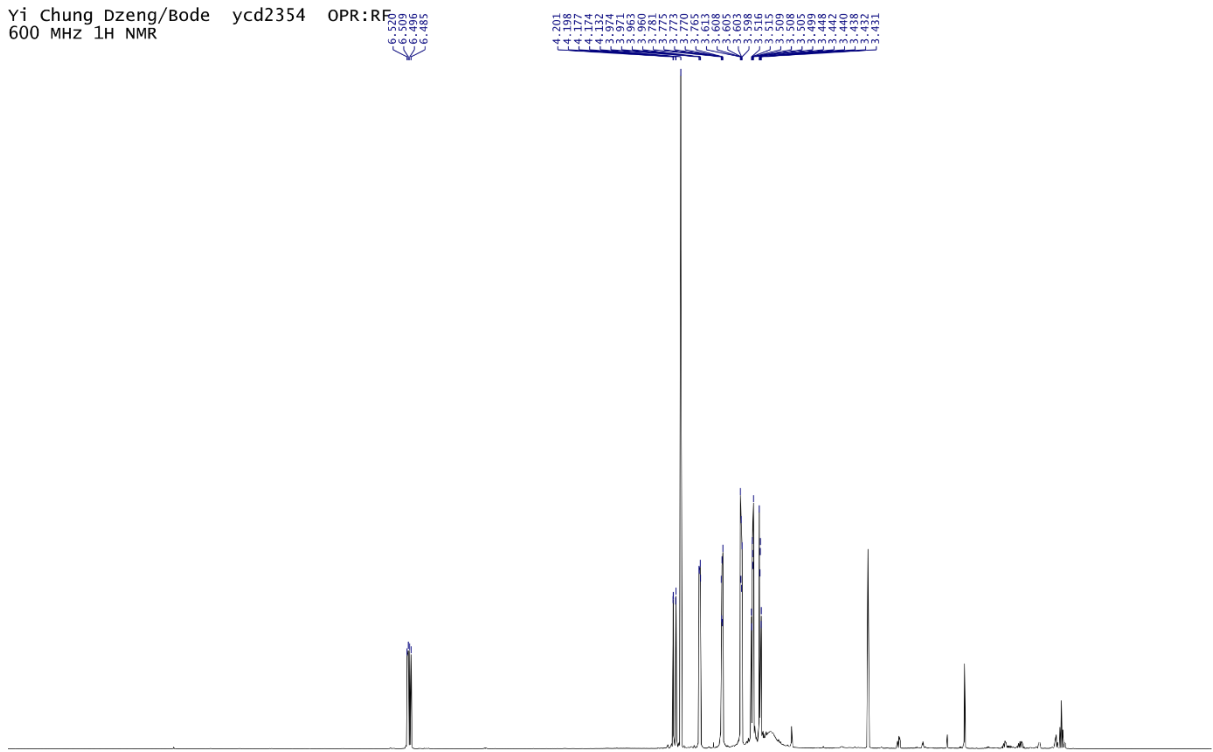
Sample 2368-S3-DMSO
Instrument AV-NEO 500 MHz
Group bode
160.5 MHz ^{11}B Spectrum
11B.ETH DMSO /opt/v bdzeng 60





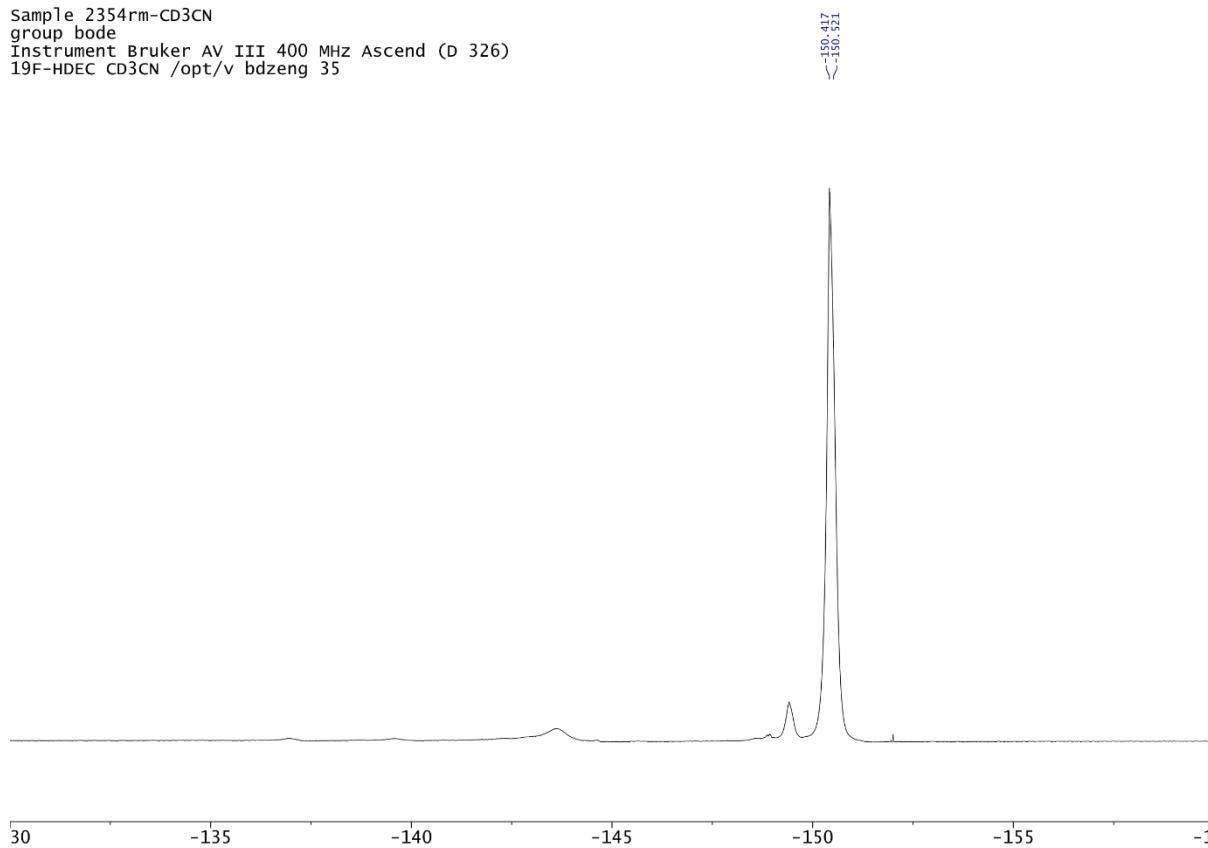
Compound 187

Yi Chung Dzeng/Bode ycd2354 OPR:RF
600 MHz 1H NMR

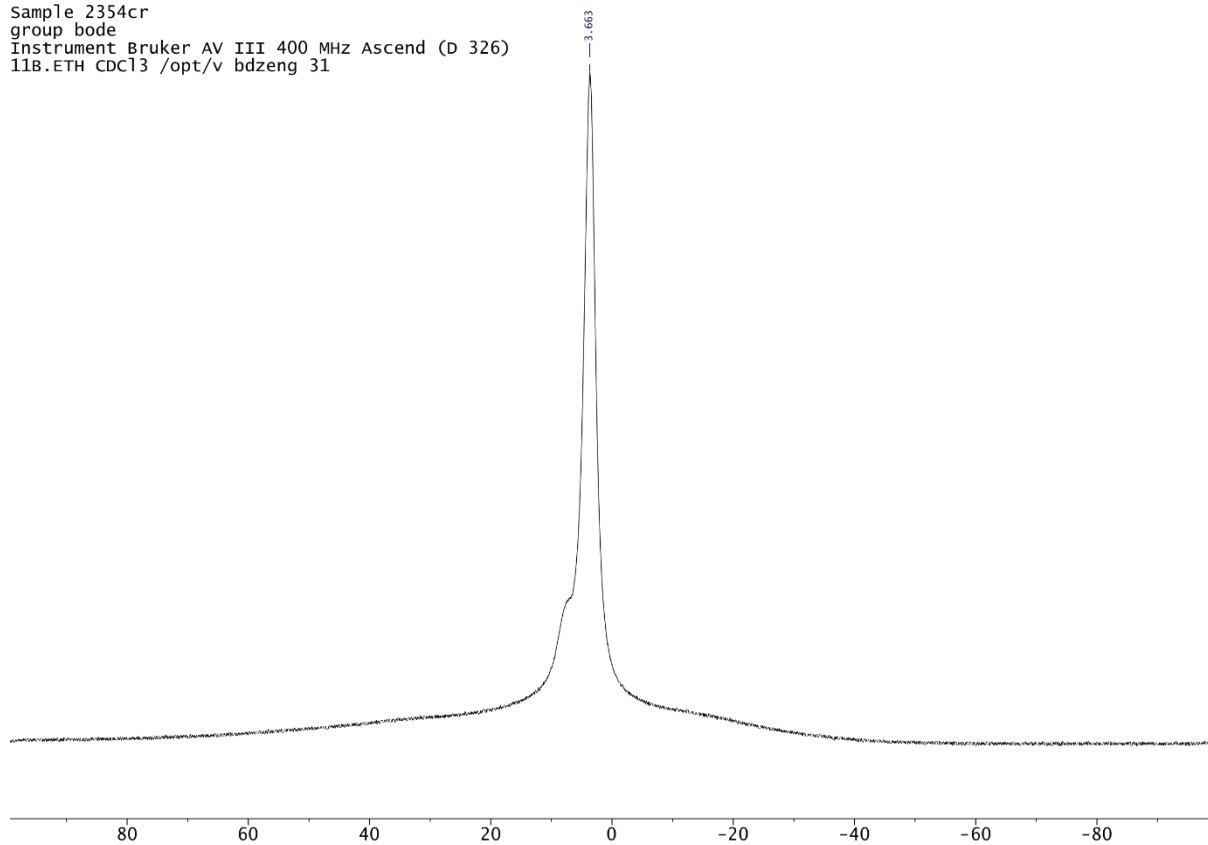


^{19}F 376 MHz

Sample 2354rm-CD3CN
group bode
Instrument Bruker AV III 400 MHz Ascend (D 326)
19F-HDEC CD3CN /opt/v bdzeng 35

 **^{11}B 128 MHz**

Sample 2354cr
group bode
Instrument Bruker AV III 400 MHz Ascend (D 326)
11B.ETH CDC13 /opt/v bdzeng 31



NMR Spectra

Compound 188

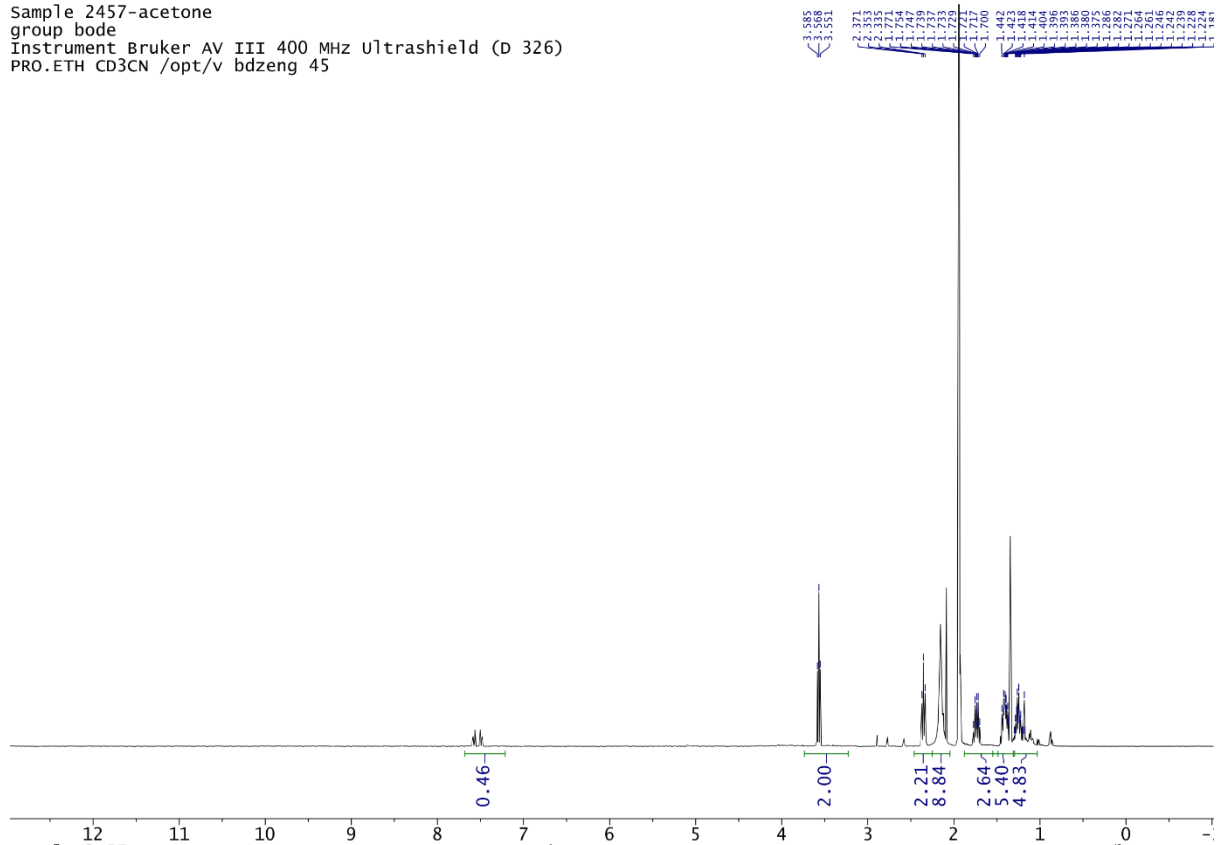
^1H 400 MHz

Sample 2457-acetone

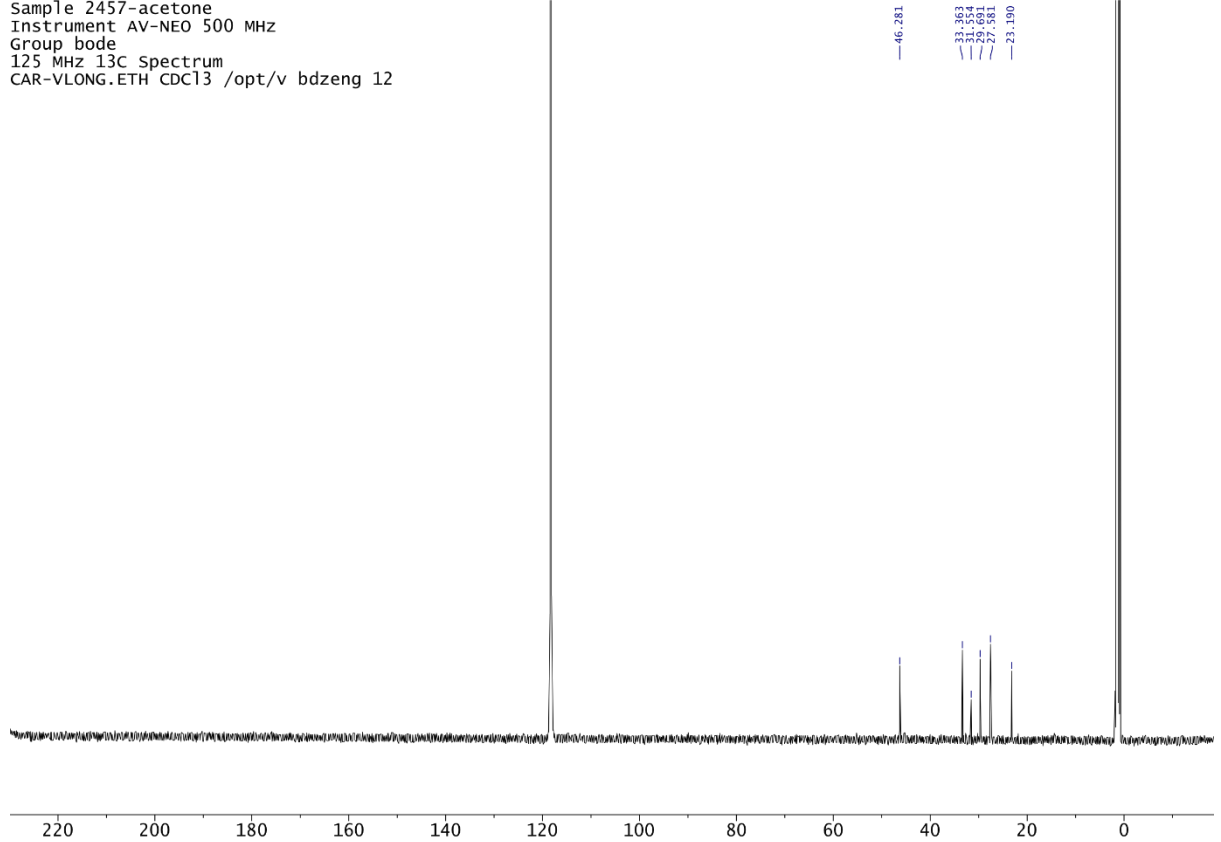
group bode

Instrument Bruker AV III 400 MHz Ultrashield (D 326)

PRO.ETH CD3CN /opt/v bdzeng 45

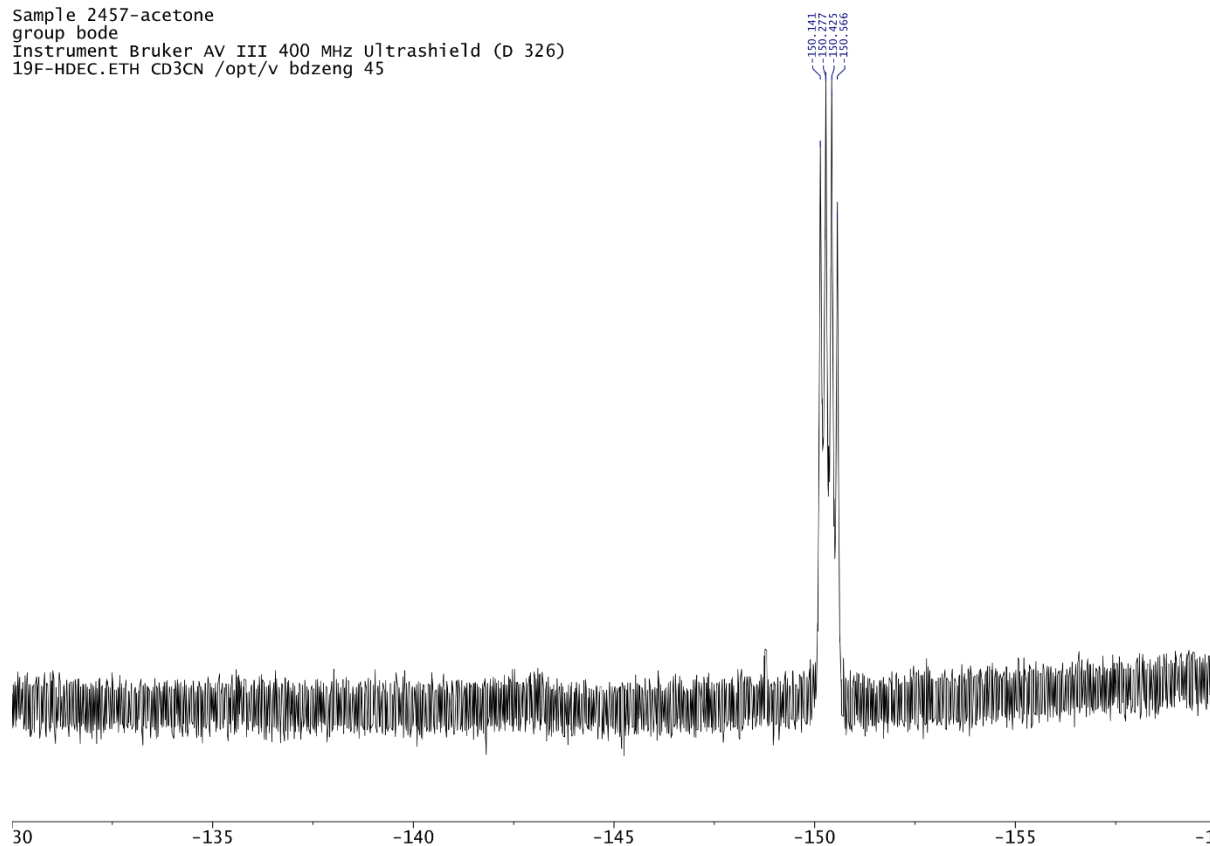


Sample 2457-acetone
Instrument AV-NEO 500 MHz
Group bode
125 MHz ^{13}C Spectrum
CAR-VLONG.ETH CDC13 /opt/v bdzeng 12



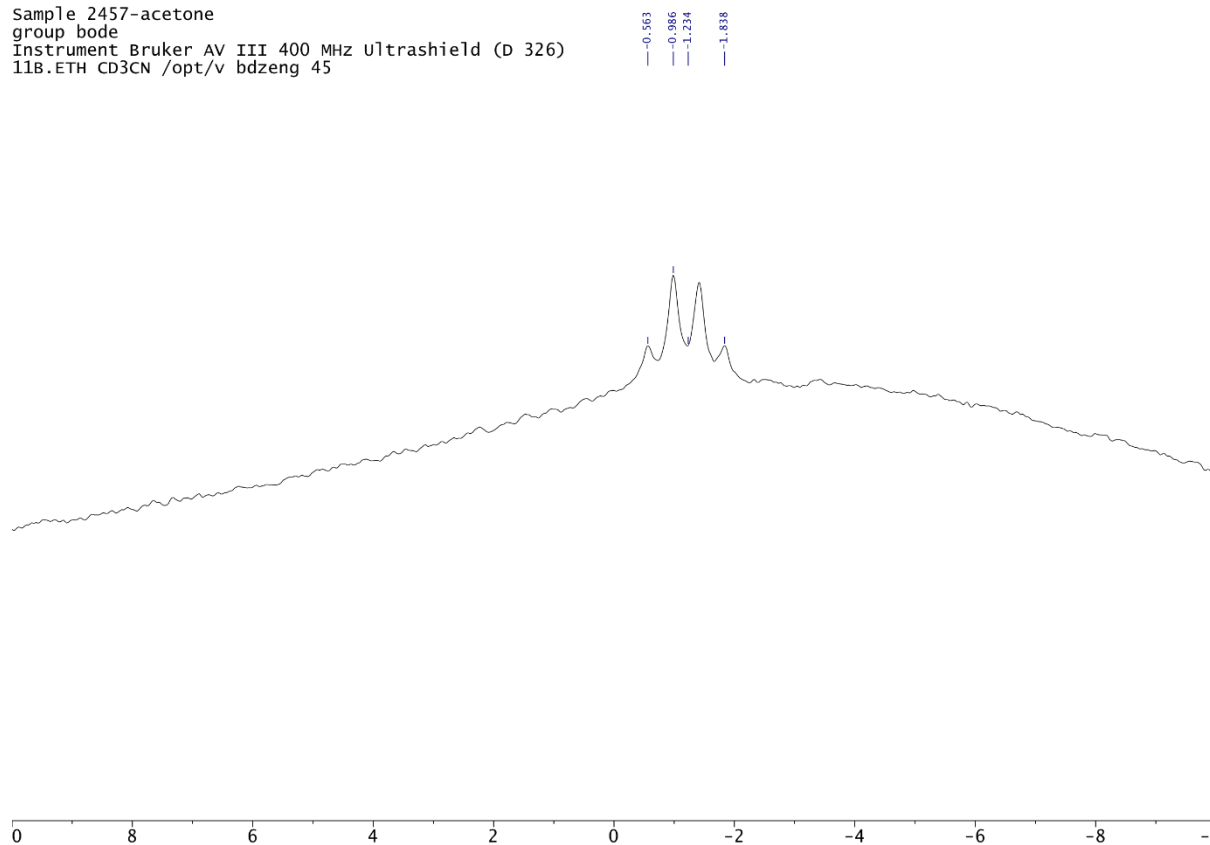
¹⁹F 376 MHz

Sample 2457-acetone
 group bode
 Instrument Bruker AV III 400 MHz Ultrashield (D 326)
 19F-HDEC.ETH CD3CN /opt/v bdzeng 45



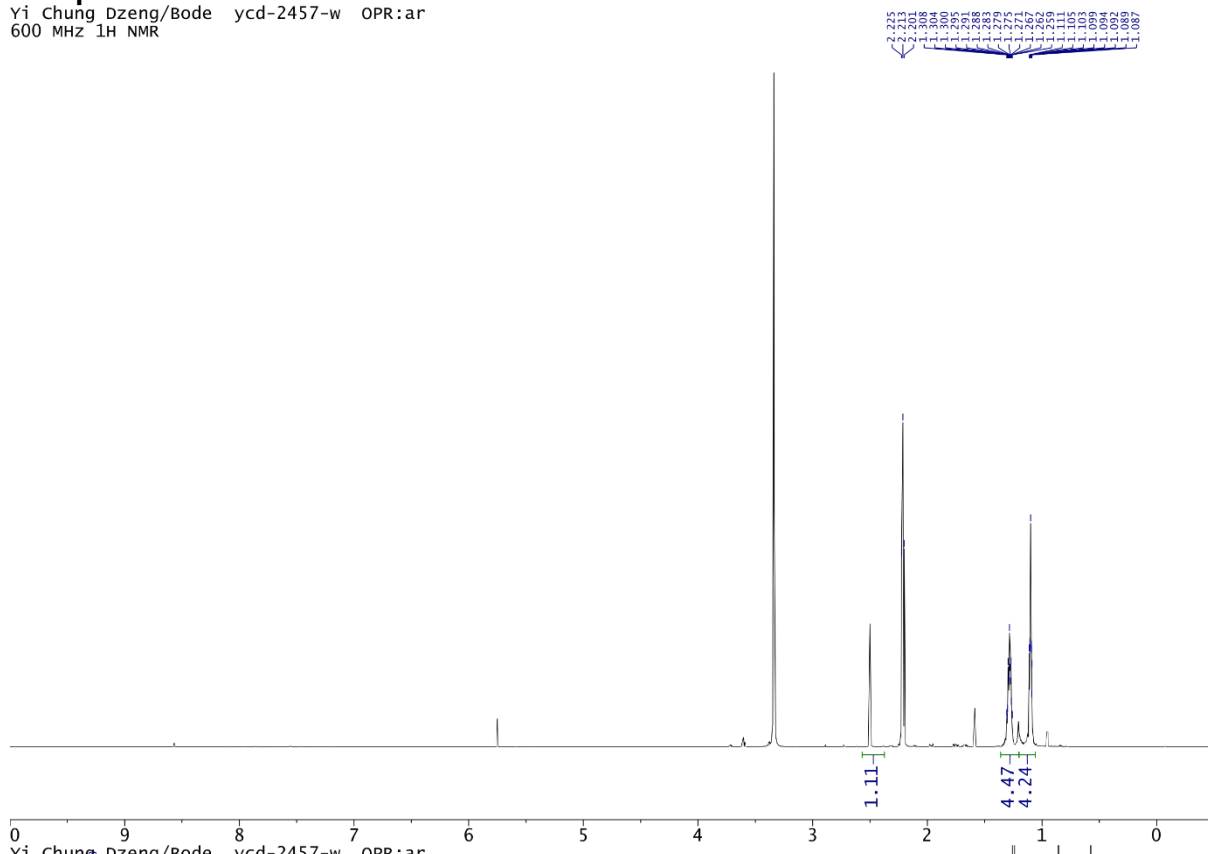
¹¹B 128 MHz

Sample 2457-acetone
 group bode
 Instrument Bruker AV III 400 MHz Ultrashield (D 326)
 11B.ETH CD3CN /opt/v bdzeng 45

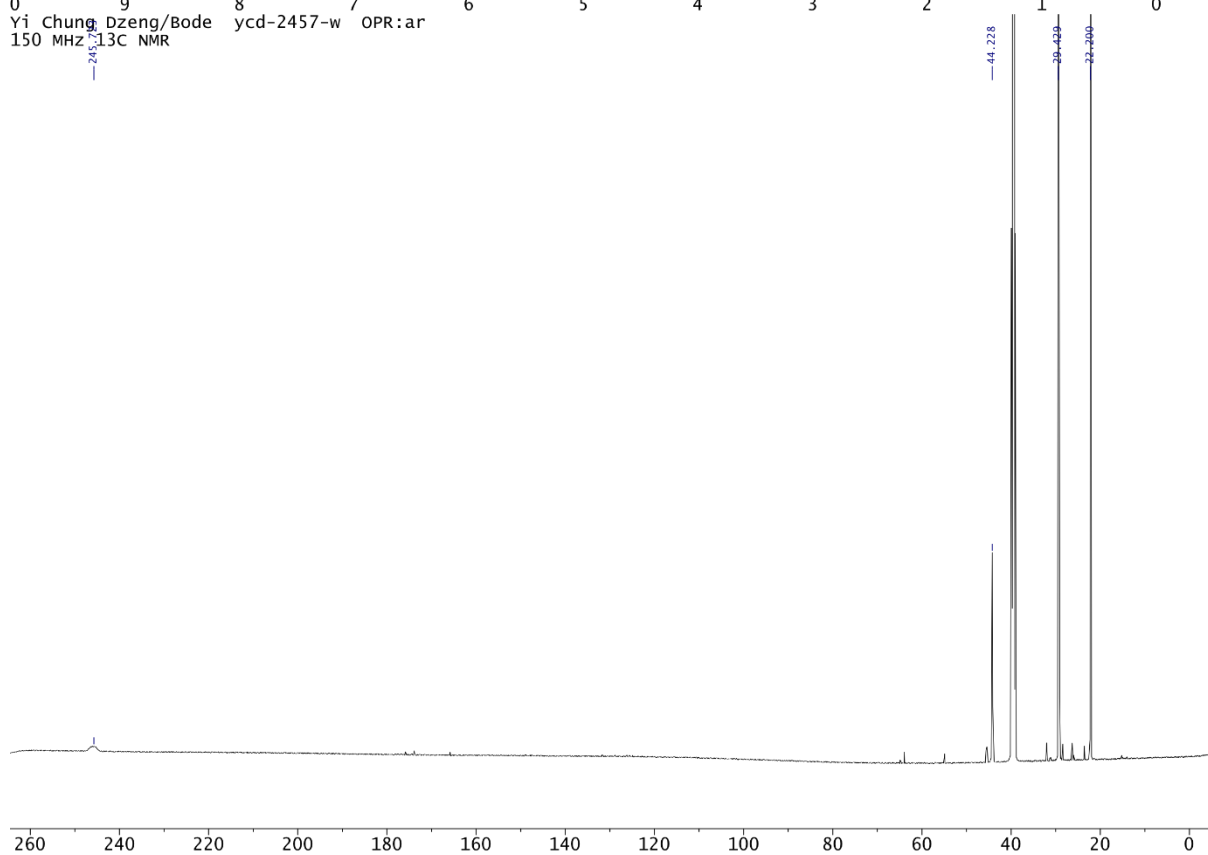


Compound 189

Yi Chung Dzeng/Bode ycd-2457-w OPR:ar
600 MHz ¹H NMR



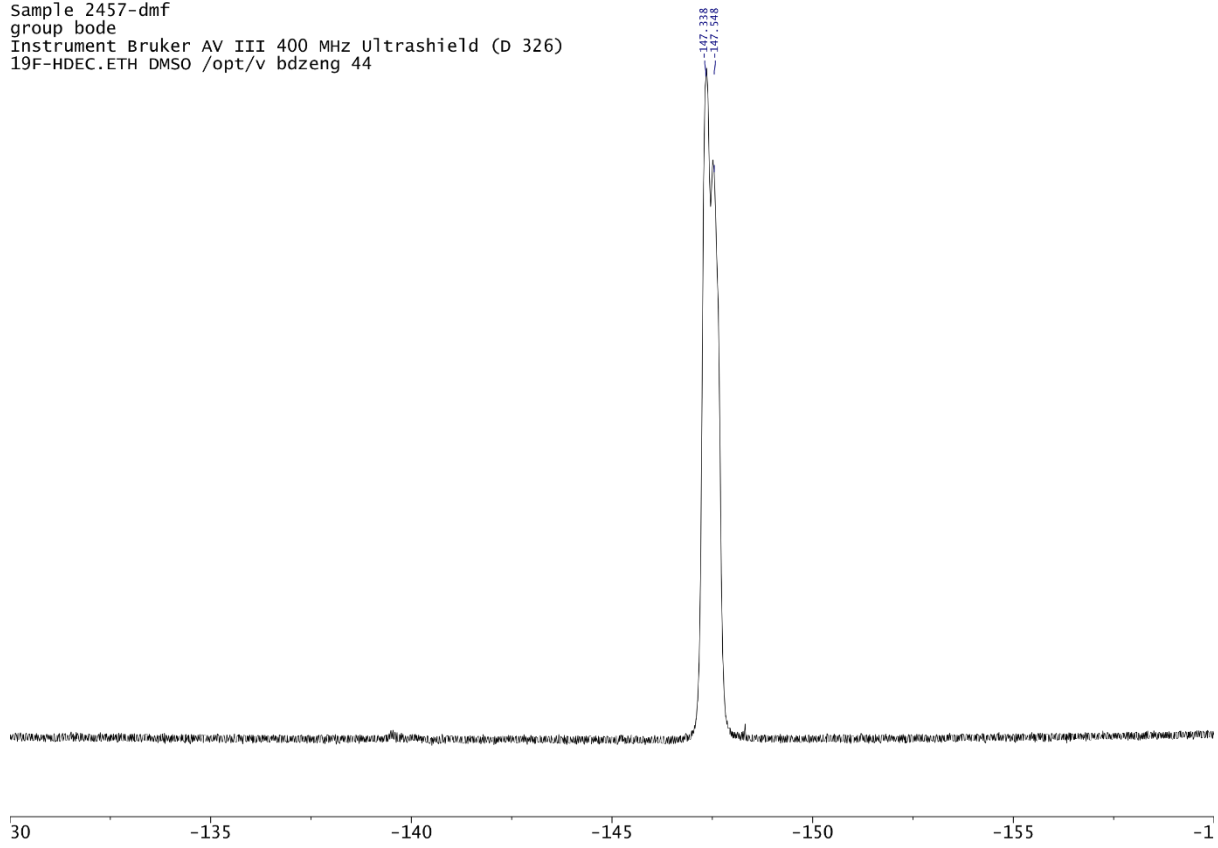
Yi Chung Dzeng/Bode ycd-2457-w OPR:ar
150 MHz ¹³C NMR



NMR Spectra

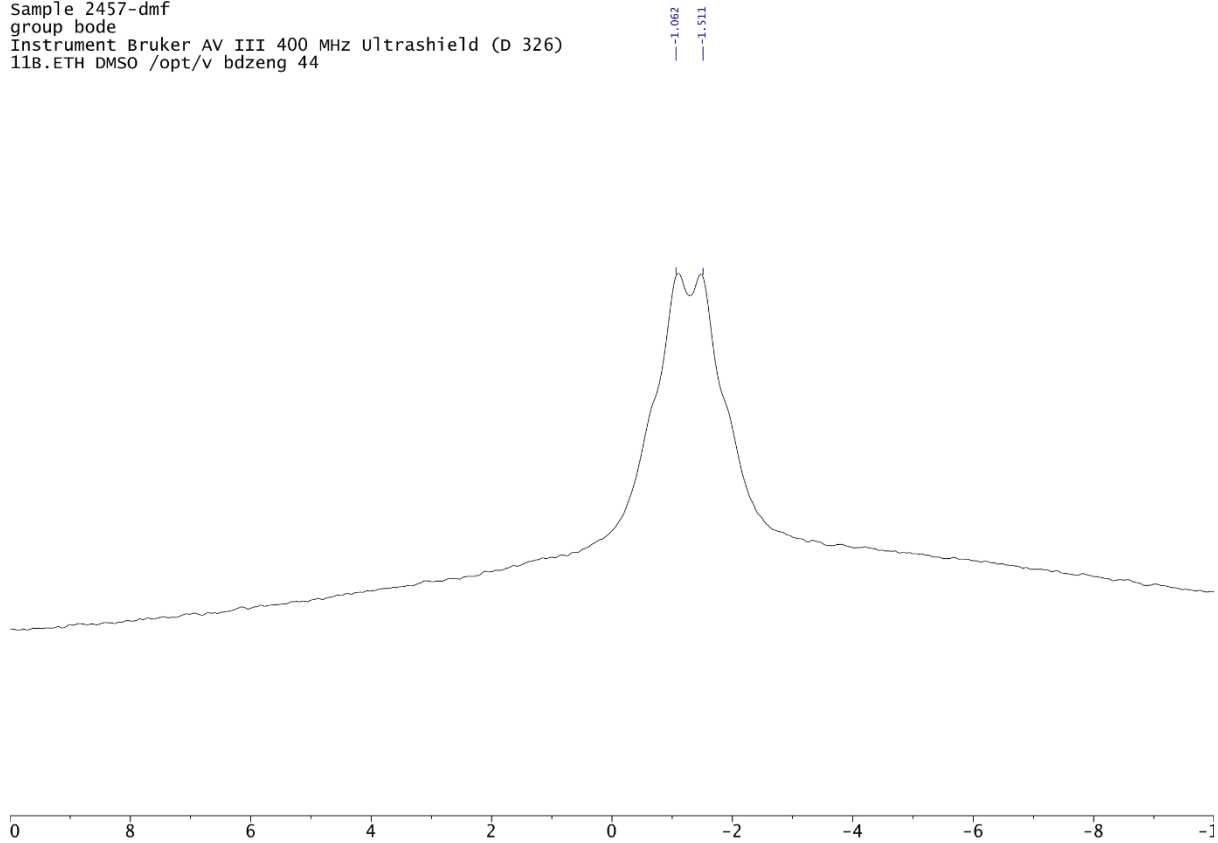
^{19}F 376 MHz

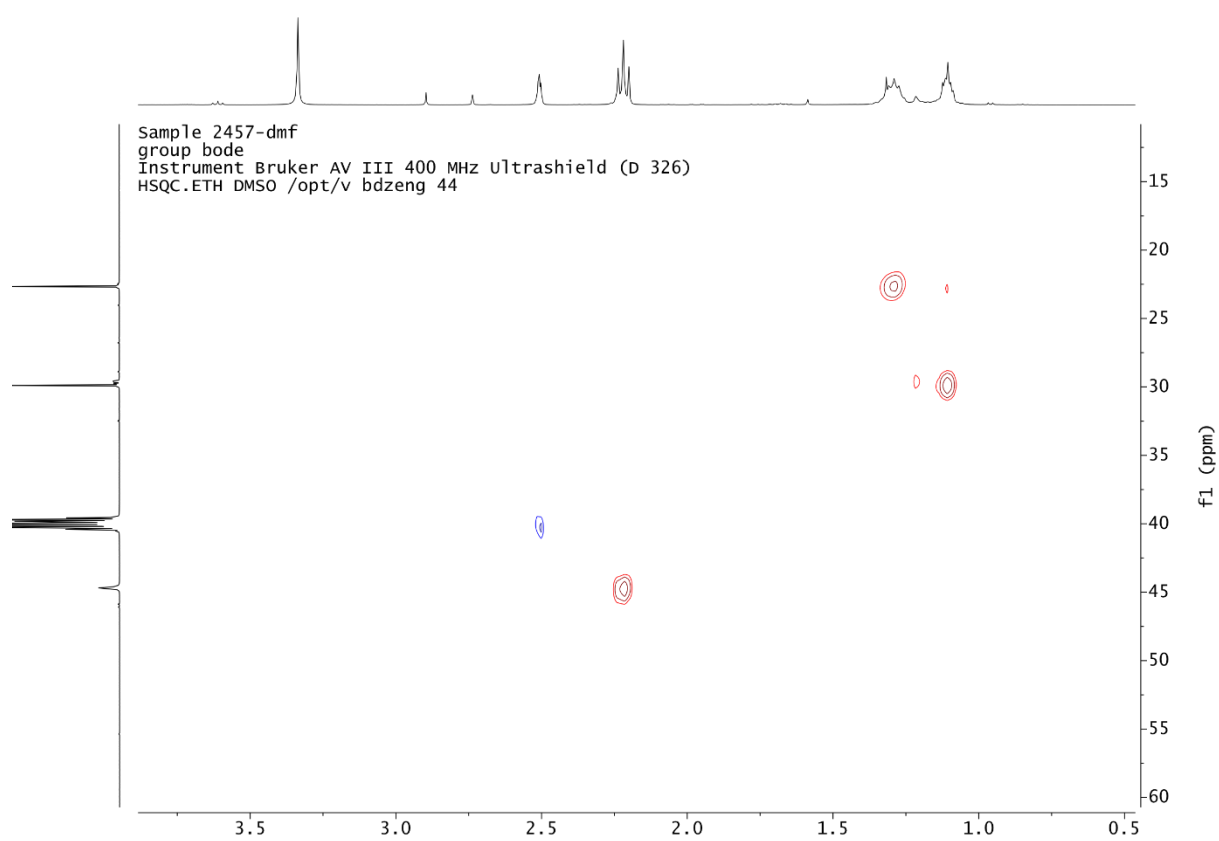
Sample 2457-dmf
group bode
Instrument Bruker AV III 400 MHz Ultrashield (D 326)
19F-HDEC.ETH DMSO /opt/v bdzeng 44



^{11}B 128 MHz

Sample 2457-dmf
group bode
Instrument Bruker AV III 400 MHz Ultrashield (D 326)
11B.ETH DMSO /opt/v bdzeng 44

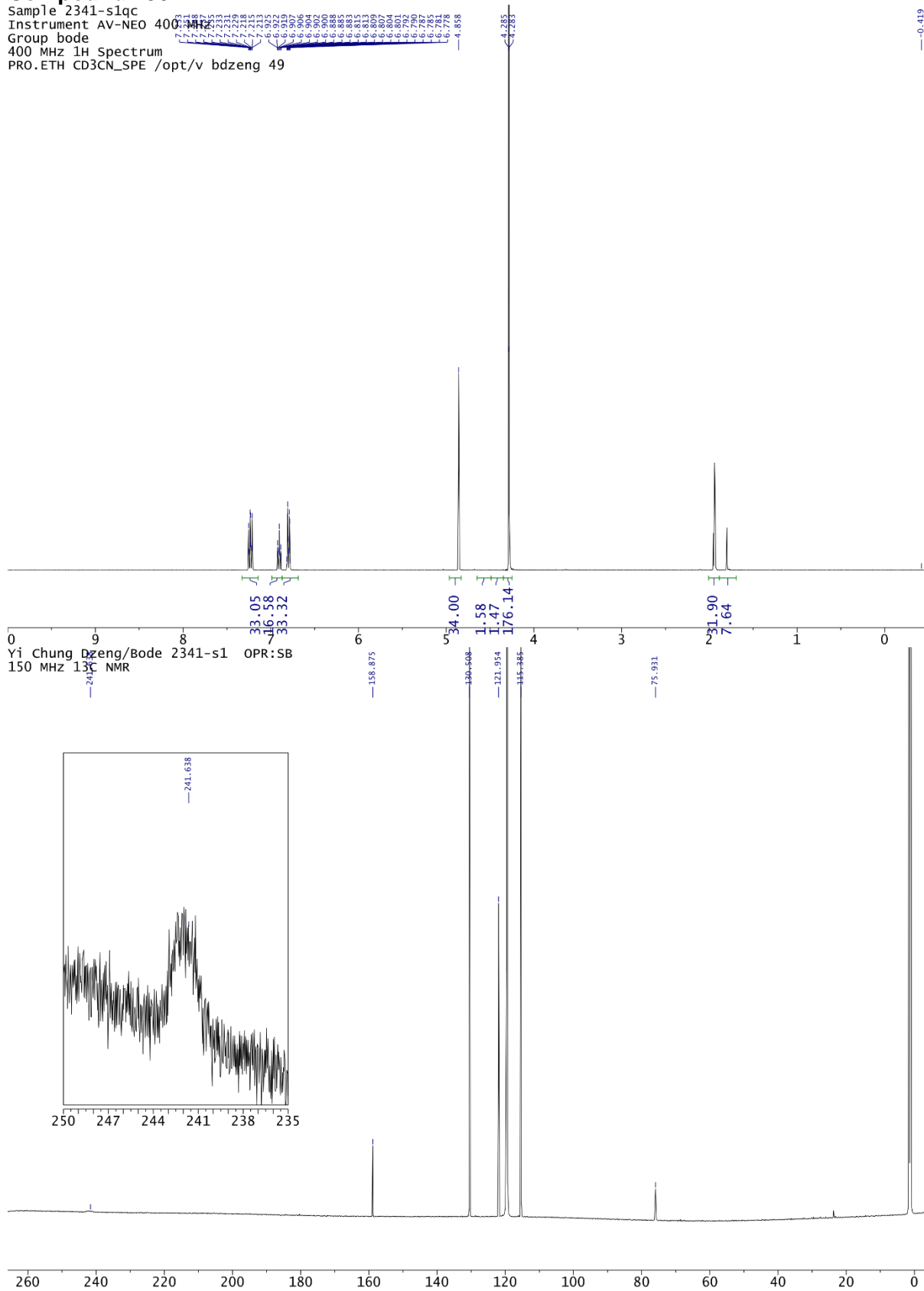




NMR Spectra

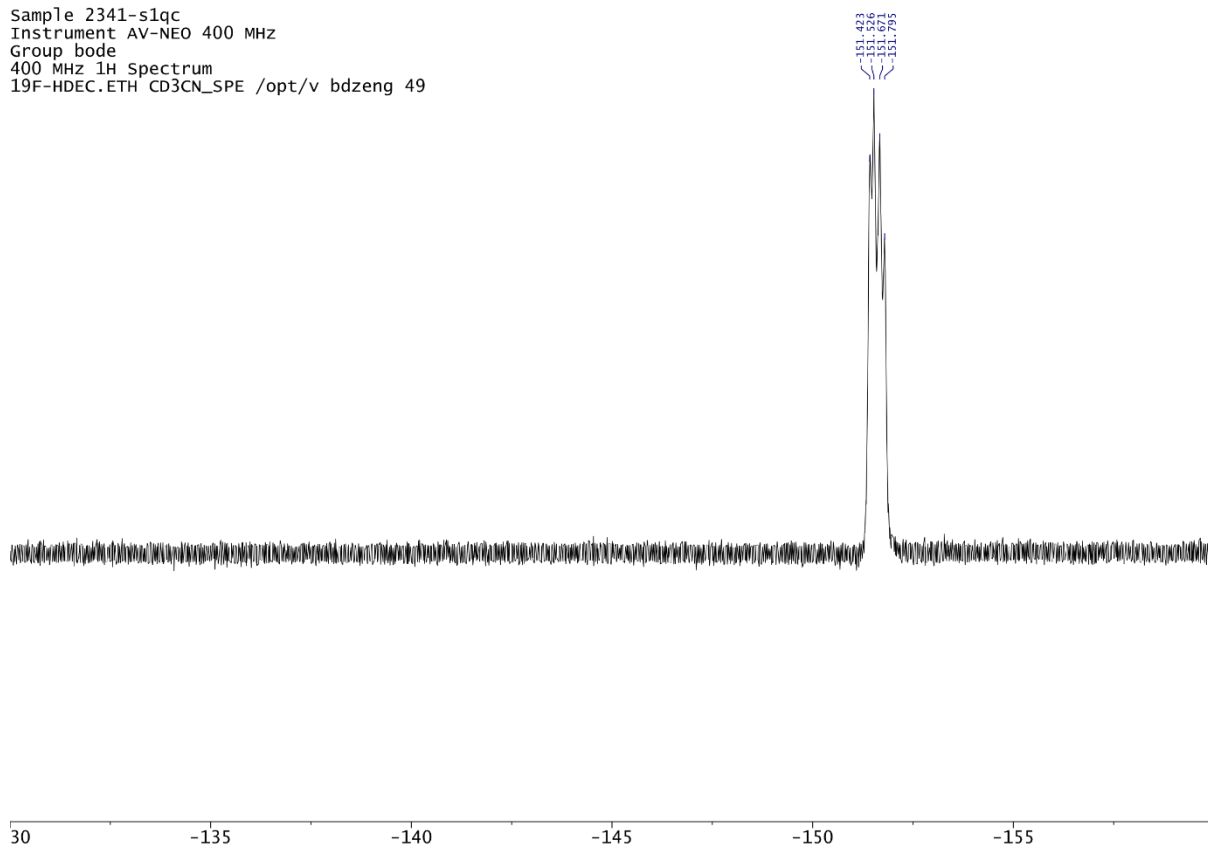
Compound 190

Sample 2341-s1qc
Instrument AV-NEO 400
Group bode
400 MHz ¹H Spectrum
PRO.ETH CD3CN_SPE /opt/v bdzeng 49



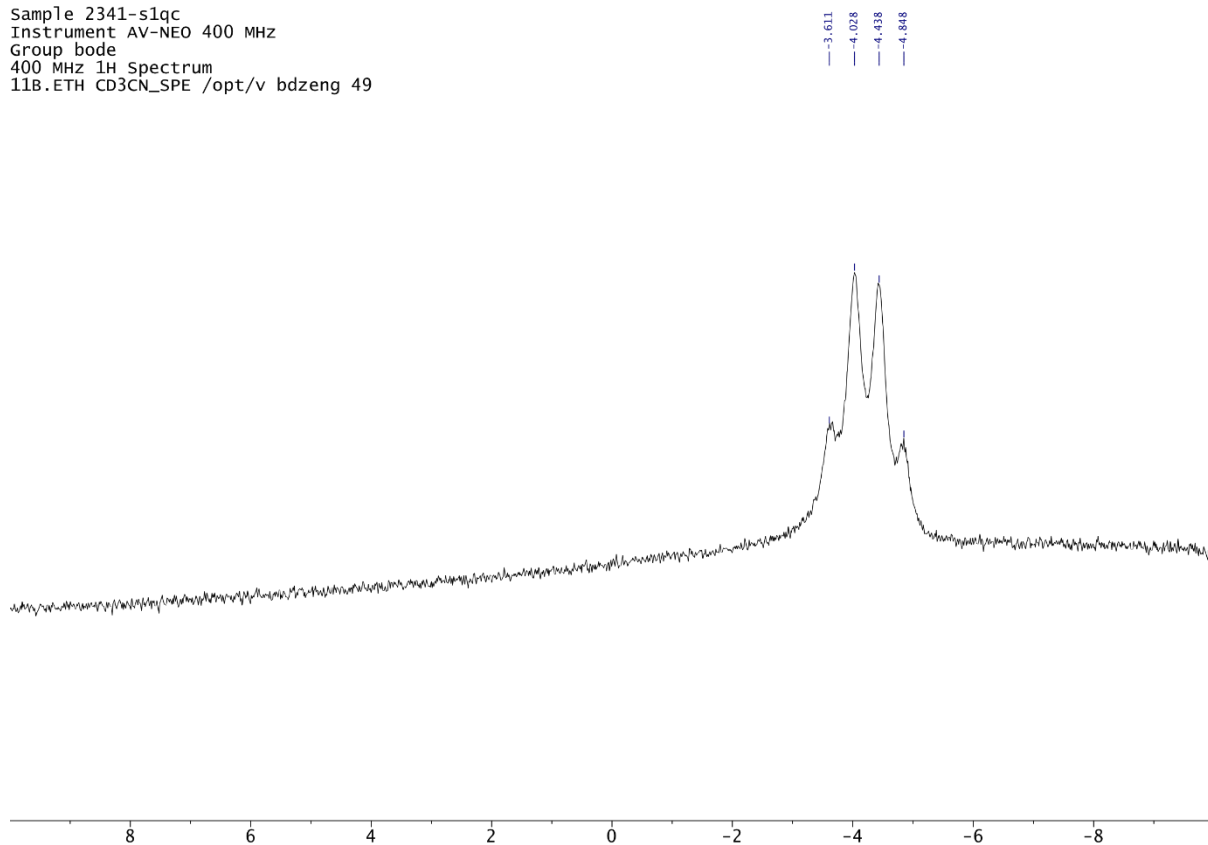
¹⁹F 376 MHz

Sample 2341-s1qc
 Instrument AV-NEO 400 MHz
 Group bode
 400 MHz 1H Spectrum
 19F-HDEC.ETH CD3CN_SPE /opt/v bdzeng 49

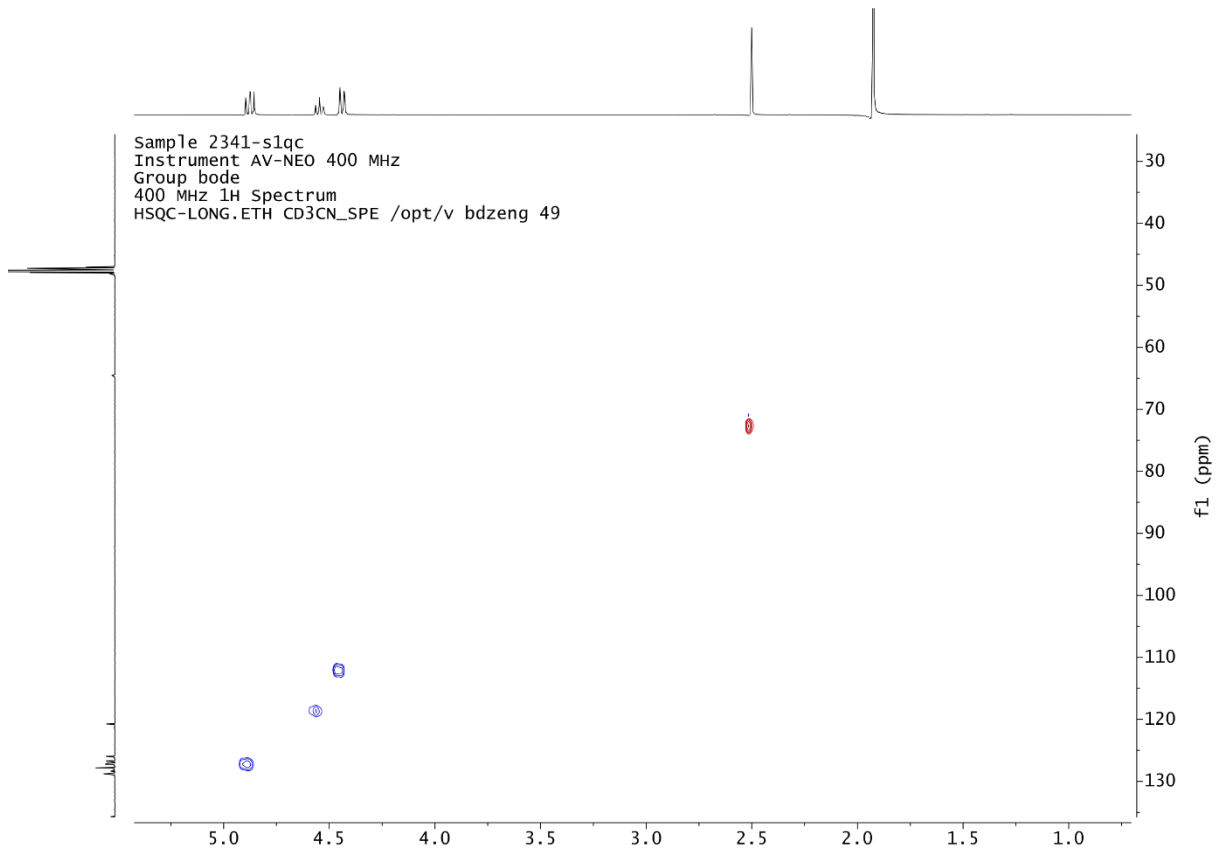


¹¹B 128 MHz

Sample 2341-s1qc
 Instrument AV-NEO 400 MHz
 Group bode
 400 MHz 1H Spectrum
 11B.ETH CD3CN_SPE /opt/v bdzeng 49

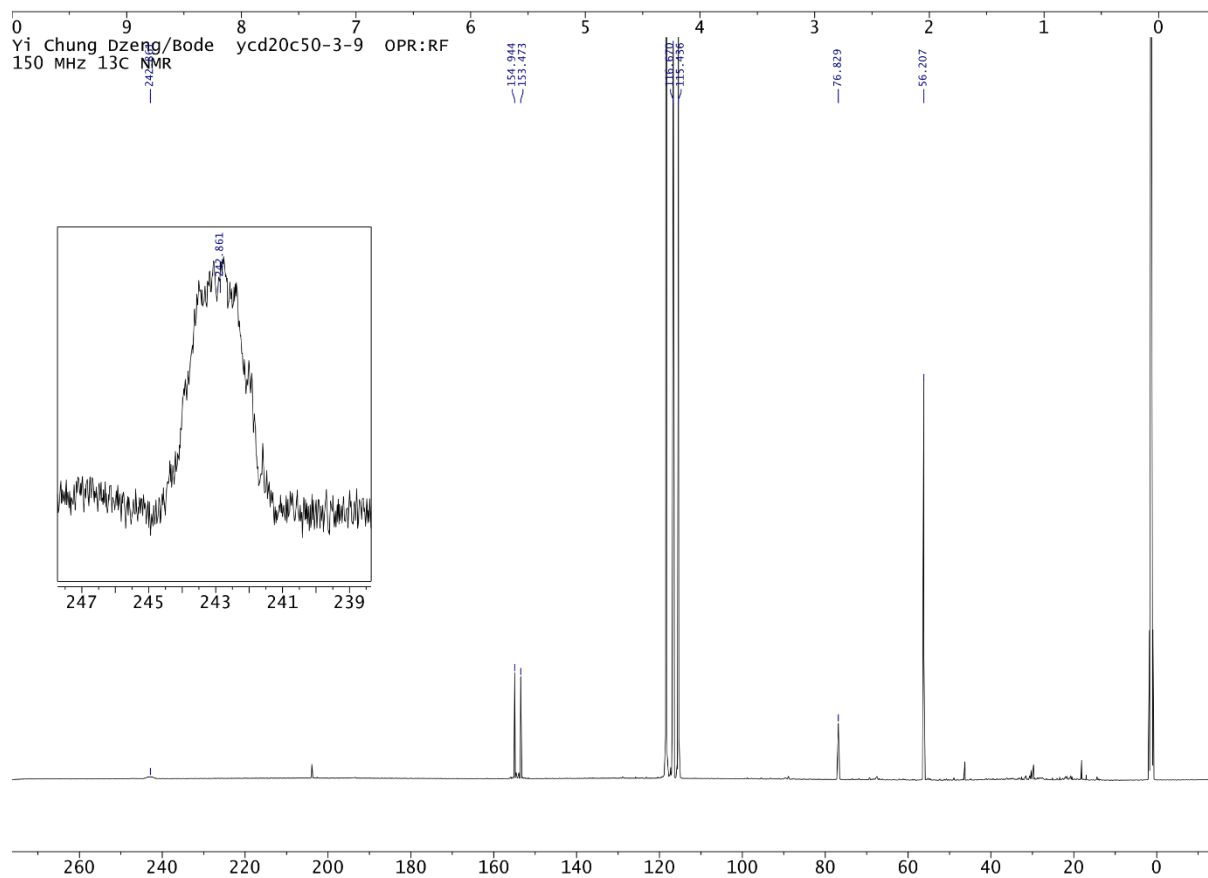
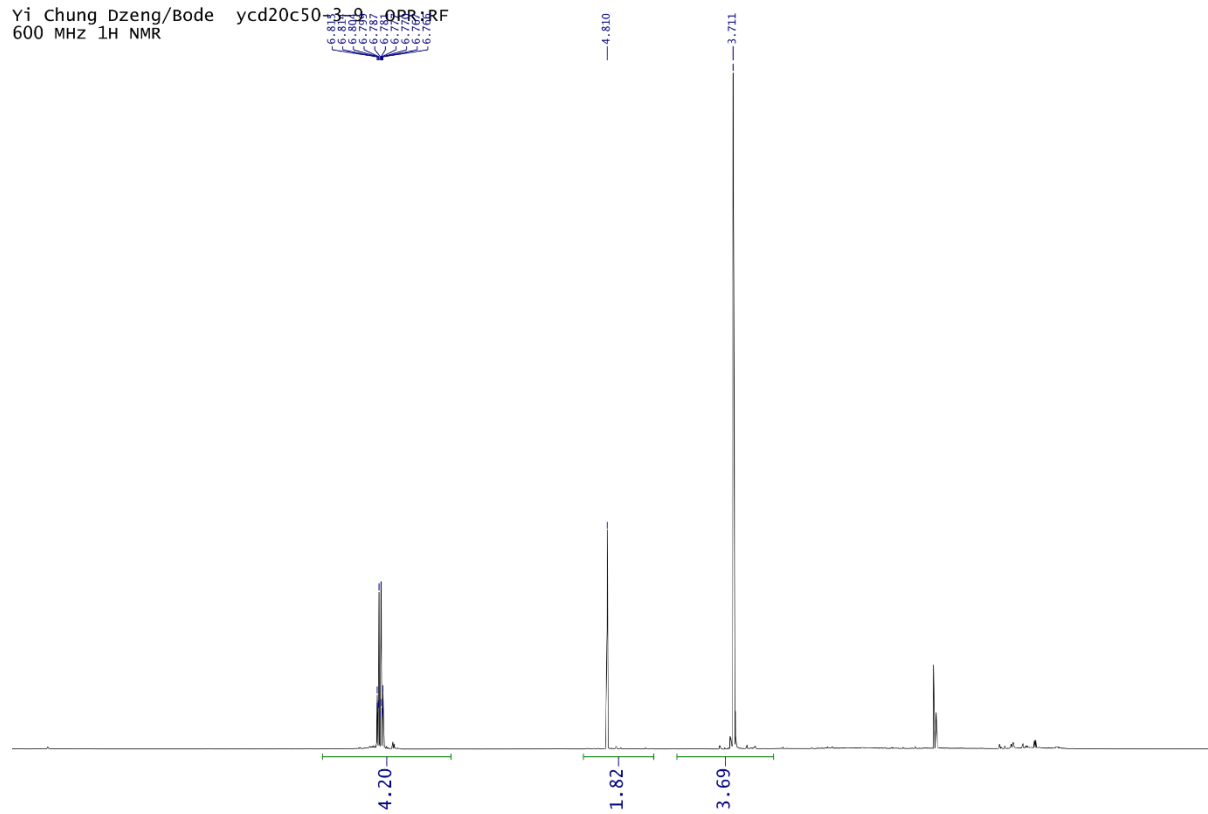


NMR Spectra



Compound 191

Yi Chung Dzung/Bode ycd20c50-3-9 OPR:RF
600 MHz 1H NMR



NMR Spectra

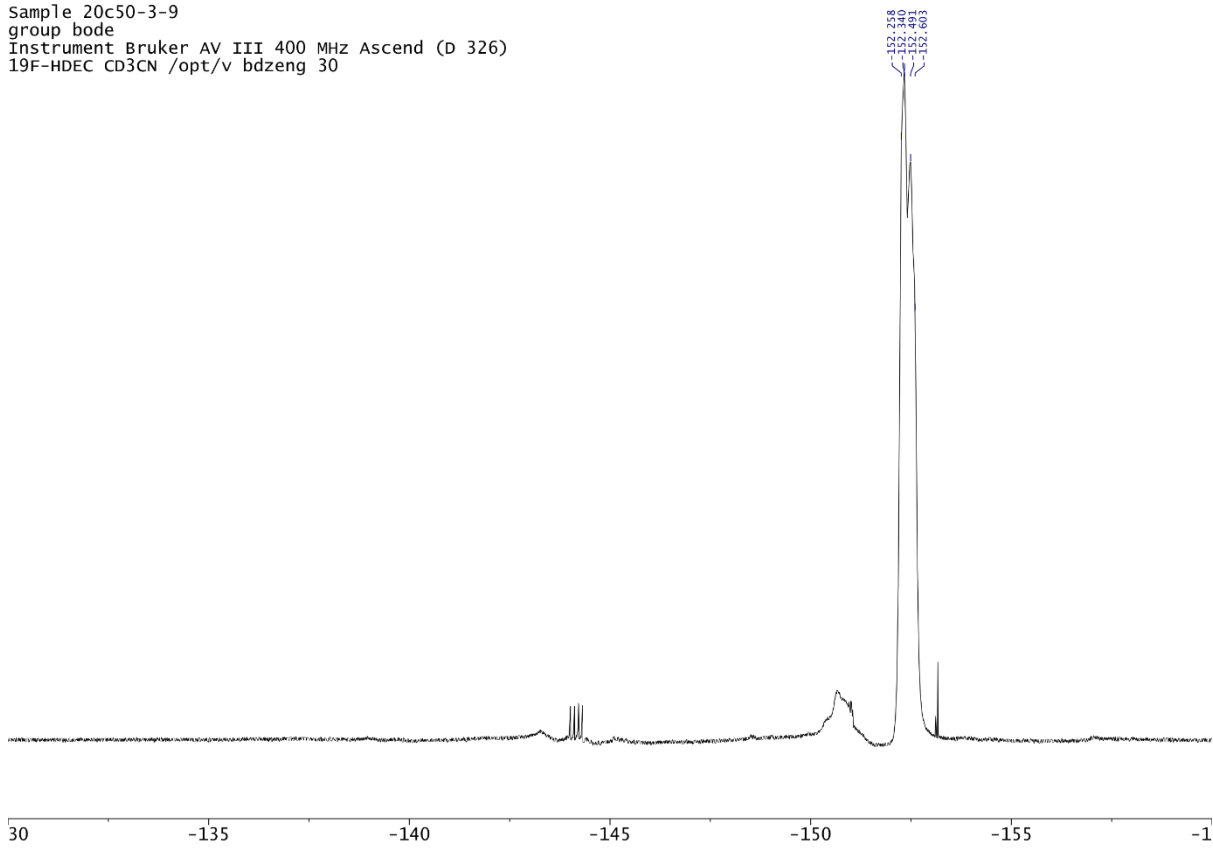
^{19}F 376 MHz

Sample 20c50-3-9

group bode

Instrument Bruker AV III 400 MHz Ascend (D 326)

^{19}F -HDEC CD $_3\text{CN}$ /opt/v bdzeng 30



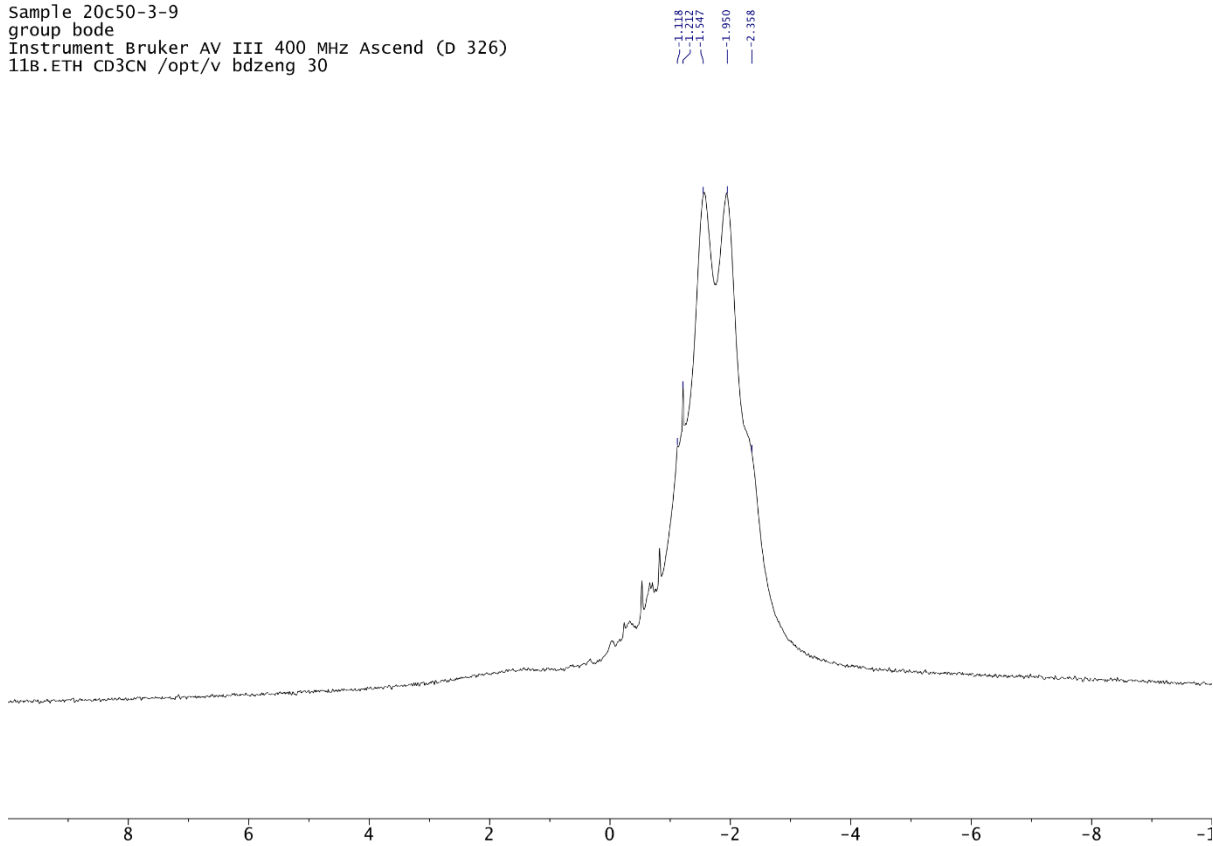
^{11}B 128 MHz

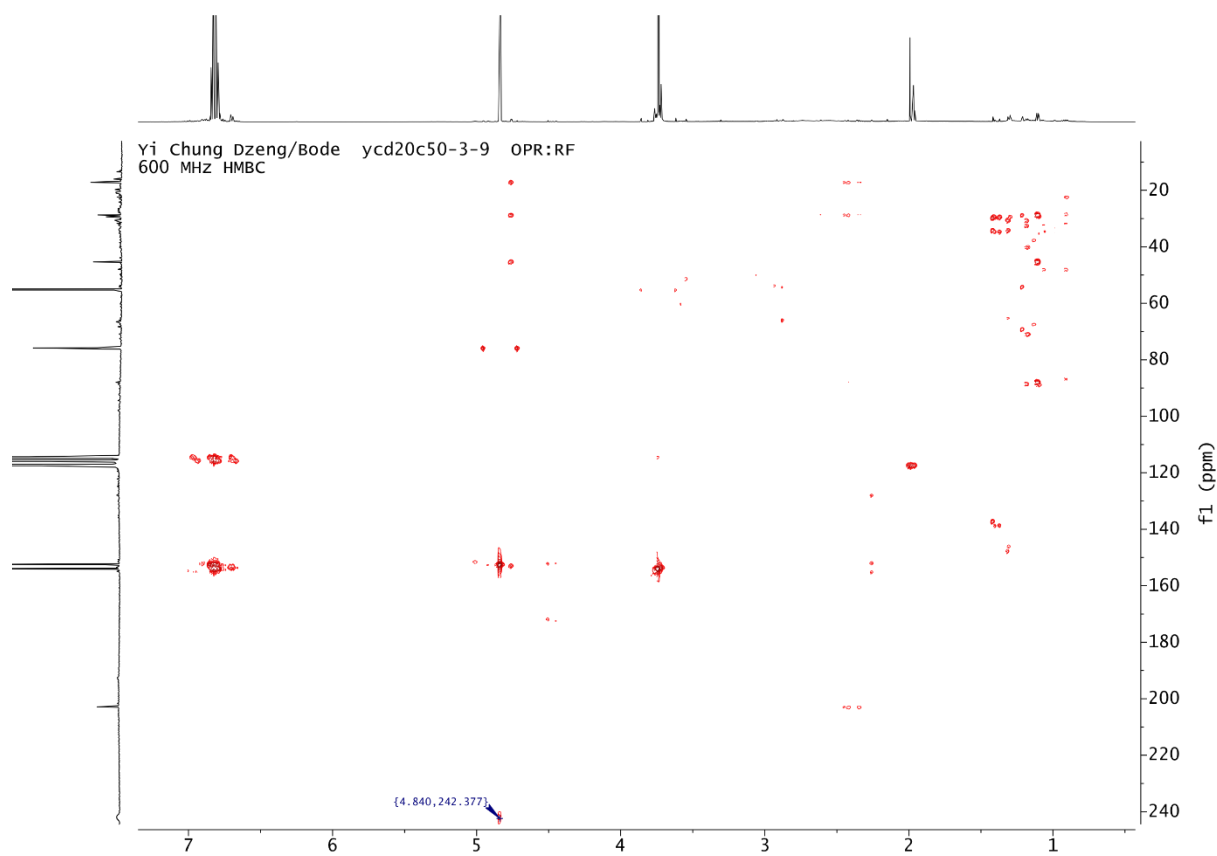
Sample 20c50-3-9

group bode

Instrument Bruker AV III 400 MHz Ascend (D 326)

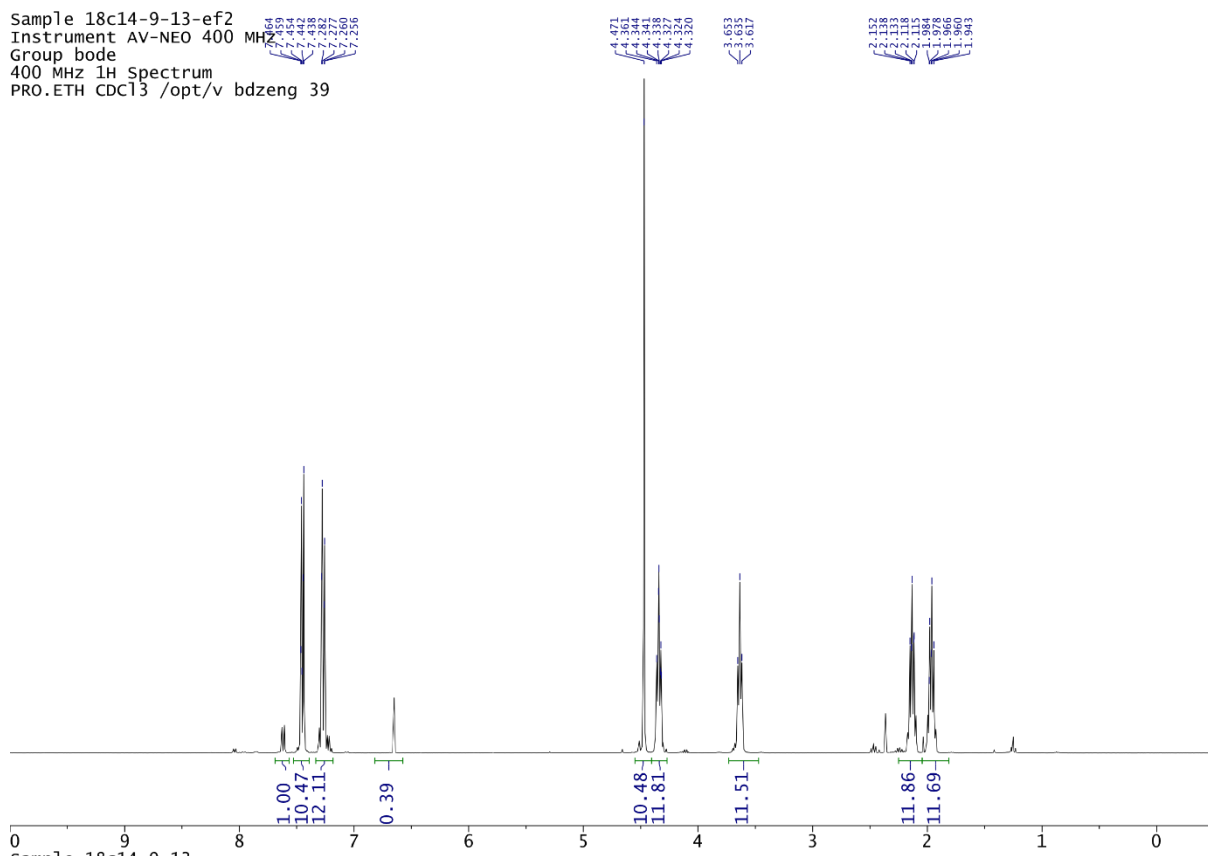
11B.ETH CD $_3\text{CN}$ /opt/v bdzeng 30



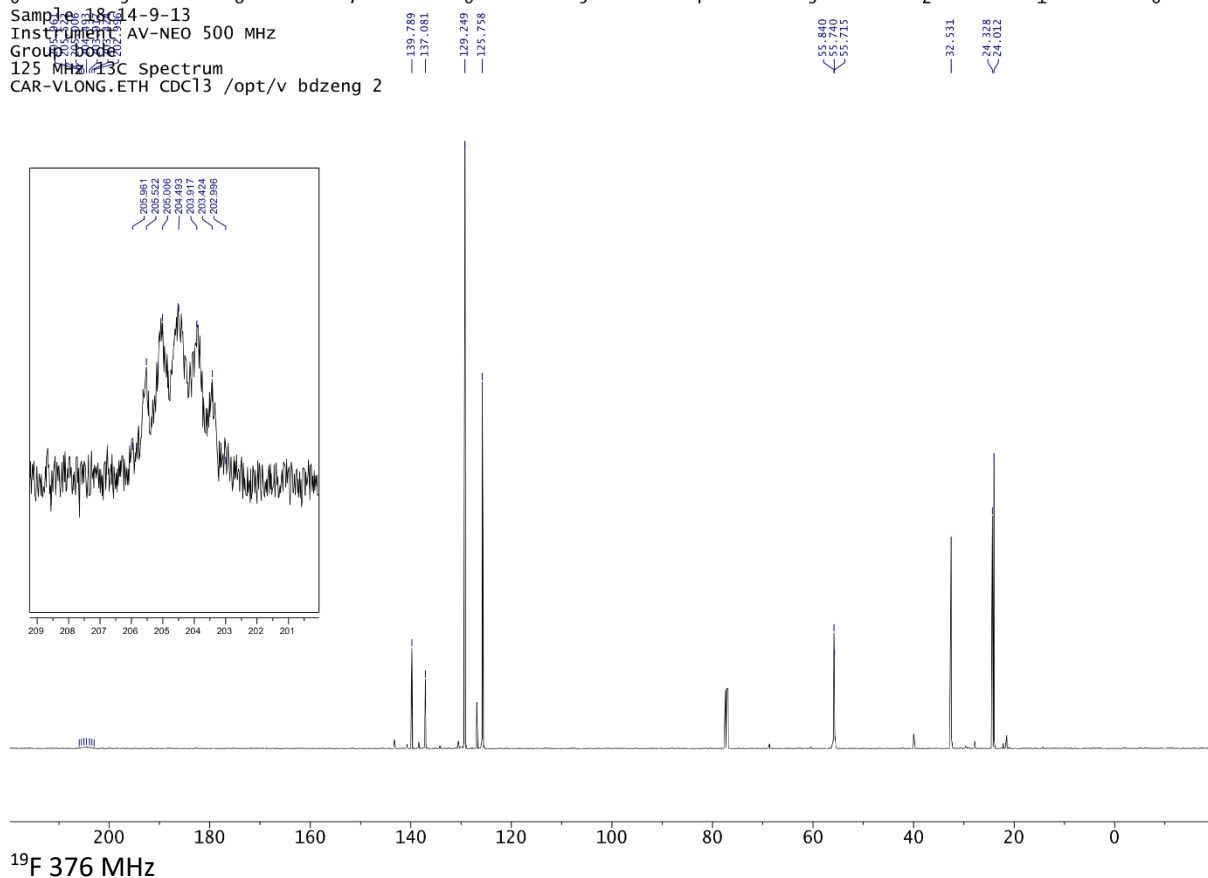


Compound 198

Sample 18c14-9-13-ef2
 Instrument AV-NEO 400 MHz
 Group bode
 400 MHz 1H Spectrum
 PRO.ETH CDC13 /opt/v bdzeng 39

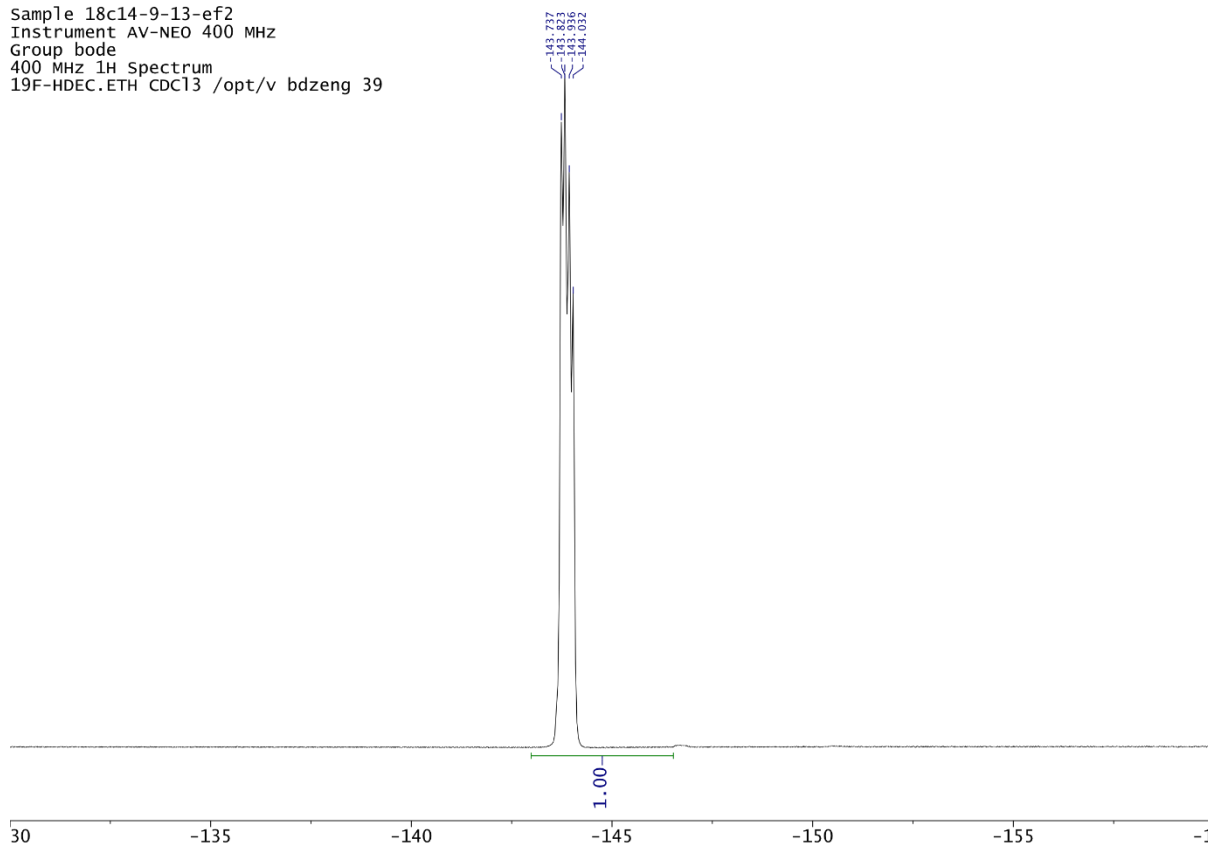


Sample 18c14-9-13
 Instrument AV-NEO 500 MHz
 Group bode
 125 MHz 13C Spectrum
 CAR-VLONG.ETH CDC13 /opt/v bdzeng 2

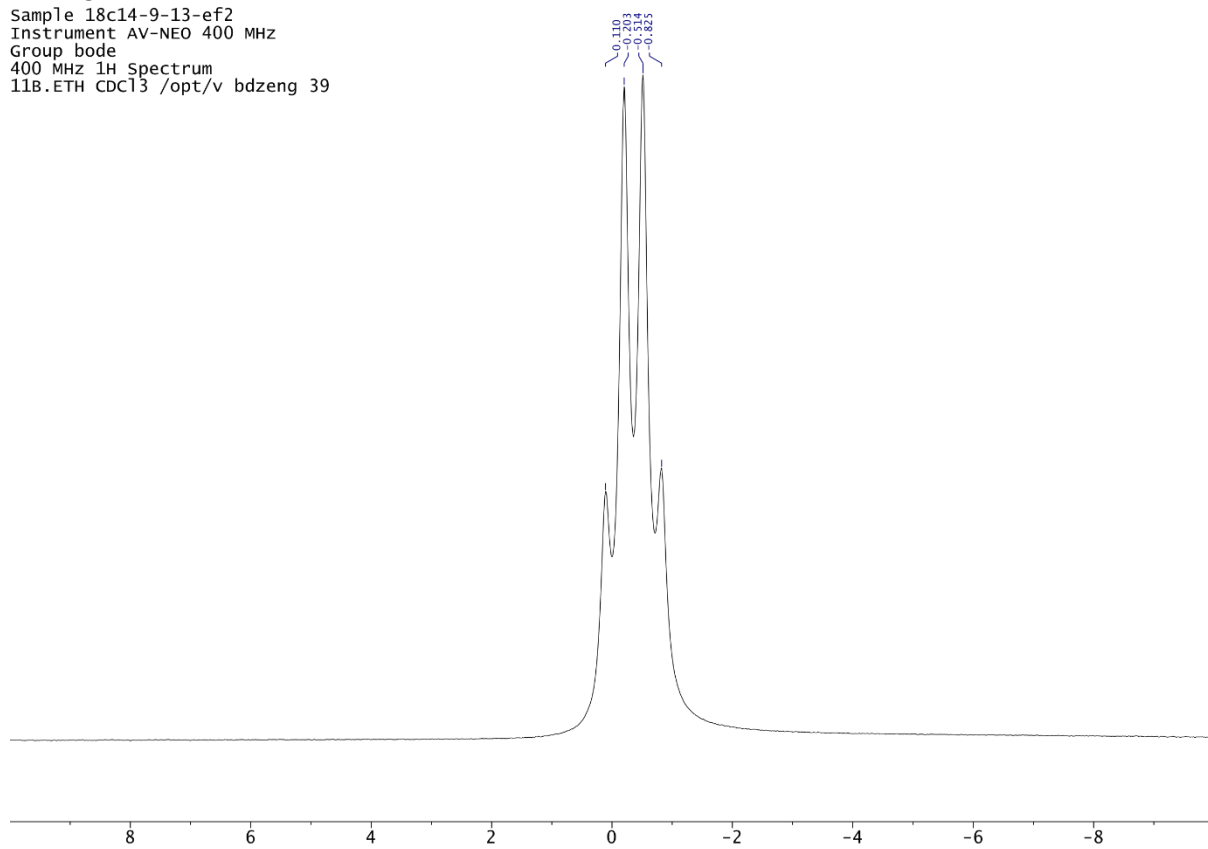


¹⁹F 376 MHz

Sample 18c14-9-13-ef2
 Instrument AV-NEO 400 MHz
 Group bode
 400 MHz 1H Spectrum
 19F-HDEC.ETH CDC13 /opt/v bdzeng 39



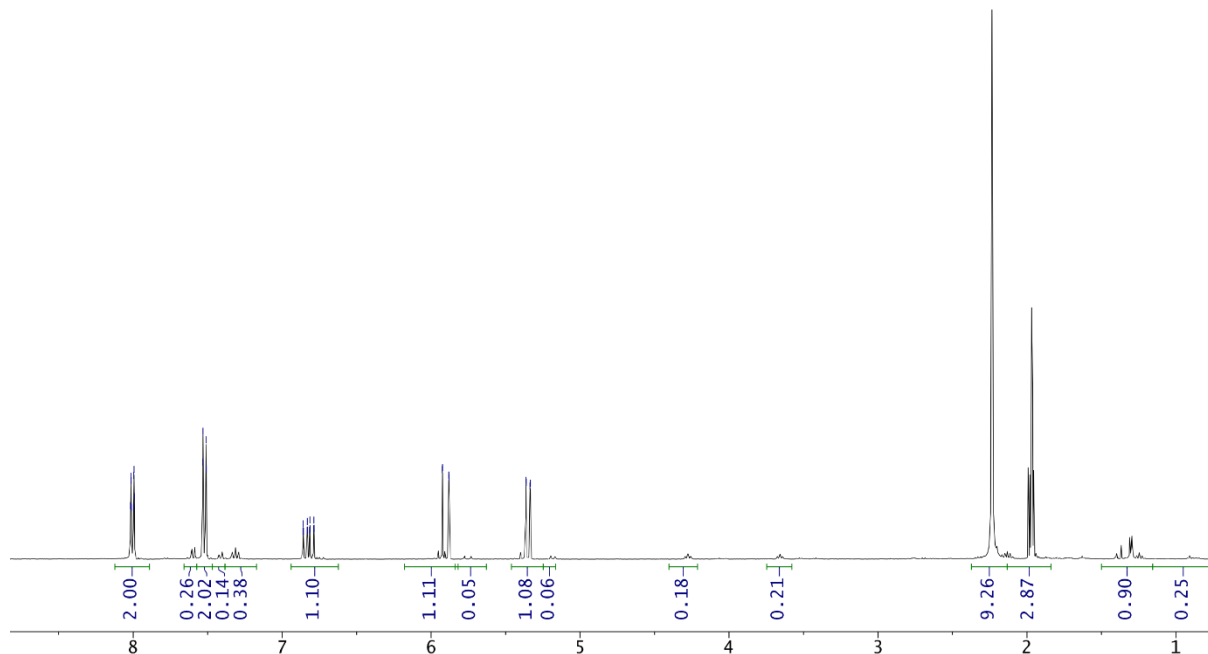
11B 128 MHz
 Sample 18c14-9-13-ef2
 Instrument AV-NEO 400 MHz
 Group bode
 400 MHz 1H Spectrum
 11B.ETH CDC13 /opt/v bdzeng 39



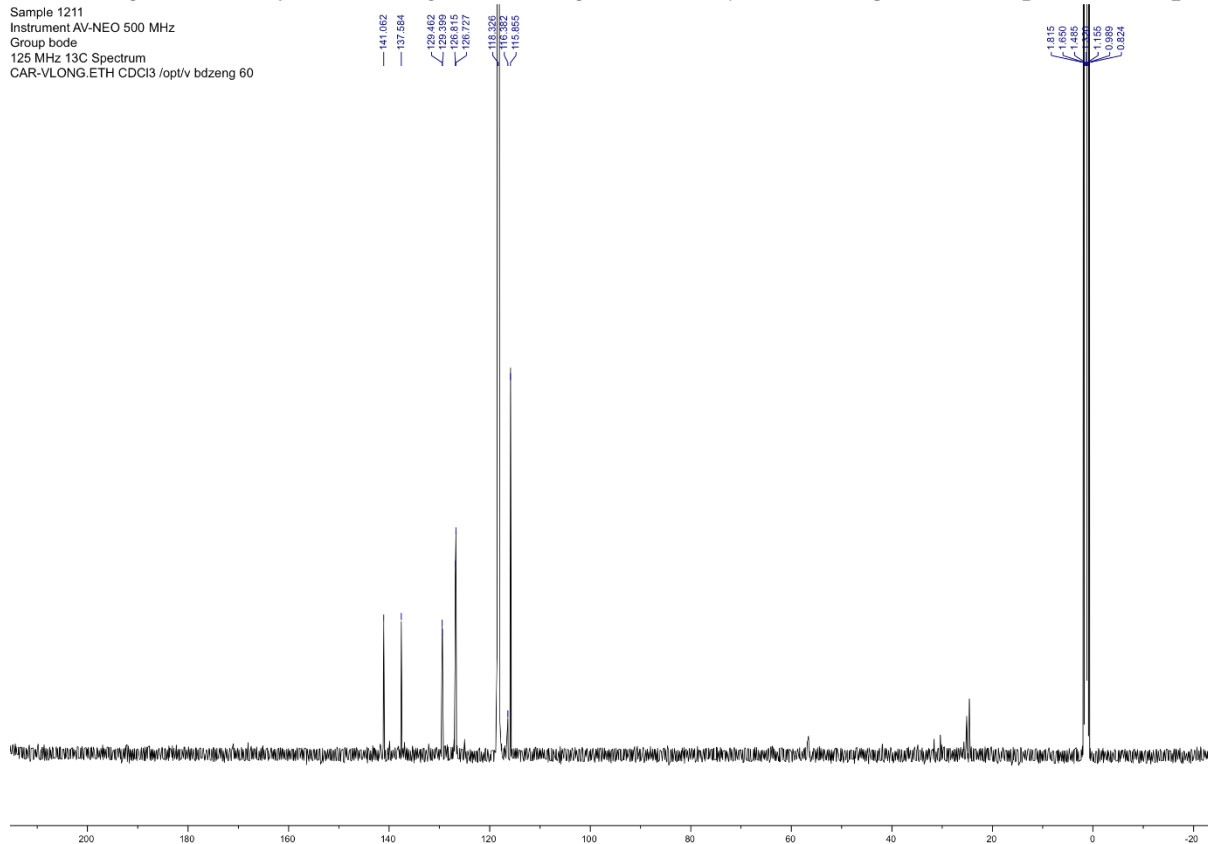
NMR Spectra

Compound 199

Sample 1221
 Instrument AV-NEO 400 MHz
 Group bode
 400 MHz 1H Spectrum
 PRO.ETH CD3CN /opt/v bdzeng 43

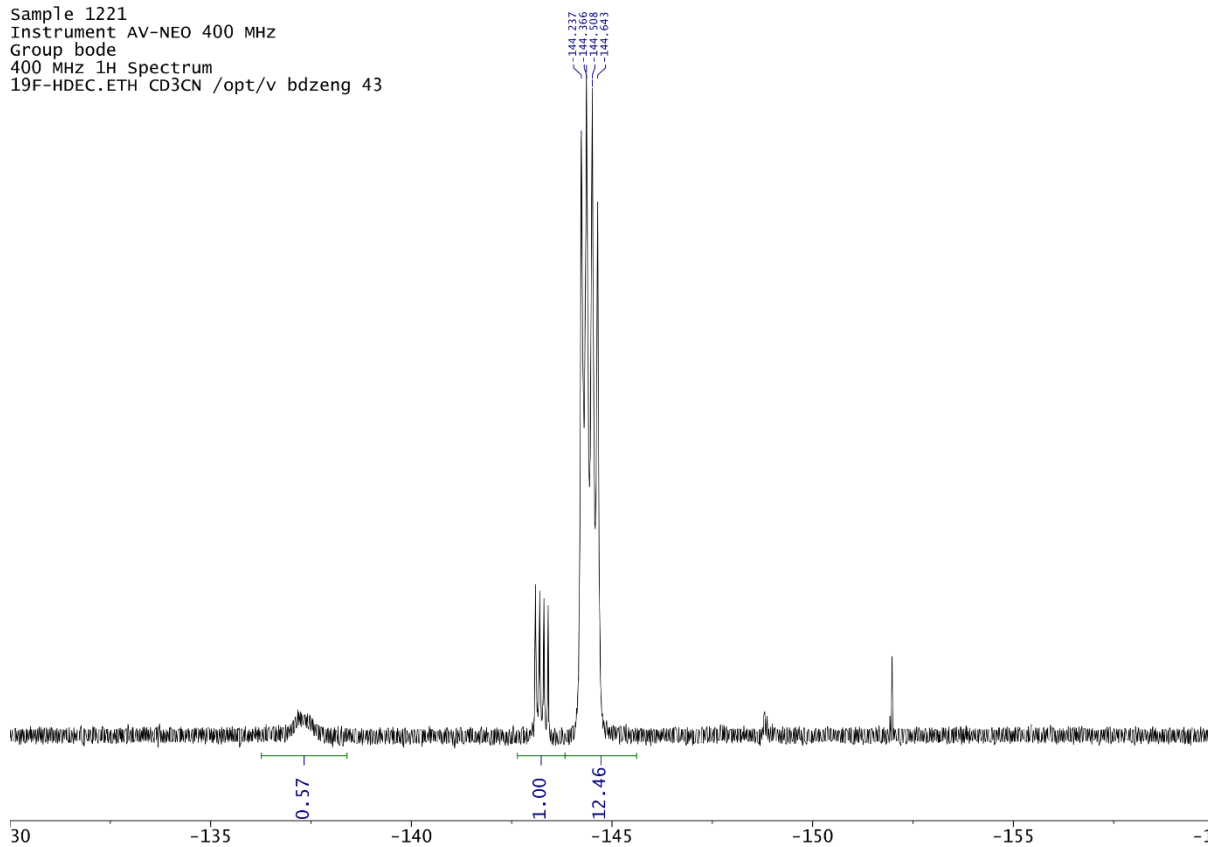


Sample 1211
 Instrument AV-NEO 500 MHz
 Group bode
 125 MHz 13C Spectrum
 CAR-VLONG.ETH CDCl3 /opt/v bdzeng 60



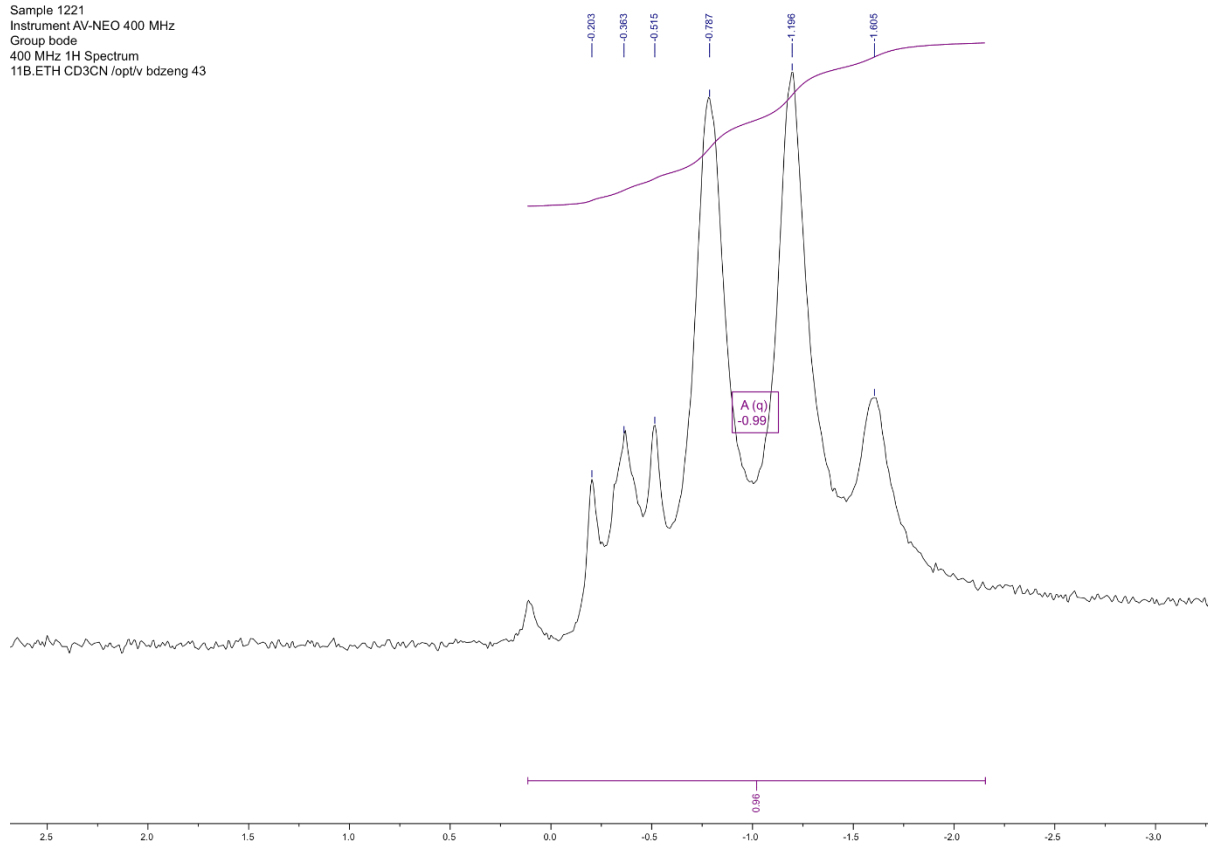
¹³C 376 MHz

Sample 1221
 Instrument AV-NEO 400 MHz
 Group bode
 400 MHz 1H Spectrum
 19F-HDEC.ETH CD3CN /opt/v bdzeng 43

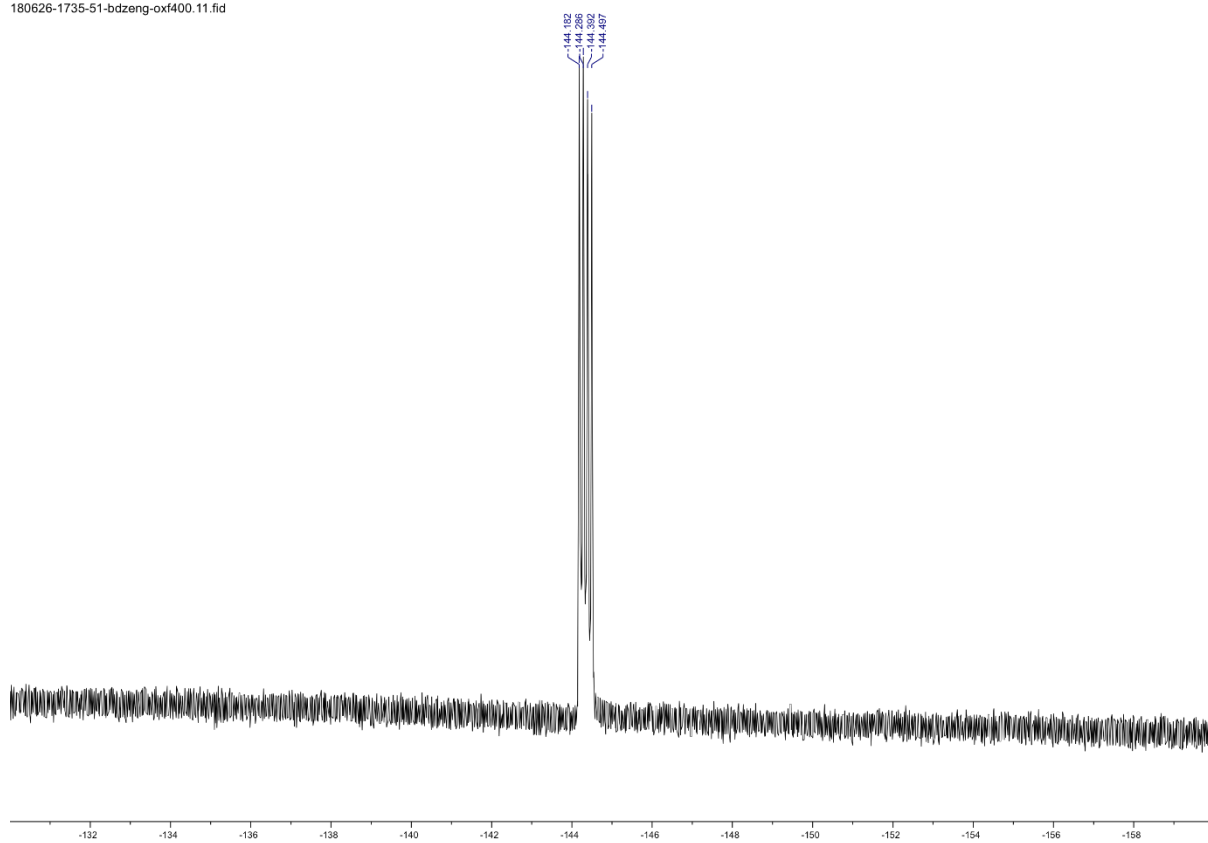


¹¹B 128 MHz

Sample 1221
 Instrument AV-NEO 400 MHz
 Group bode
 400 MHz 1H Spectrum
 11B.ETH CD3CN /opt/v bdzeng 43

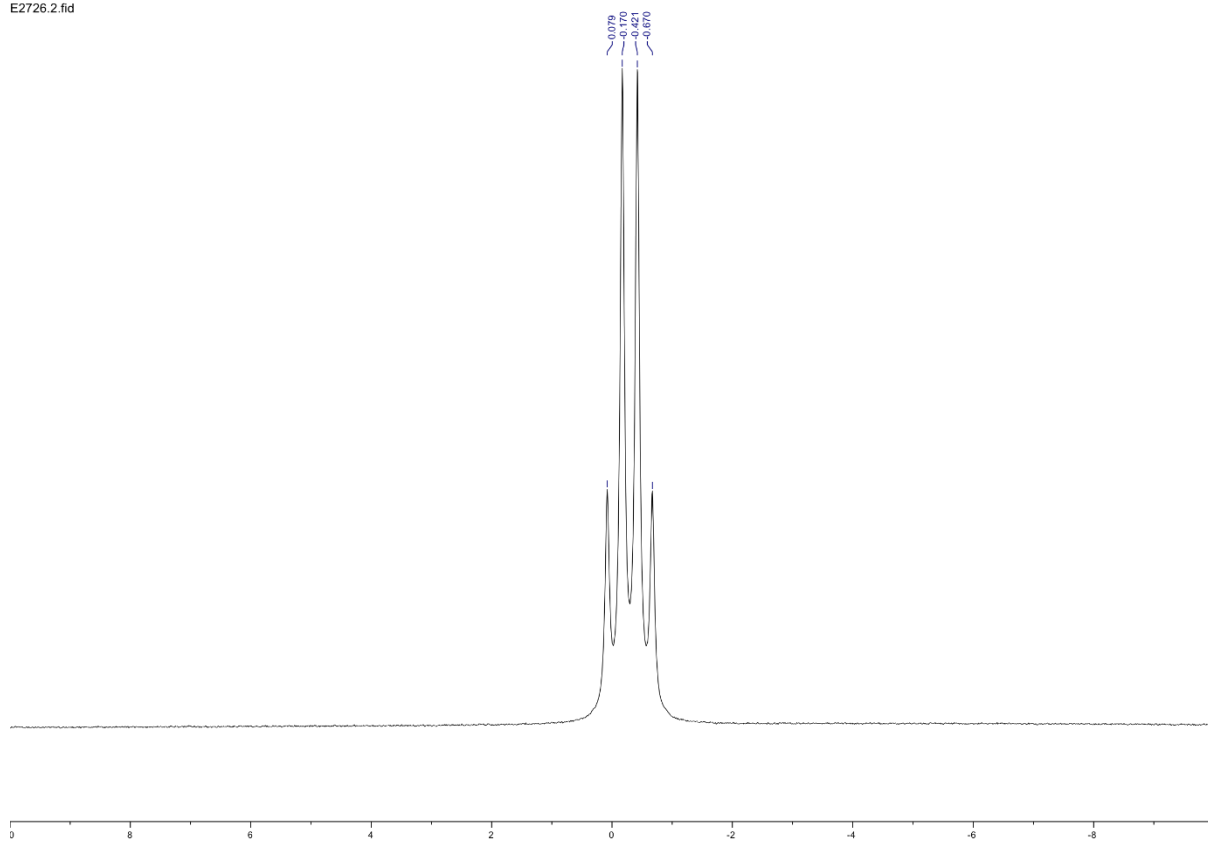


180626-1735-51-bdzeng-oxf400.11.fid

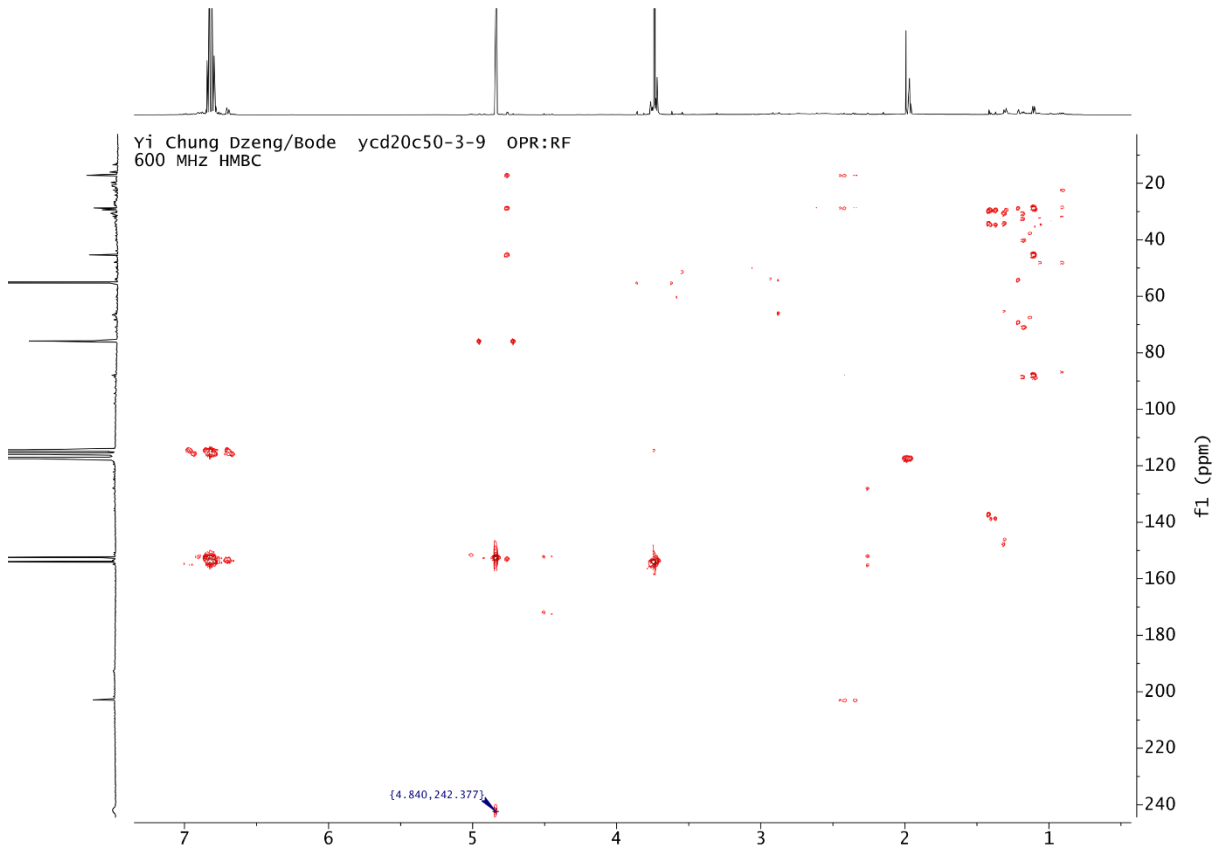


^{11}B 160 MHz

E2726.2.fid

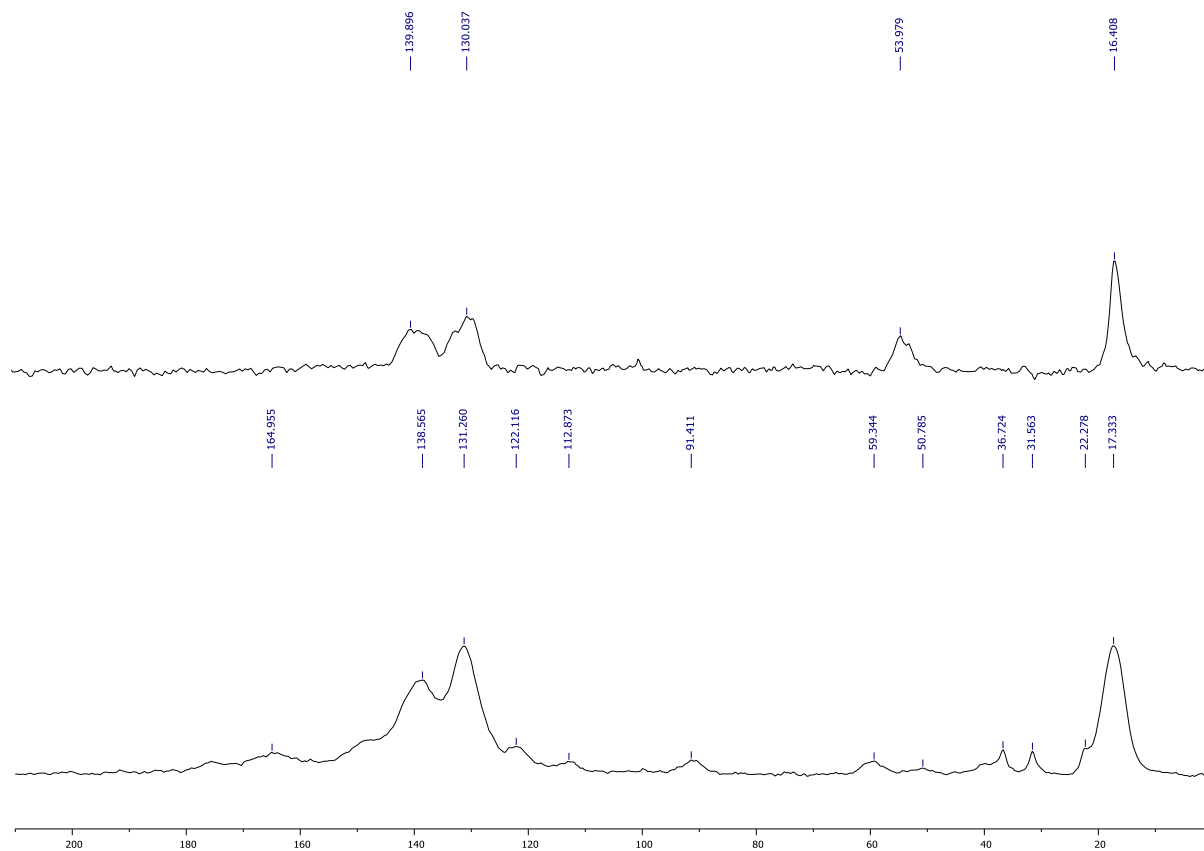


NMR Spectra



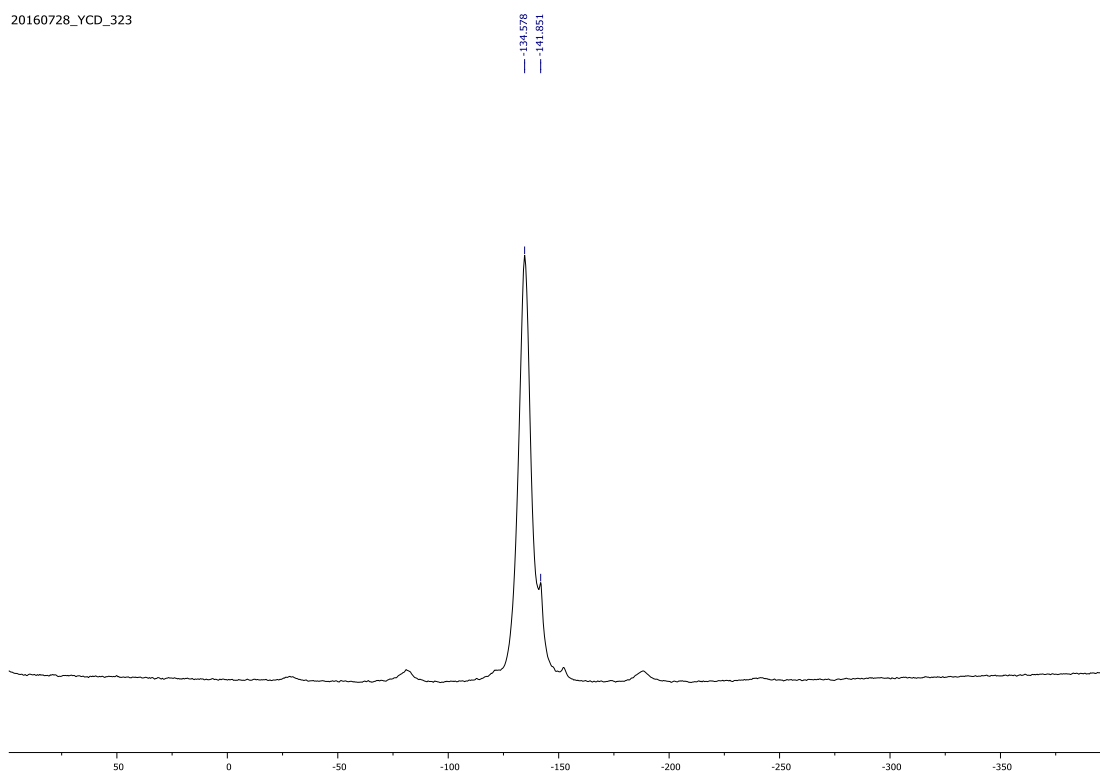
MAS SSNMR at 20kHz of the nitron from KAT 141 and hydroxylamine 124`

¹³C 100 MHz: Top: 124`, bottom: nitron.



¹⁹F 377 MHz

20160728_YCD_323



Yi-Chung Dzeng

Born: 10 Jan 1990; Nationality: Taiwan

ycdzeng@org.chem.ethz.ch
HCI F302 Vladimir-Prelog-Weg 3
8093 Zürich, Schweiz**EDUCATION/RESEARCH****ETH Zürich**

Postdoctoral associate	July 2021 - Sep 2021
PhD in Chemistry	October 2015 - June 2021
Advisor: Prof. Jefferey W. Bode	
Thesis: Dynamic Chemistry with Potassium Acyltrifluoroborates (KATs)	
Defense date: 05 May 2021	

National Taiwan University

MSc in Chemistry	June 2013 - August 2015
BSc in Chemistry	July 2008 - July 2012
Advisor: Prof. Tien-Yau Luh	
Polymer Synthesis and Conformation Dependent Photophysics	
Defense date: 14 Aug 2015	

TEACHING/NON-RESEARCH WORKING EXPERIENCE**OCP1 / OACP1**

1st / 2nd year organic chemistry lab course

ETH Zürich

OACPI TA	2016 Spring - 2017 Fall
OCPI TA	2017 Fall - 2018 Spring

Semester project supervision

Project student supervision

ETH Zürich

KAT derivatives and hydroxylamines towards vitrimers	Maria Reichenbach
Exploring a potential protecting group for Potassium Acyltrifluoroborates	Daniel Richter
Development of new KAT protection groups - II	Mike Mürli
Development of strained bicyclic hydroxylamines for faster KAT ligation	Julius Kuzmin

Organic Chemistry III

Physical Organic Chemistry and Topics in Organic Synthesis

National Taiwan University

Teaching Assistant	2010 Fall - 2011 Spring
Head Teaching Assistant	2014 Fall - 2015 Spring

Brigade CBRN Protection Officer

Compulsary Military Service as a general brigade S3 (Operational) Staff

602nd Aviation Brigade, Taiwanese Army

Second Lieutenant	2012 Summer - 2013 Summer
-------------------	---------------------------

PUBLICATIONS

Dzeng, Y.-C., Bode, J. W., A cyclic thioimidate reagent for the one-step, transition-metal free synthesis of alkyl potassium acyltrifluoroborates(KATs), manuscript in preparation

Dzeng, Y.-C., Bode, J. W., Dynamic Amide Formation by Reversible Nitron Exchange of Potassium Acyltrifluoroborates (KATs) and Hydroxylamines in Aqueous Conditions, Chem. Sci, 2021, submitted, Preprint at

ChemRxiv with doi: 10.33774/chemrxiv-2021-zm828

Tanriver, M.; Dzung, Y.-C. (co-1st authorship); Lam, E.; Bode, J. W. Mechanism-Based Design of Quinoline Potassium Acyltrifluoroborates (KATs) for Rapid Amide-Forming Ligations at Physiological pH., *J. Am. Chem. Soc.*, **2021**, accepted, doi: 10.1021/jacs.1c07354

D. Schauenburg; Divandari, M.; Neumann, K.; Spiegel, C. A.; Hackett, T.; **Dzung, Y.-C.**; Spencer, N. D.; Bode, J. W., Synthesis of Polymers Containing Potassium Acyltrifluoroborates (KATs) and Post-polymerization Ligation and Conjugation., *Angew. Chemie Int. Ed.*, **2020**, 59, 34, 14656-14663

Dzung, Y.-C.; Huang, C.-L.; Liu, Y.-H.; Lim, T.-S.; Chen, I.-C.; Luh, T.-Y., Substituent-Dependent Photophysical Properties Due to the Thorpe–Ingold Effect on Foldings of Alternating Substituted Methylene–Diethynylbenzene Copolymers: A Comparison of Carbon versus Silicon Tethers *Macromolecules* **2015**, 48, 24, 8708-8717

OTHER SKILLS AND INTERESTS

Data Processing/Visualization	Mathematica, GnuPlot
Operation Systems	Linux (or Unix-Like), MacOSX, Windows
Programming	Ruby, Bash, C/C++, Perl
Reverse Engineering	Instrument data file formats Monitoring of open-access instrument automations Numerical analysis of chemical dynamics

INSTITUTIONAL RESPONSIBILITIES

Group NMR coordinator deputy
Lab dry solvent distil management
Rotary evaporator superuser
Infrared spectrometer superuser

REFERENCE

Prof. Dr. Jeffrey W. Bode

Laboratorium für Organische Chemie, ETH Zürich
HCI F 317, Vladimir-Prelog-Weg 3, 8093 Zürich, Switzerland
bode@org.chem.ethz.ch
+41 44 633 21 03

Prof. Em. Tien-Yau Luh

Department of Chemistry, National Taiwan University
1. Roosevelt Road Sec. 4., Taipei 10617, Taiwan
tyluh@ntu.edu.tw
+886 2 3366 4088

Prof. Em. Shun-Ichi Murahashi

Department of Chemistry, Graduate School of Engineering Science, Osaka University
1-3, Machikaneyama, Toyonaka, Osaka 560-8531, Japan
mura@chem.es.osaka-u.ac.jp
+81 6 6835 5535